EFFECTS OF DIFFERENT LIGHT SPECTRA ON SECONDARY/SPECIALIZED METABOLITE ACCUMULATION AND PLANT RESISTANCE MECHANISMS

EDITED BY: Inga Mewis, Marie-Theres Hauser, Titta Katariina Kotilainen and Nadja Förster

PUBLISHED IN: Frontiers in Plant Science

frontiers Research Topics

Frontiers eBook Copyright Statement

The copyright in the text of individual articles in this eBook is the property of their respective authors or their respective institutions or funders. The copyright in graphics and images within each article may be subject to copyright of other parties. In both cases this is subject to a license granted to Frontiers.

The compilation of articles constituting this eBook is the property of Frontiers.

Each article within this eBook, and the eBook itself, are published under the most recent version of the Creative Commons CC-BY licence. The version current at the date of publication of this eBook is CC-BY 4.0. If the CC-BY licence is updated, the licence granted by Frontiers is automatically updated to the new version.

When exercising any right under the CC-BY licence, Frontiers must be attributed as the original publisher of the article or eBook, as applicable.

Authors have the responsibility of ensuring that any graphics or other materials which are the property of others may be included in the CC-BY licence, but this should be checked before relying on the CC-BY licence to reproduce those materials. Any copyright notices relating to those materials must be complied with.

Copyright and source acknowledgement notices may not be removed and must be displayed in any copy, derivative work or partial copy which includes the elements in question.

All copyright, and all rights therein, are protected by national and international copyright laws. The above represents a summary only. For further information please read Frontiers' Conditions for Website Use and Copyright Statement, and the applicable CC-BY licence.

ISSN 1664-8714
ISBN 978-2-88971-705-7
DOI 10.3389/978-2-88971-705-7

About Frontiers

Frontiers is more than just an open-access publisher of scholarly articles: it is a pioneering approach to the world of academia, radically improving the way scholarly research is managed. The grand vision of Frontiers is a world where all people have an equal opportunity to seek, share and generate knowledge. Frontiers provides immediate and permanent online open access to all its publications, but this alone is not enough to realize our grand goals.

Frontiers Journal Series

The Frontiers Journal Series is a multi-tier and interdisciplinary set of open-access, online journals, promising a paradigm shift from the current review, selection and dissemination processes in academic publishing. All Frontiers journals are driven by researchers for researchers; therefore, they constitute a service to the scholarly community. At the same time, the Frontiers Journal Series operates on a revolutionary invention, the tiered publishing system, initially addressing specific communities of scholars, and gradually climbing up to broader public understanding, thus serving the interests of the lay society, too.

Dedication to Quality

Each Frontiers article is a landmark of the highest quality, thanks to genuinely collaborative interactions between authors and review editors, who include some of the world's best academicians. Research must be certified by peers before entering a stream of knowledge that may eventually reach the public - and shape society; therefore, Frontiers only applies the most rigorous and unbiased reviews.
Frontiers revolutionizes research publishing by freely delivering the most outstanding research, evaluated with no bias from both the academic and social point of view. By applying the most advanced information technologies, Frontiers is catapulting scholarly publishing into a new generation.

What are Frontiers Research Topics?

Frontiers Research Topics are very popular trademarks of the Frontiers Journals Series: they are collections of at least ten articles, all centered on a particular subject. With their unique mix of varied contributions from Original Research to Review Articles, Frontiers Research Topics unify the most influential researchers, the latest key findings and historical advances in a hot research area! Find out more on how to host your own Frontiers Research Topic or contribute to one as an author by contacting the Frontiers Editorial Office: frontiersin.org/about/contact

EFFECTS OF DIFFERENT LIGHT SPECTRA ON SECONDARY/SPECIALIZED METABOLITE ACCUMULATION AND PLANT RESISTANCE MECHANISMS

Topic Editors:
Inga Mewis, Humboldt University of Berlin, Germany
Marie-Theres Hauser, University of Natural Resources and Life Sciences Vienna, Austria
Titta Katariina Kotilainen, Natural Resources Institute Finland (Luke), Finland
Nadja Förster, Humboldt University of Berlin, Germany

Citation: Mewis, I., Hauser, M.-T., Kotilainen, T. K., Förster, N., eds. (2021). Effects of Different Light Spectra on Secondary/Specialized Metabolite Accumulation and Plant Resistance Mechanisms. Lausanne: Frontiers Media SA.
doi: 10.3389/978-2-88971-705-7

Table of Contents

frontiers in Plant Science

ORIGINAL RESEARCH
published: 30 October 2020
doi: 10.3389/fpls.2020.579063

Beyond the Visible and Below the Peel: How UV-B Radiation Influences the Phenolic Profile in the Pulp of Peach Fruit. A Biochemical and Molecular Study

Marco Santin[1], Antonella Castagna[1,2], Begoña Miras-Moreno[3,4], Gabriele Rocchetti[3], Luigi Lucini[3], Marie-Theres Hauser[5]* and Annamaria Ranieri[1,2]*

[1] Department of Agriculture, Food and Environment, University of Pisa, Pisa, Italy, [2] Interdepartmental Research Center Nutrafood "Nutraceuticals and Food for Health", University of Pisa, Pisa, Italy, [3] Department for Sustainable Food Process, Università Cattolica del Sacro Cuore, Piacenza, Italy, [4] Council for Agricultural Research and Economics- Research Centre for Genomics and Bioinformatics, Fiorenzuola d'Arda, Italy, [5] Department of Applied Genetics and Cell Biology, University of Natural Resources and Life Sciences, Vienna, Austria

OPEN ACCESS

Edited by:
Supaart Sirikantaramas, Chulalongkorn University, Thailand

Reviewed by:
Yuepeng Han, Wuhan Botanical Garden, Chinese Academy of Sciences, China
Pengmin Li, Northwest A&F University, China

***Correspondence:**
Antonella Castagna
antonella.castagna@unipi.it
Marie-Theres Hauser
marie-theres.hauser@boku.ac.at

Specialty section:
This article was submitted to Plant Metabolism and Chemodiversity, a section of the journal Frontiers in Plant Science

Received: *01 July 2020*
Accepted: *12 October 2020*
Published: *30 October 2020*

Citation:
Santin M, Castagna A, Miras-Moreno B, Rocchetti G, Lucini L, Hauser M-T and Ranieri A (2020) Beyond the Visible and Below the Peel: How UV-B Radiation Influences the Phenolic Profile in the Pulp of Peach Fruit. A Biochemical and Molecular Study. Front. Plant Sci. 11:579063. doi: 10.3389/fpls.2020.579063

In the last decades, UV-B radiation has attracted attention due to its potential to increase nutraceutical values of fruit and vegetables, especially by inducing the accumulation of phenolics in a structure-dependent way. However, most current studies have investigated the UV-B-driven changes only in the peel or focusing on individual phenolic classes. Adopting an "-omics" approach, this work aimed to deepen the knowledge about the effects of UV-B radiation on the phenolic profile in the pulp of peach fruit. Based on these considerations, melting flesh yellow peaches (*Prunus persica* L., cv. Fairtime) were subjected to either a 10- or 60-min UV-B treatment (1.39 and 8.33 kJ m^{-2}, respectively), and sampled at different time points from the exposure. A UHPLC-ESI/QTOF-MS analysis coupled with a phenolics-specific database for the annotation of compounds and a multivariate discriminant analysis revealed a marked effect of UV-B radiation on the phenolic profiles of peach pulp. Particularly, a general, transient increase was observed after 24 h from the irradiation, especially for flavanols, flavonols, and flavones. Such behavior diverges from what was observed in the peel, where an overall increase of phenolics was observed after 36 h from the irradiation. Concerning the flavonols in the pulp, UV-B exposure stimulated a specific accumulation of isorhamnetin and kaempferol derivatives, with variations imposed by the different sugar moiety bound. Anthocyanins, which were the second most abundant flavonoid group after flavonols, displayed a general decrease after 36 h that was not attributable to specific molecules. The UV-B treatments also increased the glycoside/aglycone ratio of flavonols and anthocyanins after 24 h, by increasing the glycoside concentration of both, flavonols and anthocyanins, and decreasing the aglycone concentration of anthocyanins. In support of the biochemical results, targeted gene expression analysis by RT-qPCR revealed an UV-B-induced activation of many genes involved in the flavonoid pathway, e.g., CHS,

F3H, F3′H, DFR, as well as some MYB transcription factors and few genes involved in the UV-B perception. Generally, all the flavonoid-related and MYB genes showed a transient UV-B dose-dependent activation after 6 h from the irradiation, similarly to what was observed in the peel.

Keywords: UV-B radiation, peach fruit, *Prunus persica*, phenolics, flavonols, anthocyanins

INTRODUCTION

Peach (*Prunus persica* L.), originally domesticated in China, has become a highly appreciated fruit all over the Globe, with particular spread throughout the Mediterranean countries due to the favorable environmental conditions for its cultivation (Konopacka et al., 2010). The great popularity of peach fruit among consumers derives from both its appreciated organoleptic traits and its high nutraceutical value, thanks to the elevated content of health-promoting compounds such as polyphenols, carotenoids, and ascorbic acid (Tomás-Barberán et al., 2001; Gil et al., 2002).

Phenolic compounds represent a huge class of bioactive secondary plant metabolites, which fulfill essential functions during the lifespan of plants such as growth, reproduction, acclimation and defense (Ghasemzadeh and Ghasemzadeh, 2011; Zhang and Tsao, 2016). According to their chemical structure, functions and biosynthesis, phenolic compounds can be classified in flavonoids, lignans, phenolic acids, stilbenes, and other lower-molecular-weight compounds.

Flavonoids comprehend more than 6000 members, and surely play a key role in many defense mechanisms toward both biotic and abiotic stresses, since they possess the highest antioxidant and metal chelating activities in the phenolic group (Tolonen et al., 2002; Austin and Noel, 2003; Cheynier et al., 2013). They are commonly categorized into flavonols, isoflavonoids, flavones, flavanones, flavanols, and anthocyanidins (Ross and Kasum, 2002; Herndon et al., 2018). In plants, they are mainly glycosylated through the phenolic hydroxyls with one or multiple sugar moieties (Xiao et al., 2014; Tohge et al., 2017). The main flavonoids detected in the peach fruit are flavonols, flavan-3-ols and anthocyanins, whose concentration is strictly related to environmental factors and farming practices (Tomás-Barberán et al., 2001; Vizzotto et al., 2007; Tavarini et al., 2011; Aleixandre et al., 2013; Mokrani et al., 2016). Flavonoids provide protection against solar high-energy radiations, such as ultraviolet (UV), which can potentially damage macromolecules in plant cells through the overproduction of reactive oxygen species (ROS) (Frohnmeyer, 2003; Zhang et al., 2006; Hideg et al., 2013; Jenkins, 2014). UV-B comprehends a narrow wavelength range (280–315 nm) of the total UV radiation, whose majority is blocked by the stratospheric ozone shielding (Nunez et al., 1994; Herndon et al., 2018).

To achieve this acclimation response, UV-B activates a specific intracellular pathway mediated by the UV RESISTANCE LOCUS 8 (UVR8), a dimeric, inactive, cytoplasmic protein which acts as a UV-B-photoreceptor (Rizzini et al., 2011). Once UV-B hits UVR8, it rapidly monomerizes and the monomer interacts with the E3 ubiquitin ligase CONSTITUTIVELY PHOTOMORPHOGENIC 1 (COP1) (Favory et al., 2009). Interaction of activated UVR8 with COP1 leads to accumulation of COP1 target proteins, such as the bZIP transcription factor ELONGATED HYPOCOTYL 5 (HY5) (Favory et al., 2009; Huang et al., 2013; Lau et al., 2019). Stabilized HY5 is crucial for the regulation of numerous UV-B-induced genes, including those important for acclimation to UV-B (Ulm et al., 2004; Brown et al., 2005; Brown and Jenkins, 2008; Gruber et al., 2010; Stracke et al., 2010; Binkert et al., 2014). The expression of HY5 is also enhanced by the action of UVR8-COP1 complex, which in turn acts by over-expressing many genes involved in UV-B acclimation (Brown et al., 2005; Favory et al., 2009). Among the responsive flavonoid biosynthetic genes, *CHALCONE SYNTASE* (*CHS*), *CHALCONE ISOMERASE* (*CHI*), *FLAVANONE 3-HYDROXYLASE* (*F3H*), *DIHYDROFLAVONOL 4-REDUCTASE* (*DFR*), *ANTHOCYANIDIN SYNTHASE* (*ANS*), and *UDP-GLUCOSE:FLAVONOID 3-O-GLUCOSYLTRANSFERASE* (*UFGluT*) were found to be upregulated, together with an increase of phenolic compounds, in many fruit species such as apple (Ubi et al., 2006), tomato (Catola et al., 2017), and peach (Scattino et al., 2014; Santin et al., 2019). However, the previously cited works studied only the peel, i.e., the tissue directly exposed to UV-B radiation and thus more likely to be influenced by the treatment.

To the best of our knowledge, no studies have explored the UV-B-driven molecular and biochemical changes on the pulp of UV-B-irradiated fruit. The present work aimed to deeply investigate whether UV-B radiation influences the flavonoid profile of peach pulp and if these changes were accompanied by UVR8-dependent expression of flavonoid biosynthetic and regulatory genes.

MATERIALS AND METHODS

Plant Material and UV-B Irradiation

A set of organic peach fruit (*Prunus persica* L., cv. Fairtime) was bought in an organic supermarket and meticulously chosen to be undamaged and similar in size, color, and dimension (8.1 cm average diameter). Groups of five peaches were randomly assigned to either controls or UV-B-treated (10- or 60-min UV-B treatment) sets. UV-B exposure was conducted at 24°C in climatic chambers, each equipped with four UV-B tubes (Philips Ultraviolet-B Narrowband, TL 20W/01– RS, Koninklijke Philips Electronics, Eindhoven, Netherlands) and white light tubes (Philips F17T8/TL741). The 10- and 60-min UV-B treated fruit were subjected to a total irradiance of 6.42 kJ m^{-2} (1.39 kJ m^{-2} UV-B + 5.03 kJ m^{-2} white light) and 38.53 kJ m^{-2} (8.33 kJ m^{-2} UV-B + 30.20 kJ m^{-2} white light), respectively,

at fruit height. After the UV-B irradiation, controls and UV-B-exposed peaches were kept under white light at room temperature and sampled after 6, 12, 24, and 36 h from the end of the treatment for the molecular analysis, and after 24 and 36 h for the biochemical analysis. A portion of peach pulp (1.5 cm thick just below the skin, corresponding to approximatively one third of the fruit thickness from peel to pit) from the UV-B-exposed area was sampled with scalpels and tweezers, immediately frozen in liquid nitrogen and stored at −80°C until further analyses.

RNA Extraction and cDNA Synthesis

RNA extraction was conducted from freeze-dried peach pulp using the LiCl/CTAB protocol (Richter et al., 2017) slightly modified. Briefly, 50 mg of lyophilized pulp were finely ground and 3 mL of pre-heated RNA extraction buffer (2% [w/v] hexadecyltrimethylammonium bromide, CTAB; 2% [w/v] polyvinylpyrrolidone, PVP; 100 mM Tris/HCl pH 8.0; 25 mM EDTA; 2M NaCl; 0.5 g/L spermidine and 2.7% [v/v] 2-mercaptoethanol) were added. After an incubation of 5 min at 65°C, 3 mL of ice-cold chloroform:isoamylalcohol (24:1) were added and mixed well for 5 min. The suspension was centrifuged at 4250 *g* for 20 min at 4°C and the supernatant was washed with ice-cold chloroform:isoamylalcohol (24:1) followed by another centrifugation step. RNA precipitation was achieved by adding ice-cold 10M LiCl, and the samples were kept at 4°C overnight. By centrifuging (12000 *g* for 1 h at 4°C), the RNA pellet was isolated and then washed with 75% EtOH, dissolved in 30 μL RNAse free water and stored at −80°C. Qubit (Invitrogen) and the NanoDrop systems were used for RNA quantification, and the integrity of the isolated RNA was checked by separation on a 1.2% agarose gel. To avoid genomic DNA contamination, the RNA was incubated with 1 U RNase-free DNaseI (Fermentas) in the presence of 25 mM MgCl2 at 37°C for 30 min, as stated by Karsai et al. (2002). Reverse transcription was carried out using 1 μL of peqGOLD M-MuLV H Plus, 200 U/μL (Peqlab), in a RT master mix containing 5 x RT buffer (provided with RT enzyme), 1 mM dNTP and 50 pMol oligo(dT)18. Samples were incubated for 60 min at 37°C, then the reaction was stopped at 75°C for 5 min. The obtained cDNA was diluted five times with sterile double-distilled water, and stored at −20°C.

Real Time Quantitative PCR (RT-qPCR)

Three reference gene candidates were primarily tested [*EUKARYOTIC INITIATION FACTOR-4A* (*PpEIF4A*), *TUBULIN BETA-9 CHAIN* (*PpTUB9*), and *UBIQUITIN 5* (*PpUBQ5*)]. The threshold cycles (Ct values) for each reference gene candidate in our groups of samples are reported in **Supplementary Table S1**. NormFinder software was used to calculate the expression stability value (M) in our sample set and for selecting the most suitable reference gene (Andersen et al., 2004). According to NormFinder, *PpEIF4A* was the most stable expressed reference gene candidate (M for *PpEIF4A*: 0.032; for *PpTUB9*: 0.159; for *PpUBQ5*: 0.202). Therefore, *PpEIF4A* was used to normalize all the RT-qPCR data. The latest GenBank database and the Genome Database for Peach *Prunus persica* genome[1] were consulted to find suitable primers for *PpEIF4A*, *PpCHS*, *PpF3H*, *PpF3′H*, *PpDFR*, *PpMYB111*, *PpMYB-like*, *PpCOP1*, *PpHY5*, *PpUVR8*, based on BLAST alignments to the corresponding Arabidopsis genes as starting point (Altschul et al., 1997). The full list of primer sequences refers to Santin et al. (2019) and is reported as **Supplementary Table S2**. The Rotorgene-3000 cycler (Corbett, Qiagen, Germany) was used for the RT-qPCR runs. Each RT-qPCR reaction, performed in triplicate, was assembled in a total volume of 14 μL using the 5x HOT FIREPol EvaGreen® qPCR Mix Plus (Solis BioDyne, Tartu, Estonia). 2.8 μL of 5x HOT FIREPol EvaGreen® qPCR Mix were mixed with 0.25 μL of forward and reverse primers (each 20 μM), 1 μL of the cDNA template, and double-distilled water. The cDNA was initially denatured at 95°C for 12 min and then amplified [40 cycles: 55°C/5 s, 67°C/25 s (extension and acquisition in channel A), 76°C/6 s (acquisition in channel B), 82°C/6 s (acquisition in channel C), and denaturation at 95°C/5 s]. In addition, a standard curve using serial diluted templates (from 10^7 to 10^2, with 10^5, 10^4, and 10^3 in duplicate, and a blank) was created for each gene, to determine the PCR efficiency (**Supplementary Table S2**). In each PCR reaction, a standard curve was also inserted. Integrated Rotorgene software was used to calculate the number of copies/μL based on the gene specific standard curves, and normalization was performed with respect to the *PpEIF4A* reference gene copy number. For each gene, standard curves of known PCR amplicon copy number were designed, and serial dilutions of quantified PCR fragment were included in each run and the PCR efficiencies determined. RT-qPCR data represent means and standard errors of five independent biological replicates.

Phenolic Extraction and UHPLC-ESI-QTOF-MS Analysis

Phenolic compounds were extracted from peach pulp by using a homogenizer-assisted extraction (Santin et al., 2019). In particular, samples (1.0 g) were homogenized in 10 mL of hydro-alcoholic solution (i.e., methanol 80% v/v, acidified with 0.1% HCOOH) by using an Ultra-turrax (Ika T25, Staufen, Germany), at maximum speed for 3 min. Following centrifugation (6,000 × *g*, for 10 min at 4°C), the extracts were filtered in amber vials using 0.22 μm cellulose syringe filters, to be analyzed by ultra-high-pressure liquid chromatography (UHPLC) coupled with quadrupole time-of-flight (QTOF) mass spectrometry. In this regard, the instrumental conditions for the analysis of phenolic compounds were previously optimized (Rocchetti et al., 2019). Briefly, chromatographic separation was done in reverse phase mode, using an Agilent Zorbax Eclipse Plus C18 column (100 mm, 1.9 μm particle size). A binary mixture of acetonitrile and water (both acidified with 0.1% HCOOH) was used as mobile phase, with a gradient from 6% acetonitrile up to 94% acetonitrile in 32 min. Also, the mobile phase temperature was set to 35°C, with a flow rate of 220 μL min^{-1} and an injection volume of 6 μL. Regarding the high-resolution mass spectrometry analysis, the QTOF worked in positive (ESI +) MS-only mode, acquiring accurate masses in the 100–1200*m/z* range

[1]https://www.rosaceae.org/species/prunus_persica/genome_v2.0.a1

at a rate of 0.8 spectra/s. The QTOF was operated in dynamic range mode with a nominal mass resolution of 30,000 FWHM. Nitrogen was used as both sheath gas (10 L min^{-1} at 350°C) and drying gas (8 L min^{-1} at 330°C). The nebulizer pressure was 60 psig, nozzle voltage was 300 V, and capillary voltage was 3.5 kV. The identification of polyphenols was achieved using the software Profinder B.07 from Agilent Technologies, according to the "find-by-formula" algorithm. In particular, the annotations were recursively done against the comprehensive database Phenol-Explorer[2] and using the entire isotopic profile (including isotopic spacing and isotopic ratio, with a maximum of 5 ppm for monoisotopic mass accuracy). Therefore, a Level 2 of compound identification was achieved as set out by the COSMOS Metabolomics Standards Initiative (Salek et al., 2013; Schrimpe-Rutledge et al., 2016). The obtained dataset was further used for statistics and chemometrics. Finally, semi-quantitative information regarding the main flavonoids' subclasses were obtained by using representative standard compounds (Rocchetti et al., 2018): cyanidin (anthocyanins), catechin (flavan-3-ols and flavonols), and luteolin (flavones and other remaining subclasses), were used with this aim. Three replicates were processed ($n = 3$), and results were finally expressed as mg kg^{-1} dry weight (DW).

Statistical Analysis

Firstly, a canonical discriminant analysis (CDA) was performed starting from the whole phenolics dataset, to check the effectiveness of the UV-B treatments in modulating the phenolic concentration in both recovery time points tested. Besides, all biochemical and molecular data were analyzed by one-way ANOVA followed by Tukey–Kramer *post hoc* test at the significance level $P \leq 0.05$ to evaluate which phenolic subclasses are mainly responsive to the UV-B treatments. To elaborate and discuss the results, the recovery timepoints were deliberately kept separated to avoid the possible hiding effect of the physiological phenolic modification due to the fruit ripening process on the phenolic changes due to the UV-B exposure. All the statistical analyses were performed using JMP software (SAS Institute, Inc., Cary, NC, United States). Regarding the statistical elaboration of metabolomics-based data, the software Agilent Mass Profiler Professional B.12.06 (from Agilent Technologies) was used. In particular, phenolic compounds were filtered by abundance (min. abundance 10,000, roughly corresponding to a signal-to-noise of 5) and by frequency (retaining the compounds present in 100% of samples in at least one condition), normalized at the 75^{th} percentile and baselined to the median of each compound in the dataset.

RESULTS

UV-B-Irradiation Rearranged the Phenolic Profile in Peach Pulp

The untargeted metabolomic approach based on UHPLC-QTOF mass spectrometry allowed us to putatively annotate more than 420 phenolic compounds, which were then classified in their respective phenolic subclass. This was done to better describe the UV-B-induced effects as related to their structure and function. A comprehensive list containing all phenolics identified together with their composite mass spectrum is reported in **Supplementary Table S3**. Overall, flavonoids were found to be the most represented phenolic class, accounting for 52% of the total phenolics, followed by phenolic acids (86 compounds, 79 tyrosol equivalents, 29 lignans, and 10 stilbenes). The first step of this work was to check whether the UV-B exposures were able to induce an overall modification of the phenolic profile of both recovery time points. To this aim, a multivariate technique, the CDA, was performed including both the UV-B treatments and recovery time points (**Figure 1**). CDA represents a dimension-reduction statistical tool, which is strictly associated with the principal component analysis (PCA) but, unlike the PCA, it is usually performed when the different groups are known from the very beginning. In particular, the model tends to maximize the differences among the preassigned groups, maximizing at the same time the similarities in each group.

The CDA reported in **Figure 1** clearly showed that biological replicates fit the preassigned groups according to the phenolic dataset, with no outliers detected in the hyperspace. Robustness of this statistical analysis was assessed with four MANOVA tests (Wilk's Lambda, Roy's Largest Root Test, the Hotelling-Lawley Trace and the Pillai-Bartlett Trace), which all gave highly significant *P*-values (i.e., <0.0001). The canonical functions 1 and 2 explained 85.6 and 9.9% of the segregation, respectively. The projections of the two control groups on the canonical function 1 were overlapping, indicating that no differences are appreciable on the first canonical variable. Similarly, the 10- and the 60-min UV-B treated groups after 36 h are located on the far left of the scatterplot. The UV-B-exposed groups after 24 h, however, were the only ones that displayed a marked segregation, being the 10- and the 60-min UV-B treated groups located at the opposite sides of the control groups. Concerning the canonical function 2, the 60-min UV-B-treated groups are distributed in the upper part of the plot, being well-separated from the others. Below, the controls after 24 h do not coincide with any other set of samples, while the 10-min UV-B-treated groups, both after 24 and 36 h, and the controls after 24 h, are placed at the lowest part of the plot. The great separation of the groups in the hyperspace, especially between the UV-B-treated ones and the control ones considering the canonical 1, suggested a strong UV-B-induced modification of the phenolic profile in the pulp of peach fruit, which deserved a deepen investigation.

UV-B-Induced Flavonoid Modifications Involved Different Subclasses at Distinct Recovery Time Points

Our next step was to investigate further which phenolic subclasses were mainly responsive to the UV-B treatments, and whether the UV-B exposure might induce positive or negative modifications on such phenolic subclasses. Particularly, the attention was focused on the flavonoid family that, possess the highest antioxidant activity among phenolics and were more likely

[2]http://phenol-explorer.eu/

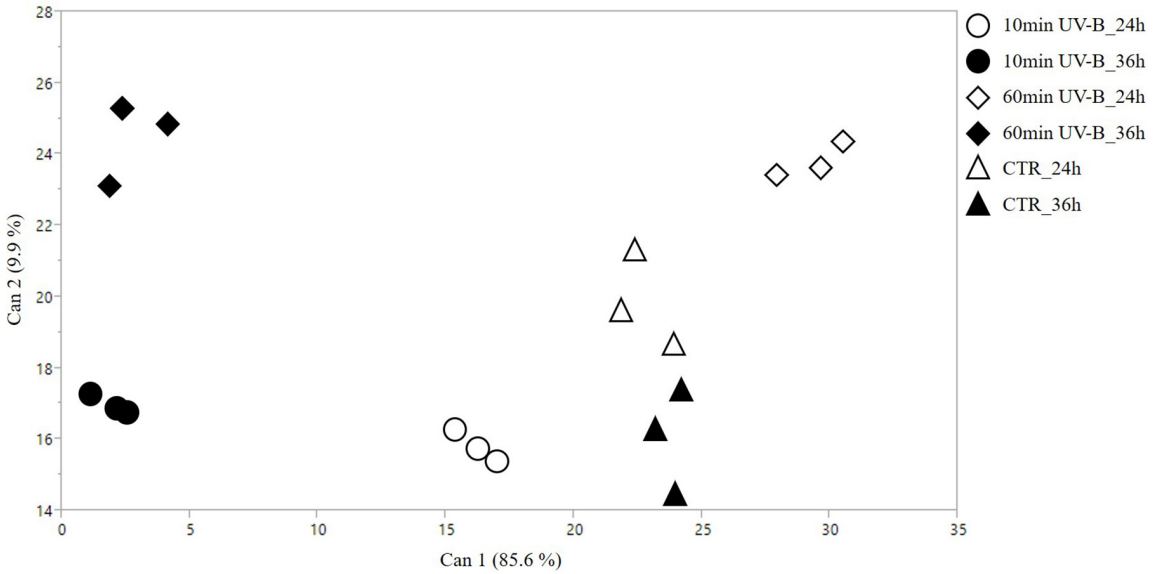

FIGURE 1 | 2D scatterplot of canonical discriminant analysis (CDA) considering the samples treated with 10 and 60 min of UV-B radiation after 24 and 36 h from the exposure, as well as the UV-B-untreated samples [controls (CTR)]. The whole phenolics dataset was used to perform this analysis. Can 1 and 2 refers to the canonical functions 1 and 2, which include all the variables to maximize the separation among the groups.

to be influenced by the UV-B radiation. The whole phenolic dataset was then rearranged combining all the compounds in their respective phenolic subclasses, and the total concentration for each subclass was calculated by summing the individual concentrations of its members. Results are graphically presented in **Figure 2**. At a first glance, it was evident that flavonols and anthocyanins represented the most abundant flavonoid subclasses in the pulp of peaches, with average concentrations in control samples of 251 and 298 mg/kg and 257 and 316 mg/kg after 24 and 36 h of incubation under white light only, respectively. Afterward, flavanols, flavones, and flavanones were the most highly concentrated ones, with average concentrations of 104, 100, and 83 mg/kg, respectively.

The UV-B treatments triggered modifications in the flavonoid profile according to the recovery times, indicating that the UV-B-induced effects were still detectable after several hours of storage. Particularly after 24 h from both the 10- and 60-min UV-B exposures (**Figure 2A**), the most responsive flavonoid classes were flavanols, flavones, flavonols, and dihydroflavonols. All these classes showed a significant increase when peaches were exposed to 60 min of UV-B (+ 123, + 70, + 55, and + 50% compared to the control group, respectively), suggesting a positive role of the UV-B radiation in enhancing such flavonoid subfamilies. Besides, the 10-min UV-B exposure was also significantly effective when considering the flavonols, which were + 43% more concentrated in the UV-B-treated group. An increasing trend occurred also regarding flavanols, flavones, and dihydroflavonols irradiated for 10 min, suggesting a dose-dependent response. The only flavonoids undergoing a decrease in both UV-B-treated groups were the dihydrochalcones.

After 36-h of recovery (**Figure 2B**), the responsive flavonoid subclasses were flavonols and flavanols. Regarding flavonols, the 60-min treatment was still effective in maintaining their concentration significantly higher than the controls (+ 52%). Flavanols, however, responded contrarily to what was observed after 24 h from the UV-B exposure. Indeed, both the UV-B-treated groups exhibited a significantly lower flavanol concentration than the controls (-55 and -47% for the 10- and the 60-min treated groups, respectively).

UV-B Radiation Was Effective in Increasing Flavonol Concentration in a Structure-Dependent Way Only After 24 h From UV-B Exposure

Since flavonols were the most abundant flavonoid class in peach pulp, thus contributing the most to the fruit quality, the next step was to investigate deeper the UV-B response of the different flavonols at the 24 and 36 h recovery time points (**Figure 3**). Sixty-one different flavonols were identified (**Supplementary Table S3**), including glycosides and aglycones, and they were grouped in relation to the respective flavonol moiety. Accordingly, 3 isorhamnetins, 18 kaempferols, 5 myricetins, 21 quercetins, and 2 spinacetins were found. Flavonols with less than two derivatives were not considered in this analysis since they were not likely contributing to the overall flavonol response. Kaempferols resulted to be the most abundant flavonol subclass in the peach pulp, with an average concentration in control samples of 72.9 mg/kg in both recovery time points, followed by isorhamnetins and quercetins (19.8 and 24.6, 41.8 and 22.8 mg/kg after 24 and 36 h, respectively). As observed in **Figure 3A**, after 24 h of recovery, the 60-min UV-B exposure was effective in increasing the concentration of spinacetins, isorhamnetins, kaempferols (+ 61, + 448, and + 95%, respectively). A not

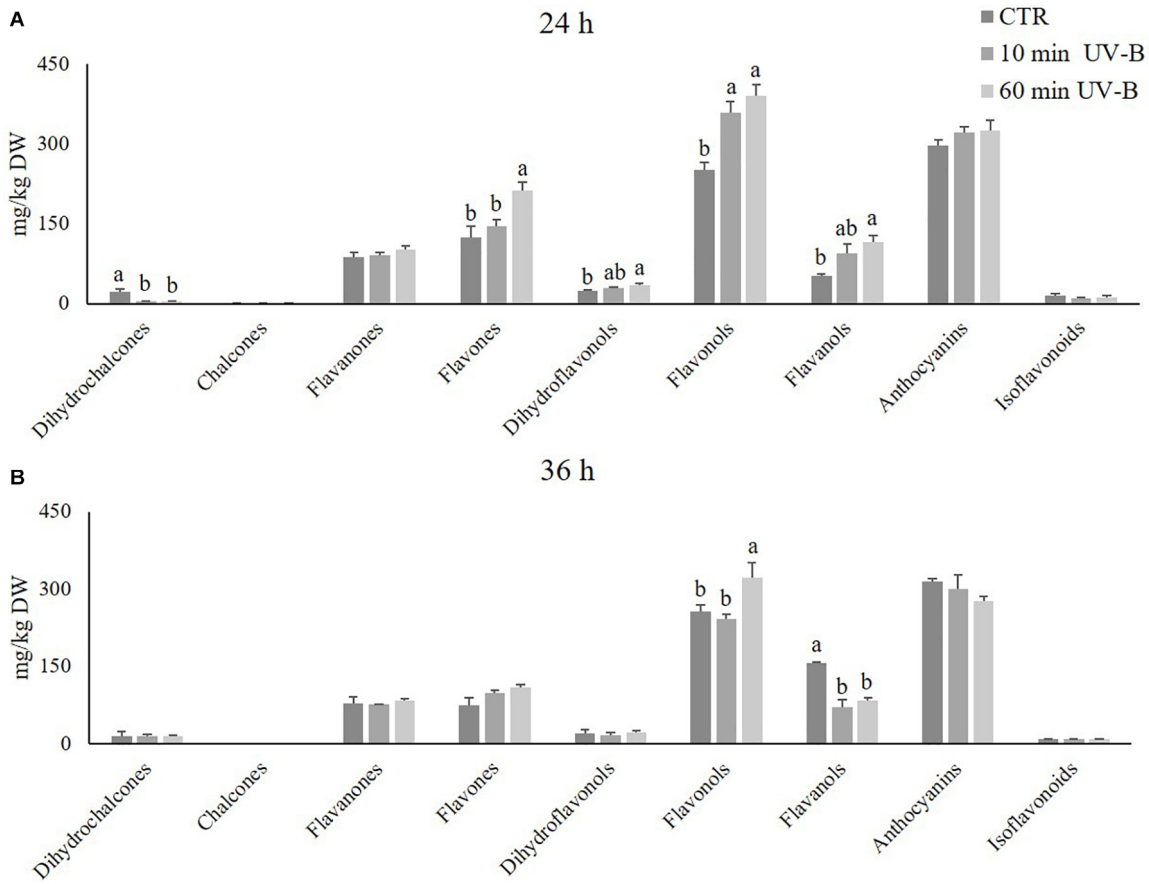

FIGURE 2 | Concentration (mg/kg DW) of several flavonoid classes (dihydrochalcones, chalcones, flavanones, flavones, dihydroflavonols, flavonols, flavanols, anthocyanins, and isoflavonoids) in the pulp of peaches exposed to UV-B radiation for either 10 or 60 min, and sampled after 24 h **(A)** and 36 h **(B)** from the exposure. Data are mean ± SE of five biological replicates. Different letters correspond to statistically significant differences according to one-way ANOVA followed by Tukey–Kramer *post hoc* test ($P \leq 0.05$).

significant tendency of increased quercetin was also detected. The 10-min UV-B treatment did not induce such accumulation of flavonols, instead being successful to determine a significant increase only for quercetins and kaempferols (+ 118 and + 66%, respectively). However, after the 36-h recovery time point (**Figure 3B**), no significant variation was observed in both the UV-B treatments for any of the flavonol subclasses detected. Since a significant accumulation after 36 h from the 60-min UV-B exposure was found for the whole class of flavonols (**Figure 2B**), it meant that the individual flavonols subclasses underwent a slight, not significant, increase, whose sum however resulted to be significantly higher compared to the controls.

Kaempferol and Isorhamnetins Glycosides Responded Differently to UV-B Radiation in Relation to Their Sugar Moiety

Since kaempferols were found to be the most abundant flavonols detected, and since they were highly UV-B-responsive in the 24-h time point after both UV-B treatments, a further exploration was conducted to study the response of individual kaempferol glycosides. As observed in **Figure 4**, **15** different kaempferol glycosides were identified, underlying the complexity of the flavonols in the pulp. All the kaempferols detected were O-glycosidically linked to sugar moieties at the C3 and/or C7 position, and most of them were di- or tri-glycosides. The most abundant kaempferols of control samples were 3-*O*-(6″-acetyl-galactoside) 7-*O*-rhamnoside, 3-*O*-galactoside 7-*O*-rhamnoside, 3-*O*-rutinoside and 3-*O*-xylosyl-glucoside, with concentrations in control samples of 10.7, 9.0, 9.0, and 8.1 mg/kg and 14.5, 7.4, 7.4, and 7.6 mg/kg after 24 and 36 h. When peaches were treated with UV-B, behavior of kaempferols differed considerably according to the substituents linked to the kaempferol moiety. After 24 h from the irradiation (**Figure 4A**), several kaempferols underwent an increase which was mostly UV-B-dose-dependent. In particular, the 60-min UV-B exposure was effective in increasing the concentration of the 3-*O*-(2″-rhamnosyl-galactoside) 7-*O*-rhamnoside (+ 189%), the 3-*O*-(6″-acetyl-galactoside) 7-*O*-rhamnoside (+ 381%), the 3-*O*-galactoside 7-*O*-rhamnoside (+ 71%), the 3-*O*-rhamnosyl-rhamnosyl-glucoside (+ 192%), the 3-*O*-rutinoside (+ 73%), the 3-*O*-xylosyl-glucoside (+ 149%), the 3-*O*-xylosyl-rutinoside (+ 190%), and the 7-*O*-glucoside (+ 97%). The 10-min UV-B

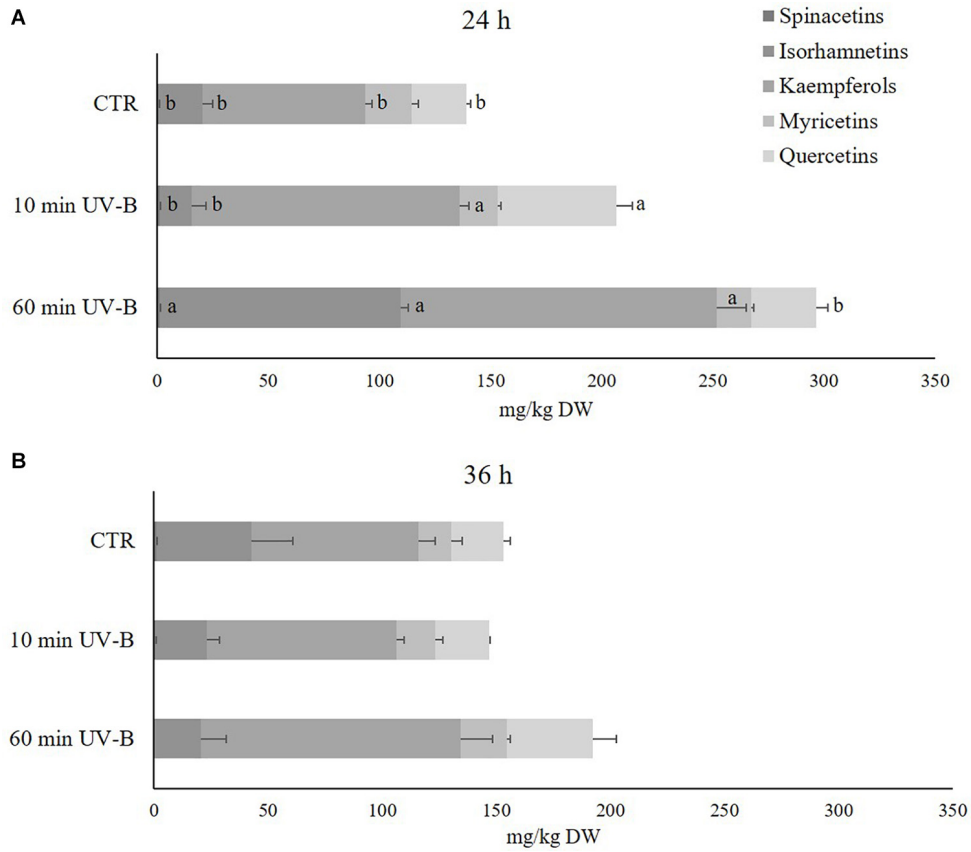

FIGURE 3 | Concentration (mg/kg DW) of different flavonols (spinacetins, isorhamnetins, kaempferols, myricetins, and quercetins) in the pulp of peaches exposed to UV-B radiation for either 10 or 60 min and sampled after 24 h **(A)** and 36 h **(B)** from the exposure. Data are mean ± SE of five biological replicates. Different letters correspond to statistically significant differences according to one-way ANOVA followed by Tukey–Kramer *post hoc* test ($P \leq 0.05$).

exposure was less effective in inducing the accumulation of kaempferols, being successful for the 3-*O*-(6″-acetyl-galactoside) 7-*O*-rhamnoside (+ 52%), the 3-*O*-galactoside 7-*O*-rhamnoside (+ 75%), and the 3-*O*-rutinoside (+ 52%). After 36 h from both the UV-B exposures (**Figure 4B**), only few significant changes were observed. In detail, the 60-min UV-B treatment induced a significant accumulation of the 3-*O*-galactoside 7-*O*-rhamnoside (+ 114%), the 3-*O*-rhamnosyl-rhamnosyl-glucoside (+ 371%), the 3-*O*-rutinoside (+ 115%), and the 3-*O*-sophoroside 7-*O*-glucoside (+ 61%). The 10-min UV-B irradiation, as observed in the 24-h recovery time point, stimulated a minor increase in terms of entity and number of kaempferols affected as compared to the 60-min UV-B irradiation. Indeed, only the 3-*O*-galactoside 7-*O*-rhamnoside and the 3-*O*-rutinoside were positively affected by the 10-min irradiation, with an increase of 100 and 102%, respectively. In addition, no kaempferols underwent a decrease following UV-B irradiation at any dose and any recovery time points, compared to the respective control. Like the kaempferols, the isorhamnetins were studied more in detail (**Figure 5**), since they underwent a massive increase after 24 h from the 60-min UV-B treatment (+ 448%). This flavonoid subclass comprised three molecules, the most abundant being a monoglycoside, the 3-*O*-rutinoside, followed by 3-*O*-glucoside 7-*O*-rhamnoside and the aglycone isorhamnetin. As observed for the kaempferols, the UV-B radiation induced more significant changes in the isorhamnetin concentration after 24 h then after 36 h of recovery. Considering the 24-h time point (**Figure 5A**), the 10-min UV-B exposure was ineffective in determining significant modifications of any of the isorhamnetin detected, while the 60-min irradiation induced an increase of the 3-*O*-rutinoside (+ 804%) and the aglycone (+ 70%). Since the 3-*O*-rutinoside was the most concentrated isorhamnetin and also the most UV-B-responsive one, it represented the main contributor to the overall increase in total isorhamnetins observed following UV-B exposure (**Figure 3A**). In the same recovery time point, the 60-min UV-B irradiation also determined a slight decrease in the 3-*O*-glucoside 7-*O*-rhamnoside (-56%). However, such decrease did not affect the total isorhamnetin due to the low concentration of this compound. Similar to the total flavonols and kaempferols, both UV-B exposures did not induce variations in any of the isorhamnetins at the 36-h recovery time point.

Total Flavonol Glycosides, but Not Aglycones, Transiently Responded to UV-B Radiation

Another interesting behavior relates the UV-B-responsiveness of the flavonol glycosides and aglycones. After having separated

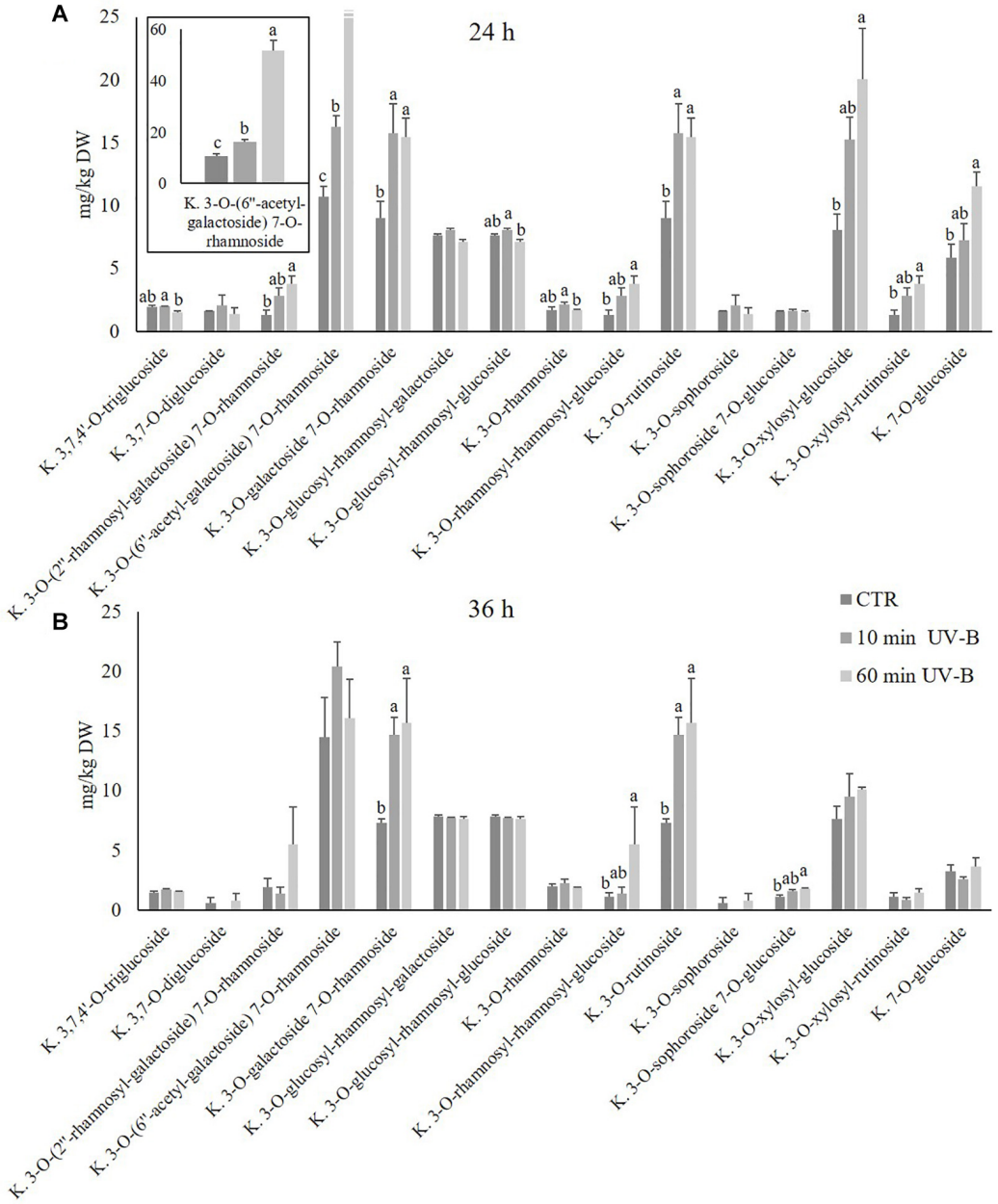

FIGURE 4 | Concentration (mg/kg DW) of different kaempferols in the pulp of peaches exposed to UV-B radiation for either 10 or 60 min and sampled after 24 h **(A)** and 36 h **(B)** from the exposure. **(A)** Kaempferol 3-*O*-(6′′-acetyl-galactoside) 7-*O*-rhamnoside was reported also in a different, framed histogram with a higher y-axis scale (0–60 mg/kg DW) for a better visualization. Data are mean ± SE of five biological replicates. Different letters correspond to statistically significant differences according to one-way ANOVA followed by Tukey–Kramer *post hoc* test ($P \leq 0.05$).

the aglycones (11) from the glycosides (54) in the dataset, the total concentrations for each group was calculated (**Table 1**). The concentration of glycosides was significantly higher than that of the aglycones, regardless of the UV-B treatment and the recovery time. Specifically, the glycoside concentration in the control groups was 21 and 45% higher than that of the aglycone in the 24 and 36 h recovery time points, respectively. As observed for the total and individual flavonols, the UV-B effects were more visible after 24 h from the irradiation also when considering the overall glycoside and aglycone concentrations. At this recovery time point, as reported in **Table 1**, both the 10- and the 60-min irradiations were effective in significantly inducing the accumulation of flavonol glycosides by 66 and 92%, respectively. On the other hand, no UV-B-induced variations in the aglycone concentrations were observed. Thus, the glycosides/aglycones ratio increased from

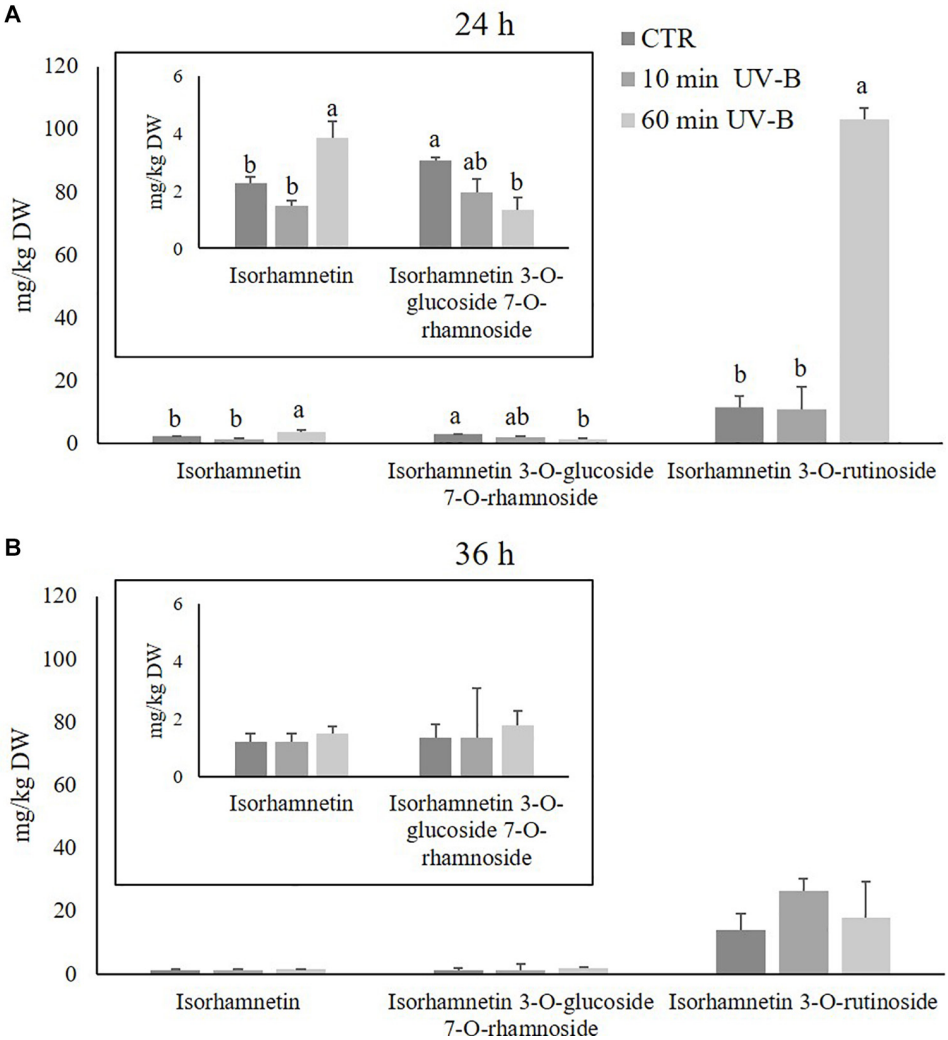

FIGURE 5 | Concentration (mg/kg DW) of different isorhamnetins in the pulp of peaches exposed to UV-B radiation for either 10 or 60 min and sampled after 24 h **(A)** and 36 h **(B)** from the exposure. **(A)** Isorhamnetin and isorhamnetin 3-*O*-glucoside 7-*O*-rhamnoside were reported also in a different, framed histogram with a lower y-axis scale (0–6 mg/kg DW) for a better visualization. Data are mean ± SE of five biological replicates. Different letters correspond to statistically significant differences according to one-way ANOVA followed by Tukey–Kramer *post hoc* test ($P \leq 0.05$).

1.2 for the controls, up to 1.9 and 2.8 in the 10- and 60-min UV-B-irradiated fruit. No variations were observed for both, the glycosides and the aglycones after 36 h from the UV-B exposures.

Total Anthocyanins Were Not Affected by UV-B Radiation While Individual Anthocyanins Responded Differently

Anthocyanins belong to the second most abundant flavonoid class, and in the light of their great importance both for humans as antioxidant and health-promoting compounds, and for plants as colored, attractive pigments for pollinators and seed dispersers, our subsequent investigation was to elucidate whether and how the UV-B treatment might have influenced individual anthocyanins. We hypothesized that, although anthocyanins as whole class might not display significant variations after UV-B exposure, different compounds belonging to the same subclass might respond differently. Sixty-one different anthocyanins, including both glycosides and aglycones, were identified (**Supplementary Table S3**). Similar to analyses of flavonols, anthocyanins were classified in 17 cyanidins, 9 delphinidins, 7 malvidins, 11 pelargonidins, 8 peonidins, and 9 petunidins. The most representative anthocyanins in the pulp of peach fruit were the pelargonidins (133.2 and 115.2 mg/kg in the 24- and 36-h recovery time points, respectively) and the cyanidins (71.1 and 80.5 mg/kg in the 36-h recovery time point, respectively), followed by delphinidins (26 and 41 mg/kg in the 24- and 36-h recovery time points, respectively), petunidins (29.5 and 22.6 mg/kg in the 24- and 36-h recovery time points, respectively), peonidins (18.7 and 33.0 mg/kg in the 24-

TABLE 1 | Concentration of total flavonol aglycones and glycosides in the UV-B-treated samples after 24 and 36 h from the UV-B exposure.

		Aglycones	Glycosides
		(mg/kg DW)	(mg/kg DW)
24 h	CTR	113.6 ± 8.3 b	137.5 ± 10.6 Ba
	10 min UV-B	121.3 ± 3.5 b	228.3 ± 41.5 Aa
	60 min UV-B	92.8 ± 10.8 b	263.5 ± 25.2 Aa
36 h	CTR	105.0 ± 18.2 b	152.2 ± 9.0 a
	10 min UV-B	97.1 ± 18.4 b	145.6 ± 7.4 a
	60 min UV-B	113.1 ± 15.4 b	180.9 ± 49.9 a

Data are mean ± SE of three biological replicates. Different letters correspond to statistically significant differences according to one-way ANOVA followed by Tukey–Kramer post hoc test ($P \leq 0.05$). Lowercase letters refer to the comparison between aglycones and glycosides, while uppercase letters refer to the comparison between the controls and the UV-B-treated groups in each recovery time point (24 or 36 h).

and 36-h recovery time points, respectively) and malvidins (18.9 and 22.6 mg/kg in the 24- and 36-h recovery time points, respectively) (**Figure 6**). Along the recovery time tested, they all underwent a slight increase in controls, especially for pelargonidins (+ 12.7 mg/kg), delphinidins (+ 11.1 mg/kg) and peonidins (+ 10.1 mg/kg), underlying the physiological modifications that such phenolic compounds might experience during storage. As observed for flavonols, the UV-B treatment was able to affect the concentration of the anthocyanin subclases differently. Indeed 24 h from the exposure, the UV-B-responsive anthocyanins were the malvidins and the pelargonidins. Malvidins underwent a significant increment in the 10-min UV-B treated samples (+ 87%). Pelargonidins, however, decreased significantly in the 10-min UV-B-irradiated peaches, while no modifications occurred after the 60-min treatment for both subclasses. At the 36-h recovery time points, the concentration of malvidins was still significantly affected by the irradiation, being 56% higher in the 60-min UV-B-treated fruit. Furthermore, the concentration of petunidins showed a trend of reduction in the 60-min UV-B-treated samples (-29%). Thus, although the total anthocyanin concentration did not show any variation (**Figure 2**), the anthocyanin profile was affected by the UV-B exposure.

UV-B Irradiation Reduced the Concentration of Anthocyanin Aglycones Without Affecting the Concentration of Glycosides

Since the ratio between glycosides and aglycones of flavonols was differentially modulated by UV-B (**Table 1**), the effect of UV-B on the ratio of anthocyanin glycosides and aglycones were determined (**Table 2**). First, also anthocyanin glycosides were more concentrated than their aglycones. Specifically, glycosides were on average 277 and 270% higher than aglycones in the 24 and 36 h recovery time points, respectively, compared to the control samples. Considering the UV-B treatments, both 10- and 60-min irradiations triggered a significant decrease in anthocyanin aglycones regardless of the recovery time point (-25 and -56% after 24 h, and -32 and -30% after 36 h, following 10- and 60-min UV-B-treatment respectively). On the other hand, anthocyanin glycosides were not significantly influenced by the UV-B radiation at any recovery time point.

Molecular Analysis Revealed Activation of Genes Involved in UV-B-Signaling and Phenylpropanoid Biosynthetic Pathways

Once elucidated that UV-B radiation was effective in modulating the flavonoid profile, with emphasis for specific flavonoid subclasses, the next step was to investigate at the molecular level expression of genes involved in the phenylpropanoid pathway. Accordingly, the transcript abundance of three UVR8-signaling related genes (*PpUVR8*, *PpCOP1*, *PpHY5*), four phenylpropanoid biosynthetic (*PpCHS*, *PpF3H*, *PpF3′H*, *PpDFR*) and two regulatory (*PpMYB111*, *PpMYB-like*) genes were investigated. The results are reported in **Figure 7**. Concerning the UVR8-signaling related genes (**Figure 7A**), UV-B radiation did not induce any variation at the transcript level of *PpUVR8* and *PpCOP1*, with respect to any recovery time points, though both genes showed a similar (not significant) increase in their expression after 24 h from the 60-min UV-B exposure compared to the control level. On the other hand, transcription of *PpHY5* significantly increased after 6 h in a dose-dependent manner (+ 77 and + 174% following 10- and 60- min UV-B irradiation, compared to the control level, respectively). In the following recovery time points, *PpHY5* transcription in both control and UV-B-treated fruit was maintained in a steady state up to 36 h, without significant variations. Contrarily to the UVR8-signaling related genes, all the phenylpropanoid biosynthetic genes tested showed a consistent UV-B-induced upregulation, especially in the early time points after UV-B exposures (**Figure 7B**). Indeed, the expression of *PpCHS*, *PpF3H*, *PpF3′H* and *PpDFR* exhibited a noteworthy increase after 6 h from the 60-min UV-B treatment compared to the control level (+ 5024, + 1285, + 317, and + 803%, respectively). The 10-min treatment was also effective in overexpressing *PpCHS* after 6 h (+ 1009%) and the UV-B-induced upregulation of this gene was detected also after 12 h from the 60-min irradiation (+ 648%). Considering the late time points, the expression of the phenylpropanoid biosynthesis genes remained stable with no significant UV-B related variations, except for the *PpF3′H*, whose transcript level increased in the 10-min UV-B-exposed fruit after 36 h (+ 163%). Among the regulatory genes, the expression of *PpMYB111* showed a similar behavior to the phenylpropanoid biosynthetic genes. In fact, a consistent upregulation was observed in the 6-h recovery time point following the 60-min UV-B-exposure (+ 139%). After this early UV-B-induced upregulation, no significant differences were detected up to 24 h from the irradiation among the treated and untreated groups, while the UV-B-exposed samples showed a higher transcript abundance after 36 h from both the 10- and 60-min irradiation (+ 71 and + 86% compared to the control, respectively). *PpMYB-like* expression slightly differed from

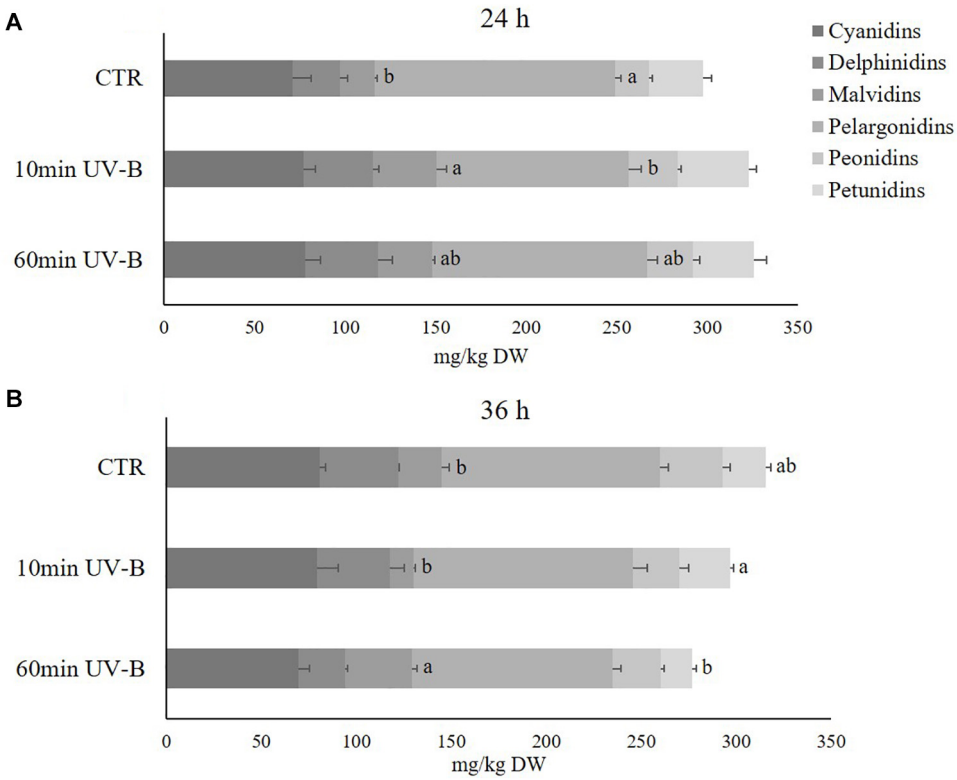

FIGURE 6 | Concentration (mg/kg DW) of different anthocyanins (cyanidins, delphinidins, malvidins, pelargonidins, peonidins, and petunidins) in the pulp of peaches exposed to UV-B radiation for either 10 or 60 min and sampled after 24 h **(A)** and 36 h **(B)** from the exposure. Data are mean ± SE of five biological replicates. Different letters correspond to statistically significant differences according to one-way ANOVA followed by Tukey–Kramer *post hoc* test ($P \leq 0.05$).

PpMYB111. Although a similar, UV-B-induced peak might be seen after 6 h in both the treated groups, such increase was not statistically significant. In contrast, the effect of UV-B radiation on *PpMYB-like* was detectable in the latter recovery time points, where a dose-dependent response was found. Its transcript level was 498 and 101% higher in the 60-min UV-B treated samples after 24 and 36 h from the irradiation, respectively, while in the 10-min treated samples, this gene showed only a trend of induction at the same recovery time points (**Figure 7C**).

TABLE 2 | Concentration of total anthocyanin aglycones and glycosides in the UV-B-treated samples after 24 and 36 h from the UV-B exposure.

		Aglicones (mg/kg DW)	Glycosides (mg/kg DW)
24 h	CTR	62.4 ± 2.4 Ab	235.1 ± 16.8 a
	10 min UV-B	46.5 ± 13.5 Bb	287.6 ± 30.8 a
	60 min UV-B	27.6 ± 11.5 Bb	288.2 ± 34.8 a
36 h	CTR	67.2 ± 2.3 Ab	248.4 ± 4.5 a
	10 min UV-B	45.6 ± 9.7 Bb	224.3 ± 28.7 a
	60 min UV-B	47.2 ± 23.4 Bb	216.8 ± 18.2 a

Data are mean ± SE of three biological replicates. Different letters correspond to statistically significant differences according to one-way ANOVA followed by Tukey–Kramer post hoc test ($P \leq 0.05$). Lowercase letters refer to the comparison between aglycones and glycosides, while uppercase letters refer to the comparison between the controls and the UV-B-treated groups in each recovery time point (24 or 36 h).

DISCUSSION

The UV-B-Driven Rearrangement of the Phenolic Profile in the Peach Pulp Differs From What Observed in the Skin

This work aimed to deeply investigate how the UV-B radiation can modify the phenolic profile in the pulp of peach fruit, focusing on the flavonoid subclasses, e.g., flavonols and anthocyanins. Besides, the UV-B-mediated responses of flavonols and anthocyanins glycosides and aglycones were studied, to determine whether such modulation might occur differently according to the linked sugar moieties. Lastly, a molecular analysis was conducted on several UVR8-signaling related and phenylpropanoid biosynthetic and regulatory genes, to understand if such modulation might be due to the UV-B photoreceptor, UVR8. Although several previous studies have deeply investigated the UV-B-induced modulation of phenolic profiles in many fruit (Luthria et al., 2006; Interdonato et al., 2011; Ruiz et al., 2016; Assumpção et al., 2018; Santin et al., 2018a, 2019) and vegetable species (Eichholz et al., 2012; Rajabbeigi et al., 2013), they principally analyzed just the outermost tissue, since

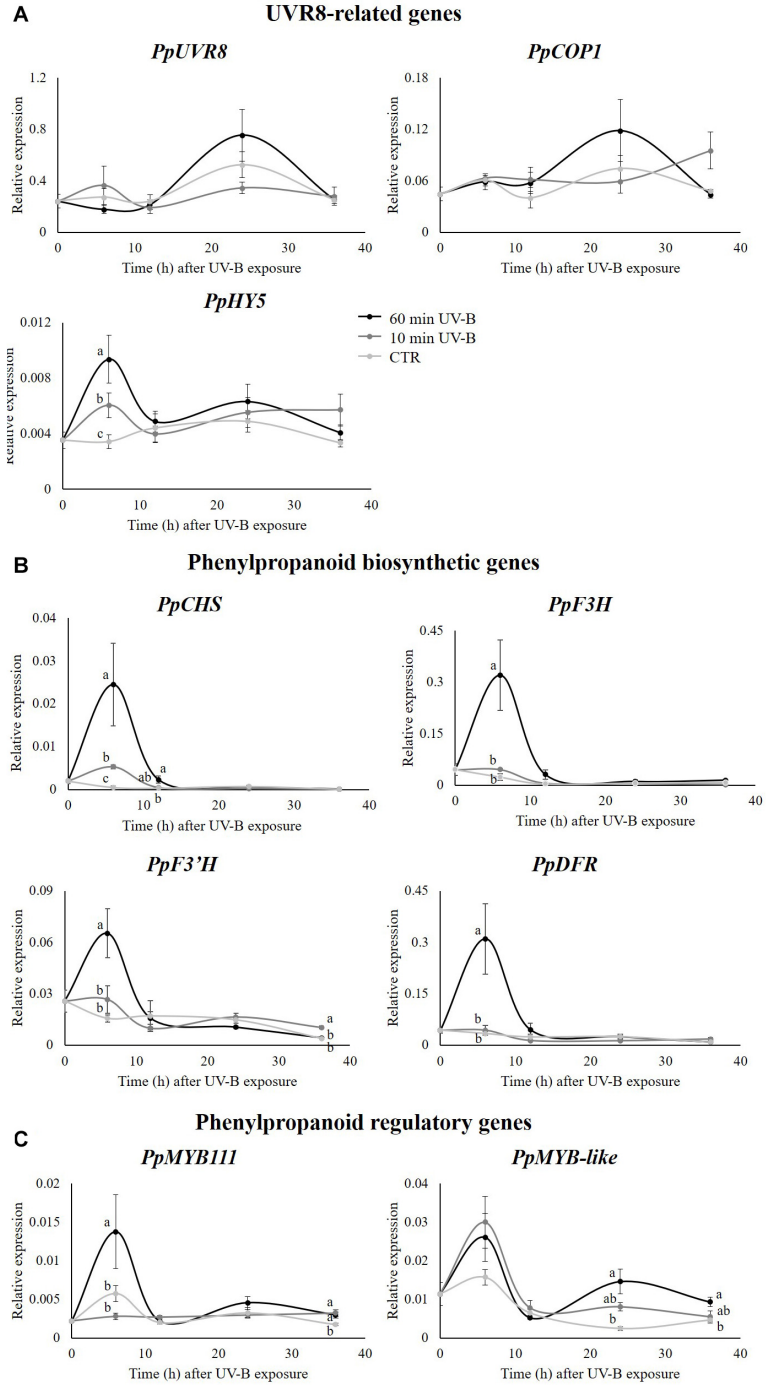

FIGURE 7 | Transcript level of: **(A)** some genes involved in UVR8 pathway (UVR8, COP1, HY5), **(B)** some structural (CHS, F3H, F30H, DFR) and **(C)** some regulatory (MYB111, MYB-like) genes involved in phenylpropanoid biosynthesis in the pulp of peaches exposed to UV-B radiation for either 10 or 60 min, and sampled after 24 and 36 h from the exposure. Data are mean ± SE of five biological replicates. Different letters correspond to statistically significant differences according to one-way ANOVA followed by Tukey–Kramer *post hoc* test ($P \leq 0.05$).

it is directly exposed to the radiation and therefore it is most likely to be influenced by the UV-B exposure. Other studies used the whole organism, risking mixing different responses the UV-B irradiation might trigger on different tissues.

In the present work, the output of the CDA (**Figure 1**) revealed that the UV-B irradiations, both for 10 and 60 min, resulted in a strong modulation of the phenolic profile in peach pulp. In addition, since UV-B-treated and control groups were separated

also in respect to recovery time points, it is reasonable to assume that also the storage time had an impact on the entire phenolic profile. A whole rearrangement of this latter was observed also in the peel of peaches exposed to similar UV-B treatments (Santin et al., 2019). Particularly, the phenolics on peach peel responded mostly after 36 h from the UV-B exposure, with 89% of the detected phenolics undergoing an increase (Santin et al., 2019). When the individual flavonoid classes were considered, a different effect was observed after 24- or 36-h recovery. After 24 h from the exposure, indeed, all the responsive flavonoid classes (flavones, dihydroflavonols, flavonols, and flavanols) exhibited a significant increase following the UV-B treatment, especially the 60-min irradiation. After 36 h, however, the significantly modulated classes were just the flavonols, which increased after the 60-min irradiation, and the flavanols, which decreased in all the UV-B-treated groups. This result was partially in contrast with what was observed by Santin et al. (2018a) in the peel of UV-B-exposed peaches, where, after a general decrease in most phenolic classes at 24 h from the UV-B exposure, a significant increase occurred 36 h from the irradiation, especially for dihydroflavonols, anthocyanins, and flavones. Besides, this effect was mainly visible in the 60-min UV-B-irradiated samples, which was the strongest treatment tested in both studies. Such discrepancy suggests a different responsiveness of the two tissues toward the UV-B radiation. As stated by Santin et al. (2019), in fact, the initial decrease in phenolic concentration in peach peel might be due to their consumption to counteract the potentially harmful UV-B-induced ROS. However, the later UVR8-induced activation of phenylpropanoid genes might have triggered the synthesis and accumulation of new phenolic compounds, as observed after 36 h. Recent studies (Santin et al., 2020) have shown that UV-B radiation does not penetrate peach peel. Thus, it is assumable that a direct UV-B-driven overproduction of ROS did not occur in the pulp. As a result, the phenolics in the pulp were not consumed by their ROS-scavenging activity but they rather increased due to the molecular activation of several genes involved in the phenylpropanoid biosynthesis and regulatory pathway, e.g., *PpCHS*, *PpF3H*, *PpF3′H*, *PpDFR* and some *PpMYB* genes, as reported in **Figure 7**.

UV-B Radiation Affects the Expression of UVR8-Related and Phenylpropanoid-Related Genes in the Peach Pulp

Influence of UV-B radiation on the level of genes involved in the flavonoid biosynthesis was elucidated in many fruit species, such as peach (Scattino et al., 2014; Zhao et al., 2017; Santin et al., 2019), apple (Ubi et al., 2006; Bai et al., 2014), and tomato (Giuntini et al., 2008; Calvenzani et al., 2010; Catola et al., 2017). In contrast to the present study, however, the transcript abundance in the cited works was investigated in the fruit tissue directly exposed to the UV-B radiation, thus likely to be influenced by the exposure. Considering that UV-B radiation was found to be blocked by the peach peel (Santin et al., 2020), the UV-B-mediated activation of phenylpropanoid-related genes described in this manuscript was probably not directly influenced by the UV-B radiation. Indeed, the *PpUVR8* and *PpCOP1* genes did not show any significant variation in response to the treatments, while the activation of *PpCOP1* was observed in peach peel (Santin et al., 2019). It is reasonable to assume that the increased transcription level of the flavonoid genes in the pulp was due to a chemical interplay between the outermost, UV-B-exposed peel and the pulp below. A possible candidate playing this role might be the *PpHY5*, which was in fact overexpressed in both the peel (Santin et al., 2019) and the pulp of the UV-B-treated samples, particularly after 6 h from the irradiation. HY5, member of the basic leucine zipper (bZIP) transcription factors, represents a key factor in the UVR8 signaling pathway, whose expression was found to be upregulated by the UVR8-COP1 complex after the UV-B perception (Ulm et al., 2004; Brown et al., 2005; Huang et al., 2012; Binkert et al., 2014). Once HY5 is stabilized in the cell, it promotes its own expression under both visible and UV-B radiation through the binding to its own promoting sequence (Abbas et al., 2014; Binkert et al., 2014). HY5 was also found to be able to translocate from the plant shoots to the roots, in order to promote and optimize the root nitrate absorption according to the environmental light conditions (Lillo, 2008; Nunes-Nesi et al., 2010; Chen et al., 2016). Though no studies have investigated a possible transport of the HY5 transcription factor among fruit tissues, it might be possible that the overproduced HY5 in the peach peel after the UV-B exposure might have reached the pulp below, triggering its own transcription and, in turn, the transcription of some flavonoid-related genes (Brown et al., 2005; Brown and Jenkins, 2007). This might have led to the accumulation of flavonoids detected after 24 h from the irradiation, such as flavanols, flavonols, and flavones. A further hypothesis that might explain the activation of UVR8- and flavonoid-related genes in the peach pulp although UV-B-protected by the peel could be that the UVR8 in the pulp is activated by wavelengths longer than UV-B, which can weakly penetrate through the peel. Accordingly, recent evidences (Rai et al., 2020) have shown that UVR8 is involved in the perception of both UV-B and UV-A up to 350 nm. However, although UV-B narrowband lamps used in this study has a weak emission within the UV-A range, the transmittance across the peel is below 1% considering both yellow and red peel portions (Santin et al., 2020), thus it is unlikely that such irradiance is able to trigger the UVR8 pathway. In addition, while other studies identified a light gradient within tissues (Seyfried and Fukshansky, 1983; Day et al., 1993), recent work in the model plant Arabidopsis demonstrates that multiple cell types contribute to UV-B signaling and that UV-B can reach the endodermis and pith of Arabidopsis stems, hypocotyls and cotyledons where the UVR8 signaling leads to local flavonoid accumulation (Bernula et al., 2017; Vanhaelewyn et al., 2019a,b).

Glycosylated Flavonols Were Differently Influences by UV-B Exposure

Responsiveness of flavonols, kaempferol glycosides, toward supplemental UV-B radiation was found also in the leaves of *Brassica napus* L. cultivars, Paroll (Olsson et al., 1998).

Concentration of kaempferol glycosides in plants grown under 800 μmol m^{-2} s^{-1} with additional 13 kJ m^{-2} day^{-1} UV-B radiation was 35% higher in the UV-B-treated plants. Moreover, the concentration of kaempferol-3-sophoroside-7-glucoside increased by 76% compared to the unirradiated plants. Interestingly, in our study, the same kaempferol glycoside was found to be accumulated in the 60-min UV-B-treated fruit after 36 h from the end of the exposure. However, other kaempferol glycosides found by Olsson et al. (1998), such as the kaempferol 3-2'''-sinapoylsophoroside-7-glucoside, were not similarly increased, underlying the differential behavior that different kaempferol glycosides might have toward UV-B exposure also in other plant species. A marked variation in the response to UV-B irradiation among the different flavonols was found also in chive (*Allium schoenoprasum* L.) cultivated under 15 mol m^{-2} d^{-1} PAR supplemented with 2 kJ m^{-2} d^{-1} UV-B radiation (Grubmüller et al., 2004). Particularly, the highest increase was observed for quercetins followed by isorhamnetins and kaempferols. Increase in flavonols was also reported in *Centella asiatica* L. Urban. grown under low (455 μmol m^{-2} s^{-1}) and high low (835 μmol m^{-2} s^{-1}) PAR, supplemented with 0.3 W m^{-2} UV-B radiation (Müller et al., 2013). Indeed, Müller et al. (2013) found that both low and high PAR conditions determined a significant increase in flavonol concentration only when supplemented with UV-B radiation. Another study on peeled onion bulbs exposed to a combination of UV-A, -B and -C radiations (18 W m^{-2}) showed a 2-fold increase in flavonol concentration (Rodov et al., 2010). Also in the peel of peach fruit, 3- and 6-h UV-B treatments (1.36 W m^{-2}) were effective in inducing a significant, strong accumulation of flavonols after 24 h from the exposure by 174 and 76%, respectively (Santin et al., 2018b). Particularly, both the kaempferols detected in that work, the 3-rutinoside and the 3-galactoside, underwent a significant increase in the UV-B-treated samples. Similarly, the kaempferol 3-rutinoside was found to be positively influenced by the UV-B radiation also in the present study. Besides, Santin et al. (2018b) observed an increase also in isorhamnetin concentration in the 3-h UV-B-treated fruit considering all the individual isorhamnetins detected, which were the 3-rutinoside, the 3-galactoside and the 3-glucoside. In the current work, isorhamnetin 3-rutinoside was likewise significantly increased after 24 h from the 60-min UV-B exposure.

The Different Anthocyanins Responded Differently to the UV-B Treatment, Although Total Anthocyanin Concentration Was Unchanged

Despite no significant variations were observed in the concentration of total anthocyanins, regardless of the recovery time point, this result derived from a differential influence played by UV-B radiation on anthocyanin subclasses. Indeed, a deeper investigation revealed that malvidins and pelargonidins significantly increased and decreased 24 h after the 10-min UV-B-treatment, respectively. After 36 h, the influenced anthocyanins were malvidins and petunidins, which decreased and increased in the 60-min UV-B-exposed peaches, respectively. These results were in contrast to what was observed in the peel of UV-B-treated peach fruit. Santin et al. (2018a) found a consistent accumulation of anthocyanins 36 h after both the 10- and the 60-min UV-B exposure (1.92- and 2.53-fold increase, respectively), and also Santin et al. (2018b) displayed a higher cyanidin-3-glucoside concentration following a 3- and 12-h UV-B-treatment. Anthocyanins play a key role in photoprotection against high-energy radiations, such as UV (Solovchenko and Schmitz-Eiberger, 2003; Guo et al., 2008; Schreiner et al., 2012). A stimulation in the anthocyanin biosynthesis following UV-B exposure, which was widely elucidated in many previous works (Marais et al., 2001; Kataoka and Beppu, 2004; Higashio et al., 2005), might not have occurred in the pulp because, being completely UV-B-shielded, did not need to boost up its defenses by accumulating newly-synthesized anthocyanins. Furthermore, in UV-B-treated apple fruit, biosynthesis of flavonols occurred faster than anthocyanins biosynthesis, leading to a higher accumulation of flavonols compared to what was observed for anthocyanins (Ban et al., 2007; Hagen et al., 2007).

UV-B Exposure Increased the Glycosides/Aglycones Ratio of Flavonols and Anthocyanins

In the present research, the UV-B treatments revealed a significant increase in the glycosides/aglycones ratio of flavonols and anthocyanins. While the glycosilated ones increased the aglycone concentration decreased. Besides, such transient effect on flavonols was noticeable only after 24 h in both UV-B treatments. Most flavonoids are normally glycosilated (Tohge et al., 2017) providing several advantages, such as increased solubility and, consequently, easier storage and reduced transportation across cell membranes (Vetter, 2000; Kytidou et al., 2020). Thus, it might be that the increased glycosides/aglycones ratio was due to the necessity of the cells to optimize the storage of the overproduced flavonoids by glycosylation. Furthermore, the stability and the bioactivity of glycosylated phytochemicals are related to the position where sugar moieties are linked, as well as the type of linkage (*O*- versus *C*-) and of sugars (Kytidou et al., 2020). Unfortunately, literature on UV-B-induced modification of glycosylation pattern is scarce. Neugart et al. (2014) found that kale plants exposed to five daily doses of 0.25 kJ m^{-2} d^{-1} UV-B radiation differentially accumulated quercetins and kaempferols depending on the sugar moiety and the degree of acetylation (whether non-, mono-, or di-acetylated flavonol). Similarly, in this work, no correlation was observed between either the type and number of sugar moieties linked to the flavonoid molecule (mono-, di-, or tri-saccharides) and the most UV-B-responsive kaempferols or isorhamnetins.

CONCLUSION

The present study provides evidence that, although UV-B radiation does not penetrate the peel of peach fruits, it rearranges

the flavonoid classes in the pulp underneath. Besides, such UV-B-induced changes of the flavonoid profiles depend on both the flavonoid class and the recovery time, and are particularly pronounced when considering the glycosides and the aglycones separately. Since UV-B-driven metabolic changes on fruits and vegetables are strictly UV-B dose- and cultivar-dependent, further "-omics" studies on other plant species are highly encouraged to extend the knowledge on how to exploit the UV-B radiation to enhance the nutraceutical value on plant-based food.

DATA AVAILABILITY STATEMENT

All datasets generated for this study are included in the article/**Supplementary Material**.

AUTHOR CONTRIBUTIONS

AR and M-TH designed the research. MS, AC, LL, GR, and BM-M carried out the experiments, analyzed the data, and wrote the manuscript. AR, LL, and M-TH helped to draft the manuscript and revised the manuscript. All authors read and approved the final manuscript.

FUNDING

The research was supported by funds of the University of Pisa. MS conducted part of the study in the laboratory of M-TH at the Department of Applied Genetics and Cell Biology, University of Natural Resources and Life Sciences which was supported by a grant of the Austrian Science Fund FWF I 1725-B16. We kindly acknowledge the technical support of Julia Richter and Nataliia Konstantinova for help with the sampling. MS was further supported by an Erasmus+ traineeship.

SUPPLEMENTARY MATERIAL

The Supplementary Material for this article can be found online at: https://www.frontiersin.org/articles/10.3389/fpls.2020.579063/full#supplementary-material

REFERENCES

Abbas, N., Maurya, J. P., Senapati, D., Gangappa, S. N., and Chattopadhyaya, S. (2014). *Arabidopsis* CAM7 and HY5 physically interact and directly bind to the HY5 promoter to regulate its expression and thereby promote photomorphogenesis. *Plant Cell* 26, 1036–1052. doi: 10.1105/tpc.113.122515

Aleixandre, J. L., Aleixandre-Tudó, J. L., Bolaños-Pizzaro, M., and Aleixandre-Benavent, R. (2013). Mapping the scientific research on wine and health (2001-2011). *J. Agric. Food Chem.* 61, 11871–11880. doi: 10.1021/jf404394e

Altschul, S., Madden, T. L., Schäffer, A. A., Zhang, J., Zhang, Z., Miller, W., et al. (1997). Gapped BLAST and PSI-BLAST: a new generation of protein database search programs. *Nucleic Acids Res.* 25, 3389–3402. doi: 10.1016/0956-7135(96)00004-7

Andersen, C. L., Jensen, J. L., and Ørntoft, T. F. (2004). Normalization of real-time quantitative reverse transcription-PCR data: a model-based variance estimation approach to identify genes suited for normalization, applied to bladder and colon cancer data sets. *Cancer Res.* 64, 5245–5250. doi: 10.1158/0008-5472.can-04-0496

Assumpção, C. F., Hermes, V. S., Pagno, C., Castagna, A., Mannucci, A., Sgherri, C., et al. (2018). Phenolic enrichment in apple skin following post-harvest fruit UV-B treatment. *Postharvest. Biol. Technol.* 138, 37–45. doi: 10.1016/j.postharvbio.2017.12.010

Austin, M. B., and Noel, J. P. (2003). The chalcone synthase superfamily of type III polyketide synthases. *Nat. Prod. Rep.* 20, 79–110. doi: 10.1039/b100917f

Bai, S., Saito, T., Honda, C., Hatsuyama, Y., Ito, A., and Moriguchi, T. (2014). An apple B-box protein, MdCOL11, is involved in UV-B- and temperature-induced anthocyanin biosynthesis. *Planta* 240, 1051–1062. doi: 10.1007/s00425-014-2129-8

Ban, Y., Honda, C., Bessho, H., Pang, X. M., and Moriguchi, T. (2007). Suppression subtractive hybridization identifies genes induced in response to UV-B irradiation in apple skin: isolation of a putative UDP-glucose 4-epimerase. *J. Exp. Bot.* 58, 1825–1834. doi: 10.1093/jxb/erm045

Bernula, P., Crocco, C. D., Arongaus, A. B., Ulm, R., Nagy, F., and Viczián, A. (2017). Expression of the UVR8 photoreceptor in different tissues reveals tissue-autonomous features of UV-B signalling. *Plant Cell Environ.* 40, 1104–1114. doi: 10.1111/pce.12904

Binkert, M., Kozma-Bognár, L., Terecskei, K., De Veylder, L., Nagy, F., and Ulm, R. (2014). UV-B-Responsive association of the *Arabidopsis* bZIP transcription factor ELONGATED HYPOCOTYL5 with target genes, including its own promoter. *Plant Cell* 26, 4200–4213. doi: 10.1105/tpc.114.130716

Brown, B. A., Cloix, C., Jiang, G. H., Kaiserli, E., Herzyk, P., Kliebenstein, D. J., et al. (2005). A UV-B-specific signaling component orchestrates plant UV protection. *Proc. Natl. Acad. Sci. U.S.A.* 102, 18225–18230. doi: 10.1073/pnas.0507187102

Brown, B. A., and Jenkins, G. I. (2007). UV-B signaling pathways with different fluence-rate response profiles are distinguished in mature *Arabidopsis* leaf tissue by requirement for UVR8, HY5, and HYH. *Plant Physiol.* 146, 576–588. doi: 10.1104/pp.107.108456

Brown, B. A., and Jenkins, G. I. (2008). UV-B signaling pathways with different fluence-rate response profiles are distinguished in mature *Arabidopsis* leaf tissue by requirement for UVR8, HY5, and HYH. *Plant Physiol.* 146, 576–588.

Calvenzani, V., Martinelli, M., Lazzeri, V., Giuntini, D., Dall 'asta, C., Galaverna, G., et al. (2010). Response of wild-type and high pigment-1 tomato fruit to UV-B depletion: xavonoid proWling and gene expression. *Planta* 231, 755–765. doi: 10.1007/s00425-009-1082-4

Catola, S., Castagna, A., Santin, M., Calvenzani, V., Petroni, K., Mazzucato, A., et al. (2017). The dominant allele Aft induces a shift from flavonol to anthocyanin production in response to UV-B radiation in tomato fruit. *Planta* 246, 263–275. doi: 10.1007/s00425-017-2710-z

Chen, X., Yao, Q., Gao, X., Jiang, C., Harberd, N. P., and Fu, X. (2016). Shoot-to-root mobile transcription factor HY5 coordinates plant carbon and nitrogen acquisition. *Curr. Biol.* 26, 640–646. doi: 10.1016/j.cub.2015.12.066

Cheynier, V., Comte, G., Davies, K. M., Lattanzio, V., and Martens, S. (2013). Plant phenolics: recent advances on their biosynthesis, genetics, andecophysiology. *Plant Physiol. Biochem.* 72, 1–20. doi: 10.1016/j.plaphy.2013.05.009

Day, T. A., Martin, G., and Vogelmann, T. C. (1993). Penetration of UV-B radiation in foliage: evidence that the epidermis behaves as a non-uniform filter. *Plant. Cell Environ.* 16, 735–741. doi: 10.1111/j.1365-3040.1993.tb00493.x

Eichholz, I., Rohn, S., Gamm, A., Beesk, N., Herppich, W. B., Kroh, L. W., et al. (2012). UV-B-mediated flavonoid synthesis in white asparagus (*Asparagus officinalis* L.). *Food Res. Int.* 48, 196–201. doi: 10.1016/j.foodres.2012.03.008

Favory, J. J., Stec, A., Gruber, H., Rizzini, L., Oravecz, A., Funk, M., et al. (2009). Interaction of COP1 and UVR8 regulates UV-B-induced photomorphogenesis and stress acclimation in *Arabidopsis*. *EMBO J.* 28, 591–601. doi: 10.1038/emboj.2009.4

Frohnmeyer, H. (2003). Ultraviolet-B radiation-mediated responses in plants. balancing damage and protection. *Plant Physiol.* 133, 1420–1428. doi: 10.1104/pp.103.030049

Ghasemzadeh, A., and Ghasemzadeh, N. (2011). Flavonoids and phenolic acids: role and biochemical activity in plants and human. *J. Med. Plants Res.* 5, 6697–6703. doi: 10.5897/JMPR11.1404

Gil, M. I., Tomás-Barberán, F. A., Hess-Pierce, B., and Kader, A. A. (2002). Antioxidant capacities, phenolic compounds, carotenoids, and vitamin C contents of nectarine, peach, and plum cultivars from California. *J. Agric. Food Chem.* 50, 4976–4982.

Giuntini, D., Lazzeri, V., Calvenzani, V., Dall'Asta, C., Galaverna, G., Tonelli, C., et al. (2008). Flavonoid profiling and biosynthetic gene expression in flesh and peel of two tomato genotypes grown under UV-B-depleted conditions during ripening. *J. Agric. Food Chem.* 56, 5905–5915. doi: 10.1021/jf8003338

Gruber, H., Heijde, M., Heller, W., Albert, A., Seidlitz, H. K., and Ulm, R. (2010). Negative feedback regulation of UV-B-induced photomorphogenesis and stress acclimation in *Arabidopsis*. *Proc. Natl. Acad. Sci. U.S.A.* 107, 20132–20137. doi: 10.1073/pnas.0914532107

Grubmüller, E., Schnitzler, W. H., and Nitz, G. M. (2004). "Differential flavonoid response to PAR and UV-B light in chive (*Allium schoenoprasum* L.)," in *VII International Symposium on Protected Cultivation in Mild Winter Climates: Production, Pest Management and Global Competition 659*, 825–830. doi: 10.17660/actahortic.2004.659.107

Guo, J., Han, W., and Wang, M. (2008). Ultraviolet and environmental stresses involved in the induction and regulation of anthocyanin biosynthesis: a review. *Afr. J. Biotechnol.* 7, 4966–4972.

Hagen, S. F., Borge, G. I. A., Bengtsson, G. B., Bilger, W., Berge, A., Haffner, K., et al. (2007). Phenolic contents and other health and sensory related properties of apple fruit (Malus domestica Borkh ., cv . Aroma): effect of postharvest UV-B irradiation. *Postharvest. Biol. Technol.* 45, 1–10. doi: 10.1016/j.postharvbio.2007.02.002

Herndon, J. M., Hoisington, R. D., and Whiteside, M. (2018). Deadly ultraviolet UV-C and UV-B penetration to earth ' s surface: human and deadly ultraviolet UV-C and UV-B penetration to earth ' s surface: human and environmental health implications. *J. Geogr. Environ. Earth Sci. Int.* 14, 1–11. doi: 10.9734/JGEESI/2018/40245

Hideg, É, Jansen, M. A. K., and Strid, Å (2013). UV-B exposure, ROS, and stress: inseparable companions or loosely linked associates? *Trends Plant Sci.* 18, 107–115. doi: 10.1016/J.TPLANTS.2012.09.003

Higashio, H., Hirokane, H., Sato, F., Tokuda, S., and Uragami, A. (2005). Effect of UV irradiation after the harvest on the content of flavonoid in vegetables. *Acta Hortic.* 682, 1007–1012. doi: 10.17660/ActaHortic.2005.682.131Ð

Huang, X., Ouyang, X., Yang, P., Lau, O. S., Chen, L., Wei, N., et al. (2013). Conversion from CUL4-based COP1-SPA E3 apparatus to UVR8-COP1-SPA complexes underlies a distinct biochemical function of COP1 under UV-B. *Proc. Natl. Acad. Sci. U.S.A.* 110, 16669–16674. doi: 10.1073/pnas.1316622110

Huang, X., Ouyang, X., Yang, P., Lau, O. S., Li, G., Li, J., et al. (2012). *Arabidopsis* FHY3 and HY5 positively mediate induction of COP1 transcription in response to photomorphogenic UV-B light. *Plant Cell* 24, 4590–4607. doi: 10.1105/tpc.112.103994

Interdonato, R., Rosa, M., Nieva, C. B., González, J. A., Hilal, M., and Prado, F. E. (2011). Effects of low UV-B doses on the accumulation of UV-B absorbing compounds and total phenolics and carbohydrate metabolism in the peel of harvested lemons. *Environ. Exp. Bot.* 70, 204–211. doi: 10.1016/j.envexpbot.2010.09.006

Jenkins, G. I. (2014). The UV-B photoreceptor UVR8: from structure to physiology. *Plant Cell* 26, 21–37. doi: 10.1105/tpc.113.119446

Karsai, A., Müller, S., Platz, S., and Hauser, M. T. (2002). Evaluation of a homemade SYBR® Green I reaction mixture for real-time PCR quantification of gene expression. *Biotechniques* 32, 790–796. doi: 10.2144/02324st05

Kataoka, I., and Beppu, K. (2004). UV irradiance increases development of red skin color and anthocyanins in "Hakuho" peach. *HortScience* 39, 1234–1237. doi: 10.21273/HORTSCI.39.6.1234

Konopacka, D., Jesionkowska, K., Kruczyńska, D., Stehr, R., Schoorl, F., Buehler, A., et al. (2010). Apple and peach consumption habits across European countries. *Appetite* 55, 478–483. doi: 10.1016/j.appet.2010.08.011

Kytidou, K., Artola, M., Overkleeft, H. S., and Aerts, J. M. F. G. (2020). Plant glycosides and glycosidases: a treasure-trove for therapeutics. *Front. Plant Sci.* 11:357. doi: 10.3389/fpls.2020.00357

Lau, K., Podolec, R., Chappuis, R., Ulm, R., and Hothorn, M. (2019). Plant photoreceptors and their signaling components compete for COP 1 binding via VP peptide motifs. *EMBO J.* 38, 1–18. doi: 10.15252/embj.2019102140

Lillo, C. (2008). Signalling cascades integrating light-enhanced nitrate metabolism. *Biochem. J.* 415, 11–19. doi: 10.1042/BJ20081115

Luthria, D. L., Mukhopadhyay, S., and Krizek, D. T. (2006). Content of total phenolics and phenolic acids in tomato (*Lycopersicon esculentum* Mill.) fruits as influenced by cultivar and solar UV radiation. *J. Food Compos. Anal.* 19, 771–777. doi: 10.1016/j.jfca.2006.04.005

Marais, E., Jacobs, G., and Holcroft, D. M. (2001). Postharvest irradiation affects colour development in bicoloured pome fruit. *Acta Hortic.* 553, 569–570. doi: 10.17660/ActaHortic.2001.553.134

Mokrani, A., Krisa, S., Cluzet, S., Da Costa, G., Temsamani, H., Renouf, E., et al. (2016). Phenolic contents and bioactive potential of peach fruit extracts. *Food Chem.* 202, 212–220. doi: 10.1016/j.foodchem.2015.12.026

Müller, V., Albert, A., Barbro Winkler, J., Lankes, C., Noga, G., and Hunsche, M. (2013). Ecologically relevant UV-B dose combined with high PAR intensity distinctly affect plant growth and accumulation of secondary metabolites in leaves of *Centella asiatica* L. *Urban. J. Photochem. Photobiol. B Biol.* 127, 161–169. doi: 10.1016/j.jphotobiol.2013.08.014

Neugart, S., Fiol, M., Schreiner, M., Rohn, S., Zrenner, R., Kroh, L. W., et al. (2014). Interaction of moderate UV-B exposure and temperature on the formation of structurally different flavonol glycosides and hydroxycinnamic acid derivatives in kale (*Brassica oleracea* var. *sabellica)*. *J. Agric. Food Chem.* 62, 4054–4062. doi: 10.1021/jf4054066

Nunes-Nesi, A., Fernie, A. R., and Stitt, M. (2010). Metabolic and signaling aspects underpinning the regulation of plant carbon nitrogen interactions. *Mol. Plant* 3, 973–996. doi: 10.1093/mp/ssq049

Nunez, M., Forgan, B., and Roy, C. (1994). Estimating ultraviolet radiation at the earth's surface. *Int. J. Biometeorol.* 38, 5–17. doi: 10.1007/BF01241798

Olsson, L. C., Veit, M., Weissenböck, G., and Bornman, J. F. (1998). Differential flavonoid response to enhanced UV-B radiation in Brassica napus. *Phytochemistry* 49, 1021–1028. doi: 10.1016/S0031-9422(98)00062-4

Rai, N., O'Hara, A., Farkas, D., Safronov, O., Ratanasopa, K., Wang, F., et al. (2020). The photoreceptor UVR8 mediates the perception of both UV-B and UV-A wavelengths up to 350 nm of sunlight with responsivity moderated by cryptochromes. *Plant Cell Environ.* 43, 1513–1527. doi: 10.1111/pce.13752

Rajabbeigi, E., Eichholz, I., Beesk, N., Ulrichs, C., Kroh, L. W., Rohn, S., et al. (2013). Interaction of drought stress and UV-B radiation - impact on biomass production and flavonoid metabolism in lettuce (Lactuca sativa L.). *J. Appl. Bot. Food Qual.* 86, 190–197. doi: 10.5073/Jabfq.2013.086.026

Richter, J., Ploderer, M., Mongelard, G., Gutierrez, L., and Hauser, M.-T. (2017). Role of CrRLK1L Cell Wall Sensors HERCULES1 and 2, THESEUS1, and FERONIA in growth adaptation triggered by heavy metals and trace elements. *Front. Plant Sci.* 8:1554. doi: 10.3389/fpls.2017.01554

Rizzini, L., Favory, J. J., Cloix, C., Faggionato, D., O'Hara, A., Kaiserli, E., et al. (2011). Perception of UV-B by the *Arabidopsis* UVR8 protein. *Science* 332, 103–106. doi: 10.1126/science.1200660

Rocchetti, G., Chiodelli, G., Giuberti, G., Ghisoni, S., Baccolo, G., Blasi, F., et al. (2018). UHPLC-ESI-QTOF-MS profile of polyphenols in Goji berries (*Lycium barbarum L.*) and its dynamics during in vitro gastrointestinal digestion and fermentation. *J. Funct. Foods.* 40, 564–572. doi: 10.1016/j.jff.2017.11.042

Rocchetti, G., Senizza, A., Gallo, A., Lucini, L., Giuberti, G., and Patrone, V. (2019). In vitro large intestine fermentation of gluten-free rice cookies containing alfalfa seed (*Medicago sativa* L.) flour: a combined metagenomic/metabolomic approach. *Food Res. Int.* 120, 312–321. doi: 10.1016/j.foodres.2019.03.003

Rodov, V., Tietel, Z., Vinokur, Y., Horev, B., and Eshel, D. (2010). Ultraviolet light stimulates flavonol accumulation in peeled onions and controls microorganisms on their surface. *J. Agric. Food Chem.* 58, 9071–9076. doi: 10.1021/jf1016016

Ross, J. A., and Kasum, C. M. (2002). DIETARY F LAVONOIDS: bioavailability, metabolic effects, and safety. *Annu. Rev. Nutr.* 22, 19–34. doi: 10.1146/annurev.nutr.22.111401.144957

Ruiz, V. E., Interdonato, R., Cerioni, L., Albornoz, P., Ramallo, J., Prado, F. E., et al. (2016). Short-term UV-B exposure induces metabolic and anatomical changes in peel of harvested lemons contributing in fruit protection against green mold.

J. Photochem. Photobiol. B Biol. 159, 59–65. doi: 10.1016/j.jphotobiol.2016.03.016

Salek, R. M., Steinbeck, C., Viant, M. R., Goodacre, R., and Dunn, W. B. (2013). The role of reporting standards for metabolite annotation and identification in metabolomic studies. *Gigascience* 2, 2–4. doi: 10.1186/2047-217X-2-13

Santin, M., Lucini, L., Castagna, A., Chiodelli, G., Hauser, M.-T., and Ranieri, A. (2018a). Post-harvest UV-B radiation modulates metabolite profile in peach fruit. *Postharvest Biol. Technol.* 139, 127–134. doi: 10.1016/j.postharvbio.2018.02.001

Santin, M., Neugart, S., Castagna, A., Barilari, M., Sarrocco, S., Vannacci, G., et al. (2018b). UV-B pre-treatment alters phenolics response to *Monilinia fructicola* infection in a structure-dependent way in peach skin. *Front. Plant Sci.* 871:1598. doi: 10.3389/fpls.2018.01598

Santin, M., Lucini, L., Castagna, A., Rocchetti, G., Hauser, M.-T., and Ranieri, A. (2019). Comparative "phenol-omics" and gene expression analyses in peach (Prunus persica) skin in response to different postharvest UV-B treatments. *Plant Physiol. Biochem.* 135, 511–519. doi: 10.1016/j.plaphy.2018.11.009

Santin, M., Ranieri, A., Hauser, M. T., Miras-Moreno, B., Rocchetti, G., Lucini, L., et al. (2020). The outer influences the inner: postharvest UV-B irradiation modulates peach flesh metabolome although shielded by the skin. *Food Chem.* 338:127782. doi: 10.1016/j.foodchem.2020.127782

Scattino, C.,Castagna, A., Neugart, S.,Chan, H. M., Schreiner, M., Crisosto, C. H., et al. (2014). Post-harvest UV-B irradiation induces changes of phenol contents and corresponding biosynthetic gene expression in peaches and nectarines. *Food Chem.* 163, 51–60. doi: 10.1016/j.foodchem.2014.04.077

Schreiner, M., Mewis, I., Huyskens-Keil, S., Jansen, M. A. K., Zrenner, R., Winkler, J. B., et al. (2012). UV-B-induced secondary plant metabolites - potential benefits for plant and human health. *CRC Crit. Rev. Plant Sci.* 31, 229–240. doi: 10.1080/07352689.2012.664979

Schrimpe-Rutledge, A. C., Codreanu, S. G., Sherrod, S. D., and McLean, J. A. (2016). Untargeted metabolomics Strategies—Challenges and emerging directions. *J. Am. Soc. Mass Spectrom.* 27, 1897–1905. doi: 10.1007/s13361-016-1469-y

Seyfried, M., and Fukshansky, L. (1983). Light gradients in plant tissue. *Appl. Opt.* 22, 1402–1408. doi: 10.1364/AO.22.001402

Solovchenko, A., and Schmitz-Eiberger, M. (2003). Significance of skin flavonoids for UV-B-protection in apple fruits. *J. Exp. Bot.* 54, 1977–1984. doi: 10.1093/jxb/erg199

Stracke, R., Favory, J. J., Gruber, H., Bartelniewoehner, L., Bartels, S., Binkert, M., et al. (2010). The *Arabidopsis* bZIP transcription factor HY5 regulates expression of the PFG1/MYB12 gene in response to light and ultraviolet-B radiation. *Plant Cell Environ.* 33, 88–103. doi: 10.1111/j.1365-3040.2009.02061.x

Tavarini, S., Gil, M. I., Tomas-Barberan, F. A., Buendia, B., Remorini, D., Massai, R., et al. (2011). Effects of water stress and rootstocks on fruit phenolic composition and physical/chemical quality in Suncrest peach. *Ann. Appl. Biol.* 158, 226–233. doi: 10.1111/j.1744-7348.2010.00457.x

Tohge, T., De Souza, L. P., and Fernie, A. R. (2017). Current understanding of the pathways of flavonoid biosynthesis in model and crop plants. *J. Exp. Bot.* 68, 4013–4028. doi: 10.1093/jxb/erx177

Tolonen, M., Taipale, M., Viander, B., Pihlava, J.-M., Korhonen, H., and Ryhänen, E.-L. (2002). Plant-derived biomolecules in fermented cabbage. *J. Agric. Food Chem.* 50, 6798–6803. doi: 10.1021/jf0109017

Tomás-Barberán, F. A., Gil, M. I., Cremin, P., Waterhouse, A. L., Hess-Pierce, B., and Kader, A. A. (2001). HPLC-DAD-ESIMS analysis of phenolic compounds in nectarines, peaches, and plums. *J. Agric. Food Chem.* 49, 4748–4760. doi: 10.1021/jf0104681

Ubi, B. E., Honda, C., Bessho, H., Kondo, S., Wada, M., Kobayashi, S., et al. (2006). Expression analysis of anthocyanin biosynthetic genes in apple skin: effect of UV-B and temperature. *Plant Sci.* 170, 571–578. doi: 10.1016/j.plantsci.2005.10.009

Ulm, R., Baumann, A., Oravecz, A., Máté, Z., Ádám, É, Oakeley, E. J., et al. (2004). Genome-wide analysis of gene expression reveals function of the bZIP transcription factor HY5 in the UV-B response of *Arabidopsis*. *Proc. Natl. Acad. Sci. U.S.A.* 101, 1397–1402. doi: 10.1073/pnas.0308044100

Vanhaelewyn, L., Bernula, P., Van Der Straeten, D., Vandenbussche, F., and Viczián, A. (2019a). UVR8-dependent reporters reveal spatial characteristics of signal spreading in plant tissues. *Photochem. Photobiol. Sci.* 18, 1030–1045. doi: 10.1039/C8PP00492G

Vanhaelewyn, L., Viczián, A., Prinsen, E., Bernula, P., Serrano, A. M., Arana, M. V., et al. (2019b). Differential UVR8 signal across the stem controls UV-B–induced inflorescence phototropism. *Plant Cell* 31, 2070–2088. doi: 10.1105/TPC.18.00929

Vetter, J. (2000). Plant cyanogenic glycosides. *Toxicon* 38, 11–36. doi: 10.1136/bmj.1.4351.729-a

Vizzotto, M., Cisneros-zevallos, L., and Byrne, D. H. (2007). Large variation found in the phytochemical and antioxidant activity of peach and plum germplasm. *J. Am. Soc. Hortic. Sci.* 132, 334–340. doi: 10.21273/jashs.132.3.334

Xiao, J., Muzashvili, T. S., and Georgiev, M. I. (2014). Advances in the biotechnological glycosylation of valuable flavonoids. *Biotechnol. Adv.* 32, 1145–1156. doi: 10.1016/j.biotechadv.2014.04.006

Zhang, H., and Tsao, R. (2016). Dietary polyphenols, oxidative stress and antioxidant and anti-inflammatory effects. *Curr. Opin. Food Sci.* 8, 33–42. doi: 10.1016/j.cofs.2016.02.002

Zhang, L., Jiao, T., Shao, X., Li, Z., and Liu, M. (2006). Aggregation of TPPS on spreading films of achiral cationic amphiphiles: effect of the charge and rigid spacer on the morphologies and supramolecular chirality. *Colloids Surfaces A Physicochem. Eng. Asp.* 284–285, 130–134. doi: 10.1021/jf100936x

Zhao, Y., Dong, W., Wang, K., Zhang, B., Allan, A. C., Lin-wang, K., et al. (2017). Differential sensitivity of fruit pigmentation to ultraviolet light between two peach cultivars. *Front. Plant Sci.* 8:1552. doi: 10.3389/fpls.2017.01552

Conflict of Interest: The authors declare that the research was conducted in the absence of any commercial or financial relationships that could be construed as a potential conflict of interest.

Copyright © 2020 Santin, Castagna, Miras-Moreno, Rocchetti, Lucini, Hauser and Ranieri. This is an open-access article distributed under the terms of the Creative Commons Attribution License (CC BY). The use, distribution or reproduction in other forums is permitted, provided the original author(s) and the copyright owner(s) are credited and that the original publication in this journal is cited, in accordance with accepted academic practice. No use, distribution or reproduction is permitted which does not comply with these terms.

frontiers in Plant Science

REVIEW
published: 15 December 2020
doi: 10.3389/fpls.2020.597642

Ultraviolet Radiation From a Plant Perspective: The Plant-Microorganism Context

Lucas Vanhaelewyn[1], Dominique Van Der Straeten[1], Barbara De Coninck[2] and Filip Vandenbussche[1]*†*

[1] Laboratory of Functional Plant Biology, Department of Biology, Ghent University, Ghent, Belgium, [2] Plant Health and Protection Laboratory, Division of Crop Biotechnics, Department of Biosystems, KU Leuven, Leuven, Belgium

OPEN ACCESS

Edited by:
Marie-Theres Hauser, University of Natural Resources and Life Sciences, Vienna, Austria

Reviewed by:
Milton Brian Traw, Nanjing University, China
Ericsson Coy-Barrera, Universidad Militar Nueva Granada, Colombia

***Correspondence:**
Lucas Vanhaelewyn
Lucas.Vanhaelewyn@UGent.be
Filip Vandenbussche
Filip.Vandenbussche@DeroosePlants.com

†Present address:
Filip Vandenbussche, Deroose Plants, Evergem, Belgium

Specialty section:
This article was submitted to Plant Metabolism and Chemodiversity, a section of the journal Frontiers in Plant Science

Received: *21 August 2020*
Accepted: *19 November 2020*
Published: *15 December 2020*

Citation:
Vanhaelewyn L, Van Der Straeten D, De Coninck B and Vandenbussche F (2020) Ultraviolet Radiation From a Plant Perspective: The Plant-Microorganism Context. Front. Plant Sci. 11:597642. doi: 10.3389/fpls.2020.597642

Ultraviolet (UV) radiation directly affects plants and microorganisms, but also alters the species-specific interactions between them. The distinct bands of UV radiation, UV-A, UV-B, and UV-C have different effects on plants and their associated microorganisms. While UV-A and UV-B mainly affect morphogenesis and phototropism, UV-B and UV-C strongly trigger secondary metabolite production. Short wave (<350 nm) UV radiation negatively affects plant pathogens in direct and indirect ways. Direct effects can be ascribed to DNA damage, protein polymerization, enzyme inactivation and increased cell membrane permeability. UV-C is the most energetic radiation and is thus more effective at lower doses to kill microorganisms, but by consequence also often causes plant damage. Indirect effects can be ascribed to UV-B specific pathways such as the UVR8-dependent upregulated defense responses in plants, UV-B and UV-C upregulated ROS accumulation, and secondary metabolite production such as phenolic compounds. In this review, we summarize the physiological and molecular effects of UV radiation on plants, microorganisms and their interactions. Considerations for the use of UV radiation to control microorganisms, pathogenic as well as non-pathogenic, are listed. Effects can be indirect by increasing specialized metabolites with plant pre-treatment, or by directly affecting microorganisms.

Keywords: ultraviolet-B, ultraviolet-A, plants, plant-microorganism interaction, ultraviolet, UV-C

INTRODUCTION

Life on Earth is exposed to the light spectrum ranging from ultraviolet-B (UV-B) to infrared wavelengths (295–2500 nm), hereafter referred to as natural radiation. The ultraviolet (UV) part of the electromagnetic spectrum comprises three classes: UV-C (200–280 nm), UV-B (280–315 nm) and UV-A (315–400 nm) with only UV-B and UV-A reaching the earth's surface. Radiation with wavelengths below 290 nm declines to undetectable levels (Schäfer and Nagy, 2006). Although UV radiation is only a minor fraction of the sunlight reaching Earth's surface, it causes significant biological effects on organisms which can affect plant-phyllosphere interactions, and indirectly plant-rhizosphere interactions, with most studies performed on UV-B (Robson et al., 2015; Carvalho and Castillo, 2018).

Land plants, fungi, and bacteria have several fundamental characteristics in common. While growing, they have minimal possibilities for rapid long-distance displacement and therefore they

usually adapt their growth and metabolism to incoming light with functionally overlapping pigments. Plants and microorganisms most often occur in the same terrestrial ecosystems with an equivalent natural climatic environment. The plant phyllosphere gets exposed to UV radiation but the optical properties – as determined by the architecture – of plants, fungi and bacteria differ. Plants have structurally organized multilayer tissues throughout their life cycle, fungi usually have mono-layered mycelia (with fruiting bodies as multi-layered exceptions), and bacteria exhibit significantly less complex organization, as single cells or biofilms. Hence the effect and impact of UV radiation on these organisms will be fundamentally different, ranging from biomolecule damage to secondary metabolite production (**Table 1**). Interestingly, these UV induced effects are usually dependent on the radiation intensity and developmental stages (Moreira-Rodriguez et al., 2017). UV irradiation has the potency to redirect the carbon flux resulting in changes in several classes of primary and secondary metabolites (recently often referred to as specialized metabolites) such as carotenoids, phenolics, glucosinolates and even chlorophylls, with associated effects in the phyllosphere (Katerova et al., 2012; Mewis et al., 2012; Heinze et al., 2018; Vandenbussche et al., 2018). Some of the specialized metabolites produced by plants in response to UV relate with defense responses and interactions with phyllosphere components (Demkura and Ballare, 2012; Mewis et al., 2012). Moreover, specialized metabolite accumulation is often ascribed to hormonal changes in the plants, especially due to an increased expression of genes of the salicylic acid (SA) and jasmonate (JA) pathways, suggesting the stimulation of defense mechanisms that potentially impact microorganisms and other leaf dwellers (Vanhaelewyn et al., 2016a; Vandenbussche et al., 2018). Much like it is the case in other eukaryotes, light and other irradiation, including the UV range, have a very diverse impact on filamentous fungal development and metabolism (Tisch and Schmoll, 2010). The UV related changes in fungal development and metabolism are orchestrated by a set of specific photosignaling pathways.

Here we review how plants, fungi and bacteria perceive and respond to UV with focus on plants and plant-microbe interactions. An overview of their response mechanisms is presented, and the consequences for their growth and survival are discussed and summarized in **Table 1**. While we do contemplate on the potential of the application of UV in plant protection, we primarily provide a broad overview on the effects and possibilities of UV radiation. Despite the increasing evidence for the occurrence and potential role of Cyanobacteria in the phyllosphere (Rigonato et al., 2012; Singh et al., 2019), they will be kept out of consideration in this manuscript. This review provides a global overview and is a basis to guide scientists and growers to make educated decisions for UV treatments in various applications.

TABLE 1 | UV perception and responses across organisms.

	Plants	Fungi	Bacteria
Photoreceptors			
UV-A	CRYs, LOV	CRYs, LOV, BLUF	CRYs, LOV-HK, BLUF
UV-B	UVR8, LOV	Yes, unknown	No
UV-C	PHOT1, (UVR8?)	?	?
Responses	DNA repair↑ Secondary metabolites↑ Defense responses↑ Growth↓ Phototropism	DNA repair↑ Pigments↑ light-dependent development↑ circadian clock Cercosporin production↑ (a) sexual reproduction↑ or ↓ Phototropism Germination↓ Conidiation↑ or ↓	DNA repair↑ Secondary metabolites↑
DNA repair	CPD Photolyase 6-4 Photolyase	CRY1 BcRadI Bcin01g08960	CPD uvrA Rul AB plasmid
Specialized metabolites	Flavones, flavonols, isoflavonoids, anthocyanins, carotenoids, pinene, artemisinin, alkaloids glucosinolates	DHN melanin, DOPA-melanin, carotenoids	Pyocyanin, siderophores, carotenoids
Defense hormones	Jasmonate Salicylic acid	N.A.	N.A.

Plants, fungi, and bacteria have similar and distinct UV responses, potentially influencing their internal relations. N.A., not applicable; ?, not reported. ↑: increases; ↓: decreases.

Detection of Ultraviolet Radiation

Living organisms developed photoreceptors in order to respond to light and optimize growth. Photoreceptors absorb specific wavelengths of radiation, triggering a cascade of events, leading to biological responses. Here we illustrate how plants and microorganisms perceive UV and summarize subsequent downstream responses. Plants have a wide set of photoreceptors, each of which has a specific absorption spectrum. Some of the known photoreceptors absorb in the ultraviolet region. UV responses are ascribed to the sensing by cryptochromes (CRYs) (Ahmad et al., 2002), phototropins (PHOTs) (Christie and Briggs, 2001; Vandenbussche et al., 2014), phytochrome A (PHYA) (Shinomura et al., 1996) and UVB-RESISTANCE 8 (UVR8) as a UV-B specific sensor (Heijde and Ulm, 2012). To date, no reports on a UV-C specific photoreceptor exist. Nevertheless, it is tempting to speculate that some of the known photoreceptors such as UVR8 and CRYs can be triggered by UV-C given their absorbance in that part of the spectrum (**Figure 1**), thus possibly playing a role in plant responses to UV-C (**Table 1**). The absorption spectrum due to chromophores in a protein context and the action spectrum of photoreceptors are very often correlated. Therefore, one can assume that photoreceptors will be triggered at any wavelength within the absorption range of the chromophore. Indeed, while phototropins are mostly regarded as blue light photoreceptors, they do display activity at wavelengths lower than 350 nm (Vandenbussche et al., 2014). Furthermore, homology of CRYs which function in the UV-A region with photolyases, is indicative for CRY activity in the UV region. It is however, noteworthy that the absorption and action spectrum for some photoreceptors are not documented below

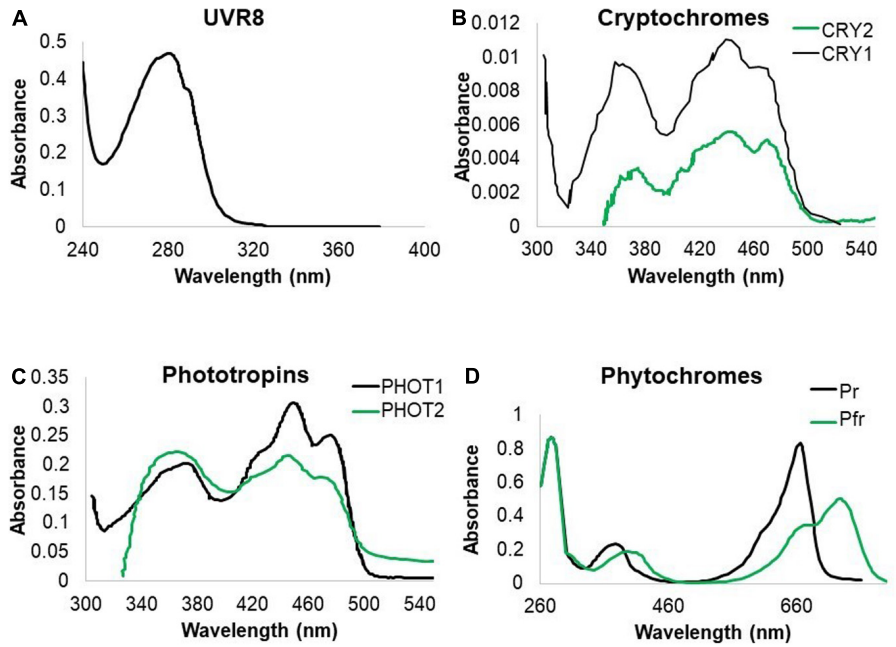

FIGURE 1 | Absorption spectra of UV-B absorbing photoreceptors in *Arabidopsis*. **(A)** UVR8 absorption is recorded in the UV-C and UV-B region of the spectrum. **(B)** CRY1 and CRY2 absorb both strongly in blue and UV-A radiation with indication that CRY1 strongly absorbs in the UV-B band. **(C)** PHOT1 and PHOT2 both absorb mainly in the blue and UV-A wavelengths of the spectrum with indications that PHOT1 also absorbs UV-B. **(D)** PHY proteins have an absorption peak in red and far red wavelengths but also absorb UV-A and UV-B (Ahmad et al., 2002; Kasahara et al., 2002; Sang et al., 2005; Christie et al., 2012).

320 nm (**Figure 1**) and therefore effects in the lower wavelengths, mediated by these photoreceptors cannot be excluded.

Comparable to plants, many fungi are exposed to natural radiation during their life cycle. Despite not being photoautotrophs, they have developed mechanisms to perceive and respond to radiation from the UV to the far-red part of the spectrum. Historically, *Phycomyces* photobiology has received a lot of attention, including its responses in the UV-range. While positive phototropism is reported for UV-A, *Phycomyces* bends away from UV-B and UV-C. These opposite responses are genetically independent (Martin-Rojas et al., 1995). Importantly, each type of UV can have major differences in responses given that UV-A activates vegetative spores of *Phycomyces* while they are killed by UV-C (Campuzano et al., 1996). Many studies on the effect of UV radiation on fungi reported direct killing of conidia. UV-A, on the other hand, promotes conidiation while sublethal doses of UV-A and UV-B reduce conidial germination (Braga et al., 2015). Additionally, UV radiation can affect hyphal growth and toxin production (Thind and Schilder, 2018).

Also bacterial survival and growth can be heavily affected by UV radiation but negative impacts rely on the diverse protection strategies bacteria developed to cope with UV-stress. UV sensitivity of bacteria is often linked with the habitat they are living in. Especially, the effect of UV radiation and UV tolerance mechanisms have been well studied in Cyanobacteria since these photosynthetic organisms cannot avoid solar energy (Rastogi et al., 2014). Finally, UV-C radiation, primarily at 245 nm, is well-known for its killing activity on microorganisms and is therefore often used for disinfection purposes (Urban et al., 2016).

UVR8 Serves as a UV-B Photoreceptor in Plants Under Natural Irradiation

Plant UVR8, with tryptophans acting as chromophores, absorbs in both the UV-B and UV-C part of the spectrum (**Figure 1A**; Christie et al., 2012). In recent years, the UVR8 pathway was well documented for the UV-B response and an array of physiological effects were ascribed to UVR8. Examples are: inhibition of hypocotyl elongation, induction of photoprotective pigment biosynthesis, increase of UV-B tolerance and augmented survival, strengthening of defense responses (Jenkins, 2017; Tossi et al., 2019), and a role in phototropism in hypocotyls and inflorescence stems (Vandenbussche et al., 2014; Vanhaelewyn et al., 2019). Upon UV-B exposure, inactive UVR8 dimers monomerize in the cytoplasm and accumulate in the nucleus where downstream signaling is induced (Kaiserli and Jenkins, 2007; Yin et al., 2016). Key components in this pathway include elongated hypocotyl 5 (HY5), HY5 homolog (HYH) and constitutively photomorphogenic 1 (COP1) (Ulm et al., 2004; Brown et al., 2005; Oravecz et al., 2006; Favory et al., 2009; Binkert et al., 2014; Yin et al., 2016). The current literature stipulates that UVR8 monomers avert the breakdown of HY5 by preventing the interaction between COP1 and HY5, leading to HY5 accumulation and signaling, accompanied with phytochrome interacting factor 5 (PIF5) and PIF4 destabilization and thus growth inhibition (Jenkins, 2017; Sharma et al., 2019; Tavridou et al., 2020). Moreover, this effect is enhanced by UVR8 binding to WRKY DNA-binding protein 36 (WRKY36), which usually acts as a HY5 transcriptional inhibitor (Liang et al., 2018). Importantly, HY5 induces flavonoid biosynthesis through

upregulation of genes such as *chalcone synthase* (*CHS*) and *flavonol synthase* (*FLS1*) and *chalcone flavanone isomerase* (*CHI*). The UVR8 dependent upregulation of flavonoid biosynthesis, mainly serves to create a sunscreen and thus contributes to the protection of macromolecules against UV-B (Jenkins et al., 2001; Hollosy, 2002; Stracke et al., 2010a; Feher et al., 2011; Binkert et al., 2014). To date, despite the homology with the guanine nucleotide exchange factors regulator of chromatin condensation (RCC), no true UVR8 is reported in fungi and bacteria, while being conserved from green algae to higher plants in the plant kingdom (Binkert et al., 2016). Besides UVR8 mediated signaling, low fluence rate UV-B, as little as 0.1 μmol $m^{-2}s^{-1}$, can activate UVR8 independent gene expression of the transcription factor *Arabidopsis* NAC domain containing protein 13 (*ANAC13*), supporting the existence of a UVR8-independent pathway in UV-B signaling. Furthermore, this regulation is also independent of PHOT, CRY, phytochromes A, B, D, COP1, and HY5/HYH (O'Hara et al., 2019).

CRYs Act as Universal Blue and UV Photoreceptors With Similar Functions

Cryptochromes are pterin and flavin based blue light photoreceptors, well-documented in animals, plants, fungi and bacteria. Interestingly, in plants CRY1 and CRY2 both absorb in the UV-A range with CRY1 even absorbing UV-B wavelengths (**Figure 1B**). Therefore, it is generally accepted that cryptochromes mediate both blue and UV responses alike. Upon activation, CRY proteins are phosphorylated, form homodimers and undergo a conformational change, exposing the C-terminus, allowing physical interactions with signaling factors such as COP1 (Yang et al., 2000, 2001; Wang et al., 2001; Sang et al., 2005) and the COP1/SPA complex (Holtkotte et al., 2017). CRYs share sequence similarity with photolyases (see further), but are – with the exception of CRY-DASH (CRY3) – missing photolyase activity necessary to repair UV-induced DNA damage (Sancar and Sancar, 1987; Ahmad and Cashmore, 1993; Selby and Sancar, 2006). Similar to PHOTs and ZEITLUPE, a circadian photoreceptor (Kim et al., 2007), CRYs have a flavin chromophore. CRYs play an important role in photomorphogenic growth responses, regulating hypocotyl and cotyledon growth, and controlling specialized metabolite production such as anthocyanins (Liu et al., 2018). CRY1 was shown to be important for defense, stress and detoxification responses. For example, in *Arabidopsis*, CRY1 promotes R protein-mediated plant resistance to *Pseudomonas syringae* (Wu and Yang, 2010).

Cryptochromes appear universal photoreceptors, present in most, if not all cellular organisms and in fungi they constitute a large class with combined or unique signaling and photolyase function [Reviewed in Cohrs and Schumacher (2017)]. In some fungi light also regulates pigment accumulation, as reported in the phytopathogenic *Botrytis cinerea* and in *Fusarium fujikuroi* pigment accumulation is known to be CRY dependent (Veluchamy and Rollins, 2008; Castrillo et al., 2013; Schumacher, 2016). Specific plant-microbe interactions as well as fungal hosts mentioned throughout the review are indicated in **Supplementary Table 1**. CRYs can steer light-dependent development of *Sclerotinia sclerotiorum* (sclerotial and apothecial development) and *F. fujikuroi* (formation of macroconidia). Moreover, CRY-DASH in *Neurospora crassa* influences light-regulated transcription and is necessary for phase entrainment of the circadian clock (Froehlich et al., 2010; Nsa et al., 2015). Some fungal CRYs belonging to the CRY-DASH family, using 5,10-methenyltetrahydrofolate (MTHF) and flavin adenine dinucleotide (FAD) as chromophores, have DNA repair activity as a photolyase (Tagua et al., 2015). In addition, the pyrimidine (6-4) pyrimidone dimers (6-4PPs) photolyase of *Cercospora zeae-maydis* is a regulator of cercosporin biosynthesis and represses the asexual reproduction by spore formation (Bluhm and Dunkle, 2008) while *Aspergillus nidulans* cyclobutane pyrimidine dimers (CPD) photolyase represses sexual development (Bayram et al., 2008). The CRY-DASH of *Trichoderma atroviride* has no clear regulatory function (Garcia-Esquivel et al., 2016) but its CPD photolyase negatively regulates its own photoinduction (Berrocal et al., 2008). Besides the cry-mediated DNA repair activity, some fungi contain true photolyases, while harboring DNA binding CRYs which are incapable of repairing damage (Froehlich et al., 2010). Thus, in fungi, CRYs and photolyases (including both CPD and 6-4 photoadduct photolyases) are not necessarily functionally separated, and one enzyme sometimes accounts for both photoreactivation and photomorphogenic functions. In *Botrytis cinerea,* blue light represses conidiation while near UV (300–400 nm) induces conidiation. However, the mechanism behind this induction remains elusive and seems to be independent from *B. cinerea* CRY receptors. In contrast, BcCRY2 even acts as a repressor of conidiation (Cohrs and Schumacher, 2017). Therefore, it has been hypothesized that *B. cinerea* contains a yet unknown photoreceptor that perceives UV-light (Cohrs and Schumacher, 2017).

Bacteria also hold several flavin based photoreceptors. To date, such proteins have been mainly classified as blue light receptors, even though their absorption spectra often show peaks into shorter wavelengths, indicating possible activation by UV-A. Some bacteria have CRY-DASH proteins, which have MTHF as antenna pigment for UV, transferring energy to FAD (Saxena et al., 2005; Moon et al., 2012). CRY activation in bacteria can affect motility and attachment, while blue light sensing using FAD (BLUF) proteins were found to control motility, adhesion, and production of exopolysaccharides and biosurfactants (Kraiselburd et al., 2017).

Light-, Oxygen, or Voltage Domains (LOV Domains) Are Universal UV-A and UV-B Photoreceptors

Phototropins were extensively investigated in relation with blue light phototropic responses but also absorb in the UV-A and UV-B region (Okajima et al., 2011; **Figure 1C**) consistent with the action spectra (Ahmad et al., 2002; Kasahara et al., 2002; Vandenbussche et al., 2014). Moreover, PHOT1 function was shown to be responsible for rapid decrease in seedling growth rate under UV-C conditions (Mageroy et al., 2010). PHOTs are membrane-associated photoreceptors which trigger a downstream signal transduction cascade (Hohm et al., 2013). *Arabidopsis* has two PHOTs, namely PHOT1 and PHOT2. These two PHOTs are very similar in structure, amino acid sequence

and domain organization (Briggs et al., 2001; Sakai et al., 2001). PHOTs consist of an N-terminal photosensory domain and a C-terminal Ser/Thr protein kinase domain for signal output. The photosensory domain consists of two LOV domains, namely LOV1 and LOV2, together referred to as LOV. Both LOV1 and LOV2 comprise 110 amino acids (Christie et al., 1998). Yet, their functions are different, LOV1 regulates receptor di/multimerization (Salomon et al., 2004) while LOV2 regulates the C-terminal Ser/Thr kinase domain (Christie et al., 2002). PHOTs have a flavin mononucleotide (FMN) chromophore which in this case binds both LOV1 and LOV2 (Christie et al., 1999). FMN is non-covalently associated with LOV in darkness, while in light conditions, FMN gets activated and binds LOV covalently through a conserved cysteine residue (Christie et al., 1999; Christie, 2007). Under the condition of moderate or high light, PHOT1 and PHOT2 conjoin to spark downstream signaling, whereas under low light conditions, PHOT1 acts as the plant's exclusive directional blue light and UV-A photoreceptor (Sakai et al., 2001). Recent work indicates that UV-B can activate PHOTs in a similar way as described under blue light (Vanhaelewyn et al., 2016b). The strength of the responses correlate with light intensity, as demonstrated for stomatal opening, leaf blade expansion and positioning of the chloroplasts (Sakai et al., 2001; Han et al., 2013).

Also in fungi, blue/UV-A photoreceptors that contain a LOV domain have been characterized. Most prominent is the White Collar Complex (WCC), a complex formed by WC1 and WC2 and named after the original mutation found in *N. crassa* with white mycelium and pigmented conidia. In *N. crassa*, the LOV domain of WC-1 binds FAD, allowing photoperception (Froehlich et al., 2002; He et al., 2002). As this protein contains a Zn finger DNA binding domain, extensive signaling routes appear unnecessary. Nevertheless, WC-1 interacts with WC-2, a non-chromophore containing Zn finger protein, to form WCC that binds promoters of light-inducible genes (He and Liu, 2005). WC-like proteins are described for multiple fungi (Lu et al., 2005; Terashima et al., 2005; Idnurm et al., 2006; Silva et al., 2006), indicating a light perception mechanism that may be conserved in a wide variety of fungi. In *Phycomyces*, the WC-1 homolog MADA (Max Delbrück A) is responsible for positive phototropism in blue light and UV-A (Campuzano et al., 1994). Mechanistically, MADA interacts with the WC-2 homolog MADB to promote the direction of growth of sporangiophores but also to regulate gene transcription in mycelia (Sanz et al., 2009). Additionally, other MAD type proteins can participate in the WCC. In *T. atroviride,* blue light receptors (BLRs), homologs of WC1 and WC2, are required for photoinduction of conidiation and gene expression regulated by blue light (Schmoll et al., 2010). Apart from WC proteins, other small LOV domain proteins in fungi include VIVID (VVD) and its homolog ENVOY1 (ENV1), regulators of WCC (Fuller et al., 2015).

In general, many plant-associated bacteria have blue light receptors. Plant pathogenic *Ralstonia*, *Pseudomonas* and *Xanthomonas* have LOV and/or BLUF proteins (Mandalari et al., 2013; Ricci et al., 2015; Kraiselburd et al., 2017). Although the effects of these proteins have been mainly studied in blue light, because of their absorbance properties (Cao et al., 2008), it is likely that UV-A has a similar mode of action. In *Xanthomonas citri*, the role of LOV proteins is related to colonizing the host plant, including exopolysaccharides, adhesin and flagellum synthesis and consequent motility, adhesion, biofilm formation and oxidative stress resistance (Kraiselburd et al., 2017). In *Pseudomonas syringae*, the role of LOV proteins appears diverse. In *P. syringae* pathovar tomato, LOV domain proteins regulate the switch to a non-motile lifestyle and growth inhibition, while in *P. syringae* pv *syringae* they are supposed to promote swarming motility (Wu et al., 2013; Kraiselburd et al., 2017).

Phytochromes Potentially Act as Minor UV Photoreceptors

Phytochromes sense red light with a bilin chromophore (Sharrock, 2008). The chromophore occurs in two interchangeable conformations, namely Pr and Pfr which have different spectral properties with major differences in the red region of the spectrum (**Figure 1D**). Pr absorbs red, and changes conformation, thereby shifting its absorption maximum into the far-red, leading to the Pfr form. This process is reversible upon absorbing far-red light. Besides red light detection, phytochromes also absorb in the UV-A and UV-B regions (**Figure 1D**) but there is limited evidence on UV induced phenotypes. Examples are UV-A-dependent chloroplast gene transcription in green leaves (Chun et al., 2001) and a role of phytochromes in UV-A induced anthocyanin biosynthesis (Oelmuller and Mohr, 1985). There are, however, no reports on PHY dependent antimicrobial responses which are provoked by UV radiation but it is tempting to speculate for a role for phytochromes in plant-microbe interactions, given that HY5 is somehow PHY regulated (van Gelderen et al., 2018), but given the lack of evidence, phytochromes will not be further elaborated here.

Also, for microorganisms, phytochromes do not seem to play an important role in UV detection and responses. Fungal phytochromes were initially discovered in the two model fungi *N. crassa* and *A. nidulans* with biliverdin as most likely natural chromophore and are now considered present throughout the Fungi kingdom (Blumenstein et al., 2005; Brandt et al., 2008). In bacteria, phytochromes are referred to as bacteriophytochromes. However, no clear UV responses are reported for these photoreceptors.

DNA DAMAGE

The exposure or application of organisms to UV light comes with risks. Besides active sensing and signal induction to UV radiation by photoreceptors, some UV induced morphological responses can be ascribed to the interaction of the high energetic UV radiation with molecules. In the UV spectrum, UV-A irradiation of plant tissues has been shown to have little DNA damaging effects because UV-A is not absorbed by DNA (**Supplementary Figure 1a**). However, DNA damage can still be indirectly caused by ROS generation issuing from photosensitizing reactions, especially by highly reactive singlet oxygen ($^1O_2$) (Alscher et al., 1997). On the other hand, higher energy UV irradiation

such as UV-B and UV-C are strongly absorbed by nuclear, mitochondrial and chloroplast DNA (**Supplementary Figure 1a**), causing similar mutations.

UV Induces Several Types of DNA Damage

Ultraviolet-B is very potent to cause chemical modifications and DNA damage in natural conditions (Sinha and Hader, 2002; Douki et al., 2003; Rastogi et al., 2010). UV-B radiation generates several distinct alterations in DNA, named photoproducts. The most likely photoproducts inducing mutations are two different lesions that unite adjacent pyrimidine residues in the same strand. The major lesions are CPDs, accounting for about 75% of UV-B mediated DNA damage (Takahashi et al., 2011), and 6-4PPs. Minor DNA damage include hydrated bases, oxidized bases and single-strand breaks (Ballare et al., 2001; Takahashi et al., 2011). Interestingly, CPDs and especially 6-4PPs cause DNA bending, with unwinding reported for 6-4PPs, causing growth retardation, lethality or mutagenesis (Tuteja et al., 2009). These types of DNA damage are usually not observed under low UV-B rates (<1 μmol $m^{-2}s^{-1}$), which are sufficient to stimulate photomorphogenic and protective responses (Kim et al., 1998; Frohnmeyer et al., 1999). Given the unstable nature of DNA and the high occurrence of CPDs, plants developed sophisticated systems to deal with this type of DNA damage.

Plants Have a Plethora of DNA Repair Possibilities

The major pathway for UV-B induced repair is the photorepair or photoreactivation. By absorbing blue/UV-A radiation, CPD photolyases and 6-4PP photolyases can monomerize the UV-B induced dimers. These photolyases specifically bind to DNA lesions and remove the CPDs and 6-4PPs (Sancar, 2003; Bray and West, 2005). Interestingly, UV-B sensitive rice cultivars were shown less able to repair CPDs as compared to resistant cultivars, while over-expression of CPD photolyase resulted in significantly higher tolerance to UV-B damage (Teranishi et al., 2012). Not surprisingly, the expression of the CPD photolyase gene (*PHR*) is predominantly controlled by UV-B in a UVR8 dependent manner, but also by UV-A and blue light in a CRY-dependent way (Li et al., 2015). In addition to the photoreactivation mechanism, there is a light-independent repair or dark repair mechanism. This mainly includes nucleotide excision repair (NER), mismatch repair (MMR), and base excision repair (BER). NER mainly recognizes conformational changes in DNA, rather than specific types of DNA damage (Boubriak et al., 2008) and is able to repair CPDs and 6-4PPs (Tuteja et al., 2001). Double strand break repair and homologous recombination, extensively reviewed before (Gill et al., 2015), are not often observed after UV damage.

Fungi Have Their Own DNA Repair Mechanisms

Among plant pathogens, the photodamage responses in *B. cinerea* have received quite some attention (**Table 1**). Like other fungi, *B. cinerea* has a functional WCC (Canessa et al., 2013). Furthermore it contains a separate functional photolyase (CRY1) and a CRY-DASH (CRY2) that does not appear to participate in photoreactivation (Cohrs and Schumacher, 2017). Apart from the afore mentioned enzymes, and true photolyases like phr in *N. crassa* (Shimura et al., 1999) and *T. atroviride* (Berrocal-Tito et al., 2007), fungi also contain other DNA repair mechanisms (Goldman et al., 2002; Inoue, 2011). The respective genes are often called MUS, for mutagen sensitive, or UVS, for UV sensitive. *Aspergillus nidulans UvsI* is an ortholog of Rev3 in yeast, a polymerase that duplicates past UV-induced lesions, thus generating mutations (Han et al., 1998). Of particular interest is the DNA repair mechanism in *N. crassa*, wherein two nucleotide excision repair pathways were found (Inoue, 2011). The first is controlled by mus-38 endonuclease (homolog of yeast Rad1 and UVH1 of *Arabidopsis thaliana*), the other by mus-18, a unique endonuclease capable of removing UV generated photoproducts (Yajima et al., 1995). These endonucleases show some functional redundancy (Hatakeyama et al., 1998). Because of the conservation of nucleotide excision repair systems in eukaryotes, it is likely that this is also the case within the fungi. In this respect, *B. cinerea* has a MUS-38 (BcRad1) ortholog, and a MUS-18 ortholog (Bcin01g08960).

Bacteria Can Also Survive UV Radiation

Comparable to plants and fungi, bacteria also possess photoreactivation properties (Kelner, 1949), which rely on rapid and efficient light dependent DNA repair by photolyase activity (Sancar, 1996). These photolyases can also be activated by blue light, as well as UV-A, owing to their pterin and flavin chromophore. Apart from photolyase activity, bacteria, including plant pathogens, have nucleotide excision repair which functions in the absence of light (Kim and Sundin, 2001; Gunasekera and Sundin, 2006; **Table 1**). Not surprisingly, phyllosphere bacteria and especially Cyanobacteria, which are exposed to solar radiation under natural conditions, show a degree of tolerance to UV-B. To this end they produce an array of enzymatic (e.g., catalase, superoxide dismutases, glutathione and ascorbate peroxidases) and non-enzymatic (carotenoids, α-tocopherols, ascorbic acid, and glutathione) antioxidants to counteract the production of ROS, an extracellular polysaccharide layer to avoid UV damage as well as the production UV-B absorbing/screening compounds such as mycosporine-like amino acids (MAAs) and scytonemin (Rastogi et al., 2014). Furthermore, *Pseudomonas* sp. have an additional method for DNA repair called mutagenic DNA repair, which helps in the protection against UV-B (Sundin and Murillo, 1999). The rulAB plasmid operon conferring this characteristic is of importance for UV-tolerance for the maintenance of the bacterial population during infection, and provides epiphytic fitness (Kim and Sundin, 2000; Cazorla et al., 2008). It is not known if DNA repair is under the control of a photosignaling pathway in bacteria.

Not All UV Inflicted Damage Can Be Repaired

Given the strong genotoxic nature of UV-C radiation and its detrimental effects on all types of microorganisms, including fungi, bacteria, and their spores, it is frequently used for its

germicidal potential. In general, the most resistant structures are fungal and bacterial spores, which need large doses of UV-C to be inactivated, while non-sporulating bacteria are more sensitive (Gayan et al., 2013). Indeed, 254 nm radiation effectively and rapidly kills a variety of bacteria (Wright et al., 2000; Ozcelik, 2007; Jones et al., 2014), but also UV-B was shown useful to kill off bacteria (Oppezzo, 2012).

UV REGULATED SPECIALIZED METABOLITES AND HORMONES, LEADING TO AUGMENTED PLANT-MICROBE INTERACTIONS

Specialized metabolites play a major role in plant-environment interactions by acting as antioxidants, signaling molecules, protective compounds against abiotic stress and pathogens, herbivore feeding deterrents and even pollinator attractants. To cope with UV-induced photodamage, organisms developed an arsenal of photoprotective molecules such as melanins (humans and animals), flavonoids (plants), mycosporines (fungi) and mycosporine-like amino acids (MAAs, Cyanobacteria, algae, and animals) (Sinha et al., 2007). The accumulation of specialized metabolites is particularly well studied upon UV-B radiation. Plant specialized metabolites are divided in three chemically distinct groups: phenolics, terpenes and nitrogen-containing compounds. The most relevant specialized metabolites that affect plant-microbe interactions in a UV context are listed below.

Phenolics Are Aromatic Benzene Ring Compounds With One or More Hydroxyl Groups Produced by Plants Mainly for Protection Against Stress

The phenolics group consists of nearly 10,000 individual compounds with a large chemical and biological diversification. Flavonoids are one of the largest classes of plant phenolics. The basic carbon skeleton consists of 15 carbons arranged in two aromatic rings, connected by a three-carbon bridge. Flavonoids are classified in different groups, mainly based on the degree of oxidation of the three-carbon bridge. Here we focus on flavones, flavonols isoflavonoids and anthocyanins. Flavones and flavonols are present in flowers and leaves of all green plants and generally absorb radiation of shorter wavelengths, with peaks in the 240–280 nm and 315–400 nm range (**Supplementary Figure 1b**; Cerovic et al., 2002). Besides a sun-screen, they can also perform antioxidant functions such as ROS scavenging near the site of generation, this is especially true for flavonoids with multiple hydroxyl groups (Gould et al., 2002; Schmitz-Hoerner and Weissenbock, 2003; Kytridis and Manetas, 2006). Upon UV-B exposure, flavonoids accumulate in the epidermal cells, leaf hairs and leaf wax (Harborne and Williams, 2000), filtering harmful UV-B rays while still ensuring passage of photosynthetically active radiation (PAR) light. Quercetin and kaempferol derivates accumulate in *Arabidopsis* seedlings (Stracke et al., 2010b) acting both as UV protectants and free-radical scavengers (Agati and Tattini, 2010). UV-B mediated flavonoid accumulation is UVR8 dependent (Demkura and Ballare, 2012; Morales et al., 2013), leading to an induction of CHS, chalcone flavanone isomerase (CHI), flavanone 3-hydroxylase (F3H) and flavonol synthase (FLS) (Hideg et al., 2013), all of which are HY5 inducible (Shin et al., 2013; Wu et al., 2019), Interestingly dihydroflavonol reductase (DFR) was only shown to be induced in UV-A conditions (Morales et al., 2013). However, the role of UVR8 in the induction of DFR transcript is not COP1 regulated under UV-B conditions (Oravecz et al., 2006) and therefore hints at an interaction between photoreceptors (Morales et al., 2013) below 350 nm (Morales et al., 2013; Rai et al., 2020). Not surprisingly, *Arabidopsis* plants missing CHS due to point mutations are much more sensitive to the effects of UV-B (Li et al., 1993).

Besides the sunscreen and antioxidant function to protect underlying photosynthetic tissues from damage, several types of flavonoids display antifungal, antibacterial and antiviral activities (van der Watt and Pretorius, 2001; Cushnie and Lamb, 2005). Generally, flavonoid accumulation leads to increased resistance against pathogens including, e.g., rust disease in cedar-apple (Lu et al., 2017) and powdery mildew in cucumber (Fofana et al., 2002; McNally et al., 2003). UV-B inducible flavones such as luteolin and apigenin have antimicrobial activity against a wide range of microorganisms and are especially known to inhibit the growth of food-borne pathogens (Cushnie and Lamb, 2005; Clayton et al., 2018). But also flavonols such as rutin are increased by UV-B treatment in *Nicotiana attenuata* and *Nicotiana longiflora* (Izaguirre et al., 2007; López-Gresa et al., 2011). They display antimicrobial activity (Pereira et al., 2007), and are induced upon *P. syringae* infection in tomato plants. Because of this widespread characteristic of flavonoids to inhibit spore germination of plant pathogens, synthetic flavonols, such as a derivative of quercetin have received extensive attention for medicinal fungal treatments (Harborne and Williams, 2000). Also chalcones such as phloretin and naringenin have been reported to display antimicrobial activities (Rauha et al., 2000; Koru et al., 2007; Vargas et al., 2013) with affected mobility of *Pseudomonas syringae pv. tomato* (Vargas et al., 2013). Further down the flavonoid pathway, anthocyanins which are usually associated with intense colors to attract insects, can also display antimicrobial effects, as they can destroy the cell wall of bacteria such as in *Salmonella* and *Escherichia coli* (Ma et al., 2019) and reduce fungal growth of e.g., *Geotrichum candidum* and *Candida albicans* (Wen et al., 2016). Similar observations were reported for leucoanthocyanidins such as leucocyanidin (Cushnie and Lamb, 2005). Furthermore, pro-anthocyanidins such as tannins (oligomeric flavonoids, as in wine) were also shown to display antimicrobial activity (Mayer et al., 2008) and against enterotoxigenic *E. coli* (Tang et al., 2017). Noteworthy, isoflavonoids are known for their phytoalexin function. The latter are antimicrobial compounds synthesized in response to fungal or bacterial infections, as well as upon pest attack. Isoflavonoids are derived from the flavonoid biosynthesis pathway via liquiritigenin or naringenin and consist of a broad structurally similar group of molecules such as isoflavones, isoflavonones, isoflavans. The isoflavonoid maackiain can inhibit the germination of plant pathogen spores

(Harborne and Williams, 2000) and relates to *B. cinerea* resistance (Stevenson and Haware, 1999).

Besides flavonoids, sinapates also accumulate at ecologically meaningful doses of UV-B. Sinapates are building blocks for lignin and can increase resistance of *Arabidopsis* to *B. cinerea* in a UVR8 dependent way (Demkura and Ballare, 2012). Interestingly, biotic stress elicits MAMP triggered immunity (MTI), which in turn inhibits the previously described flavonoid accumulation under UV-B conditions due to a biosynthetic shift of phenylalanine based molecules from flavonoids to lignin and the phytoalexin scopoletin, serving as a physical defense barrier against pathogens (Schenke et al., 2019). The flavonoid downregulation is mainly due to the downregulation of the CHS gene with prevention of histone acetylation (Zhou et al., 2017).

Flavonoid induction by UV-A is likely mainly induced through the CRY1 photoreceptor, providing that functional CRY1 is essential for chalcone synthase (CHS) expression (Fuglevand et al., 1996), with no roles described for PHOTs and UVR8 in this waveband (Verdaguer et al., 2017). Given that the absorption spectrum of UVR8 reaches into the UV-C spectrum and overlaps with the action spectrum for anthocyanin accumulation (Jiang et al., 2012), it is tempting to speculate that UV-C triggers the same pathway as in UV-B conditions (**Figure 2**).

Terpenes Are Very Volatile and Constitute the Largest Class of Specialized Metabolites

Terpenes are generally synthesized from acetyl-CoA. Importantly, some terpenes can be considered as primary metabolites since they have well defined roles in plants, for example gibberellins (diterpenes), brassinosteroids and abscisic acid, some of which are discussed below. Carotenoids are tetraterpenes that function as accessory pigments during photosynthesis and protect against photooxidation. Carotenoids are strongly induced upon UV exposure. Several plant induced carotenoids were ascribed potent anti-*Helicobacter pylori* activity, namely violaxanthin, luteoxanthin, neoxanthin, antheraxanthin, and lutein (Molnar et al., 2010). Some terpenes can act as a repellent for insects and animals (Isman, 2006; Michaelakis et al., 2009; Tholl, 2015). Recently, terpenes are receiving more attention in the Cannabis industry for their "entourage effect" for medical and olfactory properties. Monoterpene synthase (QH6) is induced by HY5 (Gangappa and Botto, 2016), QH6 converts geranyl diphosphate to β-pinene and α-pinene. Pinene is one of the several terpenes which receives major attention for its antimicrobial and antioxidant functions, and which is reported as UV-B inducible (Salehi et al., 2019). Moreover, β-caryophyllene can protect plants against fungal and bacterial pathogens (Sharma et al., 2016; Nuutinen, 2018). Antimicrobial effects of terpenes in essential oils were also reported for camphene, caryophyllene, eucalyptol, humulene, pineneterpinolene *trans*-nerolidol, eugenol, terpineol, carveol, citronellol, and geraniol (Guimaraes et al., 2019). Many of these terpenes absorb in the UV-range and some terpenes are reported as UV-B inducible. One example is the sesquiterpene (E,E)-α-farnesene, which is also increased after jasmonic acid treatment (Liu et al., 2017). Another industrially important compound is artemisinin, a UV-B and UV-C inducible sesquiterpene (Rai et al., 2011), with non-enzymatic conversions in the terpenoid metabolism (Czechowski et al., 2016). Artemisinin is well-characterized for its anti-malarial effects while its derivates are also ascribed antifungal (Galal et al., 2005) and antibacterial functions (Appalasamy et al., 2014).

Associated with their terrestrial life, many fungi have acquired the capability of synthesizing compounds that cause pigmentation. Fungi produce carotenoids and 1,8-DHN-melanin-type or DOPA-melanin (Goncalves et al., 2012). Photo-induced melanization, presumably depending on the WCC complex, has been observed for several fungi (Fuller et al., 2015). Since melanins absorb in a very broad range of wavelengths, including UV, they protect fungi and their spores from UV radiation. A melanin mutant of *Cochliobolus heterostrophus,* a pathogen of maize, was for example unable to survive in the field (Keller, 2019). In plant pathogenic *Colletotrichum* species, *Venturia inaequalis*, *Magnaporthe grisea*, and *Diplocarpon rosae,* melanin type pigments are required for efficient host invasion. Their appressoria need melanin to sustain turgor pressure in order to effectively penetrate the host leaves (Kubo and Furusawa, 1991; Steiner and Oerke, 2007; Gachomo et al., 2010). Interestingly, fungi also accumulate carotenoids for UV protection. Carotenoid accumulation in *Neurospora* strains is related to latitude and UV radiation, with higher levels at higher latitudes, correlated with increased UV. Moreover in this organism, carotenoid accumulation is associated with UV-resistance (Luque et al., 2012). For several fungi it has been reported that production of carotenoids is induced in a WC-1 dependent manner (Fuller et al., 2015).

Many plant phyllosphere bacteria, e.g., *Clavibacter michiganensis*, *Curtobacteria,* and *Methylobacteria*, are known to be chromogenic and UV tolerant (Sundin and Jacobs, 1999; Yoshida et al., 2017). In *Methylobacteria*, the UV-absorbing molecule is similar to avobenzone, a compound used in commercial sun-blockers (Yoshida et al., 2017). Although no photoprotecting UV-absorbing pigment has been described for *P. syringae*, a member of the same genus, *Pseudomonas aeruginosa* can accumulate pyocyanin, which has strong absorption in short wave UV-B and UV-C. Furthermore, many *P. syringae* strains fluoresce green and yellow under UV radiation, due to accumulation of siderophores that usually absorb in the UV-B and UV-A range (Cody and Gross, 1987; Hirano and Upper, 2000; Bultreys et al., 2001; Rombouts et al., 2016). On well-watered tea plants, *Xanthomonas* sp. are affected by UV-B, while this was not the case for *Corynebacterium aquaticum* (Gunasekera and Paul, 2007). As the presence of UV screening compounds and UV-tolerance is species specific, it is no surprise that UV can affect the bacterial diversity in the phyllosphere (Kadivar and Stapleton, 2003). Some bacteria, including Flavobacterium and many Mycobacteria and Myxococci, are capable of accumulating photoprotective pigments, including carotenoids such as phytoene and phytofluene, which absorb in blue, UV-A and

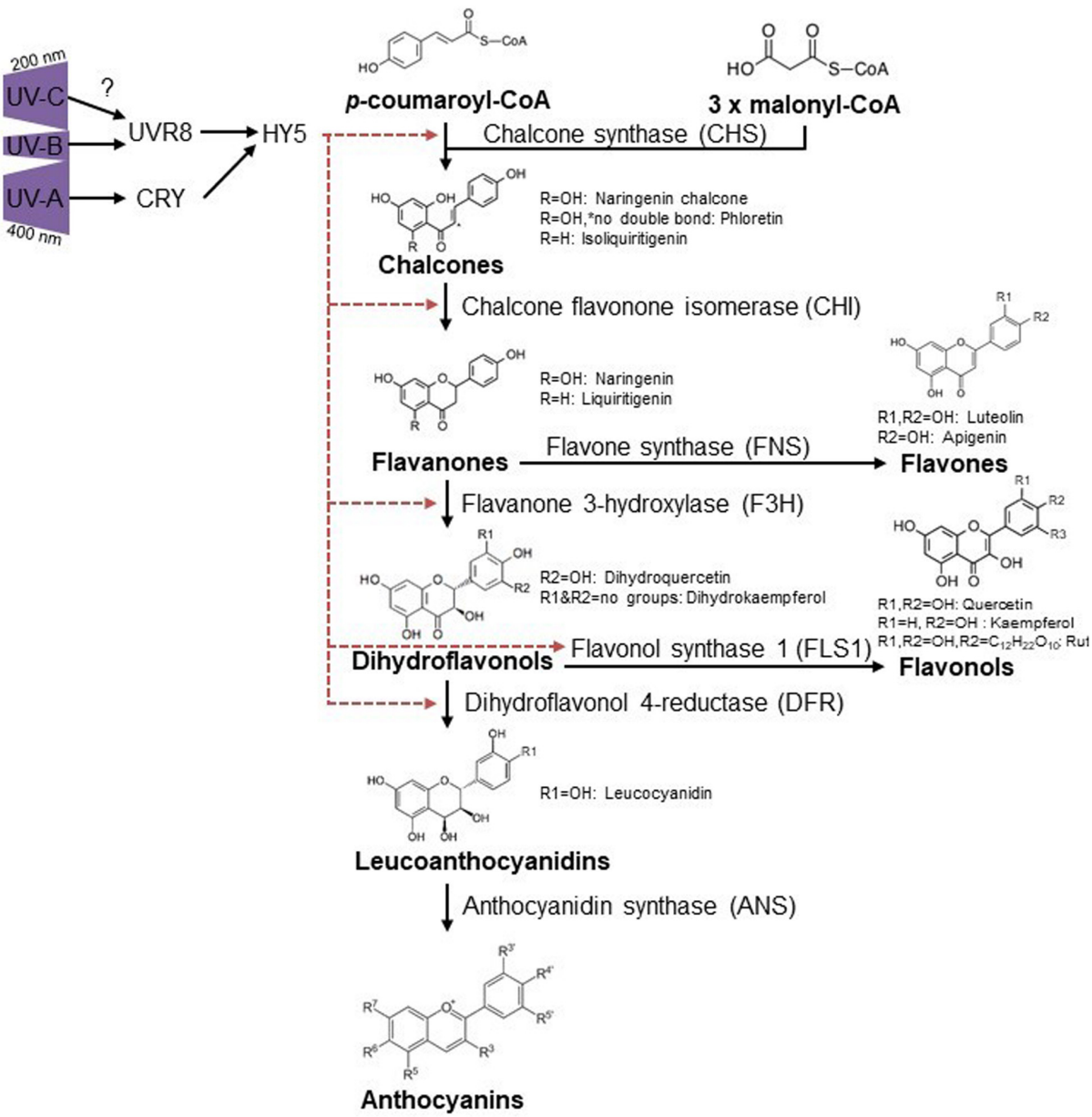

FIGURE 2 | Ultraviolet induced flavonoid accumulation is UVR8 and CRY dependent. UV-B activates UVR8 (Kaiserli and Jenkins, 2007; Yin et al., 2016) which leads to HY5 accumulation and thus diverse flavonoid biosynthesis via CHS, CHI, FH3, and FLS1 (Hideg et al., 2013). CRYs are activated via UV-A and regulate HY5, causing flavonoid accumulation in a similar way as described for UVR8 but also DFR regulation was reported for UV-A conditions (Morales et al., 2013). R-groups are indicated for substances mentioned throughout the text. Red dashed arrows indicate induction of specific enzymes by HY5.

UV-B (Batra et al., 1971). While a pterin like molecule was suggested in the activation of carotenoid biosynthesis in UV-A in Myxococcus, the action spectra for the induction of carotenoids very often points to flavin dependence, with high responses in the UV-A and blue, but also in the UV-B range (Batra et al., 1971). Common to various families of non-phototrophic bacteria, carotenoid biosynthesis is under the control of a light-releasable repressor complex, LitR-AdoB12, based on a MerR (Mercury Resistance) transcriptional regulator and adenosyl B_{12}, yet a photoperception pathway to activation of carotenoid biosynthesis has not been documented (Takano, 2016).

Nitrogen-Containing Compounds Such as Alkaloids and Glucosinolates Are Well-Known Antiherbivore Defense Metabolites

Alkaloids and glucosinolates can be toxic to humans while others are shown valuable as medicine. Most of these metabolites

are synthesized from common amino acids. The primary plant benefit of UV-B dependent upregulation of alkaloids may be related to their ability to quench singlet oxygen and thus confer protection against this toxic photosynthetic by-product (Larson and Marley, 1984). Alkaloids are generally water insoluble organic heterocyclic nitrogen compounds, some of which display antimicrobial functions (Cushnie et al., 2014). Most of the roles attributed to alkaloids are related to self-preservation of the organism and competitor inhibition. In plants, alkaloids can act as phytoanticipins and phytoalexins (plant antibiotics), thus protecting plants against infection (Gonzalez-Lamothe et al., 2009). Besides their natural function, alkaloids have inspired the development of several antibacterial drugs such as quinolones, metronidazole and bedaquiline (Bogatcheva et al., 2011; Hraiech et al., 2012; Parhi et al., 2012; Cushnie et al., 2014). Interestingly, UV-B was shown to induce certain plant alkaloids such as catharanthine (Ramani and Chelliah, 2007), lochnericine, serpentine, and ajmalicine up to 60% (Binder et al., 2009). Everything considered, it is tempting to speculate that UV treatment of plants may affect the plant-microbe interaction by inducing antimicrobial alkaloids.

Glucosinolates (GS) or mustard oil glycosides break down to release defensive substances. GS are generally found in the Brassicaceae and related families. GS are located within the vacuoles and are physically separated from β-thioglucosidase enzymes (myrosinases). Upon disruption of the plant tissue, myrosinases and GS get in contact and hydrolysis occurs, generating sulfate, glucose and an aglycone moiety. The aglycone moiety is unstable and is converted in either thiocyanates (TCs), nitriles and isothiocyanates (ITCs) (Delaquis and Mazza, 1995; Mithen, 2001; Vig et al., 2009). GS and their enzymatic hydrolysis products have been ascribed several biological activities including plant defense, especially ITCs are inhibitors of microbial activity, mainly documented in food preservation contexts (Chew, 1988; Gyawali and Ibrahim, 2014). Adverse effects were reported on insects, bacteria and fungi (Mewis et al., 2005, 2006; Halkier and Gershenzon, 2006; Saladino et al., 2016). In broccoli sprouts, UV-B irradiation affects the specialized metabolite profile in a similar way as observed during biotic stress. UV-B specifically induces glucosinolates (GS) such as 4-methoxy-indol-3-ylmethyl GS and 4-methylsulfinylbutyl GS (Mewis et al., 2012). GS hydrolysis products such as ITCs also have antibacterial effects to plant pathogenic bacteria such as *Agrobacterium tumefaciens*, *Pseudomonas tomato*, *Pseudomonas cichorii*, *Erwinia chrysanthemi*, *Xanthomonas juglandis* and *Xanthomonas campestris* (Aires et al., 2009). The modification of GS content is thus an interesting alternative to pesticide usage (Saladino et al., 2016).

In response to UV, fungi and Cyanobacteria produce mycosporine and mycosporine-like amino acids (MAAs), colorless, water-soluble compounds composed of a cycloheximine or cyclohexenone chromophore which is conjugated with a nitrogen or imino alcohol substituent (Sinha et al., 2007). Mycosporines and MAAs are UV-absorbing pigments and have a role as "sunscreen compounds" (Oren and Gunde-Cimerman, 2007) and potentially may serve as antioxidant molecules. Besides protection to UV, there is no information available whether these molecules affect plant-microbe interactions. Also fungal mycotoxins can be affected by UV radiation and have been associated with UV tolerance including, e.g., aflatoxin and citrinin produced by *Aspergillus flavus* and *Penicillium verrucosum,* respectively (Braga et al., 2015).

UV-Augmented Plant Hormones

Finally, besides the defense-related role of some UV induced specialized metabolites, there are numerous reports on the role of plant hormones against biotic stress. UV-B was studied extensively in relation to all plant hormones and was recently reviewed in Vanhaelewyn et al. (2016a). The two main plant hormones for defense responses against microorganisms are SA and JA. SA-signaling is commonly reported as important against biotrophic pathogens and is often associated with the induction of ROS (Herrera-Vasquez et al., 2015). There are numerous reports of SA biosynthesis increase and plant defense under UV-C and/or UV-B stress, in *Arabidopsis* (Yao et al., 2011; Mintoff et al., 2015), pepper (Mahdavian et al., 2008), tobacco (Yalpani et al., 1994; Yao et al., 2011), barley (Bandurska and Cieslak, 2013) and wheat (Kovacs et al., 2014) roots and leaves. In tobacco, SA increase by supplemental UV-B is probably owing to an increase in phenylalanine ammonia lyase with subsequent accumulation of downstream PATHOGENESIS RELATED PROTEINS, e.g., PR-1, PR-3, and PR-5 defense proteins (Fujibe et al., 2000). Moreover in *Arabidopsis*, *Glutaredoxin C-9* and *PR-1* are both genes induced by UV-B and SA (Herrera-Vasquez et al., 2015). This response is most likely conserved in more plant species, for example, transcriptome data of UV-B exposed broccoli sprouts, showed increased expression of *Arabidopsis* homologs of *PR-1, PR-2,* and *PR-4* (Mewis et al., 2012). This strongly suggests that UV-B mediated regulation of SA may be a way to enhance plant defense. Altogether, UV-B supplementation could be very valuable in enhancing the response to biotrophic pathogens, such as powdery mildew, e.g., in cucumber and strawberry or Magnaporthe in rice. Besides SA, the role of JA is well established in the regulation of defense against necrotrophs and herbivores. Upon UV-B exposure, JA production increases in *Arabidopsis* (Mackerness et al., 1999), mung bean cultivar HUM12 (Choudhary and Agrawal, 2014), and *Nicotiana* sp. (Izaguirre et al., 2003; Dinh et al., 2013). Nonetheless, exceptions are reported, as UV-B does not stimulate JA production in tobacco but does enhance JA dependent induction of trypsin protease inhibitors and defense (Demkura et al., 2010), similar induction of trypsin protease inhibitors and defense by UV-B was reported in tomato (Stratmann et al., 2000). The UV-B dependent upregulation of JA derivatives in some species may be more than just a beneficial side effect on plant defense; for example methylJA protects barley seedlings from UV-B stress by increasing anti-oxidant and free radical scavenging capacities, suggesting that the elevation of endogenous JA by UV-B protects plants from high level UV-B stress (Fedina et al., 2009). This may be associated with the role of JA as a trigger for specialized metabolite production (Wasternack and Strnad, 2016). Although most reports focus on UV-B and its role in inducing plant defense responses in the plants, there is increasing

evidence that also UV-C can trigger pre- and postharvest defense responses and that similar hormonal pathways are involved (Urban et al., 2016). Interestingly, very short (1s) repeated UV-C pulses stimulated plant defense responses and reduced symptom development in tomato, lettuce and pepper and grapevine upon inoculation with *B. cinerea*, *Phytophthora capsici* and *Plasmopara viticola,* respectively. Moreover, also systemic leaves showed increased resistance (Aarrouf and Urban, 2020). The effect of UV-A on plant immunity is largely unknown and has been mainly reported to stimulate biomass production and leaf size. UV-A radiation can also change the composition of phenolic compounds but less pronounced than UV-B (Verdaguer et al., 2017).

Perspectives on Practical Use of UV in Plant Protection

Ultraviolet treatment of plants can lead to increased resistance to microorganisms in diverse ways. Besides the direct damaging effects of short-wave UV radiation on organism's biomolecules, the induction of specialized plant metabolites and hormones in response to UV can also affect the plant-microbe interactions.

For direct effects on microorganisms to be effective, the radiation needs to reach the microorganism one wants to eliminate. High turbidity in liquids can render UV-C sterilization less effective (Jones et al., 2014). In contrast to UV-A and UV-B, UV-C is most potent to reduce infection pressure of plant pathogens by a process analogous to surface sterilization. Short treatments with UV-C kills microorganisms, while the plant remains unharmed. Similar to UV-C treatment, some pathogens like Cucumber powdery mildew (*Podosphaera xanthii*) are suppressed by exposing cucumber plants daily for 10 min to UV-B. Interestingly, the observed suppression effect is most significant when only UV-B is used with no background light and when UV-B is combined with red light exposure. The effect was least significant when UV-A or blue light was administered together with UV-B. Given that no additional suppression was observed when treating plants to UV-B, prior to inoculation, the observed effect is mainly directly on the pathogen, rather than induced plant resistance (Suthaparan et al., 2014). From the above we can infer that presence of UV-A prior to or during exposure, in the case of stimulation of photoprotective pigments, or during and after exposure, in the case of photoreactivation, can increase bacterial survival to UV radiation. UV-C is thus most effective if no UV-A (or blue) is present in the radiation source of use, and a subsequent red light or dark period is included. Epiphytic bacteria are more likely to be affected by the radiation than endophytic bacteria (e.g., *P. syringae* does both), because of poor penetration of UV-C radiation in plant tissues. The practical implementations in greenhouses and in the field are still under development or refinement [Clean light, Netherlands; UV-robot project PSKW (Zant et al., 2018)]. Also for *in vitro* tissue culture, possibilities exist using UV-C to lower infection pressure in growth rooms. Use for *in vitro* control of microorganisms on the plant by UV will depend on the transparency of the material of the container in which the plants are cultivated (Rao et al., 2011).

Perhaps the most promising for future applications changing plant-microbe interactions is the modulation of UV-B in the spectrum of the plant environment. The control of UVR8 in plants, and the associated specialized metabolism, combined with detrimental effects of UV-B radiation in microorganisms could provide a part of a steering mechanism for optimal plant growth and defense, which would rely on the capability of the plant of adapting much better to UV-B than the microorganisms. With the quickly developing UV-emitting LED light market, it is ever more possible to apply UV treatments to horticultural crops for various reasons. One major advantage of using UV-B supplementation is that the "treatment" can be instantaneously terminated, in contrast to the lasting impact of chemical plant growth regulators once taken up by the plant. However, the positive effects of UV to induce plant resistance should be taken with caution since some of the induced specialized metabolites which ward off microorganisms and insects may also be undesirable for human consumption, e.g., bitter taste.

We can thus conclude that UV-A is mainly neutral or even beneficial for the microorganisms, including the colonization of plants by plant pathogens, for DNA repair and processes associated with efficient infection. By contrast, UV-B and UV-C exposure leads to detrimental effects, often resulting in the death of the microbe and thus interesting for application in horticulture, provided the plant or beneficial organisms are damaged less by UV than its pathogen. Besides these detrimental effects on microorganisms, the upregulation of specialized metabolites in plants and microorganisms can affect the plant-microbe interactions in various ways. The list of advantages versus disadvantages on the use of different UV treatments in horticulture needs to be evaluated depending on a species and purpose-specific basis.

AUTHOR CONTRIBUTIONS

FV and LV conceived the project. All authors wrote the article and contributed to scientific discussion.

FUNDING

This work was supported by the research project G000515N of the Research Foundation – Flanders (FWO) to FV (as of October 2017 administratively transferred to DV) and Ghent University-Special Research Fund (Bijzonder Onderzoeksfonds) to DV. LV is a doctoral fellow of the FWO.

ACKNOWLEDGMENTS

We thank Prisca Meyer for critically reading the manuscript.

SUPPLEMENTARY MATERIAL

The Supplementary Material for this article can be found online at: https://www.frontiersin.org/articles/10.3389/fpls.2020.597642/full#supplementary-material

REFERENCES

Aarrouf, J., and Urban, L. (2020). Flashes of UV-C light: an innovative method for stimulating plant defences. *PLoS One* 15:e0235918. doi: 10.1371/journal.pone.0235918

Agati, G., and Tattini, M. (2010). Multiple functional roles of flavonoids in photoprotection. *New Phytol.* 186, 786–793. doi: 10.1111/j.1469-8137.2010.03269.x

Ahmad, M., and Cashmore, A. R. (1993). HY4 gene of *A. thaliana* encodes a protein with characteristics of a blue-light photoreceptor. *Nature* 366, 162–166. doi: 10.1038/366162a0

Ahmad, M., Grancher, N., Heil, M., Black, R. C., Giovani, B., Galland, P., et al. (2002). Action spectrum for cryptochrome-dependent hypocotyl growth inhibition in *Arabidopsis*. *Plant Physiol.* 129, 774–785. doi: 10.1104/pp.010969

Aires, A., Mota, V. R., Saavedra, M. J., Monteiro, A. A., Simoes, M., Rosa, E. A. S., et al. (2009). Initial in vitro evaluations of the antibacterial activities of glucosinolate enzymatic hydrolysis products against plant pathogenic bacteria. *J. Appl. Microbiol.* 106, 2096–2105. doi: 10.1111/j.1365-2672.2009.04181.x

Alscher, R. G., Donahue, J. L., and Cramer, C. L. (1997). Reactive oxygen species and antioxidants: relationships in green cells. *Physiol. Plant.* 100, 224–233. doi: 10.1034/j.1399-3054.1997.1000203.x

Appalasamy, S., Lo, K. Y., Ch'ng, S. J., Nornadia, K., Othman, A. S., and Chan, L. K. (2014). Antimicrobial activity of artemisinin and precursor derived from in vitro plantlets of *Artemisia annua* L. *Biomed. Res. Intern.* 2014:215872.

Ballare, C. L., Rousseau, M. C., Searles, P. S., Zaller, J. G., Giordano, C. V., Robson, T. M., et al. (2001). Impacts of solar ultraviolet-B radiation on terrestrial ecosystems of Tierra del Fuego (southern Argentina). an overview of recent progress. *J. Photochem. Photobiol. B Biol.* 62, 67–77. doi: 10.1016/s1011-1344(01)00152-x

Bandurska, H., and Cieslak, M. (2013). The interactive effect of water deficit and UV-B radiation on salicylic acid accumulation in barley roots and leaves. *Environ. Exp. Bot.* 94, 9–18. doi: 10.1016/j.envexpbot.2012.03.001

Batra, P. P., Harbin, T. L., Howes, C. D., and Bernstein, S. C. (1971). A study of the relationship of structure and activity of antimycin A in the induction of carotenoid synthesis in *Mycobacterium marinum*. *J. Biol. Chem.* 246, 7125–7130.

Bayram, O., Biesemann, C., Krappmann, S., Galland, P., and Braus, G. H. (2008). More than a repair enzyme: *Aspergillus nidulans* photolyase-like CryA is a regulator of sexual development. *Mol. Biol. Cell* 19, 3254–3262. doi: 10.1091/mbc.e08-01-0061

Berrocal, T., Mesa, J. L., Pizarro, J. L., Bazan, B., Iglesias, M., Aguayo, A. T., et al. (2008). Microporous vanadyl-arsenate with the template incorporated exhibiting sorption and catalytic properties. *Chem. Commun.* 2008, 4738–4740. doi: 10.1039/b807250g

Berrocal-Tito, G. M., Esquivel-Naranjo, E. U., Horwitz, B. A., and Herrera-Estrella, A. (2007). *Trichoderma atroviride* PHR1, a fungal photolyase responsible for DNA repair, autoregulates its own photoinduction. *Eukaryot. Cell* 6, 1682–1692. doi: 10.1128/ec.00208-06

Binder, B. Y., Peebles, C. A., Shanks, J. V., and San, K. Y. (2009). The effects of UV-B stress on the production of terpenoid indole alkaloids in *Catharanthus roseus* hairy roots. *Biotechnol. Prog.* 25, 861–865.

Binkert, M., Crocco, C. D., Ekundayo, B., Lau, K., Raffelberg, S., Tilbrook, K., et al. (2016). Revisiting chromatin binding of the *Arabidopsis* UV-B photoreceptor UVR8. *BMC Plant Biol.* 16:42. doi: 10.1186/s12870-016-0732-5

Binkert, M., Kozma-Bognar, L., Terecskei, K., De Veylder, L., Nagy, F., and Ulm, R. (2014). UV-B-responsive association of the *Arabidopsis* bZIP transcription factor ELONGATED HYPOCOTYL5 with target genes, including its own promoter. *Plant Cell* 26, 4200–4213. doi: 10.1105/tpc.114.130716

Bluhm, B. H., and Dunkle, L. D. (2008). PHL1 of *Cercospora zeae*-maydis encodes a member of the photolyase/cryptochrome family involved in UV protection and fungal development. *Fungal Genet. Biol.* 45, 1364–1372. doi: 10.1016/j.fgb.2008.07.005

Blumenstein, A., Vienken, K., Tasler, R., Purschwitz, J., Veith, D., Frankenberg-Dinkel, N., et al. (2005). The *Aspergillus nidulans* phytochrome FphA represses sexual development in red light. *Curr. Biol.* 15, 1833–1838. doi: 10.1016/j.cub.2005.08.061

Bogatcheva, E., Hanrahan, C., Nikonenko, B., de los Santos, G., Reddy, V., Chen, P., et al. (2011). Identification of SQ609 as a lead compound from a library of dipiperidines. *Bioorg. Med. Chem. Lett.* 21, 5353–5357. doi: 10.1016/j.bmcl.2011.07.015

Boubriak, I. I., Grodzinsky, D. M., Polischuk, V. P., Naumenko, V. D., Gushcha, N. P., Micheev, A. N., et al. (2008). Adaptation and impairment of DNA repair function in pollen of *Betula verrucosa* and seeds of *Oenothera biennis* from differently radionuclide-contaminated sites of Chernobyl. *Ann. Bot.* 101, 267–276. doi: 10.1093/aob/mcm276

Braga, G. U., Rangel, D. E., Fernandes, E. K., Flint, S. D., and Roberts, D. W. (2015). Molecular and physiological effects of environmental UV radiation on fungal conidia. *Curr. Genet.* 61, 405–425. doi: 10.1007/s00294-015-0483-0

Brandt, S., von Stetten, D., Gunther, M., Hildebrandt, P., and Frankenberg-Dinkel, N. (2008). The fungal phytochrome FphA from *Aspergillus nidulans*. *J. Biol. Chem.* 283, 34605–34614. doi: 10.1074/jbc.m805506200

Bray, C. M., and West, C. E. (2005). DNA repair mechanisms in plants: crucial sensors and effectors for the maintenance of genome integrity. *New Phytol.* 168, 511–528. doi: 10.1111/j.1469-8137.2005.01548.x

Briggs, W. R., Beck, C. F., Cashmore, A. R., Christie, J. M., Hughes, J., Jarillo, J. A., et al. (2001). The phototropin family of photoreceptors. *Plant Cell* 13, 993–997. doi: 10.2307/3871358

Brown, B. A., Cloix, C., Jiang, G. H., Kaiserli, E., Herzyk, P., Kliebenstein, D. J., et al. (2005). A UV-B-specific signaling component orchestrates plant UV protection. *Proc. Natl. Acad. Sci. U.S.A.* 102, 18225–18230. doi: 10.1073/pnas.0507187102

Bultreys, A., Gheysen, I., Maraite, H., and de Hoffmann, E. (2001). Characterization of fluorescent and nonfluorescent peptide siderophores produced by *Pseudomonas syringae* strains and their potential use in strain identification. *Appl. Environ. Microbiol.* 67, 1718–1727. doi: 10.1128/aem.67.4.1718-1727.2001

Campuzano, V., Galland, P., Alvarez, M. I., and Eslava, A. P. (1996). Blue-light receptor requirement for gravitropism, autochemotropism and ethylene response in *Phycomyces*. *Photochem. Photobiol.* 63, 686–694. doi: 10.1111/j.1751-1097.1996.tb05674.x

Campuzano, V., Galland, P., Senger, H., Alvarez, M. I., and Eslava, A. P. (1994). Isolation and characterization of phototropism mutants of *Phycomyces* insensitive to ultraviolet light. *Curr. Genet.* 26, 49–53. doi: 10.1007/bf00326304

Canessa, P., Schumacher, J., Hevia, M. A., Tudzynski, P., and Larrondo, L. F. (2013). Assessing the effects of light on differentiation and virulence of the plant pathogen *Botrytis cinerea*: characterization of the white collar complex. *PLoS One* 8:e84223. doi: 10.1371/journal.pone.084223

Cao, Z., Buttani, V., Losi, A., and Gartner, W. (2008). A blue light inducible two-component signal transduction system in the plant pathogen *Pseudomonas syringae* pv. tomato. *Biophys. J.* 94, 897–905. doi: 10.1529/biophysj.107.108977

Carvalho, S. D., and Castillo, J. A. (2018). Influence of light on plant-phyllosphere interaction. *Front. Plant Sci.* 9:1482. doi: 10.3389/fpls.2018.01482

Castrillo, M., Garcia-Martinez, J., and Avalos, J. (2013). Light-dependent functions of the *Fusarium fujikuroi* CryD DASH cryptochrome in development and secondary metabolism. *Appl. Environ. Microbiol.* 79, 2777–2788. doi: 10.1128/aem.03110-12

Cazorla, F. M., Codina, J. C., Abad, C., Arrebola, E., Tores, J. A., Murillo, J., et al. (2008). 62-kb plasmids harboring rulAB homologues confer UV-tolerance and epiphytic fitness to *Pseudomonas syringae* pv. *syringae* mango isolates. *Microb. Ecol.* 56, 283–291. doi: 10.1007/s00248-007-9346-7

Cerovic, Z. G., Ounis, A., Cartelat, A., Latouche, G., Goulas, Y., Meyer, S., et al. (2002). The use of chlorophyll fluorescence excitation spectra for the non-destructive in situ assessment of UV-absorbing compounds in leaves. *Plant Cell Environ.* 25, 1663–1676. doi: 10.1046/j.1365-3040.2002.00942.x

Chew, F. S. (1988). Biological effects of glucosinolates. *ACS Sym. Ser.* 380, 155–181. doi: 10.1021/bk-1988-0380.ch012

Choudhary, K. K., and Agrawal, S. B. (2014). Cultivar specificity of tropical mung bean (*Vigna radiata* L.) to elevated ultraviolet-B: changes in antioxidative defense system, nitrogen metabolism and accumulation of jasmonic and salicylic acids. *Environ. Exp. Bot.* 99, 122–132. doi: 10.1016/j.envexpbot.2013.11.006

Christie, J. M. (2007). Phototropin blue-light receptors. *Annu. Rev. Plant Biol.* 58, 21–45. doi: 10.1146/annurev.arplant.58.032806.103951

Christie, J. M., Arvai, A. S., Baxter, K. J., Heilmann, M., Pratt, A. J., O'Hara, A., et al. (2012). Plant UVR8 photoreceptor senses UV-B by tryptophan-mediated disruption of cross-dimer salt bridges. *Science* 335, 1492–1496. doi: 10.1126/science.1218091

Christie, J. M., and Briggs, W. R. (2001). Blue light sensing in higher plants. *J. Biol. Chem.* 276, 11457–11460. doi: 10.1074/jbc.r100004200

Christie, J. M., Reymond, P., Powell, G. K., Bernasconi, P., Raibekas, A. A., Liscum, E., et al. (1998). *Arabidopsis* NPH1: a flavoprotein with the properties of a photoreceptor for phototropism. *Science* 282, 1698–1701. doi: 10.1126/science.282.5394.1698

Christie, J. M., Salomon, M., Nozue, K., Wada, M., and Briggs, W. R. (1999). LOV (light, oxygen, or voltage) domains of the blue-light photoreceptor phototropin (nph1): binding sites for the chromophore flavin mononucleotide. *Proc. Natl. Acad. Sci. U.S.A.* 96, 8779–8783. doi: 10.1073/pnas.96.15.8779

Christie, J. M., Swartz, T. E., Bogomolni, R. A., and Briggs, W. R. (2002). Phototropin LOV domains exhibit distinct roles in regulating photoreceptor function. *Plant J. Cell Mol. Biol.* 32, 205–219. doi: 10.1046/j.1365-313x.2002.01415.x

Chun, L., Kawakami, A., and Christopher, D. A. (2001). Phytochrome A mediates blue light and UV-A-dependent chloroplast gene transcription in green leaves. *Plant Physiol.* 125, 1957–1966. doi: 10.1104/pp.125.4.1957

Clayton, W. A., Albert, N. W., Thrimawithana, A. H., McGhie, T. K., Deroles, S. C., Schwinn, K. E., et al. (2018). UVR8-mediated induction of flavonoid biosynthesis for UVB tolerance is conserved between the liverwort *Marchantia polymorpha* and flowering plants. *Plant J.* 96, 503–517. doi: 10.1111/tpj.14044

Cody, Y. S., and Gross, D. C. (1987). Characterization of pyoverdin(pss), the fluorescent siderophore produced by *Pseudomonas syringae* pv. *syringae*. *Appl. Environ. Microbiol.* 53, 928–934. doi: 10.1128/aem.53.5.928-934.1987

Cohrs, K. C., and Schumacher, J. (2017). The two cryptochrome/photolyase family proteins fulfill distinct roles in DNA photorepair and regulation of conidiation in the gray mold fungus *Botrytis cinerea*. *Appl. Environ. Microbiol.* 83: e00812-17.

Cushnie, T. P. T., Cushnie, B., and Lamb, A. J. (2014). Alkaloids: an overview of their antibacterial, antibiotic-enhancing and antivirulence activities. *Int. J. Antimicrob. Agents* 44, 377–386. doi: 10.1016/j.ijantimicag.2014.06.001

Cushnie, T. P. T., and Lamb, A. J. (2005). Antimicrobial activity of flavonoids. *Int. J. Antimicrob. Agents* 26, 343–356. doi: 10.1016/j.ijantimicag.2005.09.002

Czechowski, T., Larson, T. R., Catania, T. M., Harvey, D., Brown, G. D., and Graham, I. A. (2016). *Artemisia annua* mutant impaired in artemisinin synthesis demonstrates importance of nonenzymatic conversion in terpenoid metabolism. *Proc. Natl. Acad. Sci. U.S.A.* 113, 15150–15155. doi: 10.1073/pnas.1611567113

Delaquis, P. J., and Mazza, G. (1995). Antimicrobial properties of isothiocyanates in food preservation. *Food Technol. Chicago* 49, 73–84.

Demkura, P. V., Abdala, G., Baldwin, I. T., and Ballare, C. L. (2010). Jasmonate-dependent and -independent pathways mediate specific effects of solar ultraviolet b radiation on leaf phenolics and antiherbivore defense. *Plant Physiol.* 152, 1084–1095. doi: 10.1104/pp.109.148999

Demkura, P. V., and Ballare, C. L. (2012). UVR8 mediates UV-B-induced *Arabidopsis* defense responses against *Botrytis cinerea* by controlling sinapate accumulation. *Mol. Plant* 5, 642–652. doi: 10.1093/mp/sss025

Dinh, S. T., Galis, I., and Baldwin, I. T. (2013). UVB radiation and 17-hydroxygeranyllinalool diterpene glycosides provide durable resistance against mirid (*Tupiocoris notatus*) attack in field-grown *Nicotiana attenuata* plants. *Plant Cell Environ.* 36, 590–606. doi: 10.1111/j.1365-3040.2012.02598.x

Douki, T., Reynaud-Angelin, A., Cadet, J., and Sage, E. (2003). Bipyrimidine photoproducts rather than oxidative lesions are the main type of dna damage involved in the genotoxic effect of solar UVA radiation. *Biochemistry* 42, 9221–9226. doi: 10.1021/bi034593c

Favory, J. J., Stec, A., Gruber, H., Rizzini, L., Oravecz, A., Funk, M., et al. (2009). Interaction of COP1 and UVR8 regulates UV-B-induced photomorphogenesis and stress acclimation in *Arabidopsis*. *EMBO J.* 28, 591–601. doi: 10.1038/emboj.2009.4

Fedina, I., Nedeva, D., Georgieva, K., and Velitchkova, M. (2009). Methyl jasmonate counteract UV-B stress in barley seedlings. *J. Agron. Crop Sci.* 195, 204–212. doi: 10.1111/j.1439-037x.2008.00358.x

Feher, B., Kozma-Bognar, L., Kevei, E., Hajdu, A., Binkert, M., Davis, S. J., et al. (2011). Functional interaction of the circadian clock and UV RESISTANCE LOCUS 8-controlled UV-B signaling pathways in *Arabidopsis thaliana*. *Plant J.* 67, 37–48. doi: 10.1111/j.1365-313x.2011.04573.x

Fofana, B., McNally, D. J., Labbe, C., Boulanger, R., Benhamou, N., Seguin, A., et al. (2002). Milsana-induced resistance in powdery mildew-infected cucumber plants correlates with the induction of chalcone synthase and chalcone isomerase. *Physiol. Mol. Plant* 61, 121–132. doi: 10.1006/pmpp.2002.0420

Froehlich, A. C., Chen, C. H., Belden, W. J., Madeti, C., Roenneberg, T., Merrow, M., et al. (2010). Genetic and molecular characterization of a cryptochrome from the filamentous fungus *Neurospora crassa*. *Eukaryot. Cell* 9, 738–750. doi: 10.1128/ec.00380-09

Froehlich, A. C., Liu, Y., Loros, J. J., and Dunlap, J. C. (2002). White Collar-1, a circadian blue light photoreceptor, binding to the frequency promoter. *Science* 297, 815–819. doi: 10.1126/science.1073681

Frohnmeyer, H., Loyall, L., Blatt, M. R., and Grabov, A. (1999). Millisecond UV-B irradiation evokes prolonged elevation of cytosolic-free Ca2+ and stimulates gene expression in transgenic parsley cell cultures. *Plant J.* 20, 109–117. doi: 10.1046/j.1365-313x.1999.00584.x

Fuglevand, G., Jackson, J. A., and Jenkins, G. I. (1996). UV-B, UV-A, and blue light signal transduction pathways interact synergistically to regulate chalcone synthase gene expression in *Arabidopsis*. *Plant Cell* 8, 2347–2357. doi: 10.2307/3870473

Fujibe, T., Watanabe, K., Nakajima, N., Ohashi, Y., Mitsuhara, I., Yamamoto, K. T., et al. (2000). Accumulation of pathogenesis-related proteins in tobacco leaves irradiated with UV-B. *J. Plant Res.* 113, 387–394. doi: 10.1007/pl00013946

Fuller, K. K., Loros, J. J., and Dunlap, J. C. (2015). Fungal photobiology: visible light as a signal for stress, space and time. *Curr. Genet.* 61, 275–288. doi: 10.1007/s00294-014-0451-0

Gachomo, E. W., Seufferheld, M. J., and Kotchoni, S. O. (2010). Melanization of appressoria is critical for the pathogenicity of *Diplocarpon rosae*. *Mol. Biol. Rep.* 37, 3583–3591. doi: 10.1007/s11033-010-0007-4

Galal, A. M., Ross, S. A., Jacob, M., and ElSohly, M. A. (2005). Antifungal activity of artemisinin derivatives. *J. Nat. Prod.* 68, 1274–1276. doi: 10.1021/np050074u

Gangappa, S. N., and Botto, J. F. (2016). The multifaceted roles of HY5 in plant growth and development. *Mol. Plant* 9, 1353–1365. doi: 10.1016/j.molp.2016.07.002

Garcia-Esquivel, M., Esquivel-Naranjo, E. U., Hernandez-Onate, M. A., Ibarra-Laclette, E., and Herrera-Estrella, A. (2016). The *Trichoderma atroviride* cryptochrome/photolyase genes regulate the expression of blr1-independent genes both in red and blue light. *Fungal Biol.* 120, 500–512. doi: 10.1016/j.funbio.2016.01.007

Gayan, E., Manas, P., Alvarez, I., and Condon, S. (2013). Mechanism of the synergistic inactivation of *Escherichia coli* by UV-C light at mild temperatures. *Appl. Environ. Microbiol.* 79, 4465–4473. doi: 10.1128/aem.00623-13

Gill, S. S., Anjum, N. A., Gill, R., Jha, M., and Tuteja, N. (2015). DNA damage and repair in plants under ultraviolet and ionizing radiations. *Sci. World J.* 2015:250158.

Goldman, G. H., McGuire, S. L., and Harris, S. D. (2002). The DNA damage response in filamentous fungi. *Fungal Genet. Biol.* 35, 183–195. doi: 10.1006/fgbi.2002.1344

Goncalves, R. C., Lisboa, H. C., and Pombeiro-Sponchiado, S. R. (2012). Characterization of melanin pigment produced by *Aspergillus nidulans*. *World J. Microbiol. Biotechnol.* 28, 1467–1474. doi: 10.1007/s11274-011-0948-3

Gonzalez-Lamothe, R., Mitchell, G., Gattuso, M., Diarra, M. S., Malouin, F., and Bouarab, K. (2009). Plant antimicrobial agents and their effects on plant and human pathogens. *Intern. J. Mol. Sci.* 10, 3400–3419. doi: 10.3390/ijms10083400

Gould, K. S., McKelvie, J., and Markham, K. R. (2002). Do anthocyanins function as antioxidants in leaves? Imaging of H_2O_2 in red and green leaves after mechanical injury. *Plant Cell Environ.* 25, 1261–1269. doi: 10.1046/j.1365-3040.2002.00905.x

Guimaraes, A. C., Meireles, L. M., Lemos, M. F., Guimaraes, M. C. C., Endringer, D. C., Fronza, M., et al. (2019). Antibacterial activity of terpenes and terpenoids present in essential oils. *Molecules* 24:2471. doi: 10.3390/molecules24132471

Gunasekera, T. S., and Paul, N. D. (2007). Ecological impact of solar ultraviolet-B (UV-B: 320-290 nm) radiation on *Corynebacterium aquaticum* and *Xanthomonas* sp. colonization on tea phyllosphere in relation to blister blight disease incidence in the field. *Lett. Appl. Microbiol.* 44, 513–519. doi: 10.1111/j.1472-765x.2006.02102.x

Gunasekera, T. S., and Sundin, G. W. (2006). Role of nucleotide excision repair and photoreactivation in the solar UVB radiation survival of *Pseudomonas syringae* pv. *syringae* B728a. *J. Appl. Microbiol.* 100, 1073–1083. doi: 10.1111/j.1365-2672.2006.02841.x

Gyawali, R., and Ibrahim, S. A. (2014). Natural products as antimicrobial agents. *Food Control* 46, 412–429.

Halkier, B. A., and Gershenzon, J. (2006). Biology and biochemistry of glucosinolates. *Annu. Rev. Plant Biol.* 57, 303–333. doi: 10.1146/annurev.arplant.57.032905.105228

Han, I. S., Cho, H. Y., Moni, A., Lee, A. Y., and Briggs, W. R. (2013). Investigations on the photoregulation of chloroplast movement and leaf positioning in *Arabidopsis*. *Plant Cell Physiol.* 54, 48–56. doi: 10.1093/pcp/pcs098

Han, K. Y., Chae, S. K., and Han, D. M. (1998). The uvsI gene of *Aspergillus nidulans* required for UV-mutagenesis encodes a homolog to REV3, a subunit of the DNA polymerase zeta of yeast involved in translesion DNA synthesis. *FEMS Microbiol. Lett.* 164, 13–19. doi: 10.1016/s0378-1097(98)00185-2

Harborne, J. B., and Williams, C. A. (2000). Advances in flavonoid research since 1992. *Phytochemistry* 55, 481–504. doi: 10.1016/s0031-9422(00)00235-1

Hatakeyama, S., Ito, Y., Shimane, A., Ishii, C., and Inoue, H. (1998). Cloning and characterization of the yeast RAD1 homolog gene (mus-38) from *Neurospora crassa*: evidence for involvement in nucleotide excision repair. *Curr. Genet.* 33, 276–283. doi: 10.1007/s002940050337

He, Q., Cheng, P., Yang, Y., Wang, L., Gardner, K. H., and Liu, Y. (2002). White collar-1, a DNA binding transcription factor and a light sensor. *Science* 297, 840–843. doi: 10.1126/science.1072795

He, Q., and Liu, Y. (2005). Molecular mechanism of light responses in *Neurospora*: from light-induced transcription to photoadaptation. *Genes Dev.* 19, 2888–2899. doi: 10.1101/gad.1369605

Heijde, M., and Ulm, R. (2012). UV-B photoreceptor-mediated signalling in plants. *Trends Plant Sci.* 17, 230–237. doi: 10.1016/j.tplants.2012.01.007

Heinze, M., Hanschen, F. S., Wiesner-Reinhold, M., Baldermann, S., Grafe, J., Schreiner, M., et al. (2018). Effects of developmental stages and reduced UVB and Low UV conditions on plant secondary metabolite profiles in Pak Choi (*Brassica rapa* subsp. chinensis). *J. Agric. Food Chem.* 66, 1678–1692. doi: 10.1021/acs.jafc.7b03996

Herrera-Vasquez, A., Carvallo, L., Blanco, F., Tobar, M., Villarroel-Candia, E., Vicente-Carbajosa, J., et al. (2015). Transcriptional control of glutaredoxin GRXC9 expression by a salicylic acid-dependent and NPR1-independent pathway in *Arabidopsis*. *Plant Mol. Biol. Rep.* 33, 624–637. doi: 10.1007/s11105-014-0782-5

Hideg, E., Jansen, M. A., and Strid, A. (2013). UV-B exposure, ROS, and stress: inseparable companions or loosely linked associates? *Trends Plant Sci.* 18, 107–115. doi: 10.1016/j.tplants.2012.09.003

Hirano, S. S., and Upper, C. D. (2000). Bacteria in the leaf ecosystem with emphasis on *Pseudomonas syringae*-a pathogen, ice nucleus, and epiphyte. *Microbiol. Mol. Biol. Rev.* 64, 624–653. doi: 10.1128/mmbr.64.3.624-653.2000

Hohm, T., Preuten, T., and Fankhauser, C. (2013). Phototropism: translating light into directional growth. *Am. J. Bot.* 100, 47–59. doi: 10.3732/ajb.1200299

Hollosy, F. (2002). Effects of ultraviolet radiation on plant cells. *Micron* 33, 179–197. doi: 10.1016/s0968-4328(01)00011-7

Holtkotte, X., Ponnu, J., Ahmad, M., and Hoecker, U. (2017). The blue light-induced interaction of cryptochrome 1 with COP1 requires SPA proteins during *Arabidopsis* light signaling. *PLoS Genet.* 13:e1007044. doi: 10.1371/journal.pone.1007044

Hraiech, S., Bregeon, F., Brunel, J. M., Rolain, J. M., Lepidi, H., Andrieu, V., et al. (2012). Antibacterial efficacy of inhaled squalamine in a rat model of chronic *Pseudomonas aeruginosa* pneumonia. *J. Antimicrob. Chemother.* 67, 2452–2458. doi: 10.1093/jac/dks230

Idnurm, A., Rodriguez-Romero, J., Corrochano, L. M., Sanz, C., Iturriaga, E. A., Eslava, A. P., et al. (2006). The *Phycomyces* madA gene encodes a blue-light photoreceptor for phototropism and other light responses. *Proc. Natl. Acad. Sci. U.S.A.* 103, 4546–4551. doi: 10.1073/pnas.0600633103

Inoue, H. (2011). Exploring the processes of DNA repair and homologous integration in *Neurospora*. *Mutat. Res.* 728, 1–11. doi: 10.1016/j.mrrev.2011.06.003

Isman, M. B. (2006). Botanical insecticides, deterrents, and repellents in modern agriculture and an increasingly regulated world. *Annu. Rev. Entomol.* 51, 45–66. doi: 10.1146/annurev.ento.51.110104.151146

Izaguirre, M. M., Mazza, C. A., Svatos, A., Baldwin, I. T., and Ballare, C. L. (2007). Solar ultraviolet-B radiation and insect herbivory trigger partially overlapping phenolic responses in *Nicotiana attenuata* and *Nicotiana longiflora*. *Ann. Bot.* 99, 103–109. doi: 10.1093/aob/mcl226

Izaguirre, M. M., Scopel, A. L., Baldwin, I. T., and Ballare, C. L. (2003). Convergent responses to stress. Solar ultraviolet-B radiation and *Manduca sexta* herbivory elicit overlapping transcriptional responses in field-grown plants of *Nicotiana longiflora*. *Plant Physiol.* 132, 1755–1767. doi: 10.1104/pp.103.024323

Jenkins, G. I. (2017). Photomorphogenic responses to ultraviolet-B light. *Plant Cell Environ.* 40, 2544–2557. doi: 10.1111/pce.12934

Jenkins, G. I., Long, J. C., Wade, H. K., Shenton, M. R., and Bibikova, T. N. (2001). UV and blue light signalling: pathways regulating chalcone synthase gene expression in *Arabidopsis*. *New Phytol.* 151, 121–131. doi: 10.1046/j.1469-8137.2001.00151.x

Jiang, L., Wang, Y., Olof Bjorn, L., He, J. X., and Li, S. (2012). Sensing of UV-B radiation by plants. *Plant Signal. Behav.* 7, 999–1003.

Jones, L. A., Worobo, R. W., and Smart, C. D. (2014). UV light inactivation of human and plant pathogens in unfiltered surface irrigation water. *Appl. Environ. Microbiol.* 80, 849–854. doi: 10.1128/aem.02964-13

Kadivar, H., and Stapleton, A. E. (2003). Ultraviolet radiation alters maize phyllosphere bacterial diversity. *Microb. Ecol.* 45, 353–361. doi: 10.1007/s00248-002-1065-5

Kaiserli, E., and Jenkins, G. I. (2007). UV-B promotes rapid nuclear translocation of the *Arabidopsis* UV-B specific signaling component UVR8 and activates its function in the nucleus. *Plant Cell* 19, 2662–2673. doi: 10.1105/tpc.107.053330

Kasahara, M., Swartz, T. E., Olney, M. A., Onodera, A., Mochizuki, N., Fukuzawa, H., et al. (2002). Photochemical properties of the flavin mononucleotide-binding domains of the phototropins from *Arabidopsis*, rice, and *Chlamydomonas reinhardtii*. *Plant Physiol.* 129, 762–773. doi: 10.1104/pp.002410

Katerova, Z., Todorova, D., Tasheva, K., and Sergiev, I. (2012). Influence of ultraviolet radiation on plant secondary metabolite production. *Genet. Plant Physiol.* 2, 113–144.

Keller, N. P. (2019). Fungal secondary metabolism: regulation, function and drug discovery. *Nat. Rev. Microbiol.* 17, 167–180. doi: 10.1038/s41579-018-0121-1

Kelner, A. (1949). Photoreactivation of ultraviolet-irradiated *Escherichia Coli*, with special reference to the dose-reduction principle and to ultraviolet-induced mutation. *J. Bacteriol.* 58, 511–522. doi: 10.1128/jb.58.4.511-522.1949

Kim, B. C., Tennessen, D. J., and Last, R. L. (1998). UV-B-induced photomorphogenesis in *Arabidopsis thaliana*. *Plant J.* 15, 667–674. doi: 10.1046/j.1365-313x.1998.00246.x

Kim, J. J., and Sundin, G. W. (2000). Regulation of the rulAB mutagenic DNA repair operon of *Pseudomonas syringae* by UV-B (290 to 320 nanometers) radiation and analysis of rulAB-mediated mutability *in vitro* and in *planta*. *J. Bacteriol.* 182, 6137–6144. doi: 10.1128/jb.182.21.6137-6144.2000

Kim, J. J., and Sundin, G. W. (2001). Construction and analysis of photolyase mutants of *Pseudomonas aeruginosa* and *Pseudomonas syringae*: contribution of photoreactivation, nucleotide excision repair, and mutagenic DNA repair to cell survival and mutability following exposure to UV-B radiation. *Appl. Environ. Microbiol.* 67, 1405–1411. doi: 10.1128/aem.67.4.1405-1411.2001

Kim, W. Y., Fujiwara, S., Suh, S. S., Kim, J., Kim, Y., Han, L., et al. (2007). ZEITLUPE is a circadian photoreceptor stabilized by GIGANTEA in blue light. *Nature* 449, 356–360. doi: 10.1038/nature06132

Koru, O., Toksoy, F., Acikel, C. H., Tunca, Y. M., Baysallar, M., Uskudar Guclu, A., et al. (2007). In vitro antimicrobial activity of propolis samples from different geographical origins against certain oral pathogens. *Anaerobe* 13, 140–145. doi: 10.1016/j.anaerobe.2007.02.001

Kovacs, V., Gondor, O. K., Szalai, G., Majlath, I., Janda, T., and Pal, M. (2014). UV-B radiation modifies the acclimation processes to drought or cadmium in wheat. *Environ. Exp. Bot.* 100, 122–131. doi: 10.1016/j.envexpbot.2013.12.019

Kraiselburd, I., Moyano, L., Carrau, A., Tano, J., and Orellano, E. G. (2017). Bacterial photosensory proteins and their role in plant-pathogen interactions. *Photochem. Photobiol.* 93, 666–674. doi: 10.1111/php.12754

Kubo, Y., and Furusawa, I. (1991). "Melanin biosynthesis," in *The Fungal Spore and Disease Initiation in Plants and Animals*, eds G. T. Cole, and H. C. Hoch (Boston, MA: Springer), 205–218.

Kytridis, V. P., and Manetas, Y. (2006). Mesophyll versus epidermal anthocyanins as potential in vivo antioxidants: evidence linking the putative antioxidant role to the proximity of oxy-radical source. *J. Exp. Bot.* 57, 2203–2210. doi: 10.1093/jxb/erj185

Larson, R. A., and Marley, K. A. (1984). Quenching of singlet oxygen by alkaloids and related nitrogen-heterocycles. *Phytochemistry* 23, 2351–2354. doi: 10.1016/s0031-9422(00)80550-6

Li, J., Ou-Lee, T. M., Raba, R., Amundson, R. G., and Last, R. L. (1993). *Arabidopsis* flavonoid mutants are hypersensitive to UV-B irradiation. *Plant Cell* 5, 171–179. doi: 10.1105/tpc.5.2.171

Li, N., Teranishi, M., Yamaguchi, H., Matsushita, T., Watahiki, M. K., Tsuge, T., et al. (2015). UV-B-induced CPD photolyase gene expression is regulated by UVR8-dependent and -independent pathways in *Arabidopsis*. *Plant Cell Physiol.* 56, 2014–2023. doi: 10.1093/pcp/pcv121

Liang, T., Mei, S., Shi, C., Yang, Y., Peng, Y., Ma, L., et al. (2018). UVR8 interacts with BES1 and BIM1 to regulate transcription and photomorphogenesis in *Arabidopsis*. *Dev. Cell* 44, 512–523.e515.

Liu, C. C., Chi, C., Jin, L. J., Zhu, J., Yu, J. Q., and Zhou, Y. H. (2018). The bZip transcription factor HY5 mediates CRY1a-induced anthocyanin biosynthesis in tomato. *Plant Cell Environ.* 41, 1762–1775. doi: 10.1111/pce.13171

Liu, H., Cao, X., Liu, X., Xin, R., Wang, J., Gao, J., et al. (2017). UV-B irradiation differentially regulates terpene synthases and terpene content of peach. *Plant Cell Environ.* 40, 2261–2275. doi: 10.1111/pce.13029

López-Gresa, M. P., Torres, C., Campos, L., Lisón, P., Rodrigo, I., Bellés, J. M., et al. (2011). Identification of defence metabolites in tomato plants infected by the bacterial pathogen *Pseudomonas syringae*. *Environ. Exp. Bot.* 74, 216–228. doi: 10.1016/j.envexpbot.2011.06.003

Lu, Y., Chen, Q., Bu, Y., Luo, R., Hao, S., Zhang, J., et al. (2017). Flavonoid accumulation plays an important role in the rust resistance of *Malus* plant leaves. *Front. Plant Sci.* 8:1286. doi: 10.3389/fpls.2017.01286

Lu, Y. K., Sun, K. H., and Shen, W. C. (2005). Blue light negatively regulates the sexual filamentation via the Cwc1 and Cwc2 proteins in *Cryptococcus neoformans*. *Mol. Microbiol.* 56, 480–491. doi: 10.1111/j.1365-2958.2005.04549.x

Luque, E. M., Gutierrez, G., Navarro-Sampedro, L., Olmedo, M., Rodriguez-Romero, J., Ruger-Herreros, C., et al. (2012). A relationship between carotenoid accumulation and the distribution of species of the fungus *Neurospora* in spain. *PLoS One* 7:e33658. doi: 10.1371/journal.pone.0033658

Ma, Y., Ding, S., Fei, Y., Liu, G., Jang, H., and Fang, J. (2019). Antimicrobial activity of anthocyanins and catechins against foodborne pathogens *Escherichia coli* and *Salmonella*. *Food Control* 106:106712. doi: 10.1016/j.foodcont.2019.106712

Mackerness, S. A. H., Surplus, S. L., Blake, P., John, C. F., Buchanan-Wollaston, V., Jordan, B. R., et al. (1999). Ultraviolet-B-induced stress and changes in gene expression in *Arabidopsis thaliana*: role of signalling pathways controlled by jasmonic acid, ethylene and reactive oxygen species. *Plant Cell Environ.* 22, 1413–1423. doi: 10.1046/j.1365-3040.1999.00499.x

Mageroy, M. H., Kowalik, E. H., Folta, K. M., and Shinkle, J. (2010). Evidence of physiological phototropin1 (phot1) action in response to UV-C illumination. *Plant Signal. Behav.* 5, 1204–1210. doi: 10.4161/psb.5.10.12413

Mahdavian, K., Ghorbanli, M., and Kalantari, K. M. (2008). Role of salicylic acid in regulating ultraviolet radiation-induced oxidative stress in pepper leaves. *Russ. J. Plant Phys.* 55, 560–563. doi: 10.1134/s1021443708040195

Mandalari, C., Losi, A., and Gartner, W. (2013). Distance-tree analysis, distribution and co-presence of bilin- and flavin-binding prokaryotic photoreceptors for visible light. *Photochem. Photobiol. Sci.* 12, 1144–1157. doi: 10.1039/c3pp25404f

Martin-Rojas, V., Greiner, H., Wagner, T., Fukshansky, L., and Cerda-Olmedo, E. (1995). Specific tropism caused by ultraviolet C radiation in *Phycomyces*. *Planta* 197, 63–68.

Mayer, R., Stecher, G., Wuerzner, R., Silva, R. C., Sultana, T., Trojer, L., et al. (2008). Proanthocyanidins: target compounds as antibacterial agents. *J. Agric. Food Chem.* 56, 6959–6966. doi: 10.1021/jf800832r

McNally, D. J., Wurms, K. V., Labbe, C., and Belanger, R. R. (2003). Synthesis of C-glycosyl flavonoid phytoalexins as a site-specific response to fungal penetration in cucumber. *Physiol. Mol. Plant* 63, 293–303. doi: 10.1016/j.pmpp.2004.03.005

Mewis, I., Appel, H. M., Hom, A., Raina, R., and Schultz, J. C. (2005). Major signaling pathways modulate *Arabidopsis* glucosinolate accumulation and response to both phloem-feeding and chewing insects. *Plant Physiol.* 138, 1149–1162. doi: 10.1104/pp.104.053389

Mewis, I., Schreiner, M., Nguyen, C. N., Krumbein, A., Ulrichs, C., Lohse, M., et al. (2012). UV-B irradiation changes specifically the secondary metabolite profile in *Broccoli sprouts*: induced signaling overlaps with defense response to biotic stressors. *Plant Cell Physiol.* 53, 1546–1560. doi: 10.1093/pcp/pcs096

Mewis, I., Tokuhisa, J. G., Schultz, J. C., Appel, H. M., Ulrichs, C., and Gershenzon, J. (2006). Gene expression and glucosinolate accumulation in *Arabidopsis thaliana* in response to generalist and specialist herbivores of different feeding guilds and the role of defense signaling pathways. *Phytochemistry* 67, 2450–2462. doi: 10.1016/j.phytochem.2006.09.004

Michaelakis, A., Papachristos, D., Kimbaris, A., Koliopoulos, G., Giatropoulos, A., and Polissiou, M. G. (2009). Citrus essential oils and four enantiomeric pinenes against *Culex pipiens* (Diptera: Culicidae). *Parasitol. Res.* 105, 769–773. doi: 10.1007/s00436-009-1452-7

Mintoff, S. J. L., Rookes, J. E., and Cahill, D. M. (2015). Sub-lethal UV-C radiation induces callose, hydrogen peroxide and defence-related gene expression in *Arabidopsis thaliana*. *Plant Biol.* 17, 703–711. doi: 10.1111/plb.12286

Mithen, R. F. (2001). Glucosinolates and their degradation products. *Adv. Bot. Res.* 35, 213–262. doi: 10.1016/s0065-2296(01)35008-5

Molnar, P., Deli, J., Tanaka, T., Kann, Y., Tani, S., Gyemant, N., et al. (2010). Carotenoids with anti-*Helicobacter pylori* activity from golden delicious apple. *Phytother. Res.* 24, 644–648.

Moon, Y. J., Kim, S. I., and Chung, Y. H. (2012). Sensing and responding to UV-A in Cyanobacteria. *Intern. J. Mol. Sci.* 13, 16303–16332. doi: 10.3390/ijms131216303

Morales, L. O., Brosche, M., Vainonen, J., Jenkins, G. I., Wargent, J. J., Sipari, N., et al. (2013). Multiple roles for UV RESISTANCE LOCUS8 in regulating gene expression and metabolite accumulation in *Arabidopsis* under solar ultraviolet radiation. *Plant Physiol.* 161, 744–759. doi: 10.1104/pp.112.211375

Moreira-Rodriguez, M., Nair, V., Benavides, J., Cisneros-Zevallos, L., and Jacobo-Velazquez, D. A. (2017). UVA, UVB light, and methyl jasmonate, alone or combined, redirect the biosynthesis of Glucosinolates, Phenolics, Carotenoids, and chlorophylls in *Broccoli sprouts*. *Intern. J. Mol. Sci.* 18:2330. doi: 10.3390/ijms18112330

Nsa, I. Y., Karunarathna, N., Liu, X., Huang, H., Boetteger, B., and Bell-Pedersen, D. (2015). A novel cryptochrome-dependent oscillator in *Neurospora crassa*. *Genetics* 199, 233–245. doi: 10.1534/genetics.114.169441

Nuutinen, T. (2018). Medicinal properties of terpenes found in *Cannabis sativa* and *Humulus lupulus*. *Eur. J. Med. Chem.* 157, 198–228. doi: 10.1016/j.ejmech.2018.07.076

Oelmuller, R., and Mohr, H. (1985). Mode of coaction between blue/UV light and light absorbed by phytochrome in light-mediated anthocyanin formation in the milo (*Sorghum vulgare* Pers.) seedling. *Proc. Natl. Acad. Sci. U.S.A.* 82, 6124–6128. doi: 10.1073/pnas.82.18.6124

O'Hara, A., Headland, L. R., Diaz-Ramos, L. A., Morales, L. O., Strid, A., and Jenkins, G. I. (2019). Regulation of *Arabidopsis* gene expression by low fluence rate UV-B independently of UVR8 and stress signaling. *Photochem. Photobiol. Sci.* 18, 1675–1684. doi: 10.1039/c9pp00151d

Okajima, K., Matsuoka, D., and Tokutomi, S. (2011). LOV2-linker-kinase phosphorylates LOV1-containing N-terminal polypeptide substrate via photoreaction of LOV2 in *Arabidopsis* phototropin1. *FEBS Lett.* 585, 3391–3395. doi: 10.1016/j.febslet.2011.10.003

Oppezzo, O. J. (2012). Contribution of UVB radiation to bacterial inactivation by natural sunlight. *J. Photochem. Photobiol. B Biol.* 115, 58–62. doi: 10.1016/j.jphotobiol.2012.06.011

Oravecz, A., Baumann, A., Máté, Z., Brzezinska, A., Molinier, J., Oakeley, E. J., et al. (2006). CONSTITUTIVELY PHOTOMORPHOGENIC1 is required for the UV-B response in *Arabidopsis*. *Plant Cell* 18, 1975–1990. doi: 10.1105/tpc.105.040097

Oren, A., and Gunde-Cimerman, N. (2007). Mycosporines and mycosporine-like amino acids: UV protectants or multipurpose secondary metabolites? *FEMS Microbiol. Lett.* 269, 1–10. doi: 10.1111/j.1574-6968.2007.00650.x

Ozcelik, B. (2007). Fungi/bactericidal and static effects of ultraviolet light in 254 and 354 nm Wavelengths. *Res. J. Microbiol.* 2, 42–49. doi: 10.3923/jm.2007.42.49

Parhi, A., Kelley, C., Kaul, M., Pilch, D. S., and LaVoie, E. J. (2012). Antibacterial activity of substituted 5-methylbenzo[c]phenanthridinium derivatives. *Bioorg. Med. Chem. Lett.* 22, 7080–7083. doi: 10.1016/j.bmcl.2012.09.097

Pereira, J. A., Oliveira, I., Sousa, A., Valentão, P., Andrade, P. B., Ferreira, I. C. F. R., et al. (2007). Walnut (*Juglans regia* L.) leaves: Phenolic compounds, antibacterial activity and antioxidant potential of different cultivars. *Food Chem. Toxicol.* 45, 2287–2295. doi: 10.1016/j.fct.2007.06.004

Rai, N., O'Hara, A., Farkas, D., Safronov, O., Ratanasopa, K., Wang, F., et al. (2020). The photoreceptor UVR8 mediates the perception of both UV-B and

UV-A wavelengths up to 350 nm of sunlight with responsivity moderated by cryptochromes. *Plant Cell Environ.* 43, 1513–1527. doi: 10.1111/pce.13752

Rai, R., Meena, R. P., Smita, S. S., Shukla, A., Rai, S. K., and Pandey-Rai, S. (2011). UV-B and UV-C pre-treatments induce physiological changes and artemisinin biosynthesis in *Artemisia annua* L. - an antimalarial plant. *J. Photochem. Photobiol. B Biol.* 105, 216–225. doi: 10.1016/j.jphotobiol.2011.09.004

Ramani, S., and Chelliah, J. (2007). UV-B-induced signaling events leading to enhanced-production of catharanthine in *Catharanthus roseus* cell suspension cultures. *BMC Plant Biol.* 7:61. doi: 10.1186/1471-2229-7-61

Rao, B. K., Kumar, P., Rao, S., and Gurung, B. (2011). Bactericidal effect of ultraviolet C (UVC), direct and filtered through transparent plastic, on gram-positive cocci: an in vitro study. *Ostomy Wound Manag.* 57, 46–52.

Rastogi, R. P., Richa, Kumar, A., Tyagi, M. B., and Sinha, R. P. (2010). Molecular mechanisms of ultraviolet radiation-induced DNA damage and repair. *J. Nucleic Acids* 2010:592980.

Rastogi, R. P., Sinha, R. P., Moh, S. H., Lee, T. K., Kottuparambil, S., Kim, Y.-J., et al. (2014). Ultraviolet radiation and *Cyanobacteria*. *J. Photochem. Photobiol. B Biol.* 141, 154–169.

Rauha, J. P., Remes, S., Heinonen, M., Hopia, A., Kahkonen, M., Kujala, T., et al. (2000). Antimicrobial effects of Finnish plant extracts containing flavonoids and other phenolic compounds. *Int. J. Food Microbiol.* 56, 3–12. doi: 10.1016/s0168-1605(00)00218-x

Ricci, A., Dramis, L., Shah, R., Gartner, W., and Losi, A. (2015). Visualizing the relevance of bacterial blue- and red-light receptors during plant-pathogen interaction. *Environ. Microbiol. Rep.* 7, 795–802. doi: 10.1111/1758-2229.12320

Rigonato, J., Alvarenga, D. O., Andreote, F. D., Dias, A. C., Melo, I. S., Kent, A., et al. (2012). Cyanobacterial diversity in the phyllosphere of a mangrove forest. *FEMS Microbiol. Ecol.* 80, 312–322. doi: 10.1111/j.1574-6941.2012.01299.x

Robson, T. M., Klem, K., Urban, O., and Jansen, M. A. (2015). Re-interpreting plant morphological responses to UV-B radiation. *Plant Cell Environ.* 38, 856–866. doi: 10.1111/pce.12374

Rombouts, S., Volckaert, A., Venneman, S., Declercq, B., Vandenheuvel, D., Allonsius, C. N., et al. (2016). Characterization of novel bacteriophages for biocontrol of bacterial blight in leek caused by *Pseudomonas syringae* pv. *porri*. *Front. Microbiol.* 7:279. doi: 10.3389/fmicb.2016.00279

Sakai, T., Kagawa, T., Kasahara, M., Swartz, T. E., Christie, J. M., Briggs, W. R., et al. (2001). *Arabidopsis* nph1 and npl1: blue light receptors that mediate both phototropism and chloroplast relocation. *Proc. Natl. Acad. Sci. U.S.A.* 98, 6969–6974. doi: 10.1073/pnas.101137598

Saladino, F., Bordin, K., Luciano, F. B., Franzón, M. F., Mañes, J., and Meca, G. (2016). "Antimicrobial Activity of the glucosinolates," in *Glucosinolates*, eds J.-M. Mérillon, and K. G. Ramawat (Cham: Springer International Publishing), 1–26. doi: 10.1007/978-3-319-26479-0_18-1

Salehi, B., Upadhyay, S., Erdogan, O. I., Kumar, J. A., Rad, J. S., Cho, W. C., et al. (2019). Therapeutic potential of alpha- and beta-pinene: a miracle gift of nature. *Biomolecules* 9:738. doi: 10.3390/biom9110738

Salomon, M., Lempert, U., and Rudiger, W. (2004). Dimerization of the plant photoreceptor phototropin is probably mediated by the LOV1 domain. *FEBS Lett.* 572, 8–10. doi: 10.1016/j.febslet.2004.06.081

Sancar, A. (1996). DNA excision repair. *Annu. Rev. Biochem.* 65, 43–81.

Sancar, A. (2003). Structure and function of DNA photolyase and cryptochrome blue-light photoreceptors. *Chem. Rev.* 103, 2203–2237. doi: 10.1021/cr0204348

Sancar, G. B., and Sancar, A. (1987). Structure and function of DNA photolyases. *Trends Biochem. Sci.* 12, 259–261. doi: 10.1016/0968-0004(87)90130-7

Sang, Y., Li, Q. H., Rubio, V., Zhang, Y. C., Mao, J., Deng, X. W., et al. (2005). N-terminal domain-mediated homodimerization is required for photoreceptor activity of *Arabidopsis* CRYPTOCHROME 1. *Plant Cell* 17, 1569–1584. doi: 10.1105/tpc.104.029645

Sanz, C., Rodriguez-Romero, J., Idnurm, A., Christie, J. M., Heitman, J., Corrochano, L. M., et al. (2009). *Phycomyces* MADB interacts with MADA to form the primary photoreceptor complex for fungal phototropism. *Proc. Natl. Acad. Sci. U.S.A.* 106, 7095–7100. doi: 10.1073/pnas.0900879106

Saxena, C., Wang, H., Kavakli, I. H., Sancar, A., and Zhong, D. (2005). Ultrafast dynamics of resonance energy transfer in cryptochrome. *J. Am. Chem. Soc.* 127, 7984–7985. doi: 10.1021/ja0421607

Schäfer, E., and Nagy, F. (2006). *Photomorphogenesis in Plants and Bacteria: Function and Signal Transduction Mechanisms*. Dordrecht: Springer.

Schenke, D., Utami, H. P., Zhou, Z., Gallegos, M. T., and Cai, D. (2019). Suppression of UV-B stress induced flavonoids by biotic stress: is there reciprocal crosstalk? *Plant Physiol. Biochem.* 134, 53–63. doi: 10.1016/j.plaphy.2018.06.026

Schmitz-Hoerner, R., and Weissenbock, G. (2003). Contribution of phenolic compounds to the UV-B screening capacity of developing barley primary leaves in relation to DNA damage and repair under elevated UV-B levels. *Phytochemistry* 64, 243–255. doi: 10.1016/s0031-9422(03)00203-6

Schmoll, M., Esquivel-Naranjo, E. U., and Herrera-Estrella, A. (2010). *Trichoderma* in the light of day–physiology and development. *Fungal Genet. Biol.* 47, 909–916. doi: 10.1016/j.fgb.2010.04.010

Schumacher, J. (2016). DHN melanin biosynthesis in the plant pathogenic fungus *Botrytis cinerea* is based on two developmentally regulated key enzyme (PKS)-encoding genes. *Mol. Microbiol.* 99, 729–748. doi: 10.1111/mmi.13262

Selby, C. P., and Sancar, A. (2006). A cryptochrome/photolyase class of enzymes with single-stranded DNA-specific photolyase activity. *Proc. Natl. Acad. Sci. U.S.A.* 103, 17696–17700. doi: 10.1073/pnas.0607993103

Sharma, A., Sharma, B., Hayes, S., Kerner, K., Hoecker, U., Jenkins, G. I., et al. (2019). UVR8 disrupts stabilisation of PIF5 by COP1 to inhibit plant stem elongation in sunlight. *Nat. Commun.* 10:4417.

Sharma, C., Al Kaabi, J. M., Nurulain, S. M., Goyal, S. N., Kamal, M. A., and Ojha, S. (2016). Polypharmacological properties and therapeutic potential of beta-caryophyllene: a dietary phytocannabinoid of pharmaceutical promise. *Curr. Pharm. Des.* 22, 3237–3264. doi: 10.2174/1381612822666160311115226

Sharrock, R. A. (2008). The phytochrome red/far-red photoreceptor superfamily. *Genome Biol.* 9:230. doi: 10.1186/gb-2008-9-8-230

Shimura, M., Ito, Y., Ishii, C., Yajima, H., Linden, H., Harashima, T., et al. (1999). Characterization of a *Neurospora crassa* photolyase-deficient mutant generated by repeat induced point mutation of the phr gene. *Fungal Genet. Biol.* 28, 12–20. doi: 10.1006/fgbi.1999.1158

Shin, D. H., Choi, M., Kim, K., Bang, G., Cho, M., Choi, S. B., et al. (2013). HY5 regulates anthocyanin biosynthesis by inducing the transcriptional activation of the MYB75/PAP1 transcription factor in *Arabidopsis*. *FEBS Lett.* 587, 1543–1547. doi: 10.1016/j.febslet.2013.03.037

Shinomura, T., Nagatani, A., Hanzawa, H., Kubota, M., Watanabe, M., and Furuya, M. (1996). Action spectra for phytochrome A- and B-specific photoinduction of seed germination in *Arabidopsis thaliana*. *Proc. Natl. Acad. Sci. U.S.A.* 93, 8129–8133. doi: 10.1073/pnas.93.15.8129

Silva, F., Torres-Martinez, S., and Garre, V. (2006). Distinct white collar-1 genes control specific light responses in *Mucor circinelloides*. *Mol. Microbiol.* 61, 1023–1037. doi: 10.1111/j.1365-2958.2006.05291.x

Singh, P., Santoni, S., Weber, A., This, P., and Peros, J. P. (2019). Understanding the phyllosphere microbiome assemblage in grape species (*Vitaceae*) with amplicon sequence data structures. *Sci. Rep.* 9:14294.

Sinha, R. P., and Hader, D. P. (2002). UV-induced DNA damage and repair: a review. *Photochem. Photobiol. Sci.* 1, 225–236.

Sinha, R. P., Singh, S. P., and Hader, D. P. (2007). Database on mycosporines and mycosporine-like amino acids (MAAs) in fungi, cyanobacteria, macroalgae, phytoplankton and animals. *J. Photochem. Photobiol. B Biol.* 89, 29–35. doi: 10.1016/j.jphotobiol.2007.07.006

Steiner, U., and Oerke, E. C. (2007). Localized melanization of appressoria is required for pathogenicity of *Venturia inaequalis*. *Phytopathology* 97, 1222–1230. doi: 10.1094/phyto-97-10-1222

Stevenson, P. C., and Haware, M. P. (1999). Maackiain in *Cicer bijugum* Rech. f. associated with resistance to *Botrytis grey* mould. *Biochem. Syst. Ecol.* 27, 761–767. doi: 10.1016/s0305-1978(99)00023-x

Stracke, R., Favory, J. J., Gruber, H., Bartelniewoehner, L., Bartels, S., Binkert, M., et al. (2010a). The *Arabidopsis* bZIP transcription factor HY5 regulates expression of the PFG1/MYB12 gene in response to light and ultraviolet-B radiation. *Plant Cell Environ.* 33, 88–103. doi: 10.1111/j.1365-313x.2011.04670.x

Stracke, R., Jahns, O., Keck, M., Tohge, T., Niehaus, K., Fernie, A. R., et al. (2010b). Analysis of PRODUCTION OF FLAVONOL GLYCOSIDES-dependent flavonol glycoside accumulation in *Arabidopsis thaliana* plants reveals MYB11-, MYB12- and MYB111-independent flavonol glycoside accumulation. *New Phytol.* 188, 985–1000. doi: 10.1111/j.1469-8137.2010.03421.x

Stratmann, J. W., Stelmach, B. A., Weller, E. W., and Ryan, C. A. (2000). UVB/UVA radiation activates a 48 kDa myelin basic protein kinase and potentiates wound signaling in tomato leaves. *Photochem. Photobiol.* 71, 116–123. doi: 10.1562/0031-8655(2000)0710116sipuur2.0.co2

Sundin, G. W., and Jacobs, J. L. (1999). Ultraviolet radiation (UVR) sensitivity analysis and UVR survival strategies of a bacterial community from the phyllosphere of field-grown peanut (*Arachis hypogeae* L.). *Microb. Ecol.* 38, 27–38. doi: 10.1007/s002489900152

Sundin, G. W., and Murillo, J. (1999). Functional analysis of the *Pseudomonas syringae* rulAB determinant in tolerance to ultraviolet B (290-320 nm) radiation and distribution of rulAB among P. *syringae pathovars*. *Environ. Microbiol.* 1, 75–87. doi: 10.1046/j.1462-2920.1999.00008.x

Suthaparan, A., Stensvand, A., Solhaug, K. A., Torre, S., Telfer, K. H., Ruud, A. K., et al. (2014). Suppression of cucumber powdery mildew by supplemental UV-B radiation in greenhouses can be augmented or reduced by background radiation quality. *Plant Dis.* 98, 1349–1357. doi: 10.1094/pdis-03-13-0222-re

Tagua, V. G., Pausch, M., Eckel, M., Gutierrez, G., Miralles-Duran, A., Sanz, C., et al. (2015). Fungal cryptochrome with DNA repair activity reveals an early stage in cryptochrome evolution. *Proc. Natl. Acad. Sci. U.S.A.* 112, 15130–15135. doi: 10.1073/pnas.1514637112

Takahashi, M., Teranishi, M., Ishida, H., Kawasaki, J., Takeuchi, A., Yamaya, T., et al. (2011). *Cyclobutane pyrimidine* dimer (CPD) photolyase repairs ultraviolet-B-induced CPDs in rice chloroplast and mitochondrial DNA. *Plant J. Cell Mol. Biol.* 66, 433–442. doi: 10.1111/j.1365-313x.2011.04500.x

Takano, H. (2016). The regulatory mechanism underlying light-inducible production of carotenoids in nonphototrophic bacteria. *Biosci. Biotechnol. Biochem.* 80, 1264–1273. doi: 10.1080/09168451.2016.1156478

Tang, C., Xie, B. J., and Sun, Z. D. (2017). Antibacterial activity and mechanism of B-type oligomeric procyanidins from lotus seedpod on enterotoxigenic *Escherichia coli*. *J. Funct. Foods* 38, 454–463. doi: 10.1016/j.jff.2017.09.046

Tavridou, E., Pireyre, M., and Ulm, R. (2020). Degradation of the transcription factors PIF4 and PIF5 under UV-B promotes UVR8-mediated inhibition of hypocotyl growth in *Arabidopsis*. *Plant J. Cell Mol. Biol.* 101, 507–517. doi: 10.1111/tpj.14556

Teranishi, M., Taguchi, T., Ono, T., and Hidema, J. (2012). Augmentation of CPD photolyase activity in japonica and indica rice increases their UVB resistance but still leaves the difference in their sensitivities. *Photochem. Photobiol. Sci.* 11, 812–820. doi: 10.1039/c2pp05392f

Terashima, K., Yuki, K., Muraguchi, H., Akiyama, M., and Kamada, T. (2005). The dst1 gene involved in mushroom photomorphogenesis of *Coprinus cinereus* encodes a putative photoreceptor for blue light. *Genetics* 171, 101–108. doi: 10.1534/genetics.104.040048

Thind, T. S., and Schilder, A. C. (2018). Understanding photoreception in fungi and its role in fungal development with focus on phytopathogenic fungi. *Indian Phytopathol.* 71, 169–182. doi: 10.1007/s42360-018-0025-z

Tholl, D. (2015). Biosynthesis and biological functions of terpenoids in plants. *Adv. Biochem. Eng. Biotechnol.* 148, 63–106. doi: 10.1007/10_2014_295

Tisch, D., and Schmoll, M. (2010). Light regulation of metabolic pathways in fungi. *Appl. Microbiol. Biot.* 85, 1259–1277. doi: 10.1007/s00253-009-2320-1

Tossi, V. E., Regalado, J. J., Iannicelli, J., Laino, L. E., Burrieza, H. P., Escandón, A. S., et al. (2019). Beyond *Arabidopsis*: differential UV-B response mediated by UVR8 in diverse species. *Front. Plant Sci.* 10:780. doi: 10.3389/fpls.2019.00780

Tuteja, N., Ahmad, P., Panda, B. B., and Tuteja, R. (2009). Genotoxic stress in plants: shedding light on DNA damage, repair and DNA repair helicases. *Mutat. Res.* 681, 134–149. doi: 10.1016/j.mrrev.2008.06.004

Tuteja, N., Singh, M. B., Misra, M. K., Bhalla, P. L., and Tuteja, R. (2001). Molecular mechanisms of DNA damage and repair: progress in plants. *Crit. Rev. Biochem. Mol. Biol.* 36, 337–397.

Ulm, R., Baumann, A., Oravecz, A., Mate, Z., Adam, E., Oakeley, E. J., et al. (2004). Genome-wide analysis of gene expression reveals function of the bZIP transcription factor HY5 in the UV-B response of *Arabidopsis*. *Proc. Natl. Acad. Sci. U.S.A.* 101, 1397–1402. doi: 10.1073/pnas.0308044100

Urban, L., Charles, F., de Miranda, M. R. A., and Aarrouf, J. (2016). Understanding the physiological effects of UV-C light and exploiting its agronomic potential before and after harvest. *Plant Physiol. Biochem.* 105, 1–11. doi: 10.1016/j.plaphy.2016.04.004

van der Watt, E., and Pretorius, J. C. (2001). Purification and identification of active antibacterial components in *Carpobrotus edulis* L. *J. Ethnopharmacol.* 76, 87–91. doi: 10.1016/s0378-8741(01)00197-0

van Gelderen, K., Kang, C., Paalman, R., Keuskamp, D., Hayes, S., and Pierik, R. (2018). Far-red light detection in the shoot regulates lateral root development through the HY5 transcription factor. *Plant Cell* 30, 101–116. doi: 10.1105/tpc.17.00771

Vandenbussche, F., Tilbrook, K., Fierro, A. C., Marchal, K., Poelman, D., Van Der Straeten, D., et al. (2014). Photoreceptor-mediated bending towards UV-B in *Arabidopsis*. *Mol. Plant* 7, 1041–1052. doi: 10.1093/mp/ssu039

Vandenbussche, F., Yu, N., Li, W., Vanhaelewyn, L., Hamshou, M., Van Der Straeten, D., et al. (2018). An ultraviolet B condition that affects growth and defense in *Arabidopsis*. *Plant Sci.* 268, 54–63. doi: 10.1016/j.plantsci.2017.12.005

Vanhaelewyn, L., Prinsen, E., Van Der Straeten, D., and Vandenbussche, F. (2016a). Hormone-controlled UV-B responses in plants. *J. Exp. Bot.* 67, 4469–4482. doi: 10.1093/jxb/erw261

Vanhaelewyn, L., Schumacher, P., Poelman, D., Fankhauser, C., Van Der Straeten, D., and Vandenbussche, F. (2016b). REPRESSOR OF ULTRAVIOLET-B PHOTOMORPHOGENESIS function allows efficient phototropin mediated ultraviolet-B phototropism in etiolated seedlings. *Plant Sci.* 252, 215–221. doi: 10.1016/j.plantsci.2016.07.008

Vanhaelewyn, L., Viczian, A., Prinsen, E., Bernula, P., Serrano, A. M., Arana, M. V., et al. (2019). Differential UVR8 signal across the stem controls UV-B-induced inflorescence phototropism. *Plant Cell* 31, 2070–2088. doi: 10.1105/tpc.18.00929

Vargas, P., Farias, G. A., Nogales, J., Prada, H., Carvajal, V., Baron, M., et al. (2013). Plant flavonoids target *Pseudomonas syringae* pv. tomato DC3000 flagella and type III secretion system. *Environ. Microbiol. Rep.* 5, 841–850. doi: 10.1111/1758-2229.12086

Veluchamy, S., and Rollins, J. A. (2008). A CRY-DASH-type photolyase/cryptochrome from *Sclerotinia sclerotiorum* mediates minor UV-A-specific effects on development. *Fungal Genet. Biol.* 45, 1265–1276. doi: 10.1016/j.fgb.2008.06.004

Verdaguer, D., Jansen, M. A., Llorens, L., Morales, L. O., and Neugart, S. (2017). UV-A radiation effects on higher plants: exploring the known unknown. *Plant Sci.* 255, 72–81. doi: 10.1016/j.plantsci.2016.11.014

Vig, A. P., Rampal, G., Thind, T. S., and Arora, S. (2009). Bio-protective effects of glucosinolates - A review. *LWT Food Sci. Technol.* 42, 1561–1572. doi: 10.1016/j.lwt.2009.05.023

Wang, H. Y., Ma, L. G., Li, J. M., Zhao, H. Y., and Deng, X. W. (2001). Direct interaction of *Arabidopsis* cryptochromes with COP1 in light control development. *Science* 294, 154–158. doi: 10.1126/science.1063630

Wasternack, C., and Strnad, M. (2016). Jasmonate signaling in plant stress responses and development - active and inactive compounds. *N. Biotechnol.* 33, 604–613. doi: 10.1016/j.nbt.2015.11.001

Wen, H., Kang, J., Li, D., Wen, W., Yang, F., Hu, H., et al. (2016). Antifungal activities of anthocyanins from purple sweet potato in the presence of food preservatives. *Food Sci. Biotechnol.* 25, 165–171. doi: 10.1007/s10068-016-0025-7

Wright, J. R., Sumner, S. S., Hackney, C. R., Pierson, M. D., and Zoecklein, B. W. (2000). Efficacy of ultraviolet light for reducing *Escherichia coli* O157:H7 in unpasteurized apple cider. *J. Food Prot.* 63, 563–567. doi: 10.4315/0362-028x-63.5.563

Wu, L., McGrane, R. S., and Beattie, G. A. (2013). Light regulation of swarming motility in *Pseudomonas syringae* integrates signaling pathways mediated by a bacteriophytochrome and a LOV protein. *mBio* 4:e00334-13.

Wu, L., and Yang, H. Q. (2010). CRYPTOCHROME 1 is implicated in promoting r protein-mediated plant resistance to *Pseudomonas syringae* in *Arabidopsis*. *Mol. Plant* 3, 539–548. doi: 10.1093/mp/ssp107

Wu, M., Si, M., Li, X., Song, L., Liu, J., Zhai, R., et al. (2019). PbCOP1.1 contributes to the negative regulation of anthocyanin biosynthesis in Pear. *Plants* 8:39. doi: 10.3390/plants8020039

Yajima, H., Takao, M., Yasuhira, S., Zhao, J. H., Ishii, C., Inoue, H., et al. (1995). A eukaryotic gene encoding an endonuclease that specifically repairs DNA damaged by ultraviolet light. *EMBO J.* 14, 2393–2399. doi: 10.1002/j.1460-2075.1995.tb07234.x

Yalpani, N., Enyedi, A. J., Leon, J., and Raskin, I. (1994). Ultraviolet-light and ozone stimulate accumulation of salicylic-acid, pathogenesis-related proteins and virus-resistance in tobacco. *Planta* 193, 372–376.

Yang, H. Q., Tang, R. H., and Cashmore, A. R. (2001). The signaling mechanism of *Arabidopsis* CRY1 involves direct interaction with COP1. *Plant Cell* 13, 2573–2587. doi: 10.1105/tpc.13.12.2573

Yang, H. Q., Wu, Y. J., Tang, R. H., Liu, D. M., Liu, Y., and Cashmore, A. R. (2000). The C termini of *Arabidopsis* cryptochromes mediate a constitutive light response. *Cell* 103, 815–827. doi: 10.1016/s0092-8674(00)00184-7

Yao, Y. L., Danna, C. H., Zemp, F. J., Titov, V., Ciftci, O. N., Przybylski, R., et al. (2011). UV-C-Irradiated *Arabidopsis* and tobacco emit volatiles that trigger genomic instability in neighboring plants. *Plant Cell* 23, 3842–3852. doi: 10.1105/tpc.111.089003

Yin, R. H., Skvortsova, M. Y., Loubery, S., and Ulm, R. (2016). COP1 is required for UV-B-induced nuclear accumulation of the UVR8 photoreceptor. *Proc. Natl. Acad. Sci. U.S.A.* 113, E4415–E4422.

Yoshida, S., Hiradate, S., Koitabashi, M., Kamo, T., and Tsushima, S. (2017). Phyllosphere *Methylobacterium bacteria* contain UVA-absorbing compounds. *J. Photochem. Photobiol. B Biol.* 167, 168–175. doi: 10.1016/j.jphotobiol.2016.12.019

Zant, C., Klement, N., Bettayeb, B., Sahnoun, M. H., and Havard, V. (2018). "UV-robot supervision system design and development," in *Proceedings of the 25ème Colloque des Sciences de la Conception et de L'innovation (CONFERE 2018)*, Budapest.

Zhou, Z., Schenke, D., Miao, Y., and Cai, D. G. (2017). Investigation of the crosstalk between the flg22 and the UV-B-induced flavonol pathway in *Arabidopsis thaliana* seedlings. *Plant Cell Environ.* 40, 453–458. doi: 10.1111/pce.12869

Conflict of Interest: The authors declare that the research was conducted in the absence of any commercial or financial relationships that could be construed as a potential conflict of interest.

The handling editor declared a past co-authorship with one of the authors FV.

Copyright © 2020 Vanhaelewyn, Van Der Straeten, De Coninck and Vandenbussche. This is an open-access article distributed under the terms of the Creative Commons Attribution License (CC BY). The use, distribution or reproduction in other forums is permitted, provided the original author(s) and the copyright owner(s) are credited and that the original publication in this journal is cited, in accordance with accepted academic practice. No use, distribution or reproduction is permitted which does not comply with these terms.

frontiers in Plant Science

ORIGINAL RESEARCH
published: 20 January 2021
doi: 10.3389/fpls.2020.607007

Physiological and Proteomic Insights Into Red and Blue Light-Mediated Enhancement of *in vitro* Growth in *Scrophularia kakudensis*—A Potential Medicinal Plant

Abinaya Manivannan[1†], Prabhakaran Soundararajan[1†], Yoo Gyeong Park[1] and Byoung Ryong Jeong[1,2,3]*

[1] Institute of Agriculture and Life Science, Gyeongsang National University, Jinju, South Korea, [2] Division of Applied Life Science (BK21 Plus), Graduate School, Gyeongsang National University, Jinju, South Korea, [3] Research Institute of Life Science, Gyeongsang National University, Jinju, South Korea

The current study has determined the effect of red and blue lights on the enhancement of growth, antioxidant property, phytochemical contents, and expression of proteins in *Scrophularia kakudensis*. *In vitro*-grown shoot tip explants of *S. kakudensis* were cultured on the plant growth regulator-free Murashige and Skoog (MS) medium and cultured under the conventional cool white fluorescent lamp (control), blue light-emitting diodes (LED) light, or red LED light. After 4 weeks, growth, stomatal ultrastructure, total phenols and flavonoids, activities of antioxidant enzymes, and protein expressions were determined. Interestingly, blue or red LED treatment increased the shoot length, shoot diameter, root length, and biomass on comparison with the control. In addition, the LED treatments enhanced the contents of phytochemicals in the extracts. The red LED treatment significantly elicited the accumulation of flavonoids in comparison with the control. In accordance with the secondary metabolites, the LED treatments modulated the activities of antioxidant enzymes. Moreover, the proteomic insights using two-dimensional gel electrophoresis system revealed the proteins involved in transcription and translation, carbohydrate mechanism, post-translational modification, and stress responses. Taken together, the incorporation of blue or red LED during *in vitro* propagation of *S. kakudensis* can be a beneficial way to increase the plant quality and medicinal values of *S. kakudensis*.

Keywords: antioxidant enzymes, trichomes, protein, phenols, flavonoids

OPEN ACCESS

Edited by:
Inga Mewis, Humboldt University of Berlin, Germany

Reviewed by:
Titta Katariina Kotilainen, Natural Resources Institute Finland (Luke), Finland
Zia Muhammad, Quaid-i-Azam University, Pakistan

***Correspondence:**
Byoung Ryong Jeong
brjeong@gmail.com

†Present address:
Abinaya Manivannan, Vegetable Research Division, National Institute of Horticultural and Herbal Science, Rural Development Administration, Jeonju, South Korea
Prabhakaran Soundararajan, Genomics Division, Department of Agricultural Bio-Resources, National Academy of Agricultural Science, Rural Development Administration (RDA), Jeonju, South Korea

Specialty section:
This article was submitted to Plant Metabolism and Chemodiversity, a section of the journal Frontiers in Plant Science

Received: *16 September 2020*
Accepted: *16 December 2020*
Published: *20 January 2021*

Citation:
Manivannan A, Soundararajan P, Park YG and Jeong BR (2021) Physiological and Proteomic Insights Into Red and Blue Light-Mediated Enhancement of in vitro Growth in Scrophularia kakudensis—A Potential Medicinal Plant. Front. Plant Sci. 11:607007. doi: 10.3389/fpls.2020.607007

INTRODUCTION

Scrophularia kakudensis (scrophulariaceae) is a pharmaceutically important plant with several vital secondary metabolites. The extracts of *S. kakudensis* have been widely used to treat ailments such as inflammation, fever, and gastro-intestinal problems (Manivannan et al., 2015b). *S. kakudensis* consists of pharmaceutically important compounds such as acacetin and scrophulasaponins. Besides its pharmaceutical importance, *S. kakudensis* is an unexplored medicinal plant due to

inadequate healthy plant materials. Hence, improvement of the micropropagation of *S. kakudensis* by implementation of novel strategies such as the application of different light qualities during propagation could enhance the quality of plant materials. Light is the principal factor for photosynthesis and photomorphogenesis. It also entrains a cascade of reactions involved in primary and secondary metabolism, respectively, in plants. Moreover, the light signals can influence the growth and development of plants in different forms such as quality, quantity, photoperiod, and direction.

Even though several forms of light exist, in recent days, the light quality-mediated influence of physiological, biochemical, and metabolic processes has gained prime importance among plant biologists. Particularly, under an *in vitro* environment, light triggers different metabolic activities of the plant (Kozai et al., 1997). Several reports have shown an improvement of *in vitro* growth in diverse plants by various combinations of light spectra (Batista et al., 2018; Ali et al., 2019; Chen et al., 2020; Silva et al., 2020). In addition, light quality can be applied for the elicitation of vital phytochemicals with pharmaceutical importance. Recently, the application of light quality for the enhancement of secondary metabolites with medicinal importance in a controlled environment such as plant factories, green houses, and *in vitro* culture environment is increasing (Im Chung et al., 2020; Park et al., 2020; Piątczak et al., 2020; Tohidi et al., 2020). Red and blue wavelengths (650 and 450 nm, respectively) are often associated with the enhancement of physiological processes in plants (Kim et al., 2004). Moreover, plants grown under different light qualities in *in vitro* environment consisted of enhanced growth, secondary metabolites, and active antioxidant enzyme metabolism (Kozai et al., 1997; Mengxi et al., 2011; Manivannan et al., 2015a). Recently, the usage of light-emitting diodes (LEDs) over the conventional cool white fluorescent light source has been increasing due to its advantages, such as less heat radiation, energy efficiency, monochromatic spectrum, and longer life span, thus offering a wide range of applications for the plant growers (Kim et al., 2004; Samuoliene et al., 2012; Batista et al., 2018). The application of different light qualities separately or in combination influences the physiology and metabolite contents. For instance, the growth of plants cultivated under red light increased the biomass in lettuce and radish (Goins et al., 2001) and the contents of secondary metabolites in *Ajuga bracteosa* (Ali et al., 2019). Polyphenolic compounds present in plants are associated with diverse functions in growth, defense, protection from UV radiation, and reproduction (Cheynier et al., 2013; Sharma et al., 2019; Tanase et al., 2019). Moreover, the light quality-mediated stimulation of the antioxidant system resulting in the production of secondary metabolites has been shown in several plants (Chen et al., 2020; Silva et al., 2020). In green vegetables, the supplementation of blue light increased the biomass and enhanced the content of vitamin C (Li and Kubota, 2009). Similarly, the green and red LEDs enhanced the contents of sesquiterpenes and monoterpene sabinene in *in vitro* cultures of *Achillea millefolium* (Alvarenga et al., 2015). The red light elicited the levels of carvacrol content in *Plectranthus amboinicus* (Silva et al., 2017), whereas the application of blue light significantly increased the carvacrol content in *Lippia gracilis* (Lazzarini et al., 2018). The blue light enhanced the myrcene and limonene contents in *in vitro*-grown *Lippia rotundifolia*, whereas the combination of red and blue lights in 1:2.5 ratio increased the z-ocimenone metabolite content (de Hsie et al., 2019).

Although several reports have suggested the light quality-mediated modulation of growth, phytochemicals, and reactive oxygen species (ROS) metabolism, very few studies on the proteomics aspects of light quality in *in vitro*-cultured plants are available. For instance, the application of red and blue LEDs improved the maturation and conversion of somatic embryos in sugarcane (Heringer et al., 2017). According to Heringer et al. (2017), the shotgun proteomics investigation of somatic embryos in different stages revealed the up-regulation of proteins involved in the differentiation and de-differentiation process, respectively, in sugarcane. A recent comparative proteomics report by Mirzahosseini et al. (2020) suggested that the supplementation of red and blue light enhanced the wound healing response in *in vitro*-grown *Arabidopsis thaliana* by the improvement of light quality-based defense strategies such as jasmonate-independent signaling pathway. In general, proteins are the functional products of the gene which act as enzymes, primarily for various metabolisms in living organisms. In the present era of modern technologies, application of proteomics has been utilized for a better understanding of the molecular mechanism behind various biological processes in plant biology. Therefore, in the present study, red and blue light-mediated changes in physiology, phytochemicals, and protein expression were studied in the *in vitro*-grown *S. kakudensis*.

MATERIALS AND METHODS

Plant Materials and Light Treatments

The nodal explants obtained from *in vitro S. kakudensis* were sub-cultured onto the plant growth regulator-free Murashige and Skoog (MS) (Murashige and Skoog, 1962) basal medium with 3% (w/v) sucrose and 0.8% (w/v) agar and placed under either cool white fluorescent light (FL) (40-W tubes, Philips, Netherlands) or monochromatic spectral light-emitting diodes (LEDs; PSLED-1203-50A, Force Lighting Co., Ltd., Hwaseong, South Korea), such as red (621–710 nm) or blue (450–475 nm), with the light intensity of 50 μmol m^{-2} s^{-1} PPFD. The light treatments were set up in a completely randomized design with five containers per treatment containing five explants in each container. The distance between the light source and the culture container was 30 cm. Furthermore, the cultures were maintained in a single plant growth chamber with different light quality installed in separate shelves. All the cultures were maintained at 25°C under a 16-h photoperiod with 80% relative humidity. The plants were harvested after 4 weeks for physiological, biochemical, phytochemical, and proteomics analyses.

Scanning Electron Microscopy Observation

For SEM analysis, the leaf samples were fixed in 2.5% glutaraldehyde overnight at 4°C and washed with 0.1 M

phosphate-buffered saline (pH 7.0), followed by staining in 4% osmium tetroxide solution for 2 h at 4°C, and the stained samples were dehydrated in a graded series of ethanol. After dehydration, the samples were dried, gold coated, examined, and photographed under a scanning electron microscope (JSM-6380, JEOL, Tokyo, Japan) operating at 15–25 kV according to Mujib et al. (2014).

Determination of Antioxidant Enzyme Activities

The extraction of antioxidant enzymes such as superoxide dismutase (SOD), catalase (CAT), ascorbate peroxidase (APX), and phenylalanine lyase (PAL) was performed according to Manivannan et al. (2015a). The total protein content of the samples was estimated by Bradford's method (Bradford, 1976). The SOD activity was assayed by following the protocol of Giannopolitis and Ries (1977) with the nitro blue tetrazolium inhibition method. The activity of GPX was estimated based on the amount of enzyme required for the formation of tetraguaiacol per minute according to Shah et al. (2001). The activity of CAT was estimated according to the method of Cakmak and Marschner (1992). The activity of APX was estimated by following the protocol of Nakan and Asada (1981). The PAL enzyme activity was determined according to Zhan et al. (2012).

Estimation of Total Phenols and Flavonoids

The leaf samples were extracted with methanol according to Manivannan et al. (2015b), and the total phenol content of the extract was estimated by the Folin–Ciocalteu principle according to Kumaran and Karunakaran (2007). Furthermore, the total flavonoid content was determined by the aluminum chloride method mentioned by Manivannan et al. (2015a). The total phenol and flavonoids were determined from a standard gibberellic acid and quercetin calibration curve, respectively.

Proteomics

Protein Extraction

For 2D-PAGE analysis, protein extraction was carried out by following the procedure of Muneer et al. (2015). In detail, the leaf tissue (0.1 g) was homogenized in liquid nitrogen using a pre-chilled pestle and mortar. The proteins were extracted with a commercial protein extraction kit (ReadyPrep, Bio-Rad, Hercules, CA, United States) according to the instructions provided by the manufacturer. For total protein isolation, about 2 ml of extraction buffer {8 M urea, 4% 3-[(3-cholamidopropyl) dimethylammonio]-1-propanesulfonate (CHAPS), 40 mM Tris, 0.2% bio-lyte (*pI* 3-10)} was mixed with the lyophilized (0.1 g) leaf tissue. The homogenate was vortexed and sonicated with an ultrasonic probe to disrupt any interfering substances such as genomic DNA and phenolics. After sonication, the samples were centrifuged for 30 min at 4°C, and the supernatant was transferred to new Eppendorf tubes. The resultant supernatant was employed for isoelectric focusing after protein quantification with the Bradford method using a bovine serum albumin standard curve.

Isoelectric Focusing and Two-Dimensional Gel Electrophoresis

A total of 70 μg of dissolved protein sample was separated by the 2-DE in the first dimension by the isoelectric focusing on a 7-cm IPG strip (*pI* 4–7) (GE Healthcare, Little Chalfont, Buckinghamshire, United Kingdom) and the second dimension by SDS-PAGE on a Protean II unit (Bio-Rad, Hercules, CA, United States), according to methods given by Muneer et al. (2015). The samples were rehydrated for 12 h (with a 125-μl rehydration buffer containing 70 μg proteins) before focusing. For the first dimension, the rehydrated strips were focused at 20°C with 50 μA current per strip using a four-step program: step and hold—300 V for 30 min, gradient—1,000 V for 30 min, gradient—5,000 V for 1 h 30 min, and final step and hold for 1–2 h until the final voltage reached 10,000 V. The focused strips were equilibrated twice for 15 min in 10 mg ml^{-1} DTT and then in 40 mg ml^{-1} iodoacetamide prepared in an equilibration buffer containing 50 mM Tris-HCl (pH 8.8), 6 M urea, 30% (v/v) glycerol, and 2% (w/v) SDS. After equilibration, the strips were attached to the second dimension gel (12.5%) with a 0.5% low melting point agarose sealing solution. Electrophoresis was done at a constant voltage of 80 V for 4 h until the bromophenol dye front reached the end of the gel. The protein spots in the analytical gels were stained using the silver staining method.

Image Acquisition and Data Analysis

Three replicate gels from each treatment were used for image acquisition and data analysis. Spot detection, spot measurement, background subtraction, and spot matching were performed using Progenesis SameSpotsQI 2D software (ver. 4.1, Nonlinear Dynamics, Newcastle, United Kingdom) in an automatic spot detection mode to review the annotations of spots statistically using one-way analysis of variance (ANOVA) analysis ($n = 3$, $p < 0.05$) at 95% confidence level. The differentially expressed protein spots were identified as spots showing more than a twofold change in expression in comparison with the control.

In-Gel Digestion and MALDI-TOF-MS Analysis

The differentially expressed protein spots were excised manually from the gels and washed with distilled water three times. The protein spots were chopped and de-stained with 30 mM potassium ferricyanide and 100 mM sodium thiosulphate pentahydrate (1:1) by incubating at room temperature for 30 min. The de-staining reagent was removed, and the gel particles were treated with 100 μl of 50 mM NH_4HCO_3 for 5 min and dehydrated in 30 μl of acetonitrile for 5 min. After dehydration, the gel was covered with a 100-μl reduction solution (10 mM dithiothreitol in 50 mM NH_4HCO_3) and incubated for 45 min at 56°C. After the removal of the reduction solution, 100 μl of alkylation solution (100 mM iodoacetamide in 50 mM NH_4HCO_3) was added and incubated at 25°C in the dark for 30 min. Finally, the gel pieces were washed with 30 μl of 50 mM NH_4HCO_3 for 5 min and dehydrated with 30 μl of acetonitrile for 10 min. After drying using a vacuum centrifuge, the gel pieces were rehydrated in 5–10 μl of 25 mM

NH_4HCO_3 containing 5 ng μl^{-1} trypsin (Promega, Madison, WI, United States) at 37°C for 30 min. After incubation, the excess trypsin solution was replaced with 5–10 µl of 25 mM NH_4HCO_3, and digestion was carried out for a minimum of 16 h at 37°C. The digested peptides were subsequently pooled, vacuum dried, and mixed with 3 µl of sample solution (50% acetonitrile and 0.1% trifluoroacetic acid). For protein identification, the tryptic-digested peptide mixtures were targeted onto a matrix-assisted laser desorption/ionization–time-of-flight mass spectrometry (MALDI-TOF-MS) plate (AccuSpot, Shimadzu Ltd., Kyoto, Japan) and analyzed by a Voyager-DE STR mass spectrometer (Applied Biosystems, Franklin Lakes, NJ, United States) equipped with delay ion extraction.

Peptide Identification and Gene Ontology Analysis

Mass spectra were obtained over a mass range of 800–3,500 Da. Homology search was executed by matching the experimental results with both theoretical digests and sequence information from the public protein databases using the Mascot software[1]. The search parameters employed were as follows: carbamidomethyl cysteine as a fixed modification and oxidation of methionine as a variable modification, one missed cleavage site, and peptide mass tolerance of ±100 ppm. The NCBI-nr database[2] with the taxonomy Viridiplantae was employed to identify regions of similarity between sequences. The protein score employed was $-10^*\log(P)$, where P is the probability that the observed match is a random event. The spot identities were submitted to an agbase gene ontology (GO) retriever, and the resulting annotations were summarized based on the GOSlim set using GOSlim Viewer (Muneer et al., 2015).

Statistical Analysis

All the assays were performed in triplicate, and the results were averaged. Significant differences among the treatments were determined by ANOVA, followed by Duncan's multiple-range test, at a significance level of 0.05 using the Statistical Analysis System computer package (V.6.12, SAS Institute Inc., Cary, NC, United States).

RESULTS AND DISCUSSION

Influence of Light Qualities on Growth and Morphology

The light qualities influenced the growth parameters and morphology of *S. kakudensis* (**Table 1** and **Figure 1A**). Among the light treatments, the red LED treatment produced slender plants with longer stems. The red LED treatment increased the shoot length by 82.0 and 100% than the blue LED and FL treatment, respectively. Similarly, the red LED increased the stem length in *Rehmannia glutinosa*, a medicinal plant from the same Scrophulariaceae family (Manivannan et al., 2015a). Previous reports demonstrated that red light induced the levels of plant growth regulators, particularly endogenous gibberellins, which play a vital role in cell elongation by stimulating the mitosis in both apical and sub-apical meristem, which could result in taller stems (Arney and Mitchell, 1969; Toyomasu et al., 1993). On the other hand, the blue LED treatment resulted in shorter shoots with a significantly larger diameter in comparison with the other treatments. Supplementation of blue LED increased the shoot diameter by 11.5% than the FL and by 109.6% in comparison with the red LED treatment, whereas the FL treatment increased by 88.0% than the red LED treatment. Similar effects of blue light were recorded in *R. glutinosa* (Manivannan et al., 2015a), and blue light-mediated increase in biomass was reported in Chinese cabbage (Li et al., 2012). Moreover, LED treatments induced early rooting in *S. kakudensis*. Red LED enhanced the number and length of roots by 40.0 and 50.0% in comparison with the blue light, whereas roots were not observed in the control plants. The stimulation of roots in the LED treatments could be due to the involvement of photoreceptors, auxin signaling, and light piping mechanism in which the transmission of light signals occurs through the internal tissues from the aboveground shoot to the root in a wavelength-dependent manner; particularly the long-wavelength red light and far red are well transmitted (Sun et al., 2005; Canamero et al., 2006; van Gelderen et al., 2018). Similar observations were reported in *Triticum aestivum* upon blue light irradiation (Dong et al., 2014). Furthermore, the biomass of *S. kakudensis* was significantly increased by the blue LED treatment followed by the red light. In detail, the blue LED treatment enhanced the fresh weight by 91.2 and 95% in comparison with the FL and red LED treatments. Similarly, the dry weight was increased by 72.0 and 87.0% than the FL and red LED treatment, respectively. Concordantly, Wheeler et al. (1991) also suggested the effectiveness of the blue and red light sources for healthy plant growth. The improvement of fresh and dry weights by the application of blue or red LED treatment alone or in combination was reported in *Oncidium* (Mengxi et al., 2011). Overall, the use of blue or red LED during *in vitro* propagation can be beneficial for the improvement of plant production. The application of blue and red light for the *in vitro* growth of medicinal plants has been reported in *Ajuga bracteosa* (Ali et al., 2019), *Pfaffia glomerata* (Silva et al., 2020), *Fritillaria cirrhosa* (Chen et al., 2020), and *Lippia rotundifolia* (de Hsie et al., 2019).

The leaf morphology of *S. kakudensis* was also modulated by the variation in light quality (**Figure 1B**). Broader leaves were observed in the blue and red light treatments in comparison with the control FL. In general, leaves perceive the light signals from the external environment by means of specialized receptors called photoreceptors, and thus modulation in the light quality readily affects the leaf characteristics (Kim et al., 2004; Park et al., 2012). A larger leaf area increases the absorption of light, which directly influences photosynthesis (Nishimura et al., 2009). The leaf morphological observations reflected on the density of stomata (**Figure 2**). The stomatal density was significantly enhanced in the blue LED treatment than in the other treatments. Moreover, the scanning electron micrograph of a leaf revealed the occurrence of more numbers of glandular trichomes in the red and blue LED-grown leaves in comparison with the FL

[1]http://www.matrixscience.com/search_form_select.html

[2]http://www.ncbi.nlm.nih.gov/refseq

TABLE 1 | Growth traits measured after 4 weeks of light treatment in *Scrophularia kakudensis*.

Light treatment	Shoot length (cm)	Stem diameter (mm)	Length of the longest root (cm)	Number Of roots	Total fresh weight (g)	Total dry weight (mg)
FL	2.0 ± 0.03[a]b[b]	0.156 ± 0.07b	0.0 ± 0.00c	0.0 ± 0.00c	0.102 ± 0.01b	10.0 ± 0.04b
Blue LED	2.2 ± 0.05b	0.174 ± 0.02a	1.2 ± 0.01b	5.0 ± 0.07b	0.195 ± 0.04a	17.2 ± 0.02a
Red LED	4.0 ± 0.06a	0.083 ± 0.05c	1.8 ± 0.03a	7.0 ± 0.05a	0.100 ± 0.05b	9.2 ± 0.04b

FL, fluorescent lamp; LED, light-emitting diodes. [a]Values represent the mean ± SE of three replications. [b]Means followed by different letter(s) in one measurement indicate statistically significant difference at $P \leq 0.05$ by Duncan's multiple-range test.

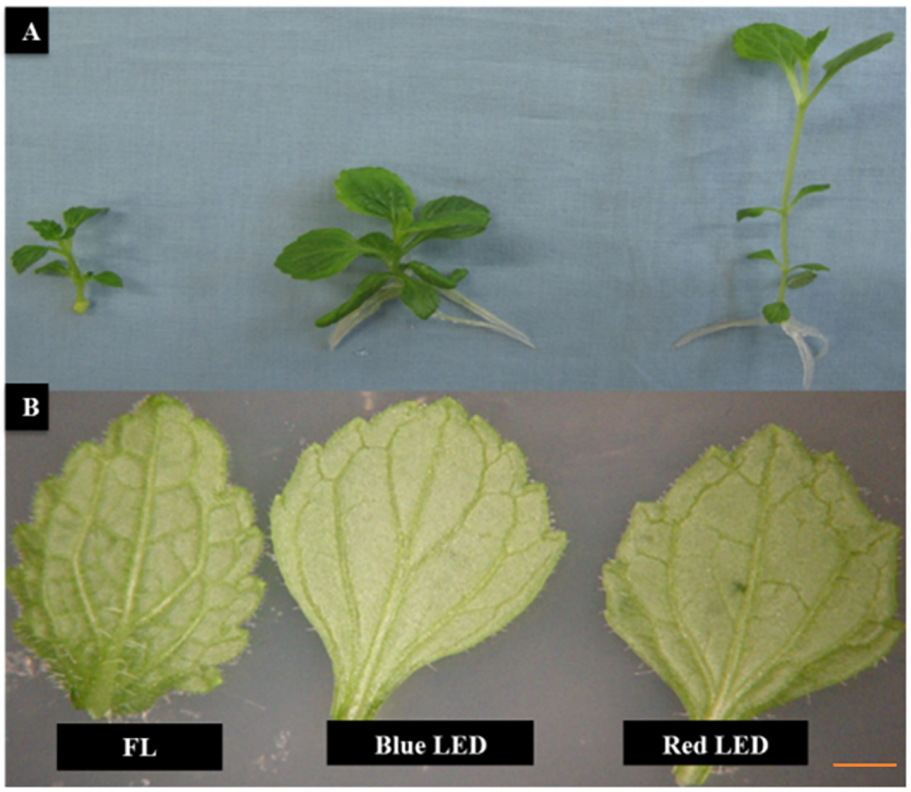

FIGURE 1 | Effect of light quality on the growth of *Scrophularia kakudensis*. Morphological differences observed in *S. kakudensis* plantlets **(A)** and variation in the leaf morphology **(B)** of *S. kakudensis* as affected by different light qualities.

(**Figure 3**). Interestingly, the increase in the density of glandular trichomes by red light was also reported in the *in vitro* cultures of *Alternanthera brasiliana* (Macedo et al., 2011). Moreover, in *Olea europaea*, the density of the trichomes was positively correlated with UV-B irradiation and considered as the defense response exhibited by plants (Liakoura et al., 1997).

Influence of Light Qualities on Redox Metabolism

The blue and the red LED treatments have positively influenced the activities of antioxidant enzymes in *S. kakudensis*. In detail, the highest SOD activity was observed upon the application of blue LED treatment followed by the red LED treatment (**Figure 4**). Generally, the antioxidant enzymes prevent the cell damages caused by the ROS by catalyzing a cascade of reactions. As the first line of defense, the SOD dismutases the O_2^{-1} radical into H_2O_2 and molecular oxygen (Gill and Tuteja, 2010). Therefore, the higher activity of SOD (H_2O_2 generator) in the blue LED treatment followed by the red LED treatment reflects the higher O_2^{-1} scavenging potential. Subsequently, the generated H_2O_2 will be eliminated by the action of GPX and CAT (H_2O_2 scavengers) (Shohael et al., 2006). These enzymes were also markedly increased upon irradiation with the blue LED and red LED than the control (**Figure 4**). Along with the above-mentioned enzymes, APX, an important enzyme involved in the ascorbate–glutathione cycle, also plays a vital role in H_2O_2 elimination. In the present study, the APX activity also followed the same trend as the other antioxidant enzymes. Similarly, the PAL enzyme activity was also increased in the blue and red LED treatments. The PAL is a key enzyme responsible for the synthesis of phenols and flavonoids *via* the phenylpropanoid pathway. Earlier reports suggested that the

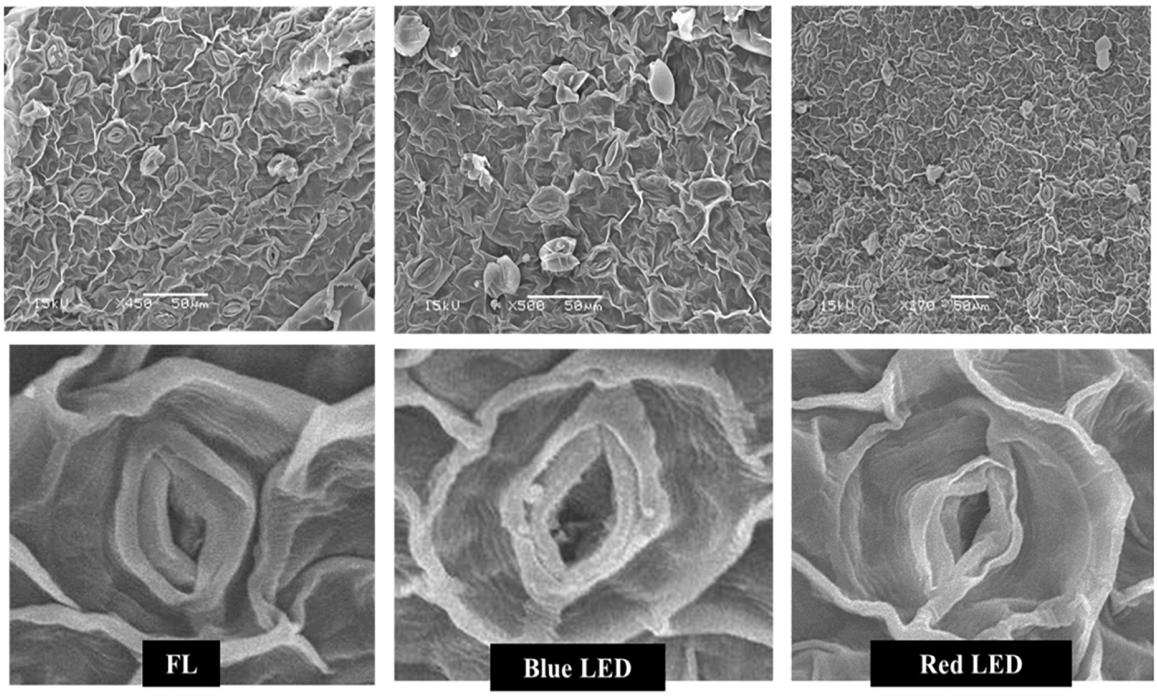

FIGURE 2 | Effect of light quality on stomatal density and structure of *in vitro*-grown *S. kakudensis*.

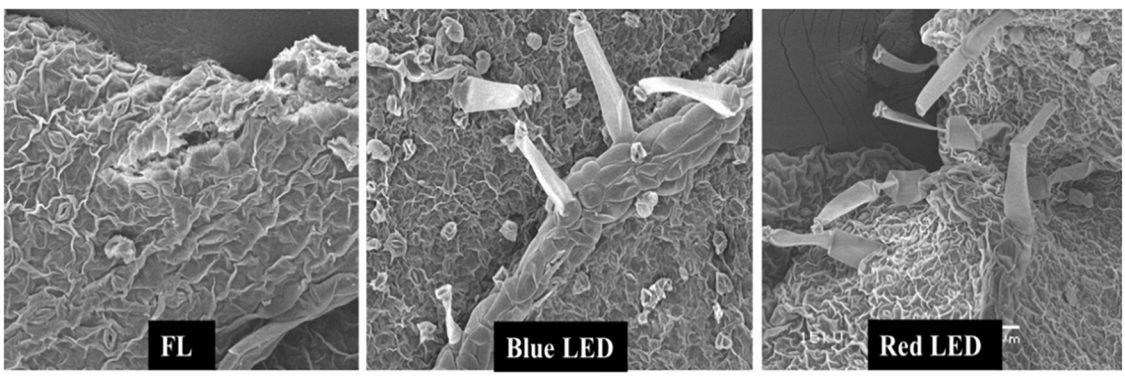

FIGURE 3 | Scanning electron micrographs of the trichomes of *in vitro*-grown *S. kakudensis* as affected by light qualities.

elevated transcriptional regulation of the PAL upon oxidative stress augments the synthesis of secondary metabolites (Zhan et al., 2012). Similarly, the supplementation of combinations of red and blue lights increased the activities of antioxidant enzymes in the *in vitro* plants of *Carpesium triste* (Zhao et al., 2020) and in the callus cultures of *Cinidium officinale* (Adil et al., 2019).

Influence of Light Qualities on the Contents of Secondary Metabolites

The light quality-mediated elicitation of secondary metabolites has gained importance in recent days, especially in medicinal plants (Alvarenga et al., 2015; Manivannan et al., 2015a). The light-mediated elicitation of phenols and flavonoids has been reported by Samuoliene et al. (2012) in lettuce. In this experiment, the contents of total phenols and flavonoids were found to be markedly higher in the blue LED treatment, followed by the red LED treatment (**Figure 5**). Notably, the blue LED immensely increased the total phenols (55.14% higher than the FL) and flavonoids (65.68% higher than the FL). The red LED treatment also resulted in the elicitation of phenols and flavonoids to 31.91 and 40.79%, respectively, than the FL. Ballaré (2014) reported that light signal influences the accumulation of phytochemicals by modulating the phenylpropanoid pathway. In general, majority of the secondary metabolites like phenols are synthesized *via* the phenylpropanoid pathway. Moreover, the accumulation of phenolic compounds by light-induced regulation of the PAL is considered as a vital mechanism behind

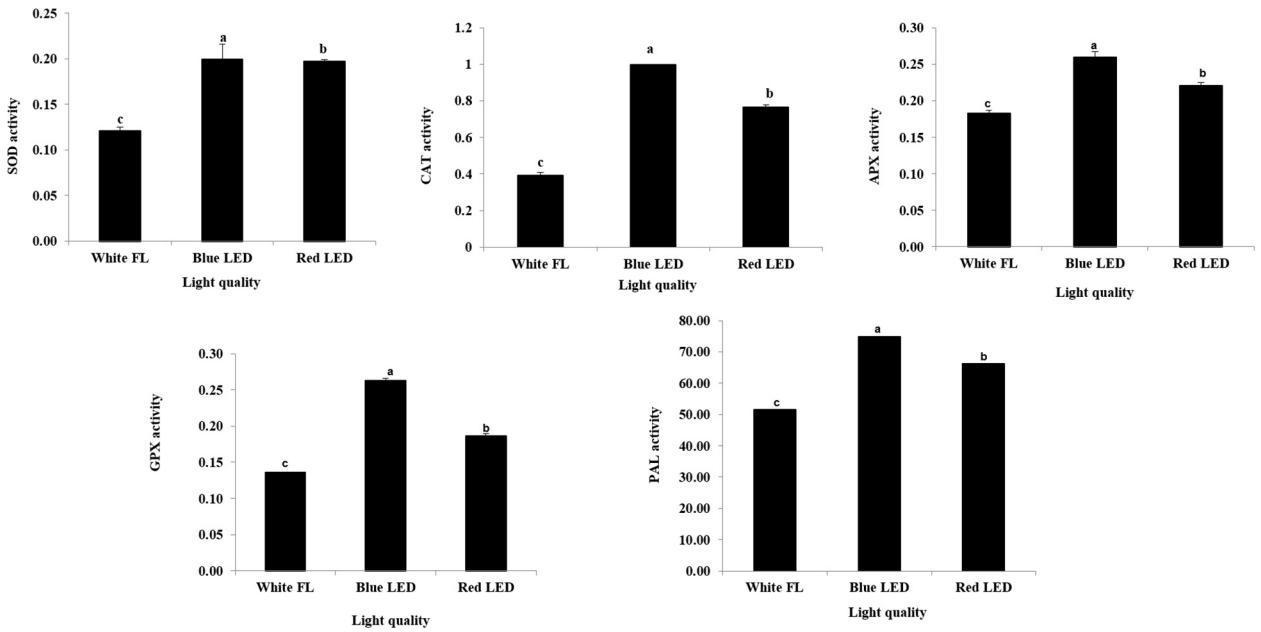

FIGURE 4 | Modulation antioxidant enzyme activities upon different light quality treatments. Data are the mean ± SE from three replicates. Different letter(s) in one measurement indicates statistically significant difference at $P \leq 0.05$ by Duncan's multiple-range test.

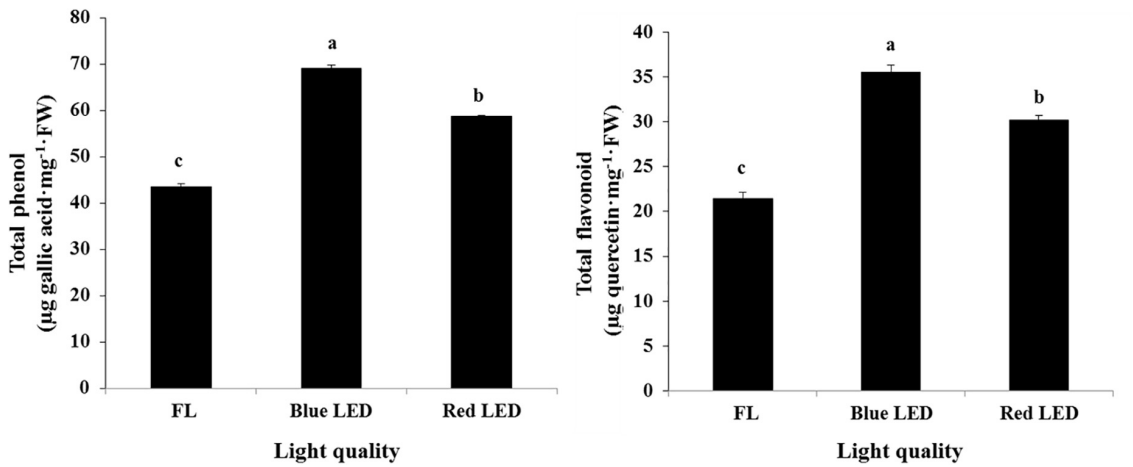

FIGURE 5 | Enhancement of total phenols and flavonoids in *S. kakudensis* upon different light quality treatments. The units of the enzymes are as follows: SOD activity (nmol NBT min^{-1} mg^{-1} protein), CAT activity (nmol H_2O_2 min^{-1} mg^{-1} protein), APX activity (nmol ascorbate oxidized min^{-1} mg^{-1} protein), GPX activity (nmol guaical min^{-1} mg^{-1} protein), and PAL activity (μmol cinnamic acid h^{-1} mg^{-1} FW). Data are the mean ± SE from three replicates. Different letters in one measurement indicate statistically significant difference at $P \leq 0.05$ by Duncan's multiple-range test.

the phytochemical elicitation (Koyama et al., 2012). This enzyme controls the biosynthesis of polyphenols by catalyzing the flux of primary metabolites into the phenylpropanoid biosynthetic pathway. Furthermore, the transcript levels of the PAL, chalcone synthase, chalcone isomerase, flavone-3-hydroxylase, flavonol synthase, flavonoid-3′-hydroxylase, anthocyanidin synthase, and dihydroflavonol-4 reductase, the key enzymes involved in the biosynthesis of important secondary metabolites, have been significantly influenced by light quality in plants (Quideau et al., 2011; Koyama et al., 2012). In *A. bracteosa*, blue light enhanced the accumulation of total polyphenol contents (Ali et al., 2019). Overall, the results illustrate the indispensable roles of red and blue LEDs over the conventional FL for the enhancement of secondary metabolites in *S. kakudensis*.

Influence of Light Qualities on Protein Expression

In addition to the above-mentioned physiological and biochemical factors, proteomics tools were utilized to investigate

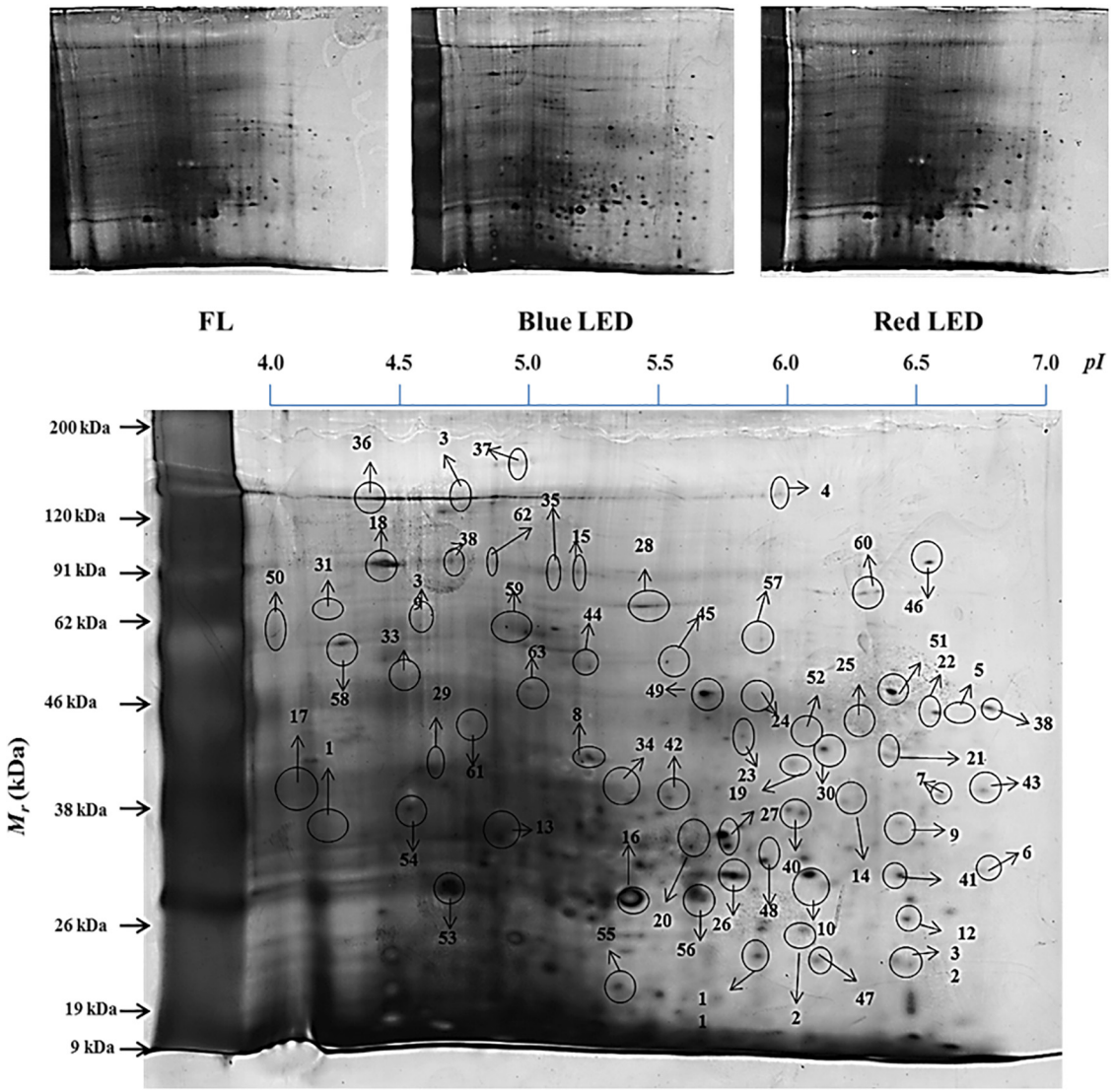

FIGURE 6 | Leaf protein profiles of *S. kakudensis* upon different light quality treatments and the master gel representation (obtained from the blue LED treatment) with identified protein spots.

the effect of light quality on *S. kakudensis* leaves (**Figure 6**). The comparative analysis of 2-DE gels analyzed by Progenesis SameSpots TotalLab (New Castle, United Kingdom) detected about 455 protein spots and was reproducibly resolved among the three replicates. Among the resolved spots, 149 protein spots were differentially expressed with more than 2.0-folds change. From the analyzed 149 spots, proteins from 63 spots were identified using MALDI-TOF-MS (ABI4800, Applied Biosystems, MA, United States). **Table 2** shows the list of identified proteins along with the corresponding spot ID, nominal mass, theoretical and calculated *pI*, accession number, MASCOT score, and sequence coverage percentage. The sequence coverage percentages of the identified proteins were in the range of 14–100%. Variation in light quality up-regulated the proteins involved in several metabolic processes, and the putative functional characterization is illustrated in **Figure 7**. The blue LED and red LED treatments up-regulated the expression levels of 30 and 25 proteins, respectively. However, the FL treatment increased the abundance of 13 protein spots.

Among the treatments, the monochromatic blue light significantly enhanced the expressions of 30 protein spots. The albino-3-like protein (spot 1), which plays a vital role in the insertion of the light-harvesting complex (LHC) proteins into the thylakoid membrane, was up-regulated by blue light. In addition, the protein is essential for the assembly and activity of LHC I and II. The abundance of a nitrogen-fixing NifU domain containing a protein (spot 2) also increased upon blue LED treatment. Chloroplastic NifU-like proteins act as molecular scaffolds in the biosynthesis of iron–sulfur clusters in plants. In *Arabidopsis*, the mutation in NifU protein resulted in the

TABLE 2 | Differentially expressed proteins identified using the MALDI-TOF MS from the leaf proteome.

Spot no.[a]	Accession number	Nominal mass (M_r)[b]	Theoretical *pI*[c]	Protein identification	Species	Sequence coverage (%)	Mascot score	Fold[d]
1	KHN29290	30,653	7.55	$ALBINO_3$-like protein 2, chloroplastic	*Glycine soja*	30	68	2.5
2	XP_007510766	32,506	6.86	Nitrogen-fixing NifU domain protein	*Bathycoccus prasinos*	56	44	3.8
3	XP_002532859	25,792	6.11	Proteasome subunit alpha type, putative	*Ricinus communis*	48	50	2.7
4	AAP46638	108,300	8.16	PG1	*Hordeum vulgare*	56	52	5.7
5	XP_007015404	27,608	5.93	20S proteasome alpha subunit G1	*Theobroma cacao*	34	49	2.4
6	AAY62983	23,313	10.24	Small ribosomal protein subunit 4, partial	*Caribaeohypnum polypterum*	48	48	6.5
7	NP_564622	34,819	9.11	RNA-binding S4 domain-containing protein	*Arabidopsis thaliana*	49	36	5.7
8	XP_003058724	31,202	9.40	NADPH-dependent 1-acyldihydroxyacetone phosphate reductase-like	*Erythranthe guttatus*	43	44	2.8
9	XP_012832543	5,912	12.49	Transmembrane protein, putative	*Medicago truncatula*	74	46	6.3
10	ACJ74207	7,631	8.04	LEA-like protein	*Solanum tuberosum*	63	35	2.1
11	EMS51364	3,387	11.01	RNA polymerase II second largest subunit	*Rhododendron viscistylum*	100	35	4.1
12	XP_011047745	90,784	5.73	Nuclear valosin-containing protein-like isoform X1	*Populus euphratica*	59	57	5.4
13	AAU88175	10,369	9.98	Disease resistance-like protein	*Coffea wightiana*	76	45	5.4
14	KMZ70332	41,940	6.56	Glyoxylate/hydroxypyruvate reductase B	*Zostera marina*	50	43	6.8
15	KMZ55951	106,021	6.18	Villin-3	*Zostera marina*	15	43	3.6
16	XP_008386513	28,563	9.40	tRNA 2′-phosphotransferase 1-like	*Malus domestica*	27	53	4.1
17	XP_010088475	27,514	5.93	Proteasome subunit alpha type-3	*Morus notabilis*	62	48	4.9
18	XP_003602824	23,398	5.54	14-3-3-like protein	*Medicago truncatula*	39	52	2.6
19	EMS62457	53,837	5.53	Aldehyde dehydrogenase family 2 member C4	*Triticum urartu*	21	45	5.1
20	XP_004979712	12,518	8.93	ER-localized cyclophilin, partial	*Triticum urartu*	56	45	4.9
21	NP_564622	34,819	9.11	RNA-binding S4 domain-containing protein	*Arabidopsis thaliana*	30	48	4.8
22	BAF01042	19,490	6.60	ACD-ScHsp26-like protein	*Tamarix hispida*	58	46	2.5
23	XP_007029049	83,906	5.99	P-loop containing nucleoside triphosphate hydrolases superfamily protein isoform 2, partial	*Theobroma cacao*	19	53	4.0
24	ABR25818	5,672	4.60	Phenylalanine ammonia-lyase, partial	*Oryza sativa Indica*	100	40	3.5
25	NP_180077	123,947	8.65	Actin-binding FH2 protein	*Arabidopsis thaliana*	32	51	3.6
26	KHN11740	12,360	6.41	Heat shock 22-kDa protein, mitochondrial	*Glycine soja*	88	51	4.5
27	AAC39472	64,970	6.22	Vacuolar protein sorting homolog	*Arabidopsis thaliana*	14	57	3.8
28	P31843	16,960	6.90	RNA-directed DNA polymerase homolog	*Oenothera berteroana*	44	54	4.4
29	NP_001150821	51,409	8.67	CIPK-like protein 1	*Zea mays*	32	53	5.0
30	XP_010094559	39,903	9.34	Protein kinase APK1B	*Morus notabilis*	36	51	3.0
31	AAS60004	2,930	11.72	Photosystem II subunit H, partial (chloroplast)	*Alstroemeria aurea*	100	40	5.2
32	AKP98463	29,663	9.61	Maturase K, partial (chloroplast)	*Duabanga grandiflora*	57	50	4.3

(Continued)

TABLE 2 | Continued

Spot no.[a]	Accession number	Nominal mass (M_r)[b]	Theoretical *pI*[c]	Protein identification	Species	Sequence coverage (%)	Mascot score	Fold[d]
33	AAS98723	23,263	10.19	Ribosomal protein subunit 4	*Touwiodendron diversifolium*	47	47	5.5
34	AES94384	16,893	7.68	RAB GTPase-like protein B1C	*Medicago truncatula*	59	46	3.3
35	XP_001417143	128,844	5.53	Predicted protein	*Ostreococcus lucimarinus*	32	36	3.2
36	CAB90625	41,311	9.32	Phosphoenolpyruvate carboxylase	*Dendrobium loddigesii*	52	48	4.0
37	XP_010091954	50,674	9.72	Chloroplastic group IIA intron splicing facilitator	*Morus notabilis*	49	56	5.2
38	AFA51060	21,277	5.73	RB protein, partial	*Solanum microdontum*	50	47	4.5
39	XP_004290877	12,296	7.79	Acetyltransferase At1g77540	*Fragaria vesca* subsp. *vesca*	88	45	4.4
40	XP_003598507	43,923	6.87	Patellin, partial	*Medicago truncatula*	22	47	7.9
41	XP_010253868	40,572	9.63	Thylakoid ADP, ATP carrier protein, chloroplastic	*Nelumbo nucifera*	42	54	5.1
42	ABU88982	56,588	9.29	Phospholipid/glycerol acyltransferase	*Helianthus annuus*	39	44	6.9
43	KEH24073	19,979	8.57	F-box protein interaction domain protein	*Medicago truncatula*	49	45	6.1
44	AFC90234	34,139	9.22	Nucleotide-binding site leucine-rich repeat protein	*Rhododendron formosanum*	53	41	6.9
45	AIU48049	43,923	6.87	Structural maintenance of chromosomes protein, partial	*Theobroma cacao*	32	42	7.2
46	AAW69888	22,267	10.19	Small ribosomal protein 4	*Zygodon bartramioides*	59	44	4.3
47	BAH80000	23,730	5.61	Putative retrotransposon protein	*Oryza sativa Indica*	50	52	6.0
48	BAD62243	49,128	11.60	Zinc knuckle domain-like	*Oryza sativa Japonica*	73	47	4.3
49	CCA60911	37,841	6.96	Phosphoenolpyruvate carboxylase, partial	*Chasmanthium latifolium*	28	44	3.4
50	AES70881	21,466	9.20	UTP-glucose-1-phosphate uridylyltransferase	*Medicago truncatula*	52	57	5.3
51	KHG14889	47,709	8.77	Advillin	*Gossypium arboreum*	45	49	4.4
52	XP_010111987	69,444	5.50	Exocyst complex component 7	*Morus notabilis*	53	56	2.2
53	CAB86074	53,160	5.65	Importin alpha-like protein	*Arabidopsis thaliana*	26	46	5.7
54	NP_567284	12,053	9.51	Putative copper transport protein	*Arabidopsis thaliana*	58	42	4.4
55	XP_003598507	50,425	9.22	DNA methyltransferase 1-associated protein,	*Ricinus communis*	50	42	4.1
56	XP_002955677	20,823	9.46	Ribulose-1,5-bisphosphate carboxylase/oxygenase	*Volvox carteri*	33	43	6.2
57	KEH35435	18,308	9.46	Proline-rich cell wall-like protein	*Medicago truncatula*	42	52	5.3
58	P09003	22,878	9.53	ATP synthase protein MI25	*Nicotiana tabacum*	58	48	5.7
59	AGC78858	22,441	10.22	Mitochondrial ATPase F(0) complex, subunit 4	*Vicia faba*	63	43	3.9
60	ACP41917	10,933	8.79	RNA polymerase IV, partial	*Heliosperma insulare*	64	37	4.1
61	XP_002311057	23,881	8.52	GTP-binding family protein	*Populus trichocarpa*	58	38	4.7
62	XP_003539430	15,545	7.66	Auxin-induced protein 6B-like	*Glycine max*	36	51	4.1
63	XP_010928981	24,551	11.62	Putative glycine-rich cell wall structural protein	*Elaeis guineensis*	69	45	4.7

[a]*The spot no. corresponds to the number labeled in the protein gel images.* [b]*Theoretical molecular mass (M_r) calculated for the peptides using MASCOT peptide mass fingerprint.* [c]*Isoelectric point of the peptides calculated using MASCOT peptide mass fingerprint.* [d]*Fold change between the treatments calculated using the Progenesis Samespot 2D software v4.1 (Nonlinear Dynamics, Newcastle, United Kingdom).*

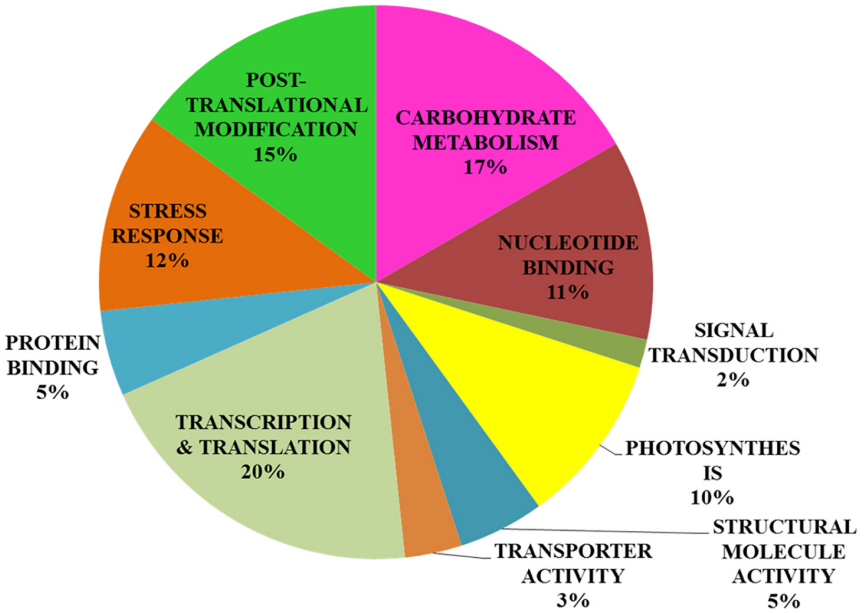

FIGURE 7 | Functional characterization of proteins identified using the matrix-assisted laser desorption/ionization–time-of-flight mass spectrometry analysis from the leaf proteome.

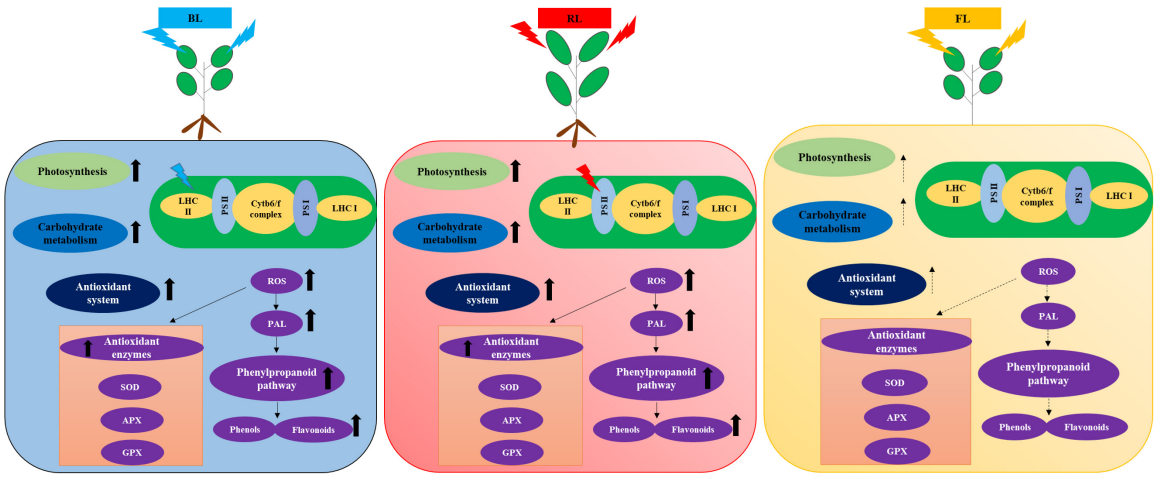

FIGURE 8 | Schematic representation of light quality-mediated effects in the photosynthesis and antioxidant system of *in vitro*-grown *S. kakudensis* hypothesized based on the outcomes of the present study. Blue light-mediated influence on the light harvesting complex II (LHC II) and red light-mediated influence on photosystem II (PS II) on the electron transport chain have been depicted based on the proteomics results. Cytb6/f complex, cytochromeb6/f complex; PS I, photosystem; PS II, photosystem II; LHC II, light-harvesting complex II; LHC I, light-harvesting complex I; SOD, superoxide dismutase; APX, ascorbate peroxidase; GPX, guaiacol peroxidase; ROS, reactive oxygen species; PAL, phenylalanine ammonia lyase.

impairment of photosynthetic electron transport and reduction of steady-state levels of photosystem I (Yabe et al., 2004). Thus, the increase in NifU protein levels in the blue LED treatment could have contributed to the enhancement of the photosynthetic mechanism in *S. kakudensis*. In addition, blue light increased the expression levels of proteasome subunits (spots 3, 5, and 17), indicating the occurrence of a stress response. In general, the 20S proteasome is composed of α and β subunits within which the target proteins are degraded to short peptides *via* a threonine protease activity (Belknap and Garbarino, 1996). The up-regulation of proteasome subunits was observed upon several abiotic stress conditions. Moreover, the blue LED treatment increased the levels of the late embryogenesis abundant (LEA) protein (spot 10). LEA was associated with resistance to various forms of stress, in particular, water stress, desiccation stress, and heat stress (Tunnacliffe and Wise, 2007). The up-regulation of RNA polymerase II (spot 11) in the blue light treatment indicated the transcriptional activation of vital genes involved

in the photosynthesis process. The enhancement in the level of phenylalanine ammonia lyase (PAL) (spot 24), an important rate-limiting enzyme in the phenylpropanoid pathway responsible for the synthesis of secondary metabolites such as phenols and flavonoids, corresponds with previous reports suggesting the elicitation of the transcripts of PAL upon the blue and red LED treatment (Rahman et al., 2015). The PAL activity tested in this experiment and the phenol contents correlate with the proteomics result. In addition, the increase in the abundance of ACD-ScHSP26 (spot 22) and heat shock protein (spot 26) also illustrates the occurrence of light-mediated stress that caused the stimulation of molecular chaperones to repair the incorrect protein folding. Protein kinase (spot 30) plays an important role in the phosphorylation of proteins. The phosphorylation of proteins can be triggered by photoreceptors, the light-signaling molecules according to Smith (2000).

In addition to the above mentioned proteins, blue light also up-regulated the expression levels of proteins such as the actin-binding FH2 protein, vacuolar protein sorting homolog, CIPK-like protein, patellin, F-box protein interaction domain, nucleotide-binding site leucine-rich repeat protein, structural maintenance of chromosome, advillin, DNA methyl transferase-1-associated protein, and mitochondrial ATPase F(0) complex. Thus, blue light imposed a stressful environment that resulted in the activation of several proteins related to stress tolerance, photosynthesis, gene regulation, post-translational modification, and secondary metabolism in *S. kakudensis*. The blue LED treatment enhanced the accumulation of phosphoenol pyruvate carboxylase (spot 36). Phosphoenol pyruvate carboxylase is a rate-limiting enzyme involved in the carbon fixation process and Crassulacean acid metabolism, a well-known adaptation mechanism in plants, especially under water stress conditions (Cushman et al., 1989). The stimulation of phosphoenol pyruvate was reported as an important strategy adopted by plants to combat the energy expense during stress (Cushman et al., 1989).

The irradiance of red LED increased the expression of small ribosomal protein (spot 6) and disease resistance protein (spot 13) which play vital roles in protein synthesis to overcome the oxidative stress caused by the external environment. Glyoxylate/hydroxyl pyruvate reductase B (spot 14) catalyzes the NADPH-dependent reduction of glyoxylate and hydroxypyruvate into glycolate and glycerate, respectively. It is indispensable for the mediation of the passage of carbons through the carbon oxidation pathway during photorespiration (Givan and Kleczkowski, 1992). In addition, red light enhanced the levels of photosystem II subunit (spot 31). PS II is a vital multi-protein enzyme involved in the photosynthetic process. Thus, the enhancement of PS II protein could improve photosynthesis. Overall, in the red LED treatment, the protein increases were associated primarily with photosynthesis, carbohydrate metabolism, protein repair, and stress resistance.

On the other hand, FL treatment improved the expressions of proteins involved in carbon fixation and photosynthesis, namely, the NADPH-dependent acyldihydroxyacetone phosphate reductase (spot 8) and phosphoenol pyruvate carboxylase (spot 49). Moreover, the GTP-binding family protein (spot 61), small ribosomal protein (spot 46), ER-localized cyclophilin (spot 20), phospholipid/glycerol acyltransferase (spot 42), exocyst complex component (spot 52), RNA polymerase IV (spot 60), auxin-induced protein (spot 62), and putative glycine-rich cell wall structural protein 1 (spot 63) were significantly increased in the control FL treatment. Thus, the regulation of the above-mentioned proteins involved in photosynthesis, post-translational modification, carbohydrate metabolism, development, and stress resistance process provides a molecular insight into the light quality-induced protein expression modulation in *S. kakudensis* leaf.

Taken together, the light quality-mediated photomorphogenesis process could facilitate the *in vitro* culture of medicinal plants like *S. kakudensis*. Moreover, the tailored use of blue and red LED lights can be utilized for the improvement of photosynthesis, photomorphogenesis, gene expression, and regulation of various metabolisms (Batista et al., 2018). The supplementation of different light qualities tends to activate the photoreceptors in plants such as red light-responsive phytochromes and blue light-mediated cryptochromes and phototrophins. These photoreceptors influence the photochemical control of various gene expressions, leading to the regulation of functional proteins in various metabolic pathways involved in the biosynthesis of primary and secondary metabolites (Batista et al., 2018). In addition, the *in vitro* culture environment poses a certain level of stress to the explants which also acts as trigger for the activation of diverse antioxidant systems in plants, leading to the elicitation of secondary metabolites with nutraceutical values. Based on the physiological, biochemical, and proteomic analysis, the application of monochromatic blue and red light influenced the photosynthetic and antioxidant system by inducing oxidative stress. The generation of excess ROS has resulted in the elicitation of antioxidant activity, which increased the contents of protective phytochemicals such as phenols and flavonoids (**Figure 8**). The proteomic analysis showed that blue and red light-mediated modulation of proteins is involved in photosynthesis, carbohydrate metabolism, and oxidative stress. Overall, the stress alleviation mechanism rendered the elicitation of secondary metabolites with medicinal value, and the red and blue lights also contributed to the physiological improvement of *S. kakudensis*.

CONCLUSION

Application of novel approaches to enhance the micropropagation of indigenous medicinal plants has been increasing in recent days. In the present study, the impact of blue and/or red LEDs on the growth, accumulation of secondary metabolites, activities of antioxidant enzymes, and protein expression of *in vitro*-grown *S. kakudensis* has been demonstrated. The outcomes suggested that the blue or red LEDs can be utilized for the improvement of *in vitro* propagation of *S. kakudensis*. Moreover, the incorporation of red and blue LEDs elicited the synthesis of secondary metabolites in *S. kakudensis*. Taken together, the light qualities can be considered as an important abiotic elicitation cue for the production of secondary metabolites with therapeutic

values. A better understanding of the molecular regulation of light quality-mediated changes at the protein level could facilitate the development of environmentally controlled regime for the production of medicinal plants with better physiological and phytochemical traits.

DATA AVAILABILITY STATEMENT

The original contributions generated for this study are included in the article/supplementary material, further inquiries can be directed to the corresponding author.

AUTHOR CONTRIBUTIONS

AM and BJ designed the experiments. AM and PS performed the experiments. AM wrote the manuscript. YP assisted in the SEM and phytochemical analysis. All authors have proofread and finalized the manuscript.

ACKNOWLEDGMENTS

PS was supported by a scholarship from the BK21 Plus Program, the Ministry of Education, South Korea.

REFERENCES

Adil, M., Ren, X., and Jeong, B. R. (2019). Light elicited growth, antioxidant enzymes activities and production of medicinal compounds in callus culture of *Cnidium officinale* Makino. *J. Photochem. Photobiol. B Biol.* 196:111509. doi: 10.1016/j.jphotobiol.2019.05.006

Ali, H., Khan, M. A., Kayani, W. K., Dilshad, E., Rani, R., and Khan, R. S. (2019). Production of biomass and medicinal metabolites through adventitious roots in *Ajuga bracteosa* under different spectral lights. *J. Photochem. Photobiol. B Biol.* 193, 109–117. doi: 10.1016/j.jphotobiol.2019.02.010

Alvarenga, I. C. A., Pacheco, F. V., Silva, S. T., Bertolucci, S. K. V., and Pinto, J. E. B. P. (2015). In vitro culture of *Achillea millefolium* L.: quality and intensity of light on growth and production of volatiles. *Plant Cell Tissue Organ. Cult.* 122, 299–308. doi: 10.1007/s11240-015-0766-7

Arney, S. E., and Mitchell, D. L. (1969). The effect of abscisic acid on stem elongation and correlative inhibition. *New Phytol.* 68, 1001–1015. doi: 10.1111/j.1469-8137.1969.tb06500.x

Ballaré, C. L. (2014). Light regulation of plant defense. *Annu. Rev. Plant Biol.* 65, 335–363. doi: 10.1146/annurev-arplant-050213-040145

Batista, D. S., Felipe, S. H. S., Silva, T. D., de Castro, K. M., Mamedes-Rodrigues, T. C., Miranda, N. A., et al. (2018). Light quality in plant tissue culture: does it matter? *Vitro Cell. Dev. Biol. Plant* 54, 195–215. doi: 10.1007/s11627-018-9902-5

Belknap, W. R., and Garbarino, J. E. (1996). The role of ubiquitin in plant senescence and stress responses. *Trends Plant Sci.* 1, 331–335. doi: 10.1016/s1360-1385(96)82593-0

Bradford, M. M. (1976). A rapid and sensitive method for the quantitation of microgram quantities of protein utilizing the principle of protein-dyebinding. *Anal. Biochem.* 72, 248–254. doi: 10.1016/0003-2697(76)90527-3

Cakmak, I., and Marschner, H. (1992). Magnesium deficiency and high light intensity enhance activities of superoxide dismutase, ascorbate peroxidase, and glutathione reductase in bean leaves. *Plant Physiol.* 98, 1222–1227. doi: 10.1104/pp.98.4.1222

Canamero, R. C., Bakrim, N., Bouly, J. P., Garay, A., Dudkin, E. E., Habricot, Y., et al. (2006). Cryptochrome photoreceptors cry1 and cry2 antagonistically regulate primary root elongation in *Arabidopsis thaliana*. *Planta* 224, 995–1003. doi: 10.1007/s00425-006-0280-6

Chen, C. C., Lee, M. R., Wu, C. R., Ke, H. J., Xie, H. M., Tsay, H. S., et al. (2020). LED lights affecting morphogenesis and isosteroidal alkaloid contents in *Fritillaria cirrhosa* D. Don—an important Chinese medicinal herb. *Plants* 9:1351. doi: 10.3390/plants9101351

Cheynier, V., Comte, G., Davies, K. M., Lattanzio, V., and Martens, S. (2013). Plant phenolics: recent advances on their biosynthesis, genetics, and ecophysiology. *Plant Physiol. Biochem.* 72, 1–20. doi: 10.1016/j.plaphy.2013.05.009

Cushman, J. C., Meyer, G., Michalowski, C. B., Schmitt, J. M., and Bohnert, H. J. (1989). Salt stress leads to differential expression of two isogenes of phosphoenolpyruvate carboxylase during crassulacean acid metabolism induction in the common ice plant. *Plant Cell* 1, 715–725. doi: 10.2307/3868962

de Hsie, B. S., Bueno, A. I. S., Bertolucci, S. K. V., de Carvalho, A. A., da Cunha, S. H. B., Martins, E. R., et al. (2019). Study of the influence of wavelengths and intensities of LEDs on the growth, photosynthetic pigment, and volatile compounds production of *Lippia rotundifolia* Cham in vitro. *J. Photochem. Photobiol. B Biol.* 198, 111577. doi: 10.1016/j.jphotobiol.2019.111577

Dong, C., Fu, Y., Liu, G., and Liu, H. (2014). Growth, photosynthetic characteristics, antioxidant capacity and biomass yield and quality of wheat (*Triticum aestivum* L.) exposed to LED light sources with different spectra combinations. *J. Agro. Crop Sci.* 200, 219–230. doi: 10.1111/jac.12059

Giannopolitis, C. N., and Ries, S. K. (1977). Superoxide dismutases. *Plant Physiol.* 59, 309–314.

Gill, S. S., and Tuteja, N. (2010). Reactive oxygen species and antioxidant machinery in abiotic stress tolerance in crop plants. *Plant Physiol. Biochem.* 48, 909–930. doi: 10.1016/j.plaphy.2010.08.016

Givan, C. V., and Kleczkowski, L. A. (1992). The enzymic reduction of glyoxylate and hydroxypyruvate in leaves of higher plants. *Plant Physiol.* 100, 552–556. doi: 10.1104/pp.100.2.552

Goins, G. D., Ruffe, L. M., Cranston, N. A., Yorio, N. C., Wheeler, R. M., and Sager, J. C. (2001). *Salad Crop Production Under Different Wavelengths of Red Light-Emitting Diodes (LEDs).* SAE Technical Paper No. 2001-01-2422. Available online at: https://doi.org/10.4271/2001-01-2422 (Accessed July 9, 2001).

Heringer, A. S., Reis, R. S., Passamani, L. Z., de Souza-Filho, G. A., Santa-Catarina, C., and Silveira, V. (2017). Comparative proteomics analysis of the effect of combined red and blue lights on sugarcane somatic embryogenesis. *Acta Physiol. Plant.* 39:52.

Im Chung, S., Kang, M. Y., and Lee, S. C. (2020). The growth and enhancement of functional ingredients for health improvement of perilla leaves using LED light source with QD application. *J. Crop Sci. Biotechnol.* 23, 163–169. doi: 10.1007/s12892-019-0361-0

Kim, S. J., Hahn, E. J., and Heo, J. W. (2004). Effects of LEDs on net photosynthetic rate, growth and leaf stomata of chrysanthemum plantlets in vitro. *Sci. Hort.* 101, 143–151. doi: 10.1016/j.scienta.2003.10.003

Koyama, K., Ikeda, H., Poudel, P. R., and Goto-Yamamoto, N. (2012). Light quality affects flavonoid biosynthesis in young berries of *Cabernet Sauvignon* grape. *Phytochemistry* 78, 54–64. doi: 10.1016/j.phytochem.2012.02.026

Kozai, T., Kubota, C., and Jeong, B. R. (1997). Environmental control for the large-scale production of plants through in vitro techniques. *Plant Cell Tissue Organ. Cult.* 51, 49–56.

Kumaran, A., and Karunakaran, R. J. (2007). In vitro antioxidant activities of methanol extracts of five *Phyllanthus* species from India. *LWT Food Sci. Technol.* 40, 344–352. doi: 10.1016/j.lwt.2005.09.011

Lazzarini, L. E. S., Bertolucci, S. K. V., Pacheco, F. V., dos Santos, J., Silva, S. T., de Carvalho, A. A., et al. (2018). Quality and intensity of light affect *Lippia gracilis* Schauer plant growth and volatile compounds in vitro. *Plant Cell Tissue Organ. Cult.* 135, 367–379. doi: 10.1007/s11240-018-1470-1

Li, H., Tang, C., Xu, Z., Liu, X., and Han, X. (2012). Effects of different light sources on the growth of non-heading Chinese cabbage (*Brassica campestris* L.). *J. Agr. Sci.* 4:262.

Li, Q., and Kubota, C. (2009). Effects of supplemental light quality on growth and phytochemicals of baby leaf lettuce. *Environ. Exp. Bot.* 67, 59–64. doi: 10.1016/j.envexpbot.2009.06.011

Liakoura, V., Stefanou, M., Manetas, Y., Cholevas, C., and Karabourniotis, G. (1997). Trichome density and its UV-B protective potential are affected by shading and leaf position on the canopy. *Environ. Exp. Bot.* 38, 223–229. doi: 10.1016/s0098-8472(97)00005-1

Macedo, A. F., Leal-Costa, M. V., Tavares, E. S., Lage, C. L. S., and Esquibel, M. A. (2011). The effect of light quality on leaf production and development of in vitro-cultured plants of *Alternanthera brasiliana* Kuntze.Environ. *Expt. Bot.* 70, 43–50. doi: 10.1016/j.envexpbot.2010.05.012

Manivannan, A., Soundararajan, P., Halimah, N., Ko, C. H., and Jeong, B. R. (2015a). Blue LED light enhances growth, phytochemical contents, and antioxidant enzyme activities of *Rehmannia glutinosa* cultured in vitro. *Hort. Environ. Biotechnol.* 56, 105–113. doi: 10.1007/s13580-015-0114-1

Manivannan, A., Soundararajan, P., Park, Y. G., and Jeong, B. R. (2015b). In vitro propagation, phytochemical analysis, and evaluation of free radical scavenging property of *Scrophularia kakudensis* Franch tissue extracts. *BioMed Res. Int.* 2015:480564. doi: 10.1155/2015/480564

Mengxi, L., Zhigang, X., Yang, Y., and Yijie, F. (2011). Effects of different spectral lights on Oncidium PLBs induction, proliferation, and plant regeneration. *Plant Cell Tissue Organ. Cult.* 106, 1–10. doi: 10.1007/s11240-010-9887-1

Mirzahosseini, Z., Shabani, L., Sabzalian, M. R., and Dayanandan, S. (2020). Comparative physiological and proteomic analysis of Arabidopsis thaliana revealed differential wound stress responses following the exposure to different LED light sources. *Environ. Exp. Bot.* 169:103895. doi: 10.1016/j.envexpbot.2019.103895

Mujib, A., Tonk, D., and Ali, M. (2014). Plant regeneration from protoplasts in Indian local *Coriandrum sativum* L.: scanning electron microscopy and histological evidences for somatic embryogenesis. *Plant Cell Tissue Organ Cult.* 117, 323–334. doi: 10.1007/s11240-014-0442-3

Muneer, S., Ko, C. H., Prabhakaran, S., Manivnnan, A., Park, Y. G., and Jeong, B. R. (2015). Proteomic study related to vascular connections in watermelon scions grafted onto bottle-gourd rootstock under different light intensities. *PLoS One* 1:e0120899. doi: 10.1371/journal.pone.0120899

Murashige, T., and Skoog, F. (1962). A revised medium of rapid growth and bioassay with tobacco tissue cultures. *Physiol. Plant.* 15, 473–497. doi: 10.1111/j.1399-3054.1962.tb08052.x

Nakan, Y., and Asada, K. (1981). Hydrogen peroxide is scavenged by ascorbate-specific peroxidase in spinach chloroplasts. *Plant Cell Physiol.* 22, 867–880.

Nishimura, T., Ohyama, K., Goto, E., and Inagaki, N. (2009). Concentration of perillaldehyde, limonene, and anthocyanin of Perilla plants as affected by light quality under controlled environments. *Sci. Hort.* 122, 134–137. doi: 10.1016/j.scienta.2009.03.010

Park, S. Y., Bae, J. H., and Oh, M. M. (2020). Manipulating light quality to promote shoot growth and bioactive compound biosynthesis of *Crepidiastrum denticulatum* (Houtt.) Pak & Kawano cultivated in plant factories. *J. Appl. Res. Med. Aromat. Plants* 16:100237. doi: 10.1016/j.jarmap.2019.100237

Park, Y. G., Park, J. E., Hwang, S. J., and Jeong, B. R. (2012). Light source and CO_2 concentration affect growth and anthocyanin content of lettuce under controlled environment. *Hort. Environ. Biotechnol.* 53, 460–466. doi: 10.1007/s13580-012-0821-9

Piątczak, E., Kuźma, Ł, Kozłowska, W., Lisiecki, P., Szemraj, M., Płachno, B. J., et al. (2020). Phenylethanoid and iridoid glycosides production in *Rehmannia elata* NE Brown ex Prein. in vitro shoot cultures and their biological activity. *Ind. Crops Prod.* 158:113050. doi: 10.1016/j.indcrop.2020.113050

Quideau, S., Deffieux, D., Douat−Casassus, C., and Pouységu, L. (2011). Plant polyphenols: Chemical properties, biological activities, and synthesis. *Angew. Chem. Int. Ed. Engl.* 50, 586–621. doi: 10.1002/anie.201000044

Rahman, A., Wallis, C., and Uddin, W. (2015). Silicon induced systemic defense responses in perennial ryegrass against infection by *Magnaporthe oryzae*. *Phytopathology* 105, 748–757. doi: 10.1094/phyto-12-14-0378-r

Samuoliene, G., Sirtautas, R., Brazaityte, A., and Duchovskis, P. (2012). LED lighting and seasonality effects antioxidant properties of baby leaf lettuce. *Food Chem.* 134, 1494–1499. doi: 10.1016/j.foodchem.2012.03.061

Shah, K., Kumar, R. G., Verma, S., and Dubey, R. S. (2001). Effect of cadmium on lipid peroxidation, superoxide anion generation and activities of antioxidant enzymes in growing rice seedlings. *Plant Sci.* 161, 1135–1144. doi: 10.1016/s0168-9452(01)00517-9

Sharma, A., Shahzad, B., Rehman, A., Bhardwaj, R., Landi, M., and Zheng, B. (2019). Response of phenylpropanoid pathway and the role of polyphenols in plants under abiotic stress. *Molecules* 24:2452. doi: 10.3390/molecules24132452

Shohael, A. M., Ali, M. B., Yu, K. W., Hahn, E., Islam, R., and Paek, K. Y. (2006). Effect of light on oxidative stress, secondary metabolites and induction of antioxidant enzymes in *Eleutherococcus senticosus* somatic embryos in bioreactor. *Process Biochem.* 41, 1176–1185.

Silva, S. T., Bertolucci, S. K. V., da Cunha, S. H. B., Lazzarini, L. E. S., Tavares, M. C., and Pinto, J. E. B. P. (2017). Effect of light and natural ventilation systems on the growth parameters and carvacrol content in the in vitro cultures of *Plectranthus amboinicus* (Lour.) Spreng. *Plant Cell Tissue Organ Cult.* 129, 501–510. doi: 10.1007/s11240-017-1195-6

Silva, T. D., Batista, D. S., Fortini, E. A., de Castro, K. M., Felipe, S. H. S., Fernandes, A. M., et al. (2020). Blue and red light affects morphogenesis and 20-hydroxyecdisone content of in vitro *Pfaffia glomerata* accessions. *J. Photochem. Photobiol. B Biol.* 203:111761. doi: 10.1016/j.jphotobiol.2019.111761

Smith, H. (2000). Phytochromes and light signal perception by plants-an emerging synthesis. *Nature* 407, 585–591. doi: 10.1038/35036500

Sun, Q., Yoda, K., and Suzuki, H. (2005). Internal axial light conduction in the stems and roots of herbaceous plants.J. *Expt. Bot.* 56, 191–203.

Tanase, C., Bujor, O. C., and Popa, V. I. (2019). "Phenolic natural compounds and their influence on physiological processes in plants," in *Polyphenols in Plants*, 2nd Edn, ed. R. R. Watson (Cambridge, MA: Academic Press.), 45–58. doi: 10.1016/b978-0-12-813768-0.00003-7

Tohidi, B., Rahimmalek, M., Arzani, A., and Sabzalian, M. R. (2020). Thymol, carvacrol, and antioxidant accumulation in Thymus species in response to different light spectra emitted by light-emitting diodes. *Food Chem.* 307:125521. doi: 10.1016/j.foodchem.2019.125521

Toyomasu, T., Tsuji, H., Yamane, H., Nakayama, M., Yamaguchi, I., Murofushi, N., et al. (1993). Light effects on endogenous levels of gibberellins in photoblastic lettuce seeds. *J. Plant Growth Regul.* 12, 85–90. doi: 10.1007/bf00193238

Tunnacliffe, A., and Wise, M. J. (2007). The continuing conundrum of the LEA proteins. *Naturwissenschaften* 94, 791–812. doi: 10.1007/s00114-007-0254-y

van Gelderen, K., Kang, C., and Pierik, R. (2018). Light signaling, root development, and plasticity. *Plant Physiol.* 176, 1049–1060. doi: 10.1104/pp.17.01079

Wheeler, R. M., Mackowiak, C. L., and Sager, J. C. (1991). Soybean stem growth under high-pressure sodium with supplemental blue lighting. *Agron. J.* 83, 903–906. doi: 10.2134/agronj1991.00021962008300050024x

Yabe, T., Morimoto, K., Kikuchi, S., Nishio, K., Terashima, I., and Nakai, M. (2004). The *Arabidopsis* chloroplastic NifU-like protein CnfU, which can act as an iron-sulfur cluster scaffold protein, is required for biogenesis of ferredoxin and photosystem I. *Plant Cell* 16, 993–1007. doi: 10.1105/tpc.020511

Zhan, L., Li, Y., Hu, J. Q., Pang, L. Y., and Fan, H. P. (2012). Browning inhibition and quality preservation of fresh-cut romaine lettuce exposed to high intensity light. *Innov. Food Sci. Emerg. Technol.* 14, 70–76. doi: 10.1016/j.ifset.2012.02.004

Zhao, J., Park, Y. G., and Jeong, B. R. (2020). Light Quality Affects Growth and Physiology of *Carpesium triste* Maxim. *Cult. Vitro. Agric.* 10:258. doi: 10.3390/agriculture10070258

Conflict of Interest: The authors declare that the research was conducted in the absence of any commercial or financial relationships that could be construed as a potential conflict of interest.

Copyright © 2021 Manivannan, Soundararajan, Park and Jeong. This is an open-access article distributed under the terms of the Creative Commons Attribution License (CC BY). The use, distribution or reproduction in other forums is permitted, provided the original author(s) and the copyright owner(s) are credited and that the original publication in this journal is cited, in accordance with accepted academic practice. No use, distribution or reproduction is permitted which does not comply with these terms.

frontiers in Plant Science

ORIGINAL RESEARCH
published: 28 January 2021
doi: 10.3389/fpls.2020.611247

Blue Light Treatment but Not Green Light Treatment After Pre-exposure to UV-B Stabilizes Flavonoid Glycoside Changes and Corresponding Biological Effects in Three Different Brassicaceae Sprouts

Susanne Neugart[1], Petra Majer[2], Monika Schreiner[3] and Éva Hideg[4]*

[1] Division Quality and Sensory of Plant Products, Georg-August-Universität Göttingen, Göttingen, Germany, [2] Institute of Plant Biology, Biological Research Centre, Hungarian Academy of Sciences, Szeged, Hungary, [3] Leibniz Institute of Vegetable and Ornamental Crops e.V., Grossbeeren, Germany, [4] Department of Plant Biology, University of Pécs, Pécs, Hungary

OPEN ACCESS

Edited by:
Marie-Theres Hauser, University of Natural Resources and Life Sciences Vienna, Austria

Reviewed by:
Myung-Min OH, Chungbuk National University, South Korea
Alexei E. Solovchenko, Lomonosov Moscow State University, Russia

***Correspondence:**
Susanne Neugart
susanne.neugart@uni-goettingen.de

Specialty section:
This article was submitted to Plant Metabolism and Chemodiversity, a section of the journal Frontiers in Plant Science

Received: *28 September 2020*
Accepted: *10 December 2020*
Published: *28 January 2021*

Citation:
Neugart S, Majer P, Schreiner M and Hideg É (2021) Blue Light Treatment but Not Green Light Treatment After Pre-exposure to UV-B Stabilizes Flavonoid Glycoside Changes and Corresponding Biological Effects in Three Different Brassicaceae Sprouts. Front. Plant Sci. 11:611247. doi: 10.3389/fpls.2020.611247

Ultraviolet-B (UV-B; 280–315 nm) radiation induces the biosynthesis of secondary plant metabolites such as flavonoids. Flavonoids could also be enhanced by blue (420–490 nm) or green (490–585 nm) light. Flavonoids act as antioxidants and shielding components in the plant's response to UV-B exposure. They are shown to quench singlet oxygen and to be reactive to hydroxyl radical. The aim was to determine whether treatment with blue or green light can alter flavonoid profiles after pre-exposure to UV-B and whether they cause corresponding biological effects in Brassicaceae sprouts. Based on their different flavonoid profiles, three vegetables from the Brassicaceae were selected. Sprouts were treated with five subsequent doses (equals 5 days) of moderate UV-B (0.23 kJ m^{-2} day^{-1} $UV\text{-}B_{BE}$), which was followed with two subsequent (equals 2 days) doses of either blue (99 μmol m^{-2} s^{-1}) or green (119 μmol m^{-2} s^{-1}) light. In sprouts of kale, kohlrabi, and rocket salad, flavonoid glycosides were identified by HPLC-DAD-ESI-MS^n. Both *Brassica oleracea* species, kale and kohlrabi, showed mainly acylated quercetin and kaempferol glycosides. In contrast, in rocket salad, the main flavonol glycosides were quercetin glycosides. Blue light treatment after the UV-B treatment showed that quercetin and kaempferol glycosides were increased in the *B. oleracea* species kale and kohlrabi while—contrary to this—in rocket salad, there were only quercetin glycosides increased. Blue light treatment in general stabilized the enhanced concentrations of flavonoid glycosides while green treatment did not have this effect. Blue light treatment following the UV-B exposure resulted in a trend

of increased singlet oxygen scavenging for kale and rocket. The hydroxyl radical scavenging capacity was independent from the light quality except for kale where an exposure with UV-B followed by a blue light treatment led to a higher hydroxyl radical scavenging capacity. These results underline the importance of different light qualities for the biosynthesis of reactive oxygen species that intercept secondary plant metabolites, but also show a pronounced species-dependent reaction, which is of special interest for growers.

Keywords: LEDs (light emitting diode), kale, UV-radiation, kohlrabi, rocket salad

INTRODUCTION

Plants have photosensory mechanisms to detect ultraviolet-B (UV-B; 280–315 nm) radiation (Heijde and Ulm, 2012; Jenkins, 2014) and therefore protect and repair sensitive targets from direct and indirect UV-induced injury (Britt, 1996; Jansen and Bornman, 2012). One line of defense is the increased biosynthesis of flavonoids and hydroxycinnamic acids (Jansen et al., 2008; Neugart and Schreiner, 2018). However, the impact of moderate UV-B, below ecologically summer day doses, during cultivation is less investigated (Schreiner et al., 2012; Neugart and Schreiner, 2018). Changes in the biosynthesis of flavonoid glycosides and hydroxycinnamic acid derivatives in response to UV-B depends on the chemical structure of the compounds (Olsson et al., 1998; Neugart et al., 2012a, 2014; Harbaum-Piayda et al., 2016). Light-emitting diodes (LEDs) are the most innovative light sources and create new possibilities for indoor cultivation. Blue and red LEDs were the first choice for manufacturers as these wavelengths are efficiently absorbed by chlorophylls (Kaiser et al., 2019). It is a widespread but erroneous belief that plants simply prefer blue and red light and poorly absorb green light (Smith et al., 2017). Less than 50% of green light (500–600 nm range) is reflected by plant chloroplasts, and green light reaches deeper leaf tissues more efficiently than blue or red wavelengths, which are shielded with chlorophyll-containing layers (Terashima et al., 2009). It was shown recently that flavonoid biosynthesis can be enhanced by blue light (420–490 nm) or green light (490–585 nm), but species differ in their response. While blue light treatment (30–100 μmol m^{-2} s^{-1}) of lettuce resulted in higher total phenols (Johkan et al., 2010; Samuoliene et al., 2017), higher doses of blue light within the light spectrum (200 μmol m^{-2} s^{-1}) resulted in a reduction of total phenolics in lamb's lettuce (Wojciechowska et al., 2015). For green light treatment (30 μmol m^{-2} s^{-1}) of lettuce, an increase of total phenolics was reported by the same authors. While UV-B radiation activates the UVR8 photoreceptor, blue and partly green light trigger the cryptochromes among other blue light receptors (Fuglevand et al., 1996; Heijde and Ulm, 2012; Jenkins, 2014; Tissot and Ulm, 2020). Extraordinarily, the light signaling of these photoreceptors, both UVR8 and cryptochromes, is mediated through COP1 operating as signaling center (Lau and Deng, 2012). While indoor farming offers the chance to tailor make light spectra in the visible spectrum, UV LEDs are not commonly used due to higher costs. One idea to overcome this issue is to have UV bulbs for the UV-B treatment and later on use visible light to stabilize or further increase the UV effects. There are no information how structurally different flavonol glycosides and hydroxycinnamic acids respond to different light qualities after pre-exposure with UV-B. Therefore, some basic principles need to be investigated for the later development of recipes.

The effect of light conditions during growth on flavonoids is of special importance, because these compounds act as antioxidants and shielding components in the plant's response to UV-B exposure (Edreva, 2005; Agati et al., 2013; Waterman et al., 2017) and are well-known antioxidants in human nutrition (Pan et al., 2010). Flavonoids are structurally diverse polyphenols that are ubiquitous in plants where they naturally occur as glycosides. *Brassica* vegetable leaves have high concentrations of flavonoids and hydroxycinnamic acids (Neugart et al., 2012a). The main flavonoids of Brassicaceae are quercetin and kaempferol glycosides. In kale, kaempferol glycosides show different antioxidant activities dependent on their chemical structure (Fiol et al., 2012). Rocket salad is known for high concentrations of quercetin glycosides (Martínez-Sánchez et al., 2007).

Flavonoids, as antioxidants, can quench singlet oxygen *in vivo* (Triantaphylides and Havaux, 2009) and are also reactive to other reactive oxygen species (ROS) such as hydroxyl radicals (Husain et al., 1987). Glycosylation reduces the antioxidant activity of flavonoids and affects the accumulation, stability, and solubility of flavonoids (Gachon et al., 2005; Bowles et al., 2006). The intracellular accumulation at sites of ROS production underlines the important antioxidant properties of flavonoids (Hernandez et al., 2009). Remarkably, it was previously shown that hydroxycinnamic acids act as scavengers of ROS induced by UV-B radiation (Edreva, 2005). Many studies investigated the overall antioxidant activity (such as TEAC) among different *Brassica* vegetables (Podsedek, 2007) or focus on total phenolic content and specific radical scavenging capacities (Li et al., 2011). Nevertheless, there are less scavenging information on plant-specific ROS such as singlet oxygen and hydroxyl radical and their correlation to flavonoid glycosides.

The ability of plants to accumulate protective UV-absorbing compounds such as flavonoids in response to days or weeks of exposure to UV is well known (Searles et al., 2001). It was shown that epidermal flavonoids are more important in response to UV-A and UV-B than mesophyll flavonoids and even epidermal hydroxycinnamic acids (Burchard et al., 2000; Kolb et al., 2001). However, it was also shown that flavonoids can absorb light in the lower wavelength region of the visible spectrum, e.g., blue light (Gitelson et al., 2017), which can result in higher

flavonoid concentrations (Matysiak and Kowalski, 2019). In addition, the absorption spectra of flavonoids depend on their chemical structure (Stochmal and Oleszek, 2007). Nevertheless, flavonoids such as rutin (absorption maxima at 260 and 360 nm) and hydroxycinnamic acids such as chlorogenic acid (absorption maximum at 320 nm) are relevant UV-absorbing compounds (Solovchenko and Merzlyak, 2008). How specific complex flavonoid glycosides and hydroxycinnamic acids contribute to the absorption capacity is still largely unclear, but will support non-destructive measurements of flavonoids in the future.

We hypothesize that (i) UV-B pre-exposure leads to an increase in flavonoid glycosides and hydroxycinnamic acids with high antioxidant activity, (ii) blue and green light after UV-B pre-exposure contributes to obtain the higher concentrations of flavonoid glycosides and hydroxycinnamic acids, (iii) these light-induced changes in flavonoid and hydroxycinnamic acid profiles result in an increased ROS scavenging capacity and increased absorption ability, and (iv) there are specific species within the Brassicaceae family. This knowledge will be transferable to recipes for indoor use and subsequent storage conditions, as it is important to increase not only the yield but also phenolic compounds that can act as color, flavor, and health-promoting compounds.

MATERIALS AND METHODS

Three Brassicaceae vegetables, namely, kale (*Brassica oleracea* var. *sabellica*) kohlrabi (*Brassica oleracea* var. *gongylodes* L.), and rocket salad (*Diplotaxis tenuifolia*), were cultivated in a controlled environment, in a greenhouse, for the UV treatment. Afterward, they were transferred to climate chamber for the LED treatment. The first part of this experiment was carried out in the greenhouse at Grossbeeren (Germany, 52.37°N 13.33°E) under partly overcast skies with glass that is blocking UV. PAR was on average 306 μmol m^{-2} s^{-1} with intra- and inter-day variations [natural sunlight plus Lamps (SON-T Agro 400)]. Temperature was set at 22°C from 8:00 to 21:00 and 18°C from 21:00 to 8:00. The sprouts (3 days after sowing) were treated with five subsequent doses of moderate UV-B provided by UV-B fluorescence light sources (TL 40W 12 RS, Philips, Hamburg, Germany). The UV-B dose was 0.23 kJ m^{-2} day^{-1} UV-B_{BE} per day (total: 1.15 kJ m^{-2} day^{-1} UV-B_{BE}) at a distance of 60 cm from 10:30 to 12:00 each day. The lamps were moving above the samples being applied to an irrigation system, which at the same time results in an balanced UV radiation treatment among the samples. To calculate the biologically effective UV-B, the generalized plant action spectrum (Caldwell, 1971) was used. UV-B radiation was determined using an UV-B sensor (type DK-UVB 1.3-051, deka Sensor + Technologie, Teltow, Germany) with a spectral range of 265–315 nm. Afterward, a subset of the 8-day-old sprouts pre-treated with UV got two subsequent doses (6 h each from 8:00 to 14:00) of blue (450 nm–99 μmol m^{-2} s^{-1}) or green (510 nm–119 μmol m^{-2} s^{-1}) light (**Figure 1**). In addition to the blue or green LEDs, white LEDs (400–700 nm) were present in the climate chamber with 100 μmol m^{-2} s^{-1} from 6:00 to 18:00 to ensure further growth of the plants (**Figure 1**). Temperature was 22°C from 8:00 to 21:00 and 18°C from 21:00 to 8:00. A sampling fraction of three biological replicates, each one tray of sprouts grown from 3 g of seeds, was harvested after an acclimatization period of 24 h after the last treatment.

Flavonoid glycosides and hydroxycinnamic acids were identified and quantified by HPLC-ESI-MS^n (Neugart et al., 2012b). The modified method follows in brief, and lyophilized samples (20 mg) were extracted with 1.2 ml of 60% aqueous methanol in three steps. The extract was evaporated to dryness and the residue was dissolved in 200 μl of 10% methanol and then filtered through a Spin-X filter (cellulose acetate membrane filter) for the HPLC analysis. An HPLC series 1100 from Agilent (Waldbronn, Germany) consisting of a degasser, binary pump, autosampler, column oven, and photodiode array detector was used to quantify the flavonoid glycosides. For identification purposes, an ion trap mass spectrometer (Agilent series 1100 MSD) was used with ESI as an ion source in negative ionization mode. Nitrogen was the dry gas (12 L/min, 350°C) and nebulizer gas (40 psi). Helium was the inert collision gas in the ion trap. The following gradient was used for eluent B (100% acetonitrile) at a temperature of 30°C: 5–7% (0–12 min), 7–9% (12–25 min), 9–12% (25–45 min), 12–15% (45–100 min), 15% isocratic (100–150 min), 15–50% (150–155 min), 50% isocratic (155–165 min), 50–5% (165–170 min), 5% isocratic (170–175 min). The flow was performed using 0.4 ml min^{-1}, and the measured detector wavelength for the quantification was set at 370 nm for non-acylated flavonol glycosides and 330 nm for acylated flavonol glycosides. The standards quercetin-3-*O*-glucoside and the corresponding 3-*O*-glucosides of kaempferol and isorhamnetin (Carl Roth GmbH, Karlsruhe, Germany) were used to obtain an external calibration curve in the range of 0.1–10 mg 100 ml^{-1}.

Singlet oxygen ($^1O_2$) and hydroxyl radical ($^{\bullet}OH$) scavenging capacities by photospectrometric methods (Majer and Hideg, 2012). In singlet oxygen scavenging capacity measurements, *p*-nitrosodimethylaniline (RNO) is bleached by a product of the reaction between singlet oxygen and histidine, which can be followed by monitoring the decrease in RNO absorption at 440 nm. Reaction mixtures contained 10 mM methylene blue, 15 mM RNO, and 10 mM histidine in 50 mM phosphate buffer (pH 7.0). Singlet oxygen scavenging capacities of plant extracts were measured based on their abilities to inhibit the above reaction and were quantified as millimolar Trolox equivalents per gram of dry matter. The hydroxyl radical scavenging capacity was determined by measuring the ability of leaf extracts to inhibit the formation of the strongly fluorescent 2-hydroxyterephthalate (HTPA) in a reaction between terephthalate (1,4-benzenedicarboxylic acid, TPA) and hydroxyl radical. HTPA fluorescence was measured at room temperature with a Quanta Master QM-1 spectrofluorometer (Photon Technology Inc., Birmingham, NJ, United States), using 315-nm excitation and 420-nm emission. The 2.5-ml reaction mixture contained 500 mM TPA, 10 mM EDTA, 10 mM $FeSO_4$, 100 mM AA, and 100 mM H_2O_2 in a 50 mM Na-phosphate buffer (pH 7.2). Hydroxyl radical scavenging of each plant extract was characterized by its half-inhibitory concentration on HTPA formation. The method was calibrated with ethanol, which is a

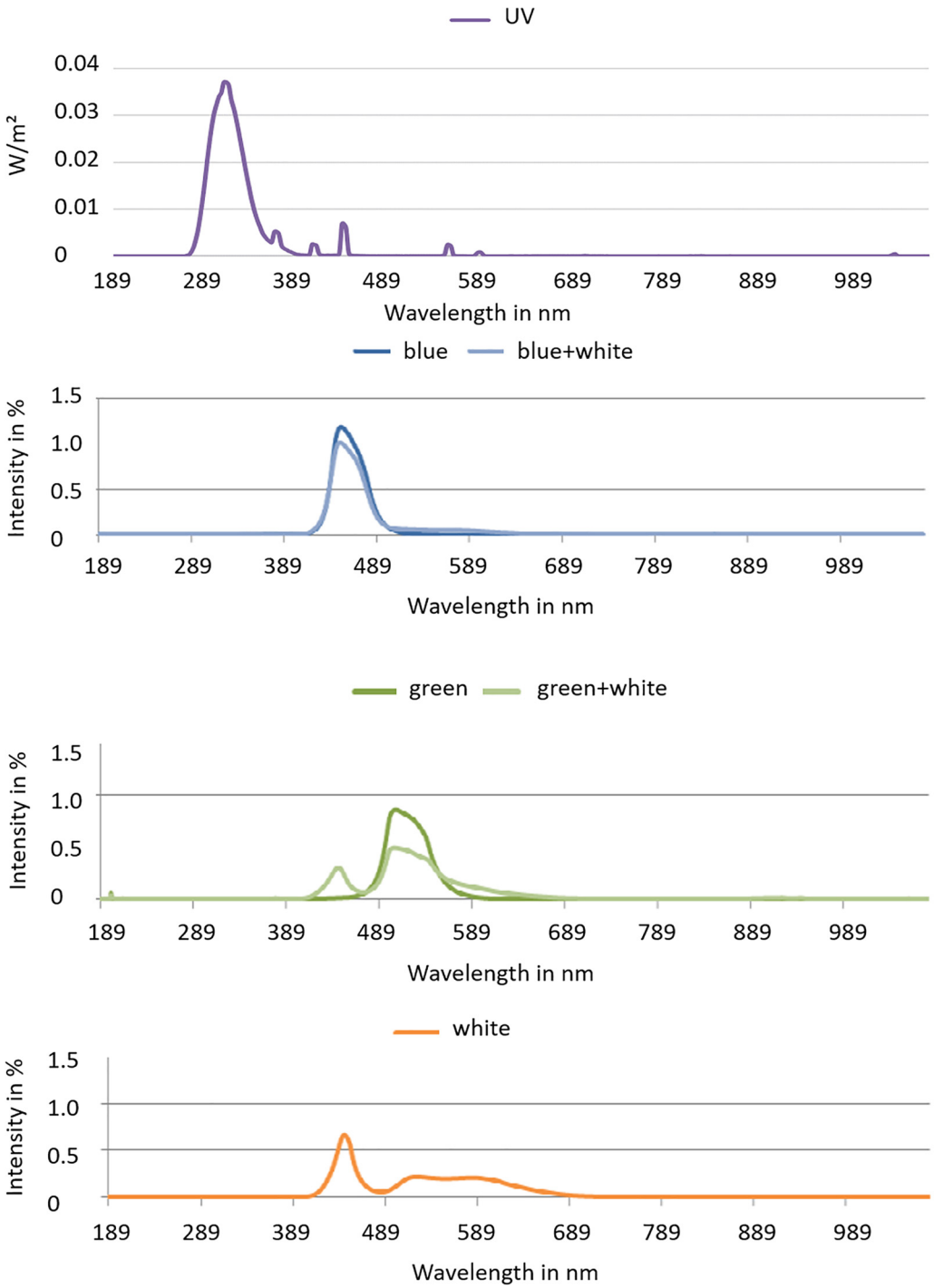

FIGURE 1 | Spectra of blue and green LEDs with and without white light and the white light spectrum used in the climate chambers.

strong hydroxyl radical scavenger, and specific hydroxyl radical neutralizing capacities of leaf extracts were given as millimolar ethanol equivalents per gram of dry matter.

The absorption spectra of the extracts were determined according to Mirecki and Teramura (1984). Twenty milligrams of freeze-dried powder was extracted with acidified methanol and used for spectrophotometric determination of total UV-B absorption ($A_{280-315\ nm}$) which is linked to the phenolic content. All absorption measurements were carried out using a Shimadzu UV-1601 spectrophotometer.

All measurements were done on three independent biological replicates and two technical replicates in the lab.

To analyze variance (ANOVA), Tukey's Honest Significant Difference (HSD) test was used to calculate significant differences at a significance level of $p \leq 0.05$.

RESULTS

Effect of Light Quality on Structurally Different Flavonoid Glycosides and Hydroxycinnamic Acids

The flavonol glycoside and hydroxycinnamic acid profiles varied within the three Brassicaceae vegetables. In total, kale (**Figure 2** and **Supplementary Table 1**) and kohlrabi (**Figure 2** and **Supplementary Table 2**) were characterized by acylated quercetin and kaempferol glycosides based on the 3-*O*-sophoroside-7-*O*-glycosides. Rocket salad (**Figure 3** and **Supplementary Table 3**) had mainly acylated quercetin glycosides based on the quercetin-3,3′,4′-triglucoside. Generally, the response of flavonol glycosides and hydroxycinnamic acids to the different light treatments was distinctly dependent on their chemical structure. In kale, caffeoylquinic acid and feruloyl glucoside were increased by UV-B exposure and remain high after blue light treatment but not after green light treatment (**Figure 2** and **Supplementary Table 1**). Interestingly, gentiobiosides acylated only with sinapoyl residues were found in high concentrations in kale plants, but mixtures of sinapoyl- and feruloyl-acylated gentiobiosides appeared in high concentrations in plants exposed to UV-B and subsequently to blue light treatment. For non-acylated flavonol glycosides, including quercetin, kaempferol, and isorhamnetin glycosides, an increase was found after UV-B exposure and was mostly stable after two doses of blue light but not green light (**Figure 2** and **Supplementary Table 1**). The same was true for most of the acylated quercetin and kaempferol glycosides (**Figure 2** and **Supplementary Table 1**). Nevertheless, for quercetin-3-feruloyl-sphoroside-7-glucoside, kaempferol-3-caffeoyl-sophoroside-7-glucoside, and kaempferol-3-caffeoyl-sophoroside-7-diglucoside, the highest concentrations were found after UV-B exposure followed by blue light treatment. Although kale and kohlrabi showed similar flavonoid and hydroxycinnamic acid profiles, the response of both to treatment was species-specific. In kohlrabi, hydroxycinnamic acids were rarely affected by UV-B exposure (**Figure 2** and **Supplementary Table 2**). However, hydroxycinnamic acid monoglycosides, namely, caffeoyl-glucoside, sinapoyl-glucoside, and disinapoyl-glucoside, were increased after UV-B exposure followed by the exposure to green light. In contrast, mainly non-acylated quercetin glycosides (quercetin-3-sophoroside and quercetin-3-triglucoside) were increased by two- to threefold in response to UV-B (**Figure 2** and **Supplementary Table 2**). Blue as well as green light after

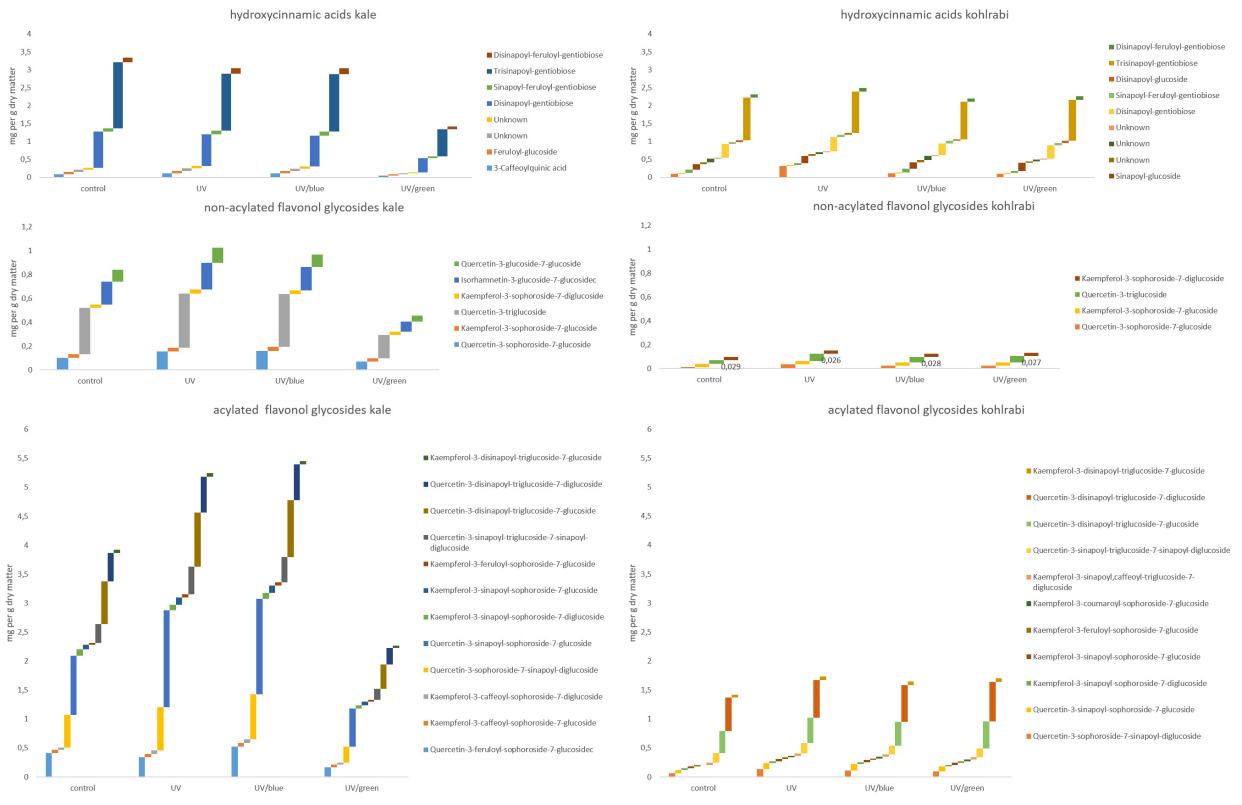

FIGURE 2 | Hydroxycinnamic acids, non-acylated flavonol glycosides, and acylated flavonol glycosides of kale and kohlrabi grown under different irradiation qualities (control, UV, UV plus blue, and UV plus green). For statistics, see **Supplementary Tables 1**, **2**.

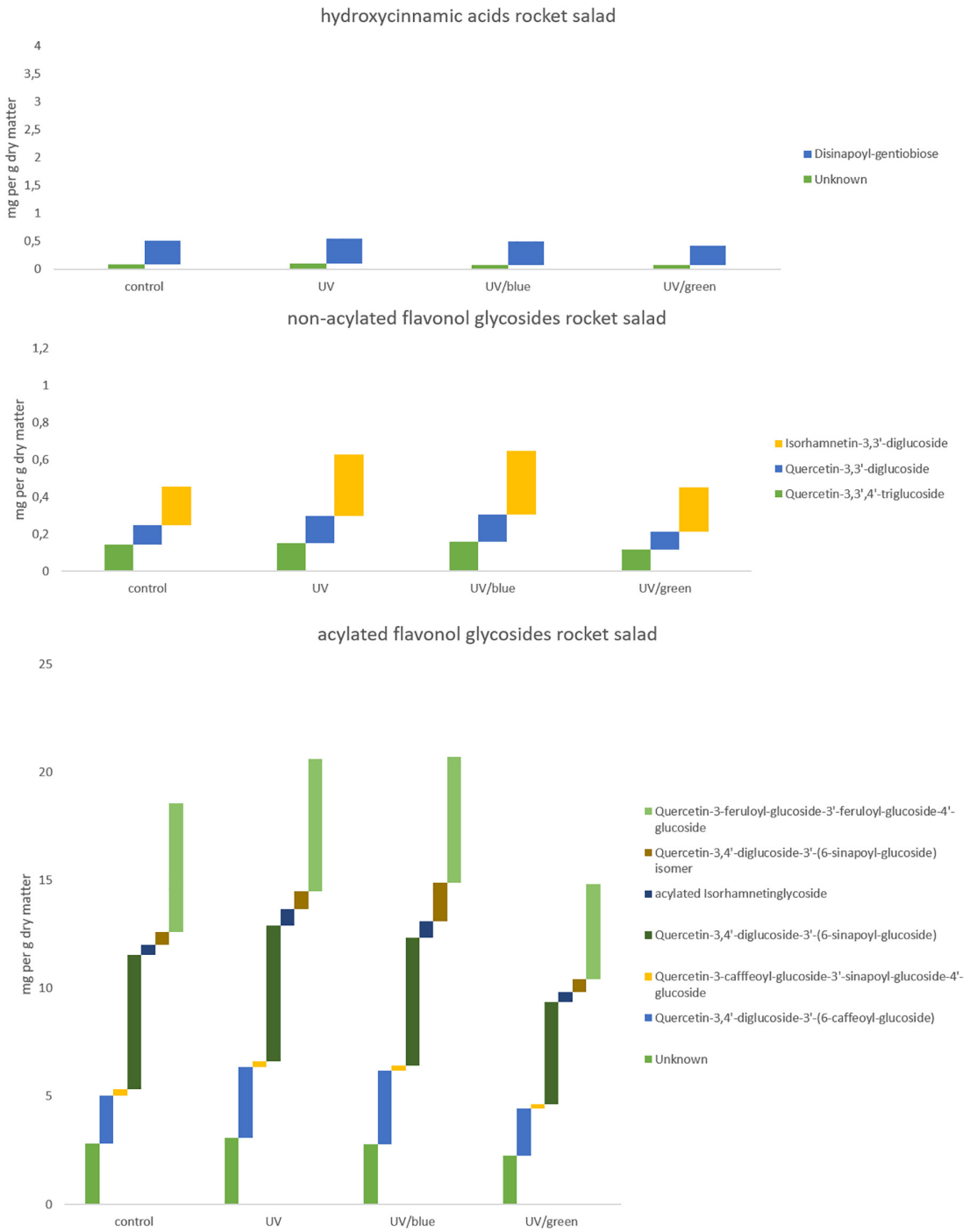

FIGURE 3 | Hydroxycinnamic acids, non-acylated flavonol glycosides, and acylated flavonol glycosides of rocket salad grown under different irradiation qualities (control, UV, UV plus blue, and UV plus green). For statistics see **Supplementary Table 3**.

the UV-B exposure resulted in a decrease of the non-acylated quercetin glycosides. Furthermore, in kohlrabi, the most acylated quercetin and kaempferol triglycosides and tetraglycosides were increased by UV-B exposure and were still high after two subsequent doses of blue light, but no green light (**Figure 2** and **Supplementary Table 2**). Nevertheless, quercetin and kaempferol pentaglycosides were not affected by UV-B exposure or blue and green light. The values are still high after two subsequent doses of blue light but not with green light instead. In rocket salad, several flavonol glycosides and hydroxycinnamic acids were increased by 1.2- to 2-fold due to the exposure with UV-B, e.g., quercetin-3′,4′-diglucoside-3′-(6-caffeoyl-glucoside)

(**Figure 3** and **Supplementary Table 3**). The values are still high after two subsequent doses of blue light, but not with green light instead.

Effect of Light Quality on ROS Scavenging Capacity

In the present study, kale and kohlrabi, in general, showed a higher singlet oxygen scavenging capacity than rocket salad (**Figure 4**). Both kale and kohlrabi belong to the *Brassica* genus while rocket salad is *Diplotaxis* species. The results reveal a strong species-specific response of sprouts to the different light qualities regarding singlet oxygen scavenging capacity. For hydroxyl radical scavenging capacity, no species-specific response was detected in the *Brassica* sprouts. UV-B exposure resulted in higher singlet oxygen scavenging capacity in rocket but not kale and kohlrabi (**Figure 4**). Blue light treatment following the UV-B exposure did not result in a significant increase of singlet oxygen scavenging for kale and rocket but in a trend toward an increase. Green light treatment after UV-B exposure showed similar singlet oxygen scavenging as the control for all three *Brassicaceae* sprouts. The hydroxyl radical scavenging capacity was independent from the light quality except for kale, where an exposure with UV-B followed by a blue light treatment led to a higher hydroxyl radical scavenging capacity. In kale, non-acylated as well as acylated quercetin and kaempferol glycosides of very different chemical structures contributed to the singlet oxygen-scavenging capacity including kaempferol-3-caffeoyl-sophoroside-7-glucoside and its corresponding tetraglycoside (**Table 1**). In kohlrabi, however, there was not a single compound that contributed significantly to singlet oxygen scavenging capacity (**Table 2**), whereas in rocket salad, almost all the compounds measured, most of them quercetin glycosides and disinapoyl and trisinapoyl geniobiosides, have contributed to

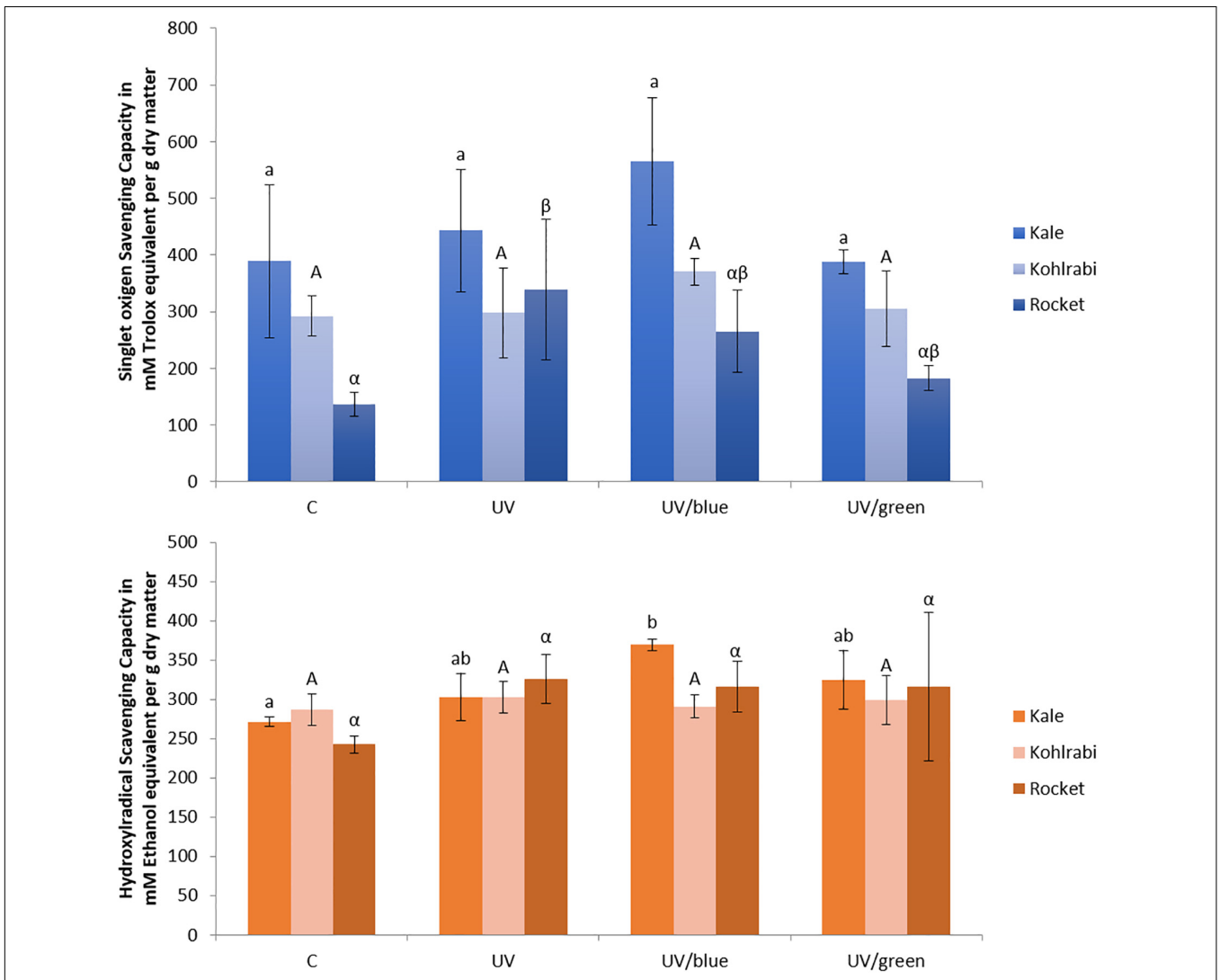

FIGURE 4 | Singlet oxygen scavenging capacity and hydroxyl radical scavenging capacity of three Brassiceae species grown under different irradiation qualities (control, UV plus blue, and UV plus green). Different letters represent significant differences ($p \leq 0.05$ by Tukey's HSD test) between the treatment ($n = 3$).

TABLE 1 | Correlation of hydroxycinnamic acid derivatives and flavonol glycosides (mg g^{-1} dry weight) and biological functions as antioxidants (singlet oxygen scavenging capacity and hydroxyl radical scavenging capacity) and ultraviolet radiation shielding (absorbance) in kale.

	Retention time	Singlet oxygen scavenging capacity	Hydroxyl radical scavenging capacity	Absorbance
Hydroxycinnamic acid derivatives				
3-Caffeoylquinic acid	6.2	0.352184	0.051560	−0.061421
Feruloyl-glucosidec	11.6	0.381948	0.081930	−0.087946
Unknown	20.5	0.208944	−0.227761	−0.312001
Unknown	23.5	0.293131	−0.063830	−0.151934
Disinapoyl-gentiobiose	37.0	0.190063	−0.287159	**−0.426992**
Sinapoyl-feruloyl-gentiobiose	37.6	0.385117	0.072049	−0.121618
Trisinapoyl-gentiobiose	44.1	0.204305	−0.273807	**−0.409741**
Disinapoyl-feruloyl-gentiobiose	44.8	0.363088	0.045728	−0.082927
Non-acylated flavonol glycosides				
Quercetin-3-sophoroside-7-glucoside	8.6	**0.449189**	0.283069	0.202812
Kaempferol-3-sophoroside-7-glucoside	9.2	0.378105	0.085331	−0.069357
Quercetin-3-triglucoside	9.4	0.332416	−0.011929	−0.120216
Kaempferol-3-sophoroside-7-diglucoside	10.0	**0.458391**	0.327639	0.255956
Isorhamnetin-3-glucoside-7-glucosidec	11.0	0.221753	−0.188276	−0.206147
Quercetin-3-glucoside-7-glucoside	19.8	0.160116	−0.200319	−0.212897
Acylated flavonol glycosides				
Quercetin-3-feruloyl-sophoroside-7-glucosidec	12.9	0.383240	0.205756	−0.059238
Kaempferol-3-caffeoyl-sophoroside-7-glucoside	13.2	**0.501781**	0.317331	0.092935
Kaempferol-3-caffeoyl-sophoroside-7-diglucoside	13.5	**0.465506**	**0.452818**	0.365073
Quercetin-3-sophoroside-7-sinapoyl-diglucoside	14.6	0.364968	0.161180	0.057482
Quercetin-3-sinapoyl-sophoroside-7-glucoside	14.8	**0.408538**	0.253602	0.170001
Kaempferol-3-sinapoyl-sophoroside-7-diglucoside	16.1	0.153452	−0.224867	−0.379953
Kaempferol-3-sinapoyl-sophoroside-7-glucoside	16.6	**0.431807**	0.355216	0.297535
Kaempferol-3-feruloyl-sophoroside-7-glucoside	16.9	**0.514344**	**0.552080**	**0.458408**
Quercetin-3-sinapoyl-triglucoside-7-sinapoyl-diglucoside	29.1	0.356813	0.103971	0.036905
Quercetin-3-disinapoyl-triglucoside-7-glucoside	30.3	**0.408943**	0.165905	0.046120
Quercetin-3-disinapoyl-triglucoside-7-diglucoside	30.4	0.390050	0.100338	0.010353
Kaempferol-3-disinapoyl-triglucoside-7-glucoside	31.7	0.345852	0.024576	−0.076607

Results include three biological replicates each measured as technical duplicates. Bold values indicate significant correlations $p \leq 0.05$.

the singlet oxygen scavenging capacity (**Table 3**). None of the Brassicaceae species studied had a large amount of compounds with hydroxyl radical scavenging capacity (**Tables 1–3**).

Effect of Light Quality on Absorption Ability

The extracts of Brassicaceae vegetables showed lower absorption intensities in kohlrabi compared to kale and rocket (**Figure 5**). In kale, the absorption was higher in UV-B-exposed plants and was additionally increased by the blue and green light treatment, whereas in kohlrabi, there was a clear UV-B exposure effect but no further increase following the blue and green light treatment. In rocket salad, the absorption was only slightly increased by UV-B exposure and not further increased by blue or green light treatment. Nevertheless, for kale, negative correlations of absorption and the hydroxycinnamic acid derivatives disinapoyl-gentiobioside as well as trisinapoly gentiobioside were found, whereas kaempferol-3-feruloyl-sophorroside-7-glucoside was the only flavonol glycoside to contribute to the absorption (**Table 1**). In contrast, in kohlrabi caffeoyl-glucoside, sinapoyl-glucoside and disnapoyl-feruloyl-gentiobioside contributed to the higher absorption alongside with several non-acylated quercetin glycosides and acylated quercetin and kaempferol glycosides (**Table 2**). In rocket salad, none of the soluble flavonol glycosides and hydroxycinnamic acid derivatives contributed to absorbance changes, which were very small (**Table 3**).

DISCUSSION

Effect of Light Quality on Structurally Different Flavonoid Glycosides and Hydroxycinnamic Acids

The results on the chemical structures identified and quantified are in line with the literature on *Brassica* species (Ferreres et al., 2009; Lin and Harnly, 2009; Olsen et al., 2009; Schmidt et al., 2010; Cartea et al., 2011; Kyriacou et al., 2020) and rocket salad (Martínez-Sánchez et al., 2007; Pasini et al., 2012; Bell and Wagstaff, 2014). UV-B exposure can lead to an up to 2 fold increase of phenolic compounds in *Brassica* species and rocket salad as previously found in the literature

TABLE 2 | Correlation of hydroxycinnamic acid derivatives and flavonol glycosides (mg g^{-1} dry weight) and biological functions as antioxidants (singlet oxygen scavenging capacity and hydroxyl radical scavenging capacity) and ultraviolet radiation shielding (absorbance) in kohlrabi.

	Retention time	Singlet oxygen scavenging capacity	Hydroxyl radical scavenging capacity	Absorbance
Hydroxycinnamic acid derivatives				
3-Caffeoylquinic acid	6.2	−0.101751	0.137149	0.188011
Caffeoyl-glucoside	6.6	0.300800	0.139749	**0.446213**
Feruloyl-glucoside	11.6	−0.018152	−0.001907	−0.298706
Sinapoyl-glucoside	13.2	0.078954	0.048242	**0.700352**
Unknown	20.6	0.136176	0.244739	−0.158513
Unknown	22.1	−0.031982	0.027816	−0.271488
Unknown	24.2	−0.172506	0.284134	0.042835
Disinapoyl-gentiobiose	37.0	−0.084294	0.145878	0.080536
Sinapoyl-Feruloyl-gentiobiose	37.6	0.154490	0.138082	0.271076
Disinapoyl-glucoside	41.5	−0.091963	−0.038959	0.122176
Trisinapoyl-gentiobiose	44.1	−0.239872	0.206963	−0.092451
Disinapoyl-feruloyl-gentiobiose	44.8	0.072664	0.047670	**0.415865**
Non-acylated flavonol glycosides				
Quercetin-3-sophoroside-7-glucoside	8.6	0.202437	0.124999	**0.508333**
Kaempferol-3-sophoroside-7-glucoside	9.2	0.147052	0.097162	0.371887
Quercetin-3-triglucoside	9.4	0.124553	0.022812	**0.569440**
Kaempferol-3-sophoroside-7-diglucoside	10.5	−0.178689	−0.035190	−0.363275
Acylated flavonol glycosides				
Quercetin-3-sophoroside-7-sinapoyl-diglucoside	14.5	0.071770	0.034289	**0.490458**
Quercetin-3-sinapoyl-sophoroside-7-glucoside	14.9	0.070899	−0.202322	0.166614
Kaempferol-3-sinapoyl-sophoroside-7-diglucoside	16.1	0.264322	0.061002	0.196169
Kaempferol-3-sinapoyl-sophoroside-7-glucoside	16.6	0.308640	0.102392	**0.491060**
Kaempferol-3-feruloyl-sophoroside-7-glucoside	16.9	0.337465	0.100600	**0.493892**
Kaempferol-3-coumaroyl-sophoroside-7-glucoside	17.2	0.255314	−0.004100	**0.694317**
Kaempferol-3-sinapoyl,caffeoyl-triglucoside-7-diglucoside	28.4	0.006828	−0.023776	−0.211027
Quercetin-3-sinapoyl-triglucoside-7-sinapoyl-diglucoside	29.1	−0.181499	0.012428	0.057980
Quercetin-3-disinapoyl-triglucoside-7-glucoside	30.3	−0.056011	−0.021571	0.375379
Quercetin-3-disinapoyl-triglucoside-7-diglucoside	30.4	−0.035954	−0.005042	0.352710
Kaempferol-3-disinapoyl-triglucoside-7-glucoside	31.7	0.127330	−0.011764	**0.673996**

Results include three biological replicates each measured as technical duplicates. Bold values indicate significant correlations $p \leq 0.05$.

(Reifenrath and Mueller, 2007; Harbaum-Piayda et al., 2010; Mormile et al., 2019; **Table 4**). Additionally, an effect dependent on the specific chemical structure as well as the dose and duration of the UV-B treatment was shown (Olsson et al., 1998; Neugart et al., 2012a, 2014; Groenbaek et al., 2014; Rechner et al., 2016). The present study shows that kaempferol glycosides such as kaempferol-3-caffeoyl-sophoroside-7-glucoside of *Brassica* species and quercetin glycosides in rocket salad are involved in the UV and blue light response. Nevertheless, blue light was not able to further increase flavonoid glycosides and hydroxycinnamic acids in Brassicaceae sprouts. However, in broccoli, kaempferol-3-feruloyl-sphoroside-7-glucoside and kaempferol-3-caffeoyl-sophoroside-7-glucoside were increased after blue light treatment alone, without any UV pre-treatment (Rechner et al., 2017). Blue light was able to increase total phenolics of lettuce (Johkan et al., 2010). Furthermore, in basil, lettuce and arugula flavonoid glycosides and hydroxycinnamic acids reacted to blue light based on their chemical structure, mainly based on the aglycone as trigger (Taulavuori et al., 2016, 2018). An effect of the glycosylation pattern or the acylated hydroxycinnamic acid has not been found in the present study but was previously discussed for kale juvenile plants or broccoli juvenile plants treated with UV-B (Neugart et al., 2014; Rechner et al., 2016). Furthermore, blue light was able to increase sinapoyl derivatives and kaempferol glycosides of *Arabidopsis thaliana* with a clear pattern that kaempferol glycosides including glucose are increased, while those not including glucose but rhamnose are not (Brelsford et al., 2019). The fact that complex flavonoid glycosides, e.g., quercetin and kaempferol pentaglycosides from kohlrabi, are not affected by the light treatment was previously found in broccoli (Rechner et al., 2016). It is worth noting that the blue-to-red ratio should be 1:3 or higher to increase flavonoid glycosides and hydroxycinnamic acids (Pennisi et al., 2019). Such ratios were not reached in the present study and might explain why no further increase of flavonoid glycosides and hydroxycinnamic acid derivatives was found. However, green light seems to reduce plant response in general (Folta and Maruhnich, 2007), even though there had also been reports that green light in addition to blue and red light can increase total phenols in lettuce (Bian et al., 2018). In accordance with the

TABLE 3 | Correlation of hydroxycinnamin acid derivatives and flavonol glycosides (mg g^{-1} dry weight) and biological functions as antioxidants (singlet oxygen scavenging capacity and hydroxyl radical scavenging capacity) and ultraviolet radiation shielding (absorbance) in rocket salad.

	Retention time	Singlet oxygen scavenging capacity	Hydroxyl radical scavenging capacity	Absorbance
Hydroxycinnamic acid derivatives				
Unknown	22.0	**0.662612**	0.151068	0.181309
Disinapoyl-gentiobiose	37.0	**0.596333**	0.027661	0.059041
Trisinapoyl-gentiobiose	44.1	**0.618794**	0.050132	0.132872
Non-acylated flavonol glycosides				
Quercetin-3,3′,4′-triglucoside	7.0	**0.522826**	−0.008168	−0.039766
Quercetin-3,3′-diglucoside	19.8	**0.780204**	0.295542	0.095067
Isorhamnetin-3,3′-diglucoside	21.8	**0.748274**	0.402655	0.236553
Acylated flavonol glycosides				
Unknown	13.1	**0.596496**	0.078941	0.124960
Quercetin-3,4′-diglucoside-3′-(6-caffeoyl-glucoside)	15.8	**0.782141**	0.338902	0.115805
Quercetin-3-cafffeoyl-glucoside-3′-sinapoyl-glucoside-4′-glucoside	19.3	0.224488	−0.257167	−0.084739
Quercetin-3,4′-diglucoside-3′-(6-sinapoyl-glucoside)	25.9	**0.471698**	−0.084599	−0.037693
Acylated isorhamnetin glycoside	33.4	**0.825667**	**0.428811**	0.089431
Quercetin-3,4′-diglucoside-3′-(6-sinapoyl-glucoside) isomer	33.8	0.194651	−0.001776	0.203347
Quercetin-3-feruloyl-glucoside-3′-feruloyl-glucoside-4′-glucoside	35.2	**0.538342**	−0.027237	−0.012547

Bold values indicate significant correlations $p \leq 0.05$.

results of the present study in broccoli plants radiated with green light without any treatment of UV-B, structurally different flavonoid glycosides and hydroxycinnamic acids were in the same concentrations of the control plants (Rechner et al., 2017). This is true although green light (119 μmol m^{-2} s^{-1}) had a higher intensity than blue light (99 μmol m^{-2} s^{-1}) due to technical limitations in the climate chamber. Generally, there is the assumption that higher intensities of blue and green light are needed to actually increase flavonoid glycosides and hydroxycinnamic acid derivatives.

Even though kale and kohlrabi had similar flavonoid and hydroxycinnamic acid profiles, the response of both to the treatment was species-specific (**Figure 1**). In Chinese kale, 100 μmol m^{-2} s^{-1} of blue light treatment were not enough to increase total phenolics (Li et al., 2019), while in pak choi, it was enough to lead to an increase of total phenolics (Zheng et al., 2018). In lamb's lettuce, the increase of blue light in the light spectrum even decreased the total phenolics (Wojciechowska et al., 2015). It is therefore possible that either the intensity of blue light was too low for kohlrabi or kohlrabi uses other defense mechanisms such as waxes.

Effect of Light Quality on ROS Scavenging Capacity

Leaves are good sources of flavonoid glycosides, which, alongside with other compounds such as carotenoids and vitamins, contribute to a high singlet oxygen scavenging capacity (Ribeiro et al., 2015). Ascorbic acid and quercetin contribute to the hydroxyl radical scavenging capacity of Indian olive (Panja et al., 2014). This leads to the conclusion that other compounds must be involved. In the present study, the results reveal a strong species-specific response of sprouts to the different light qualities dependent on the high variation of flavonoid glycosides and hydroxycinnamic acids within the species. Recent results showed a strong correlation between flavonols and singlet oxygen scavenging capacity, as shown here for kale and rocket salad, but also revealed that glycosides of flavonols are less effective as their aglycones (Agati et al., 2007; Majer et al., 2014; Csepregi and Hideg, 2018). Hydroxycinnamic acids had about 10% of singlet oxygen scavenging capacity compared to quercetin and kaempferol (Csepregi and Hideg, 2018). In the Brassicaceae sprouts, no correlation of hydroxycinnamic acids and the singlet oxygen scavenging capacity and hydroxyl radical scavenging capacity was found as previously described for hydroxycinnamic acids ferulic acid and *p*-coumaric acid of millet cultivars (Chandrasekara and Shahidi, 2011). In wild strawberries, different cultivars showed a strong correlation of singlet oxygen scavenging capacity and hydroxyl radical scavenging capacity (Wang et al., 2007), a trend that is also seen in the data presented here. Furthermore, in strawberries, numerous hydroxycinnamic acids as well as quercetin and kaempferol glycosides were increased with higher temperatures, in line with the singlet oxygen scavenging capacity and hydroxyl radical scavenging capacity (Wang and Zheng, 2001). None of the Brassicaceae species studied showed a large amount of compounds contributing to the hydroxyl radical scavenging capacity. Concomitantly, Majer et al. (2010) found no correlation between total phenolic content and hydroxyl radical scavenging capacity in tobacco leaves assuming other compounds involved in the quenching of hydroxyl radical. Hydroxycinnamic acids, although highly concentrated in the *Brassica* sprouts (Heinze et al., 2018), had no specific effects on the scavenging capacity to plant-specific ROS.

Effect of Light Quality on Absorption Ability

In addition to their role as antioxidants, flavonoids act as UV shielding components (Edreva, 2005). Kaempferol, quercetin,

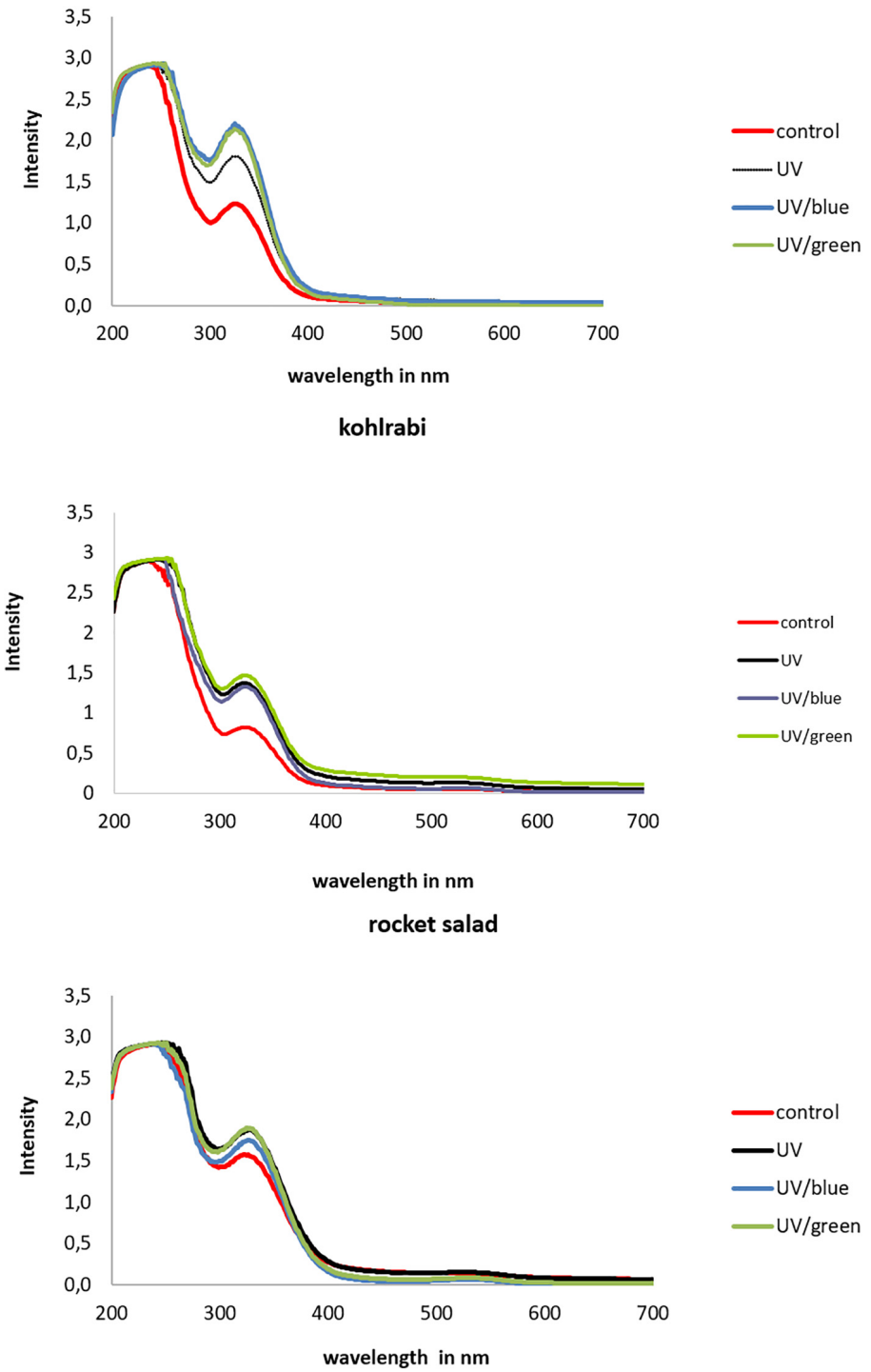

FIGURE 5 | Absorption of three Brassiceae species grown under different irradiation qualities (control, UV, UV plus blue, and UV plus green).

and isorhamnetin absorb longer wavelength in the UV radiation (350–400 nm) better than higher energized UV-B (280–315 nm). Absorption spectra of flavonol glycosides are shifted slightly toward shorter wavelengths compared to their corresponding aglycones (Majer et al., 2014). However, the role of structurally different flavonol glycosides in the UV shielding function of

TABLE 4 | Overview of the effects of UV, blue, and green light on flavonoid glycosides and hydroxycinnamic acid derivatives.

Species	Irradiation treatment	Induced changes in phenolic compounds UV light	References
Pak choi (*Brassica rapa* ssp. *chinensis*)	0.35 W m^{-2} UV-B	Kaempferol glycosides ↑ Malates of hydroxycinnamic acids	Harbaum-Piayda et al., 2010
Rocket salad (Eruca sativa)	No UV vs 60% UV transmission	Quercetin glycosides ↑ Luteoloin glycosides ↑ Apigenin glycosides ↑ Hydroxycinnamic acids ↓-	Mormile et al., 2019
Kale (*Brassica oleracea* var. *sabellica*)	0.22-0.88 kJ m^{-2} day^{-1} $UV\text{-}B_{BE}$ (single dose)	Quercetin glycosides ↓ Kaemperol glycosides ↑↓ (depending on glycosylation and acylation pattern)	Neugart et al., 2012b
Kale (*Brassica oleracea* var. *sabellica*)	0.25–1.25 kJ m^{-2} day^{-1} $UV\text{-}B_{BE}$	Quercetin glycosides ↑ Kaemperol glycosides ↑↓ (depending on glycosylation and acylation pattern)	Neugart et al., 2014
Canola (*Brassica napus*)	2 kJ m^{-2} day^{-1} $UV\text{-}B_{BE}$	Quercetin glycosides ↓ Kaemperol glycosides ↑↓ (depending on glycosylation and acylation pattern)	Olsson et al., 1998
Broccoli (*Brassica oleracea* var. *italica* Plenck)	2.9 kJ m^{-2} day^{-1} UV-B	Quercetin glycosides ↑- Kaempferol glycosides ↑- Hydroxycinnamic acids ↓-	Rechner et al., 2016
Nasturtium (*Nasturtium officinale*), Mustard (*Sinapis alba*)	1.12 W m^{-2} UV-B	Quercetin glycosides ↑ Kaempferol glycosides ↑ Hydroxycinnamic acids -	Reifenrath and Mueller, 2007
Species	**Irradiation treatment**	**Induced changes in phenolic compounds blue light**	**References**
Arabidopsis thaliana	PAR 168 μmol m^{-2} s^{-1} plus 32 μmol m^{-2} s^{-1} far red, blue light attenuated by film	Kaempferol glycosides ↑- Hydroxycinnamic acids ↑	Brelsford et al., 2019
Red leaf lettuce (*Lactuca sativa* L.)	100 μmol m^{-2} s^{-1}	Total phenols ↑ Antocyanins ↑	Johkan et al., 2010
Chinese kale (*Brassica alboglabra*)	0–150 μmol m^{-2} s^{-1}	Total phenols ↑ Antocyanins ↑	Li et al., 2019
Broccoli (*Brassica oleracea* var. *italica* Plenck)	50 μmol m^{-2} s^{-1} blue light	Quercetin glycosides - Kaempferol glycosides ↑- Hydroxycinnamic acids -	Rechner et al., 2017
Red leaf lettuce (*Lactuca sativa*) Basil (*Ocimum basilicum*)	300 μmol m^{-2} s^{-1} (blue enhanced)	Quercetin glycosides ↑- Hydroxycinnamic acids ↑-	Taulavuori et al., 2016
Basil (*Ocimum basilicum*), arugula (*Eruca sativa*), and bloody dock (*Rumex sanguineus*)	300 μmol m^{-2} s^{-1} (blue enhanced)	Apigenin glycosides ↑- Luteolin glycosides ↑- Hydroxycinnamic acids ↑-	Taulavuori et al., 2018
Lamb's lettuce (*Valerianella locusta*)	200 μmol m^{-2} s^{-1} 50% red and 50% blue, 70% red and 30% blue, 90% red and 10% blue	Total phenols ↓	Wojciechowska et al., 2015
Pak choi (*Brassica rapa* ssp. *chinensis*)	0–150 μmol m^{-2} s^{-1}	Total phenols ↑ Antocyanins ↑	Zheng et al. (2018)
Species	**Irradiation treatment**	**Induced changes in phenolic compounds green light**	**References**
Lettuce (*Lactuca sativa* L.)	Red:blue:green = 1:1:1 150 μmol m^{-2} s^{-1}	Total phenols ↑	Bian et al., 2018
Broccoli (*Brassica oleracea* var. *italica* Plenck)	50 μmol m^{-2} s^{-1} blue light	Quercetin glycosides - Kaempferol glycosides - Hydroxycinnamic acids -	Rechner et al., 2017

leaves is still not clear. UV-B as well as blue and green light treatment resulted in a slight shift of the band I assuming a better shielding activity (Edreva, 2005). Hydroxycinnamic acids with absorption maxima between 320 and 330 nm serve specific UV-B screening functions much better (Harborne and Williams, 2000). The results on kale and kohlrabi, once more

underlines the species-specific response although the compounds were comparable in the two *Brassica oleracea* species. In the model plant *Arabidopsis thaliana*, the absorption at 330 nm was higher in a UV-tolerant mutant, in line with the reduced UV-B transmittance (Bieza and Lois, 2001). Kohlrabi, as a plant, might use also other defense mechanisms such as leaf hairs or waxes. In general, hydroxycinnamic acids have a higher UV-A and especially UV-B absorption compared to the flavonoid aglycones quercetin and kaempferol (Csepregi and Hideg, 2018). However, it is to be mentioned that glycosylation of flavonoid aglycones, which is commonly found in plants, resulted in a lower UV absorption capacity of these compounds (Csepregi and Hideg, 2018). Furthermore, in the absence of flavonoids, hydroxycinnamic acid derivatives were found to take over the absorption of UV radiation especially in the UV-A range (Stelzner et al., 2019). In total, the absorbance seemed to be less important in the defense against UV compared to the antioxidant activity as previously shown in linden leaves (Majer et al., 2014). Nevertheless, cell wall-bound phenolics were not investigated here and might play a major role in the UV response based on absorption.

CONCLUSION

UV radiation resulted in the enhancement of a number of hydroxycinnamic acids and quercetin as well as kaempferol glycosides in different *Brassicaceae* vegetable sprouts. In kale, the glycosylation pattern had no effect on the UV-B response. In kohlrabi, tri- and tetraglycosides are involved in the UV-B response, whereas pentaglycosides are not, which is clearly highlighting the effect of the glycosylation pattern. Blue light treatment after pre-exposure with UV resulted in constantly high concentrations of the most hydroxycinnamic acids and quercetin and kaempferol glycosides in three *Brassicaceae* sprouts, but no further increase. Green light, in general, resulted in a decrease of most flavonol glycosides and hydroxycinnamic acids to the control level. This result underlines the importance of different light qualities on the biosynthesis of flavonoids and hydroxycinnamic acids and their fast response to changing environments. The enhancement of the singlet oxygen scavenging capacity or the hydroxyl radical scavenging capacity was very low and often only a trend even though some hydroxycinnamic acids or quercetin and kaempferol glycosides were increased 1.2- to 2-fold. However, sprouts seem to be protected by high concentrations of hydroxycinnamic acids compared to adult plants. The shift in the absorption band highlights the role of flavonol glycosides and hydroxycinnamic acids as shielding compounds in the UV-A and UV-B range. Nevertheless, the investigated sprouts showed species-specific responses in the absorption also reflecting the chemically different structures of the hydroxycinnamic acids and quercetin and kaempferol glycosides, as well as other possible defense mechanisms. Regarding the use of UV light and blue or green light in vertical farming to improve secondary plant metabolites that correlate with quality traits, a combination of UV light and subsequent blue light is possible, but requires further specifications, especially regarding the intensity of blue light.

DATA AVAILABILITY STATEMENT

The original contributions presented in the study are included in the article/**Supplementary Material**, further inquiries can be directed to the corresponding author/s.

AUTHOR CONTRIBUTIONS

SN and MS designed the experiment. SN conducted the experiment and wrote the first draft of the manuscript. PM measured and evaluated the singlet oxygen and hydroxyl radical scavenging capacity as well as absorbance. ÉH contributed in the discussion of biological functions. All authors revised and approved the manuscript.

FUNDING

ÉH wishes to thank the National Research, Development, and Innovation Office for support (grant no. KH-129615). This work was supported by grant no. STSM-FA0906-9730.

ACKNOWLEDGMENTS

We thank Sarah Farrherr for support of the flavonoid analysis.

SUPPLEMENTARY MATERIAL

The Supplementary Material for this article can be found online at: https://www.frontiersin.org/articles/10.3389/fpls.2020.611247/full#supplementary-material

REFERENCES

Agati, G., Brunetti, C., Di Ferdinando, M., Ferrini, F., Pollastri, S., and Tattini, M. (2013). Functional roles of flavonoids in photoprotection – new evidence, lessons from the past. *Plant Physiol. Biochem.* 72, 35–45. doi: 10.1016/j.plaphy.2013.03.014

Agati, G., Matteini, P., Goti, A., and Tattini, M. (2007). Chloroplast-located flavonoids can scavenge singlet oxygen. *New Phytol.* 174, 77–89. doi: 10.1111/j.1469-8137.2007.01986.x

Bell, L., and Wagstaff, C. (2014). Glucosinolates, myrosinase hydrolysis products, and flavonols found in rocket (*Eruca sativa* and *Diplotaxis tenuifolia*). *J. Agric. Food Chem.* 62, 4481–4492. doi: 10.1021/jf501096x

Bian, Z., Cheng, R., Wang, Y., Yang, Q., and Lu, C. (2018). Effect of green light on nitrate reduction and edible quality of hydroponically grown lettuce (*Lactuca sativa* L.) under short-term continuous light from red and blue light-emitting diodes. *Environ. Exp. Bot.* 153, 63–71. doi: 10.1016/j.envexpbot.2018.05.010

Bieza, K., and Lois, R. (2001). An *Arabidopsis* mutant tolerant to lethal ultraviolet-B levels shows constitutively elevated accumulation of flavonoids and other phenolics. *Plant Physiol.* 126, 1105–1115. doi: 10.1104/pp.126.3.1105

Bowles, D., Lim, E. K., Poppenberger, B., and Vaistij, F. E. (2006). Glycosyltransferases of lipophilic small molecules. *Annu. Rev.*

Plant Biol. 57, 567–597. doi: 10.1146/annurev.arplant.57.032905.105429

Brelsford, C. C., Morales, L. O., Nezval, J., Kotilainen, T. K., Hartikainen, S. M., Aphalo, P. J., et al. (2019). Do UV-A radiation and blue light during growth prime leaves to cope with acute high light in photoreceptor mutants of *Arabidopsis thaliana*? *Physiol. Plant.* 165, 537–554. doi: 10.1111/ppl.12749

Britt, A. B. (1996). DNA damage and repair in plants. *Annu. Rev. Plant Physiol. Plant Mol. Biol.* 47, 75–100. doi: 10.1146/annurev.arplant.47.1.75

Burchard, P., Bilger, W., and Weissenbock, G. (2000). Contribution of hydroxycinnamates and flavonoids to epidermal shielding of UV-A and UV-B radiation in developing rye primary leaves as assessed by ultraviolet-induced chlorophyll fluorescence measurements. *Plant Cell Environ.* 23, 1373–1380. doi: 10.1046/j.1365-3040.2000.00633.x

Caldwell, M. M. (1971). "Solar UV irradiation and the growth and development of higher plants," in *Photophysiology VI*, ed. Giese, 131–177.

Cartea, M. E., Francisco, M., Soengas, P., and Velasco, P. (2011). Phenolic compounds in *Brassica* vegetables. *Molecules* 16, 251–280. doi: 10.3390/molecules16010251

Chandrasekara, A., and Shahidi, F. (2011). Inhibitory activities of soluble and bound millet seed phenolics on free radicals and reactive oxygen species. *J. Agric. Food Chem.* 59, 428–436. doi: 10.1021/jf103896z

Csepregi, K., and Hideg, É (2018). Phenolic compound diversity explored in the context of photo-oxidative stress protection. *Phytochem. Anal.* 29, 129–136. doi: 10.1002/pca.2720

Edreva, A. (2005). The importance of non-photosynthetic pigments and cinnamic acid derivatives in photoprotection. *Agric. Ecosyst. Environ.* 106, 135–146. doi: 10.1016/j.agee.2004.10.002

Ferreres, F., Fernandes, F., Oliveira, J. M. A., Valentão, P., Pereira, J. A., and Andrade, P. B. (2009). Metabolic profiling and biological capacity of *Pieris brassicae* fed with kale (*Brassica oleracea* L. var. *acephala*). *Food Chem. Toxicol.* 47, 1209–1220. doi: 10.1016/j.fct.2009.02.014

Fiol, M., Adermann, S., Neugart, S., Rohn, S., Mügge, C., Schreiner, M., et al. (2012). Highly glycosylated and acylated flavonols isolated from kale (*Brassica oleracea* var. *sabellica*) — structure–antioxidant activity relationship. *Food Res. Int.* 47, 80–89. doi: 10.1016/j.foodres.2012.01.014

Folta, K. M., and Maruhnich, S. A. (2007). Green light: a signal to slow down or stop. *J. Exp. Bot.* 58, 3099–3111. doi: 10.1093/jxb/erm130

Fuglevand, G., Jackson, J. A., and Jenkins, G. I. (1996). UV-B, UV-A, and blue light signal transduction pathways interact synergistically to regulate chalcone synthase gene expression in *Arabidopsis*. *Plant Cell* 8, 2347–2357. doi: 10.1105/tpc.8.12.2347

Gachon, C. M. M., Langlois-Meurinne, M., and Saindrenan, P. (2005). Plant secondary metabolism glycosyltransferases: the emerging functional analysis. *Trends Plant Sci.* 10, 542–549. doi: 10.1016/j.tplants.2005.09.007

Gitelson, A., Chivkunova, O., Zhigalova, T., and Solovchenko, A. (2017). In situ optical properties of foliar flavonoids: implication for non-destructive estimation of flavonoid content. *J. Plant Physiol.* 218, 258–264. doi: 10.1016/j.jplph.2017.08.009

Groenbaek, M., Jensen, S., Neugart, S., Schreiner, M., Kidmose, U., and Lakkenborg Kristensen, H. (2014). Influence of cultivar and fertilizer approach on curly kale (*Brassica oleracea* L. var. *sabellica*). 1. Genetic diversity reflected in agronomic characteristics and phytochemical concentration. *J. Agric. Food Chem.* 62, 11393–11402. doi: 10.1021/jf503096p

Harbaum-Piayda, B., Palani, K., and Schwarz, K. (2016). Influence of postharvest UV-B treatment and fermentation on secondary plant compounds in white cabbage leaves. *Food Chem.* 197, 47–56. doi: 10.1016/j.foodchem.2015.10.065

Harbaum-Piayda, B., Walter, B., Bengtsson, G. B., Hubbermann, E. M., Bilger, W., and Schwarz, K. (2010). Influence of pre-harvest UV-B irradiation and normal or controlled atmosphere storage on flavonoid and hydroxycinnamic acid contents of pak choi (*Brassica campestris* L. ssp *chinensis* var. *communis*). *Postharvest Biol. Technol.* 56, 202–208. doi: 10.1016/j.postharvbio.2010.01.003

Harborne, J. B., and Williams, C. A. (2000). Advances in flavonoid research since 1992. *Phytochemistry* 55, 481–504. doi: 10.1016/s0031-9422(00)00235-1

Heijde, M., and Ulm, R. (2012). UV-B photoreceptor-mediated signalling in plants. *Trends in Plant Sci.* 17, 230–237. doi: 10.1016/j.tplants.2012.01.007

Heinze, M., Hanschen, F. S., Wiesner-Reinhold, M., Baldermann, S., Grafe, J., Schreiner, M., et al. (2018). Effects of developmental stages and reduced UVB and low UV conditions on plant secondary metabolite profiles in pak choi (*Brassica rapa* subsp. *chinensis*). *J. Agric. Food Chem.* 66, 1678–1692. doi: 10.1021/acs.jafc.7b03996

Hernandez, I., Alegre, L., van Breusegem, F., and Munne-Bosch, S. (2009). How relevant are flavonoids as antioxidants in plants? *Trends Plant Sci.* 14, 125–132. doi: 10.1016/j.tplants.2008.12.003

Husain, S. R., Cillard, J., and Cillard, P. (1987). Hydroxyl radical scavenging activity of flavonoids. *Phytochemistry* 26, 2489–2491. doi: 10.1016/s0031-9422(00)83860-1

Jansen, M. A. K., and Bornman, J. F. (2012). UV-B radiation: from generic stressor to specific regulator. *Physiol. Plant.* 145, 501–504. doi: 10.1111/j.1399-3054.2012.01656.x

Jansen, M. A. K., Hectors, K., O'Brien, N. M., Guisez, Y., and Potters, G. (2008). Plant stress and human health: do human consumers benefit from UV-B acclimated crops? *Plant Sci.* 175, 449–458. doi: 10.1016/j.plantsci.2008.04.010

Jenkins, G. I. (2014). The UV-B photoreceptor UVR8: from structure to physiology. *Plant Cell* 26, 21–37. doi: 10.1105/tpc.113.119446

Johkan, M., Shoji, K., Goto, F., Hashida, S., and Yoshihara, T. (2010). Blue light-emitting diode light irradiation of seedlings improves seedling quality and growth after transplanting in red leaf lettuce. *Hortic. Sci.* 45, 1809–1814. doi: 10.21273/hortsci.45.12.1809

Kaiser, E., Ouzounis, T., Giday, H., Schipper, R., Heuvelink, E., and Marcelis, L. F. M. (2019). Adding blue to red supplemental light increases biomass and yield of greenhouse-grown tomatoes, but only to an optimum. *Front. Plant Sci.* 9:2002. doi: 10.3389/fpls.2018.02002

Kolb, C. A., Kaser, M. A., Kopecky, J., Zotz, G., Riederer, M., and Pfundel, E. E. (2001). Effects of natural intensities of visible and ultraviolet radiation on epidermal ultraviolet screening and photosynthesis in grape leaves. *Plant Physiol.* 127, 863–875. doi: 10.1104/pp.010373

Kyriacou, M. C., El-Nakhel, C., Pannico, A., Graziani, G., Soteriou, G. A., Giordano, M., et al. (2020). Phenolic constitution, phytochemical and macronutrient content in three species of microgreens as modulated by natural fiber and synthetic substrates. *Antioxidants (Basel)* 9:252. doi: 10.3390/antiox9030252

Lau, O. S., and Deng, X. W. (2012). The photomorphogenic repressors COP1 and DET1: 20 years later. *Trends Plant Sci.* 17, 584–593. doi: 10.1016/j.tplants.2012.05.004

Li, H., Zhang, M., and Ma, G. (2011). Radical scavenging activity of flavonoids from *Trollius chinensis* Bunge. *Nutrition* 27, 1061–1065. doi: 10.1016/j.nut.2011.03.005

Li, Y., Zheng, Y., Liu, H., Zhang, Y., Hao, Y., Song, S., et al. (2019). Effect of supplemental blue light intensity on the growth and quality of Chinese kale. *Hortic. Environ. Biotechnol.* 60, 49–57. doi: 10.1007/s13580-018-0104-1

Lin, L.-Z., and Harnly, J. M. (2009). Identification of the phenolic components of collard greens, kale, and Chinese broccoli. *J. Agric. Food Chem.* 57, 7401–7408. doi: 10.1021/jf901121v

Majer, P., and Hideg, E. (2012). Developmental stage is an important factor that determines the antioxidant responses of young and old grapevine leaves under UV irradiation in a greenhouse. *Plant Physiol. Biochem.* 50, 15–23. doi: 10.1016/j.plaphy.2011.09.018

Majer, P., Neugart, S., Krumbein, A., Schreiner, M., and Hideg, É (2014). Singlet oxygen scavenging by leaf flavonoids contributes to sunlight acclimation in *Tilia platyphyllos*. *Environ. Exp. Bot.* 100, 1–9. doi: 10.1016/j.envexpbot.2013.12.001

Majer, P., Stoyanova, S., and Hideg, E. (2010). Do leaf total antioxidant capacities (TAC) reflect specific antioxidant potentials? A comparison of TAC and reactive oxygen scavenging in tobacco leaf extracts. *J. Photochem. Photobiol. B Biol.* 100, 38–43. doi: 10.1016/j.jphotobiol.2010.04.007

Martínez-Sánchez, A., Llorach, R., Gil, M. I., and Ferreres, F. (2007). Identification of new flavonoid glycosides and flavonoid profiles to characterize rocket leafy salads (*Eruca vesicaria* and *Diplotaxis tenuifolia*). *J. Agric. Food Chem.* 55, 1356–1363. doi: 10.1021/jf063474b

Matysiak, B., and Kowalski, A. (2019). White, blue and red LED lighting on growth, morphology and accumulation of flavonoid compounds in leafy greens. *Zemdirbyste* 103, 281–286. doi: 10.13080/z-a.2019.106.036

Mirecki, R. M., and Teramura, A. H. (1984). Effects of ultraviolet-B irradiance on soybean: the dependence of plant-sensitivity on the photosynthetic photon flux-density during and after leaf expansion. *Plant Physiol.* 74, 475–480. doi: 10.1104/pp.74.3.475

Mormile, P., Rippa, M., Graziani, G., and Ritieni, A. (2019). Use of greenhouse-covering films with tailored UV-B transmission dose for growing 'medicines' through plants: rocket salad case. *J. Sci. Food Agric.* 99, 6931–6936. doi: 10.1002/jsfa.9980

Neugart, S., Fiol, M., Schreiner, M., Rohn, S., Zrenner, R., Kroh, L. W., et al. (2014). Interaction of moderate UV-B exposure and temperature on the formation of structurally different flavonol glycosides and hydroxycinnamic acid derivatives in Kale (*Brassica oleracea* var. *sabellica*). *J. Agric. Food Chem.* 62, 4054–4062. doi: 10.1021/jf4054066

Neugart, S., Kläring, H.-P., Zietz, M., Schreiner, M., Rohn, S., Kroh, L. W., et al. (2012a). The effect of temperature and radiation on flavonol aglycones and flavonol glycosides of kale (*Brassica oleracea* var. *sabellica*). *Food Chem.* 133, 1456–1465. doi: 10.1016/j.foodchem.2012.02.034

Neugart, S., and Schreiner, M. (2018). UVB and UVA as eustressors in horticultural and agricultural crops. *Sci. Hortic.* 234, 370–381. doi: 10.1016/j.scienta.2018.02.021

Neugart, S., Zietz, M., Schreiner, M., Rohn, S., Kroh, L. W., and Krumbein, A. (2012b). Structurally different flavonol glycosides and hydroxycinnamic acid derivatives respond differently to moderate UV-B radiation exposure. *Physiol. Plant.* 145, 582–593. doi: 10.1111/j.1399-3054.2012.01567.x

Olsen, H., Aaby, K., and Borge, G. I. A. (2009). Characterization and quantification of flavonoids and hydroxycinnamic acids in curly kale (*Brassica oleracea* L. convar. *acephala* var. *sabellica*) by HPLC-DAD-ESI-MS^n. *J. Agric. Food Chem.* 57, 2816–2825. doi: 10.1021/jf803693t

Olsson, L. C., Veit, M., Weissenbock, G., and Bornman, J. F. (1998). Differential flavonoid response to enhanced UV-B radiation in *Brassica napus*. *Phytochemistry* 49, 1021–1028. doi: 10.1016/s0031-9422(98)00062-4

Pan, M. H., Lai, C. S., and Ho, C. T. (2010). Anti-inflammatory activity of natural dietary flavonoids. *Food Funct.* 1, 15–31. doi: 10.1039/c0fo00103a

Panja, S., Chaudhuri, D., Baban Ghate, N., Le Minh, H., and Mandal, N. (2014). In vitro assessment of phytochemicals, antioxidant and DNA protective potential of wild edible fruit of *Elaeagnus latifolia* Linn. *Fruits* 69, 303–314. doi: 10.1051/fruits/2014019

Pasini, F., Verardo, V., Caboni, M. F., and D'Antuono, L. F. (2012). Determination of glucosinolates and phenolic compounds in rocket salad by HPLC-DAD-MS: evaluation of *Eruca sativa* Mill. and *Diplotaxis tenuifolia* L. genetic resources. *Food Chem.* 133, 1025–1033. doi: 10.1016/j.foodchem.2012.01.021

Pennisi, G., Blasioli, S., Cellini, A., Maia, L., Crepaldi, A., Braschi, I., et al. (2019). Unraveling the role of red:blue led lights on resource use efficiency and nutritional properties of indoor grown sweet basil. *Front. Plant Sci.* 10:305. doi: 10.3389/fpls.2019.00305

Podsedek, A. (2007). Natural antioxidants and antioxidant capacity of *Brassica* vegetables: a review. *LWT Food Sci. Technol.* 40, 1–11. doi: 10.1016/j.lwt.2005.07.023

Rechner, O., Neugart, S., Schreiner, M., Wu, S., and Poehling, H. M. (2016). Different narrow-band light ranges alter plant secondary metabolism and plant defense response to aphids. *J. Chem. Ecol.* 42, 989–1003. doi: 10.1007/s10886-016-0755-2

Rechner, O., Neugart, S., Schreiner, M., Wu, S., and Poehling, H.-M. (2017). Can narrow-bandwidth light from UV-A to green alter secondary plant metabolism and increase *Brassica* plant defenses against aphids? *PLoS One* 12:e0188522. doi: 10.1371/journal.pone.0188522

Reifenrath, K., and Mueller, C. (2007). Species-specific and leaf-age dependent effects of ultraviolet radiation on two *Brassicaceae*. *Phytochemistry* 68, 875–885. doi: 10.1016/j.phytochem.2006.12.008

Ribeiro, A. B., Berto, A., Chisté, R. C., Freitas, M., Visentainer, J. V., and Fernandes, E. (2015). Bioactive compounds and scavenging capacity of extracts from different parts of *Vismia cauliflora* against reactive oxygen and nitrogen species. *Pharm. Biol.* 53, 1267–1276. doi: 10.3109/13880209.2014.974063

Samuoliene, G., Virsile, A., Brazaityte, A., Jankauskiene, J., Sakalauskiene, S., Vastakaite, V., et al. (2017). Blue light dosage affects carotenoids and tocopherols in microgreens. *Food Chem.* 228, 50–56. doi: 10.1016/j.foodchem.2017.01.144

Schmidt, S., Zietz, M., Schreiner, M., Rohn, S., Kroh, L. W., and Krumbein, A. (2010). Identification of complex, naturally occurring flavonoid glycosides in kale (*Brassica oleracea* var. *sabellica*) by high-performance liquid chromatography diode-array detection/electrospray ionization multi-stage mass spectrometry. *Rapid Commun. Mass Spectrom.* 24, 2009–2022. doi: 10.1002/rcm.4605

Schreiner, M., Mewis, I., Huyskens-Keil, S., Jansen, M. A. K., Zrenner, R., Winkler, J. B., et al. (2012). UV-B-induced secondary plant metabolites – potential benefits for plant and human health. *Crit. Rev. Plant Sci.* 31, 229–240. doi: 10.1080/07352689.2012.664979

Searles, P. S., Flint, S. D., and Caldwell, M. M. (2001). A meta-analysis of plant field studies simulating stratospheric ozone depletion. *Oecologia* 127, 1–10. doi: 10.1007/s004420000592

Smith, H. L., McAusland, L., and Murchie, E. H. (2017). Don't ignore the green light: exploring diverse roles in plant processes. *J. Exp. Bot.* 68, 2099–2110. doi: 10.1093/jxb/erx098

Solovchenko, A. E., and Merzlyak, M. N. (2008). Screening of visible and UV radiation as a photoprotective mechanism in plants. *Russ. J. Plant Physiol.* 55:719. doi: 10.1134/S1021443708060010

Stelzner, J., Roemhild, R., Garibay-Hernández, A., Harbaum-Piayda, B., Mock, H.-P., and Bilger, W. (2019). Hydroxycinnamic acids in sunflower leaves serve as UV-A screening pigments. *Photochem. Photobiol. Sci.* 18, 1649–1659. doi: 10.1039/c8pp00440d

Stochmal, A., and Oleszek, W. (2007). Effect of acylation of flavones with hydroxycinnamic acids on their spectral characteristics. *Nat. Prod. Commun.* 2, 571–574.

Taulavuori, K., Hyöky, V., Oksanen, J., Taulavuori, E., and Julkunen-Tiitto, R. (2016). Species-specific differences in synthesis of flavonoids and phenolic acids under increasing periods of enhanced blue light. *Environ. Exp. Bot.* 121, 145–150. doi: 10.1016/j.envexpbot.2015.04.002

Taulavuori, K., Pyysalo, A., Taulavuori, E., and Julkunen-Tiitto, R. (2018). Responses of phenolic acid and flavonoid synthesis to blue and blue-violet light depends on plant species. *Environ. Exp. Bot.* 150, 183–187. doi: 10.1016/j.envexpbot.2018.03.016

Terashima, I., Fujita, T., Inoue, T., Chow, W. S., and Oguchi, R. (2009). Green light drives leaf photosynthesis more efficiently than red light in strong white light: revisiting the enigmatic question of why leaves are green. *Plant Cell Physiol.* 50, 684–697. doi: 10.1093/pcp/pcp034

Tissot, N., and Ulm, R. (2020). Cryptochrome-mediated blue-light signalling modulates UVR8 photoreceptor activity and contributes to UV-B tolerance in *Arabidopsis*. *Nat. Commun.* 11:1323. doi: 10.1038/s41467-020-15133-y

Triantaphylides, C., and Havaux, M. (2009). Singlet oxygen in plants: production, detoxification and signaling. *Trends Plant Sci.* 14, 219–228. doi: 10.1016/j.tplants.2009.01.008

Wang, S. Y., Lewers, K. S., Bowman, L., and Ding, M. (2007). Antioxidant activities and anticancer cell proliferation properties of wild strawberries. *J. Am. Soc. Hort. Sci.* 132, 647–658. doi: 10.21273/JASHS.132.5.647

Wang, S. Y., and Zheng, W. (2001). Effect of plant growth temperature on antioxidant capacity in strawberry. *J. Agric. Food Chem.* 49, 4977–4982. doi: 10.1021/jf0106244

Waterman, M. J., Nugraha, A. S., Hendra, R., Ball, G. E., Robinson, S. A., and Keller, P. A. (2017). Antarctic moss biflavonoids show high antioxidant and ultraviolet-screening activity. *J. Nat. Prod.* 80, 2224–2231. doi: 10.1021/acs.jnatprod.7b00085

Wojciechowska, R., Bugosz-Grochowska, O., Kołton, A., and Żupnik, M. (2015). Effects of LED supplemental lighting on yield and some quality parameters of lamb's lettuce grown in two winter cycles. *Sci. Hortic.* 187, 80–86. doi: 10.1016/j.scienta.2015.03.006

Zheng, Y., Zhang, Y., Liu, H., Li, Y., Liu, Y., Hao, Y., et al. (2018). Supplemental blue light increases growth and quality of greenhouse pak choi depending on cultivar and supplemental light intensity. *J. Integr. Agric.* 17, 2245–2256. doi: 10.1016/S2095-3119(18)62064-7

Conflict of Interest: The authors declare that the research was conducted in the absence of any commercial or financial relationships that could be construed as a potential conflict of interest.

Copyright © 2021 Neugart, Majer, Schreiner and Hideg. This is an open-access article distributed under the terms of the Creative Commons Attribution License (CC BY). The use, distribution or reproduction in other forums is permitted, provided the original author(s) and the copyright owner(s) are credited and that the original publication in this journal is cited, in accordance with accepted academic practice. No use, distribution or reproduction is permitted which does not comply with these terms.

frontiers in Plant Science

REVIEW
published: 01 February 2021
doi: 10.3389/fpls.2021.611893

A Review of Strawberry Photobiology and Fruit Flavonoids in Controlled Environments

*Rachael Warner, Bo-Sen Wu, Sarah MacPherson and Mark Lefsrud**

Department of Bioresource Engineering, McGill University, Sainte-Anne-de-Bellevue, QC, Canada

Rapid technology development in controlled environment (CE) plant production has been applied to a large variety of plants. In recent years, strawberries have become a popular fruit for CE production because of their high economic and nutritional values. With the widespread use of light-emitting diode (LED) technology in the produce industry, growers can manipulate strawberry growth and development by providing specific light spectra. Manipulating light intensity and spectral composition can modify strawberry secondary metabolism and highly impact fruit quality and antioxidant properties. While the impact of visible light on secondary metabolite profiles for other greenhouse crops is well documented, more insight into the impact of different light spectra, from UV radiation to the visible light spectrum, on strawberry plants is required. This will allow growers to maximize yield and rapidly adapt to consumer preferences. In this review, a compilation of studies investigating the effect of light properties on strawberry fruit flavonoids is provided, and a comparative analysis of how light spectra influences strawberry's photobiology and secondary metabolism is presented. The effects of pre-harvest and post-harvest light treatments with UV radiation and visible light are considered. Future studies and implications for LED lighting configurations in strawberry fruit production for researchers and growers are discussed.

Keywords: LED, light spectrum, secondary metabolite, UV, visible light

OPEN ACCESS

Edited by:
Marie-Theres Hauser, University of Natural Resources and Life Sciences Vienna, Austria

Reviewed by:
Vance Whitaker, University of Florida, United States
Giovanni Agati, Nello Carrara Institute of Applied Physics (IFAC), Italy

****Correspondence:***
Mark Lefsrud
mark.lefsrud@mcgill.ca

Specialty section:
This article was submitted to Plant Metabolism and Chemodiversity, a section of the journal Frontiers in Plant Science

Received: *29 September 2020*
Accepted: *06 January 2021*
Published: *01 February 2021*

Citation:
Warner R, Wu B-S, MacPherson S and Lefsrud M (2021) A Review of Strawberry Photobiology and Fruit Flavonoids in Controlled Environments. Front. Plant Sci. 12:611893. doi: 10.3389/fpls.2021.611893

INTRODUCTION

Strawberry (*Fragaria* × *ananassa*) is a valuable crop cultivated worldwide. All strawberry species belong to the genus *Fragaria* and are members of *Rosaceae*, a family that contains many economically significant crops, primarily fruits such as apple (*Malus domestica*), pear (*Pyrus communis*), and peach (*Prunas persica*). The most cultivated strawberry species produced in North America is *F.* × *ananassa*, arising from breeding between two species: *F.* × *virginiana* and *F.* × *chiloensis* (Stewart and Folta, 2010). Strawberry fruits provide a wide range of sensory elicitation and health benefits to the consumer, including high fiber, micronutrient, and ascorbic acid content (Giampieri et al., 2012; Afrin et al., 2016; Battino et al., 2016). Additionally, strawberry fruits are part of a growing trend that highlights plant-derived antioxidants for their proven health benefits (Nile and Park, 2014). These consumer-liking and health-promoting properties have consequently led to strawberry's strong economic role in the fruit industry.

In 2016, the global total production of strawberries was over US$17.7 billion, and this value has substantially increased over the last 10 years (FAO, 2016).

The production of strawberry fruit and their nutritional value are highly impacted by the surrounding environment; therefore, strawberries are often produced in controlled environments (CEs) where lighting and temperature are controlled (Samtani et al., 2019). The use of artificial lighting is a common approach for flower initiation and improved fruit yield (López-Aranda et al., 2011; Hidaka et al., 2014). The critical photoperiod for strawberry flower initiation varies depending upon cultivars and interactions with temperature (Bradford et al., 2010; López-Aranda et al., 2011; Heide et al., 2013). Inhibition of flower initiation at high temperature has been reported for strawberry plants with flowering habits under different photoperiods (Ito and Saito, 1962; Heide, 1977; Serçe and Hancock, 2005). As such, it is suggested that it is inadequate to classify strawberry cultivars solely based on their flowering habits (i.e., short-day, long-day, and day length-insensitive) without considering temperature effects (Durner et al., 1984). Artificial light properties, including wavelength and intensity, also play an important role in strawberry fruit production and quality (Nadalini et al., 2017; Zahedi and Sarikhani, 2017). For instance, sole blue light treatment enhances strawberry (*F.* × *ananassa* cv. Elsanta) fruit production, approximately 25% more than other light sources (Nadalini et al., 2017). End-of-day 735-nm radiation treatment results in a higher strawberry sucrose level (Zahedi and Sarikhani, 2017). These studies have proven that the use of artificial lighting systems allows growers to optimize fruit production and meet consumers' sensory desires (Nadalini et al., 2017; Zahedi and Sarikhani, 2017).

Plant-derived antioxidants are produced through secondary metabolic pathways, and act as an essential protective barrier against both biotic and abiotic stressors, including light stress (Pocock, 2015; Nadalini et al., 2017). Secondary metabolites such as flavonoids and quinones protect plants from oxidation caused by free radical scavenging (Lü et al., 2010). The extent of secondary metabolite accumulation further influences plant and fruit features, such as specific coloration and antioxidant properties that consumers adore (Akula and Ravishankar, 2011). The high level of total antioxidant capacity contained in strawberry fruit enables the neutralization of free radicals and reduces oxidative stress in the human body (Afrin et al., 2016). The most prevalent secondary metabolites in strawberry fruits are flavonoids, including anthocyanins (Aaby et al., 2012), which are associated with antioxidative and anti-inflammatory properties. Flavonoids predominantly protect plants from UV radiation (Panche et al., 2016), and anthocyanins protect plants from blue and green light (Landi et al., 2020a). In recent years, known antioxidant properties of strawberry fruit have prompted the rise of its global consumption.

Considering the important role that strawberry plants play in the fruit industry, several reviews on strawberry production have been conducted, including flower initiation, development, handling, flavor profile, and health benefits (López-Aranda et al., 2011; Heide et al., 2013; Afrin et al., 2016; Baicu and Popa, 2018; Yan et al., 2018). However, there is limited information available on the impact of light properties on strawberry productivity and secondary metabolite accumulation. Secondary metabolite accumulation in strawberries is impacted by interactive effects between light wavelengths, developmental stages, and lighting strategies (i.e., pre-harvesting and post-harvesting; Erkan et al., 2008; Kadomura-Ishikawa et al., 2013). To this end, this review attempts to compile and compare available research on the impact of light properties within the wavelength ranges of UV radiation (<380 nm) to the visible light spectrum (380–730 nm) on strawberry fruit production, as well as the major group of secondary metabolites, flavonoid compounds. This may lead to improved strawberry fruit production and quality with additional health values in antioxidant activity, while possibly allowing for knowledge transfer to other berry plants grown in CEs.

FLAVONOID PROFILE AND FUNCTION IN STRAWBERRY FRUITS

Plant secondary metabolites have several functions in light signaling and defending against abiotic stresses (Thirumurugan et al., 2018). The most prevalent class of secondary metabolites in strawberry fruits is phenolic compounds, which have at least one phenol unit (aromatic organic ring) in their chemical structures. Phenolic compounds are further divided into different sub-groups, including coumarins, flavonoids, phenolic acids, and tannins. Flavonoids are widely found in foods and beverages of plant origin (i.e., fruits and vegetables; Rozema et al., 2002; Delgado et al., 2019). Flavonoids are easily recognized as flower pigments – they are responsible for the color and aroma of flowers (Dewick, 2001). Flavonoids can be further sub-classified to different subgroups: anthocyanins, flavonols, and flavanols (Aaby et al., 2012; Alvarez, 2014). Over 10,000 flavonoids have been reported, representing the third largest group of naturally occurred secondary metabolites, after terpenoids and alkaloids (Martens et al., 2010). Most flavonoids absorb wavelengths between 315 and 400 nm; therefore, they play an important role in UV radiation screening and as antioxidants for plants (Kotilainen et al., 2009). Sunlight and UV radiation exposure directly impact the extent of flavonoid accumulation in plants (Downey et al., 2006).

Anthocyanins

Anthocyanins are the most prevalent phenolic compound found in the outer cell layers of various fruits, constituting up to 40% of total phenols in some strawberry cultivars (Aaby et al., 2012). In strawberry, the major anthocyanin is pelargonidin 3-glucoside, with reported anti-inflammatory effects (Da Silva et al., 2007; Amini et al., 2017). Although anthocyanin accumulation is implicated in UV–B protection (280–315 nm), it also occurs under stress conditions involving visible light and far-red radiation (Carvalho and Folta, 2016; Dou et al., 2017). Anthocyanins are the pigments responsible for coloration in flowers and fruits, often serving as visual signal for insect-mediated pollination and seed dispersers (Turturică et al., 2015).

Anthocyanin stability largely depends on light, temperature, pH, and the co-pigmentation with other flavonoids (i.e., flavonols; Martens et al., 2010; Turturică et al., 2015). Anthocyanin color is pH-dependent because of its ionic nature; anthocyanin pigments appear red under acidic conditions and blue under alkaline conditions (Khoo et al., 2017). In strawberry plants, anthocyanin accumulates quickly in the late stages of ripening, beginning when fruits turn from white to red and increase more than 10-fold in red, ripe berries (Kadomura-Ishikawa et al., 2013). These phytochemicals largely contribute to antioxidant capacity, impacting the nutritional benefits of the fruit (Aaby et al., 2012; Kadomura-Ishikawa et al., 2013). About 70% of total antioxidant capacity comes from anthocyanins, highlighting its importance among plant secondary metabolites (Wang and Millner, 2009; Giampieri et al., 2012).

Flavonols

Flavonols are abundantly found in a variety of fruits and vegetables including apples, grapes, and berries, and are reportedly associated with antioxidant potential and reduced risk of vascular disease in humans (Panche et al., 2016). In cultivated strawberry, the major flavonols are quercetin and kaempferol (Labadie et al., 2020). Flavonols are often the main flavonoids at the beginning of the fruit development, but at the ripening stage the flavonoid pathway switches to anthocyanin production (Chassy et al., 2012). Compared to anthocyanins, flavonols contribute more to antioxidant protection against UV-B radiation (Ferreyra et al., 2012; Zoratti et al., 2014); however, they are more sensitive to light properties (Carbone et al., 2009). Studies have reported that flavonol accumulation is highly reduced under shadow treatment in grape (*Vitis vinifera*) skins and is influenced by light levels in grape berry (*Vitis berlandieri* × *V. vinifera*; Pereira et al., 2006; Matus et al., 2009). Apart from functioning as a tissue-protector against UV radiation, flavonols act as flower pigments that attract and defend against insects (Gronquist et al., 2001). Flavonols influence plants' responses to gravity, but these effects were observed in mutants only (Owens et al., 2008).

Flavanols

Flavanols, also called flavan-3-ols, are the most common dietary flavonoids. They are used as functional ingredients in food processing to control microbial levels and provide oxidative stability (Aron and Kennedy, 2008). Flavanols consist of monomeric units (i.e., catechins and epicatechin), in addition to oligomeric and polymeric compounds (proanthocyanidins, also called condensed tannins; Al-Dashti et al., 2018). Like anthocyanins and flavonols, flavanol accumulation is developmental stage-dependent (Zhang et al., 2013). For instance, supplemental UV radiation increases flavanol content during development but not in mature grape berries (*V. vinifera* cv. Cabernet Sauvignon). Flavanols help plants protect against harmful pathogens, such as microbes and fungi, as well as insects and herbivorous animals (Aron and Kennedy, 2008). As for flavanols' dietary effects, they may improve vascular function and nitric oxide availability, as well as modulate metabolism and respiration (Al-Dashti et al., 2018). Being flavanol polymers, it has been reported that proanthocyanidins possess antioxidative and cardio-preventive properties (Monagas et al., 2010).

PLANT PHOTOMORPHOGENETIC RESPONSES AND FLAVONOID BIOSYNTHESIS UNDER UV RADIATION

Biologically active radiation extends from 300 to 800 nm. UV radiation lies in the wavelength range below 380 nm, followed by the visible spectrum between 380 and 720 nm. Outdoors or in an environment lit without supplemental light, approximate 6% of solar radiation is UV radiation, comprising 95% UV-A radiation (315–380 nm) and 5% of UV-B radiation (280–315 nm). UV-C radiation (<280 nm) does not penetrate to Earth's surface because of the ozone layer. Currently, the major focus of UV radiation-plant investigations is on the UV-B wavelength range, and the number of studies targeting UV-A radiation is relatively small (Verdaguer et al., 2017).

Secondary metabolite formation, including phenolic compounds and antioxidants, is a plant's response to UV-A and UV-B radiation (Caldwell and Britz, 2006), and most flavonoids absorb light in the UV-A radiation range (Cerovic et al., 2002). High levels of UV radiation can cause damage to plants at different levels, including DNA and lipids, leading to impaired gene transcription and photosynthesis (Kunz et al., 2006; Khudyakova et al., 2017). Plant responses to UV-A and UV-B radiation are summarized in **Figure 1A**. UV radiation alters plant morphology and biomass accumulation during both vegetative and reproductive stages (Müller-Xing et al., 2014; Bernal et al., 2015), and UV-A radiation is perceived by several photoreceptors, including cryptochromes and phytochromes (**Figure 1B**; Mockler et al., 2003; Folta and Carvalho, 2015). Cryptochromes (cry1 and cry2) are flavin-type blue light photoreceptors (320–500 nm) that have been implicated in numerous developmental and circadian signaling pathways (Banerjee and Batschauer, 2005; Jones, 2018). Phytochromes (phyA to phyE) are light-sensitive proteins with photo-reversible conformers: Pr and Pfr (Folta and Carvalho, 2015). Phytochrome Pr, the inactive form of phytochrome, has a primary absorption peak at 660 nm and a secondary absorption peak located at 380 nm. Absorption peaks of the active form shift approximately 20–70 nm, toward longer wavelengths (408 and 730 nm; Stutte et al., 2009).

The mechanisms underlying this process are poorly investigated in plants, and varied plant responses to UV-A radiation regarding leaf size, morphology and biomass accumulation are reported (Biswas and Jansen, 2012; Kataria and Guruprasad, 2012; Verdaguer et al., 2017). Leaf size is one of the most important determinants of light capture and productivity. Increased rosette size was observed under different accessions of *Arabidopsis thaliana* grown indoors under 1.59 W m^{-2} UV-A radiation and 30 µmol m^{-2} s^{-1} of white light (4,000 K; Biswas and Jansen, 2012). The use of UV-blocking films further revealed that UV-A radiation increases total leaf area in soybean

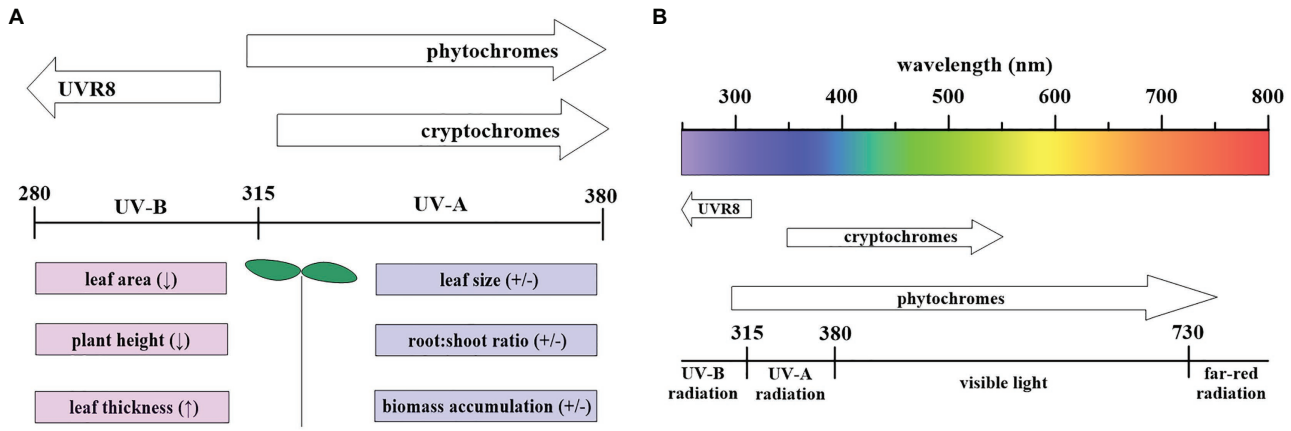

FIGURE 1 | (A) Plant responses to UV-A and UV-B radiation, with both positive and negative effects induced by UV-A radiation. **(B)** Plant photoreceptors involved in flower initiation with their corresponding spectral regions, adapted from Folta and Carvalho (2015) and Jones (2018).

(*Glycine max*) when grown in a greenhouse (Zhang et al., 2014). To the contrary, the solar spectrum, without UV-A and UV-B radiation, induced a larger leaf size when compared to UV-A and UV-B radiation in different varieties of sorghum (*Sorghum bicolor*; Kataria and Guruprasad, 2012). Published data shows no clear link between the impact of UV-A radiation and biomass accumulation, as inconsistent responses have been reported for UV-A-mediated biomass responses (Kataria and Guruprasad, 2012; Zhang et al., 2014). Some studies demonstrated stimulatory effects on biomass accumulation under UV-A radiation (Bernal et al., 2013; Zhang et al., 2014), while others reported inhibitory effects (Kataria et al., 2013). One study concluded that the genotype determines UV-A-mediated responses in plants; however, the study was solely conducted using *A. thaliana* ecotypes (Cooley et al., 2001).

Such contradictory findings may be due to changes in morphology and photosynthetic activity, as well as accumulation of secondary metabolites (Verdaguer et al., 2017). Apart from the impact of plant physiological properties on UV-A radiation, different UV-A radiation conditions might contribute to these conflicting findings. Most UV-A-mediated response studies were conducted with UV-blocking films and the solar spectrum as radiation sources (Zhang et al., 2014; Khudyakova et al., 2017). The use of UV-blocking films only enables the reflection of a certain percentage of UV radiation from solar radiation, and their cut-off wavelengths vary depending on the manufacturer (Katsoulas et al., 2020). In this scenario, although all studies reported the same radiation treatments (i.e., UV-A radiation), radiation spectra might differ. Distinct UV spectra and radiation properties could potentially lead to different plant responses. Furthermore, users cannot select for specific wavelengths passing through the UV-blocking films, as is possible with bandpass optical filters (i.e., blocking UV-A radiation only). As such, UV-A + UV-B treatments are often used as a baseline to compare and discuss the impact of UV-A radiation. Although potential interactive effects between UV-A and UV-B radiation have not yet been reported, they should still be considered and determined with future research.

The most frequently reported UV-B-induced morphological changes are a decrease in leaf area and/or an increase in leaf thickness (**Figure 1A**; Klem et al., 2012; Robson and Aphalo, 2012; Doupis et al., 2016). UV-B radiation results in leaf changes (i.e., chlorosis, necrosis, and desiccation), and declines in plant height and shoot growth. These observations may serve as a protective mechanism since UV-B can damage photosystems (Gupta et al., 2017). Additionally, secondary metabolite responses differ under UV-B radiation (Schreiner et al., 2012; Hectors et al., 2014). For instance, polyamine and tocopherol levels upregulate quickly (within less than 24 h) in *A. thaliana* (Hectors et al., 2014), whereas flavonoids accumulate at a lower rate, with steady states usually reached after several days (Kusano et al., 2011). Furthermore, dose-dependent responses by flavonoids have been reported; a moderate UV-B dose (ambient radiation) induces flavonoid rutin production, which decreases under both reduced and enhanced UV-B dosage. Ambient UV-B dosage stimulates rutin accumulation, and accumulated rutin is more evident in buckwheat (*Fagopyrum esculentum*) leaves than in flowers (Kreft et al., 2002; Jansen et al., 2008). This suggests that different protectants respond differently based on UV radiation dosage, and that the relative abundance of different flavonoid species differs after UV radiation treatment, implying that distinct dose-response curves for each individual flavonoid compounds exist (Reifenrath and Müller, 2007).

UV-B radiation is perceived by the UV-B photoreceptor UV resistance locus 8 (UVR8), which promotes pest resistance and increases flavonoid accumulation. Under a low dose of UV-B radiation, UVR8 photoreceptor signaling is mediated through the RING-finger type ubiquitin E3 ligase CONSTITUTIVE PHOTOMORPHOGENIC1 (COP1; **Figure 2**; Lau and Deng, 2012; Peng et al., 2013). COP1 promotes the expression of ELONGATED HYPOCOTYL5 (HY5) in *A.thaliana* (Lau and Deng, 2012) and apple (*Malus* × *domestica*; Peng et al., 2013). Specifically, the presence of low UV-B

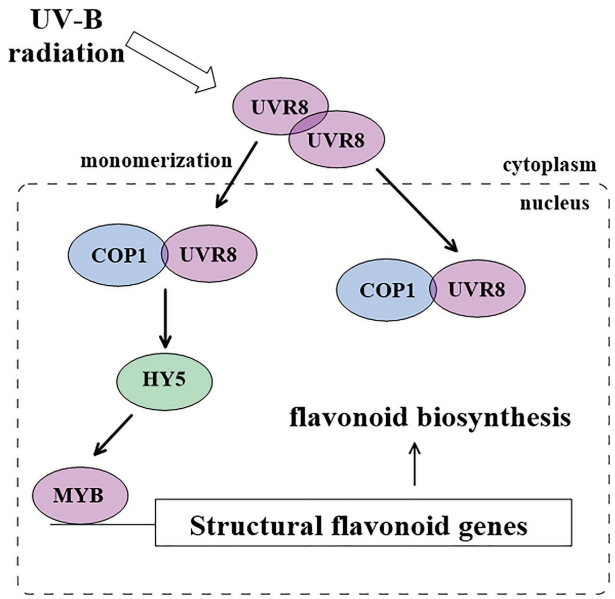

FIGURE 2 | Proposed mechanism for UV-B signaling pathway in flavonoid biosynthesis.

radiation results in UVR8 monomerization, and UVR8 monomers interact with COP1 to initiate the UV-B signaling pathway. The UVR8-COP1 complex then activates HY5 binding to the promoter region of different R2R3 MYBs, and this leads to flavonoid accumulation in the nucleus (Peng et al., 2013; Jenkins, 2017). Under a high dose of UV-B radiation, UV-B signaling may occur independently of UVR8, possibly *via* mitogen-activated protein kinase (MAPK) signaling (Besteiro et al., 2011).

The negative effects of UV-C radiation on plant development are well established (Urban et al., 2016). Overexposure of UV-C radiation can lead to shortened shelf-life for fresh produce and a reduction in photosynthetic efficiency (De Oliveira et al., 2016; Li et al., 2019). UV-C radiation inflicts considerable damage on lipids and DNA; hence, it is often credited with the most bactericidal activity within the UV wavelength range (Santos et al., 2013). In the context of plant secondary metabolism, it is important to note that UV-C radiation induces the accumulation of phenolics and flavonoids (Nigro et al., 2000; Erkan et al., 2008). However, because of higher energy contained in each photon, the focus on UV-C plant applications for secondary metabolites is largely placed on low doses and on pre- and post-harvesting treatments (Urban et al., 2016).

THE IMPACT OF UV RADIATION ON STRAWBERRY FRUIT FLAVONOIDS

Two approaches are often used to manipulate wavelength in CE production: UV-blocking films (i.e., pure polyethylene) and light-emitting diodes (LEDs; Singh et al., 2015; Katsoulas et al., 2020). Both technologies can manipulate wavelengths, yet they have different constraints and effective spectrum ranges. Earlier studies have reported the impact of UV dosage (combined UV-A and UV-B radiation) on strawberry fruit flavonoid levels, predominantly using UV-blocking films (Josuttis et al., 2010; Tsormpatsidis et al., 2011). Strawberry (cvs. Everest, Elsanta) fruits grown under films with high UV transparency (UV-A + UV-B) have higher anthocyanin and phenolic content (cyanidin 3-glucoside, quercetin 3-glucuronide, and kaempferol 3-glucoside) than the strawberry fruits grown under UV-blocking film (Josuttis et al., 2010; Tsormpatsidis et al., 2011). Moreover, UV radiation affects strawberry fruit firmness and color, in which fruit ripened with UV radiation was smaller, firmer, and darker compared to fruit grown under UV-blocking film (Tsormpatsidis et al., 2010; Ordidge et al., 2012). These earlier studies provide insightful information on the impact of UV radiation on strawberry fruit quality and flavonoid contents. However, reported effects on the impact of UV radiation include both UV-A and UV-B radiation. Specific wavelength or radiation treatments within the UV wavelength range cannot be achieved by using solar UV radiation and UV-blocking films. It is unknown if interactive effects within the UV range exist for strawberry flavonoid accumulation.

Unlike UV-blocking films, LEDs offer higher controllability of light properties, such as specific wavelength(s), photoperiod adjustment, and a wide range of intensities (Zoratti et al., 2014; Alrifai et al., 2019; Wu et al., 2019). Many recent studies show the potential of manipulating plant growth and regulating plant secondary metabolite profiles with LED lighting on numerous greenhouse crops within the visible spectrum (Stewart and Folta, 2010; Cocetta et al., 2017; Landi et al., 2020b). In recent years, steady progress has been made regarding wall-plug efficiency and the life-span of UV-LEDs (Kneissl, 2016). UV-LEDs may be superior to UV-blocking films when investigating UV radiation. However, the majority of strawberry studies using UV-LEDs is for enhanced strawberry fruit production, not insect and disease control (Kanto et al., 2009; Suthaparan et al., 2016). To our knowledge, only one study using UV-LED on strawberry (cvs. Maehyang and Seolhyang) flavonoid level has been reported to date, demonstrating that anthocyanin content increased in the Seolhyang cultivar when irradiated with combined 254, 306, and 352-nm LED radiation (Kim et al., 2011). Insufficient data suggest there is a clear lack of studies in this regard, and further study is required to elucidate the impact of narrow UV-A and UV-B spectra on strawberry flavonoids and other secondary metabolite accumulation.

Studies on strawberry secondary metabolites and UV-C radiation have concentrated on pre- and post-harvest treatment (Erkan et al., 2008; Xu et al., 2017a, 2019). This might be because of the availability of UV-C radiation sources (i.e., UV discharge lamps with a major peak at 255 nm) and the adverse effect of UV-C radiation on plant development (Kim et al., 2011). Low dose UV-C radiation at the post-harvesting stage has been applied to many valuable crops to reduce postharvest losses due to fungal growth and fruit decay (Marquenie et al., 2002). This UV-C radiation treatment is recognized as an effective method to enhance secondary metabolite concentrations in strawberry fruit within the food industry (Xu et al., 2017a; Saini and Keum, 2018; Li et al., 2019). UV-C radiation improves

the antioxidant capacity and reduces softening of fresh-cut strawberry fruit (Erkan et al., 2008; Pombo et al., 2009; Li et al., 2019). Erkan et al. (2008) first observed that low dose UV-C radiation (0.43–4.30 kJ m^{-2}) promoted the antioxidant capacity and phenolic content in strawberry fruit storage at 10°C (post-harvest), yet few effects were observed for anthocyanin accumulation. A recent study reported that both total phenolic compounds and anthocyanin in strawberry fruit significantly increased (>20%) with post-harvest treatment using UV-C radiation at 4°C (Li et al., 2019). Low dose UV-C radiation (4.1 kJ m^{-2}) slowed down strawberry fruit softening and degradation (Pombo et al., 2009).

Unlike post-harvest treatment, pre-harvest treatment with UV-C radiation is a relatively new approach to improving fruit quality that shows promise (Xie et al., 2015; Severo et al., 2017; Xu et al., 2017a). With UV-C radiation, strawberry fruit exhibit an increase in sucrose, ascorbic acid, and phytochemical profiles (ellagic acid and kaempferol-3-glucuronide). It is possible that UV-C radiation might affect fruit quality *via* the action of plant hormones, as it may be involved in abscisic acid signaling. A recent study showed that pre-harvest UV-C radiation of strawberries had a dose-dependent effect on secondary metabolite levels. Upon harvest, strawberry fruit that underwent UV-C radiation had a higher overall level of anthocyanins and flavonols at 15 kJ m^{-2}, and this level dropped to that of the control under the highest UV-C dose (29.4 kJ m^{-2}; Xu et al., 2017b). However, pre-harvest UV-C radiation also induced a decrease in volatile compounds responsible for aroma, impacting its flavor profile (Severo et al., 2017; **Table 1**).

THE IMPACT OF VISIBLE LIGHT AND FAR-RED RADIATION ON STRAWBERRY DEVELOPMENT AND FLAVONOID ACCUMULATION

Key transcription factors for flavonoid biosynthesis have been identified in many fruit crops, such as apple, grapevine, and woodland strawberry (Jaillon et al., 2007; Velasco et al., 2010; Shulaev et al., 2011). These studies indicate that R2R3 MYB transcription factors are the primary regulators of fruit flavonoid biosynthesis in response to changing light conditions within the visible light spectrum. Contrary to its positive regulator role under UV-radiation, COP1 acts as a repressor of flavonoid biosynthesis under visible light (Shulaev et al., 2011; Zoratti et al., 2014). Specifically, COP1 is exported from the nucleus to the cytoplasm, allowing nuclear-localized transcription factors to accumulate and induce expression of genes that are directly regulated by R2R3 MYB transcription factors (Lau and Deng, 2012; Zoratti et al., 2014). Within the visible spectrum, blue light most prominently affects fruit flavonoid accumulation, particularly anthocyanins in unripe strawberries (Zoratti et al., 2014). The relevance of blue light photoreceptors and anthocyanin accumulation was demonstrated at the molecular level, and it was observed that the elevated expression of phototropin 2 FaPHOT2 corresponded to an increase in anthocyanin content (Kadomura-Ishikawa et al., 2013), In addition, blue light leads to overexpression of cryptochrome, resulting in anthocyanin accumulation (Giliberto et al., 2005). Blue light is perceived by cryptochromes that influence different plant developmental

TABLE 1 | Strawberry anthocyanin, phenolic, and plant responses under UV radiation compared to control lighting (solar spectrum without UV radiation).

Light spectrum	Cultivar	Intensity and duration	Temperature (°C)	Response	Reference
Solar UV-A + UV-B	Everest and Elsanta	Solar radiation (70% UV transmission)	19.5	Anthocyanin ↑ (cyanidin 3-glucoside) Flavonols ↑ (quercetin 3-glucuronide and kaempferol 3-glucoside)	Josuttis et al., 2010
	Elsanta	Solar radiation (81% UV transmission)	-	Anthocyanin ↑ Flavonoid ↑ phenolic ↑	Tsormpatsidis et al., 2011
	Elsanta	Solar radiation (60–78% UV transmission)	-	Anthocyanins ↑ Phenolics↑ Ellagic acid ↑	Ordidge et al., 2012
UV-C (255 nm)	Candiss	1.70–10.2 kJ m^{-2} (4 min 8 s per week)	-	Early flowering	Forges et al., 2020
	Albion	9.6–15 kJ m^{-2} (18–29 min per 3 days)	20	Anthocyanins ↑ Flavonols ↑	Xu et al., 2017b
	Benihoppe	4.0 kJ m^{-2}	4	Total phenolic compounds ↑ Anthocyanin ↑ Antioxidant capacity ↑	Li et al., 2019
	Allstar	0.43–4.30 kJ m^{-2} (1, 5, and 10 min, once)	5–10	Phenolic content ↑ Anthocyanins Δ	Erkan et al., 2008
UV LEDs (254, 306, and 352-nm LEDs)	Seolhyang and Maehyang	16.4 W m^{-2} (8 and 16 min per 2 days)	-	Anthocyanins ↑ Phenolics↑ (cv.Seolhyang only)	Kim et al., 2011

All solar UV radiation and UV-light-emitting diode (LED) studies comprise pre-harvest treatment, while all UV-C radiation studies include post-harvest treatment (↑: increase, ↓: decrease).

steps, including flowering induction and fruit secondary metabolite production (Fantini and Facella, 2020). Increases in flavonoid/anthocyanin biosynthesis with blue light have been reported in tomato (*Solanum lycopersicum* cv. Moneymaker; Lopez et al., 2012) and grape (cv. Malbec; Gonzalez et al., 2015). The impact of blue light and supplemental red light on anthocyanin accumulation has also been investigated in many greenhouse crops (Liu et al., 2018).

Attention on strawberry secondary metabolites is mainly placed on anthocyanin accumulation in CE agriculture, and investigations are mainly conducted with two approaches: (i) sole LED lighting as a growing light with post-harvest treatment; and (ii) different lighting strategies that result in different strawberry phenolic compound/anthocyanin biosynthesis responses (Kadomura-Ishikawa et al., 2013; Miao et al., 2016; Nadalini et al., 2017). **Table 2** summarizes current research on the modulation of strawberry flavonoid and fruit productivity under the visible spectrum. Opposed to other greenhouse crops, conflicting data for blue-light-mediated responses and strawberry fruit flavonoid accumulation exist. It appears that blue light is not the most effective wavelength for anthocyanin production in strawberry fruit (Besteiro et al., 2011; Piovene et al., 2015; Nadalini et al., 2017). Blue LED light (e.g., 436 and 470-nm light) induces a higher number of flower clusters and increases final yield for strawberry plants (Nadalini et al., 2017; Magar et al., 2018). A reduction in anthocyanin (pelargonidin-3-glucoside) and phenolic concentrations was observed in strawberry fruit grown under sole 436-nm LED light when compared to the fluorescent light spectrum, with peaks at 430, 450, 540, and 620 nm (Nadalini et al., 2017). Different ratios of 630 and 450 nm (0.7–5.5) LED light has no impact on flavonoid concentrations for strawberry fruit when compared to fluorescent light (Piovene et al., 2015). In the same study, lower flavonoid concentrations were reported in basil leaves (*Ocimum basilicum*) grown under red and blue LED light when compared to basil grown under fluorescent light. The authors concluded that the impact of blue light on flavonoid biosynthesis is species-dependent (Nadalini et al., 2017). Light bandwidth might also attribute to varied responses under blue light. Contrary to other strawberry studies, Miao et al. (2016) reported increased anthocyanins (cyanidin 3-glucoside) in the strawberry cultivar "Yueli" grown under blue plastic film (Miao et al., 2016). Although details of the blue light spectrum used in this study are not known, it is possible that the blue light produced with blue plastic film has a broad spectrum that is similar to the one from UV-blocking films. A broader spectrum of blue light (>25 nm LED bandwidth) could lead to overexpression of both phototropin and cryptochrome, two main blue light photoreceptors. Further investigation into the impact of blue light bandwidths, as well as how blue light influences flavonoid accumulation in different strawberry plant tissues, may answer this question.

In the presence of red light and far-red radiation, activated photoreceptors (phytochromes) repress COP1 function and allow its export from the nucleus, thus inducing flavonoid gene expression (Lau and Deng, 2012; Tossi et al., 2019). The impact of red light on strawberry secondary metabolites and development was reported by Choi et al. (2015), who compared the flavonoid and phenolic compounds of strawberry (cv. Daewang) when grown under 448, 634, and 661-nm LED light in a growth chamber, and with supplementary light in a plastic greenhouse. Upon fruit maturation and testing, higher levels of total phenolic compounds were observed under red light (634 + 661 nm) treatment in the growth chamber, yet there was no significant difference in the amount of anthocyanin and flavonoid between any of the treatments. This was confirmed in a later study with 666-nm LED and strawberry (cv. Elsanta; Nadalini et al., 2017). Similar to the conflicting data obtained with the blue film, opposite anthocyanin responses to "red light" produced with red film and red LED light were reported (Miao et al., 2016). Strawberry (cv. Yueli) grown under red film had a significant impact on total anthocyanin concentration and individual anthocyanins (pelargonidin 3-glucoside and pelargonidin 3-malonylglucoside; Miao et al., 2016). Although the detailed light spectrum under these plastic films was not presented (Miao et al., 2016), differences in secondary metabolite responses to light spectrum imply that specific wavelengths can differentially affect secondary metabolite accumulation in strawberry plants.

Unlike LED light in the visible spectrum, sole far-red radiation has less impact on secondary metabolite accumulation. Yet, it plays an import role in flowering and has proven an effective method for improved flowering with short duration at the end of the day (Zahedi and Sarikhani, 2016, 2017). The authors tested the end-of-day approach with 735-nm LED radiation using different exposure durations and temperatures on various developmental stages for strawberry (cv. Paros). They concluded that flowering can be induced in 12-week old and older strawberry plants through 32 daily cycles of 735-nm LED radiation at a cooler temperature (Zahedi and Sarikhani, 2016). A similar conclusion on flowering initiation was made when end-of-day lighting was combined with mixed red light and far-red radiation (Rantanen et al., 2014).

Although beyond the scope of this review, it is noteworthy to mention that purple light, with different ratios of red and blue LED light as well as intensity, results in increased stolon production, higher photosynthetic activity, and fruit productivity in strawberry plant (Nhut et al., 2003; Wu et al., 2009; Piovene et al., 2015; Naznin et al., 2016). An increase in strawberry flowering and fruit yield occurs with full-spectrum and white LED light (Hidaka et al., 2013; Díaz-Galián et al., 2020). In addition to the purple light spectrum, intensity is critical for influencing strawberry growth (Zhou et al., 2005; Choi et al., 2015). This response appears cultivar-dependent (Smeets, 1976, 1980). An increased daily light integral result in higher dry matter accumulation, propagation efficiency, and quality of strawberry runner plants (Miyazawa et al., 2009; Zheng et al., 2019). In summary, the importance of wavelength and its bandwidth should be emphasized and light spectra with different emitting wavelengths and lighting strategies clearly affect flavonoid content and fruit productivity in strawberry plants. The shift from broad-spectrum to narrow spectrum artificial lighting system is gaining momentum, but there is a paucity of studies comparing broad-spectrum to

TABLE 2 | Strawberry anthocyanin, phenolic, and plant responses under the assigned light exposition compared to control (white light produced by fluorescent lamps; [1]: post-harvesting treatment, [2]: supplemental lighting, ↑: increase, Δ: same as control, ↓: decrease).

Light spectrum	Cultivar	Wavelength (nm)	Intensity	Temperature (°C)	Response	Reference
Blue light (380–500 nm)	Yueli	blue plastic film	-	-	Anthocyanins ↑	Miao et al., 2016
	Elsanta	436	100 μmol·m^{-2}·s^{-1}	22–25	Fruit yield ↑ Anthocyanin↓	Nadalini et al., 2017
	Pechka	470[1]	80 μmol·m^{-2}·s^{-1}	>16	Fruit yield ↑	Magar et al., 2018
Red light (630–700 nm)	Daewang	634 + 661	200 μmol·m^{-2}·s^{-1}	10–25	Total phenolic compounds ↑ Flavonoids and anthocyanins Δ	Choi et al., 2015
	Yueli	red plastic film	-	-	Anthocyanins ↑	Miao et al., 2016
	Pechka	640[1]	80 μmol·m^{-2}·s^{-1}	>16	Flower ↓	Magar et al., 2018
	Elsanta	666	100 μmol·m^{-2}·s^{-1}	22–25	Total phenolic compounds ↓	Nadalini et al., 2017
Purple light (blue + red light)	Albion	449 + 661 (ratio 1:19)	120 μmol·m^{-2}·s^{-1}	16–21	Fruit yield ↑	Naznin et al., 2016
	Akihime	450 + 660 (ratio 3:7)	60 μmol·m^{-2}·s^{-1}	25	Fruit yield ↑	Nhut et al., 2003
Far-red radiation	Paros	735[2]	15 μmol·m^{-2}·s^{-1}	-	Flower ↑ (low temperature)	Zahedi and Sarikhani, 2016
Full spectrum	Fortuna	450 + 650*	70–120 μmol·m^{-2}·s^{-1}	15	Flower ↑	Díaz-Galián et al., 2020
	Fukuoka S6	White LED[2]	>400 μmol·m^{-2}·s^{-1}	25	Fruit yield ↑	Hidaka et al., 2013

**With narrow-spectrum and broad-spectrum of 650 nm LED light.*

narrow-spectrum light. This is compounded by conflicting findings for the blue-light-mediated response in strawberry fruit. More CE research could further elucidate the impact of different wavelengths and underlying mechanisms, while determining interactions with temperature-dependent processes, to improve fruit properties, including yield, quality, and nutritional value.

UV RADIATION AND PHOTOBIOLOGICAL SAFETY

UV radiation triggers the accumulation of flavonoids and other secondary metabolites (Caldwell and Britz, 2006). However, widespread use remains elusive, mainly caused by a limited selection of UV radiation sources and the photobiological hazard it presents to humans (Voke, 1999). Several types of UV radiation sources (i.e., gas-discharge lamps, fluorescent bulbs, and LEDs) are not often used in plant photobiology studies. UV gas-discharge lamps radiate a sharp 255-nm spectrum, and are accompanied by many disadvantages, including low radiation output and limited effective radiation area (Sarigiannis et al., 2012). These disadvantages limit further investigation into the impact of UV radiation on plants. Unlike conventional UV radiation sources, UV-LEDs available on the market have a wide range of wavelength selection. By adding aluminum nitride (AlN) to the GaN diodes, emitting UV wavelengths ranges cover from 220 to 380 nm. Unlike earlier UV devices with less than a 100-h lifespan (L50, 50% of light bulbs fail at 100 h), current UV-LEDs emitting at 280–310 nm now boast a lifespan of at least 3,000 h (Würtele et al., 2011; Fujioka et al., 2014; Kneissl, 2016), with some exceeding more than 10,000 h (Glaab et al., 2015). Although these UV-LEDs still have lower reliability and longevity than LEDs in visible spectrum, they have become an emerging radiation source for research involving UV germicidal irradiation, such as water treatment and microbial inactivation (Song et al., 2016; Kebbi et al., 2020).

A major concern when applying UV radiation in plant production facilities is UV photobiology safety. While employing any UV radiation source, there is a potential risk of being exposed to hazardous ocular and skin UV radiation (Ichihashi et al., 2003; Laube et al., 2004), and UV photobiology safety precautions for users are necessary (Lau, 2013). Controls to prevent skin and eye injuries should be placed, and protective housing that restricts or reduces UV exposure is an effective approach. If personnel requires to entering UV-radiation environment, personal protective equipment is highly recommended. Many international bodies have published guidelines that assess and evaluate photobiological eye safety based on wavelength and exposure (European Union, 2006; International Electrotechnical Commission, 2006). For radiation between 180 and 400 nm, the exposure limit is 30 J cm^{-2} within 8-h per day. Note that when users assess the UV radiation environment, spectral weighting functions need to be applied. Sunglasses provide adequate, as most sunglasses are able to greatly reduce the amount of UV radiation (Tuchinda et al., 2006; Wu and Lefsrud, 2018).

CONCLUDING REMARKS AND FUTURE OUTLOOK

Here, we review aspects of photobiology and flavonoid accumulation that are relevant to strawberry plant production. Studies showing our interest in enhancing strawberry plant growth, development, metabolites, and crop status span nearly 100 years. Information on photobiology research can be utilized to tailor artificial light spectra, which can target the development of flavonoid content in strawberry fruits. More specifically that different wavelengths will elicit varied responses in the growth and quality of fruit production. Practically applied, optimized

light recipes reduce the necessary electrical inputs, while increasing the crop yields and quality. Pre-harvesting UV treatment combined the UV-A to UV-C wavelengths is a powerful tool for stimulating flavonoid biosynthesis in strawberry fruits; however, UV-C radiation alone impacts flavor profile. In post-harvesting treatments, UV-C radiation shows promising results on enhancing secondary metabolites. We expect that UV LEDs will be increasingly used to stimulate desirable fruit metabolites, while requiring only short doses (minutes per day) to elicit a response. Evidence indicates that blue LED light can enhance flavonoid accumulation in greenhouse crops, but this is not explicitly seen with strawberry plants. Blue-light-mediated responses in strawberry fruit flavonoid accumulation are bandwidth-dependent, rather than wavelength-dependent. Based on literature reported, a spectrum with board blue light spectrum or with multiple peaks in the blue wavelength range targeting both phototropin and cryptochrome is optimal and recommended for enhancing flavonoid accumulation. Understanding the action spectrum (or spectral dose-response curve) of flavonoid biosynthesis in different tissues is important to improve the precision of flavonoid production and the antioxidant capacity in strawberry CE production, making these "super foods" more super. Continued investigation of this variation in flavonoid response to light spectrum will provide important knowledge on light signaling machinery, such as COP1-mediated pathways, in strawberry, and possibly other fruit producing species.

Based on research reviewed, we believe there is value in pursuing further research on the implication of light spectra on strawberry secondary metabolites to improve crop quality for human health. The following areas should be considered for further study to fill knowledge gaps: (1) the impact of pre-harvest UV-A on secondary metabolite accumulation. Flavonoids absorb majorly in the UV-A spectrum, yet there is minimal research available on the direct impact of UV-A on flavonoid accumulation in strawberries. (2) Further investigations into the impact of pre-harvest UV-C radiation, considering post-harvest research is very promising. UV-C LED sources with different wavelengths are highly available, and the accessibility to both researchers and producers make results more accessible. (3) Determination of the impact of specific visible light wavelengths across both cultivars and temperature, especially with white LED light. (4) Investigations into blue: red light ratios in purple lighting during vegetative growth and flowering to determine impact on secondary metabolite profile in strawberries. (5) Degradation monitoring of flavonoids during post-harvest storage and transport, to determine timeframe of benefits imposed by augmented light spectrum.

AUTHOR CONTRIBUTIONS

RW and B-SW led the writing of this paper. B-SW and SM were the major editors. SM and ML contributed over 40% of the writing for the paper. ML is the correspondence point person. All authors contributed to the article and approved the submitted version.

ACKNOWLEDGMENTS

We would like to thank Mitacs (grant number IT16220) and Gardyn Inc. for their continuous support and funding of this project.

REFERENCES

Aaby, K., Mazur, S., Nes, A., and Skrede, G. (2012). Phenolic compounds in strawberry (*Fragaria x ananassa* Duch.) fruits: composition in 27 cultivars and changes during ripening. *Food Chem.* 132, 86–97. doi: 10.1016/j.foodchem.2011.10.037

Afrin, S., Gasparrini, M., Forbes-Hernandez, T. Y., Reboredo-Rodriguez, P., Mezzetti, B., Varela-LóPez, A., et al. (2016). Promising health benefits of the strawberry: a focus on clinical studies. *J. Agric. Food Chem.* 64, 4435–4449. doi: 10.1021/acs.jafc.6b00857

Akula, R., and Ravishankar, G. A. (2011). Influence of abiotic stress signals on secondary metabolites in plants. *Plant Signal. Behav.* 6, 1720–1731. doi: 10.4161/psb.6.11.17613

Al-Dashti, Y. A., Holt, R. R., Stebbins, C. L., Keen, C. L., and Hackman, R. M. (2018). Dietary flavanols: a review of select effects on vascular function, blood pressure, and exercise performance. *J. Am. Coll. Nutr.* 37, 553–567. doi: 10.1080/07315724.2018.1451788

Alrifai, O., Hao, X., Marcone, M. F., and Tsao, R. (2019). Current review of the modulatory effects of LED lights on photosynthesis of secondary metabolites and future perspectives of microgreen vegetables. *J. Agric. Food Chem.* 67, 6075–6090. doi: 10.1021/acs.jafc.9b00819

Alvarez, M. A. (ed.) (2014). "Plant secondary metabolism" in *Plant biotechnology for health*. Springer, 15–31.

Amini, A. M., Muzs, K., Spencer, J. P., and Yaqoob, P. (2017). Pelargonidin-3-O-glucoside and its metabolites have modest anti-inflammatory effects in human whole blood cultures. *Nutr. Res.* 46, 88–95. doi: 10.1016/j.nutres.2017.09.006

Aron, P. M., and Kennedy, J. A. (2008). Flavan-3-ols: nature, occurrence and biological activity. *Mol. Nutr. Food Res.* 52, 79–104. doi: 10.1002/mnfr.200700137

Baicu, A. A., and Popa, M. E. (2018). Trends in prolonging the post-harvest life of strawberries–a review. *The Annals of the University Dunarea de Jos of Galati Fascicle VI-Food Technology* 42, 9–16.

Banerjee, R., and Batschauer, A. (2005). Plant blue-light receptors. *Planta* 220, 498–502. doi: 10.1007/s00425-004-1418-z

Battino, M., Forbes-Hernandez, T., Gasparrini, M., Afrin, S., Mezzetti, B., and Giampieri, F. (2016). The effects of strawberry bioactive compounds on human health. *Acta Hortic.* 1156, 355–362. doi: 10.17660/ActaHortic.2017.1156.54

Bernal, M., Llorens, L., Badosa, J., and Verdaguer, D. (2013). Interactive effects of UV radiation and water availability on seedlings of six woody Mediterranean species. *Physiol. Plant.* 147, 234–247. doi: 10.1111/j.1399-3054.2012.01660.x

Bernal, M., Verdaguer, D., Badosa, J., Abadía, A., Llusià, J., Peñuelas, J., et al. (2015). Effects of enhanced UV radiation and water availability on performance, biomass production and photoprotective mechanisms of *Laurus nobilis* seedlings. *Environ. Exp. Bot.* 109, 264–275. doi: 10.1016/j.envexpbot.2014.06.016

Besteiro, M. A. G., Bartels, S., Albert, A., and Ulm, R. (2011). Arabidopsis MAP kinase phosphatase 1 and its target MAP kinases 3 and 6 antagonistically determine UV-B stress tolerance, independent of the UVR8 photoreceptor pathway. *Plant J.* 68, 727–737. doi: 10.1111/j.1365-313X.2011.04725.x

Biswas, D. K., and Jansen, M. A. (2012). Natural variation in UV-B protection amongst *Arabidopsis thaliana* accessions. *Emir. J. Food Agric.* 24, 621–631. doi: 10.9755/ejfa.v24i6.621631

Bradford, E., Hancock, J. F., and Warner, R. M. (2010). Interactions of temperature and photoperiod determine expression of repeat flowering in strawberry. *J. Am. Soc. Hortic. Sci.* 135, 102–107. doi: 10.21273/JASHS.135.2.102

Caldwell, C. R., and Britz, S. J. (2006). Effect of supplemental ultraviolet radiation on the carotenoid and chlorophyll composition of green house-grown leaf lettuce (*Lactuca sativa L.*) cultivars. *J. Food Compos. Anal.* 19, 637–644. doi: 10.1016/j.jfca.2005.12.016

Carbone, F., Preuss, A., De Vos, R. C., D'amico, E., Perrotta, G., Bovy, A. G., et al. (2009). Developmental, genetic and environmental factors affect the expression of flavonoid genes, enzymes and metabolites in strawberry fruits. *Plant Cell Environ.* 32, 1117–1131. doi: 10.1111/j.1365-3040.2009.01994.x

Carvalho, S., and Folta, K. (2016). Green light control of anthocyanin production in microgreens. *Acta Hortic.* 1134, 13–18. doi: 10.17660/ActaHortic.2016.1134.2

Cerovic, Z., Ounis, A., Cartelat, A., Latouche, G., Goulas, Y., Meyer, S., et al. (2002). The use of chlorophyll fluorescence excitation spectra for the non-destructive in situ assessment of UV-absorbing compounds in leaves. *Plant Cell Environ.* 25, 1663–1676. doi: 10.1046/j.1365-3040.2002.00942.x

Chassy, A. W., Adams, D. O., Laurie, V. F., and Waterhouse, A. L. (2012). Tracing phenolic biosynthesis in *Vitis vinifera* via in situ C-13 labeling and liquid chromatography–diode-array detector–mass spectrometer/mass spectrometer detection. *Anal. Chim. Acta* 747, 51–57. doi: 10.1016/j.aca.2012.08.012

Choi, H. G., Moon, B. Y., and Kang, N. J. (2015). Effects of LED light on the production of strawberry during cultivation in a plastic greenhouse and in a growth chamber. *Sci. Hortic.* 189, 22–31. doi: 10.1016/j.scienta.2015.03.022

Cocetta, G., Casciani, D., Bulgari, R., Musante, F., Kołton, A., Rossi, M., et al. (2017). Light use efficiency for vegetables production in protected and indoor environments. *Eur. Phys. J. Plus* 132:43. doi: 10.1140/epjp/i2017-11298-x

Cooley, N. M., Higgins, J., Holmes, M., and Attridge, T. (2001). Ecotypic differences in responses of *Arabidopsis thaliana* L. to elevated polychromatic UV-A and UV-B+ A radiation in the natural environment: a positive correlation between UV-B+ A inhibition and growth rate. *J. Photochem. Photobiol. B* 60, 143–150. doi: 10.1016/S1011-1344(01)00140-3

Da Silva, F. L., Escribano-Bailón, M. T., Alonso, J. J. P., Rivas-Gonzalo, J. C., and Santos-Buelga, C. (2007). Anthocyanin pigments in strawberry. *LWT-Food Sci. Technol.* 40, 374–382. doi: 10.1016/j.lwt.2005.09.018

De Oliveira, I. R., Crizel, G. R., Severo, J., Renard, C. M., Chaves, F. C., and Rombaldi, C. V. (2016). Preharvest UV-C radiation influences physiological, biochemical, and transcriptional changes in strawberry cv. Camarosa. *Plant Physiol. Biochem.* 108, 391–399. doi: 10.1016/j.plaphy.2016.08.012

Delgado, A. M., Issaoui, M., and Chammem, N. (2019). Analysis of main and healthy phenolic compounds in foods. *J. AOAC Int.* 102, 1356–1364. doi: 10.5740/jaoacint.19-0128

Dewick, P. M. (ed.) (2001). "The shikimate pathway: aromatic amino acids and phenylpropanoids" in *Medicinal natural products: A biosynthetic approach. 2nd Edn.* (Chichester, UK: John Wiley & Sons, Ltd), 137–186.

Díaz-Galián, M. V., Torres, M., Sanchez-Pagán, J. D., Navarro, P. J., Weiss, J., and Egea-Cortines, M. (2020). Enhancement of strawberry production and fruit quality by blue and red LED lights in research and commercial greenhouses. S. Afr. J. Bot. doi: 10.1016/j.sajb.2020.05.004 (in press).

Dou, H., Niu, G., Gu, M., and Masabni, J. G. (2017). Effects of light quality on growth and phytonutrient accumulation of herbs under controlled environments. *Horticulturae* 3:36. doi: 10.3390/horticulturae3020036

Doupis, G., Bosabalidis, A., and Patakas, A. (2016). Comparative effects of water deficit and enhanced UV-B radiation on photosynthetic capacity and leaf anatomy traits of two grapevine (*Vitis vinifera* L.) cultivars. *Theor. Exp. Plant Physiol.* 28, 131–141. doi: 10.1007/s40626-016-0055-9

Downey, M. O., Dokoozlian, N. K., and Krstic, M. P. (2006). Cultural practice and environmental impacts on the flavonoid composition of grapes and wine: a review of recent research. *Am. J. Enol. Vitic.* 57, 257–268.

Durner, E. F., Barden, J., Himelrick, D., and Poling, E. (1984). Photoperiod and temperature effects on flower and runner development in day-neutral, junebearing, and everbearing strawberries. *J. Am. Soc. Hortic. Sci.* 109, 396–400.

Erkan, M., Wang, S. Y., and Wang, C. Y. (2008). Effect of UV treatment on antioxidant capacity, antioxidant enzyme activity and decay in strawberry fruit. *Postharvest Biol. Technol.* 48, 163–171. doi: 10.1016/j.postharvbio.2007.09.028

European Union (2006). Directive 2006/25/EC of the European Parliament and of the Council of 5 April 2006 on the minimum health and safety requirements regarding the exposure of workers to risks arising from physical agents (artificial optical radiation). Official Journal of the European Union 114, 38–59.

Fantini, E., and Facella, P. (2020). Cryptochromes in the field: how blue light influences crop development. *Physiol. Plant.* 169, 336–346. doi: 10.1111/ppl.13088

FAO (2016). FAOSTAT online database [Online]. Available: http://www.fao.org/faostat/en/#data/QV (Accessed June 30 2020).

Ferreyra, M. L. F., Rius, S., and Casati, P. (2012). Flavonoids: biosynthesis, biological functions, and biotechnological applications. *Front. Plant Sci.* 3:222. doi: 10.3389/fpls.2012.00222

Folta, K. M., and Carvalho, S. D. (2015). Photoreceptors and control of horticultural plant traits. *HortScience* 50, 1274–1280. doi: 10.21273/HORTSCI.50.9.1274

Forges, M., Bardin, M., Urban, L., Aarrouf, J., and Charles, F. (2020). Impact of UV-C radiation applied during plant growth on pre-and post-harvest disease sensitivity and fruit quality of strawberry. *Plant Dis.* 104, 3239–3247. doi: 10.1094/PDIS-02-20-0306-RE

Fujioka, A., Asada, K., Yamada, H., Ohtsuka, T., Ogawa, T., Kosugi, T., et al. (2014). High-output-power 255/280/310 nm deep ultraviolet light-emitting diodes and their lifetime characteristics. *Semicond. Sci. Technol.* 29:084005. doi: 10.1088/0268-1242/29/8/084005

Giampieri, F., Tulipani, S., Alvarez-Suarez, J. M., Quiles, J. L., Mezzetti, B., and Battino, M. (2012). The strawberry: composition, nutritional quality, and impact on human health. *Nutrition* 28, 9–19. doi: 10.1016/j.nut.2011.08.009

Giliberto, L., Perrotta, G., Pallara, P., Weller, J. L., Fraser, P. D., Bramley, P. M., et al. (2005). Manipulation of the blue light photoreceptor cryptochrome 2 in tomato affects vegetative development, flowering time, and fruit antioxidant content. *Plant Physiol.* 137, 199–208. doi: 10.1104/pp.104.051987

Glaab, J., Ploch, C., Kelz, R., Stölmacker, C., Lapeyrade, M., Ploch, N. L., et al. (2015). Temperature induced degradation of InAlGaN multiple-quantum well UV-B LEDs. *Mater. Res. Soc. Symp. Proc.* 1792:mrss 15–2102646. doi: 10.1557/opl.2015.446

Gonzalez, C. V., Fanzone, M. L., Cortés, L. E., Bottini, R., Lijavetzky, D. C., Ballare, C. L., et al. (2015). Fruit-localized photoreceptors increase phenolic compounds in berry skins of field-grown *Vitis vinifera* L. cv. Malbec. *Phytochemistry* 110, 46–57. doi: 10.1016/j.phytochem.2014.11.018

Gronquist, M., Bezzerides, A., Attygalle, A., Meinwald, J., Eisner, M., and Eisner, T. (2001). Attractive and defensive functions of the ultraviolet pigments of a flower (*Hypericum calycinum*). *Proc. Natl. Acad. Sci. U. S. A.* 98, 13745–13750. doi: 10.1073/pnas.231471698

Gupta, S. K., Sharma, M., Deeba, F., and Pandey, V. (2017). "Plant response: UV-B avoidance mechanisms" in *UV-B radiation: From environmental stressor to regulator of plant growth*. eds. V. P. Singh, S. M. Prasad and P. Parihar (West Sussex, UK: Wiley-Blackwell), 217–258.

Hectors, K., Van Oevelen, S., Geuns, J., Guisez, Y., Jansen, M. A., and Prinsen, E. (2014). Dynamic changes in plant secondary metabolites during UV acclimation in *Arabidopsis thaliana*. *Physiol. Plant.* 152, 219–230. doi: 10.1111/ppl.12168

Heide, O. M. (1977). Photoperiod and temperature interactions in growth and flowering of strawberry. *Physiol. Plant.* 40, 21–26. doi: 10.1111/j.1399-3054.1977.tb01486.x

Heide, O., Stavang, J., and Sønsteby, A. (2013). Physiology and genetics of flowering in cultivated and wild strawberries–a review. *J. Hortic. Sci. Biotechnol.* 88, 1–18. doi: 10.1080/14620316.2013.11512930

Hidaka, K., Dan, K., Imamura, H., Miyoshi, Y., Takayama, T., Sameshima, K., et al. (2013). Effect of supplemental lighting from different light sources on growth and yield of strawberry. *Environ. Control Biol.* 51, 41–47. doi: 10.2525/ecb.51.41

Hidaka, K., Okamoto, A., Araki, T., Miyoshi, Y., Dan, K., Imamura, H., et al. (2014). Effect of photoperiod of supplemental lighting with light-emitting diodes on growth and yield of strawberry. *Environ. Control Biol.* 52, 63–71. doi: 10.2525/ecb.52.63

Ichihashi, M., Ueda, M., Budiyanto, A., Bito, T., Oka, M., Fukunaga, M., et al. (2003). UV-induced skin damage. *Toxicology* 189, 21–39. doi: 10.1016/S0300-483X(03)00150-1

International Electrotechnical Commission (2006). "Photobiological safety of lamps and lamp systems (IEC 62471)." Geneva: IEC.

Ito, H., and Saito, T. (1962). Studies on the flower formation in the strawberry plants. *Tohoku J. Agr. Res.* 13, 191–203.

Jaillon, O., Aury, J. -M., Noel, B., Policriti, A., Clepet, C., Casagrande, A., et al. (2007). The grapevine genome sequence suggests ancestral hexaploidization in major angiosperm phyla. *Nature* 449, 463–467. doi: 10.1038/nature06148

Jansen, M. A., Hectors, K., O'brien, N. M., Guisez, Y., and Potters, G. (2008). Plant stress and human health: do human consumers benefit from UV-B acclimated crops? *Plant Sci.* 175, 449–458. doi: 10.1016/j.plantsci.2008.04.010

Jenkins, G. I. (2017). Photomorphogenic responses to ultraviolet-B light. *Plant Cell Environ.* 40, 2544–2557. doi: 10.1111/pce.12934

Jones, M. A. (2018). Using light to improve commercial value. *Hortic. Res.* 5:47. doi: 10.1038/s41438-018-0049-7

Josuttis, M., Dietrich, H., Treutter, D., Will, F., LinnemannstöNs, L., and KrüGer, E. (2010). Solar UVB response of bioactives in strawberry (*Fragaria× ananassa* Duch. L.): a comparison of protected and open-field cultivation. *J. Agric. Food Chem.* 58, 12692–12702. doi: 10.1021/jf102937e

Kadomura-Ishikawa, Y., Miyawaki, K., Noji, S., and Takahashi, A. (2013). Phototropin 2 is involved in blue light-induced anthocyanin accumulation in *Fragaria x ananassa* fruits. *J. Plant Res.* 126, 847–857. doi: 10.1007/s10265-013-0582-2

Kanto, T., Matsuura, K., Yamada, M., Usami, T., and Amemiya, Y. (2009). UV-B radiation for control of strawberry powdery mildew. *Acta Hortic.* 842, 359–362. doi: 10.17660/ActaHortic.2009.842.68

Kataria, S., and Guruprasad, K. (2012). Intraspecific variations in growth, yield and photosynthesis of sorghum varieties to ambient UV (280–400 nm) radiation. *Plant Sci.* 196, 85–92. doi: 10.1016/j.plantsci.2012.07.011

Kataria, S., Guruprasad, K., Ahuja, S., and Singh, B. (2013). Enhancement of growth, photosynthetic performance and yield by exclusion of ambient UV components in C_3 and C_4 plants. *J. Photochem. Photobiol. B* 127, 140–152. doi: 10.1016/j.jphotobiol.2013.08.013

Katsoulas, N., Bari, A., and Papaioannou, C. (2020). Plant responses to UV blocking greenhouse covering materials: a review. *Agronomy* 10:1021. doi: 10.3390/agronomy10071021

Kebbi, Y., Muhammad, A. I., Sant'ana, A. S., Do Prado-Silva, L., Liu, D., and Ding, T. (2020). Recent advances on the application of UV-LED technology for microbial inactivation: progress and mechanism. *Compr. Rev. Food Sci. Food Saf.* 19, 3501–3527. doi: 10.1111/1541-4337.12645

Khoo, H. E., Azlan, A., Tang, S. T., and Lim, S. M. (2017). Anthocyanidins and anthocyanins: colored pigments as food, pharmaceutical ingredients, and the potential health benefits. *Food Nutr. Res.* 61:1361779. doi: 10.1080/16546628.2017.1361779

Khudyakova, A. Y., Kreslavski, V. D., Shirshikova, G. N., Zharmukhamedov, S. K., Kosobryukhov, A. A., and Allakhverdiev, S. (2017). Resistance of *Arabidopsis thaliana* L. photosynthetic apparatus to UV-B is reduced by deficit of phytochromes B and A. *J. Photochem. Photobiol. B* 169, 41–46. doi: 10.1016/j.jphotobiol.2017.02.024

Kim, S. -K., Bae, R. -N., and Chun, C. -H. (2011). Changes in bioactive compounds contents of 'Maehyang' and 'Seolhyang' strawberry fruits by UV light illumination. *Korean J. Hortic. Sci. Technol.* 29, 172–180.

Klem, K., Ač, A., Holub, P., Kováč, D., Špunda, V., Robson, T. M., et al. (2012). Interactive effects of PAR and UV radiation on the physiology, morphology and leaf optical properties of two barley varieties. *Environ. Exp. Bot.* 75, 52–64. doi: 10.1016/j.envexpbot.2011.08.008

Kneissl, M. (2016). "A brief review of III-nitride UV emitter technologies and their applications" in *III-nitride ultraviolet emitters*. eds. M. Kneissl and J. Rass (Heidelberg: Springer), 1–25.

Kotilainen, T., Venäläinen, T., Tegelberg, R., Lindfors, A., Julkunen-Tiitto, R., Sutinen, S., et al. (2009). Assessment of UV biological spectral weighting functions for phenolic metabolites and growth responses in silver birch seedlings. *Photochem. Photobiol.* 85, 1346–1355. doi: 10.1111/j.1751-1097.2009.00597.x

Kreft, S., Štrukelj, B., Gaberščik, A., and Kreft, I. (2002). Rutin in buckwheat herbs grown at different UV-B radiation levels: comparison of two UV spectrophotometric and an HPLC method. *J. Exp. Bot.* 53, 1801–1804. doi: 10.1093/jxb/erf032

Kunz, B. A., Cahill, D. M., Mohr, P. G., Osmond, M. J., and Vonarx, E. J. (2006). Plant responses to UV radiation and links to pathogen resistance. *Int. Rev. Cytol.* 255, 1–40. doi: 10.1016/S0074-7696(06)55001-6

Kusano, M., Tohge, T., Fukushima, A., Kobayashi, M., Hayashi, N., Otsuki, H., et al. (2011). Metabolomics reveals comprehensive reprogramming involving two independent metabolic responses of Arabidopsis to UV-B light. *Plant J.* 67, 354–369. doi: 10.1111/j.1365-313X.2011.04599.x

Labadie, M., Vallin, G., Petit, A., Ring, L., Hoffmann, T., Gaston, A., et al. (2020). Metabolite quantitative trait loci for flavonoids provide new insights into the genetic architecture of strawberry (*Fragaria x ananassa*) fruit quality. *J. Agric. Food Chem.* 68, 6927–6939. doi: 10.1021/acs.jafc.0c01855

Landi, M., Agati, G., Fini, A., Guidi, L., Sebastiani, F., and Tattini, M. (2020a). Unveiling the shade nature of cyanic leaves: a view from the "blue absorbing side" of anthocyanins. *Plant Cell Environ.* 1–11. doi: 10.1111/pce.13818 [Epub ahead of print]

Landi, M., Zivcak, M., Sytar, O., Brestic, M., and Allakhverdiev, S. I. (2020b). Plasticity of photosynthetic processes and the accumulation of secondary metabolites in plants in response to monochromatic light environments: a review. *Biochim. Biophys. Acta Bioenerg.* 1861:148131. doi: 10.1016/j.bbabio.2019.148131

Lau, E. K. (2013). "Understanding radiation safety of high-intensity light-emitting diodes" in *2013 IEEE Symposium on Product Compliance Engineering (ISPCE)*; October 7–9, 2013; Austin, TX, USA, 1–3.

Lau, O. S., and Deng, X. W. (2012). The photomorphogenic repressors COP1 and DET1: 20 years later. *Trends Plant Sci.* 17, 584–593. doi: 10.1016/j.tplants.2012.05.004

Laube, T., Apel, H., and Koch, H. -R. (2004). Ultraviolet radiation absorption of intraocular lenses. *Ophthalmology* 111, 880–885. doi: 10.1016/j.ophtha.2003.08.031

Li, M., Li, X., Han, C., Ji, N., Jin, P., and Zheng, Y. (2019). UV-C treatment maintains quality and enhances antioxidant capacity of fresh-cut strawberries. *Postharvest Biol. Technol.* 156:110945. doi: 10.1016/j.postharvbio.2019.110945

Liu, Y., Tikunov, Y., Schouten, R. E., Marcelis, L. F., Visser, R. G., and Bovy, A. (2018). Anthocyanin biosynthesis and degradation mechanisms in *Solanaceous* vegetables: a review. *Front. Chem.* 6:52. doi: 10.3389/fchem.2018.00052

Lopez, L., Carbone, F., Bianco, L., Giuliano, G., Facella, P., and Perrotta, G. (2012). Tomato plants overexpressing cryptochrome 2 reveal altered expression of energy and stress-related gene products in response to diurnal cues. *Plant Cell Environ.* 35, 994–1012. doi: 10.1111/j.1365-3040.2011.02467.x

López-Aranda, J. M., Soria, C., Santos, B. M., Miranda, L., Domínguez, P., and Medina-Mínguez, J. J. (2011). Strawberry production in mild climates of the world: a review of current cultivar use. *Int. J. Fruit Sci.* 11, 232–244. doi: 10.1080/15538362.2011.608294

Lü, J. M., Lin, P. H., Yao, Q., and Chen, C. (2010). Chemical and molecular mechanisms of antioxidants: experimental approaches and model systems. *J. Cell. Mol. Med.* 14, 840–860. doi: 10.1111/j.1582-4934.2009.00897.x

Magar, Y., Ohyama, K., Noguchi, A., Amaki, W., and Furufuji, S. (2018). Effects of light quality during supplemental lighting on the flowering in an everbearing strawberry. *Acta Hortic.* 1206, 279–284. doi: 10.17660/ActaHortic.2018.1206.39

Marquenie, D., Lammertyn, J., Geeraerd, A., Soontjens, C., Van Impe, J., Nicolaı, B., et al. (2002). Inactivation of conidia of *Botrytis cinerea* and *Monilinia fructigena* using UV-C and heat treatment. *Int. J. Food Microbiol.* 74, 27–35. doi: 10.1016/S0168-1605(01)00719-X

Martens, S., Preuß, A., and Matern, U. (2010). Multifunctional flavonoid dioxygenases: flavonol and anthocyanin biosynthesis in *Arabidopsis thaliana* L. *Phytochemistry* 71, 1040–1049. doi: 10.1016/j.phytochem.2010.04.016

Matus, J. T., Loyola, R., Vega, A., Peña-Neira, A., Bordeu, E., Arce-Johnson, P., et al. (2009). Post-veraison sunlight exposure induces MYB-mediated transcriptional regulation of anthocyanin and flavonol synthesis in berry skins of *Vitis vinifera*. *J. Exp. Bot.* 60, 853–867. doi: 10.1093/jxb/ern336

Miao, L., Zhang, Y., Yang, X., Xiao, J., Zhang, H., Zhang, Z., et al. (2016). Colored light-quality selective plastic films affect anthocyanin content, enzyme activities, and the expression of flavonoid genes in strawberry (*Fragaria× ananassa*) fruit. *Food Chem.* 207, 93–100. doi: 10.1016/j.foodchem.2016.02.077

Miyazawa, Y., Hikosaka, S., Goto, E., and Aoki, T. (2009). Effects of light conditions and air temperature on the growth of everbearing strawberry during the vegetative stage. *Acta Hortic.* 842, 817–820. doi: 10.17660/ActaHortic.2009.842.180

Mockler, T., Yang, H., Yu, X., Parikh, D., Cheng, Y. -C., Dolan, S., et al. (2003). Regulation of photoperiodic flowering by Arabidopsis photoreceptors. *Proc. Natl. Acad. Sci. U. S. A.* 100, 2140–2145. doi: 10.1073/pnas.0437826100

Monagas, M., Urpi-Sarda, M., Sánchez-Patán, F., Llorach, R., Garrido, I., Gómez-Cordovés, C., et al. (2010). Insights into the metabolism and microbial biotransformation of dietary flavan-3-ols and the bioactivity of their metabolites. *Food Funct.* 1, 233–253. doi: 10.1039/c0fo00132e

Müller-Xing, R., Xing, Q., and Goodrich, J. (2014). Footprints of the sun: memory of UV and light stress in plants. *Front. Plant Sci.* 5:474. doi: 10.3389/fpls.2014.00474

Nadalini, S., Zucchi, P., and Andreotti, C. (2017). Effects of blue and red LED lights on soilless cultivated strawberry growth performances and fruit quality. *Eur. J. Hortic. Sci.* 82, 12–20. doi: 10.17660/eJHS.2017/82.1.2

Naznin, M., Lefsrud, M., Gravel, V., and Hao, X. (2016). Using different ratios of red and blue LEDs to improve the growth of strawberry plants. *Acta Hortic.* 1134, 125–130. doi: 10.17660/ActaHortic.2016.1134.17

Nhut, D. T., Takamura, T., Watanabe, H., Okamoto, K., and Tanaka, M. (2003). Responses of strawberry plantlets cultured in vitro under superbright red and blue light-emitting diodes (LEDs). *Plant Cell Tissue Organ Cult.* 73, 43–52. doi: 10.1023/A:1022638508007

Nigro, F., Ippolito, A., and Lattanzio, V., Di Venere, D., and Salerno, M. (2000). Effect of ultraviolet-C light on postharvest decay of strawberry. *J. Plant Pathol.* 82, 29–37.

Nile, S. H., and Park, S. W. (2014). Edible berries: bioactive components and their effect on human health. *Nutrition* 30, 134–144. doi: 10.1016/j.nut.2013.04.007

Ordidge, M., García-Macías, P., Battey, N. H., Gordon, M. H., John, P., Lovegrove, J. A., et al. (2012). Development of colour and firmness in strawberry crops is UV light sensitive, but colour is not a good predictor of several quality parameters. *J. Sci. Food Agric.* 92, 1597–1604. doi: 10.1002/jsfa.4744

Owens, D. K., Alerding, A. B., Crosby, K. C., Bandara, A. B., Westwood, J. H., and Winkel, B. S. (2008). Functional analysis of a predicted flavonol synthase gene family in Arabidopsis. *Plant Physiol.* 147, 1046–1061. doi: 10.1104/pp.108.117457

Panche, A., Diwan, A., and Chandra, S. (2016). Flavonoids: an overview. *J. Nutr. Sci.* 5:e47. doi: 10.1017/jns.2016.41

Peng, T., Saito, T., Honda, C., Ban, Y., Kondo, S., Liu, J. H., et al. (2013). Screening of UV-B-induced genes from apple peels by SSH: possible involvement of MdCOP1-mediated signaling cascade genes in anthocyanin accumulation. *Physiol. Plant.* 148, 432–444. doi: 10.1111/ppl.12002

Pereira, G. E., Gaudillere, J. -P., Pieri, P., Hilbert, G., Maucourt, M., Deborde, C., et al. (2006). Microclimate influence on mineral and metabolic profiles of grape berries. *J. Agric. Food Chem.* 54, 6765–6775. doi: 10.1021/jf061013k

Piovene, C., Orsini, F., Bosi, S., Sanoubar, R., Bregola, V., Dinelli, G., et al. (2015). Optimal red: blue ratio in led lighting for nutraceutical indoor horticulture. *Sci. Hortic.* 193, 202–208. doi: 10.1016/j.scienta.2015.07.015

Pocock, T. (2015). Light-emitting diodes and the modulation of specialty crops: light sensing and signaling networks in plants. *HortScience* 50, 1281–1284. doi: 10.21273/HORTSCI.50.9.1281

Pombo, M. A., Dotto, M. C., Martínez, G. A., and Civello, P. M. (2009). UV-C irradiation delays strawberry fruit softening and modifies the expression of genes involved in cell wall degradation. *Postharvest Biol. Technol.* 51, 141–148. doi: 10.1016/j.postharvbio.2008.07.007

Rantanen, M., Kurokura, T., Mouhu, K., Pinho, P., Tetri, E., Halonen, L., et al. (2014). Light quality regulates flowering in FvFT1/FvTFL1 dependent manner in the woodland strawberry *Fragaria vesca*. *Front. Plant Sci.* 5:271. doi: 10.3389/fpls.2014.00271

Reifenrath, K., and Müller, C. (2007). Species-specific and leaf-age dependent effects of ultraviolet radiation on two *Brassicaceae*. *Phytochemistry* 68, 875–885. doi: 10.1016/j.phytochem.2006.12.008

Robson, T. M., and Aphalo, P. J. (2012). Species-specific effect of UV-B radiation on the temporal pattern of leaf growth. *Physiol. Plant.* 144, 146–160. doi: 10.1111/j.1399-3054.2011.01546.x

Rozema, J., Björn, L. O., Bornman, J., Gaberščik, A., Häder, D. -P., Trošt, T., et al. (2002). The role of UV-B radiation in aquatic and terrestrial ecosystems—an experimental and functional analysis of the evolution of UV-absorbing compounds. *J. Photochem. Photobiol. B* 66, 2–12. doi: 10.1016/S1011-1344(01)00269-X

Saini, R. K., and Keum, Y. -S. (2018). Significance of genetic, environmental, and pre-and postharvest factors affecting carotenoid contents in crops: a review. *J. Agric. Food Chem.* 66, 5310–5324. doi: 10.1021/acs.jafc.8b01613

Samtani, J. B., Rom, C. R., Friedrich, H., Fennimore, S. A., Finn, C. E., Petran, A., et al. (2019). The status and future of the strawberry industry in the United States. *HortTechnology* 29, 11–24. doi: 10.21273/HORTTECH04135-18

Santos, A. L., Oliveira, V., Baptista, I., Henriques, I., Gomes, N. C., Almeida, A., et al. (2013). Wavelength dependence of biological damage induced by UV radiation on bacteria. *Arch. Microbiol.* 195, 63–74. doi: 10.1007/s00203-012-0847-5

Sarigiannis, D., Karakitsios, S., Antonakopoulou, M., and Gotti, A. (2012). Exposure analysis of accidental release of mercury from compact fluorescent lamps (CFLs). *Sci. Total Environ.* 435, 306–315. doi: 10.1016/j.scitotenv.2012.07.026

Schreiner, M., Mewis, I., Huyskens-Keil, S., Jansen, M., Zrenner, R., Winkler, J., et al. (2012). UV-B-induced secondary plant metabolites-potential benefits for plant and human health. *Crit. Rev. Plant Sci.* 31, 229–240. doi: 10.1080/07352689.2012.664979

Serçe, S., and Hancock, J. F. (2005). Inheritance of day-neutrality in octoploid species of *Fragaria*. *J. Am. Soc. Hortic. Sci.* 130, 580–584. doi: 10.21273/JASHS.130.4.580

Severo, J., De Oliveira, I. R., Bott, R., Le Bourvellec, C., Renard, C. M., Page, D., et al. (2017). Preharvest UV-C radiation impacts strawberry metabolite content and volatile organic compound production. *LWT-Food Sci. Technol.* 85, 390–393. doi: 10.1016/j.lwt.2016.10.032

Shulaev, V., Sargent, D. J., Crowhurst, R. N., Mockler, T. C., Folkerts, O., Delcher, A. L., et al. (2011). The genome of woodland strawberry (*Fragaria vesca*). *Nat. Genet.* 43, 109–116. doi: 10.1038/ng.740

Singh, D., Basu, C., Meinhardt-Wollweber, M., and Roth, B. (2015). LEDs for energy efficient greenhouse lighting. *Renew. Sust. Energ. Rev.* 49, 139–147. doi: 10.1016/j.rser.2015.04.117

Smeets, L. (1976). Effect of light intensity on stamen development in the strawberry cultivar 'Glasa'. *Sci. Hortic.* 4, 255–260. doi: 10.1016/0304-4238(76)90048-0

Smeets, L. (1980). Effect of the light intensity during flowering on stamen development in the strawberry cultivars 'Karina'and 'Sivetta'. *Sci. Hortic.* 12, 343–346. doi: 10.1016/0304-4238(80)90049-7

Song, K., Mohseni, M., and Taghipour, F. (2016). Application of ultraviolet light-emitting diodes (UV-LEDs) for water disinfection: a review. *Water Res.* 94, 341–349. doi: 10.1016/j.watres.2016.03.003

Stewart, P. J., and Folta, K. M. (2010). A review of photoperiodic flowering research in strawberry (*Fragaria* spp.). *Crit. Rev. Plant Sci.* 29, 1–13. doi: 10.1080/07352680903436259

Stutte, G. W., Edney, S., and Skerritt, T. (2009). Photoregulation of bioprotectant content of red leaf lettuce with light-emitting diodes. *HortScience* 44, 79–82. doi: 10.21273/HORTSCI.44.1.79

Suthaparan, A., Solhaug, K., Bjugstad, N., Gislerød, H., Gadoury, D., and Stensvand, A. (2016). Suppression of powdery mildews by UV-B: application frequency and timing, dose, reflectance, and automation. *Plant Dis.* 100, 1643–1650. doi: 10.1094/PDIS-12-15-1440-RE

Thirumurugan, D., Cholarajan, A., Raja, S. S., and Vijayakumar, R. (2018). "An introductory chapter: secondary metabolites" in *Secondary metabolites-sources and applications*. ed. R. Vijayakumar (London, UK: IntechOpen), 3–21.

Tossi, V. E., Regalado, J. J., Iannicelli, J., Laino, L. E., Burrieza, H. P., Escandón, A. S., et al. (2019). Beyond Arabidopsis: differential UV-B response mediated by UVR8 in diverse species. *Front. Plant Sci.* 10:780. doi: 10.3389/fpls.2019.00780

Tsormpatsidis, E., Henbest, R., Battey, N. H., and Hadley, P. (2010). The influence of ultraviolet radiation on growth, photosynthesis and phenolic levels of green and red lettuce: potential for exploiting effects of ultraviolet radiation in a production system. *Ann. Appl. Biol.* 156, 357–366. doi: 10.1111/j.1744-7348.2010.00393.x

Tsormpatsidis, E., Ordidge, M., Henbest, R. G., Wagstaffe, A., Battey, N. H., and Hadley, P. (2011). Harvesting fruit of equivalent chronological age and fruit position shows individual effects of UV radiation on aspects of the strawberry ripening process. *Environ. Exp. Bot.* 74, 178–185. doi: 10.1016/j.envexpbot.2011.05.017

Tuchinda, C., Srivannaboon, S., and Lim, H. W. (2006). Photoprotection by window glass, automobile glass, and sunglasses. *J. Am. Acad. Dermatol.* 54, 845–854. doi: 10.1016/j.jaad.2005.11.1082

Turturică, M., Oancea, A. M., Râpeanu, G., and Bahrim, G. (2015). Anthocyanins: naturally occuring fruit pigments with functional properties. *The Annals of the University Dunarea de Jos of Galati Fascicle VI-Food Technology* 39, 9–24.

Urban, L., Charles, F., De Miranda, M. R. A., and Aarrouf, J. (2016). Understanding the physiological effects of UV-C light and exploiting its agronomic potential before and after harvest. *Plant Physiol. Biochem.* 105, 1–11. doi: 10.1016/j.plaphy.2016.04.004

Velasco, R., Zharkikh, A., Affourtit, J., Dhingra, A., Cestaro, A., Kalyanaraman, A., et al. (2010). The genome of the domesticated apple (*Malus*× *domestica* Borkh.). *Nat. Genet.* 42, 833–839. doi: 10.1038/ng.654

Verdaguer, D., Jansen, M. A., Llorens, L., Morales, L. O., and Neugart, S. (2017). UV-A radiation effects on higher plants: exploring the known unknown. *Plant Sci.* 255, 72–81. doi: 10.1016/j.plantsci.2016.11.014

Voke, J. (1999). Radiation effects on the eye. Part 3b-ocular effects of ultraviolet radiation. *OT* 8, 37–40.

Wang, S. Y., and Millner, P. (2009). Effect of different cultural systems on antioxidant capacity, phenolic content, and fruit quality of strawberries (*fragaria*× *aranassa* duch.). *J. Agric. Food Chem.* 57, 9651–9657. doi: 10.1021/jf9020575

Wu, B. -S., Hitti, Y., Macpherson, S., Orsat, V., and Lefsrud, M. G. (2019). Comparison and perspective of conventional and LED lighting for photobiology and industry applications. *Environ. Exp. Bot.* 171:103953. doi: 10.1016/j.envexpbot.2019.103953

Wu, C., Hsu, S., Chang, M., and Fang, W. (2009). Effect of light environment on runner plant propagation of strawberry. *Acta Hortic.* 907, 297–302. doi: 10.17660/ActaHortic.2011.907.48

Wu, B. -S., and Lefsrud, M. G. (2018). Photobiology eye safety for horticultural LED lighting: transmittance performance of eyewear protection using high-irradiant monochromatic LEDs. *J. Occup. Environ. Hyg.* 15, 133–142. doi: 10.1080/15459624.2017.1395959

Würtele, M., Kolbe, T., Lipsz, M., Külberg, A., Weyers, M., Kneissl, M., et al. (2011). Application of GaN-based ultraviolet-C light emitting diodes–UV LEDs–for water disinfection. *Water Res.* 45, 1481–1489. doi: 10.1016/j.watres.2010.11.015

Xie, Z., Charles, M. T., Fan, J., Charlebois, D., Khanizadeh, S., Rolland, D., et al. (2015). Effects of preharvest ultraviolet-C irradiation on fruit phytochemical profiles and antioxidant capacity in three strawberry (*Fragaria*× *ananassa* Duch.) cultivars. *J. Sci. Food Agric.* 95, 2996–3002. doi: 10.1002/jsfa.7064

Xu, Y., Charles, M. T., Luo, Z., Mimee, B., Tong, Z., Roussel, D., et al. (2019). Preharvest UV-C treatment affected postharvest senescence and phytochemicals alternation of strawberry fruit with the possible involvement of abscisic acid regulation. *Food Chem.* 299:125138. doi: 10.1016/j.foodchem.2019.125138

Xu, Y., Charles, M. T. R. S., Luo, Z., Mimee, B., Veronneau, P. -Y., Rolland, D., et al. (2017b). Preharvest ultraviolet C irradiation increased the level of polyphenol accumulation and flavonoid pathway gene expression in strawberry fruit. *J. Agric. Food Chem.* 65, 9970–9979. doi: 10.1021/acs.jafc.7b04252

Xu, Y., Charles, M. T., Luo, Z., Roussel, D., and Rolland, D. (2017a). Potential link between fruit yield, quality parameters and phytohormonal changes in preharvest UV-C treated strawberry. *Plant Physiol. Biochem.* 116, 80–90. doi: 10.1016/j.plaphy.2017.05.010

Yan, J. W., Ban, Z. J., Lu, H. Y., Li, D., Poverenov, E., Luo, Z. S., et al. (2018). The aroma volatile repertoire in strawberry fruit: a review. *J. Sci. Food Agric.* 98, 4395–4402. doi: 10.1002/jsfa.9039

Zahedi, S. M., and Sarikhani, H. (2016). Effect of far-red light, temperature, and plant age on morphological changes and induction of flowering of a 'June-bearing'strawberry. *Hortic. Environ. Biotechnol.* 57, 340–347. doi: 10.1007/s13580-016-0018-8

Zahedi, S., and Sarikhani, H. (2017). The effect of end of day far-red light on regulating flowering of short-day strawberry (*Fragaria*× *ananassa* Duch. cv. Paros) in a long-day situation. *Russ. J. Plant Physiol.* 64, 83–90. doi: 10.1134/S1021443717010198

Zhang, L., Allen, L. H. Jr., Vaughan, M. M., Hauser, B. A., and Boote, K. (2014). Solar ultraviolet radiation exclusion increases soybean internode lengths and plant height. *Agric. For. Meteorol.* 184, 170–178. doi: 10.1016/j.agrformet.2013.09.011

Zhang, Z. -Z., Che, X. -N., Pan, Q. -H., Li, X. -X., and Duan, C. -Q. (2013). Transcriptional activation of flavan-3-ols biosynthesis in grape berries by UV irradiation depending on developmental stage. *Plant Sci.* 208, 64–74. doi: 10.1016/j.plantsci.2013.03.013

Zheng, J., He, D., and Ji, F. (2019). Effects of light intensity and photoperiod on runner plant propagation of hydroponic strawberry transplants under LED lighting. *Int. J. Agric. Biol. Engin.* 12, 26–31. doi: 10.25165/j.ijabe.20191205.5265

Zhou, Y. -H., Guo, D. -P., Zhu, Z. -J., and Qian, Q. -Q. (2005). Effects of in vitro rooting environments and irradiance on growth and photosynthesis of strawberry plantlets during acclimatization. *Plant Cell Tissue Organ Cult.* 81, 105–108. doi: 10.1007/s11240-004-2775-9

Zoratti, L., Karppinen, K., Escobar, A. L., Häggman, H., and Jaakola, L. (2014). Light-controlled flavonoid biosynthesis in fruits. *Front. Plant Sci.* 5:534. doi: 10.3389/fpls.2014.00534

Conflict of Interest: The authors declare that this study was funded in part by Gardyn Inc. The funder was not involved in study design, collection, data analysis, the drafting of this manuscript, or the decision to submit it for refereed publication.

Copyright © 2021 Warner, Wu, MacPherson and Lefsrud. This is an open-access article distributed under the terms of the Creative Commons Attribution License (CC BY). The use, distribution or reproduction in other forums is permitted, provided the original author(s) and the copyright owner(s) are credited and that the original publication in this journal is cited, in accordance with accepted academic practice. No use, distribution or reproduction is permitted which does not comply with these terms.

frontiers in Plant Science

ORIGINAL RESEARCH
published: 12 February 2021
doi: 10.3389/fpls.2020.610174

The Physiological Response of Lettuce to Red and Blue Light Dynamics Over Different Photoperiods

Giedrė Samuolienė, Akvilė Viršilė, Jurga Miliauskienė, Perttu J. Haimi, Kristina Laužikė, Aušra Brazaitytė and Pavelas Duchovskis*

Lithuanian Research Centre for Agriculture and Forestry, Institute of Horticulture, Babtai, Lithuania

OPEN ACCESS

Edited by:
Inga Mewis, Humboldt University of Berlin, Germany

Reviewed by:
Thomas J. Bach, Université de Strasbourg, France
Qichang Yang, Chinese Academy of Agricultural Sciences, China

***Correspondence:**
Giedrė Samuolienė
giedre.samuoliene@lammc.lt

Specialty section:
This article was submitted to Plant Metabolism and Chemodiversity, a section of the journal Frontiers in Plant Science

Received: *25 September 2020*
Accepted: *28 December 2020*
Published: *12 February 2021*

Citation:
Samuolienė G, Viršilė A, Miliauskienė J, Haimi PJ, Laužikė K, Brazaitytė A and Duchovskis P (2021) The Physiological Response of Lettuce to Red and Blue Light Dynamics Over Different Photoperiods. Front. Plant Sci. 11:610174. doi: 10.3389/fpls.2020.610174

This study aimed to evaluate the effect of dynamic red and blue light parameters on the physiological responses and key metabolites in lettuce and also the subsequent impact of varying light spectra on nutritive value. We explored the metabolic changes in carotenes, xanthophylls, soluble sugars, organic acids, and antioxidants; the response of photosynthetic indices [photosynthetic (Pr) and transpiration (Tr) rates]; and the intracellular to ambient CO_2 concentration ratios (C_i/C_a) in lettuce (*Lactuca sativa* L. "Lobjoits Green Cos"). They were cultivated under constant (con) or parabolic (dyn) blue (B, 452 nm) and/or red (R, 662 nm) light-emitting diode (LED) photosynthetic photon flux densities (PPFDs) at 12, 16, and 20 h photoperiods, maintaining consistent daily light integrals (DLIs) for each light component in all treatments, at 2.3 and 9.2 mol m^{-2} per day for blue and red light, respectively. The obtained results and principal component analysis (PCA) confirmed a significant impact of the light spectrum, photoperiod, and parabolic profiles of PPFD on the physiological response of lettuce. The 16 h photoperiod resulted in significantly higher content of xanthophylls (neoxanthin, violaxanthin, lutein, and zeaxanthin) in lettuce leaves under both constant and parabolic blue light treatments (BconRdyn 16 h and BdynRdyn 16 h, respectively). Lower PPFD levels under a 20 h photoperiod (BdynRdyn 20 h) as well as higher PPFD levels under a 12 h photoperiod (BdynRdyn 12 h) had a pronounced impact on leaf gas exchange indices (Pr, Tr, C_i/C_a), xanthophylls, soluble sugar contents, and antioxidant properties of lettuce leaves. The parabolic PPFD lighting profile over a 16 h photoperiod (BdynRdyn 16 h) led to a significant decrease in C_i/C_a, which resulted in decreased Pr and Tr, compared with constant blue or red light treatments with the same photoperiod (BconRdyn and BdynRcon 16 h). Additionally, constant blue lighting produced higher α + β-carotene and anthocyanin (ARI) content and increased carotenoid to chlorophyll ratio (CRI) but decreased biomass accumulation and antioxidant activity.

Keywords: xanthophylls, carotenes, soluble sugars, organic acids, antioxidant activity, photosynthesis, dynamic light, photoperiod

INTRODUCTION

The effects of light on plants are complex, as it controls photosynthesis, plant growth, and developmental processes. Plants generally absorb radiation in the visible electromagnetic spectrum; however, not the entire spectrum of light is beneficial (Hasan et al., 2017). Under controlled environmental conditions, the mixed application of red and blue light-emitting diodes (LEDs) is usually the first choice where plant growth is a priority (Shen et al., 2014; Bantis et al., 2018). Red and blue LEDs can act as a principal light source, with the potential to improve photosynthesis by stimulating the stomatal activity, which can enhance dry mass and yield (Sabzalian et al., 2014). Various studies have demonstrated that controlled amounts or specific spectra of light affect photosynthetic characteristics (Dong et al., 2014; Samuolienė et al., 2020), metabolism (Samuolienė et al., 2013; Lee et al., 2016), and antioxidant properties (Samuolienė et al., 2012; Lekkham et al., 2016). However, these experiments are typically performed in controlled environment chambers with constant irradiance during the day and abrupt transitions between light and dark at dawn and dusk. In natural environments, plants are adapted to diurnal fluctuations in irradiance and light quality, with gradual shifts between light and dark at the beginning and the end of the day. Moreover, the light in controlled environment chambers differs from natural sunlight in several ways, including qualitative spectral and quantitative intensity changes over the course of the day (Annunziata et al., 2017).

The light-dependent reactions of photosynthesis involve electron and proton transfer from water to $NADP^+$ to form NADPH, whereas the dark-dependent reactions involve the fixation of CO_2 into carbohydrates *via* the Calvin–Benson cycle, regenerating ADP and $NADP^+$ (Johnson, 2016). Concentrations of Mg^{2+}, pH, and thioredoxin play a key role in regulating the activity of the Calvin–Benson cycle enzymes, ensuring that the activity of the light-dependent and light-independent reactions are closely coordinated. Pigment molecules (chlorophylls *a* and *b*, β-carotene, zeaxanthin, neoxanthin, violaxanthin, and lutein), located in the thylakoid membrane, absorbing red and blue light, induce the process of photosynthesis. Moderate stress caused by different environmental factors, including light, influences the metabolism of carotenoids (Fanciullino et al., 2014), as some carotenoids play a key role in the dissipation of excess absorbed energy through the xanthophyll cycle. In light-collecting antennae, carotenoids absorb light in the blue and green region, transferring the absorbed energy to the chlorophylls, thus increase photosynthetic efficiency by expanding the range of wavelengths absorbed (Mozzo et al., 2008; García-Plazaola et al., 2012). Furthermore, exposed to excessive radiation, xanthophylls quench the singlet excited state of chlorophyll in photosystem II (Robert et al., 2004). This process, named non-photochemical quenching, is linked to the xanthophyll cycle (García-Plazaola et al., 2012); preventing photodamage, it allows plants to acclimate to variable levels of light. Additionally, many carotenoids act as antioxidants. For instance, zeaxanthin can protect membrane surfaces from hydrophilic oxidants (Johnson, 2016), Xanthophylls are precursors of abscisic acid, which modulates stress and developmental processes (Chernys and Zeevaart, 2000), and by quenching excited chlorophyll molecules, β-carotene exerts an effective photoprotective action (Johnson, 2016).

Plants rely on both rapid response and delayed mechanisms to dynamically acclimate to their environment. Immediate and sensitive responses involve redox and ROS, while delayed responses are related to the accumulation of sugars which can reduce photoinhibition and the associated production of ROS in photosynthetic tissues (Fanciullino et al., 2014). The overall parameter intensities from both response types are integrated to realize appropriate long-term acclimation (Dietz, 2015). Sugars, as the end products of photosynthesis (Stein and Granot, 2019), are information-rich signaling molecules involved in the mechanisms that balance carbohydrate supply and usage in growth and storage processes. For instance, glucose coordinates internal sugar signals with external light conditions (Moore et al., 2003). There are several sugar-sensing mechanisms, including sensory systems for hexoses, sucrose, and raffinose, with increasing evidence suggesting that sugar contents are monitored in the plastids (Häusler et al., 2014). Additionally, photosynthesizing cell metabolisms respond quickly to changes in photosynthetic conditions, in particular, light, temperature, or CO_2 availability, which in turn depends on the state of stomatal opening (Dietz, 2015). However, contradictory data on the effect of soluble sugars on the synthesis of carotenoids reflect the distinct strategies in the leaves as a function of light influence (Urban and Alphonsout, 2007). The former leads to a benefit of carotenoids to increase protection against photodamage, leading to a loss of carotenoids when senescence is triggered (Fanciullino et al., 2014).

The aim of this study was to evaluate the effect of dynamic red and blue light parameters on lettuce physiological response and metabolite contents and thereby its impact on nutritive value.

MATERIALS AND METHODS

Growing Conditions

Lettuce (*Lactuca sativa* L. cv. "Lobjoits Green Cos") was grown in a growth chamber in peat substrate (Profile 1, JSC Durpeta, Lithuania) (pH 6, accuracy ± 0.01 pH units). The average concentrations of nutrients (mg L^{-1}) in the substrate were as follows: N, 110; P_2O_5, 50; and K_2O, 160. The microelements Fe, Mn, Cu, B, Mo, and Zn were also present. Electrical conductivity (EC) varied between 1.0 and 2.5 mS cm^{-1} (±0.03 m). One seed was seeded into a 120 ml vessel, and 28 plants for each treatment were analyzed. Plants were watered as needed. Experiments were performed in a walk-in controlled environment growth chamber (4 × 6 m). Day/night temperatures of +21/17 ± 2°C were established, and the relative humidity was maintained at 50–60%.

LED fixtures, consisting of commercially available LEDs with emission wavelengths (λ) of blue (λ = 452 nm, LedEngin LZ1-00B200, Osram Sylvania, United States) and red (λ = 662 nm, Luxeon Rebel LXM3-PD01-0300, Lumileds, United States), were used for lettuce lighting. Plants grew under constant (con) or parabolic (dyn) blue (B) and/or red (R) LED photosynthetic

photon flux density (PPFD) at 12, 16, and 20 h photoperiods, but the same daily light integral (DLI; 2.3 and 9.2 mol m^{-2} per day for B and R) was maintained for each light component in all treatments (**Figure 1**). PPFD was measured and regulated at the vessel level by using a photometer–radiometer (RF-100, Sonopan, Poland).

Determination of Pigments

Xanthophylls (neoxanthin, violaxanthin, lutein, and zeaxanthin), carotenes (carotenes α and β), and chlorophylls (chlorophylls *a* and *b*) were extracted using 80% acetone (1 g of sample ground with liquid N_2 and 10 ml of solvent), centrifuged (5 min, 4,000 rpm), and filtered through a 0.45-μm nylon membrane syringe filter (VWR International, United States). The contents of carotenes, xanthophylls, and chlorophylls were evaluated using a Shimadzu HPLC (Japan) instrument equipped with a diode array detector (SPD-M 10A VP) on a YMC Carotenoid column (3 μm particle size, 150 × 4.0 mm) (YMC, Japan). The mobile phase consisted of A (80% methanol, 20% water) and B (100% ethyl acetate). The gradient was as follows: 0 min; 20% B, 2.5 min; 22.5% B, 20–22.5 min; 50% B, 24–26 min; 80% B, 31–34 min; 100% B, 42–47 min; and 20% B, flow rate 1 ml min^{-1} (Edelenbos et al., 2001). The diode array detector was employed at 440 nm, and the absorption spectra of xanthophylls, carotenes, and chlorophylls were identified using an external standard calibration method.

Determination of Sugars

About 0.5 g of fresh plant tissue was ground and diluted with deionized H_2O. The extraction was carried out for 4 h at room temperature with mixing. Samples were centrifuged at 14,000*g* for 15 min. A clean-up step to remove soluble proteins (Brons and Olieman, 1983) was performed prior to the chromatographic analysis. Briefly, 1 ml of the supernatant was mixed with 1 ml 0.01% (w/v) ammonium acetate in acetonitrile and incubated for 30 min at +4°C. The samples were centrifuged at 14,000*g* for 15 min and filtered through a 0.22 μm PTPE syringe filter (VWR International, United States). Sugars were analyzed according to Ma et al. (2014) with modifications. The analyses were performed on a Shimadzu HPLC (Japan) instrument equipped with an evaporative light scattering detector (ELSD). Separation of fructose, glucose, sucrose, and maltose was performed on a Shodex VG-50 4D HPLC column with deionized water (mobile phase A) and acetonitrile (mobile phase B) gradient. The gradient was maintained at 88% B for 13 min, changed linearly to 70% B in 9 min, kept at 70% B for 1 min, and raised back to 88% B for 2 min, and the column was equilibrated to 88% B for 5 min. The flow rate was 0.8 ml min^{-1}.

Determination of Organic Acids

Approximately 0.5 g of fresh plant tissue was homogenized and diluted with deionized H_2O (1:10) (w/v) and heated in a water bath for 30 min at +50°C. The extract was centrifuged at 10,000 rpm for 15 min and filtered through a 0.22 μm PTPE syringe filter (VWR International, United States). Organic acids were analyzed according to Wang et al. (2014) with modifications. The analyses were performed on a Shimadzu HPLC (Japan) instrument equipped with a refractive index detector. Separation of oxalic, oxaloacetic, malic, ascorbic, folic, citric, succinic, and fumaric acids was performed on a C18 column (4.6 mm × 250 mm, 5 μm) (Nucleodur) with 0.05 M sulfuric acid in deionized water isocratic elution. The flow rate

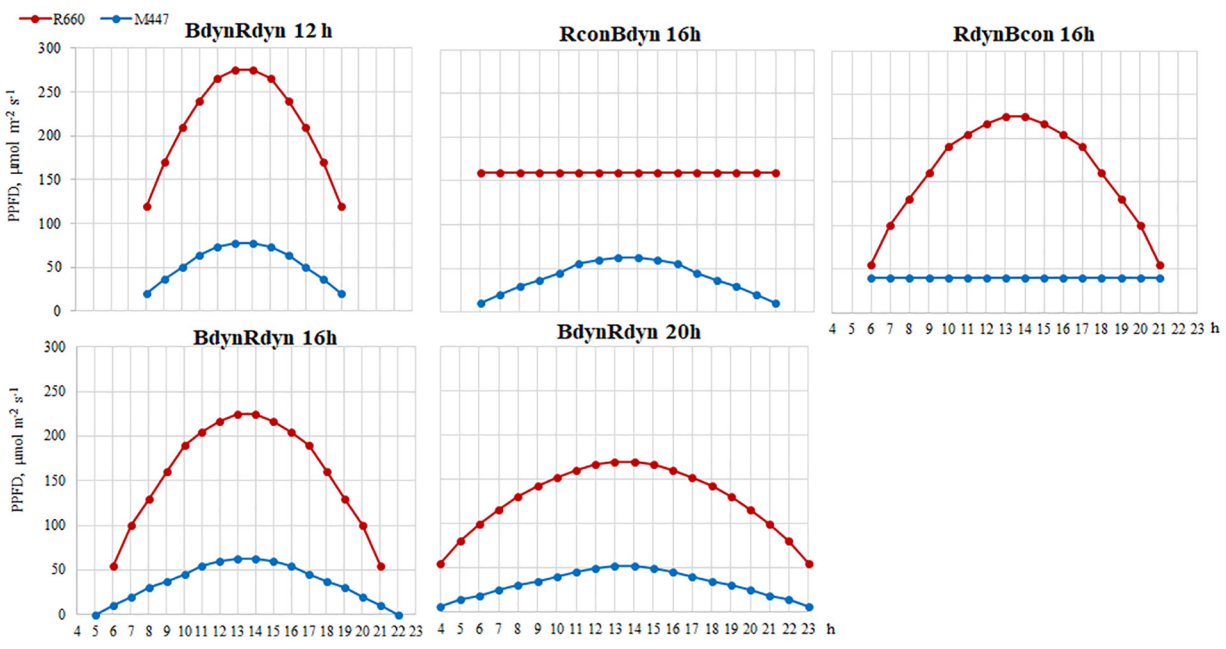

FIGURE 1 | Experimental setup of parabolic and constant light profiles. Photosynthetic photon flux densities (PPFDs) and photoperiods of the applied light-emitting diode (LED) spectra. B, blue, 452 nm; R, red, 662 nm. Total PPFD, 200 μmol m^{-2} s^{-1} which corresponds to daily light integral (DLI) of 11.5 m^{-2} per day.

was 0.5 ml min^{-1}. The peak was detected at 210 nm and identified using an external calibration method.

Determination of Antioxidant Activity

The antioxidant activity of lettuce leaves was evaluated using DPPH (2-diphenyl-1-picrylhydrazyl), ABTS [2,2′-azino-bis (3-ethylbenzothiazoline-6-sulfonic acid) diammonium salt], and an Fe^{2+} reducing antioxidant power (FRAP) assay (Kraujalytė et al., 2013). Extracts were prepared by grinding the plant material with liquid nitrogen and dilution with 80% methanol 1:10 (w/v). After 24 h, the extracts were filtered through cellulose filters.

The DPPH free radical scavenging activity was determined by mixing a diluted extract with 0.06 M methanolic DPPH solution and monitoring radical quenching every minute for 16 min to measure the absorbance at 515 nm (M501, Camspec, United Kingdom). The results are presented as DPPH free radical scavenging activity, μmol g^{-1} of fresh plant weight.

The ABTS radical solution was prepared by mixing 50 ml of 2 mM ABTS with 200 μl 70 mM $K_2S_2O_8$, allowing the mixture to stand in the dark at room temperature for 16 h before use. The working solution was diluted to obtain an initial absorbance of AU 0.700 at 734 nm (M501, Camspec, United Kingdom); 100 μl of the samples were mixed with 2 ml ABTS solution and absorbance was monitored for 11 min. The results are presented as ABTS free radical scavenging activity, μmol g^{-1} of fresh plant weight.

For the FRAP assay, the working reagent was prepared by mixing acetate buffer (300 mM, pH 3.6), a solution of 10 mM 2,4,6-tripyridyl-s-triazine (TPTZ) in 40 mM HCl, and 20 mM $FeCl_3 \times 6H_2O$ at 10:1:1 (v/v/v). Twenty microliters of the sample was mixed with 3 ml of working solution and incubated in the dark for 30 min. Then, the absorbance at 593 nm was read. The antioxidant power was expressed as Trolox equivalent antioxidant capacity (TEAC, μmol Trolox per g^{-1} of fresh plant weight) and Fe^{2+} antioxidant capacity (Fe^{2+} μmol g^{-1} of fresh plant weight).

Leaf Gas Exchange Indices

Photosynthetic rate (Pr, μmol CO_2 m^{-2} s^{-1}), transpiration rate (Tr, mmol H_2O m^{-2} s^{-1}), and the intercellular to ambient CO_2 concentration ratio (C_i/C_a) were measured on the third developed leaf, using a portable photosynthesis system (LI-COR 6400XT, United States) under the conditions at +21°C, with a CO_2 concentration of 400 μmol mol^{-1} and 60% relative humidity. Artificial irradiation was supplied to the leaf using different LEDs (665 and 470 nm), but their respective intensities were the same for PPFD 1,000 μmol m^{-2} s^{-1}. Photosynthesis was measured from 9 to 12 a.m.

Spectral Reflectance Indices

Spectral reflectance was measured using a leaf spectrometer (CID Bio-Science, United States) from 9 to 12 a.m. Reflection spectra obtained from the leaves were used to calculate the carotenoid reflectance index (CRI) and the anthocyanin reflectance index (ARI).

CRI, which shows carotenoid to chlorophyll ratio, was evaluated using the following formula:

$$CRI = (1/\rho 510) - (1/\rho 700) \quad (1)$$

ARI evaluates changes in anthocyanin amount:

$$ARI = (1/\rho 550) - (1/\rho 700) \quad (2)$$

where ρ510, ρ550, and ρ570 represent the leaf reflectance integrated over a 10 nm wavelength band centered on 510, 550, and 570 nm, respectively.

Biometric Measurements

At the end of the experiment, plant fresh mass (FW) was determined by harvesting leaves from five different plants per light treatment. Leaf area (LA) was determined using a leaf area meter (AT Delta-T Devices, United Kingdom). Dry weight (DW) was weighed after tissue dehydration at +70°C for 48 h (Venticell-BMT, Czech Republic).

Statistical Analysis

Data were processed using the XLSTAT software (Addinsoft, France), using one-way analysis of variance, ANOVA, and Tukey's (HSD) test at confidence level $p = 0.05$. Multivariate principal component analysis (PCA) was performed. The results are presented in a PCA scatterplot that indicates distinct levels of metabolites, antioxidant activity, and photosynthetic indices in lettuce subjected to constant or dynamic red and blue light at different photoperiods and a correlation circle (based on Pearson's correlation matrix) that summarizes the metabolic relations between investigated metabolites, antioxidants, and photosynthetic systems.

RESULTS

The Effect of Light Conditions on Leaf Pigments, Soluble Sugars, Photosynthetic Indices and Growth Characteristics

A parabolic PPFD profile of 16 h BdynRdyn 16 h resulted in a significant accumulation of Violax (**Figure 2A**) and hexoses (Fru and Glu) (**Figure 2D**), along with a significant decrease in pigment reflectance indexes (CRI and ARI) (**Figure 2C**), C_i/C_a, Pr, and Tr (**Figure 2E**). However, the trend of Neox accumulation was similar to constant blue (BconRdyn 16 h) lighting (**Figure 1A**). The 16 h photoperiod under BdynRdyn and BdynRcon treatments resulted in a significant increase of lettuce fresh weight (11.1%) and leaf area (16.8%) (**Figure 2F**). However, neither parabolic or constant PPFD patterns nor the duration of photoperiod had a significant effect on the accumulation of chlorophylls (Chl *a*, Chl *b*), sucrose, or maltose (**Figures 2B,D**). Higher PPFD levels under a 12 h photoperiod (BdynRdyn 12 h) significantly reduced the accumulation of neoxanthin (23.4%), violaxanthin (19.5%), lutein, and zeaxanthin (11.6%). However, the total amounts of xanthophylls were similar

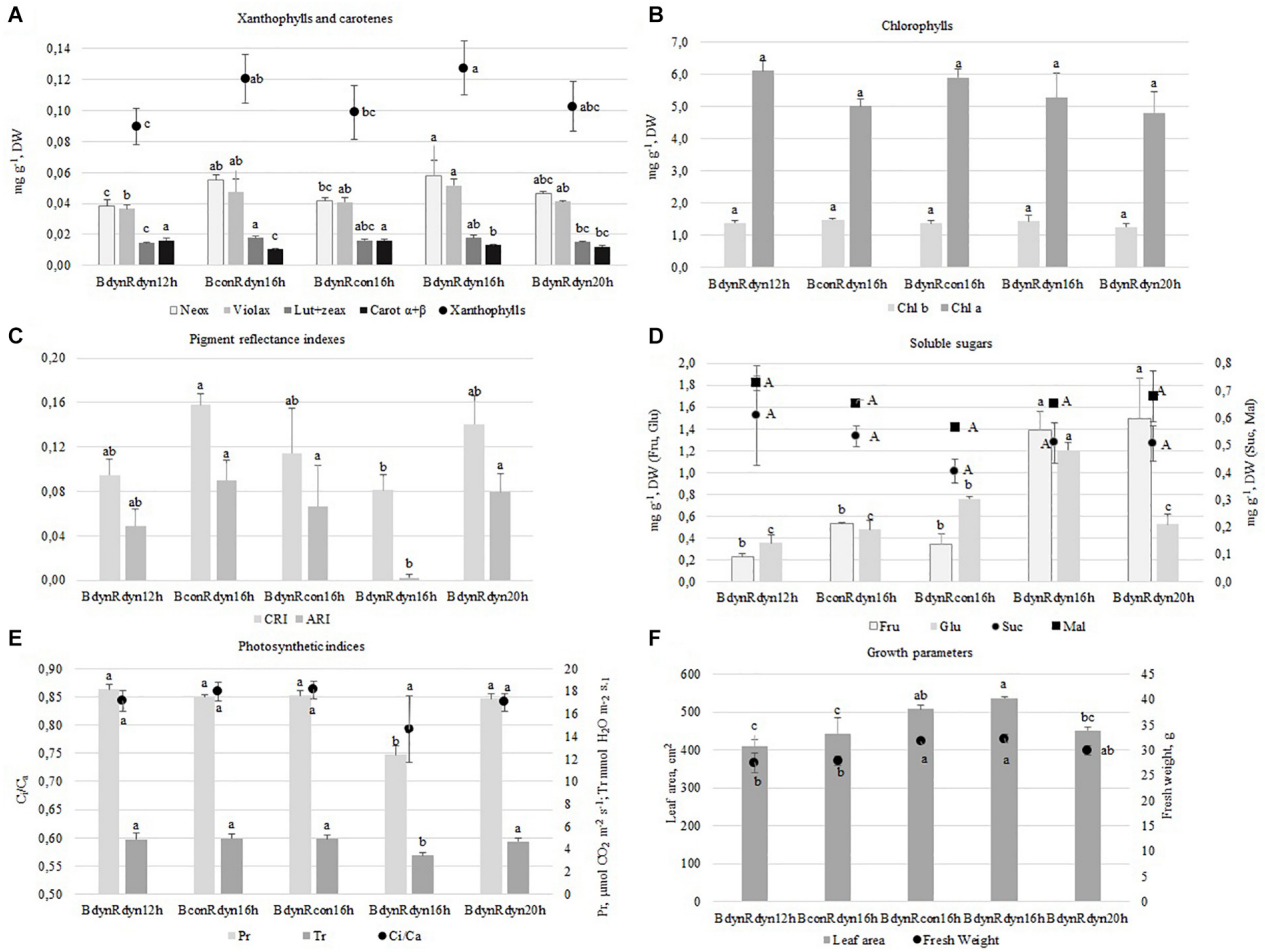

FIGURE 2 | The effect of light conditions on leaf pigments **(A,B,D)**, soluble sugars **(C)**, photosynthetic indices **(E)**, and growth characteristics **(F)** of lettuce. Plants grew under constant (con) or parabolic (dyn) blue (B, 452 nm) and/or red (R, 662 nm) LED PPFD at 12, 16, and 20 h photoperiods, but the same DLI; 2.3 and 9.2 mol m^{-2} per day for B and R. The data were processed using the XLSTAT software and Tukey's (HSD) test at confidence level $p = 0.05$ (biological replicates, $n = 5$). Neox, neoxanthin; Violax, violaxanthin; Lut + zeax, lutein and zeaxanthin; Carot α + β, α- and β-carotenes; Chl *a*, Chl *b*, chlorophylls *a* and *b*; Fru, fructose; Glu, glucose; Suc, sucrose; Mal, maltose; CRI, carotenoid/chlorophyll ratio; ARI, anthocyanin amount; Pr, photosynthetic rate; Tr, transpiration rate; C_i/C_a, intercellular to ambient CO_2 concentration.

to those accumulated under lower PPFD levels under a 20 h photoperiod (BdynRdyn 20 h) or under the constant red (BdynRcon 16 h) PPFD treatment. Constant blue (BconRdyn 16 h) significantly reduced (31.0%), whereas constant red (BdynRcon 16 h) significantly increased (21.9%) the contents of α + β-carotenes (**Figure 2A**). Under a 12 h photoperiod, hexose accumulated in amounts more than two times lower (0.58 mg g^{-1} DW) than sucrose, compared with other treatments (1.1–2.6 mg g^{-1} DW) (**Figure 1D**).

The Effect of Light Conditions on the Variation of Organic Acid Content and Antioxidant Response

Substantial amounts of oxalic, malic, and citric acids (7.4–0.5 mg g^{-1} DW) were found in lettuce, with folic and fumaric acids present as a second major group (0.19–0.05 mg g^{-1} DW), while oxaloacetic, succinic, and ascorbic acids were present in the smallest amounts (0.034–0.003 mg g^{-1} DW) (**Figures 3A,B**). The accumulation of oxalic, citric, and fumaric acids significantly (2.2 times) increased under a 12 h photoperiod. Constant blue (BconRdyn 16 h) resulted in a significant increase in oxalic and oxaloacetic acids (2.2 times both), while parabolic blue (BdynRdyn 16 h) led to a significant increase in folic acid (2.3 times). No significant differences in malic, succinic, or ascorbic acids were found.

The trends of antioxidant activity in response to lighting treatments, based on different assays, were similar (**Figure 3C**). Constant blue (BconRdyn 16 h) light resulted in the lowest values of DPPH, $ABTS^{+}$, and FRAP (3.5, 3.9, and 8.9 mmol TE g^{-1}). Significantly, the highest antioxidant capacity was found under a 20 h photoperiod using the FRAP assay (12.0 mmol TE g^{-1}); however, a significant decrease (18.8%) was conditioned only under constant blue (BconRdyn 16 h) treatments. The

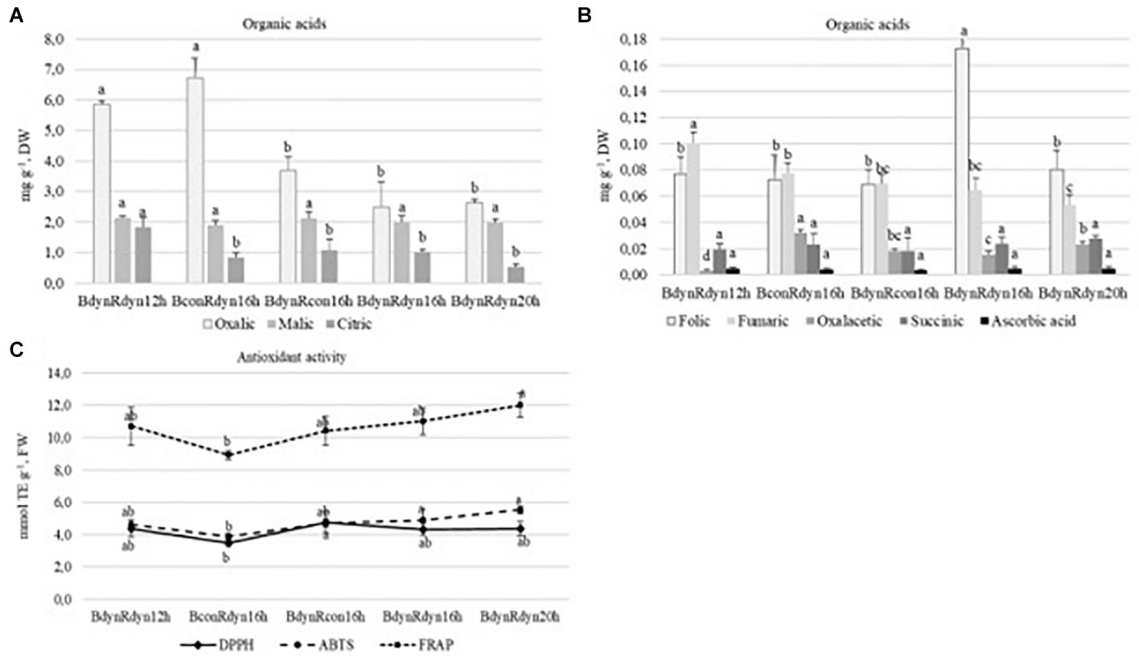

FIGURE 3 | The effect of light conditions on the variation of organic acid **(A,B)** content and antioxidant response with a focus on DPPH, ABTS, and FRAP assays **(C)** of lettuce. Plants grew under constant (con) or parabolic (dyn) blue (B, 452 nm) and/or red (R, 662 nm) LED PPFD at 12, 16, and 20 h photoperiods, but the same DLI; 2.3 and 9.2 mol m^{-2} per day for B and R. The data were processed using the XLSTAT software and Tukey's (HSD) test at confidence level $p = 0.05$ (biological replicates, $n = 5$).

$ABTS^{+}$ assay showed an antioxidant activity of 5.5 mmol TE g^{-1}, whereas the $DPPH^{\bullet}$ assay showed no significant differences in lettuce extracts compared with the 12- or 16 h parabolic blue and red light profiles (BdynRdyn).

Light Affected Differences in Metabolic, Antioxidant, and Photosynthetic Response

The PCA score scatterplot (**Figure 4**) shows the average coordinates of carotenes, xanthophylls, soluble sugars, organic acids, antioxidant activity, and photosynthetic indices in lettuce under constant, parabolic blue and/or red light at 12, 16, and 20 h photoperiods. The first two factors (F1 vs. F2) of the PCA explained 65.97 and 68.57% of the total variance in the photoperiod (**Figure 4A**) and lighting profile (**Figure 4B**) responses, respectively. F1 explained approximately 42%, whereas F2 explained 24–26% of the total variability. In terms of the F1 score, the plant responses to parabolic blue and red lighting (BdynRdyn) under the 16 and 20 h photoperiods were clearly distinct from the responses to the 12 h photoperiod (**Figure 4A**). F1 scores from the 16 h photoperiods (**Figure 1B**) with parabolic (BdynRdyn) and constant (BconRdyn) blue light treatments were clearly distinct from those with the same photoperiod and parabolic blue and red light treatments.

The agglomerative hierarchical cluster (AHC) analysis was used to divide the responses to the light profile and photoperiod data into groups of increasing dissimilarity (**Figure 5**). These divisions correspond to the PCA output with the following three clusters: cluster 1 (BconRdyn 16 h, BdynRdyn 12 h, and BdynRcon 16 h), cluster 2 (BdynRdyn 16 h), and cluster 3 (BdynRdyn 20 h). Six clusters of metabolic, photosynthetic, and antioxidant responses were identified. In contrast to cluster 1, clusters 2 and 3, both groups which included parabolic blue and red light profiles (BdynRdyn) at 16 and 20 h photoperiods, were characterized by low C_i/C_a, Pr, Tr, Chl *a*, DPPH, oxalic, and fumaric acid values and low or medium malic acid, sucrose, and α- and β-carotene content. All analyzed metabolites were in cluster 1 or cluster 2, except for Chl *a* (C3) and oxalic acid (C6). The highest similarity among metabolites was found in cluster 1. Fumaric acid, anthocyanin amount, violaxanthin, and neoxanthin were grouped into cluster C1-1; succinic acid, oxaloacetic acid, carotenes α + β, lutein + zeaxanthin, and ascorbic acid were grouped into cluster C1–2; and maltose, carotenoid/chlorophyll ratio, and folic acid were grouped into cluster C1–3.

A negative correlation between xanthophylls (Neox, Violax, Lut + zeax) and the 12 h photoperiod treatment was found, with the opposite pattern for the 16 h photoperiod treatment. A positive correlation between photosynthetic response (Pr, Tr, C_i/C_a) and the 12 h photoperiod was found (**Table 1**). A negative correlation between antioxidant properties (ABTS, FRAP), growth parameters (LA, FW), and the 12 h photoperiod was observed. A positive correlation between LA, FW, and the 16 h photoperiod was found. In contrast to the parabolic blue and red light profiles (BdynRdyn), a positive correlation between Pr,

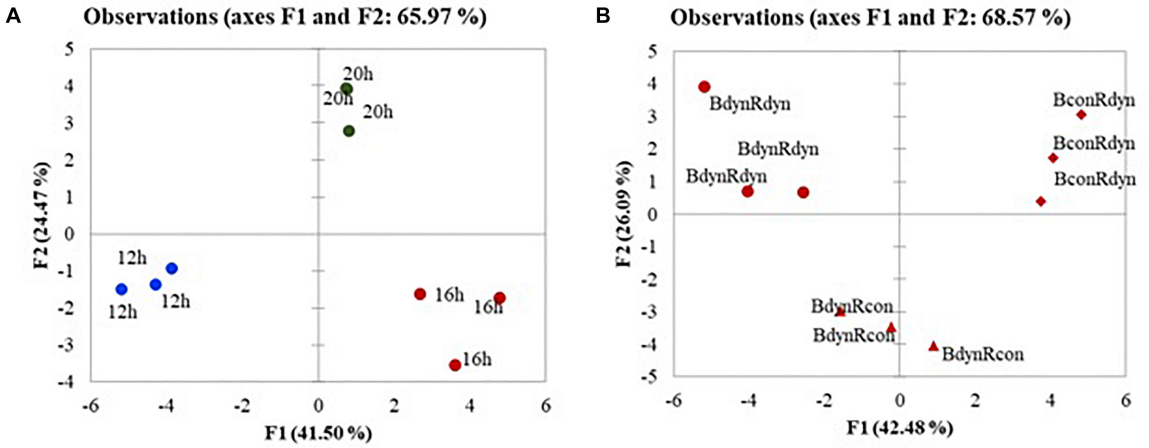

FIGURE 4 | The PCA scatterplot analysis in lettuce, indicating distinct differences in metabolites, antioxidants, and photosynthetic indices depending on lighting conditions in lettuces subjected to parabolic or constant red and blue lighting **(B)** at different photoperiods **(A)**, but similar DLA. Plants grew under constant (con) or parabolic (dyn) blue (B, 452 nm) and/or red (R, 662 nm) LED PPFD at 12, 16, and 20 h photoperiods, but the same DLI; 2.3 and 9.2 mol m^{-2} per day for B and R. The data were processed using the XLSTAT software and Tukey's (HSD) test at confidence level $p = 0.05$ (biological replicates, $n = 5$).

Tr, C_i/C_a, and constant blue light (BconRdyn) or constant red (BdynRcon) light was observed. A negative correlation between antioxidant properties (DPPH, ABTS, FRAP), growth parameters (LA, FW), and constant blue light (BconRdyn) was found, while a parabolic light profile (BdynRdyn) led to a positive correlation.

A positive correlation was found between xanthophylls (Neox, Violax, Lut + zeax) and photoperiod, with the content of these compounds increasing as the length of the light cycle increased (12–16 h). The opposite pattern was observed between photosynthetic response (Pr, Tr, C_i/C_a) and photoperiod (**Table 1**). Similarly, antioxidant properties (ABTS, FRAP) and growth parameters (LA, FW) increased with increasing photoperiod (12–16 h). Pr, Tr, and C_i/C_a increased under the constant blue (BconRdyn) or constant red (BdynRcon) light treatments compared with the other light treatments. The same was true for antioxidant properties (DPPH, ABTS, FRAP) and growth parameters (LA, FW) under the parabolic light profile BdynRdyn, with the opposite responses observed for treatments with the constant blue (BconRdyn) light profile.

DISCUSSION

Photosynthetic Response and Primary Metabolism

When plants acclimate to changing light conditions, physiological responses are the first to occur, leading to morphological, photosynthetic, and metabolic changes. Detailed knowledge about the photosynthetic pigment pool is critical for understanding the light-harvesting mechanism and photoacclimation potential of plants. The modulation and balance of photosynthetic pigment contents are part of the photosynthesis process and contribute to attaining proper equilibrium between the energy input and output (Ruban et al., 2011). Changing the photoperiod under parabolic red and blue light profiles (BdynRdyn) had a significant effect on the accumulation of neoxanthin and violaxanthin. The 12 and 16 h photoperiods led to a significant decrease and increase, respectively, in the xanthophyll content (**Figure 2A**). Although chlorophylls are the main light-capturing antennae pigments, changes in neoxanthin and violaxanthin ratio should act as a signal for light-harvesting antennae efficiency, finally resulting in acclimations to the lighting environment and lower tendencies to switch to the photoprotective mode (Gruszecki, 2010). No significant differences among chlorophylls *a* and *b*, lutein, and zeaxanthin content were found. However, parabolic blue and red light under a 16 h photoperiod led to a significant decrease in the carotenoid to chlorophyll ratio (CRI). The trend of the response of carotenes and chlorophylls to all lighting conditions in this study was the same (**Figures 2A–C**). Thus, it can be presumed that under parabolic red and blue light profiles, the xanthophyll cycle pigments may lead to dissipation of excess energy, with carotenoids concurrently dissipating the excitation energy from chlorophyll, limiting the possible light damage to membranes.

Accumulation of soluble carbohydrates is associated with decreased photosynthesis and increased photoinhibition in the leaves (Urban and Alphonsout, 2007), and this negative feedback effect was also observed in the present study (**Figures 2D,E**). Apel and Hirt (2004) suggested that the inhibiting effect of soluble sugar accumulation on the Calvin cycle leads to the formation of singlet oxygen in PS II. Fanciullino et al. (2014) supposed that glucose stimulates the synthesis of carotenoids, especially xanthophylls, which are involved in the protection of photosystems against photooxidative stress. However, AHC analysis did not show any direct connections between glucose (cluster C2) and carotenoids (cluster C1) (**Figure 5**). It is known that glucose and fructose are primary, while sucrose and starch are the major end products of photosynthetic activity in most plants. The process of sucrose and starch formation does not depend on light because sucrose can be synthesized from glucose

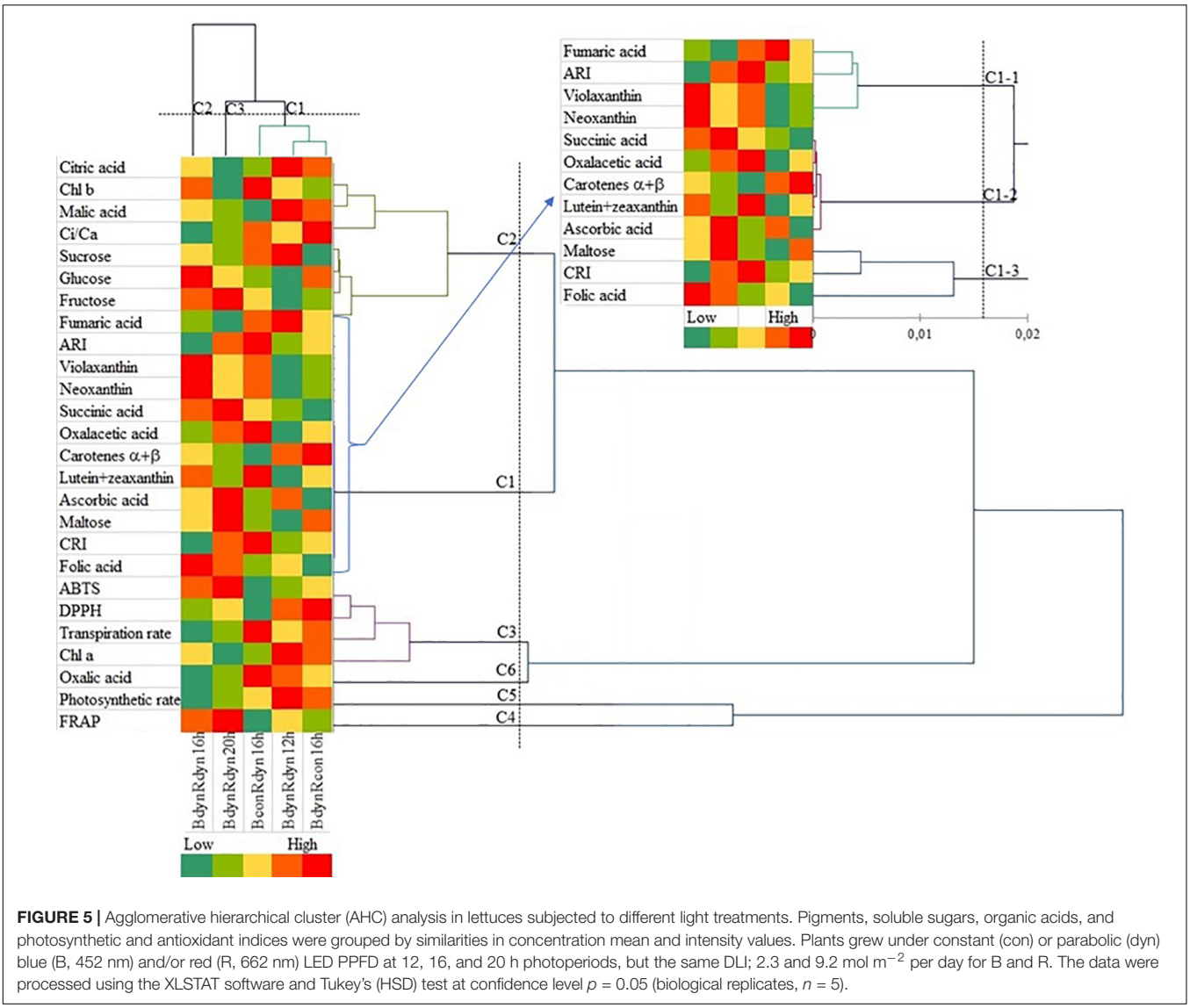

FIGURE 5 | Agglomerative hierarchical cluster (AHC) analysis in lettuces subjected to different light treatments. Pigments, soluble sugars, organic acids, and photosynthetic and antioxidant indices were grouped by similarities in concentration mean and intensity values. Plants grew under constant (con) or parabolic (dyn) blue (B, 452 nm) and/or red (R, 662 nm) LED PPFD at 12, 16, and 20 h photoperiods, but the same DLI; 2.3 and 9.2 mol m^{-2} per day for B and R. The data were processed using the XLSTAT software and Tukey's (HSD) test at confidence level $p = 0.05$ (biological replicates, $n = 5$).

and fructose in the dark and without chlorophyll (Stein and Granot, 2019). We also obtained similar results; neither sucrose nor maltose was affected by different light profiles or photoperiod (**Figure 2D**), indicating that the synthesis of disaccharides is a process independent from photosynthesis. Meanwhile, AHC analysis showed a similar trend of sucrose accumulation and C_i/C_a, which was opposite to the trend of fructose and glucose accumulation (**Figure 5**). A strong negative correlation between C_i/C_a and parabolic blue and red light under a 16 h photoperiod was found, while other light profiles or durations resulted in a weak correlation (**Table 1**). Thus, the stomatal behavior regulation might depend on both external environmental and internal signaling cues (Lawson and Blatt, 2014). Annunziata et al. (2017) found that the accumulation of starch in *Arabidopsis* grown under artificial light with a sinusoidal light profile was more intensive at the end of the day compared with that grown under constant irradiance or natural light. Parabolic lighting (BdynRdyn 16 h) led to a significant increase in fructose and glucose (**Figure 2D**), compared with other lighting treatments, suggesting that plants avoid C starvation before photosynthesis starts after the dark period (Stitt and Zeeman, 2012). However, the decrease in C_i/C_a resulted in a significant decrease in photosynthetic and transpiration rates (**Figure 2**) under a parabolic blue and red lighting treatment with a 16 h photoperiod (**Figure 2E**). McAusland et al. (2013) suggested that stomatal responses tend to be slower than photosynthetic responses, leading to suboptimal responses in stomatal conductance and photosynthetic rate, resulting in lower carbon gain. The decrease in photosynthetic rate and stomatal conductance observed over longer time scales, related to red light changes toward the end of the day, may be explained by sugar import into guard cells (Matthews et al., 2020). Sucrose transported to the guard cells is cleaved in the apoplasts to produce hexoses, which are sensed by hexokinase, which in turn signals for the stomatal closure response (Kelly et al., 2013). In contrast to that for red light, the stomatal blue light response, which has been reported to not

require photosynthesis (Hiyama et al., 2017), is important for stomatal opening in the morning, when the irradiance spectrum is steeped in blue wavelengths. These findings suggest that light is only required for the reactions involving the primary phases of CO_2 utilization during photosynthesis. Chen et al. (2019) found that a dynamic red/blue light environment had no positive effects on glucose and fructose accumulation in lettuce, in contrast to its effect on sucrose, and they also found that monochromatic lighting had the opposite effect. Our results show that hexoses were more sensitive to the lighting profile than sucrose or maltose (**Figure 2D**). These differences may be due to differences in DLI: the DLI was maintained at 11.54 mol m^{-2} per day in the current study, whereas Chen et al. (2019) used 7.49 mol m^{-2} per day. The highest total soluble sugar content under parabolic blue and red light was found in the 16 h photoperiod (BdynRdyn 16 h) treatment, which showed a significantly higher fresh weight and new leaf area formation (**Figures 2D,F**). Other results have shown that alternating red and blue light at intervals resulted in better yield and taste. Moreover, the duration of the interval between red and blue light largely influenced the dynamics between the signal and response pathways (Chen et al., 2019).

Antioxidant Response and Secondary Metabolism

Environmental fluctuations and external stress are the main factors enhancing the antioxidant response. While most studies have indicated that red and blue components are more effective against antioxidant responses, these treatments were performed on *in vitro* callus cultures and only constant monochromatic spectral lights were investigated (Nazir et al., 2020; Usman et al., 2020). Nam et al. (2018) showed that blue light, compared with red or fluorescent, could be applied to enhance flavonoid levels and antioxidant activity in common buckwheat sprouts. A significant increase in antioxidant activity, based on the DPPH assay, was found in microgreens, such as red pak choi and basil, under 25 and 33% of constant blue light (Vaštakaitė et al., 2015). Son and Oh (2013) also stated that the antioxidant capacity (expressed as TEAC) of both red and green leaf lettuces grown under high ratios of blue LED (such as 59, 47, and 35% B) was significantly higher than the lower blue to red ratio. Antioxidant activity in response to parabolic or constant light profiles was evaluated by employing antioxidant assays, mainly DPPH, ABTS, and FRAP assays. Compared with the other treatments, the lowest antioxidant activity of all the assays was recorded under constant blue and parabolic red light treatments with the 16 h photoperiod (**Figure 3C**). The increase in antioxidant capacity and induced accumulation of phenolic compounds under additional irradiation of blue LEDs in combination with red light was explained by the decreased growth of lettuce (Stutte et al., 2009; Johkan et al., 2010; Son and Oh, 2013). However, such tendencies were not observed among changes in lettuce fresh weight or leaf area (**Figure 2F**) and antioxidant activity (**Figure 3C**) in the present study.

The reason for the apparent C deficiency, or more specifically, the deficiency in organic acids, in plants grown under natural light is unclear (Annunziata et al., 2017). Plants adapted their C metabolism in response to sunny and cloudy days balancing their C and N metabolism. Sucrose signaling metabolites have been implicated in C/N interactions through activation of phosphoenolpyruvate carboxylase and nitrate reductase and increased anaplerotic flux of C into organic acids (Figueroa et al., 2016). However, sucrose did not differ significantly (**Figure 2D**) between lighting treatments; moreover, AHC analysis did not show any similarities with organic acids, except for malic and citric acids (**Figure 5**). The changes in organic acid content (**Figures 3A,B**) suggest that metabolism of organic acids may be less robust to changes in light intensity

TABLE 1 | Correlation between photosynthetic indices, antioxidant activity, growth parameters, and lighting conditions.

	BdynRdyn			16 h		
	12 h	**16 h**	**20 h**	**BconRdyn**	**BdynRcon**	**BdynRdyn**
Neox	−0.673*	0.768*	−0.094	0.277	−0.796*	0.518*
Violax	−0.701*	0.899*	−0.199	0.098	−0.664*	0.567*
Lut + zeax	−0.475*	0.831*	−0.356	0.365	−0.589*	0.223
Chl *a*	0.683*	−0.099	−0.584	−0.513*	0.663*	−0.150
Chl *b*	0.146	0.406*	−0.551	0.309*	−0.334*	0.024
Pr	0.600*	−0.973*	0.373	0.470*	0.513*	−0.982*
Tr	0.544*	−0.878*	0.335	0.478*	0.458*	−0.935*
C_i/C_a	0.329*	−0.611*	0.282	0.344*	0.391*	−0.734*
DPPH	0.019	−0.022	0.003	−0.772*	0.622*	0.150
ABTS	−0.538*	−0.163	0.701	−0.782*	0.277	0.505*
FRAP	−0.403*	−0.163	0.566	−0.798*	0.195	0.603*
LA	−0.742*	0.927*	−0.184	−0.838*	0.184	0.654*
FW	−0.756*	0.739*	0.017	−0.944*	0.389	0.555*

Correlation coefficient (r) for the pairs of investigated parameters (n = 3 for each parameter) is presented. Correlations marked with asterisk mark (*) are significant at $p < 0.05$. B, blue, 452 nm; R, red, 662 nm; dyn, parabolic profile; con, constant profile; Neox, neoxanthin; Violax, violaxanthin; Lut + zeax, lutein and zeaxanthin; Chl a, Chl b, chlorophylls a and b; Pr, photosynthetic rate; Tr, transpiration rate; C_i/C_a, intercellular to ambient CO_2 concentration; LA, leaf area; FW, fresh weight.

profiles than to photoperiod. Ascorbic acid is involved in many plant physiological processes, including photosynthesis or transmembrane electron transport (Plumb et al., 2018). In agreement, AHC analysis showed close similarity among ascorbic acid, lutein, zeaxanthin, and carotenes (cluster C1–2) (**Figure 5**). On the other hand, neither parabolic nor constant lighting profiles or different photoperiods (it should be stated that DLI was the same in all treatments) had a significant effect on ascorbic acid accumulation (**Figure 3B**). A significant increase in ascorbic acid was mainly obtained by extending the continuous light for 48 (Zhou et al., 2012) or 72 h (Yabuta et al., 2007). Moreover, in agreement with Yabuta et al. (2007), the dissimilarity among hexoses, sucrose (cluster C2), and ascorbic acid (cluster C1) (**Figure 5**) shows that photosynthetic electron transport in chloroplasts is highly related to ascorbic acid pool size regulation in the leaves but is independent of sugars.

CONCLUSION

The results obtained and the PCA analysis confirmed the significant impact of both photoperiod and the parabolic profiles of PPFD distribution on lettuce physiological response. A 16 h photoperiod resulted in significantly higher xanthophyll content (neoxanthin, violaxanthin, lutein, and zeaxanthin) in lettuce leaves under both constant and parabolic blue light treatments (BconRdyn 16 h; BdynRdyn 16 h). Lower and higher PPFD levels under a 20 and 12 h photoperiod (BdynRdyn 20 h, BdynRdyn 12 h), respectively, and maintaining the same DLI had a pronounced reducing impact on photosynthetic indices (Pr, Tr, C_i/C_a), xanthophylls, soluble sugar contents, and antioxidant properties of lettuce leaves. Parabolic lighting (BdynRdyn 16 h) led to a significant decrease in C_i/C_a, resulting in decreased photosynthetic and transpiration rates, compared with constant blue or red light PPFD over the same photoperiod (BconRdyn, BdynRcon at 16 h). Moreover, under constant blue lighting, higher carotenes α + β, anthocyanin (ARI) content, and CRI were obtained, but these were accompanied by decreased biomass accumulation and antioxidant activity.

DATA AVAILABILITY STATEMENT

The original contributions presented in the study are included in the article/supplementary material, further inquiries can be directed to the corresponding author/s.

AUTHOR CONTRIBUTIONS

GS: data analysis, writing of the manuscript. AV: joint coordination of the experiment, modeling of light parameters, and data summarizing JM: spectrophotometric analysis, biometric measurements, and data summarizing. PH: chromatographic analysis. KL: photosynthesis and optical indices measurements, data summarizing. AB and PD: the realization of lighting schedules in vegetative experiments, data analysis All authors read and approved the final version of the manuscript.

FUNDING

This research was funded by a grant (No. S-MIP-17-23) from the Research Council of Lithuania.

ACKNOWLEDGMENTS

We would like to thank Editage (www.editage.com) for English language editing.

REFERENCES

Annunziata, M. G., Aplet, F., Carillo, P., Krause, U., Feil, R., Mengin, V., et al. (2017). Getting back to nature: a reality check for experiments in controlled environments. *J. Exp. Bot.* 68, 4463–4477.doi: 10.1093/jxb/erx220

Apel, K., and Hirt, H. (2004). Reactive oxygen species: metabolism, oxidative stress, and signal transduction. *Annu. Rev. Plant Biol.* 55, 373–399.doi: 10.1146/annurev.arplant.55.031903.141701

Bantis, F., Smirnakou, S., Ouzounis, T., Koukounaras, A., Ntagkas, N., and Radoglou, K. (2018). Current status and recent achievements in the field of horticulture with the use of light-emitting diodes (LEDs). *Sci. Hort.* 235, 437–451.doi: 10.1016/j.scienta.2018.02.058

Brons, C., and Olieman, C. (1983). Study of the high-performance liquid chromatographic separation of reducing sugars, applied to the determination of lactose in milk. *J. Chromatogr.* 259, 79–86.doi: 10.1016/S0021-9673(01)87980-2

Chen, X.-L., Wang, L.-C., Li, T., Yang, Q.-C., and Guo, W.-Z. (2019). Sugar accumulation and growth of lettuce exposed to different lighting modes of red and blue LED light. *Sci. Rep* 9:969. doi: 10.1038/s41598-019-43498-8

Chernys, J. T., and Zeevaart, J. A. D. (2000). Characterization of the 9-cisepoxycarotenoid dioxygenase gene family and the regulation of abscisic acid biosynthesis in avocado. *Plant Physiol.* 124, 343–353.doi: 10.1104/pp.124.1.343

Dietz, K.-J. (2015). Efficient high light acclimation involves rapid processes at multiple mechanistic levels. *J. Exp. Bot.* 66, 2401–2414.doi: 10.1093/jxb/eru505

Dong, C., Fu, Y., Liu, G., and Liu, H. (2014). Growth, photosynthetic characteristics, antioxidant capacity and biomass yield and quality of wheat (*Triticum aestivum* L.) exposed to LED light sources with different spectra combinations. *J. Agron. Crop Sci.* 200, 219–230.doi: 10.1111/jac.12059

Edelenbos, M., Christensen, L. P., and Grevsen, K. (2001). HPLC determination of chlorophyll and carotenoid pigments in processed green pea cultivars (*Pisum sativum* L.). *J. Agric. Food Chem.* 49, 4768–4774.doi: 10.1021/jf010569z

Fanciullino, A. L., Bidel, L. P. R., and Urban, L. (2014). Carotenoid responses to environmental stimuli: integrating redox and carbon controls into a fruit model. *Plant Cell Environ.* 37, 273–289.doi: 10.1111/pce.12153

Figueroa, C. M., Feil, R., Ishihara, H., Watanabe, M., Kölling, K., Krause, U., et al. (2016). Trehalose 6-phosphate coordinates organic and amino acid metabolism with carbon availability. *Plant J.* 85, 410–423.doi: 10.1111/tpj.13114

García-Plazaola, J., Esteban, R., Fernández-Marín, B., Kranner, I., and Porcar-Castell, A. (2012). Thermal energy dissipation and xanthophyll cycles beyond the *Arabidopsis* model. *Photosynth. Res.* 113, 89–103.doi: 10.1007/s11120-012-9760-7

Gruszecki, W. I. (2010). Light-driven regulatory mechanisms in the photosynthetic antenna complex LHCII. *Biochem. Soc. Trans.* 38, 702–704.doi: 10.1042/bst0380702

Hasan, M. M., Bashir, T., Ghosh, R., Lee, S. K., and Bae, H. (2017). An overview of LEDs' effects on the production of bioactive compounds and crop quality. *Molecules.* 22:1420.doi: 10.3390/molecules22091420

Häusler, R. E., Heinrichs, L., Schmitz, J., and Flügge, U. I. (2014). How sugars might coordinate chloroplast and nuclear gene expression during acclimation to high light intensities. *Mol. Plant.* 7, 1121–1137.doi: 10.1093/mp/ssu064

Hiyama, A., Takemiya, A., Munemasa, S., Okuma, E., Sugiyama, N., Tada, Y., et al. (2017). Blue light and CO_2 signals converge to regulate light-induced stomatal opening. *Nat. Commun.* 8:1284. doi: 10.1038/s41467-017-01237-5

Johkan, M., Shoji, K., Goto, F., Hashida, S., and Yoshihara, T. (2010). Blue light-emitting diode light irradiation of seedlings improves seedling quality and growth after transplanting in red leaf lettuce. *HortScience* 45, 1809–1814.doi: 10.21273/HORTSCI.45.12.1809

Johnson, M. P. (2016). Photosynthesis. *Essays Biochem.* 60, 255–273. doi: 10.1042/EBC20160016

Kelly, G., Moshelion, M., David-Schwartz, R., Halperin, O., Wallach, R., Attia, Z., et al. (2013). Hexokinase mediates stomatal closure. *Plant J.* 75, 977–988.doi: 10.1111/tpj.12258

Kraujalytė, V., Venskutonis, P. R., Pukalskas, A., Česonienė, L., and Daubaras, R. (2013). Antioxidant properties and polyphenolic compositions of fruits from different European cranberrybush (*ViburnuB opulus* L.) genotypes. *Food Chem.* 141, 3695–3702.doi: 10.1016/j.foodchem.2013.06.054

Lawson, T., and Blatt, M. R. (2014). Stomatal size, speed, and responsiveness impact on photosynthesis and water use efficiency. *Plant Physiol.* 164, 1556–1570.doi: 10.1104/pp.114.237107

Lee, M. K., Arasu, M. V., Park, S., Byeon, D. H., Chung, S. O., Park, S. U., et al. (2016). LED lights enhance metabolites and antioxidants in Chinese cabbage and kale. *Braz. Arch. Biol. Technol.* 59:e16150546. doi: 10.1590/1678-4324-2016150546

Lekkham, P., Srilaong, V., Pongprasert, N., and Kondo, S. (2016). Anthocyanin concentration and antioxidant activity in light-emitting diode (LED)-treated apples in a greenhouse environmental control system. *Fruits* 71, 269–274.doi: 10.1051/fruits/2016022

Ma, C., Sun, Z., Chen, C., Zhang, L., and Zhu, S. (2014). Simultaneous separation and determination of fructose, sorbitol, glucose and sucrose in fruits by HPLC–ELSD. *Food Chem.* 145, 784–788.doi: 10.1016/j.foodchem.2013.08.135

Matthews, J. S. A., Vialet-Chabrand, S., and Lawson, T. (2020). Role of blue and red light in stomatal dynamic behaviour. *J. Exp. Bot.* 71, 2253–2269.doi: 10.1093/jxb/erz563

McAusland, L., Davey, P. A., Kanwal, N., Baker, N. R., and Lawson, T. (2013). A novel system for spatial and temporal imaging of intrinsic plant water use efficiency. *J. Exp. Bot.* 64, 4993–5007.doi: 10.1093/jxb/ert288

Moore, B., Zhou, L., Rolland, F., Hall, Q., Cheng, W.-H., Liu, Y.-X., et al. (2003). Role of the Arabidopsis glucose sensor HXK1 in nutrient, light, and hormonal signaling. *Science* 300, 332–336.doi: 10.1126/science.1080585

Mozzo, M., Dall'Osto, L., Hienerwadel, R., Bassi, R., and Croce, R. (2008). Photoprotection in the antenna complexes of Photosystem II: role of individual xanthophylls in chlorophyll triplet quenching. *J. Biol. Chem.* 283, 6184–6192. doi: 10.1074/jbc.M708961200

Nam, T. G., Dae-Ok, K., and Seok, H. E. (2018). Effects of light sources on major flavonoids and antioxidant activity in common buckwheat sprouts. *Food Sci. Biotechnol.* 27, 169–176.doi: 10.1007/s10068-017-0204-1

Nazir, M., Ullah, M. A., Younas, M., Siddiquah, A., Shah, M., Giglioli-Guivarc'h, N., et al. (2020). Light-mediated biosynthesis of phenylpropanoid metabolites and antioxidant potential in callus cultures of purple basil (*Ocimum basilicum* L. var purpurascens). *Plant Cell Tissue Organ. Cult.* 142, 107–120.doi: 10.1007/s11240-020-01844-z

Plumb, W., Townsend, A. J., Rasool, B., Alomrani, S., Razak, N., Karpinska, B., et al. (2018). Ascorbate-mediated regulation of growth, photoprotection and photoinhibition in *Arabidopsis thaliana*. *J. Exp. Bot.* 69, 2823–2835.doi: 10.1093/jxb/ery170

Robert, B., Horton, P., Pascal, A. A., and Ruban, A. V. (2004). Insights into the molecular dynamics of plant light-harvesting proteins in vivo. *Trends Plant Sci.* 9, 385–390.doi: 10.1016/j.tplants.2004.06.006

Ruban, A. V., Johnson, M. P., and Duffy, C. D. P. (2011). Natural light harvesting: principles and environmental trends. *Energ. Environ. Sci.* 4, 1643–1650.doi: 10.1039/C0EE00578A

Sabzalian, M. R., Heydarizadeh, P., Zahedi, M., Boroomand, A., Agharokh, M., Sahba, M. R., et al. (2014). High performance of vegetables, flowers, and medicinal plants in a red-blue LED incubator for indoor plant production. *Agron. Sustain. Dev.* 34, 879–886.doi: 10.1007/s13593-014-0209-6

Samuolienė, G., Brazaitytė, A., Sirtautas, R., Viršilė, A., Sakalauskaitė, J., Sakalauskienė, S., et al. (2013). LED illumination affects bioactive compounds in romaine baby leaf lettuce. *J. Sci. Food Agric.* 93, 3286–3291.doi: 10.1002/jsfa.6173

Samuolienė, G., Sirtautas, R., Brazaitytė, A., and Duchovskis, P. (2012). LED lighting and seasonality effects antioxidant properties of baby leaf lettuce. *Food Chem.* 134, 1494–1499.doi: 10.1016/j.foodchem.2012.03.061

Samuolienė, G., Viršilė, A., Haimi, P., and Miliauskienė, J. (2020). Photoresponse to different lighting strategies during red leaf lettuce growth. *J. Photochem. Photobiol. B Biol.* 202, 111726.doi: 10.1016/j.jphotobiol.2019.111726

Shen, Y. Z., Guo, S. S., Ai, W. D., and Tang, Y. K. (2014). Effects of illuminants and illumination time on lettuce growth, yield and nutritional quality in a controlled environment. *Life Sci. Space Res.* 2, 38–42. doi: 10.1016/j.lssr.2014.06.001

Son, K.-H., and Oh, M.-M. (2013). Leaf shape, growth, and antioxidant phenolic compounds of two lettuce cultivars grown under various combinations of blue and red light-emitting diodes. *HortScience* 48, 988–995.doi: 10.21273/HORTSCI.48.8.988

Stein, O., and Granot, D. (2019). An overview of sucrose synthases in plants. *Front. Plant Sci.* 10:95. doi: 10.3389/fpls.2019.00095

Stitt, M., and Zeeman, S. C. (2012). Starch turnover: pathways, regulation and role in growth. *Cur. Opin. Plant Biol.* 15, 282–292. doi: 10.1016/j.pbi.2012.03.016

Stutte, G. W., Edney, S., and Skerritt, T. (2009). Photoregulation of bioprotectant content of red leaf lettuce with light-emitting diodes. *HortScience* 44, 79–82.doi: 10.21273/HORTSCI.44.1.79

Urban, L., and Alphonsout, L. (2007). Girdling decreases photosynthetic electron fluxes and induces sustained photoprotection in mango leaves. *Tree Physiol.* 27, 345–352.doi: 10.1093/treephys/27.3.345

Usman, H., Ullah, M. A., Jan, H., Siddiquah, A., Drouet, S., Anjum, S., et al. (2020). Interactive effects of wide-spectrum monochromatic lights on phytochemical production, antioxidant and biological activities of *Solanum xanthocarpum* callus cultures. *Molecules* 25:2201.doi: 10.3390/molecules25092201

Vaštakaitė, V., Viršilė, A., Brazaitytė, A., Samuolienė, G., Jankauskienė, J., Sirtautas, R., et al. (2015). The effect of blue light dosage on growth and antioxidant properties of microgreens. *Sodinink. Daržinink.* 34, 25–35.

Wang, Y., Wang, J., Chang, W., Zhao, Z., and Cao, J. (2014). HPLC method for the simultaneous quantification of the major organic acids in Angeleno plum fruit. *IOP Conf. Ser. Mater. Sci. Eng.* 62:012035. doi: 10.1088/1757-899X/62/1/012035

Yabuta, Y., Mieda, T., Rapolu, M., Nakamura, A., Motoki, T., Maruta, T., et al. (2007). Light regulation of ascorbate biosynthesis is dependent on the photosynthetic electron transport chain but independent of sugars in *Arabidopsis*. *J. Exp. Bot.* 58, 2661–2671.doi: 10.1093/jxb/erm124

Zhou, W. L., Liu, W. K., and Yang, Q. C. (2012). Quality changes in hydroponic lettuce grown under pre-harvest short-duration continuous light of different intensities. *J. Hortic. Sci. Biotechnol.* 87, 429–434. doi: 10.1080/14620316.2012.11512890

Conflict of Interest: The authors declare that the research was conducted in the absence of any commercial or financial relationships that could be construed as a potential conflict of interest.

Copyright © 2021 Samuolienė, Viršilė, Miliauskienė, Haimi, Laužikė, Brazaitytė and Duchovskis. This is an open-access article distributed under the terms of the Creative Commons Attribution License (CC BY). The use, distribution or reproduction in other forums is permitted, provided the original author(s) and the copyright owner(s) are credited and that the original publication in this journal is cited, in accordance with accepted academic practice. No use, distribution or reproduction is permitted which does not comply with these terms.

frontiers in Plant Science

ORIGINAL RESEARCH
published: 26 February 2021
doi: 10.3389/fpls.2021.611236

Increase of Yield, Lycopene, and Lutein Content in Tomatoes Grown Under Continuous PAR Spectrum LED Lighting

Dennis Dannehl[1], Thomas Schwend[2], Daniel Veit[3] and Uwe Schmidt[1]*

[1] Division Biosystems Engineering, Faculty of Life Sciences, Albrecht Daniel Thaer - Institute of Agricultural and Horticultural Sciences, Humboldt-Universität zu Berlin, Berlin, Germany, [2] BLV Licht-und Vakuumtechnik GmbH, Steinhöring, Germany, [3] Max Planck Institute for Chemical Ecology, Jena, Germany

Light emitting diodes (LEDs) are an energy efficient alternative to high-pressure sodium (HPS) lighting in tomato cultivation. In the past years, we have learned a lot about the effect of red and blue LEDs on plant growth and yield of tomatoes. From previous studies, we know that plants absorb and utilize most of the visible spectrum for photosynthesis. This part of the spectrum is referred to as the photosynthetically active radiation (PAR). We designed a LED fixture with an emission spectrum that partially matches the range of 400 to 700 nm and thus partially covers the absorption spectrum of photosynthetic pigments in tomato leaves. Tomato plants grown under this fixture were significantly taller and produced a higher fruit yield (14%) than plants grown under HPS lighting. There was no difference in the number of leaves and trusses, leaf area, stem diameter, the electron transport rate, and the normalized difference vegetation index. Lycopene and lutein contents in tomatoes were 18% and 142% higher when they were exposed to the LED fixture. However, the ß-carotene content was not different between the light treatments. Transpiration rate under LED was significantly lower (40%), while the light use efficiency (LUE) was significantly higher (19%) compared to HPS lighting. These data show that an LED fixture with an emission spectrum covering the entire PAR range can improve LUE, yields, and content of secondary metabolites in tomatoes compared to HPS lighting.

Keywords: LED lighting, secondary metabolites, tomato, supplementary lighting, full spectrum LED, carotenoids, greenhouse

OPEN ACCESS

Edited by:
Titta Katariina Kotilainen, Natural Resources Institute Finland (Luke), Finland

Reviewed by:
Christine Becker, Hochschule Geisenheim University, Germany
Georgios Ntinas, Hellenic Agricultural Organisation (HAO), Greece

****Correspondence:***
Dennis Dannehl
Dennis.Dannehl@agrar.hu-berlin.de

Specialty section:
This article was submitted to Plant Metabolism and Chemodiversity, a section of the journal Frontiers in Plant Science

Received: *28 September 2020*
Accepted: *08 February 2021*
Published: *26 February 2021*

Citation:
Dannehl D, Schwend T, Veit D and Schmidt U (2021) Increase of Yield, Lycopene, and Lutein Content in Tomatoes Grown Under Continuous PAR Spectrum LED Lighting. Front. Plant Sci. 12:611236. doi: 10.3389/fpls.2021.611236

INTRODUCTION

Tomato is one of the most important greenhouse crops in the world. They are an important dietary source of carotenoids, a class of compounds that may have beneficial effects on human health, e.g., the reduction in the occurrence of inflammations and human prostate cancer (Kotake-Nara et al., 2001; Jacob et al., 2008). Tomatoes are nowadays also produced during winter season. We owe this to the development of supplementary greenhouse lightening. For the last 60 years high-pressure sodium (HPS) lamps were the working horse of the greenhouse industry due to their long operating life and low acquisition costs (Ouzounis et al., 2018). However, in the past years, light emitting diodes (LEDs) have become increasingly important as a more energy efficient alternative, in particular for tomato cultivation, which requires a daily light integral of up to 25 mol m^{-2} d^{-1}

(Moe et al., 2005). Furthermore, in contrast to HPS lighting, which emits dominantly yellow and orange and very little blue light (∼5%) (Terfa et al., 2013), LED lighting can be designed to meet to photosynthesis action spectrum of the crop (Jou et al., 2015). The action spectrum of tomato leaves is well known (McCree, 1971). The photosynthesis action spectrum shows two peaks in the red and blue part of the visible spectrum that coincide with chlorophyll absorption. However, photosynthesis occurs over the entire range of wavelengths between 400 to 700 nm. The effect of these wavelengths is mediated by carotenoids, a diverse group of pigments, which are associated with the light harvesting complex (Frank and Cogdell, 1993; Hashimoto et al., 2016).

Although the role of carotenoids in photosynthesis is well appreciated, wavelengths other than red and blue had rarely been used in academic studies on the effect of LED lightings in tomato production. Consequently, there is a lot of information about the effect of red and blue light used as overhead-lighting, inter-lighting or hybrid-lighting (LEDs + HPS) on plant growth and yield of tomatoes (Dueck et al., 2011; Hogewoning et al., 2012; Gajc-Wolska et al., 2013; Gomez et al., 2013; Deram et al., 2014; Gómez and Mitchell, 2015; Tewolde et al., 2016; Gilli et al., 2018; Lanoue et al., 2019; Paponov et al., 2019). These studies showed that photosynthesis under a combination of red and blue light tends to be higher than under HPS lighting, but fruit yield is equal. It is not quite clear why there is no increase in fruit harvest under red and blue LEDs. Some studies also included additional far-red light (Hao et al., 2015; Zhang et al., 2019). Additional far-red light in combination with red LEDs and HPS appears to increase total fruit number. It has also been shown that the exposure to supplementary red and blue LED lighting increases the lycopene and ß-carotene content (Xie et al., 2019; Ngcobo et al., 2020).

To our best knowledge, only one research group studied the effects of spectrally optimized LED-lighting on algae growth (Ng et al., 2020). However, no information is available on the effects of continuous PAR spectrum LEDs on tomato growth and the tomato carotenoid content.

In order to study the effect of a continuous PAR spectrum on tomato growth and plant responses, such as light use efficiency, transpiration mass flow density and the concentrations of different carotenoids in tomatoes, a new LED fixture was designed. The emission spectrum of the fixture matches the waveband from 400 to 750 nm and in certain areas approximates the absorption spectrum of photosynthetic pigments in tomato leaves. This fixture was used to grow tomato plants in a greenhouse and compare the morphological and -physiological responses to plants grown under HPS lighting.

MATERIALS AND METHODS

Supplementary Lighting

We designed a fixture with an emission spectrum that matches partially the PAR spectral range and in some parts approximates the absorption spectrum of photosynthetic pigments in tomato leaves (**Figure 1**). The leaf absorption spectrum was measured in acetone (Lichtenthaler and Wellburn, 1983). The LED fixture consisted of 14 LEDs (Roschwege GmbH, Greifenstein, Germany) combined with zoom lenses (B & M Optics GmBH, Limburg, Germany), which have a radiation angle of 60° to achieve an average light intensity of 55 μmol $m^{-2}s^{-1}$ at a distance of 1.8 m between the lamp and the bottom. The LED fixture consisted of three warm white LED's (3000 K), 3 cool white LED's (6000 K), two blue and red multichip LEDs (380 – 840 nm), 2 LED's (630 nm), 3 LED's (660 nm) and 1 LED (720 nm). Each LED had 10 W. The LED fixture had the following dimension: width = 20 cm, length = 50 cm, depth = 15 cm. This LED system was compared with a high-pressure sodium lamp (HPS) (SON-T Agro 400, Koninklijke Philips N.V., Amsterdam, Netherlands), which had 400 W. The HPS emission spectrum is displayed in **Figure 1**. In a distance of 1.8 m, the photosynthetic active radiation of the LED and HPS fixture was the same.

Plant Material and Experimental Setup

Tomato plants (*Solanum lycopersicum* L., cv. Purezza) (Syngenta AG, Basel, Switzerland) were planted into a 75 m^2 compartment of an experimental Venlo-type greenhouse at Humboldt-Universität zu Berlin. The seeds were germinated for 2 weeks in perlite (Perligran premium, Knauf Aquapanel GmbH, Dortmund, Germany) (October 11, 2018). The seedlings were transferred to 7.5 L containers filled with a horticultural substrate (substrate 1, Klasmann-Deilmann GmbH, Geeste, Germany). The plants were grown under the same conditions (temperature 23°C; relative humidity 80%, HPS lighting for 12 h from 6 am to 6 pm) until they reached a height of approximately 20 cm. This plant development stage was the starting point for the lighting experiments (November 22, 2018).

The experiments consisted of two light treatments, which were replicated three times. Each plot had the size of 1 m^2 and contained five plants. The distance between plots was 3 m. The floor level heating was set at a target temperature of 23°C during the day and 18°C during the night. The ventilation was opened above 24°C. During the experiments, the temperature did not fall below the set night temperature. The maximum daytime temperature was reached in April and was 26.7°C. The energy screen was closed if the global radiation was below 3 W m^{-2}. Plants were fertilized when required. In detail, the substrate moisture was measured with an analog tensiometer (Tensiometer, Step Systems GmbH, Nürnberg, Germany). If a suction tension of 120 hPa in the substrate was exceeded, watering was carried out until the nutrient solution ran out of the pot. The nutrient solution was prepared according to the protocol of Göhler and Molitor (2002). Supplementary LED and HPS lighting were used between 6.00 am and midnight if the solar photosynthetic photon flux density (PPFD) was below 360 μmol m^{-2} s^{-1}.

Assessment of Plant Growth and Yield

The average plant height, internode distance, stem diameter, number of trusses and leaves, as well as the leaf area were recorded during the first six weeks of cultivation. The number of leaves and trusses were counted, and all other parameters were

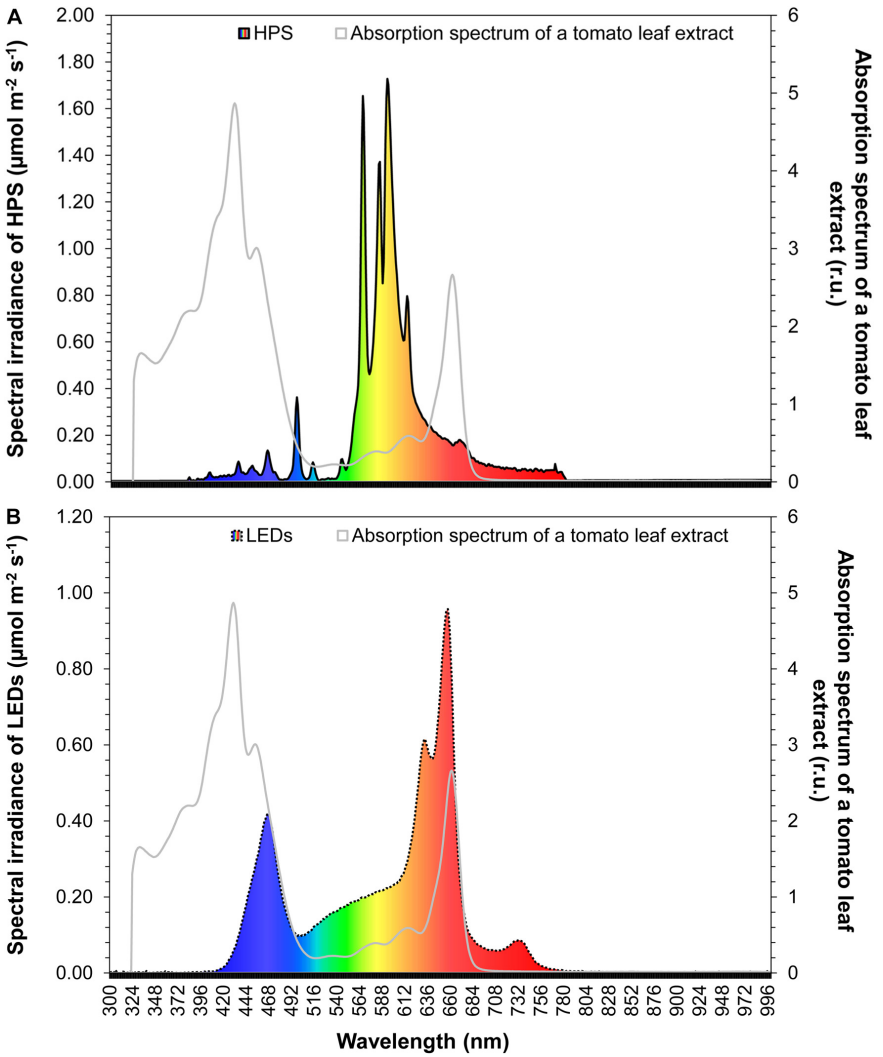

FIGURE 1 | Comparison of the HPS **(A)** and LED **(B)** light spectrum with the absorption spectrum of a tomato leaf extract. Tomato leaves were extracted in acetone.

measured with normal tools like a folding ruler and a caliper. Leaf area was calculated according to Dannehl et al. (2015). Leaf area per plant (m^2 $plant^{-1}$) is the sum of individual leaves. The stem diameter was measured at a height of 10 cm above ground. Tomatoes were harvested at ripening stage 10 (according to the Organisation for Economic Co-operation and Development, OECD colour gauge), counted and weighed. As such, the weight of each fruit was categorized according to different weight classes: marketable fruit > 50 g and non-marketable fruit ≤ 50 g. The end of cultivation was April 7, 2019.

Light Use Efficiency, Transpiration Mass Flow Density, and Leaf Temperature

The light use efficiency (LUE) and transpiration mass flow density caused by both light treatments were measured using two gas exchange systems (BERMONIS, Steinbeis GmbH & Co. KG, Stuttgart, Germany) and recorded all 30 s. Each gas exchange system consisted of 10 leaf chambers. As such, 10 leaf chambers were distributed on five plants of each light treatment. One leaf chamber was attached to the first and one to the second fully developed leaf of each randomly selected plant. Simultaneously, PPFD was measured (Li-190R, LICOR, Lincoln, NE, United States) at each leaf chamber. This was done three times between 8.00 pm and midnight for a period of 1 week, starting on 6 February. LUE is here defined as CO_2 uptake (µmol CO_2 m^{-2} s^{-1}) divided by the incident PPFD (µmol m^{-2} s^{-1}) and expressed as µmol CO_2 $µmol^{-1}$ PPFD. The transpiration mass flow density was measured with the same experimental setup using the BERMONIS system and expressed as mg m^{-2} s^{-1}.

Leaf temperatures were measured under both light treatments with thermoelements during five consecutive weeks (starting point 16 weeks after sowing), where mean values were calculated per week. Five thermoelements were fixed on the first fully developed leaf of five different plants.

Optical Readings

A portable, hand-held spectrophotometer (Pigment Analyzer PA-1101/801, Control in Applied Physiology GbR, Falkensee, Germany) equipped with photodiode arrays and a NIR spectrometer (MMS1 NIR enh., Carl Zeiss, Germany) were used to measure the reflectance spectra of tomato leaves in the visible and near infrared range between 402 and 1048 nm with a spectral resolution of 3.3 nm. An integrated light cup equipped with LEDs, capturing the entire recorded wavelength range, served as the light source. Spectralon (20% certified, Labsphere Ltd., North Sutton, NH, United States) was used as the white reference to calibrate this device. During three consecutive weeks (starting point 16 weeks after sowing), five measurements were taken from the first fully developed leaf of every plant in the plot, and the average reflectance indices were used for the estimation of the normalized difference vegetation index (NDVI). The NDVI was calculated as NDVI = $(I_{NIR}\text{-}I_{Red})/(I_{NIR} + I_{Red})$; we used I_{750} for I_{NIR} and I_{680} for I_{Red} as described by Richardson et al. (2002). At the same measuring dates as mentioned in NDVI measurements, nine randomly selected leaflets per light treatment group were used to measure the electron-transport rate (ETR). This was measured non-destructively using a pulse-amplitude modulated device (IMAGING MAXI-PAM, M-series, Heinz Walz GmbH, Eltrich, Germany) on dark adapted leaflets (20 min). Among others, this method was used to study the photosynthetic performance of plants. Based on these data, conclusions on plant health or stress factors can be drawn (Baker, 2008). The ETR was calculated as follows: ETR = Y (II) x PPFD x 0.84 × 0.5. In this context, Y (II) is defined as quantum efficiency of photosystem two (PS II). The factor 0.84 derives from the assumption that 84% of the incident PPFD is absorbed by the leaves. The factor 0.5 indicates the average energy distribution between PS I and PS II (Stemke and Santiago, 2011).

Chemical Analysis

To measure the carotenoid concentrations of tomatoes, 15 tomatoes (>70 g) were harvested randomly from different plants in each plot at ripening stage 9. This sampling was repeated three times in three consecutive weeks, starting 22 weeks after sowing. The harvested tomatoes were homogenized with a blender (Kenwood HB856, De'Longhi Deutschland GmbH, Neu-Isenburg, Germany). Lycopene, ß-carotene, and lutein were extracted using the method of Fish et al. (2002). Afterward, the extracts were measured spectrophotometrically in transmission geometry in the range from 350 to 850 nm in a resolution of 1 nm (Lambda 950; Perkin-Elmer, United States). These data were used to calculate the lycopene, ß-carotene, and lutein concentrations using iterative multiple linear regressions (iMLRs), a method developed by Pflanz and Zude (2008).

Data Analysis

All data represent mean values and standard deviations. The normal distribution of the data was tested using the Kolmogorov–Smirnov test. These tests were followed by student's *t*-tests to calculate significant differences at a significant level of $p \leq 0.05$. Standard deviations are illustrated by ± in tables and bars in figures. Significant differences are displayed with different small letters. All statistical tests were calculated using SPSS, package version 26.0.

RESULTS

Duration of Artificial Light Exposure

Supplementary lighting was provided for 420 h in January, 412 h in February, 371 h in March, and 250 h in April. The ratio of daylight to supplementary lighting exposure changed as follows: 1:3 in January, 1:4 in February, 1:2 in March, and 1:1 in April.

Plant Growth and Yield

Plants grown under LED lighting became significantly taller compared to those grown under HPS lighting eight weeks after sowing (**Table 1**). The difference in plant height was 6.5 cm two weeks after the beginning of the experiment and 11 cm by the end. The internodes of plants grown under LEDs were on average 1 cm longer, but the stems were equally thick (**Table 1**).

There was no significant difference in the number of leaves and leaf area per plant, except for a short period at the beginning of growth in weeks 8 and 9 after sowing, when the leaf area of plants exposed to LED light was smaller. Despite having the same number of trusses as plants grown under HPS, marketable yield of plants grown under LED lighting was significantly higher (by 257.8 gram per plant) compared to that caused by HPS lighting. Non-marketable fruits were not found for both light treatments. The average fruit weight was also higher under LED lighting (**Table 1**).

Effects on Leaf Temperature, LUE, Transpiration Mass Flow Density, ETR, and NDVI

As plants grew toward the supplementary lighting, leaf temperatures increased from 19.9°C to 21.7°C under LED lighting and from 20.7°C to 23.2°C under HPS lighting (**Table 2**). The leaf temperature of plants exposed to LED light was always significantly lower, 0.8°C at the beginning and 1.5°C at the end of measurements (**Table 2**).

Figure 2 shows the average LUE of the supplementary lighting without daylight during a period of 3 weeks. Although the PPFD was identical from both lighting systems, the LED fixture significantly increased the light use efficiency of the plants by 20% compared to those that grew under the HPS lighting. In contrast, the transpiration mass flow density of the tomato plants under LED exposure (20.15 mg m^2 s^{-1}) was lower than that of the tomato plants under HPS exposure (28.03 mg m^2 s^{-1}). A significantly higher transpiration mass flow density (by 39%) caused by HPS lighting was calculated (**Figure 2**).

Neither LEDs nor HPS lighting led to a significant change in the values regarding the calculated electron transport rate and NDVI. The values of both parameters were almost identical and were 0.9 and 21.0, respectively (**Figure 3**).

TABLE 1 | Effects of different supplementary lightings on plant development and yield of tomato plants.

			Weeks after sowing					
Plant parameter	**Unit**	**Light treatment**	**6**	**7**	**8**	**9**	**10**	**11**
Plant height	cm	LEDs	24.1 ± 1.9a	51.0 ± 4.1a	82.1 ± 5.3b	112.4 ± 9.1b	143.4 ± 10.9b	172.1 ± 9.2b
		HPS	24.2 ± 1.6a	48.5 ± 4.1a	75.6 ± 5.8a	104.5 ± 8.5a	131.9 ± 7.9a	161.1 ± 6.3a
Internode distance	cm	LEDs	3.5 ± 0.3a	7.3 ± 0.7b	8.7 ± 0.7b	9.4 ± 0.9b	9.5 ± 0.8b	9.8 ± 0.6b
		HPS	3.2 ± 0.4a	6.2 ± 0.7a	7.7 ± 0.6a	8.4 ± 0.7a	8.5 ± 0.3a	8.7 ± 0.4a
Stem diameter	cm	LEDs	6.3 ± 0.4a	7.4 ± 0.3a	7.8 ± 0.5a	8.5 ± 0.4a	8.9 ± 0.6a	9.5 ± 0.5a
		HPS	6.2 ± 0.5a	7.2 ± 0.2a	7.7 ± 0.3a	8.4 ± 0.5a	8.9 ± 0.3a	9.3 ± 0.6a
Trusses	number plant^{-1}	LEDs	0.0 ± 0.0a	0.0 ± 0.0a	0.0 ± 0.0a	1.0 ± 0.0a	2.0 ± 0.0a	3.1 ± 0.3a
		HPS	0.0 ± 0.0a	0.0 ± 0.0a	0.0 ± 0.0a	1.0 ± 0.0a	2.0 ± 0.0a	3.1 ± 0.3a
Leaves	number plant^{-1}	LEDs	3.8 ± 0.4a	5.1 ± 0.3a	7.6 ± 0.5a	9.9 ± 0.6a	13.4 ± 0.5a	15.4 ± 0.9a
		HPS	3.8 ± 0.3a	5.1 ± 0.3a	7.8 ± 0.4a	10.2 ± 0.4a	13.6 ± 0.5a	16.0 ± 0.5a
Leafarea	cm^2 plant^{-1}	LEDs	489.3 ± 60.9a	965.1 ± 99.9a	1713.0 ± 132.7a	2872.0 ± 186.0a	4946.0 ± 351.3a	6674.9 ± 431.5a
		HPS	509.6 ± 52.1a	975.1 ± 90.6a	1863.4 ± 124.5b	3243.6 ± 228.4b	5346.8 ± 482.9a	7196.3 ± 589.2a
			End of the experiments					
Yield	g plant^{-1}	LEDs	2102.1 ± 159.0b					
		HPS	1844.3 ± 91.8a					
Fruit weight	g fruit^{-1}	LEDs	96.7 ± 5.2a					
		HPS	92.4 ± 5.4a					

Values represent means of three plots per light treatment (n = 3) ± standard deviation. Values followed by the same letter do not differ significantly according to student's t-tests ($p < 0.05$).

Effects on Carotenoids

There were significant differences in the carotenoid concentrations between the light treatments. The lycopene concentration of tomatoes grown under LED lighting was 18% higher (910.3 versus 773.8 μg lycopene g^{-1} DW) and the lutein concentration was more than two times higher (24.7 versus 10.2 μg lutein g^{-1} DW) (**Table 3**). The ß-carotene concentrations of tomatoes, on the other hand, were similar (44.4 versus 46.2 μg g^{-1} DW).

DISCUSSION

Plant Growth and Yield Under Different Supplementary Lightings

In this article, we provide evidence that LED lighting with an emission spectrum that partially matches the range of 400 to 700 nm can accelerate plant growth and increase the yield of tomatoes. Similar results in terms of the stem development were demonstrated for cucumbers, sweet basil, and tomatoes when a combination of blue, green, and red LEDs (Särkkä et al., 2017); blue, yellow, and red LEDs (Carvalho et al., 2016); or only green LEDs combined with daylight (Snowden et al., 2016) was used, respectively. Our yield data, however, are different to others, who have reported that a LED lighting with an emission spectrum that is optimized for chlorophyll absorption (blue and red) produces similar or even less yield than HPS lighting (Dueck et al., 2011; Gomez et al., 2013; Fanwoua et al., 2019). Although

TABLE 2 | Leaf temperature (°C) under LED and HPS lighting.

	Weeks after sowing				
Light treatment	**16**	**17**	**18**	**19**	**20**
LEDs	19.9 ± 0.1	20.8 ± 0.2	21.2 ± 0.1	21.3 ± 0.2	21.7 ± 0.3
HPS	20.7 ± 0.1	21.8 ± 0.5	22.2 ± 0.2	22.5 ± 0.5	23.2 ± 0.8

Data represent mean values of five repetitions in five consecutive weeks (n = 5). Differences in leaf temperature were evaluated using student's t-tests. Different small letters illustrate significant differences ($p < 0.05$).

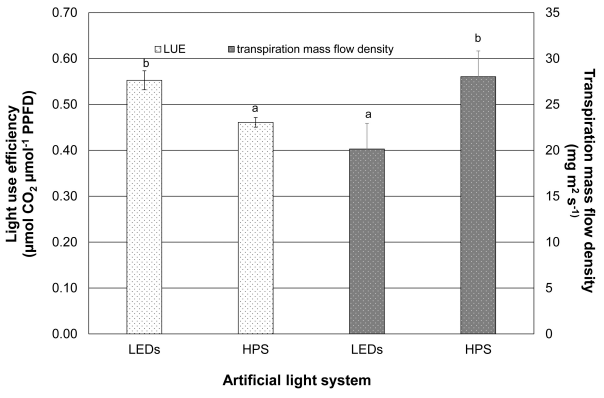

FIGURE 2 | Light use efficiency and transpiration mass flow density caused by LEDs and HPS lighting. Data represent mean values of three repetitions ($n = 3$). Light use efficiency and transpiration mass flow density were tested using student's *t*-tests. Different small letters indicate significant differences ($p < 0.05$).

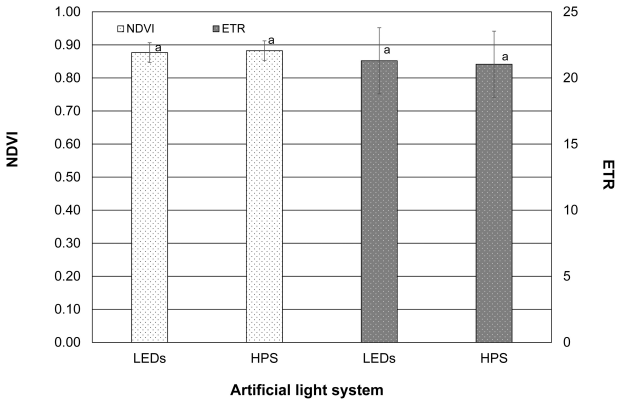

FIGURE 3 | Normalized difference vegetation index (NDVI) and electron transport rate (ETR) of tomato leaves exposed to LEDs and HPS lighting. Data represent mean values of three repetitions in three consecutive weeks ($n = 3$). NDVI and ETR were tested using student's *t*-tests. Different small letters illustrate significant differences ($p < 0.05$).

TABLE 3 | Influence of LEDs and HPS supplementary lighting on carotenoid concentration in tomatoes.

	Carotenoid concentration in tomatoes (μg g^{-1} DW)		
Light treatment	**Lycopene**	**ß-carotene**	**Lutein**
LEDs	910.3 ± 53.3b	44.4 ± 3.0a	24.7 ± 3.3b
HPS	773.8 ± 45.1a	46.2 ± 3.5a	10.2 ± 3.0a

Values represent means of three repetitions per light treatment in three consecutive weeks (n = 3) ± standard deviation. Values followed by the same letter do not differ significantly according to student's t-tests (p < 0.05).

the cultivation conditions in these studies differ substantially from ours (most used interlight, different cultivar), our data suggest that a full spectrum offers advantages over a simple red and blue emission spectrum in tomato plants. Evidence that more complex spectra can increase tomato yield was also provided by Kim et al. (2019), who showed that adding far-red to red and blue increases yield. Kim et al. (2019) attributed the effect of far-red light to an increase in photosynthesis, an effect that is well known in the literature as Emerson effect (Emerson, 1957). An over-proportional increase in photosynthesis due to changes in the spectrum, like for instance the addition of far-red to red light, results in an increase in light use efficiency. In our study, we found that the light use efficiency under a continuous PAR spectrum LED lighting was higher than under HPS lighting, indicating that the additional wavelengths are not only absorbed but actively used for photosynthesis. This conclusion is in agreement with Yang et al. (2016), who found that the addition of yellow light to blue and red light can greatly enhance the LUE of purple cabbage. The LUE can be affected by plant stress. For instance, water deficiency, photoinhibition, or low light quality can reduce photosynthesis despite a sufficiently high PPFD. An indicator for plant stress is ETR. ETR is reduced when plants suffer from water stress (Ögren and Öquist, 1985) or exposure to monochromatic light (Wang et al., 2009; Xiaoying et al., 2012). More complex spectra have higher ETR (Xiaoying et al., 2012). Another indicator is NDVI. NDVI increases when the chlorophyll concentration in a canopy increases (Yoder and Waring, 1994; Gitelson et al., 2003). Therefore, NDVI can be used to monitor vitality, especially senescence of leaves. In this study, we did not find differences in NDVI or ETR. Therefore, we can exclude that the plants were stressed. These data support our conclusion that the LUE is higher under the LED lighting because the wavelengths are effectively used for photosynthesis. In summary, the data presented here show that the absorption of the additional wavelengths of the continuous PAR spectrum LED leads to higher photosynthesis and consequently longer plants and higher fruit yield.

Photosynthesis is more than photon absorption. For instance, gas exchange at the stomata and RuBisCo activity are of vital importance to photosynthesis. The latter increases with higher leaf temperatures. HPS lighting emits ample infra-red radiation, which is not captured by the photosystem but increases leaf temperature instead (Nelson and Bugbee, 2015). Infra-red radiation can have a substantial effect on photosynthesis and yield (Hernández and Kubota, 2015; Bergstrand et al., 2016). In our experiment, we measured the expected 1.5°C higher leaf temperature under HPS, and as a consequence, a higher transpiration rate was also found in other studies (Dueck et al., 2011; Gajc-Wolska et al., 2013; Kim et al., 2019). Sage and Sharkey (1987) had shown that the rate of carbon dioxide uptake (e.g., photosynthesis) increased with increasing temperatures, until it reaches a critical point, after which it rapidly decreases. The critical point of tomatoes is between 25°C and 27°C. In our study, the leaf temperature under HPS lighting was higher than under LEDs, but lower than 25°C. One, therefore, can expect that the activity of the photosystem, the Calvin cycle activity, and the gas exchange are higher under HPS. However, it appears that the temperature advantage is not sufficient to compensate for the effects of the LED spectrum.

Since there is no evidence that the LED spectrum promoted photosynthesis downstream of the photosystem, via control of stomata opening for instance, it is most likely that the additional wavelengths are effectively used for nicotinamide adenine dinucleotide phosphate reduction.

High photosynthesis is a prerequisite but not a guarantee for high yield. There is sometimes surprisingly little correlation between photosynthesis measured at a single leaf and total plant biomass or fruit yield. Therefore, horticulturists prefer to use the leaf area index to model and predict plant growth (Heuvelink et al., 2004). The leaf area depends on a variety of parameters, of which light spectral quality is one. Red light tends to increase leaf area, while blue light tends to decrease it (Bantis et al., 2018). These effects are not mediated by photosynthesis, but by photoreceptors (Kami et al., 2010). However, in our study there was no difference in leaf area despite a significant difference in tomato yield. Therefore, these data indicate that the effect of the spectrum is not mediated by alternative pathways (e.g., photoreceptors) but via the photosystem.

We know from other studies that effects of the spectra on photosynthesis can vary between species and even between

varieties (Ouzounis et al., 2016). It is at the moment not clear how this diversity will be handled in the future. Perhaps, one way is to find common responses on a physiological or molecular level that allow the prediction of plant responses.

Effects on Carotenoids of Tomatoes

Generally, the concentrations of carotenoids in tomatoes were consistent with those reported in literature (Frusciante et al., 2007). The biosynthesis of lycopene and lutein was affected by the different light treatments. The lycopene and lutein concentrations of tomatoes grown under LED lighting were 18 and 142%, respectively, higher than that grown under HPS lighting (**Table 3**). The increase in lycopene of tomatoes caused by a combination of blue and red LEDs was also demonstrated by Ngcobo et al. (2020). They also found that these LEDs caused a higher concentration of ß-carotene than a combination of yellow and blue or red LEDs, while the ß-carotene concentration in the present study did not change when illuminated with LEDs or HPS lighting. The regulation of carotenoid biosynthesis in ripening tomato fruits has been extensively studied (Bramley, 2002). In green tissue, lycopene is further converted to ß-carotene by lycopene cyclases. Therefore, ß-carotene and lutein levels increase during the first days of fruits ripening, long before lycopene appears (Ntagkas et al., 2020). However, during the later stage of tomato fruit ripening, the mRNA of the lycopene ß- and ε-cyclase enzymes are downregulated (Pecker et al., 1996; Ronen et al., 1999). As a consequence, lycopene accumulates, while the ß-carotene level starts decreasing. In contrast to the intermediate product ß-carotene, lutein levels stay constant after the metabolism is shifted to lycopene production. One, therefore, can assume that the differences in lutein content manifest before the fruits ripen, while differences in ß-carotene levels are a combination of early formation and later conversion. Aherne et al. (2009), furthermore, showed that the geographical origin has a strong influence on the ß-carotene concentration and that this influence is higher than that of the variety. This study indicates that cultivation and environmental conditions, such as light intensity, light spectrum, and fruit temperature, affect the regulation of the ß-carotene biosynthesis pathway in tomatoes.

In a previous article, we have shown that tomatoes grown in optimized climate conditions increase photosynthesis and ß-carotene concentration in fruit (Dannehl et al., 2014). These data indicate that photosynthesis provides the molecular precursors for the biosynthesis of ß-carotene in fruit and subsequently lutein and lycopene. It is therefore reasonable to assume that the increase of lycopene and lutein concentrations in this study is driven by a higher LUE caused by the continuous PAR spectrum LED-fixture. Beside photosynthesis, there is ample evidence that lycopene biosynthesis in tomatoes is also regulated by photoreceptors. Alba et al. (2000) reported that red light promotes and far-red light reduces lycopene biosynthesis and that this effect is mediated by photochromes. Xie et al. (2019) have analyzed tomatoes exposed to blue and red LEDs on a gene expression level using qRT-PCR. They found out that blue and red light increased the lycopene concentration in tomatoes by inducing light receptors that modulate phytochrome-interacting factors and ELONGATED HYPOCOTYL 5 activations to mediate phytoene synthase 1 (*PSY*). *PSY* is the main enzyme in the carotenoid pathway (Bramley, 2002). Furthermore, they found that blue light showed a much stronger effect than red light. Li and Kubota (2009) and Ouzounis et al. (2015) also showed that the concentration of carotenoids in green lettuce increased when blue light was supplemented. Ntagkas et al. (2020), on the other hand, showed that the spectrum has no effect on the lutein concentration. Blue light appears to promote the lutein content more than red light for instance. However, the data are insufficient to explain the increase in lutein in our experiment. It is therefore possible that the higher proportion of blue light, and perhaps a lower percentage of far-red light, emitted by our LED fixture had an additional effect on the lycopene and lutein concentrations, but we think that the main effect is an increase in LUE. As to why the ß-carotene concentration is constant while the other carotenes increase, our data do not provide a simple explanation. Ntagkas et al. (2020) showed that zeaxanthin, the product of ß-carotene conversion, increases in tomato fruits under blue and white light. These data indicate that ß-carotene is further converted under white light. Therefore, it is likely that the initially higher ß-carotene levels under white light were later converted to zeaxanthin. At a later stage of fruit development zeaxanthin levels in tomato fruits also drop rapidly, indicating that either the conversion is inhibited or the degradation accelerated. These findings may indicate that ß-carotene levels reach a steady-state toward the end of fruit ripening. However, at the moment, there are no data supporting this hypothesis.

Beside light, it is also known that an increase in mean ambient temperature from 18°C to 22°C favors the accumulation of carotenoids in tomatoes (Krumbein et al., 2006). Since the leaf temperature was increased under the influence of HPS lighting, it can be assumed that the fruit temperature was also increased. However, Krumbein's study also shows that a temperature increase of 2°C has no effect. Since we only measured a maximum temperature increase of 1.5°C regarding the leaf temperature, the temperature influence on the carotenoid accumulation can be neglected.

CONCLUSION

In this article, we show that LED with an emission spectrum that partially matches the PAR range is more effective than HPS supplementary lighting. Based on our results, it can be concluded that our LED fixture positively affected plant growth and LUE, increasing the yield and concentrations of lycopene and lutein. In comparison to HPS lighting, the LED spectrum reduced the transpiration mass flow density, while keeping the electron transport rate and the normalized difference vegetation index at the same level.

In recent years, white LEDs have become more and more efficient, so that more manufacturers have begun to incorporate them into their fixtures. Our data clearly show that from a horticultural point of view, the use of continuous PAR spectrum

LEDs can be considered as a useful tool, as not only the yield but also the carotenoid concentration in tomatoes can be improved.

DATA AVAILABILITY STATEMENT

The original contributions presented in the study are included in the article/supplementary material, further inquiries can be directed to the corresponding author/s.

AUTHOR CONTRIBUTIONS

DD brought up the idea, contributed to the study conception and design, acquisition, statistical analysis, and interpretation of data, and writing of the manuscript, and discussed with the reviewers and editors to modify the manuscript. TS made recommendations and suggestions and discussed with the reviewers and editor to modify the manuscript. DV manufactured the full spectrum LED fixture. US made recommendations and modified the manuscript. All authors contributed to the article and approved the submitted version.

FUNDING

This research was funded by the Federal Ministry of Education and Research/PtJ Project Management Agency in the frame of Agricultural Systems of the Future (CUBES Circle).

ACKNOWLEDGMENTS

We acknowledge the support by the German Research Foundation (DFG) and the Open Access Publication Fund of Humboldt-Universität zu Berlin. We would also like to thank the gardeners of the Humboldt-Universität zu Berlin for their plant care and Wofgang Pfeifer, our technician, who supported us with his many years of experience.

REFERENCES

Aherne, S. A., Jiwan, M. A., Daly, T., and O'brien, N. M. (2009). Geographical location has greater impact on carotenoid content and bioaccessibility from tomatoes than variety. *Plant Foods Hum. Nutr.* 64, 250–256. doi: 10.1007/s11130-009-0136-x

Alba, R., Cordonnier-Pratt, M.-M., and Pratt, L. H. (2000). Fruit-localized phytochromes regulate lycopene accumulation independently of ethylene production in tomato. *Plant Physiol.* 123, 363–370. doi: 10.1104/pp.123.1.363

Baker, N. R. (2008). Chlorophyll fluorescence: a probe of photosynthesis in vivo. *Annu. Rev. Plant Biol.* 59, 89–113. doi: 10.1146/annurev.arplant.59.032607.092759

Bantis, F., Smirnakou, S., Ouzounis, T., Koukounaras, A., Ntagkas, N., and Radoglou, K. (2018). Current status and recent achievements in the field of horticulture with the use of light-emitting diodes (LEDs). *Scientia Horticulturae* 235, 437–451. doi: 10.1016/j.scienta.2018.02.058

Bergstrand, K. J., Mortensen, L. M., Suthaparan, A., and Gislerød, H. R. (2016). Acclimatisation of greenhouse crops to differing light quality. *Scientia Horticulturae* 204, 1–7. doi: 10.1016/j.scienta.2016.03.035

Bramley, P. M. (2002). Regulation of carotenoid formation during tomato fruit ripening and development. *J. Exp. Bot.* 53, 2107–2113. doi: 10.1093/jxb/erf059

Carvalho, S. D., Schwieterman, M. L., Abrahan, C. E., Colquhoun, T. A., and Folta, K. M. (2016). Light quality dependent changes in morphology, antioxidant capacity, and volatile production in sweet basil (*Ocimum basilicum*). *Front. Plant Sci.* 7:1328.

Dannehl, D., Josuttis, M., Huyskens-Keil, S., Ulrichs, C., and Schmidt, U. (2014). Comparison of different greenhouse systems and their impacts on plant responses of tomatoes. *Gesunde Pflanzen* 66, 111–119. doi: 10.1007/s10343-014-0322-0

Dannehl, D., Rocksch, T., and Schmidt, U. (2015). Modelling to estimate the specific leaf area of tomato leaves ('Pannovy'). *Acta Horticulturae* 1099, 79–86. doi: 10.17660/actahortic.2015.1099.5

Deram, P., Lefsrud, M. G., and Orsat, V. (2014). Supplemental lighting orientation and red-to-blue ratio of light-emitting diodes for greenhouse tomato production. *HortScience* 49, 448–452. doi: 10.21273/hortsci.49.4.448

Dueck, T. A., Janse, J., Eveleens, B. A., Kempkes, F. L. K., and Marcelis, L. F. M. (2011). Growth of tomatoes under hybrid LED and HPS lighting. *Acta Horticulturae* 952, 335–342. doi: 10.17660/actahortic.2012.952.42

Emerson, R. (1957). Dependence of yield of photosynthesis in long-wave red on wavelength and intensity of supplementary light. *Science* 125, 746–746.

Fanwoua, J., Vercambre, G., Buck-Sorlin, G. H., Dieleman, J. A., de Visser, P., and Génard, M. (2019). Supplemental LED lighting affects the dynamics of tomato fruit growth and composition. *Scientia Horticulturae* 256:108571. doi: 10.1016/j.scienta.2019.108571

Fish, W., Perkins-Veazie, P., and Collins, J. K. (2002). A quantitative assay for lycopene that utilizes reduced volumes of organic solvents. *J. Food Compost. Anal.* 15, 309–317. doi: 10.1006/jfca.2002.1069

Frank, H. A., and Cogdell, R. J. (1993). "The photochemistry and function of carotenoids in photosynthesis," in *Carotenoids in Photosynthesis*, eds A. J. Young and G. Britton (London: Springer), 252–326. doi: 10.1007/978-94-011-2124-8_8

Frusciante, L., Carli, P., Ercolano, M. R., Pernice, R., Di Matteo, A., Fogliano, V., et al. (2007). Antioxidant nutritional quality of tomato. *Mol. Nutr. Food Res.* 51, 609–617. doi: 10.1002/mnfr.200600158

Gajc-Wolska, J., Kowalczyk, K., Metera, A., Mazur, K., Bujalski, D., and Hemka, L. (2013). Effect of supplementary lighting on selected physiological parameters and yielding of tomato plants. *Folia Horticulturae* 25, 153–159. doi: 10.2478/fhort-2013-0017

Gilli, C., Camps, C., and Fleury, Y. (2018). Supplemental lighting in tomato crop on substrate in Swiss conditions. *Acta horticulturae* 1271, 93–100. doi: 10.17660/actahortic.2020.1271.13

Gitelson, A. A., Gritz, Y., and Merzlyak, M. N. (2003). Relationships between leaf chlorophyll content and spectral reflectance and algorithms for non-destructive chlorophyll assessment in higher plant leaves. *J. Plant Physiol.* 160, 271–282. doi: 10.1078/0176-1617-00887

Göhler, F., and Molitor, H.-D. (2002). *Erdelose Kulturverfahren im Gartenbau*. Stuttgart: Eugen Ulmer.

Gómez, C., and Mitchell, C. A. (2015). Growth responses of tomato seedlings to different spectra of supplemental lighting. *HortScience* 50, 112–118. doi: 10.21273/hortsci.50.1.112

Gomez, C., Morrow, R. C., Bourget, C. M., Massa, G. D., and Mitchell, C. A. (2013). Comparison of intracanopy light-emitting diode towers and overhead high-pressure sodium lamps for supplemental lighting of greenhouse-grown tomatoes. *HortTechnology* 23, 93–98. doi: 10.21273/horttech.23.1.93

Hao, X. M., Guo, X., Zheng, J., Celeste, L., Kholsa, S., and Chen, X. (2015). Response of greenhouse tomato to different vertical spectra of LED lighting under overhead high pressure sodium and plasma lighting. *Acta Horticulturae* 1170, 1003–1110. doi: 10.17660/actahortic.2017.1170.129

Hashimoto, H., Uragami, C., and Cogdell, R. J. (2016). Carotenoids and photosynthesis. *Carotenoids Nat.* 79, 111–139.

Hernández, R., and Kubota, C. (2015). Physiological, morphological, and energy-use efficiency comparisons of LED and HPS supplemental lighting for cucumber transplant production. *HortScience* 50, 351–357. doi: 10.21273/hortsci.50.3.351

Heuvelink, E., Bakker, M. J., Elings, A., Kaarsemaker, R. C., and Marcelis, L. F. M. (2004). Effect of leaf area on tomato yield. *Acta Horticulturae* 691, 43–50. doi: 10.17660/actahortic.2005.691.2

Hogewoning, S. W., Trouwborst, G., Meinen, E., and van Ieperen, W. (2012). Finding the optimal growth-light spectrum for greenhouse crops. *Acta Horticulturae* 956, 357–363. doi: 10.17660/actahortic.2012.956.41

Jacob, K., Periago, M. J., Bohm, V., and Berruezo, G. R. (2008). Influence of lycopene and vitamin C from tomato juice on biomarkers of oxidative stress and inflammation. *Br. J. Nutr.* 99, 137–146. doi: 10.1017/s0007114507791894

Jou, J.-H., Lin, C.-C., Li, T.-H., Li, C.-J., Peng, S.-H., Yang, F.-C., et al. (2015). Plant growth absorption spectrum mimicking light sources. *Materials* 8, 5265–5275. doi: 10.3390/ma8085240

Kami, C., Lorrain, S., Hornitschek, P., and Fankhauser, C. (2010). "Light-regulated plant growth and development," in *Current Topics in Developmental Biology*, ed. G. Schatten (Amsterdam: Elsevier), 29–66. doi: 10.1016/s0070-2153(10)91002-8

Kim, H. J., Lin, M. Y., and Mitchell, C. A. (2019). Light spectral and thermal properties govern biomass allocation in tomato through morphological and physiological changes. *Environ. Exp. Bot.* 157, 228–240. doi: 10.1016/j.envexpbot.2018.10.019

Kotake-Nara, E., Kushiro, M., Zhang, H., Sugawara, T., Miyashita, K., and Nagao, A. (2001). Carotenoids affect proliferation of human prostate cancer cells. *J. Nutr.* 131, 3303–3306. doi: 10.1093/jn/131.12.3303

Krumbein, A., Schwarz, D., and Kläring, H. P. (2006). Effects of environmental factors on carotenoid content in tomato (*Lycopersicon esculentum* (L.) mill.) grown in a greenhouse. *J. Appl. Bot. Food Q. Angewandte Botanik* 80, 160–164.

Lanoue, J., Zheng, J., Little, C., Thibodeau, A., Grodzinski, B., and Hao, X. (2019). Alternating red and blue light-emitting diodes allows for injury-free tomato production with continuous lighting. *Front. Plant Sci.* 10:1114.

Li, Q., and Kubota, C. (2009). Effects of supplemental light quality on growth and phytochemicals of baby leaf lettuce. *Environ. Exp. Bot.* 67, 59–64. doi: 10.1016/j.envexpbot.2009.06.011

Lichtenthaler, H. K., and Wellburn, A. R. (1983). Determinations of total carotenoids and chlorophylls a and b of leaf extracts in different solvents. *Biochem. Soc. Trans.* 11, 591–592. doi: 10.1042/bst0110591

McCree, K. J. (1971). The action spectrum, absorptance and quantum yield of photosynthesis in crop plants. *Agric. Meteorol.* 9, 191–216. doi: 10.1016/0002-1571(71)90022-7

Moe, R., Grimstad, S. O., and Gislerod, H. R. (2005). The use of artificial light in year round production of greenhouse crops in Norway. *Acta Horticulturae* 711, 35–42. doi: 10.17660/actahortic.2006.711.2

Nelson, J. A., and Bugbee, B. (2015). Analysis of environmental effects on leaf temperature under sunlight, high pressure sodium and light emitting diodes. *PLoS One* 10:e0138930. doi: 10.1371/journal.pone.0138930

Ng, F.-L., Phang, S.-M., Lan, B. L., Kalavally, V., Thong, C.-H., Chong, K.-T., et al. (2020). Optimised spectral effects of programmable LED arrays (PLA) s on bioelectricity generation from algal-biophotovoltaic devices. *Sci. Rep.* 10:16105.

Ngcobo, B. L., Bertling, I., and Clulow, A. D. (2020). Preharvest illumination of cherry tomato reduces ripening period, enhances fruit carotenoid concentration and overall fruit quality. *J. Hortic. Sci. Biotechnol.* 95, 617–627. doi: 10.1080/14620316.2020.1743771

Ntagkas, N., de Vos, R. C., Woltering, E. J., Nicole, C., Labrie, C., and Marcelis, L. F. (2020). Modulation of the tomato fruit metabolome by LED light. *Metabolites* 10:266. doi: 10.3390/metabo10060266

Ögren, E., and Öquist, G. (1985). Effects of drought on photosynthesis, chlorophyll fluorescence and photoinhibition susceptibility in intact willow leaves. *Planta* 166, 380–388. doi: 10.1007/bf00401176

Ouzounis, T., Giday, H., Kjær, K. H., and Ottosen, C. O. (2018). LED or HPS in ornamentals? a case study in roses and campanulas. *Eur. J. Hortic. Sci.* 83, 166–172. doi: 10.17660/ejhs.2018/83.3.6

Ouzounis, T., Heuvelink, E., Ji, Y., Schouten, H. J., Visser, R. G. F., and Marcelis, L. F. M. (2016). Blue and red LED lighting effects on plant biomass, stomatal conductance, and metabolite content in nine tomato genotypes. *Acta Horticulturae* 1134, 251–258. doi: 10.17660/actahortic.2016.1134.34

Ouzounis, T., Razi Parjikolaei, B., Fretté, X., Rosenqvist, E., and Ottosen, C.-O. (2015). Predawn and high intensity application of supplemental blue light decreases the quantum yield of PSII and enhances the amount of phenolic acids, flavonoids, and pigments in *Lactuca sativa*. *Front. Plant Sci.* 6:19. doi: 10.18052/www.scipress.com/ilns.68.19

Paponov, M., Kechasov, D., Lacek, J., Verheul, M. J., and Paponov, I. A. (2019). Supplemental LED inter-lighting increases tomato fruit growth through enhanced photosynthetic light use efficiency and modulated root activity. *Front. Plant Sci.* 10:1656.

Pecker, I., Gabbay, R., Cunningham, F. X., and Hirschberg, J. (1996). Cloning and characterization of the cDNA for lycopene β-cyclase from tomato reveals decrease in its expression during fruit ripening. *Plant Mol. Biol.* 30, 807–819. doi: 10.1007/bf00019013

Pflanz, M., and Zude, M. (2008). Spectrophotometric analyses of chlorophyll and single carotenoids during fruit development of tomato (*Solanum lycopersicum* L.) by means of iterative multiple linear regression analysis. *Appl. Optics* 47, 5961–5970. doi: 10.1364/ao.47.005961

Richardson, A. D., Duigan, S. P., and Berlyn, G. P. (2002). An evaluation of noninvasive methods to estimate foliar chlorophyll content. *New Phytol.* 153, 185–194. doi: 10.1046/j.0028-646X.2001.00289.x

Ronen, G., Cohen, M., Zamir, D., and Hirschberg, J. (1999). Regulation of carotenoid biosynthesis during tomato fruit development: expression of the gene for lycopene epsilon-cyclase is down-regulated during ripening and is elevated in the mutant Delta. *Plant J.* 17, 341–351. doi: 10.1046/j.1365-313x.1999.00381.x

Sage, R. F., and Sharkey, T. D. (1987). The effect of temperature on the occurrence of O2 and CO2 insensitive photosynthesis in field grown plants. *Plant Physiol.* 84, 658–664. doi: 10.1104/pp.84.3.658

Särkkä, L. E., Jokinen, K., Ottosen, C. O., and Kaukoranta, T. (2017). Effects of HPS and LED lighting on cucumber leaf photosynthesis, light quality penetration and temperature in the canopy, plant morphology and yield. *Agric. Food Sci.* 26, 102–110.

Snowden, M. C., Cope, K. R., and Bugbee, B. (2016). Sensitivity of seven diverse species to blue and green light: interactions with photon flux. *PLoS One* 11:e163121.

Stemke, J. A., and Santiago, L. S. (2011). Consequences of light absorptance in calculating electron transport rate of desert and succulent plants. *Photosynthetica* 49, 195–200. doi: 10.1007/s11099-011-0026-y

Terfa, M. T., Solhaug, K. A., Gislerød, H. R., Olsen, J. E., and Torre, S. (2013). A high proportion of blue light increases the photosynthesis capacity and leaf formation rate of Rosa×hybrida but does not affect time to flower opening. *Physiol. Plant.* 148, 146–159. doi: 10.1111/j.1399-3054.2012.01698.x

Tewolde, F. T., Lu, N., Shiina, K., Maruo, T., Takagaki, M., Kozai, T., et al. (2016). Nighttime supplemental LED inter-lighting improves growth and yield of single-truss tomatoes by enhancing photosynthesis in both winter and summer. *Front. Plant Sci.* 7:448.

Wang, H., Gu, M., Cui, J., Shi, K., Zhou, Y., and Yu, J. (2009). Effects of light quality on CO2 assimilation, chlorophyll-fluorescence quenching, expression of Calvin cycle genes and carbohydrate accumulation in *Cucumis sativus*. *J. Photochem. Photobiol. B Biol.* 96, 30–370. doi: 10.1016/j.jphotobiol.2009.03.010

Xiaoying, L., Shirong, G., Taotao, C., Zhigang, X., and Tezuka, T. (2012). Regulation of the growth and photosynthesis of cherry tomato seedlings by different light irradiations of light emitting diodes (LED). *Afr. J. Biotechnol.* 11, 6169–6177.

Xie, B. Y., Wei, J. J., Zhang, Y. T., Song, S. W., Wei, S. U., Sun, G. W., et al. (2019). Supplemental blue and red light promote lycopene synthesis in tomato fruits. *J. Integr. Agric.* 18, 590–598. doi: 10.1016/s2095-3119(18)62062-3

Yang, B., Zhou, X., Xu, R. A., Wang, J., Lin, Y., Pang, J., et al. (2016). Comprehensive analysis of photosynthetic characteristics and quality improvement of purple cabbage under different combinations of monochromatic light. *Front. Plant Sci.* 7:1788.

Yoder, B. J., and Waring, R. H. (1994). The normalized difference vegetation index of small douglas-fir canopies with varying chlorophyll concentrations. *Remote Sens. Environ.* 49, 81–91. doi: 10.1016/0034-4257(94)90061-2

Zhang, Y. T., Zhang, Y. Q., Yang, Q., and Tao, L. (2019). Overhead supplemental far-red light stimulates tomato growth under intra-canopy lighting with LEDs. *J. Integr. Agric.* 18, 62–69. doi: 10.1016/s2095-3119(18)62130-6

Conflict of Interest: TS was employed by BLV Licht-und Vakuumtechnik GmbH.

The remaining authors declare that the research was conducted in the absence of any commercial or financial relationships that could be conducted as a potential conflict of interest.

Copyright © 2021 Dannehl, Schwend, Veit and Schmidt. This is an open-access article distributed under the terms of the Creative Commons Attribution License (CC BY). The use, distribution or reproduction in other forums is permitted, provided the original author(s) and the copyright owner(s) are credited and that the original publication in this journal is cited, in accordance with accepted academic practice. No use, distribution or reproduction is permitted which does not comply with these terms.

frontiers in Plant Science

ORIGINAL RESEARCH
published: 26 February 2021
doi: 10.3389/fpls.2021.623314

Narrowband Blue and Red LED Supplements Impact Key Flavor Volatiles in Hydroponically Grown Basil Across Growing Seasons

Hunter A. Hammock, Dean A. Kopsell and Carl E. Sams**

Department of Plant Sciences, The University of Tennessee, Knoxville, Knoxville, TN, United States

The use of light-emitting diodes (LEDs) in commercial greenhouse production is rapidly increasing because of technological advancements, increased spectral control, and improved energy efficiency. Research is needed to determine the value and efficacy of LEDs in comparison to traditional lighting systems. The objective of this study was to establish the impact of narrowband blue (B) and red (R) LED lighting ratios on flavor volatiles in hydroponic basil (*Ocimum basilicum* var. "Genovese") in comparison to a non-supplemented natural light (NL) control and traditional high-pressure sodium (HPS) lighting. "Genovese" basil was chosen because of its high market value and demand among professional chefs. Emphasis was placed on investigating concentrations of important flavor volatiles in response to specific ratios of narrowband B/R LED supplemental lighting (SL) and growing season. A total of eight treatments were used: one non-supplemented NL control, one HPS treatment, and six LED treatments (peaked at 447 nm/627 nm, ±20 nm) with progressive B/R ratios (10B/90R, 20B/80R, 30B/70R, 40B/60R, 50B/50R, and 60B/40R). Each SL treatment provided 8.64 mol · m^{-2} · d^{-1} (100 μmol · m^{-2} · s^{-1}, 24 h · d^{-1}). The daily light integral (DLI) of the NL control averaged 9.5 mol · m^{-2} · d^{-1} during the growth period (ranging from 4 to 18 mol · m^{-2} · d^{-1}). Relative humidity averaged 50%, with day/night temperatures averaging 27.4°C/21.8°C, respectively. Basil plants were harvested 45 days after seeding, and volatile organic compound profiles were obtained by gas chromatography–mass spectrometry. Total terpenoid concentrations were dramatically increased during winter months under LED treatments, but still showed significant impacts during seasons with sufficient DLI and spectral quality. Many key flavor volatile concentrations varied significantly among lighting treatments and growing season. However, the concentrations of some compounds, such as methyl eugenol, were three to four times higher in the control and decreased significantly for basil grown under SL treatments. Maximum concentrations for each compound varied among lighting treatments, but most monoterpenes and diterpenes evaluated were highest under 20B/80R to 50B/50R. This study shows that supplemental narrowband light treatments from LED sources may be used to manipulate secondary metabolic resource allocation. The application of narrowband LED SL has great potential for improving overall flavor quality of basil and other high-value specialty herbs.

Keywords: controlled environment, narrowband LEDs, flavor volatiles, *Ocimum basilicum*, secondary metabolism, supplemental lighting

OPEN ACCESS

Edited by:
Inga Mewis,
Humboldt University of Berlin, Germany

Reviewed by:
Aušra Brazaitytė,
Lithuanian Research Centre for Agriculture and Forestry, Lithuania
Akvile Virsile,
Institute of Horticulture, Lithuanian Research Centre for Agriculture and Forestry, Lithuania
Rita Maggini,
University of Pisa, Italy

****Correspondence:***
Carl E. Sams
carlsams@utk.edu
Hunter A. Hammock
hhammoc1@vols.utk.edu

Specialty section:
This article was submitted to Plant Metabolism and Chemodiversity, a section of the journal Frontiers in Plant Science

Received: *29 October 2020*
Accepted: *12 January 2021*
Published: *26 February 2021*

Citation:
Hammock HA, Kopsell DA and Sams CE (2021) Narrowband Blue and Red LED Supplements Impact Key Flavor Volatiles in Hydroponically Grown Basil Across Growing Seasons. Front. Plant Sci. 12:623314. doi: 10.3389/fpls.2021.623314

INTRODUCTION

Plants have the ability to sense and respond to specific narrowband wavelengths within the ambient spectrum, ranging from ultraviolet-C (UV-C) (200–280 nm) to far-red (720–780 nm) regions (Galvao and Fankhauser, 2015; Carvalho et al., 2016). They use specialized pigment-proteins called photoreceptors, which react to changes in light intensity and spectra. This promotes physiological and biochemical changes that allow the plant to better adapt to the surrounding environment, further enhancing chances of survival/reproduction (Galvao and Fankhauser, 2015). Responses from abiotic stressors (i.e., changes in light intensity and spectra) prompt a diverse range of photomorphogenic responses across many plant species (Massa et al., 2008; Carvalho et al., 2016; Montgomery, 2016). Stimulation of phytochromes, cryptochromes, and phototropins has been shown to up- and down-regulate metabolic pathways that directly influence plant growth, development, and secondary metabolism (Briggs and Huala, 1999; Christie, 2007; Galvao and Fankhauser, 2015).

The solar radiation spectrum that has the most direct impact on plant growth and development includes three parts: UV light, visible (VS) light, and infrared (IR) light (McCree, 1973). Photosynthetically active radiation wavelengths (300–700 nm) are mostly absorbed by leaf tissues, and the majority of light absorption by chlorophyll pigments and quantum yield of photosynthesis occur primarily in the blue (B) and red (R) regions of the VS light spectrum (Morrow, 2008; Pimputkar et al., 2009; Kopsell et al., 2014). UV-C radiation includes 200–280 nm and is harmful to plants; however, UV-C is mostly blocked by the atmosphere, and most radiation of this type does not reach the earth's surface. Lighting sources that produce high-level UV-C radiation may be harmful to plants/animals and should generally be avoided in horticulture applications. UV-B radiation includes 280–315 nm and is only harmful to plants under intense applications. UV-B exposure has the potential to increase secondary metabolite production, in addition to pigment bleaching and degradation of flavor volatiles/carotenoids/other secondary metabolites at intense levels. UV-A radiation includes 315–380 nm and has controversial impacts on plant morphology and secondary metabolite production. The range of 380–400 nm contains the transition from UV-A to the VS light spectrum. Chlorophyll and carotenoid pigments begin to absorb light within this range.

Wavelengths ranging from 400 to 520 nm contain violet, blue, and green light. Chlorophyll pigments obtain peak energy absorption at these wavelengths and strongly influence vegetative growth and development. Cryptochromes and phototropins are both B light receptors (Briggs and Christie, 2002). Cryptochromes act as signaling mechanisms that regulate circadian rhythms and prompt many physiological and morphological changes; phototropins control chloroplast movements to maximize absorption of specific wavelengths (Christie, 2007; Chaves et al., 2011; Kopsell et al., 2014). Changes in specific B wavelengths that target phototropins or cryptochromes have the ability to impact primary and secondary metabolism, volatile production, carotenoid and chlorophyll pigment bioaccumulation, circadian rhythms, stomatal opening/closing, intermodal length, leaf area and thickness, and intracellular structure configurations/positioning (Lichtenthaler, 1987; Frank and Cogdell, 1996; Briggs and Huala, 1999; Briggs and Christie, 2002; Christie, 2007; Abney et al., 2013; Kopsell and Sams, 2013; Metallo et al., 2018; Bantis et al., 2020; Samuoliene et al., 2020). Intensity changes to specific B wavelengths that target phytochromes have also been shown to impact germination rates, vegetative and reproductive growth/development, leaf size/thickness, phenolic and antioxidant pathways, etc. (Li and Kubota, 2009; Olle and Viršile, 2013; Landi et al., 2020). Exposure to UV light and specific B wavelengths have been shown to result in higher concentrations of favorable flavor volatiles in many high-value crops such as mint (*Mentha piperita*) (Lucchesi et al., 2004; Hikosaka et al., 2010; Treadwell et al., 2011), thyme (*Thymus vulgaris*) (Lee et al., 2005), strawberries *(Fragaria* × *ananassa)* (Colquhoun et al., 2013), chives (*Allium fistulosum*) (Abney et al., 2013), lettuce (*Lactuca sativa* L.) (Baumbauer et al., 2019; Chen et al., 2019; Kong et al., 2019; Yan et al., 2019; Zhang et al., 2019; Samuoliene et al., 2020), and basil (*Ocimum basilicum*) (Loughrin and Kasperbauer, 2003; Kopsell et al., 2005; Lee et al., 2005; Deschamps and Simon, 2006; Chalchat and Ozcan, 2008; Hussain et al., 2008; Klimánková et al., 2008; Bantis et al., 2016; Carvalho et al., 2016).

The range of 520–610 nm contains green, yellow, and orange wavelengths, which has limited influence on vegetative growth and development. Some studies have found that special wavebands within this range have specific impacts on plant development and secondary metabolite production, but additional research should be conducted to determine practical uses for specific wavebands within this range.

The range of 610–720 nm contains R wavelengths, and high levels of absorption occur at this range. These wavelengths strongly influence vegetative growth, photosynthesis, and reproductive growth. Phytochromes are mostly R light photoreceptors that control physiological responses via R and far-red wavelengths (Chaves et al., 2011). R light closely aligns with the maximum absorption for chlorophyll and matches the absorption peaks of various phytochemicals and secondary pigments (Goins et al., 1997; Pimputkar et al., 2009). Literature suggests that the interaction between cryptochromes/phytochromes/other accessory pigments and various wavelengths is not fully understood and should be researched further (Tennessen et al., 1994; Goins et al., 1997; Briggs and Huala, 1999; Morrow, 2008; Pimputkar et al., 2009; Chaves et al., 2011; Fraikin et al., 2013). Other unidentified photoreceptors may be influenced by the addition of these wavelengths.

The range of 720–1,000 nm contain far-red and IR wavelengths that directly impact germination and flowering. Wavelengths greater than 1,000 nm contain IR radiation, which is primarily converted into heat energy. These wavebands are not particularly useful to plants for primary or secondary metabolism and are not used for photosynthesis (McCree, 1973; Barta et al., 1992; Goins et al., 1997; Briggs and Huala, 1999;

Lucchesi et al., 2004; Morrow, 2008; Abney et al., 2013; Tuan et al., 2013; Kopsell et al., 2014).

Secondary metabolites contain a wide range of chemical compound classes that serve many functions in plants, most of which involve adaptation to environmental stress (Bourgaud et al., 2001). In plant tissues, the synthesis of secondary metabolites is significantly impacted by environmental conditions in addition to many physiological, biochemical, and genetic factors (Bourgaud et al., 2001; Lefsrud et al., 2008). Light intensity and spectral quality are two of the most influential factors on secondary metabolism (Kopsell et al., 2005; Kopsell et al., 2014), and changes in light intensity and spectral quality directly impact plant physiology and biochemistry (Colquhoun et al., 2013; Bian et al., 2015; Landi et al., 2020).

Volatile organic compounds (VOCs) are defined as carbon-containing molecules that have high vapor pressure at ordinary room temperatures. Low boiling points, chemical structure, and other physical properties determine the high vapor pressures of volatile compounds (Taylor, 1996). These compounds include both naturally occurring and manmade compounds. A large number of scents, flavors, odors, and aromas are VOCs. The majority of VOCs found in nature are produced by plants, with isoprene being the base unit (i.e., isoprenoids). These compounds play an important role in plant signaling, defense, pollinator attraction, etc. (Kesselmeier and Staudt, 1999). Stabilization, volatilization, and plant-controlled emission of these compounds are directly impacted by genetics, as well as many abiotic and biotic factors such as temperature, sunlight, turgor pressure, stomatal opening, humidity, pest and pathogen pressures, etc. (Kesselmeier and Staudt, 1999; Klimánková et al., 2008). Emission occurs almost exclusively at the leaf's surface through open stomata, but certain defense compounds may be released if physical damage occurs (Yousif et al., 1999). Aromatic and flavor compounds usually have low molecular weights (<300 Da), which directly contributes to their volatility along with chemical structure and high vapor pressures. Flavors affect both taste and smell, whereas fragrances (aroma) affect only smell (Fahlbusch et al., 2003). The terms *flavor* and *aroma* tend to denote naturally occurring compounds, whereas fragrance typically refers to synthetic compounds (Fahlbusch et al., 2003). Some studies have been performed on basil flavor volatiles, and substantial volatile profiles have been established using a variety of analytical techniques (Charles and Simon, 1990; Barbieri et al., 2004; Kopsell et al., 2005; Deschamps and Simon, 2006; Raimondi et al., 2006; Politeo et al., 2007; Chalchat and Ozcan, 2008; Hussain et al., 2008; Klimánková et al., 2008; Olfati et al., 2012; Tarchoune et al., 2013; Bantis et al., 2016).

Basil is a highly valued, annual culinary and medicinal herb that has a complex aroma profile preferred by top restaurants and professional chefs. Basil is rich in antioxidants and phenolic compounds that have been shown to possess human health benefits (Kopsell et al., 2005; Kopsell and Sams, 2013; Kim et al., 2016). The Genovese cultivar is considered valuable because of its popularity and highly desirable flavor/aroma profiles, with extensive use in culinary dishes and manufacturing productions (i.e., essential oils, soaps, etc.). In comparison to other herbs, basil contains a wide variety of compounds that are nutritionally significant to humans, including terpenes, flavonoids, carotenoids, volatile compounds, etc. (Bourgaud et al., 2001; Hussain et al., 2008). In previous surveys, basil has been reported as having one of the highest antioxidant concentrations compared to other popular herbs and spices (Kopsell et al., 2005; Lee et al., 2005; Politeo et al., 2007), increasing potential health benefits for consumers. To date, only a few studies have been conducted using a supplemental dichromatic light-emitting diode (LED) lighting source to influence basil sensory quality and VOC flavor profiles across seasons.

The advancement of LED technology provides researchers the opportunity to investigate how narrowband wavelengths fundamentally impact plant metabolism and development (Darko et al., 2014). Purposefully manipulating spectral quality in order to promote increases in secondary metabolic production has been shown to increase the nutritional value of specialty herb crops and benefit overall consumer health (Lefsrud et al., 2006; Kopsell et al., 2015; Bantis et al., 2016; Kopsell et al., 2017). Both B and R wavelengths evaluated in this study were chosen because they closely match absorption spectrums of chlorophyll and carotenoid compounds; they have direct impacts on photosynthesis and promote significant increases in overall biomass accumulation across a variety of plant species. In addition, secondary metabolic pathways may be influenced by the supplementation of specific B and R wavelengths (Colquhoun et al., 2013; Carvalho et al., 2016). These various metabolic pathways are interconnected with primary metabolism, which has the potential to impart a variety of antagonistic and synergistic effects on metabolic products that have sensory/nutritional value for humans (Kesselmeier and Staudt, 1999; Lee et al., 2005; Deschamps and Simon, 2006). A recent report indicates that basil plants grown under various narrowband wavelengths had significant concentration changes in specific volatile classes and that LED narrowband lighting may manipulate specific secondary metabolic pathways of basil under certain conditions (Carvalho et al., 2016). Another study indicated that B and R light significantly increased a variety of volatile fatty acid derivatives, volatile phenylpropanoids/benzenoids, and volatile terpenes in preharvest/postharvest tea leaves, including key flavor volatiles such as linalool, eugenol, 2-phenylethanol, etc. (Fu et al., 2015), all of which share similar pathways across species and prove relevant for the flavor and aroma of basil.

A wide range of narrowband wavelengths should be further investigated to determine potential impacts across many plant species, in addition to full-spectrum light sources. This will provide necessary information to develop effective "light recipes" that can be added for optimal growth across a variety of plant species in unfavorable growing seasons. Conflicting results have been found in relation to the suggested ratios, intensities, and daily light integral (DLI) of narrowband blue/red wavelengths for optimal plant growth and secondary metabolite production, indicating a need to further investigate the interaction between supplemental lighting (SL) and plant physiology and morphology.

The primary objective of this study was to determine the impact of progressive B/R supplemental narrowband wavelength

ratios on the production of key flavor volatiles and sensory quality of basil under greenhouse conditions. Emphasis was placed on determining the optimal ratio of B/R wavelengths for VOC bioaccumulation and how changes in spectral quality/DLI impact secondary metabolic resource partitioning. Because primary and secondary metabolism are directly linked to the intensity and spectral quality of available natural light (NL), seasonal differences are expected for primary and secondary metabolism (Banthorpe et al., 1972; Kang et al., 2009; Wink, 2010; Sugimoto et al., 2012; Olle and Viršile, 2013; Carvalho et al., 2016); however, few studies have determined the relationship between specific B/R wavelengths, key flavor volatiles in basil, and impact of changing DLI/spectral quality across growing seasons in addition to narrowband SL treatments (Wink, 2010; Buchanan et al., 2015).

MATERIALS AND METHODS

Cultural Techniques and Environmental Growing Conditions

This project was conducted at The University of Tennessee Institute of Agriculture in Knoxville, TN (35°56′44.5″N, 83°56′17.3″W). Growing dates for six separate experimental cycles occurred from August 2015 to June 2016 and have been labeled as growing seasons. "Genovese" basil seeds (Johnny's Select Seeds, Winslow, ME, United States) were germinated in peat moss based cubes (2 × 2 × 6 cm) (Park's Bio Dome Sponges, Hodges, SC, United States) at 28.3°C and 95% RH. The "Genovese" variety of sweet basil was specifically chosen because of its unique flavor profile, high market demand, and preference among professional chefs. After 2 weeks, seedlings were transplanted into 8 × 8 × 9-cm plastic pots using 1 part peat moss (Black Gold Canadian Sphagnum Peat Moss, Agawam, MA, United States) to 3 parts perlite (Krum Horticultural Perlite, Hodgkins, IL, United States) potting mix. Relative humidity during the growth period averaged 55%. Across all six growing seasons, day temperatures averaged 27.4°C, whereas night temperatures averaged 21.8°C. Daily and nightly temperature averages were taken across 1 full year (August 2015 to August 2016) to determine capacity of greenhouse heating/cooling systems and averaged 29.4°C/23.8°C, respectively. The DLI of the NL control averaged 9.5 mol · m^{-2} · d^{-1} across all growing cycles (ranging from 4 to 18 mol · m^{-2} · d^{-1}). Specific growing parameters for each growing season may be found in **Table 1**.

Changes to key flavor volatiles were evaluated in response to specific ratios of narrowband B/R (peaked at 447 nm/627 nm, ±20 nm) LED light. Light emission spectra from natural sunlight (**Figure 1A**) and all SL treatments (**Figure 1B**) were taken across growing seasons with an Apogee PS-200 Spectroradiometer (Apogee, Logan, UT, United States). The NL control was used to establish baseline growth and development parameters under non-supplemented conditions as well as determine changes to plant physiology in response to variations in spectral quality/intensity across growing seasons. **Table 1** shows average DLIs across growing season as well as the average NL intensity of B/R narrowband wavelengths that were evaluated in this experiment (447 nm/627 nm). A total of seven SL treatments were applied immediately after seedling transplant: one HPS treatment and six LED treatments with progressive B/R ratios [10B/90R, 20B/80R, 30B/70R, 40B/60R, 50B/50R, and 60B/40R (Orbital Technologies, Madison, WI, United States)]. Each SL treatment provided 8.64 mol · m^{-2} · d^{-1} across all growing seasons (100 μmol · m^{-2} · s^{-1}, 24 h · d^{-1}).

Basil plants were grown in ebb and flow hydroponic systems and subirrigated for 5 min each day with a full-strength, modified Hoagland's solution. Nutrient solution elemental concentrations were as follows (ppm): N (207.54), P (50.87), K (298.23), Ca (180.15), Mg (77.10), S (136.45), Fe (3.95), Mn (0.90), Zn (0.40), Mo (0.09), Cu (0.90), and B (0.90). The fertility regimen was kept constant across the duration of all seasons. Total growth time lasted approximately 45 days across all six experimental cycles. Like many commercial

TABLE 1 | Important environmental parameters across growing cycles.

	September	November	January	March	April	June
Growing season	8/14/15–9/29/15	10/14/15–11/19/15	12/16/15–01/29/16	2/10/16–3/15/16	3/11/16–4/28/16	5/16/16–6/23/16
Average day temp (°C)	27.33	26.84	25.83	25.85	26.95	27.84
Average night temp (°C)	23.61	20.62	19.11	21.01	21.94	22.56
Average relative humidity	55%	55%	50%	55%	55%	60%
Average NL Daily Light integral (DLI) (mol · m^{-2} · d^{-1})	9.81	3.26	4.65	8.62	11.99	14.55
Average day length (h)	12.98	10.35	9.93	11.65	13.20	14.27
Average natural blue 447 nm (±10 nm) intensity at noon (μmol · m^{-2} · s^{-1})	13.8	12.2	10.3	12.1	13.3	14.5
Average natural red 627 nm (±10 nm) intensity at noon (μmol · m^{-2} · s^{-1})	14.8	13.2	10.8	13.5	14.4	15.6

All crops grown under greenhouse conditions at The University of Tennessee Institute of Agriculture in Knoxville, TN, United States (35°56′44.5″N, 83°56′17.3″W).

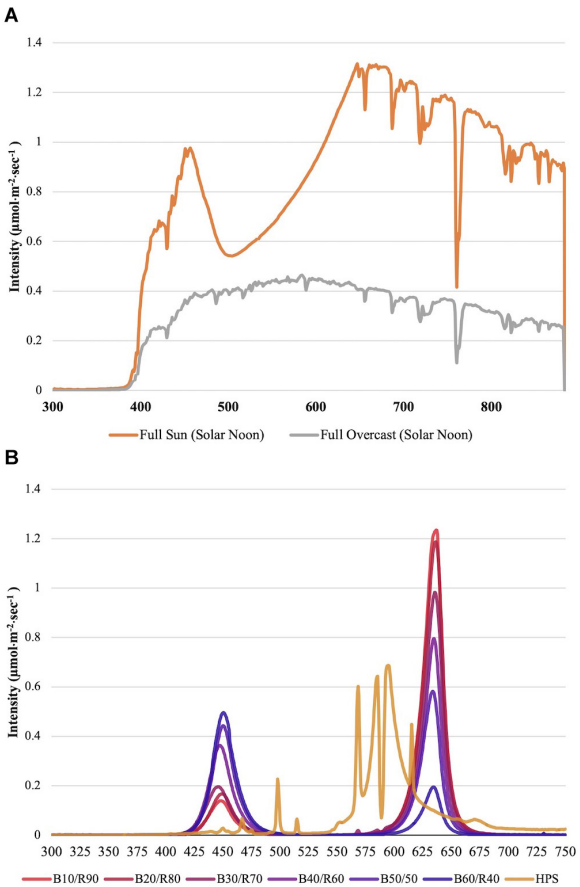

FIGURE 1 | (A) Natural light spectra in greenhouse averaged across all six growing seasons, ranging from 300 to 875 nm. Values were taken at solar noon with three replicates for full sun and overcast for each experimental run. The daily light integral (DLI) of the NL control averaged 9.5 mol · m^{-2} · d^{-1} across all growing cycles (ranging from 4 to 18 mol · m^{-2} · d^{-1}). **(B)** Emission spectra of LED and HPS treatments from 300 to 750 nm. All supplemental lighting (SL) treatments provided exactly 8.64 mol · m^{-2} · d^{-1} (100 µmol · m^{-2} · s^{-1}, 24 h · d^{-1}). All lighting treatments were measured with a PS-200 Apogee Spectroradiometer to confirm intensity of specific treatment wavelengths throughout all growing seasons. Readings were taken at midnight in order to exclude underlying natural solar spectra. LED treatments provided narrowband progressive blue (B)/red (R) lighting ratios (10B/90R, 20B/80R, 30B/70R, 40B/60R, 50B/50R, 60B/40R, expressed as % artificial light intensity), while the high pressure sodium (HPS) treatment provided broadband light.

basil-growing operations, harvest occurred as the first signs of change from vegetative to reproductive growth were observed (i.e., 8–10 nodes). **Figure 2** provides a visual representation of morphological and developmental changes imparted by SL treatments.

Gas Chromatography–Mass Spectrometry Headspace Volatile Analysis

Three grams of fresh leaf tissue (two basil plants per sample rep, 1.5 g of representative material from each plant, nodes 4 and 8) were placed in 20-mL borosilicate glass vials then immediately sealed and placed onto a Network Headspace Sampler (Agilent G1888, Santa Clara, CA, United States). Six sample reps were used per treatment. Samples were heated to 80°C for 10 min and then pressurized with helium (Air Gas, analytical purity) to 95.21 kPa for 1 min. The tube was then vented for 1 min into the headspace transfer line (110°C) and injected (port at 250°C) into the gas chromatography (GC) (Agilent Technologies 6890N Network GC System). The volatiles were separated by an HP-5MS capillary column [(5%-phenyl)-methylpolysiloxane, length: 30 m, internal diameter: 0.250 mm, film thickness: 1 µm, Agilent Technologies)] using analytical purity helium carrier gas at 95.21 kPa with constant column pressure. At the start of data acquisition, temperature was held at 40°C for 5 min, ramped up from 40 to 250°C (5°C per min), and then held constant for the duration of the run. Total run time was 70 min, including post-run and cool-down phases. After sample separation and column elution, the analytes were passed through a mass selective detector (Agilent Technologies 5973 Network Mass Selective Detector) at 250°C and collected over the course of the sample run. The transfer line, ion source, and quadrupole temperatures were 250, 230, and 170°C, respectively. The full scan mass range was set to 40–550 m/z (threshold: 150).

Agilent ChemStation was used for data collection and processing. More than 200 separate compounds were identified throughout this experiment, but emphasis was placed on key flavor compounds (i.e., shown in the literature to be important for human sensory perception) that have been calibrated to our GC–mass spectrometry (MS) and HP-5MS column using analytical standards (Sigma–Aldrich, St. Louis, MO, United States) to determine leaf tissue concentrations of key VOCs on a fresh plant weight basis. The MS spectra from analytical standards and fresh samples were compared to NIST, ADMIS, and our custom basil reference library created from calibrated analytical standards to confirm peak identity and retention times. MassHunter Workstation Software Version B.06.00 (Agilent Technologies, Inc., 2012) was used to automatically integrate peaks. Relative peak areas were automatically adjusted based on analytical standards and multiple library references.

Statistical Analyses

A randomized complete block design was used for this experiment. All data sets were analyzed by generalized linear model and mixed-model analysis of variance procedures using the statistical software SAS (version 9.4, SAS Institute, Cary, NC, United States). Design and Analysis macro (DandA.sas), created by Dr. Arnold Saxton, was utilized in addition to Tukey adjustment, regression analysis, and univariate/normalization procedures to provide additional statistical insights on the complete data set. Treatments were separated by least significant difference (LSD) at $\alpha = 0.05$. Because of the overwhelming number of compounds analyzed, only statically significant separations were reported from this study. Key volatiles were analyzed and presented on a fresh mass (FM) basis in comparison to micromolar calibration curves created from analytical standards. All volatile concentrations units are reported in micromolarity of analyte concentration per g of fresh leaf tissue

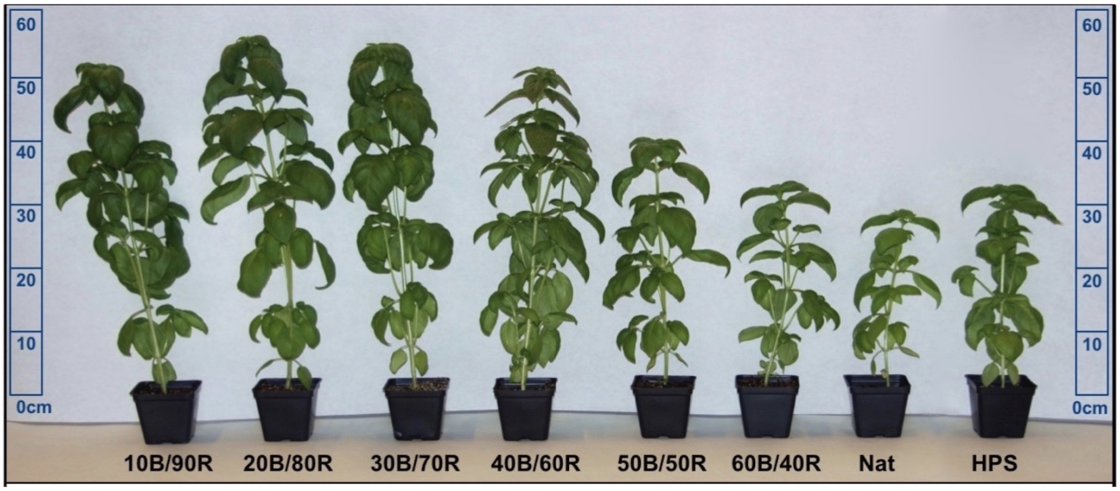

FIGURE 2 | Visual representation of LED lighting impacts on morphology of hydroponically grown "Genovese" basil (*Ocimum basilicum* var. "Genovese"). Photo taken immediately before June season harvest and shows comparison of variations in height, canopy size, leaf area, and pigmentation after being exposed to supplemental blue (B)/red (R) LED ratios, natural light (NL) control (Nat), and broad-spectrum HPS supplemental lighting (SL). A non-supplemented NL control was used to account for daily light integral (DLI) and spectral quality variations across seasons. All treatments (except control) were provided 100 $\mu mol \cdot m^{-2} \cdot s^{-1}$ of supplemental light from transplant to harvest.

($\mu M \cdot g^{-1}$ FM) to most accurately represent VOC emissions from the collected headspace sample above fresh plant tissues under specific reproducible analytical conditions.

RESULTS

(R)-(+)-limonene concentrations were significantly different across season ($P \leq 0.0001$; $F = 115.43$), treatment ($P \leq 0.0001$; $F = 14.90$), and season × treatment interaction ($P = 0.0050$; $F = 1.76$). (S)-(−)-limonene concentrations were significantly impacted by season ($P \leq 0.0001$; $F = 52.86$), treatment ($P \leq 0.0001$; $F = 14.03$), and season × treatment interaction ($P \leq 0.0001$; $F = 2.32$). The optimal LED treatment for increasing both limonene compound concentrations was 40B/60R (**Figure 3A**). In general, (S)-(−)-limonene and (R)-(+)-limonene concentrations differed by a factor of 7–10 times across treatments, with (R)-(+)-limonene being the more intense flavor volatile in terms of analytical response (**Figure 3A**). Concentration ratios of (S)-(−)-limonene and (R)-(+)-limonene were not significantly different across all lighting treatments, which demonstrates that varying B/R light treatments do not modify the ratio of (S)-(−)-limonene and (R)-(+)-limonene produced, but rather the quantity. (S)-(−)-limonene concentrations were highest during the winter growing seasons (January–March) (**Figure 3B**). Average natural DLIs were much lower during this time in comparison to other growing seasons, which shows that the supplemental B/R wavelengths have greater impact on secondary metabolism when DLI is lower for this specific compound. November had the lowest concentration of overall terpenoid compounds across all seasons. (R)-(+)-limonene did not follow the same trend across growing seasons as its enantiomer (**Figure 3B**); ratios of R/S limonene varied across all growing seasons and did not follow any definitive patterns. September showed the highest concentrations of (R)-(+)-limonene, a six times increase over June, which was the lowest concentration observed across all growing seasons.

α-Pinene concentrations were significantly impacted by season ($P \leq 0.0001$; $F = 56.98$), treatment ($P \leq 0.0001$; $F = 9.46$), and season × treatment interaction ($P \leq 0.0010$; $F = 1.96$). All LED treatments were significantly higher than the NL control. HPS treatment concentration was not significantly different than the control and did not separate from some of the LED treatments (**Figure 4A**). The highest concentrations were found in early fall, whereas the lowest concentrations were found in late spring, both significantly different than any other growing season (**Figure 4B**). β-Pinene concentrations were significantly impacted by season ($P \leq 0.0001$; $F = 42.03$), treatment ($P \leq 0.0001$; $F = 10.25$), and season × treatment interaction ($P = 0.0017$; $F = 1.90$). All LED treatments were significantly higher than the NL control. HPS treatment was not significantly different than the control and did not separate from some of the LED treatments. The LED treatments show a regression trend, with 40B/60R being the optimal B/R ratio for pinene bioaccumulation (**Figure 4A**). The highest concentrations were found in early fall, whereas the lowest concentrations were found in early winter and late spring; late spring had significantly lower concentrations, almost five times difference than the best season (September) (**Figure 4B**). Concentration totals of limonene and pinene compounds followed similar patterns to one another across season.

Methyl eugenol (ME) showed significant impacts across season ($P \leq 0.0001$; $F = 23.48$), treatment ($P \leq 0.0001$; $F = 14.14$), and season × treatment interaction ($P \leq 0.0001$; $F = 2.37$). ME showed an inverse relationship to LED lighting treatments and

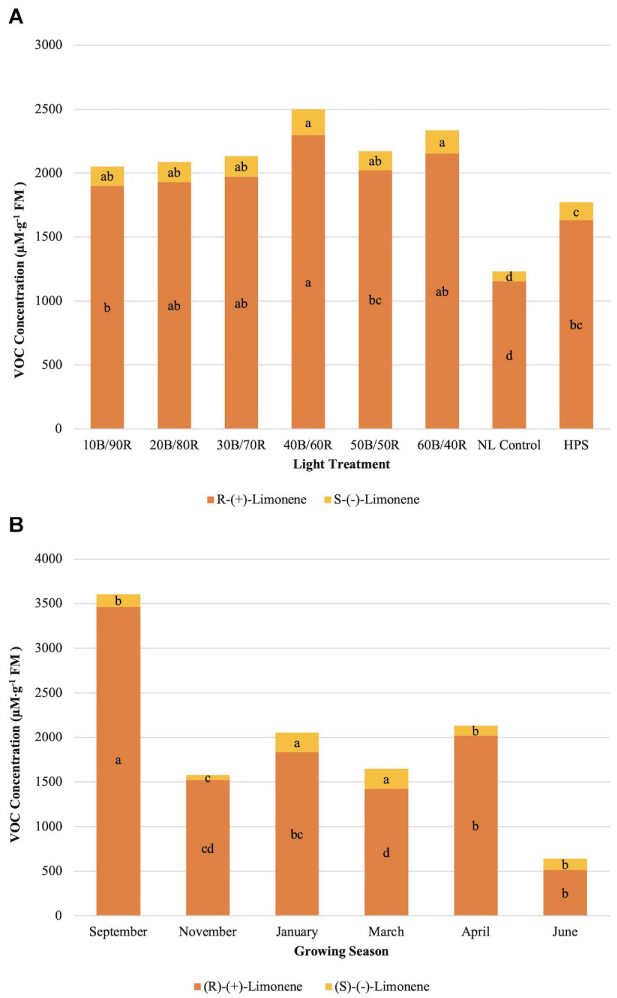

FIGURE 3 | Influence of **(A)** greenhouse lighting treatments and **(B)** growing season on (R)-(+)-limonene and (S)-(−)- Limonene concentrations ($\mu M \cdot g^{-1}$ FM) of hydroponically grown "Genovese" basil (*Ocimum basilicum* var. "Genovese"). Six LED treatments with progressive blue (B)/red (R) ratios (10B/90R, 20B/80R, 30B/70R, 40B/60R, 50B/50R, 60B/40R, expressed as % artificial light intensity), and the high-pressure sodium (HPS) treatment provided supplemental light at 8.64 mol $\cdot m^{-2} \cdot d^{-1}$ (100 μmol $\cdot m^{-2} \cdot s^{-1}$, 24 h $\cdot d^{-}1$). The daily light integral (DLI) of the NL control averaged 9.5 mol $\cdot m^{-2} \cdot d^{-1}$ during the growth period (ranging from 4 to 18 mol $\cdot m^{-2} \cdot d^{-1}$). Supplemental lighting was then compared to the natural light (NL) control. Values were analyzed using Tukey protected LSD, and those followed by the same letter are not significantly different ($\alpha = 0.05$).

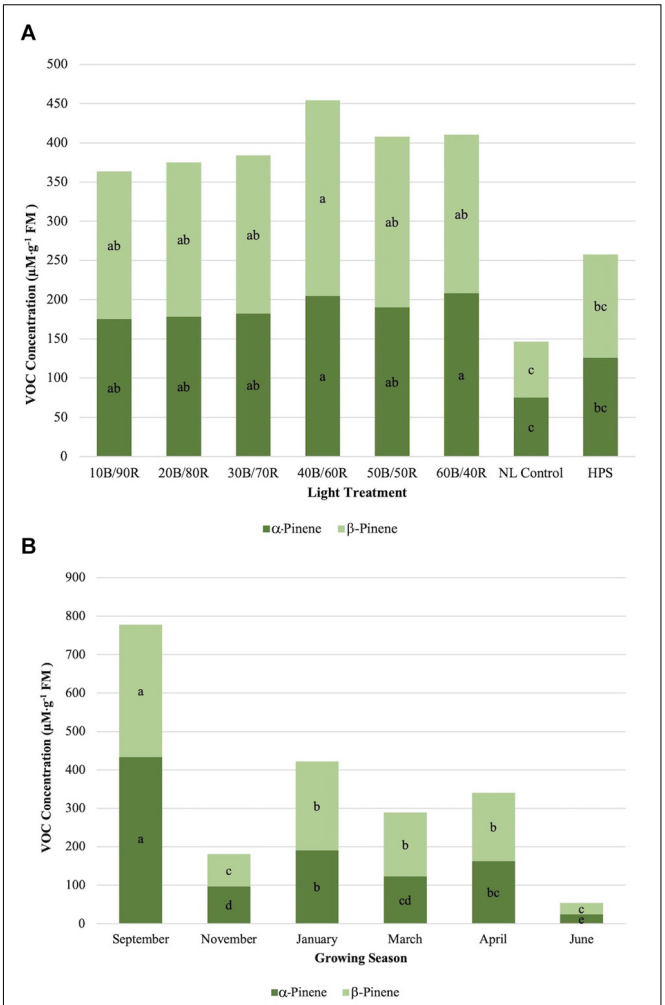

FIGURE 4 | Influence of **(A)** greenhouse lighting treatments and **(B)** growing season on α-pinene and β-pinene concentrations ($\mu M \cdot g^{-1}$ FM) of hydroponically grown "Genovese" basil (*Ocimum basilicum* var. "Genovese"). Six LED treatments with progressive blue (B)/red (R) ratios (10B/90R, 20B/80R, 30B/70R, 40B/60R, 50B/50R, 60B/40R, expressed as % artificial light intensity), and the high-pressure sodium (HPS) treatment provided supplemental light at 8.64 mol $\cdot m^{-2} \cdot d^{-1}$ (100 μmol $\cdot m^{-2} \cdot s^{-1}$, 24 h $\cdot d^{-}1$). The daily light integral (DLI) of the NL control averaged 9.5 mol $\cdot m^{-2} \cdot d^{-1}$ during the growth period (ranging from 4 to 18 mol $\cdot m^{-2} \cdot d^{-1}$). Supplemental lighting was then compared to the natural light (NL) control. Values were analyzed using Tukey protected LSD, and those followed by the same letter are not significantly different ($\alpha = 0.05$).

NL control in comparison to other key flavor volatiles evaluated in this study (**Figure 5A**). Many of the compounds evaluated (i.e., isoprenoids) show a regression relationship between the LED lighting treatments peaking around 40B/60R and the NL control showing the lowest concentrations. The opposite was true for ME, as the NL control showed the highest concentrations in comparison to any other treatment, whereas the 40B/60R had the lowest concentrations. March and April had the statistically lower concentrations of ME as compared to the four other seasons (**Figure 5B**).

Eucalyptol concentrations were impacted by season ($P \leq 0.0001$; $F = 47.47$), treatment ($P \leq 0.0001$; $F = 16.20$), and season × treatment interaction ($P = 0.0007$; $F = 2.00$). All LED treatment concentrations were higher than the NL control. HPS treatment showed some separation for optimal LED treatments, but did not separate from other LED treatments. 40B/60R produced the highest eucalyptol concentrations, with nearly 1-mM emission per gram of fresh leaf tissue. The HPS treatment separated from the NL control (**Figure 6A**). Early fall concentrations were higher than winter and spring seasons and

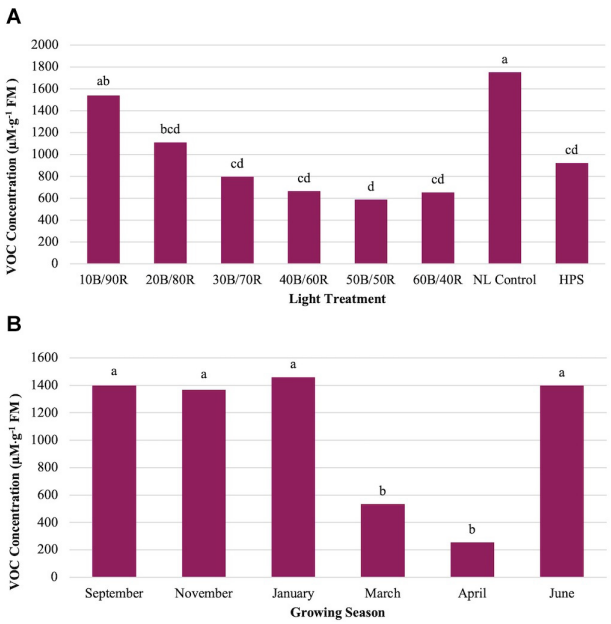

FIGURE 5 | Influence of **(A)** greenhouse lighting treatments and **(B)** growing season on Methyl Eugenol concentrations ($\mu M \cdot g^{-1}$ FM) of hydroponically grown "Genovese" basil (*Ocimum basilicum* var. "Genovese"). Six LED treatments with progressive blue (B)/red (R) ratios (10B/90R, 20B/80R, 30B/70R, 40B/60R, 50B/50R, 60B/40R, expressed as % artificial light intensity), and the high-pressure sodium (HPS) treatment provided supplemental light at 8.64 mol $\cdot m^{-2} \cdot d^{-1}$ (100 μmol $\cdot m^{-2} \cdot s^{-1}$, 24 h $\cdot$ d−1). The daily light integral (DLI) of the NL control averaged 9.5 mol $\cdot m^{-2} \cdot d^{-1}$ during the growth period (ranging from 4 to 18 mol $\cdot m^{-2} \cdot d^{-1}$). Supplemental lighting was then compared to the natural light (NL) control. Values were analyzed using Tukey protected LSD, and those followed by the same letter are not significantly different ($\alpha = 0.05$).

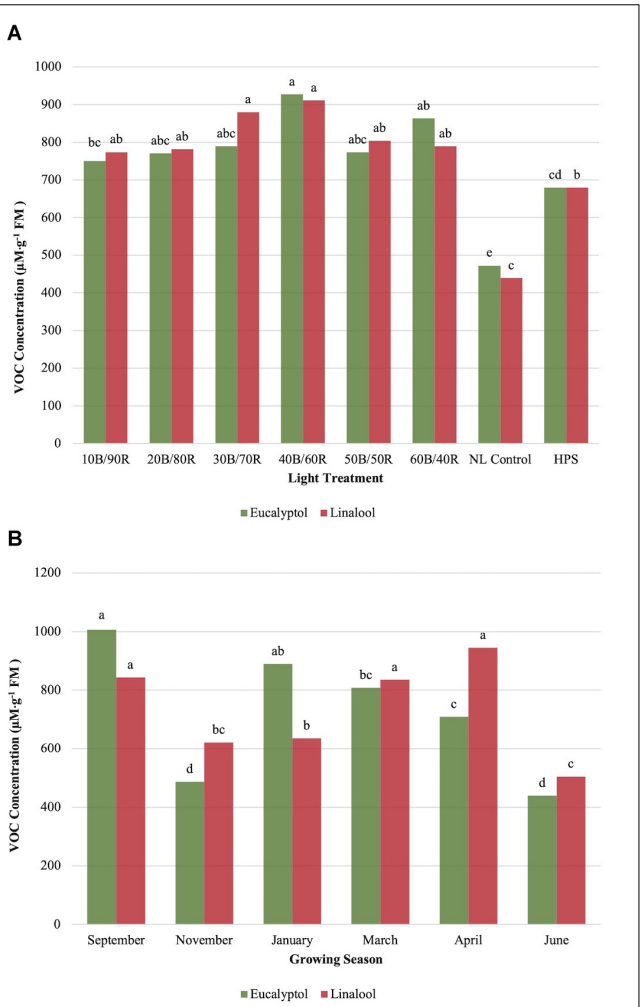

FIGURE 6 | Influence of **(A)** greenhouse lighting treatments and **(B)** growing season on eucalyptol and linalool concentrations ($\mu M \cdot g^{-1}$ FM) of hydroponically grown "Genovese" basil (*Ocimum basilicum* var. "Genovese"). Six LED treatments with progressive blue (B)/red (R) ratios (10B/90R, 20B/80R, 30B/70R, 40B/60R, 50B/50R, 60B/40R, expressed as % artificial light intensity), and the high-pressure sodium (HPS) treatment provided supplemental light at 8.64 mol $\cdot m^{-2} \cdot d^{-1}$ (100 μmol $\cdot m^{-2} \cdot s^{-1}$, 24 h $\cdot$ d−1). The daily light integral (DLI) of the NL control averaged 9.5 mol $\cdot m^{-2} \cdot d^{-1}$ during the growth period (ranging from 4 to 18 mol $\cdot m^{-2} \cdot d^{-1}$). Supplemental lighting was then compared to the natural light (NL) control. Values were analyzed using Tukey protected LSD, and those followed by the same letter are not significantly different ($\alpha = 0.05$).

generally followed the pattern observed by other monoterpenes evaluated in this experiment (**Figure 6B**).

Linalool concentrations were significantly impacted by season ($P \leq 0.0001$; $F = 28.24$), treatment ($P \leq 0.0001$; $F = 16.52$), and season × treatment interaction ($P = 0.0398$; $F = 1.48$). Concentrations peaked around 40B/60R, and this lighting treatment did not separate from other LED lighting treatments. All LED treatments were significantly higher than NL control (**Figure 6A**). September, March, and April had statistically higher concentrations than the other three seasons (**Figure 6B**).

α-Humulene concentrations were significantly impacted by season ($P \leq 0.0001$; $F = 34.34$), treatment ($P \leq 0.0001$; $F = 12.29$), and season × treatment interaction ($P \leq 0.0001$; $F = 3.20$). All LED treatments were significantly higher than the NL control and HPS treatment; however, none of the LED treatments separated from one another, and the control/HPS treatment did not separate (**Figure 7A**). Volatile emission from LED treatments was approximately 10 $\mu M \cdot g^{-1}$ FM higher than control and HPS. Linalool and α-humulene concentrations showed significance across growing seasons, with the highest concentrations in September, March, and April (**Figures 6B**, 7B). The lowest concentrations for both isoprenoid compounds were found in June.

1,3,6-Octatriene,3,7- dimethy-,(E) showed significant season ($P \leq 0.0001$; $F = 40.80$) and treatment ($P \leq 0.0001$; $F = 5.99$) differences. The (Z) conformation did not show any significant changes across lighting treatments and was not presented in this study. The (E) conformation did show significant differences between the 40B/60R treatment and the HPS treatment/NL control (**Figure 7A**). Approximately 1.8 times concentration increase was observed for the (E) conformation between the best LED treatment (40B/60R) and the NL control. The concentration of the 40B/60R treatment was higher than the HPS treatment;

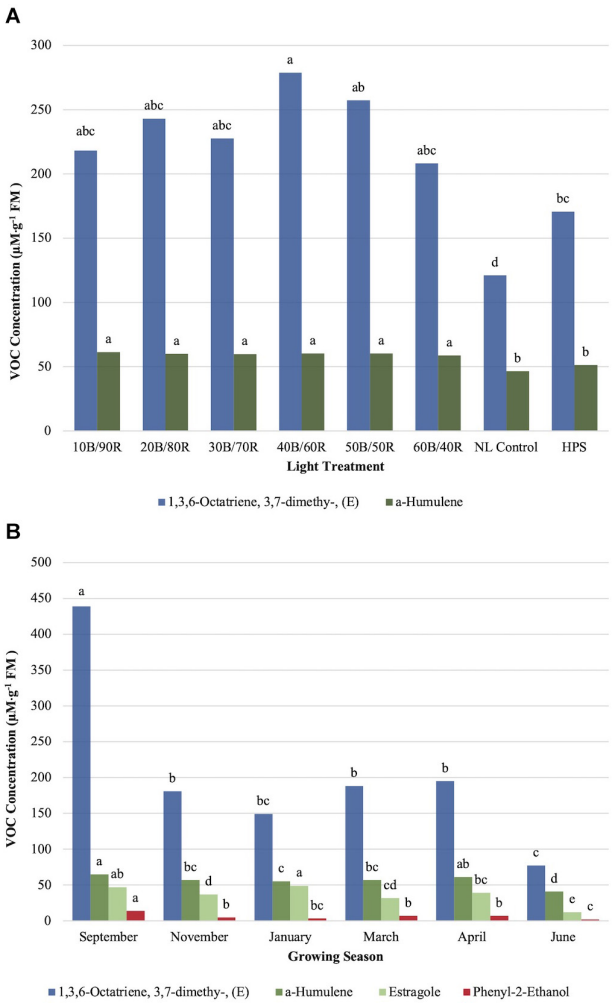

FIGURE 7 | Influence of **(A)** greenhouse lighting treatments and **(B)** growing season on moderate concentration VOCs ($\mu M \cdot g^{-1}$ FM) of hydroponically grown "Genovese" basil (*Ocimum basilicum* var. "Genovese"). Six LED treatments with progressive blue (B)/red (R) ratios (10B/90R, 20B/80R, 30B/70R, 40B/60R, 50B/50R, 60B/40R, expressed as % artificial light intensity), and the high-pressure sodium (HPS) treatment provided supplemental light at 8.64 mol $\cdot m^{-2} \cdot d^{-1}$ (100 μmol $\cdot m^{-2} \cdot s^{-1}$, 24 h $\cdot d^{-1}$). The daily light integral (DLI) of the NL control averaged 9.5 mol $\cdot m^{-2} \cdot d^{-1}$ during the growth period (ranging from 4 to 18 mol $\cdot m^{-2} \cdot d^{-1}$). Supplemental lighting was then compared to the natural light (NL) control. Values were analyzed using Tukey protected LSD, and those followed by the same letter are not significantly different ($\alpha = 0.05$).

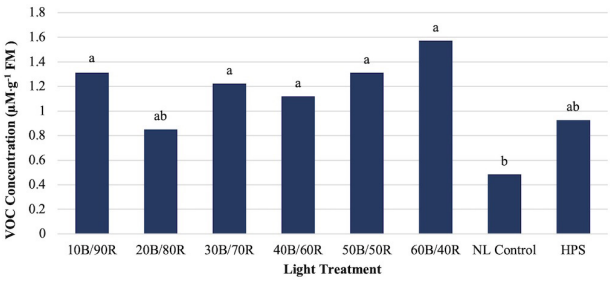

FIGURE 8 | Influence of greenhouse lighting treatments on hexanal concentrations ($\mu M \cdot g^{-1}$ FM) of hydroponically grown "Genovese" basil (*Ocimum basilicum* var. "Genovese"). Six LED treatments with progressive blue (B)/red (R) ratios (10B/90R, 20B/80R, 30B/70R, 40B/60R, 50B/50R, 60B/40R, expressed as % artificial light intensity), and the high-pressure sodium (HPS) treatment provided supplemental light at 8.64 mol $\cdot m^{-2} \cdot d^{-1}$ (100 μmol $\cdot m^{-2} \cdot s^{-1}$, 24 h $\cdot d^{-1}$). The daily light integral (DLI) of the NL control averaged 9.5 mol $\cdot m^{-2} \cdot d^{-1}$ during the growth period (ranging from 4 to 18 mol $\cdot m^{-2} \cdot d^{-1}$). Supplemental lighting was then compared to the natural light (NL) control. Values were analyzed using Tukey protected LSD, and those followed by the same letter are not significantly different ($\alpha = 0.05$).

the HPS treatment did not separate from most of the other LED treatments but did separate from the NL control. The (E) conformation of 1,3,6-octatriene showed seasonal concentration changes, but the (Z) conformation did not show any significant concentration changes across season. September had the highest concentrations, six times higher than the June growing season, which had the lowest concentration of any growing season observed (**Figure 7B**).

Estragole concentrations were significantly impacted by season ($P \leq 0.0001$; $F = 36.57$) and season × treatment interaction ($P = 0.0017$; $F = 1.89$) but did not show significant impacts across treatments ($P = 0.1127$; $F = 1.64$). Midwinter and early fall had the highest levels of estragole, whereas late spring/early summer showed significantly lower levels than all the other seasons (**Figure 7B**).

Hexanal concentrations were significantly impacted by season ($P \leq 0.0001$; $F = 76.86$), treatment ($P \leq 0.0001$; $F = 4.12$), and season × treatment interaction ($P = 0.0002$; $F = 2.14$). Some LED treatments showed separation from the control, but concentrations were relatively low across all treatments as compared to many of the other key flavor volatiles (**Figure 8**).

Total concentrations of key flavor volatiles analyzed in this experiment were significantly impacted by lighting treatment ($P \leq 0.0001$; $F = 81.21$). Total concentrations of VOCs ranged from approximately 4,200–5,800 $\mu M \cdot g^{-1}$ FM (**Figure 9**). The highest total concentration of VOCs was under the 40B/60R and 10B/90R treatments. The HPS treatment was significantly lower than all LED treatments. The lowest concentration was under the NL control.

DISCUSSION

As expected, there were significant differences to VOC profiles across lighting treatments as well as growing season. Even though greenhouses protect from winter weather and poor climate conditions, outside environmental conditions have significant influence on crop production quality and yields. Some factors that may impact volatile concentrations across growing seasons include reduced NL intensity, inferior spectral quality, increased cloud cover, day/night temperature reductions and fluctuations (including difference in day/night temperature, DIF), and changes in relative humidity. SL significantly increased collective terpenoid concentrations during winter months. SL treatments caused significant changes to many VOC concentrations even

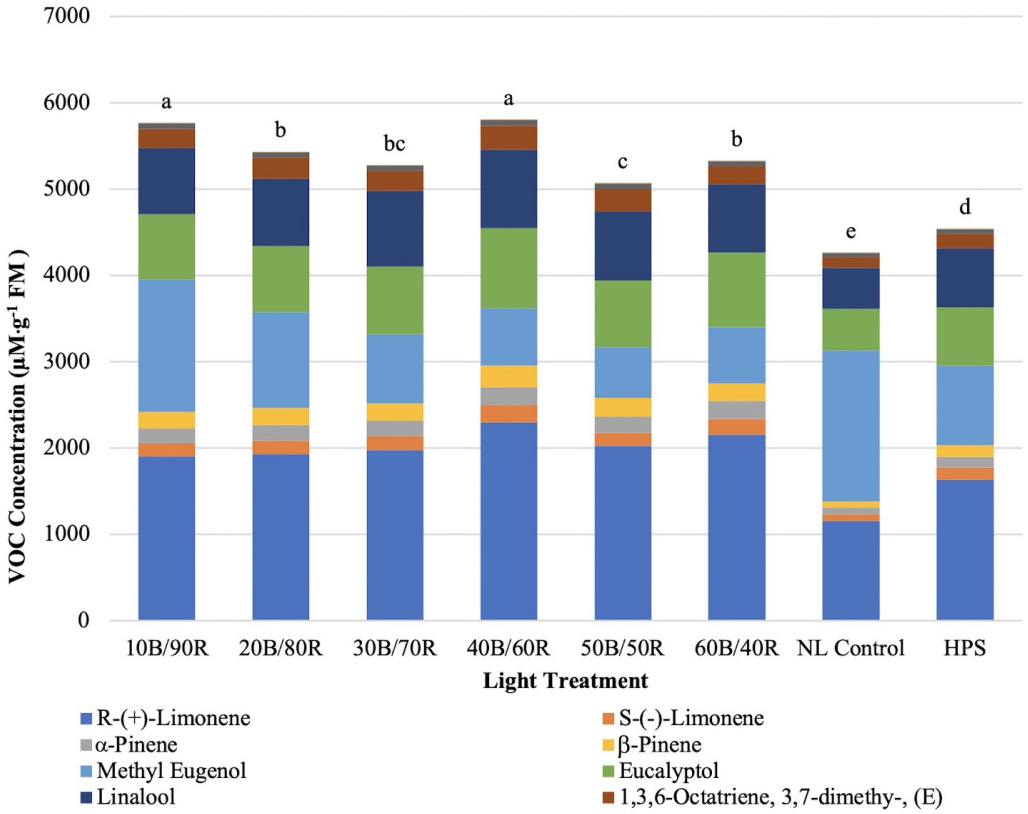

FIGURE 9 | Influence of greenhouse lighting treatments on total key flavor VOC concentrations ($\mu M \cdot g^{-1}$ FM) of hydroponically grown "Genovese" basil (*Ocimum basilicum* var. "Genovese"). Six LED treatments with progressive blue (B)/red (R) ratios (10B/90R, 20B/80R, 30B/70R, 40B/60R, 50B/50R, 60B/40R, expressed as % artificial light intensity), and the high-pressure sodium (HPS) treatment provided supplemental light at 8.64 mol $\cdot m^{-2} \cdot d^{-1}$ (100 μmol $\cdot m^{-2} \cdot s^{-1}$, 24 h $\cdot d^{-1}$). The daily light integral (DLI) of the NL control averaged 9.5 mol $\cdot m^{-2} \cdot d^{-1}$ during the growth period (ranging from 4 to 18 mol $\cdot m^{-2} \cdot d^{-1}$). Supplemental lighting was then compared to the natural light (NL) control. Values were analyzed using Tukey protected LSD, and those followed by the same letter are not significantly different ($\alpha = 0.05$).

during seasons with much higher DLI (close to full saturation for basil) and more favorable NL spectral quality. Key flavor volatiles in basil within specific classes (terpenoids vs. phenols) of secondary metabolites had opposing changes in concentration across growing seasons and followed some general trends that coincide with many studies that investigate the impact of abiotic factors (i.e., DLI and spectral quality) on crop production and physiology (McCree, 1973; Smith, 1982; Lange et al., 2000; Briggs and Christie, 2002; Loughrin and Kasperbauer, 2003; Leonard et al., 2010; Gouvea et al., 2012; Olle and Viršile, 2013; Ouzounis et al., 2015b; Kopsell et al., 2017).

Many of the compounds explored in this study include abundant isoprenoids and phenylpropanoids found in edible tissues from basil that profoundly impact human sensory experience (i.e., flavor and aroma). (S)-(−)-limonene and (R)-(+)-limonene are two important flavor compounds that have significant influence on the sensory perception of basil. (S)-(−)-limonene is said to have an orange like aroma, whereas (R)-(+)-limonene has a stronger lemon/citrus aroma (Larsen et al., 2016). Both monoterpenes possess similar bioactivities (i.e., detection threshold and intensity of sensory response). The combination of these two limonene compounds, in addition to other volatile compounds, contributes to overall citrus flavor. Changes in the relative concentrations of these flavor volatiles determine the "type" of citrus flavor that is perceived by humans as well as the intensity. Both (S)-(−)-limonene and (R)-(+)-limonene concentrations were impacted by lighting treatment and season. This suggests that spectral quality and DLI have a direct impact on secondary pathways upstream from the R/S conformation point and produce higher volumes of both compounds (i.e., increased production of isoprene subunits required for monoterpene production).

November had the highest concentrations of total limonene compounds across all seasons, which may be explained by higher NL intensity during the first stage of development and lower NL intensity as the growing season progressed into late fall. Day/night temperature averages were maintained with a few degrees throughout the growing season. While greenhouses reduce temperature variation across growing seasons, it is nearly impossible for any type of environmental control system to completely eliminate variations in humidity and temperature across all growing seasons. Minute temperature variations are

expected across growing seasons, but do not provide basis for the stark contrast between generalized LED treatment concentrations and HPS treatment concentrations. It is also possible that secondary metabolic carryover effects were experienced from the seedling stage into later growth periods. Multiple studies have found that specific wavelength, light intensities, and temperature variations at the seedling stage can impact secondary metabolism and resource partitioning for specific classes of terpenoids at later stages of development (Massa et al., 2008; Randall and Lopez, 2014; Bantis et al., 2016, 2020; Carvalho et al., 2016; Jishi et al., 2016; Matsuda et al., 2016).

Total concentrations of both compounds did not follow any physiological-based pattern across growing seasons. This is somewhat unexpected as both limonene compounds are so closely related in terms of chemical structure, biosynthesis, bioactivity in humans, and importance in flavor for basil/other herbaceous and citrus crops. This phenomenon of seasonal variation is mostly a result of the interaction between DLI and spectral quality (i.e., the ratio of supplemental/NL at different times of the year), which in turn controls a specific mechanism or pathway up-/down-regulation at the point in the metabolic pathway that determines the R/S conformation. Passive volatilization or other physical chemistry-based phenomena alone cannot explain the differences in limonene compound concentrations across treatments and seasons, as emission would theoretically be similar for both; unless a specific mechanism or active process is responsible for biosynthesizing and/or emitting one volatile over the other as a result of environmental changes. Leaf temperatures were recorded and maintained with 2°C across all treatments and growing seasons, which further reduces the likelihood that passive volatilization is responsible.

α-Pinene and β-pinene are two other monoterpenes that have significant influence on the flavor and aroma of basil, both of which are impacted by the total concentration of all pinene compounds present as well as the concentration ratio of different pinene isomers in relation to one another. Pinene compounds are primarily found in pine resin, and they are one of the most abundant terpenoids in nature (Noma et al., 2010). These compounds have high biological activities in mammals (both beneficial medical properties, as well as moderate toxicity levels) and strongly repel insects. α-Pinene and β-pinene concentrations were impacted by treatment and season. Concentration totals of limonene and pinene compounds followed similar patterns to one another across season, both of which belong to the same chemical class (monoterpenes) and are made in the same pathway deriving from isoprene subunits. Independent of lighting treatment, slightly higher levels of β-pinene were observed in comparison to α-pinene (i.e., ratio of α/β). These ratios remained consistent across lighting treatments but were significantly different across season, further suggesting that changes in both DLI and spectral quality influence secondary metabolism, and these variables have interacting effects on VOC production.

Methyl eugenol (ME) is a phenolic compound that possesses a strong, spicy, herbaceous aroma, which greatly contributes to the flavor and aroma of basil. This compound also has valuable medicinal properties and many human health benefits (Lee et al., 2005). It can be described as having a clove-like flavor and is used extensively in the pharmaceutical and cosmetic industries. This compound has been labeled as an antioxidant, antimutagenic, antigenotoxic, and anti-inflammatory and even has the potential to reduce the recurrence of certain cancers (Carvalho et al., 2016). While ME shows a clear pattern across treatments, it does not show a pattern with increasing DLI across seasons, suggesting that spectral quality has greater influence on ME concentrations when compared to DLI (**Figures 5A,B**). March and April growing seasons showed the lowest ME concentrations. All other growing seasons (September, November, January, June) showed elevated concentrations and did not statistically separate (**Figure 5B**). This was unexpected as there is less ambient NL and inferior spectral quality at the start of the November and January growing seasons as compared to the March and April season. Further, June had the highest DLI, but ME concentrations were not significantly different from the other optimal seasons. ME may be released through passive volatilization in higher quantities due to changes in light intensity and spectral quality because of its high boiling point and vapor pressure. ME is derived from a separate secondary metabolic pathway (may be derived from a variety of pathways, but dominant biosynthesis occurs from the precursor amino acid L-tyrosine and is converted into a variety of eugenol conformations through multistep biosynthesis) as compared to the other terpene-based compounds created from the isoprenoid pathway. This suggests that spectral quality has a direct impact on the resource partitioning in this secondary pathway, specifically tyrosine and other enzymes that are used to synthesize eugenol and other phenolic compounds. These results are consistent with similar studies that investigated the impact of LED lighting on flavor volatiles and resource partitioning of other secondary metabolites (Loughrin and Kasperbauer, 2003; Colquhoun et al., 2013; Samuolienė et al., 2013; Carvalho et al., 2016). Overall concentrations of terpene-based compounds showed concentration increases with the addition of B wavelengths (peaking around 40B/60R and diminishing greatly after that), while ME generally showed concentration decreases with the addition of supplementary B light, which is consistent with results from a similar study (Carvalho et al., 2016). The unexpected changes across seasons may also be a result of varying broad-spectrum light quality and wavelengths not supplemented in the B/R regiment (i.e., variations of other B/R, yellows, greens, oranges, etc.) during certain times of the year. While basil does not exhibit photoperiodic responses toward reproductive growth, many plants have a variety of metabolic processes that are regulated by the interaction of light intensity, duration, and spectral quality, all of which may have an impact on sensory perception (i.e., flavor and aroma) (Banthorpe et al., 1972; Buchanan et al., 2015; Ouzounis et al., 2015a). It is also possible that the B/R treatments had a much more pronounced impact on monoterpene synthesis during winter/early spring months from reduced day-length and light intensity/spectral quality, which diverted resources away from the pathway that synthesizes eugenol compounds. Eugenol, isoeugenol, ME, and several other isomeric compounds should be further investigated to determine the impact of wavelength and intensity on the ratios of these specific compounds and/or overall concentrations of this class

of metabolic products in comparison to other classes, as they all have impacts on flavor and aroma in basil. The benefits (i.e., increase of other terpenoids that are important to flavor) that result from the addition of supplementary wavelengths may outweigh the net loss of ME and other phenolic compounds that are also important to flavor. It is important to note that ME can be somewhat toxic and unpalatable at levels found even in naturally occurring sources; reducing the amount of ME or other somewhat toxic/unpalatable compounds may give growers the opportunity to create designer flavors while optimizing the health benefits of their crop (Reverchon, 1997; Fahlbusch et al., 2003). The biological activities, sensory impacts, and overall health benefits of each key flavor/aroma compound should be further investigated to determine which compounds are most important for basil quality and human sensory perception; in turn, this information may be used to determine the optimal spectrum and intensity of SL treatments to improve flavor and aroma profiles of basil and other high-value greenhouse crops.

Eucalyptol, or 1,8-cineole, is another monoterpene that is closely related in both chemical/physical properties and structure to pinene, limonene, and other secondary metabolites produced from isoprene subunits (Buchanan et al., 2015). Eucalyptol is the primary VOC that influences flavor in a variety of basil cultivars. In general, this compound followed the same pattern as other monoterpenes evaluated in this experiment. Eucalyptol is the most abundant flavor volatile found in basil leaf tissues, accounting for greater than 50% of GC-MS response area in a variety of studies (Loughrin and Kasperbauer, 2003; Lee et al., 2005; Klimánková et al., 2008; Claudia et al., 2013; Tarchoune et al., 2013; Bantis et al., 2016; Carvalho et al., 2016). It has a spicy, energizing, camphoraceous aroma with a cooling mint-like taste. Biological activity related to this compound is extremely high, in addition to moderate toxicity levels at relatively low concentrations. For these reasons, this compound is used in extremely low concentrations when manufacturing food products and cosmetics.

The aroma of linalool can be described as sweet and floral, similar to fruity-pebbles cereal. It has been shown to possess antioxidant and anti-inflammatory properties in addition to numerous other health benefits (Randall and Lopez, 2014; Carvalho et al., 2016). Linalool is a critical component in the overall flavor of basil and many other herbaceous crops. Linalool concentrations were significant impacted by treatment and growing season. Patterns with linalool concentration changes were consistent with other terpenoids in this, as well as other studies involving basil, mint, and other high-value crops (Lee et al., 2005; Galeotti et al., 2008; Colquhoun et al., 2013; Carvalho et al., 2016). α-Humulene is one of the primary chemical constituents that results in the flavor and aroma of flowering cones of the hops plant and many other herbaceous crops. This compound and its reaction products are essential for brewing processes and are responsible for the hoppy flavor and aroma in beer and other fermented products. This sesquiterpene can be found in many other plants in the Lamiaceae family and has relative impacts on flavor and aroma in many basil cultivars/varieties (Lee et al., 2005). Linalool and α-humulene concentrations showed significance across growing seasons, with the highest concentrations in September, March, and April. The lowest concentrations for both isoprenoid compounds were found in June. As they are both created with fundamental isoprene units and found in the same pathway. Concentration levels between the two were found approximately 10:1 linalool:α-humulene and remained constant across all seasons, with less than 5% variance across all seasonal concentration ratios. This is expected, as linalool is a monoterpene and α-humulene is a sesquiterpene, both of which are synthesized primarily in the same metabolic pathway. It was also unexpected that eucalyptol and linalool did not show similar patterns across seasons, suggesting an interaction between varying DLIs and spectral qualities impacting monoterpene synthesis.

1,3,6-Octatriene,3,7- dimethy-,(Z) and 1,3,6-octatriene,3,7-dimethy-,(E) were measured across lighting treatments, both of which exhibit an herbaceous and terpene-based aroma. Limited information was available regarding sensory perception of these compounds, concentrations within basil, the impact of LED lighting treatments on these compounds, or any combination of these areas of study. Only the (E) conformation showed significant differences across treatment and season. Phenyl-2-ethanol has a pleasant floral odor and is used extensively in the food and beverage industries. Early fall concentrations were higher than any other season, whereas late spring/early summer were the lowest. Hexanal is considered an aliphatic aldehyde and is used extensively in the food industry to produce fruity flavors. It has a fruity herbaceous odor that also resembles fresh cut grass. Hexanal concentrations were significantly impacted by treatment and season. Some LED treatments showed separation from the control, but concentrations were relatively low across all treatments. Despite having relatively low concentrations as compared to other flavor volatiles in basil, they have a great importance in flavor perception because of their high biological activities in humans.

These results are consistent with our ongoing conclusion that the combination of both spectral quality and DLI influences secondary metabolism at various points in isoprenoid and phenylpropanoid pathways. Various studies that have investigated narrowband wavelengths in relation to pinene isomers, monoterpene hydrocarbon compounds, and broad secondary metabolic resource partitioning (i.e., phenylpropanoids, sesquiterpenoids, other isoprenoids, etc.) are congruent with the findings of this study (Loughrin and Kasperbauer, 2001; Loughrin and Kasperbauer, 2003; Deschamps and Simon, 2006; Klimánková et al., 2008; Colina-Coca et al., 2013; Colquhoun et al., 2013; Olle and Viršile, 2013; Samuolienė et al., 2013; Tarchoune et al., 2013; Darko et al., 2014; Ouzounis et al., 2014; Selli et al., 2014; Du et al., 2015; Fu et al., 2015; Carvalho et al., 2016).

CONCLUSION

No matter the intended use, sweet basil is highly appreciated for its aroma and flavor. High yields and overall quality are critical foundations of successful commercial growing operations. A variety of quality parameters have been established for the

flavor and aroma of many high-value herbaceous crops. The delicate flavor and aroma of basil are a result of the specific and complex ratios of chemical compounds produced through primary and secondary metabolic processes directly related to environmental conditions and genetic makeup (Lachowicz et al., 1996; Samuolienė et al., 2009; Ouzounis et al., 2014). The impacts of environmental stressors, growing season, and cultivar chemotype are reflected in VOC profiles, which is a direct result of changes to secondary metabolism. The results of this experiment demonstrate that manipulating spectral quality with narrowband supplements can be used to alter secondary metabolic resource allocation (i.e., flavor profile), regardless of season.

Overall, eucalyptol, (R)-(+)-limonene, linalool, and ME showed the highest calibrated concentration abundance in basil for this experiment, approximately 1–3 mM · g^{-1} FM headspace emission across a variety of seasons and treatments. All other flavor volatiles were found in lower concentrations, within the range of 1.0–0.01 mM · g^{-1} FM headspace emission. (R)-(+)-limonene, α-pinene, β-pinene, eucalyptol, and phenyl-2-ethanol showed similar concentration patterns across growing seasons (**Figures 3B**, **4B**, **6B**, **7B**). September showed the highest concentrations of these compounds, whereas November and June showed the lowest concentrations. While the specific concentrations of these individual compounds found in plant tissue varied greatly, they all followed similar concentration ratios as growing seasons progressed (in contrast to phenylpropanoids). The ratios of two important flavor compounds, α-pinene and β-pinene, were similar across lighting treatments but varied across growing seasons, which demonstrates the complex interactions between spectral quality/DLI and the impact they have on secondary metabolism. The use of B/R supplements in addition to natural spectral quality and DLI has the ability to influence flavor volatile profiles and alter secondary metabolic resource partitioning in hydroponically grown sweet basil.

DATA AVAILABILITY STATEMENT

The raw data supporting the conclusions of this article will be made available by the authors, without undue reservation.

AUTHOR CONTRIBUTIONS

HH developed the hypothesis, experimental design, data collection, lab analysis, statistical analysis, and prepared and edited the original manuscript. DK provided input on hypothesis and experimental design, review and editing of the manuscript. CS developed the hypothesis, experimental design, data evaluation, statistical analysis, and review and editing of the manuscript. All the authors contributed to the article and approved the submitted version.

REFERENCES

Abney, K. R., Kopsell, D. A., Sams, C. E., Zivanovic, S., and Kopsell, D. E. (2013). UV-B radiation impacts shoot tissue pigment composition in *Allium fistulosum* L. cultigens. *Sci. World J.* 2013:513867. doi: 10.1155/2013/513867

Banthorpe, D. V., Charlwood, B. V., and Francis, M. J. (1972). The biosynthesis of monoterpenes. *Chem. Rev.* 72, 115–155. doi: 10.1021/cr60276a002

Bantis, F., Koukounaras, A., Siomos, A. S., Fotelli, M. N., and Kintzonidis, D. (2020). Bichromatic red and blue LEDs during healing enhance the vegetative growth and quality of grafted watermelon seedlings. *Sci. Hortic.* 261:109000. doi: 10.1016/j.scienta.2019.109000

Bantis, F., Ouzounis, T., and Radoglou, K. (2016). Artificial LED lighting enhances growth characteristics and total phenolic content of *Ocimum* basilicum, but variably affects transplant success. *Sci. Hortic.* 198, 277–283. doi: 10.1016/j.scienta.2015.11.014

Barbieri, S., Elustondo, M., and Urbicain, M. (2004). Retention of aroma compounds in basil dried with low pressure superheated steam. *J. Food Eng.* 65, 109–115. doi: 10.1016/j.foodeng.2004.01.003

Barta, D. J., Tibbitts, T. W., Bula, R. J., and Morrow, R. C. (1992). Evaluation of light emitting diode characteristics for a space-based plant irradiation source. *Adv. Space Res.* 12, 141–149. doi: 10.1016/0273-1177(92)90020-x

Baumbauer, D. A., Schmidt, C. B., and Burgess, M. H. (2019). Leaf lettuce yield is more sensitive to low daily light integral than kale and Spinach. *HortScience* 54, 2159–2162. doi: 10.21273/hortsci14288-19

Bian, Z. H., Yang, Q. C., and Liu, W. K. (2015). Effects of light quality on the accumulation of phytochemicals in vegetables produced in controlled environments: a review. *J. Sci. Food Agric.* 95, 869–877. doi: 10.1002/jsfa.6789

Bourgaud, F., Gravot, A., Milesi, S., and Gontier, E. (2001). Production of plant secondary metabolites: a historical perspective. *Plant Sci.* 161, 839–851. doi: 10.1016/s0168-9452(01)00490-3

Briggs, W. R., and Christie, J. M. (2002). Phototropins 1 and 2: versatile plant blue-light receptors. *Trends Plant Sci.* 7, 204–210. doi: 10.1016/s1360-1385(02)02245-8

Briggs, W. R., and Huala, E. (1999). Blue-light photoreceptors in higher plants. *Annu. Rev. Cell Dev. Biol.* 15, 33–62. doi: 10.1146/annurev.cellbio.15.1.33

Buchanan, B., Gruissem, W., and Jones, R. (2015). *Biochemistry and Molecular Biology of Plants*, 2nd Edn. Hoboken, NJ: Wiley Blackwell.

Carvalho, S. D., Schwieterman, M. L., Abrahan, C. E., Colquhoun, T. A., and Folta, K. M. (2016). Light quality dependent changes in morphology, antioxidant capacity, and volatile production in sweet Basil (*Ocimum* basilicum). *Front. Plant Sci.* 7:1328. doi: 10.3389/fpls.2016.01328

Chalchat, J. C., and Ozcan, M. M. (2008). Comparative essential oil composition of flowers, leavesand stems of basil (*Ocimum* basilicum L.) used as herb. *Food Chem.* 110, 501–503. doi: 10.1016/j.foodchem.2008.02.018

Charles, D. J., and Simon, J. E. (1990). Comparison of extraction methods for the rapid-determination of essential oil content and composition of Basil. *J. Am. Soc. Hortic. Sci.* 115, 458–462. doi: 10.21273/jashs.115.3.458

Chaves, I., Pokorny, R., Byrdin, M., Hoang, N., Ritz, T., Brettel, K., et al. (2011). The cryptochromes: blue light photoreceptors in plants and animals. *Annu. Rev. Plant Biol.* 62, 335–364. doi: 10.1146/annurev-arplant-042110-103759

Chen, Y., Li, T., Yang, Q., Zhang, Y., Zou, J., Bian, Z., et al. (2019). UVA radiation is beneficial for yield and quality of indoor cultivated lettuce. *Front. Plant Sci.* 10:1563. doi: 10.3389/fpls.2019.01563

Christie, J. M. (2007). Phototropin blue-light receptors. *Annu. Rev. Plant Biol.* 58, 21–45. doi: 10.1146/annurev.arplant.58.032806.103951

Claudia, K., Maggini, R., and Pardossi, A. (2013). Influence of nitrogen nutrition on growth and accumulation of rosmarinic acid in sweet basil (*Ocimum basilicum* L.) grown in hydroponic culture. *Aust. J. Crop Sci.* 7, 321–327.

Colina-Coca, C., Gonzalez-Pena, D., Vega, E., de Ancos, B., and Sanchez-Moreno, C. (2013). Novel approach for the determination of volatile compounds in processed onion by headspace gas chromatography-mass spectrometry (HS GC-MS). *Talanta* 103, 137–144. doi: 10.1016/j.talanta.2012.10.022

Colquhoun, T. A., Schwieterman, M. L., Gilbert, J. L., Jaworski, E. A., Langer, K. M., Jones, C. R., et al. (2013). Light modulation of volatile organic compounds

from petunia flowers and select fruits. *Postharvest Biol. Technol.* 86, 37–44. doi: 10.1016/j.postharvbio.2013.06.013

Darko, E., Heydarizadeh, P., Schoefs, B., and Sabzalian, M. R. (2014). Photosynthesis under artificial light: the shift in primary and secondary metabolism. *Philos. Trans. R. Soc. B Biol. Sci.* 369:20130243. doi: 10.1098/rstb.2013.0243

Deschamps, C., and Simon, J. E. (2006). Terpenoid essential oil metabolism in Basil (*Ocimum* basilicumL.) following elicitation. *JEOR* 18, 618–621. doi: 10.1080/10412905.2006.9699183

Du, X., Song, M., Baldwin, E., and Rouseff, R. (2015). Identification of sulphur volatiles and GC-olfactometry aroma profiling in two fresh tomato cultivars. *Food Chem.* 171, 306–314. doi: 10.1016/j.foodchem.2014.09.013

Fahlbusch, K.-G., Hammerschmidt, F.-J., Panten, J., Pickenhagen, W., Schatkowski, D., Bauer, K., et al. (2003). "Flavors and fragrances," in *Ullmann's Encyclopedia of Industrial Chemistry*, (Weinheim: Wiley-VCH Verlag GmbH), 341–358. doi: 10.1002/14356007.a11_141

Fraikin, G. Y., Strakhovskaya, M. G., and Rubin, A. B. (2013). Biological photoreceptors of light-dependent regulatory processes. *Biochemistry* 78, 1238–1253. doi: 10.1134/S0006297913110047

Frank, H. A., and Cogdell, R. J. (1996). Carotenoids in photosynthesis. *Photochem. Photobiol.* 63, 257–264. doi: 10.1111/j.1751-1097.1996.tb03022.x

Fu, X., Chen, Y., Mei, X., Katsuno, T., Kobayashi, E., Dong, F., et al. (2015). Regulation of formation of volatile compounds of tea (*Camellia sinensis*) leaves by single light wavelength. *Sci. Rep.* 5:16858. doi: 10.1038/srep16858

Galeotti, F., Barile, E., Curir, P., Dolci, M., and Lanzotti, V. (2008). Flavonoids from carnation (*Dianthus caryophyllus*) and their antifungal activity. *Phytochem. Lett.* 1, 44–48. doi: 10.1016/j.phytol.2007.10.001

Galvao, V. C., and Fankhauser, C. (2015). Sensing the light environment in plants: photoreceptors and early signaling steps. *Curr. Opin. Neurobiol.* 34, 46–53. doi: 10.1016/j.conb.2015.01.013

Goins, G. D., Yorio, N. C., Sanwo, M. M., and Brown, C. S. (1997). Photomorphogenesis, photosynthesis, and seed yield of wheat plants grown under red light-emitting diodes (LEDs) with and without supplemental blue lighting. *J. Exp. Bot.* 48, 1407–1413. doi: 10.1093/jxb/48.7.1407

Gouvea, D. R., Gobbo-Neto, L., Sakamoto, H. T., Lopes, N. P., Lopes, J. L. C., Meloni, F., et al. (2012). Seasonal variation of the major secondary metabolites present in the extract of eremanthus mattogrossensis less (*Asteraceae*: *Vernonieae*) leaves. *Química Nova* 35, 2139–2145. doi: 10.1590/s0100-40422012001100007

Hikosaka, S., Ito, K., and Goto, E. (2010). Effects of ultraviolet light on growth, essential oil concentration, and total antioxidant capacity of Japanese mint. *Environ. Control Biol.* 48, 185–190. doi: 10.2525/ecb.48.185

Hussain, A. I., Anwar, F., Hussain Sherazi, S. T., and Przybylski, R. (2008). Chemical composition, antioxidant and antimicrobial activities of basil (*Ocimum* basilicum) essential oils depends on seasonal variations. *Food Chem.* 108, 986–995. doi: 10.1016/j.foodchem.2007.12.010

Jishi, T., Kimura, K., Matsuda, R., and Fujiwara, K. (2016). Effects of temporally shifted irradiation of blue and red LED light on cos lettuce growth and morphology. *Sci. Hortic.* 198, 227–232. doi: 10.1016/j.scienta.2015.12.005

Kang, Y., Khan, S., and Ma, X. (2009). Climate change impacts on crop yield, crop water productivity and food security – A review. *Prog. Nat. Sci.* 19, 1665–1674. doi: 10.1016/j.pnsc.2009.08.001

Kesselmeier, J., and Staudt, M. (1999). Biogenic volatile organic compounds (VOC): an overview on emission, physiology and ecology. *J. Atmos. Chem.* 33, 23–88. doi: 10.1023/a:1006127516791

Kim, M. J., Moon, Y., Kopsell, D. A., Park, S., Tou, J. C., and Waterland, N. L. (2016). Nutritional value of crisphead 'Iceberg' and romaine lettuces (*Lactuca sativa* L.). *J. Agric. Sci.* 8, 1–10. doi: 10.5539/jas.v8n11p1

Klimánková, E., Holadová, K., Hajšlová, J., Čajka, T., Poustka, J., and Koudela, M. (2008). Aroma profiles of five basil (*Ocimum* basilicum L.) cultivars grown under conventional and organic conditions. *Food Chem.* 107, 464–472. doi: 10.1016/j.foodchem.2007.07.062

Kong, Y., Schiestel, K., and Zheng, Y. (2019). Pure blue light effects on growth and morphology are slightly changed by adding low-level UVA or far-red light: a comparison with red light in four microgreen species. *Environ. Exp. Bot.* 157, 58–68. doi: 10.1016/j.envexpbot.2018.09.024

Kopsell, D. A., Kopsell, D. E., and Curran-Celentano, J. (2005). Carotenoid and chlorophyll pigments in sweet basil grown in the field and greenhouse. *HortScience* 40, 1230–1233. doi: 10.21273/hortsci.40.5.1230

Kopsell, D. A., and Sams, C. E. (2013). Increases in shoot tissue pigments, glucosinolates, and mineral elements in sprouting broccoli after exposure to short-duration blue light from light emitting diodes. *J. Am. Soc. Hortic. Sci.* 138, 31–37. doi: 10.21273/jashs.138.1.31

Kopsell, D. A., Sams, C. E., Barickman, T. C., and Morrow, R. C. (2014). Sprouting broccoli accumulate higher concentrations of nutritionally important metabolites under narrow-band light-emitting diode lighting. *J. Am. Soc. Hortic. Sci.* 139, 469–477. doi: 10.21273/jashs.139.4.469

Kopsell, D. A., Sams, C. E., and Morrow, R. C. (2015). Blue wavelengths from LED lighting increase nutritionally important metabolites in specialty crops. *HortScience* 50, 1285–1288. doi: 10.21273/hortsci.50.9.1285

Kopsell, D. A., Sams, C. E., and Morrow, R. C. (2017). Interaction of light quality and fertility on biomass, shoot pigmentation and xanthophyll cycle flux in Chinese kale. *J Sci Food Agric* 97, 911–917. doi: 10.1002/jsfa.7814

Lachowicz, K. J., Jones, G. P., Briggs, D. R., Bienvenu, F. E., Palmer, M. V., Ting, S. S. T., et al. (1996). Characteristics of essential oil from Basil (*Ocimum* basilicumL.) grown in Australia. *J. Agric. Food Chem.* 44, 877–881. doi: 10.1021/jf9405214

Landi, M., Zivcak, M., Sytar, O., Brestic, M., and Allakhverdiev, S. I. (2020). Plasticity of photosynthetic processes and the accumulation of secondary metabolites in plants in response to monochromatic light environments: a review. *Biochim. Biophys. Acta Bioenerg.* 1861:148131. doi: 10.1016/j.bbabio.2019.148131

Lange, B. M., Rujan, T., Martin, W., and Croteau, R. (2000). Isoprenoid biosynthesis: the evolution of two ancient and distinct pathways across genomes. *Proc. Natl. Acad. Sci. U.S.A.* 97, 13172–13177. doi: 10.1073/pnas.240454797

Larsen, S. T., Hougaard, K. S., Hammer, M., Alarie, Y., Wolkoff, P., Clausen, P. A., et al. (2016). Effects of R-(+)-and S-(-)-limonene on the respiratory tract in mice. *Hum. Exp. Toxicol.* 19, 457–466. doi: 10.1191/096032700682694233

Lee, S. J., Umano, K., Shibamoto, T., and Lee, K. G. (2005). Identification of volatile components in basil (*Ocimum basilicum* L.) and thyme leaves (*Thymus vulgaris* L.) and their antioxidant properties. *Food Chem.* 91, 131–137. doi: 10.1016/j.foodchem.2004.05.056

Lefsrud, M. G., Kopsell, D. A., Kopsell, D. E., and Randle, W. M. (2006). Kale carotenoids are unaffected by, whereas biomass production, elemental concentrations, and selenium accumulation respond to, changes in selenium fertility. *J. Agric. Food Chem.* 54, 1764–1771. doi: 10.1021/jf052478y

Lefsrud, M. G., Kopsell, D. A., and Sams, C. E. (2008). Irradiance from distinct wavelength light-emitting diodes affect secondary metabolites in kale. *HortScience* 43, 2243–2244. doi: 10.21273/hortsci.43.7.2243

Leonard, E., Ajikumar, P. K., Thayer, K., Xiao, W. H., Mo, J. D., Tidor, B., et al. (2010). Combining metabolic and protein engineering of a terpenoid biosynthetic pathway for overproduction and selectivity control. *Proc. Natl. Acad. Sci. U.S.A.* 107, 13654–13659. doi: 10.1073/pnas.1006138107

Li, Q., and Kubota, C. (2009). Effects of supplemental light quality on growth and phytochemicals of baby leaf lettuce. *Environ. Exp. Bot.* 67, 59–64. doi: 10.1016/j.envexpbot.2009.06.011

Lichtenthaler, H. K. (1987). [34] chlorophylls and carotenoids: pigments of photosynthetic biomembranes. *Methods Enzymol.* 148:350–382. doi: 10.1016/0076-6879(87)48036-1

Loughrin, J. H., and Kasperbauer, M. J. (2001). Light reflected from colored mulches affects aroma and phenol content of sweet Basil (*Ocimum basilicum* L.) leaves. *J. Agric. Food Chem.* 49, 1331–1335. doi: 10.1021/jf0012648

Loughrin, J. H., and Kasperbauer, M. J. (2003). Aroma content of fresh basil (*Ocimum* basilicum L.) leaves is affected by light reflected from colored mulches. *J. Agric. Food Chem.* 51, 2272–2276. doi: 10.1021/jf021076c

Lucchesi, M. E., Chemat, F., and Smadja, J. (2004). Solvent-free microwave extraction of essential oil from aromatic herbs: comparison with conventional hydro-distillation. *J. Chromatogr. A* 1043, 323–327. doi: 10.1016/j.chroma.2004.05.083

Massa, G. D., Kim, H.-H., Wheeler, R. M., and Mitchell, C. A. (2008). Plant Productivity in Response to LED Lighting. *HortScience* 43, 1951–1956. doi: 10.21273/hortsci.43.7.1951

Matsuda, R., Yamano, T., Murakami, K., and Fujiwara, K. (2016). Effects of spectral distribution and photosynthetic photon flux density for overnight LED light irradiation on tomato seedling growth and leaf injury. *Sci. Hortic.* 198, 363–369. doi: 10.1016/j.scienta.2015.11.045

McCree, K. J. (1973). The measurement of photosynthetically active radiation. *Sol. Energy* 15, 83–87. doi: 10.1016/0038-092x(73)90010-8

Metallo, R. M., Kopsell, D. A., Sams, C. E., and Bumgarner, N. R. (2018). Influence of blue/red vs. white LED light treatments on biomass, shoot morphology, and quality parameters of hydroponically grown kale. *Sci. Hortic.* 235, 189–197. doi: 10.1016/j.scienta.2018.02.061

Montgomery, B. L. (2016). Mechanisms and fitness implications of photomorphogenesis during chromatic acclimation in cyanobacteria. *J. Exp. Bot.* 67, 4079–4090. doi: 10.1093/jxb/erw206

Morrow, R. C. (2008). LED lighting in horticulture. *HortScience* 43, 1947–1950. doi: 10.21273/hortsci.43.7.1947

Noma, Y., Hashimoto, T., Uehara, S., and Asakawa, Y. (2010). Microbial transformation of isopinocampheol and caryophyllene oxide. *Flavour Fragr. J.* 25, 161–170. doi: 10.1002/ffj.1988

Olfati, J. A., Khasmakhi-Sabet, S. A., and Shabani, H. (2012). Nutrient solutions on yield and quality of basil and cress. *Int. J. Veg. Sci.* 18, 298–304. doi: 10.1080/19315260.2011.642475

Olle, M., and Viršile, A. (2013). The effects of light-emitting diode lighting on greenhouse plant growth and quality. *Agr. Food Sci.* 22, 223–234. doi: 10.23986/afsci.7897

Ouzounis, T., Fretté, X., Rosenqvist, E., and Ottosen, C.-O. (2014). Spectral effects of supplementary lighting on the secondary metabolites in roses, chrysanthemums, and campanulas. *J. Plant Physiol.* 171, 1491–1499. doi: 10.1016/j.jplph.2014.06.012

Ouzounis, T., Razi Parjikolaei, B., Frette, X., Rosenqvist, E., and Ottosen, C. O. (2015a). Predawn and high intensity application of supplemental blue light decreases the quantum yield of PSII and enhances the amount of phenolic acids, flavonoids, and pigments in Lactuca sativa. *Front. Plant Sci.* 6:19. doi: 10.3389/fpls.2015.00019

Ouzounis, T., Rosenqvist, E., and Ottosen, C.-O. (2015b). spectral effects of artificial light on plant physiology and secondary metabolism: a review. *HortScience* 50, 1128–1135. doi: 10.21273/hortsci.50.8.1128

Pimputkar, S., Speck, J. S., DenBaars, S. P., and Nakamura, S. (2009). Prospects for LED lighting. *Nat. Photonics* 3, 179–181. doi: 10.1038/nphoton.2009.32

Politeo, O., Jukic, M., and Milos, M. (2007). Chemical composition and antioxidant capacity of free volatile aglycones from basil (*Ocimum* basilicum L.) compared with its essential oil. *Food Chem.* 101, 379–385. doi: 10.1016/j.foodchem.2006.01.045

Raimondi, G., Orsini, F., Maggio, A., De Pascale, S., and Barbieri, G. (2006). Yield and quality of hydroponically grown sweet basil cultivars. *Acta Hortic.* 723, 353–359. doi: 10.17660/ActaHortic.2006.723.48

Randall, W. C., and Lopez, R. G. (2014). Comparison of supplemental lighting from high-pressure sodium lamps and light-emitting diodes during bedding plant seedling production. *HortScience* 49, 589–595. doi: 10.21273/hortsci.49.5.589

Reverchon, E. (1997). Supercritical fluid extraction and fractionation of essential oils and related products. *J. Supercrit. Fluid* 10, 1–37. doi: 10.1016/S0896-8446(97)00014-4

Samuolienė, G., Brazaitytė, A., Sirtautas, R., Viršilė, A., Sakalauskaitė, J., Sakalauskienė, S., et al. (2013). LED illumination affects bioactive compounds in romaine baby leaf lettuce. *J. Sci. Food Agric.* 93, 3286–3291. doi: 10.1002/jsfa.6173

Samuolienė, G., Urbonaviciūtė, A., Brazaitytė, A., Jankauskienė, J., Duchovskis, P., Bliznikas, Z., et al. (2009). The benefits of red LEDs: improved nutritional quality due to accelerated senescence in lettuce. *Sci. Work Lith. Inst. Hortic. Lith. Univ. Agric.* 28, 111–120.

Samuoliene, G., Virsile, A., Haimi, P., and Miliauskiene, J. (2020). Photoresponse to different lighting strategies during red leaf lettuce growth. *J. Photochem. Photobiol. B* 202:111726. doi: 10.1016/j.jphotobiol.2019.111726

Selli, S., Kelebek, H., Ayseli, M. T., and Tokbas, H. (2014). Characterization of the most aroma-active compounds in cherry tomato by application of the aroma extract dilution analysis. *Food Chem.* 165, 540–546. doi: 10.1016/j.foodchem.2014.05.147

Smith, H. (1982). Light quality, photoperception, and plant strategy. *Annu. Rev. Plant Physiol. Plant Mol. Biol.* 33, 481–518. doi: 10.1146/annurev.pp.33.060182.002405

Sugimoto, M., Kawakami, M., Robert, M., Soga, T., and Tomita, M. (2012). Bioinformatics tools for mass spectroscopy-based metabolomic data processing and analysis. *Curr. Bioinform.* 7, 96–108. doi: 10.2174/157489312799304431

Tarchoune, I., Baatour, O., Harrathi, J., Cioni, P. L., Lachaal, M., Flamini, G., et al. (2013). Essential oil and volatile emissions of basil (*Ocimum* basilicum) leaves exposed to NaCl or Na2SO4 salinity. *J. Plant Nutr. Soil Sci.* 176, 748–755. doi: 10.1002/jpln.201200278

Taylor, A. J. (1996). Volatile flavor release from foods during eating. *Crit. Rev. Food Sci. Nutr.* 36, 765–784. doi: 10.1080/10408399609527749

Tennessen, D. J., Singsaas, E. L., and Sharkey, T. D. (1994). Light-emitting diodes as a light source for photosynthesis research. *Photosynth. Res.* 39, 85–92. doi: 10.1007/BF00027146

Treadwell, D. D., Hochmuth, G. J., Hochmuth, R. C., Simonne, E. H., Sargent, S. A., Davis, L. L., et al. (2011). Organic fertilization programs for greenhouse fresh-cut Basil and spearmint in a soilless media trough system. *HortTechnology* 21, 162–169. doi: 10.21273/horttech.21.2.162

Tuan, P. A., Thwe, A. A., Kim, Y. B., Kim, J. K., Kim, S. J., Lee, S., et al. (2013). Effects of white, blue, and red light-emitting diodes on carotenoid biosynthetic gene expression levels and carotenoid accumulation in sprouts of tartary buckwheat (*Fagopyrum tataricum* Gaertn.). *J. Agric. Food Chem.* 61, 12356–12361. doi: 10.1021/jf4039937

Wink, M. (2010). *Biochemistry of Plant Secondary Metabolism*, Vol. 40. Hoboken, NJ: Wiley.

Yan, Z., He, D., Niu, G., and Zhai, H. (2019). Evaluation of growth and quality of hydroponic lettuce at harvest as affected by the light intensity, photoperiod and light quality at seedling stage. *Sci. Hortic.* 248, 138–144. doi: 10.1016/j.scienta.2019.01.002

Yousif, A. N., Scaman, C. H., Durance, T. D., and Girard, B. (1999). Flavor volatiles and physical properties of vacuum-microwave- and air-dried sweet basil (*Ocimum* basilicum L.). *J. Agric. Food Chem.* 47, 4777–4781. doi: 10.1021/jf990484m

Zhang, M., Whitman, C. M., and Runkle, E. S. (2019). Manipulating growth, color, and taste attributes of fresh cut lettuce by greenhouse supplemental lighting. *Sci. Hortic.* 252, 274–282. doi: 10.1016/j.scienta.2019.03.051

Conflict of Interest: The authors declare that the research was conducted in the absence of any commercial or financial relationships that could be construed as a potential conflict of interest.

Copyright © 2021 Hammock, Kopsell and Sams. This is an open-access article distributed under the terms of the Creative Commons Attribution License (CC BY). The use, distribution or reproduction in other forums is permitted, provided the original author(s) and the copyright owner(s) are credited and that the original publication in this journal is cited, in accordance with accepted academic practice. No use, distribution or reproduction is permitted which does not comply with these terms.

frontiers in Plant Science

REVIEW
published: 31 May 2021
doi: 10.3389/fpls.2021.620021

Cannabinoids and Terpenes: How Production of Photo-Protectants Can Be Manipulated to Enhance *Cannabis sativa* L. Phytochemistry

*Vincent Desaulniers Brousseau, Bo-Sen Wu, Sarah MacPherson, Victorio Morello and Mark Lefsrud**

Department of Bioresource Engineering, McGill University, Sainte-Anne-de-Bellevue, QC, Canada

Cannabis sativa L. is cultivated for its secondary metabolites, of which the cannabinoids have documented health benefits and growing pharmaceutical potential. Recent legal cannabis production in North America and Europe has been accompanied by an increase in reported findings for optimization of naturally occurring and synthetic cannabinoid production. Of the many environmental cues that can be manipulated during plant growth in controlled environments, cannabis cultivation with different lighting spectra indicates differential production and accumulation of medically important cannabinoids, including Δ^9-tetrahydrocannabinol (Δ^9-THC), cannabidiol (CBD), and cannabigerol (CBG), as well as terpenes and flavonoids. Ultraviolet (UV) radiation shows potential in stimulating cannabinoid biosynthesis in cannabis trichomes and pre-harvest or post-harvest UV treatment merits further exploration to determine if plant secondary metabolite accumulation could be enhanced in this manner. Visible LED light can augment THC and terpene accumulation, but not CBD. Well-designed experiments with light wavelengths other than blue and red light will provide more insight into light-dependent regulatory and molecular pathways in cannabis. Lighting strategies such as subcanopy lighting and varied light spectra at different developmental stages can lower energy consumption and optimize cannabis PSM production. Although evidence demonstrates that secondary metabolites in cannabis may be modulated by the light spectrum like other plant species, several questions remain for cannabinoid production pathways in this fast-paced and growing industry. In summarizing recent research progress on light spectra and secondary metabolites in cannabis, along with pertinent light responses in model plant species, future research directions are presented.

Keywords: light emitting diode, light spectrum, light wavelength, photobiology, secondary metabolites, tetrahydrocannabinol, ultraviolet

OPEN ACCESS

Edited by:
Inga Mewis, Humboldt University of Berlin, Germany

Reviewed by:
Radmila Pavlovic, University of Milan, Italy
Waseem Gul, ElSohly Laboratories Inc, United States

****Correspondence:***
Mark Lefsrud
mark.lefsrud@mcgill.ca

Specialty section:
This article was submitted to Plant Metabolism and Chemodiversity, a section of the journal Frontiers in Plant Science

Received: *21 October 2020*
Accepted: *07 May 2021*
Published: *31 May 2021*

Citation:
Desaulniers Brousseau V, Wu B-S, MacPherson S, Morello V and Lefsrud M (2021) Cannabinoids and Terpenes: How Production of Photo-Protectants Can Be Manipulated to Enhance Cannabis sativa L. Phytochemistry. Front. Plant Sci. 12:620021. doi: 10.3389/fpls.2021.620021

INTRODUCTION

Secondary metabolites from plants, animals, and microorganisms drive many medical and pharmacological applications, building on thousands of years of traditional medicine (Stojanoski, 1999). In depth characterization of isolated plant secondary metabolites (PSM) for medical treatment started at least 200 years ago, and it has progressed exponentially during the last

30 to 40 years (Okada et al., 2010). One notable and historical medical application is the isolation of morphine from poppy (*Papaver somniferum*) seed oil in the early 1800s (Krishnamurti and Rao, 2016). This alkaloid and its derivatives, opiates, are used for managing pain, yet they have contributed to a deadly and costly opioid crisis because of their addictive nature (Dasgupta et al., 2018).

The cannabis plant (*Cannabis sativa* L.) possesses more than 500 known PSM, including cannabinoids, terpenes, and flavonoids (Elsohly et al., 2017; Solymosi and Köfalvi, 2017; Gonçalves et al., 2019). Research on cannabis PSM has grown rapidly because of therapeutic potential. The cannabinoid Δ^9-tetrahydrocannabinol (Δ^9-THC), a hallmark of medical cannabis, reportedly exerts anticancer (White et al., 1976), antibacterial (Van Klingeren and Ten Ham, 1976), antiemetic (Garb, 1981), and analgesic action *via* modulation of the endocannabinoid system (Mao et al., 2000), and it remains a possible alternative to opiates for managing neuropathies and treatment-resistant spasticity (Abrams, 2019). Specific cannabinoid-terpenoid ratios from herbal extracts have shown further promise (Gonçalves et al., 2019), and provide support for the "entourage effect," the postulated synergistic action of cannabinoids and terpenes with notable examples in pain management (Johnson et al., 2010), analgesia (Gallily et al., 2015), cancer (Blasco-Benito et al., 2018), and severe epilepsy (Goldstein, 2016).

Prior to cannabis legalization, our knowledge of cannabis PSM production primarily stemmed from illegal production operations (Vanhove et al., 2011). Over the last few years, enormous progress has been made toward advancing cannabis-related medicine (Hutchison et al., 2019) and cannabis biotechnology (i.e., productivity and molecular biology) (Hesami et al., 2020). Phytochemical characterization of a given cultivar (or the newly coined term "chemovar"), including biochemical and pharmacological properties, could drive this next era of medicine forward (Russo, 2019), but thorough understanding of cannabis PSM production and accumulation mechanisms are required. Contemporary medicine highlights cannabinoids, terpenes, and flavonoids as promising PSMs for treating multiple ailments (Aliferis and Bernard-Perron, 2020).

Evidence suggests that growing conditions (i.e., light, nutrients, temperature, and microbiome) can be manipulated to improve and optimize production of specific compounds. Light triggers plant secondary metabolism and PSM accumulation, although how optical and spectral properties (i.e., wavelength, bandwidth, and intensity) impact cannabis PSM production remains unclear (Hawley, 2018; Magagnini et al., 2018; Namdar et al., 2019). This review aims to bridge the gap between light properties and cannabis PSM production, by recalling PSM origin and function in plants. An overview of the cannabis PSM biosynthesis, including cannabinoid, terpene, and flavonoid, is provided in the support of the "entourage effect" (Baron, 2018; Tomko et al., 2020). Available light study findings on cannabis PSM production in response to different light treatments are summarized, with an emphasis on ultraviolet (UV) radiation during plant growth.

EVOLUTIVE PERSPECTIVE OF PLANT SECONDARY METABOLITES

PSM are assembled from primary metabolite precursors (Seca and Pinto, 2019). These PSM are not essential to plants' survival; rather, they allow plants to withstand abiotic and biotic stress (drought or water stress, light or predatory stress) (Bourgaud et al., 2001). PSM molecular pathways are conserved between plant families through gene clusters. Genome sequencing has shown that these gene clusters are highly conserved between plants of different families because of their shared evolutive origin (Nützmann et al., 2016). In *C. sativa* L., cannabinoid and terpene biosynthesis reportedly contributes to protection against UV radiation and chemical stressors created to combat insects (Pate, 1994; Benelli et al., 2018).

PSM likely evolved in an environment where biotic stressors played a lesser role in driving evolutive adaptation (Tossi et al., 2019). By looking at other PSM functions and their role in the plant's response to abiotic stress, one theory states that to survive in shallow water, ancestral algae evolved mechanisms to survive in an environment with elevated UV radiation (<380 nm), a primordial abiotic stressor (Akula and Ravishankar, 2011; Jenkins, 2017). UV radiation leads to damaged DNA and photosystems, resulting in reduced production (Teramura, 1983). Plants evolved mechanisms to protect against this radiation stress by accumulating phenolic and terpenoid compounds that absorb UV radiation and acted as sunscreen in leaves (Rozema et al., 2002). This allowed photosynthetic organisms to grow in new ecological niches, while exposing themselves to increasing UV radiation (Tossi et al., 2019). This theory is supported by the apparition of a highly conserved receptor, UV-B Resistance 8 (UVR8) in terrestrial plants that mediates plant photomorphogenesis in response to UV radiation (Jenkins, 2017; Tossi et al., 2019). Parallel to the abiotic stress response, the large diversity of PSM can also be explained by exposure to biotic stress and

Abbreviations: CBC, cannabichromene; CBCA, cannabichromentic acid; CBCAS, cannabichromentic acid synthase; CBDAS, cannabidiolic acid synthase; CBD, cannabidiol; CBDA, cannabidiolic acid; CBG, cannabigerol; CBGA, cannabigerolic acid; CBL, cannabicyclol; CBLA, cannabicyclolic acid; CBN, cannabinol; CBNA, cannabinolic acid; CHS, chalcone synthase; CHI, chalcone isomerase; CsOMT21, *C. sativa* L. O-methyltransferase 21; CsPT3, *C. sativa* L. prenyltransferase 3; C4H, cinnamate 4-hydroxylase; C3H, p-coumaroyl-CoA 3-hydroxylase; DMAPP, dimethylallyl pyrophosphate; DXS, 1-deoxy d-xylulose-5-phosphate synthase; DXP, 1-deoxy-D-xylulose 5- phosphate; FNS, flavone synthase; FPP, farnesyl diphosphate; FPPS, farnesyl diphosphate synthase; F3'H, flavonoid 3'-hydrolase; G3P, glyceraldehyde 3-phosphate; GPP, geranyl pyrophosphate; GPPS, geranyl pyrophosphate synthase; HEDS or HvCHS, homoeriodictyol/eriodictyol synthase; HPS, high pressure sodium; IPP, isopentenyl diphosphate; IPPi, isopentenyl-diphosphate delta-isomerase; LED, light-emitting diode; LS, limonene synthase; MEP, methylerythritol phosphate; MEV, mevalonate; OA, olivetolic acid; OAC, olivetolic acid cyclase; OMT, SAM-methyltransferase; PAL, phenylalanine ammonia-lyase; PSM, plant secondary metabolite; PT4, geranylpyrophosphate: olivetolate geranyltransferase 4; Δ^8-THC, Δ^8-tetrahydrocannabinol; Δ^9-THC (or THC), Δ^9-tetrahydrocannabinol; THCA, tetrahydrocannabinolic acid; THCAS, tetrahydrocannabinolic acid synthase; THCV, tetrahydrocannabivarin; TPS, terpene synthase; TK, tetraketide; TKS, tetraketide synthase; UV, ultraviolet; 4CL, 4-Coumarate:CoA ligase.

the co-evolution of insects and plants during terrestrialization in the Neoproterozoic era (1,000 to 541 million years ago) (Theis and Lerdau, 2003; Labandeira, 2005). Plants evolved attractant and deterrent cues through their PSM to favor pollination and decrease predation (Kessler and Halitschke, 2007). Studies report that cannabis PSM extracts, specifically hemp extracts, effectively repel insects (Mcpartland, 1997; Benelli et al., 2018). The cannabis microbiome also influences plant metabolism. A recent review highlights promising avenues of PSM modulation in cannabis through endophytes (Taghinasab and Jabaji, 2020).

TRICHOMES AND CANNABIS PROFILING

Trichomes

Trichomes form a large group of plant structures that are uni- or multicellular epidermal appendages, classified by their origin, form, function, and secretion (Werker, 2000). These structures are responsible for synthesis and storage of cannabinoids and terpenes in *C. sativa* L., accumulating in resin heads (Hudson, 1963). They protect plants from light stress (Lydon et al., 1987), high heat (Levin, 1973; Lapinjoki et al., 1991), and herbivore pressure (Pillemer and Tingey, 1976; Alahakoon et al., 2016). Other mechanisms, including water absorption through dew collection, salt secretion, and alluring function, are reported (Werker, 2000).

All aerial parts of the cannabis plant are covered with trichomes, and can be classified as either "glandular" or "non-glandular" (Dayanandan and Kaufman, 1976). Glandular trichomes contain more bioactive/psychoactive compounds than non-glandular trichomes (Raman et al., 2017; Livingston et al., 2020). Glandular trichomes are found on all anatomical plant parts except the hypocotyl and cotyledon, and non-glandular trichomes are found on stems, leaves, petioles, stipules, bract, and tepals (Raman et al., 2017).

Glandular trichome classification relates to morphological traits and composition of the chemical substance secreted (Werker, 2000). Three types of glandular trichomes in the cannabis plant are described and size-differentiated: capitate-stalked, capitate-sessile, and bulbous trichomes (Dayanandan and Kaufman, 1976; Hammond and Mahlberg, 1977). Capitate-stalked trichomes are found exclusively on flowering regions, whereas capitate-sessile and bulbous trichomes are found everywhere except the hypocotyl and cotyledon (Raman et al., 2017). In *C. sativa* L., high THC-containing strains had a bigger resin head on their glandular trichomes than in low-THC industrial hemp (Small and Naraine, 2016). Capitate-stalked glandular trichomes have more secretory disc cells than other plants and secrete specialized metabolites in the subcuticular oil storage cavity, instead of through pores formed in the cuticle (Tissier, 2012; Huchelmann et al., 2017). Excretory cells secrete a resin in a subcuticular cavity (Small and Naraine, 2016). This resin contains high concentrations of the economically important cannabinoids, with psychoactive and medicinal properties (Dayanandan and Kaufman, 1976; Small and Naraine, 2016). Optimal cannabinoid and terpene biosynthesis in glandular trichomes is of paramount importance to bud quality (El-Alfy et al., 2010; Friedman and Devinsky, 2015).

Cannabinoids and Cannabis Profiling

Cannabinoids, also called meroterpenes or terpenophenols, are PSM synthesized by members of the *Cannabaceae* family, and several other plant species, including *Echinacea purpurea, Echinacea angustifolia, Acmella oleracea, Helichrysum umbraculigerum,* and *Radula marginata* (Bauer et al., 2008). More than 20% of isolated cannabis PSMs are cannabinoids (Chandra et al., 2017). The two major cannabinoids, Δ^9-THC and cannabidiol (CBD), are used to classify cannabis (Bruci et al., 2012; Piluzza et al., 2013; Hilderbrand, 2018), and differentiation between marijuana and hemp is often based on Δ^9-THC content from cannabis biomass. Cannabis extract with a Δ^9-THC percentage greater than 0.3% is classified as a medical marijuana product, whereas *C. sativa* L. with a Δ^9-THC content of less than 0.3% is cultivated as hemp (Hilderbrand, 2018). Three *C. sativa* L. chemotypes have further been distinguished and classified, determined by the relative proportions of Δ^9-THC and CBD: drug-type (Δ^9-THC is the predominant cannabinoid, known as marijuana), intermediate-type (both Δ^9-THC and CBD are predominant), and fiber-type (CBD is the predominant cannabinoid, known as hemp) (Bruci et al., 2012; Piluzza et al., 2013). This differentiation based on cannabinoid content or cannabis cultivars is inadequate, particularly for the medical industry, since it does not reflect or match the therapeutic and medical properties (Russo, 2019). The term "chemovar," which considers the specific ratios of cannabinoids, flavonoids, and terpenes, will likely be a better tool in the development of cannabis-assisted medicine (Baron, 2018).

CANNABIS PSMs AND BIOSYNTHESIS

Changes in PSM biosynthesis during ontological development of cannabis are well-studied, starting with cannabinoid and monoterpene concentrations in flowers in the first weeks of the flowering phase, and ending with almost four times the quantity in a matter of 7 weeks (Aizpurua-Olaizola et al., 2016). At least 113 cannabinoids and 120 terpenes have been identified (Elsohly and Slade, 2005; Elsohly and Gul, 2014; Ahmed et al., 2015), and they are heavily concentrated in virgin female inflorescence (Turner et al., 1980). PSMs are usually extracted from this, as maximal PSM accumulation is often found in glandular trichomes. Other studies have concentrated on determining the role that flavonoids play in cannabis physiology, and how cannabis-specific flavonoids may be exploited (Barrett et al., 1985; Pollastro et al., 2018).

Cannabinoids

Figure 1 shows the cannabinoid biosynthesis pathway and precursor formation. Primary biosynthesis steps are impacted by UV radiation and blue light (Dolzhenko et al., 2010; Booth et al., 2017; Jin et al., 2019; Nazari and Zarinkamar, 2020). Cannabinoid biosynthesis starts as isopentenyl diphosphate (IPP), formed from glyceraldehyde 3-phosphate (G3P), and pyruvate in plastids (Mcgarvey and Croteau, 1995). Formation of IPP in plastids is

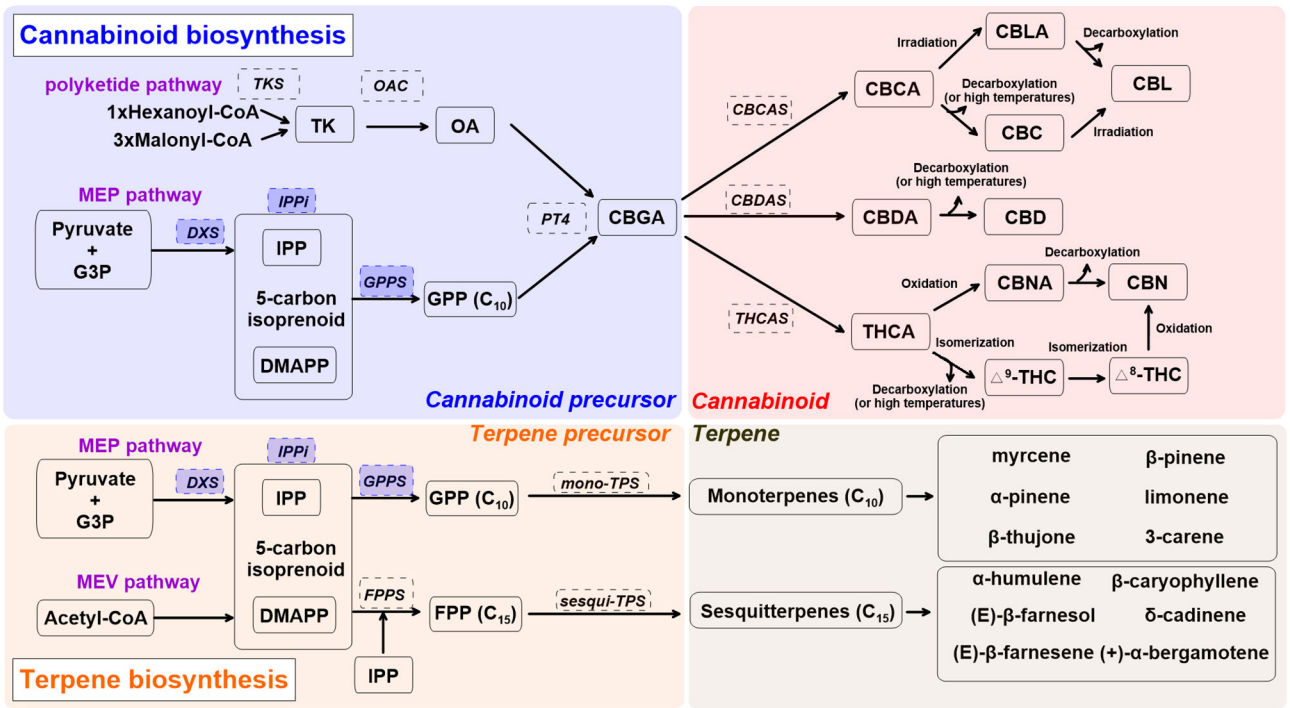

FIGURE 1 | A simplified overview of cannabinoid and terpene biosynthesis pathways in cannabis (*Cannabis sativa* L.), derived from recent reviews (Hazekamp, 2007; Degenhardt et al., 2017; Sirikantaramas and Taura, 2017; Jin et al., 2019). Enzymes are in dashed line box. Enzymes in shaded blue boxes are upregulated by UV radiation and blue light in Lamiaceae. Cannabis precursor (shade blue): CBDA, cannabidiolic acid; DMAPP, dimethylallyl pyrophosphate; G3P, glyceraldehyde 3-phosphate; GPP, geranyl pyrophosphate; GPPS, geranyl pyrophosphate synthase; MEP, methylerythritol phosphate; PT4, geranylpyrophosphate: olivetolate geranyltransferase 4; IPP, isopentenyl diphosphate; IPPi, isopentenyl-diphosphate delta-isomerase; OA, olivetolic acid; OAC, olivetolic acid cyclase; TK, tetraketide; TKS, tetraketide synthase. Cannabinoid (shade red): CBC, cannabichromene; CBCA, cannabichromentic acid; CBCAS, cannabichromentic acid synthase; CBDAS, cannabidiolic acid synthase; CBD, cannabidiol; CBG, cannabigerol; CBGA, cannabigerolic acid; CBL, cannabicyclol; CBLA, cannabicyclolic acid; CBN, cannabinol; CBNA: cannabinolic acid; Δ^8-THC, Δ^8-tetrahydrocannabinol; Δ^9-THC (or THC), Δ^9-tetrahydrocannabinol; THCA, tetrahydrocannabinolic acid. Terpene precursor (shade orange): FPP, farnesyl diphosphate; FPPS, farnesyl diphosphate synthase; MEV, mevalonate; TPS, terpene synthase.

ensured by 1-deoxy d-xylulose-5-phosphate synthase (DXS), part of the methylerythritol phosphate (MEP) pathway (Lichtenthaler, 1999). The 5-carbon isoprenoid then is linked with isopentenyl diphosphate (IPP) and dimethylallyl pyrophosphate (DMAPP) through isopentenyl-diphosphate delta-isomerase (IPPi). These are condensed into geranyl diphosphate (GPP, C_{10}) *via* GPP synthase (GPPS) (Ruzicka, 1953; Hunter, 2007). GPP also acts as a precursor for monoterpene biosynthesis. The enzymes DXS, IPPi, and GPPS are upregulated by UV radiation and blue light in peppermint (*Mentha x piperita*) and water mint (*Mentha aquatica*) (Dolzhenko et al., 2010; Nazari and Zarinkamar, 2020).

Olivetolic acid (OA) sets cannabinoid and monoterpene biosynthesis apart. It is produced through a type III polyketide synthase, leading to formation of the cannabinoid precursor, cannabigerolic acid (CBGA) (Gagne et al., 2012). The first step of OA formation is ensured by a unique tetraketide synthase (TKS) and olivetolic acid cyclase (OAC) (Luo et al., 2019). This step uses 1 hexanoyl-CoA and 3 malonyl-CoA to form OA *via* a tetraketide (TK) intermediate. OA is then prenylated by geranylpyrophosphate: olivetolate geranyltransferase 4 (PT4) to form the central precursor molecule CBGA, which can then be further modified into constituents such as Δ^9-THC, CBD, and cannabichromene (CBC) (Flores-Sanchez and Verpoorte, 2008b; Luo et al., 2019). CBGA is converted to cannabidiolic acid (CBDA), tetrahydrocannabinolic acid (THCA), and cannabichromentic acid (CBCA) by cannabidiolic acid synthase (CBDAS), tetrahydrocannabinolic acid synthase (THCAS), and cannabichromentic acid synthase (CBCAS), respectively. During these steps, cannabinoids are naturally converted from their acid forms during storage or heating (decarboxylation) as non-enzymatic catalyzed reactions (Veress et al., 1990). THCA and CBDA reactions are oxygen-dependent and produce hydrogen peroxide, as opposed to the CBCA reaction, which is oxygen-independent and can be inhibited by hydrogen peroxide (Sirikantaramas et al., 2004; Taura et al., 2007; Degenhardt et al., 2017).

CBCA is most actively synthesized in young cannabis seedlings and can be found in both drug-type and fiber-type cannabis plants, yet its concentration is relatively low compared to other cannabinoids (Kushima et al., 1980; Chandra et al., 2017). CBCA is converted to CBC (Gaoni and Mechoulam, 1966), cannabicyclolic (CBL), and cannabicyclolic acid (CBLA) through irradiation or decarboxylation (Shoyama et al., 1972). CBDA is the precursor of CBD, and THCA is the acidic precursor

of Δ^9-THC. THCA can be converted to Δ^8-THC, cannabinol (CBN), and cannabinolic acid (CBNA) (Mechoulam and Gaoni, 1965; Elsohly and Slade, 2005).

Terpenes

Terpenes are a large class of organic molecules responsible for flower aroma; they include β-caryophyllene, limonene, and linalool, which are present in 50 to 70% of all studied plants (Knudsen et al., 2006; Booth et al., 2017). For monoterpene biosynthesis, GPPS condenses one unit of IPP and DMAPP to form GPP, and GPP is converted into monoterpene form *via* mono-terpene synthase (TPS). Sesquiterpene biosynthesis requires two units of IPP to be added to a DMAPP unit. This sequential modification of DMAPP is ensured by farnesyl diphosphate synthase (FPPS) (Kulkarni et al., 2013). FPP is converted into sesquiterpenes *via* sesqui-TPS (Booth et al., 2017). Involvement of other enzymes such as cytochrome P450s leads to more complex terpenes (diterpenes, C_{20}) (Grof, 2018; Booth and Bohlmann, 2019).

Independent of the inflorescence stage, major monoterpenes found in indoor-grown *C. sativa* L. "Finola" are α-pinene, β-pinene, β-ocimene, limonene, myrcene, and terpinolene (Booth and Bohlmann, 2019). Major sesquiterpenes expressed in trichomes are α-humulene, β-caryophyllene, bergamotene, and farnesene. As inflorescence matures, monoterpene accumulation increases relative to sesquiterpenes (**Figure 1**) (Booth et al., 2017). Although more than 120 terpenes have been identified in *C. sativa* L., many (including corresponding TPS genes) require further characterization (Aizpurua-Olaizola et al., 2016; Booth and Bohlmann, 2019). Since robust analytical standards are lacking, reported terpene profiles in *C. sativa* L. may contain some unknown terpene compounds, especially sesquiterpenes. A recent study reported more than 30 different TPS genes in the "Purple Kush" genome, and only 9 of 30 have been characterized (Günnewich et al., 2007; Booth et al., 2017). Elucidation of the underlying mechanisms surrounding terpene biosynthesis in cannabis plants may lead to further exploration and different medical applications for this PSM group (Aliferis and Bernard-Perron, 2020).

Terpenoids (a modified class of terpenes with different functional groups) are by far the most diverse group, with at least 80,000 different compounds (Christianson, 2017; Zhou and Pichersky, 2020). In recent years, cannabis terpenoids have slowly gained interest (Arena et al., 2016; Booth et al., 2017; Mudge et al., 2019). Studies have reported that terpenoids are powerful metabolites that have an interactive effect (or an "entourage effect") with cannabinoid receptors (Gertsch et al., 2008). However, terpene composition in cannabis resin is dependent upon genetic, environmental, and developmental factors, and highly variable terpene profiles additionally exist between individual plants (Fischedick et al., 2010; Hazekamp and Fischedick, 2012; Booth et al., 2017). Terpene diversity in cannabis resin is responsible for scent and flavor qualities of cannabis flowers (Booth et al., 2017).

Flavonoids

Members of the phenol family, flavonoids, form an important PSM group that aids in the plant's responses to sunlight and UV radiation (Downey et al., 2006; Warner et al., 2021). More than 20 flavonoid types in *C. sativa* L. have been identified, such as quercetin and kaempferol (Brenneisen, 2007). Others, such as cannflavins A, B, and C, are uniquely found in cannabis (Barrett et al., 1985, 1986; Radwan et al., 2008). Cannabis-specific flavonoids show promising therapeutic effects because of their anti-inflammatory activities (Barrett et al., 1985, 1986).

Cannabis-specific flavonoid biosynthesis is not well-established. **Figure 2** shows the proposed biosynthetic pathway(s) for cannflavin A and B in *C. sativa* L. (Flores-Sanchez and Verpoorte, 2008b; Rea et al., 2019). The general pathway for cannflavin biosynthesis begins with *p*-coumaroyl-CoA derived from phenylalanine, phenylalanine ammonia-lyase (PAL), cinnamate 4-hydroxylase (C4H), and 4-Coumarate:CoA ligase (4CL). *p*-coumaroyl is covered to luteolin and cannflavin A and B via regiospecific methylation and prenylation reactions (Rea et al., 2019). Alternate routes for cannflavin A/B biosynthesis, beginning with feruloyl-CoA or caffeoyl-CoA with 3 malonyl-CoA, are also proposed (Flores-Sanchez and Verpoorte, 2008b). Although it has not been reported in *C.sativa* L., upregulated chalcone synthase (CHS) gene expression is observed in several plant species under abiotic stress such as UV radiation, as well as biotic stressors such as bacterial or fungal infection (Lipphardt et al., 1988; Dao et al., 2011).

Unlike cannabinoids and terpenes, flavonoid spatial and temporal distribution in cannabis plants does not follow the same pattern (Aizpurua-Olaizola et al., 2016). Rather, higher flavonoid content is reported in *C. sativa* L. leaves than other plant tissues (Flores-Sanchez and Verpoorte, 2008a; Jin et al., 2020). Apart from this, flavonoid concentration seems to decrease with plant tissue age (both leaves and inflorescence), in which higher flavonoid content is observed in young cannabis plants (Flores-Sanchez and Verpoorte, 2008a; Drinić et al., 2018). Low flavonoid content in cannabis oil and seeds is reported (Frassinetti et al., 2018; Moccia et al., 2019; Siano et al., 2019), while flavonoids are absent in glandular trichomes (Flores-Sanchez and Verpoorte, 2008b).

Recent studies show that flavonoid accumulation in inflorescence is variety-dependent and could be an indicator of the susceptibility of the variety to oxidative stress (Pavlovic et al., 2019; Giupponi et al., 2020). Pavlovic et al. (2019) reported the hemp variety "Futura 75" had higher cannabispiran concentration than "Finola." This variety-dependent response is displayed elsewhere, where the hemp variety "Carmagnola Cs" has up to 25% more total phenol content (TPC) than other varieties, such as "Kompolti" (Izzo et al., 2020). Harnessing the radical scavenger activity and screening ability of flavonoids against UV radiation is a promising means of increasing flavonoid production in medical varieties (Agati and Tattini, 2010). Although it is out of the scope in this review, it is still worth to mention that the differences in the flavonoid quantifying methodologies, such as solvents used, matrix to solvent ratio, and characterization methods may result in

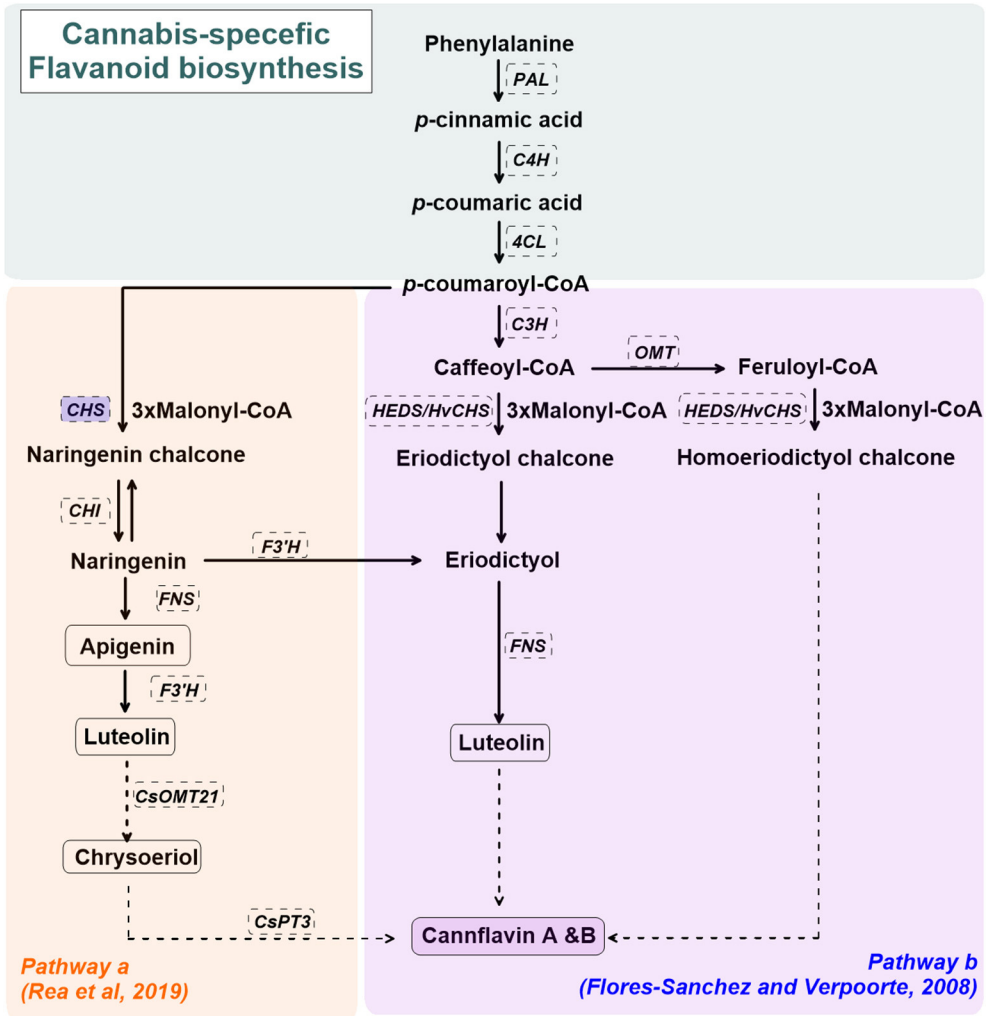

FIGURE 2 | A simplified overview of the cannabis flavonoids, cannflavin A&B, pathway(s) in cannabis (*Cannabis sativa* L.), derived from Flores-Sanchez and Verpoorte (2008b) and Rea et al. (2019). Enzymes are in dashed line box. Enzymes in shaded blue boxes are upregulated by UV radiation in *Arabidopsis thaliana.* Dashed arrows represent proposed enzymatic reactions. CHS, chalcone synthase; CHI, chalcone isomerase; CsOMT21, *C. sativa* L. O-methyltransferase 21; CsPT3, *C. sativa* L. prenyltransferase 3; C4H, cinnamate 4-hydroxylase; C3H, p-coumaroyl-CoA 3-hydroxylase; FNS, flavone synthase; F3'H, flavonoid 3'-hydrolase; HEDS or HvCHS, homoeriodictyol/eriodictyol synthase; OMT, SAM-methyltransferase; PAL, phenylalanine ammonia-lyase; 4CL, 4-Coumarate:CoA ligase.

flavonoid concentration discrepancies (Drinić et al., 2018; Frassinetti et al., 2018; Pellati et al., 2018).

THE IMPACT OF LIGHT SPECTRUM ON CANNABIS PSM PRODUCTION

Plants respond to light stress by producing and accumulating PSM (Thirumurugan et al., 2018). The impact of UV radiation (>380 nm) and the visible light spectrum (380–740 nm) on PSM in greenhouse-grown crops has been well-studied (Urban et al., 2016; Gupta et al., 2017; Alrifai et al., 2019). However, the specific effects of light, including light properties (wavelength and intensity) and fixture configuration (i.e., overhead and subcanopy lighting) on cannabis PSM and phytochemistry is limited and not well-understood (Andre et al., 2016). These studies primarily focused on PSM accumulation in leaves rather than floral biomass. **Table 1** summarizes available studies aimed at determining the impact of light spectrum and lighting configurations on cannabinoid and terpene accumulation.

UV Radiation and PSM

Different wavelength ranges in UV radiation result in varying cannabinoid accumulation (Lydon et al., 1987; Magagnini et al., 2018). It has been nearly four decades since the first study suggesting that UV-B (280–315 nm) radiation affects cannabinoid accumulation in cannabis plants (Lydon et al., 1987). UV-B radiation did not impact cannabinoid content in both drug- and fiber-type cannabis plants, with the exception of Δ^9-THC in bud tissues of drug-type cannabis plants. When the daily dosage of UV-B radiation increased from 0 to 13.4 kJ m^{-2},

TABLE 1 | A comparison of cannabis PSM yield data compiled with overhead, subcanopy, or supplemental lighting.

	Wavelength		Light intensity	Increased PSM	References
	Treatment	**Control**			
Cannabinoids	Supplemental UV-B radiation	Mercury-vapor lamp and sunlight[a]	6.7 and 13.4 kJ m^{-2}	Δ^9-THC	Lydon et al., 1987
	Subcanopy 440+660 nm	440+660 nm[a]	50–500 $\mu mol \cdot m^{-2} \cdot s^{-1}$	CBGA and Δ^9-THC	Hawley, 2018
	Subcanopy 440+530+660 nm	440+660 nm[a]	50–500 $\mu mol \cdot m^{-2} \cdot s^{-1}$	CBGA and Δ^9-THC	Hawley, 2018
	410, 460, 540 +670 nm[a]	HPS[a]	450 $\mu mol \cdot m^{-2} \cdot s^{-1}$	CBD, CBG, Δ^9-THC, and THCV	Magagnini et al., 2018
	450+630 nm[a]	HPS[a]	450 $\mu mol \cdot m^{-2} \cdot s^{-1}$	CBD and Δ^9-THC	Magagnini et al., 2018
	~450+650 nm[a,F] (high blueand low red)	HPS[a,F]	90 $\mu mol \cdot m^{-2} \cdot s^{-1}$	CBGA and Δ^9-THC	Namdar et al., 2019
	Solar radiation (1,200 m ASL)	Solar radiation (130 m ASL)	–	CBDA	Giupponi et al., 2020[b]
	Full-spectrum LEDs	HPS	900 $\mu mol \cdot m^{-2} \cdot s^{-1}$	No impacts	Westmoreland et al., 2021[b]
Terpenes	Subcanopy 440+660 nm	440+660 nm[a]	50–500 $\mu mol \cdot m^{-2} \cdot s^{-1}$	*cis*-nerolidol	Hawley, 2018
	Subcanopy 440+530+660 nm	440+660 nm[a]	50–500 $\mu mol \cdot m^{-2} \cdot s^{-1}$	**Upper canopy:** α-pinine, limonene, myrcene, linalool, and cis-nerolidol **Lower canopy:** α-pinine, borneol, and *cis* -nerolidol	Hawley, 2018
	~450+650 nm[a, V] (high blueand low red)	Fluorescent lamp[a,V]	180–200 $\mu mol \cdot m^{-2} \cdot s^{-1}$	Total terpene	Namdar et al., 2019
	Solar radiation (1,200 m ASL)	Solar radiation (130 m ASL)	–	β-myrcene, α-/β-pinene and limonene	Giupponi et al., 2020[b]

[a]*Overhead lighting;* [b]*fiber-type cannabis (hemp); ASL, above sea level; CBD, cannabidiol; CBG, cannabigerol; CBGA, cannabigerolic acid; F, flowering stage;* Δ^9*-THC,* Δ^9*-tetrahydrocannabinol; THCV, tetrahydrocannabivarin; V, vegetative stage.*

the Δ^9-THC content increased from 25 to 32% (Lydon et al., 1987), suggesting that Δ^9-THC was a UV-B photo-protectant (Pate, 1994). It was further noted that UV-B radiation increases trichome numbers. Altitude may be equally important. Increased solar UV radiation results in higher CBDA, terpene, and cannaflavin content in the hemp variety "Kompolti" (Giupponi et al., 2020). Notably, UV radiation sources used in both studies had relatively broad spectra, compared to electrical UV radiation sources, such UV-discharge lamps and light-emitting diodes (LEDs). It is unknown if there is was an interactive effect between UV-A (315–380 nm) and UV-B radiation, as a high percentage of UV-A radiation was present in both the UV-B and control light treatments (Mirecki and Teramura, 1984; Lydon et al., 1987; Giupponi et al., 2020). A subsequent study examined the impact of UV-A radiation on cannabinoid accumulation, and reported increased cannabinoid levels other than Δ^9-THC (Magagnini et al., 2018). Low percentages of UV-A radiation (2%) from full-spectrum LED arrays induced an increase of several cannabinoids, including CBD, CBG, Δ^9-THC, and tetrahydrocannabivarin (THCV), compared to a high pressure sodium (HPS) lamp that contained 1% of UV-A radiation (Magagnini et al., 2018). Clearly, more studies are required to clarify the impact of UV radiation on cannabis PSM accumulation.

Visible Light and PSM

The impact of visible light on cannabis PSM accumulation has been investigated with different lighting configurations and different wavelengths (Hawley, 2018; Magagnini et al., 2018; Namdar et al., 2019) (**Table 1**). A high percentage of blue light cause increased cannabinoid content in cannabis inflorescence (drug-type cannabis, high amount of THC) (Hawley, 2018; Namdar et al., 2019; Danziger and Bernstein, 2021). Hawley (2018) examined the impact of subcanopy lighting with two different light spectra, 440 + 660 nm (blue + red, BR) and 440 + 530 + 660 nm (blue+ green + red, BGR), on cannabinoid and terpene accumulation. Increased Δ^9-THC content and high CBGA levels were observed under both subcanopy BR and BGR lighting. Subcanopy BGR lighting had a higher impact on terpene accumulation than BR lighting, on both upper and lower canopies (Hawley, 2018). Increased CBGA content under LED lighting was similarly reported (Namdar et al., 2019; Danziger and Bernstein, 2021). During the flowering stage, light treatment with rich-blue light from overhead blue-red LED fixtures increased CBGA content and the CBGA: THCA ratio (Namdar et al., 2019).

Conflicting results on the interactive effects between blue light and cannabinoid content, however, were reported recently in fiber-type cannabis (hemp)

(Wei et al., 2021; Westmoreland et al., 2021). Westmoreland et al. (2021) investigated the impact of light spectra on fiber-type cannabis and reported that neither CBD nor THC accumulation was impacted by spectral quality. The authors reported that this was likely caused by high light level (900 $\mu mol \cdot m^{-2} \cdot s^{-1}$) used as the saturation state of photoreceptors was reached, resulting in low sensitivity of cannabinoid accumulation to spectral quality (Westmoreland et al., 2021). Wei et al. (2021) also reported that no significant correlation between blue light fraction and cannabinoid yield was found in fiber-type cannabis; however, note that in this study the light levels used was between 28 and 540 $\mu mol \cdot m^{-2} \cdot s^{-1}$. As such, it is unknown that whether such variation on the interactive effect between spectral quality and cannabinoid accumulation is caused by light levels or cannabis chemotypes. Apart from blue light, supplemental green light induced cannabis PSM accumulation, including Δ^9-THC and terpenes (limonene, linalool, and myrcene) (Hawley, 2018). No physiological theories explain how supplemental green light induces cannabis PSM accumulation. Clearly, both spectral properties and cannabis chemotype used highly impact cannabinoid accumulation, and further investigation on the links between spectral properties, cannabis chemotype, and photoreceptor is required to clarify the spectral effects.

PHOTOBIOLOGY AND MOLECULAR PATHWAYS IN *C. SATIVA* L. PSM BIOSYNTHESIS

Light regimes are elemental to *C. sativa* L. cultivation, as different wavelengths of light activate various light-dependent responses and related gene expression *via* photoreceptors and enzymes (Eichhorn Bilodeau et al., 2019; Aliferis and Bernard-Perron, 2020). Although the studies on cannabis growth and photobiology has expanded in the last few years, a comprehensive review by Aliferis and Bernard-Perron (2020) concludes that how light spectra influence cannabis metabolomics is still largely unknown. In particular, how cannabis PSM biosynthesis is impacted by monochromatic light requires further investigation, as most studies to date were conducted under mixed wavelength or full-spectrum light conditions.

Figure 3 summarizes what is known of wavelengths and corresponding *C. sativa* L. PSM responses. UV radiation, one of the most effective wavelength ranges that induces cannabinoid biosynthesis (THC, THCV, CBD, and CBG), is perceived by several photoreceptors including UVR8, cryptochromes, and phototropins (Sager et al., 1988; Galvão and Fankhauser, 2015). Few studies have attempted to identify the regulatory elements of PSM biosynthetic pathway in cannabis plants (Marks et al., 2009; Bassolino et al., 2020). Some candidate regulatory genes for both cannabinoid and flavonoid biosynthesis(s) have been pinpointed and regulatory proteins identified; CsMYB77 and CsMYB94 for cannabinoid biosynthesis and CsbHLH112 and CsbHLH113 for flavonoid biosynthesis (Bassolino et al., 2020). Both MYB and bHLH superfamilies play key roles in the regulation of secondary metabolism (Hong, 2016). Follow up studies are required to place these cannabis proteins in the cannabinoid and flavonoid

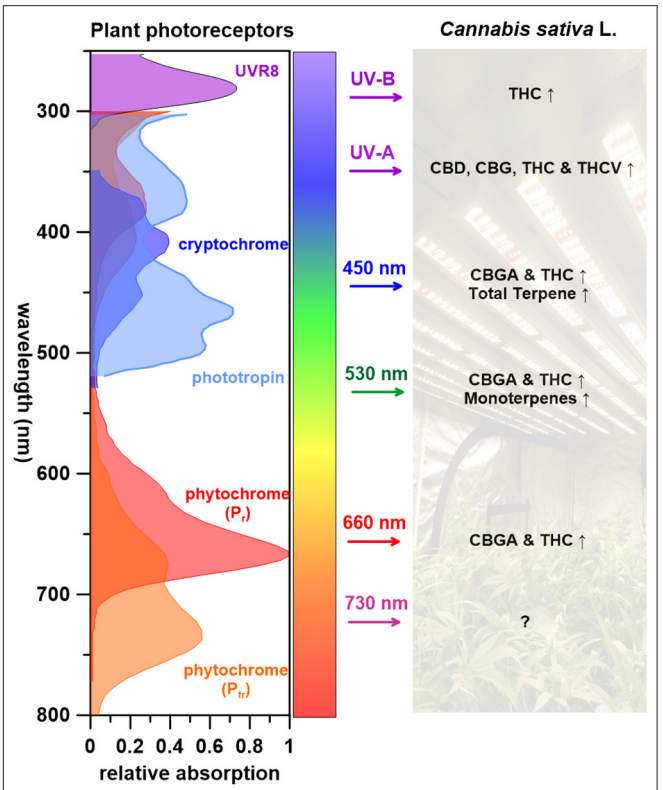

FIGURE 3 | The impact of wavelengths on *Cannabis sativa* L. PSM responses, with corresponding photoreceptors (↑: increase, Δ: varying depended on light treatments, ↓: decrease, ?: unknown).

metabolic pathways. As for terpenes, although several studies indicate that UV-B radiation effects higher monoterpene content in plants that contain glandular trichomes (Johnson et al., 1999; Maffei and Scannerini, 2000), this has not yet been reported in *C. sativa* L. to our knowledge.

It has been proposed that light-dependent reactions for photosynthesis occur and supply energy for metabolic activity in tomato (*Solanum lycopersicum*) type VI glandular trichomes (Balcke et al., 2017). Using this as a precedence, it may be of interest to evaluate the global carbon and energy balance in *C. sativa* L. with different wavelengths of light to further elucidate trichome productivity and phytochemistry. Visible light (450, 530, and 660 nm) leads to increased CBGA, THC and terpene contents in *C. sativa* L. (**Figure 3**). When shifting wavelengths from UV radiation to the visible spectrum, cannabinoid precursor CBGA levels increases, yet no impact on THC is observed (Hawley, 2018; Namdar et al., 2019). Although Veress et al. (1990) reported that CBGA conversion to cannabinoids are non-enzymatic catalyzed reactions that naturally occurring postharvest during storage or heating (decarboxylation), it appears that light wavelengths can impact specific cannabinoid potency.

How visible light affects terpene biosynthesis remains elusive due to limited studies and terpene diversity (monoterpenes, sesquiterpene, and diterpenes). Drawing from previous studies

of other crops may provide some insight and future direction for cannabis terpene production (Kessler and Kalske, 2018). When grown under blue LEDs, sage (*Pervoskia abrotanoides*, from the *Lamiaceae* family), sees its relative monoterpene content increase 3-fold upon exposure, with notable increases of α-thujene, α-pinene, and β-pinene. It was concluded that blue light could generally promote monoterpene content in *P. abrotanoides*, while augmented production of only one monoterpene, limonene, was observed in *P. atriplicifolia.* In this species, red light increased β-myrcene and cis-ocimene content (Ghaffari et al., 2019).

A nascent legal industry with proprietary value slows access to reliable information on indoor cannabis production, postharvest practices and processing of cannabis and cannabis-derived products. Apart from controlling environment (light, temperature, nutrients, microbiome etc.) to boost plant phytochemistry, optimal use of light pre- and post-harvest should be considered. For example, UV radiation could be used at the end of the flowering stage or before harvest to increase PSM production. More studies on how light can be manipulated during plant production and post-harvest for consistent PSM production and accumulation are anticipated.

CONCLUDING REMARKS

Here we review known aspects of photobiology that are relevant to PSM production in *C. sativa* L., as cannabis research and development efforts are shifting from plant yield performance to manipulating cannabinoid, terpene, and flavonoid content. It is clear that light spectra can be manipulated to target specific cannabis PSM accumulation in different cannabis tissues (leaves and buds), resulting in altered potencies. Practically applied, optimized light regimes should reduce necessary electrical inputs while increasing cannabis PSM yields and quality. UV radiation is a powerful tool for stimulating cannabinoid biosynthesis in cannabis trichomes, while visible light alone impacts specific cannabinoid biosynthesis pathways and PSM profiles. UV radiation impacts terpene biosynthesis in other model plants, and this could be useful for cannabis plants. We expect that UV and blue LEDs will be increasingly used to stimulate desirable cannabis PSMs, as they have been widely applied and tailored to other high-value crops. The majority of cannabis studies are conducted under blue- and red-light mixtures, leaving a large sum of wavelengths in the visible spectrum untouched. Current evidence indicates that visible LED light can enhance CBG, THC, and terpene accumulation, but this is not explicitly seen with CBD. Gene regulatory and molecular pathways affecting cannabis metabolomics under monochromatic light remain elusive. Lighting strategies such as subcanopy lighting and varying light spectra for different plant growing stages and plant architecture can lower energy consumption and optimize cannabis PSM production, eventually improving the precision of cannabis PSM production, as well as therapeutic capacities.

Based on research reviewed, a few experimental directions are proposed to bridge knowledge gaps in cannabis lighting and PSM accumulation research: (1) The impact of narrow-spectrum light on cannabis PSM accumulation. Light spectrum greatly impacts cannabis PSM accumulation, yet there is minimal research available on the impact of narrow-spectrum light as most studies were conducted under either dichromatic or full-spectrum lighting. (2) Further investigations into the impact of high light in drug-type cannabis growth and its PSM accumulation, as our current knowledge in cannabis lighting is based on experimentation conducted under 500 $\mu mol \cdot m^{-2} \cdot s^{-1}$. (3) The impact of pre-harvest UV radiation treatment on cannabis PSM accumulation. UV LED sources with different wavelengths are highly available, and the accessibility to both researchers and producers make results more accessible.

AUTHOR CONTRIBUTIONS

VD and B-SW led the writing of this paper. B-SW and SM were the major editors. SM, VM, and ML contributed over 50% of the writing for the paper. ML is the correspondence point person. All authors contributed to the article and approved the submitted version.

ACKNOWLEDGMENTS

The authors would like to thank NSERC (CRDPF 543704-19 and CREATE 543319-2020) and EXKA Inc. for their continuous support and funding of this project.

REFERENCES

Abrams, D. I. (2019). Should oncologists recommend cannabis? *Curr. Treat. Options Oncol.* 20:59. doi: 10.1007/s11864-019-0659-9

Agati, G., and Tattini, M. (2010). Multiple functional roles of flavonoids in photoprotection. *New Phytol.* 186, 786–793. doi: 10.1111/j.1469-8137.2010.03269.x

Ahmed, S. A., Ross, S. A., Slade, D., Radwan, M. M., Khan, I. A., and Elsohly, M. A. (2015). Minor oxygenated cannabinoids from high potency *Cannabis sativa* L. *Phytochemistry* 117, 194–199. doi: 10.1016/j.phytochem.2015.04.007

Aizpurua-Olaizola, O., Soydaner, U., ÖztüRk, E., Schibano, D., Simsir, Y., Navarro, P., et al. (2016). Evolution of the cannabinoid and terpene content during the growth of *Cannabis sativa* plants from different chemotypes. *J. Nat. Prod.* 79, 324–331. doi: 10.1021/acs.jnatprod.5b00949

Akula, R., and Ravishankar, G. A. (2011). Influence of abiotic stress signals on secondary metabolites in plants. *Plant Signal. Behav.* 6, 1720–1731. doi: 10.4161/psb.6.11.17613

Alahakoon, U., Adamson, J., Grenkow, L., Soroka, J., Bonham-Smith, P., and Gruber, M. (2016). Field growth traits and insect-host plant interactions of two transgenic canola (Brassicaceae) lines with elevated trichome numbers. *Can. Entomol.* 148:603. doi: 10.4039/tce.2016.9

Aliferis, K. A., and Bernard-Perron, D. (2020). Cannabinomics: application of metabolomics in Cannabis (*Cannabis sativa* L.) research and development. *Front. Plant Sci.* 11:554. doi: 10.3389/fpls.2020.00554

Alrifai, O., Hao, X., Marcone, M. F., and Tsao, R. (2019). Current review of the modulatory effects of LED lights on photosynthesis of secondary metabolites and future perspectives of microgreen vegetables. *J. Agric. Food Chem.* 67, 6075–6090. doi: 10.1021/acs.jafc.9b00819

Andre, C. M., Hausman, J.-F., and Guerriero, G. (2016). *Cannabis sativa*: the plant of the thousand and one molecules. *Front. Plant Sci.* 7:19. doi: 10.3389/fpls.2016.00019

Arena, C., Tsonev, T., Doneva, D., De Micco, V., Michelozzi, M., Brunetti, C., et al. (2016). The effect of light quality on growth, photosynthesis, leaf anatomy and volatile isoprenoids of a monoterpene-emitting herbaceous species (*Solanum lycopersicum* L.) and an isoprene-emitting tree (*Platanus orientalis* L.). *Environ. Exp. Bot.* 130, 122–132. doi: 10.1016/j.envexpbot.2016.05.014

Balcke, G. U., Bennewitz, S., Bergau, N., Athmer, B., Henning, A., Majovsky, P., et al. (2017). Multi-omics of tomato glandular trichomes reveals distinct features of central carbon metabolism supporting high productivity of specialized metabolites. *Plant Cell* 29, 960–983. doi: 10.1105/tpc.17.00060

Baron, E. P. (2018). Medicinal properties of cannabinoids, terpenes, and flavonoids in cannabis, and benefits in migraine, headache, and pain: an update on current evidence and cannabis science. *Headache* 58, 1139–1186. doi: 10.1111/head.13345

Barrett, M., Gordon, D., and Evans, F. (1985). Isolation from *Cannabis sativa* L. of cannflavin—a novel inhibitor of prostaglandin production. *Biochem. Pharmacol.* 34, 2019–2024. doi: 10.1016/0006-2952(85)90325-9

Barrett, M., Scutt, A., and Evans, F. (1986). Cannflavin A and B, prenylated flavones from *Cannabis sativa* L. *Experientia* 42, 452–453. doi: 10.1007/BF02118655

Bassolino, L., Buti, M., Fulvio, F., Pennesi, A., Mandolino, G., Milc, J., et al. (2020). *In silico* identification of MYB and bHLH families reveals candidate transcription factors for secondary metabolic pathways in *Cannabis sativa L. Plants* 9:1540. doi: 10.3390/plants9111540

Bauer, R., Woelkart, K., and Salo-Ahen, O. M. (2008). CB receptor ligands from plants. *Curr. Top. Med. Chem.* 8, 173–186. doi: 10.2174/156802608783498023

Benelli, G., Pavela, R., Lupidi, G., Nabissi, M., Petrelli, R., Kamte, S. L. N., et al. (2018). The crop-residue of fiber hemp cv. Futura 75: from a waste product to a source of botanical insecticides. *Environ. Sci. Pollut. Res.* 25, 10515–10525. doi: 10.1007/s11356-017-0635-5

Blasco-Benito, S., Seijo-Vila, M., Caro-Villalobos, M., Tundidor, I., Andradas, C., García-Taboada, E., et al. (2018). Appraising the "entourage effect": antitumor action of a pure cannabinoid versus a botanical drug preparation in preclinical models of breast cancer. *Biochem. Pharmacol.* 157, 285–293. doi: 10.1016/j.bcp.2018.06.025

Booth, J. K., and Bohlmann, J. (2019). Terpenes in *Cannabis sativa*–From plant genome to humans. *Plant Sci.* 284, 67–72. doi: 10.1016/j.plantsci.2019.03.022

Booth, J. K., Page, J. E., and Bohlmann, J. (2017). Terpene synthases from *Cannabis sativa*. *PLoS ONE* 12:e0173911. doi: 10.1371/journal.pone.0173911

Bourgaud, F., Gravot, A., Milesi, S., and Gontier, E. (2001). Production of plant secondary metabolites: a historical perspective. *Plant Sci.* 161, 839–851. doi: 10.1016/S0168-9452(01)00490-3

Brenneisen, R. (2007). "Chemistry and analysis of phytocannabinoids and other Cannabis constituents," in *Marijuana and the Cannabinoids,* ed M. A. Elsohly. (Totowa, NJ: Human Press), 17–49. doi: 10.1007/978-1-59259-947-9_2

Bruci, Z., Papoutsis, I., Athanaselis, S., Nikolaou, P., Pazari, E., Spiliopoulou, C., et al. (2012). First systematic evaluation of the potency of *Cannabis sativa* plants grown in Albania. *For. Sci. Int.* 222, 40–46. doi: 10.1016/j.forsciint.2012.04.032

Chandra, S., Lata, H., and Elsohly, M. A. (2017). *Cannabis sativa L.-Botany and Biotechnology.* Cham: Springer. doi: 10.1007/978-3-319-54564-6

Christianson, D. W. (2017). Structural and chemical biology of terpenoid cyclases. *Chem. Rev.* 117, 11570–11648. doi: 10.1021/acs.chemrev.7b00287

Danziger, N., and Bernstein, N. (2021). Light matters: effect of light spectra on cannabinoid profile and plant development of medical cannabis (*Cannabis sativa* L.). *Indus. Crops Prod.* 164:113351. doi: 10.1016/j.indcrop.2021.113351

Dao, T., Linthorst, H., and Verpoorte, R. (2011). Chalcone synthase and its functions in plant resistance. *Phytochem. Rev.* 10:397. doi: 10.1007/s11101-011-9211-7

Dasgupta, N., Beletsky, L., and Ciccarone, D. (2018). Opioid crisis: no easy fix to its social and economic determinants. *Am. J. Public Health* 108, 182–186. doi: 10.2105/AJPH.2017.304187

Dayanandan, P., and Kaufman, P. B. (1976). Trichomes of *Cannabis sativa* L. (*Cannabaceae*). *Am. J. Bot.* 63, 578–591. doi: 10.1002/j.1537-2197.1976.tb11846.x

Degenhardt, F., Stehle, F., and Kayser, O. (2017). "The biosynthesis of cannabinoids," in *Handbook of Cannabis and Related Pathologies,* ed V. R. Preedy (Cambridge, MA, Elsevier), 13–23. doi: 10.1016/B978-0-12-800756-3.00002-8

Dolzhenko, Y., Bertea, C. M., Occhipinti, A., Bossi, S., and Maffei, M. E. (2010). UV-B modulates the interplay between terpenoids and flavonoids in peppermint (*Mentha× piperita* L.). *J. Photochem. Photobiol. B Biol.* 100, 67–75. doi: 10.1016/j.jphotobiol.2010.05.003

Downey, M. O., Dokoozlian, N. K., and Krstic, M. P. (2006). Cultural practice and environmental impacts on the flavonoid composition of grapes and wine: a review of recent research. *Am. J. Enol. Viticult.* 57, 257–268.

Drinić, Z., Vidović, S., Vladić, J., Koren, A., Kiprovski, B., and Sikora, V. (2018). Effect of extraction solvent on total polyphenols content and antioxidant activity of *Cannabis sativa* L. *Lekovite Sirovine* 38, 17–21. doi: 10.5937/leksir1838017D

Eichhorn Bilodeau, S., Wu, B.-S., Rufyikiri, A.-S., Macpherson, S., and Lefsrud, M. (2019). An update on plant photobiology and implications for cannabis production. *Front. Plant Sci.* 10:296. doi: 10.3389/fpls.2019.00296

El-Alfy, A. T., Ivey, K., Robinson, K., Ahmed, S., Radwan, M., Slade, D., et al. (2010). Antidepressant-like effect of Δ^9-tetrahydrocannabinol and other cannabinoids isolated from *Cannabis sativa L. Pharmacol. Biochem. Behav.* 95, 434–442. doi: 10.1016/j.pbb.2010.03.004

Elsohly, M., and Gul, W. (2014). "Constituents of *Cannabis sativa*," in *Handbook of Cannabis*, ed R. G. Pertwee (Oxford: Oxford University Press), 3–22. doi: 10.1093/acprof:oso/9780199662685.003.0001

Elsohly, M. A., Radwan, M. M., Gul, W., Chandra, S., and Galal, A. (2017). "Phytochemistry of *Cannabis sativa L.*," in *Phytocannabinoids*, eds A. D. Kinghorn, H. Falk, S. Gibbons, J. I. Kobayashi, and W. Herz (Cham: Springer), 1–36. doi: 10.1007/978-3-319-45541-9_1

Elsohly, M. A., and Slade, D. (2005). Chemical constituents of marijuana: the complex mixture of natural cannabinoids. *Life Sci.* 78, 539–548. doi: 10.1016/j.lfs.2005.09.011

Fischedick, J. T., Hazekamp, A., Erkelens, T., Choi, Y. H., and Verpoorte, R. (2010). Metabolic fingerprinting of *Cannabis sativa L.*, cannabinoids and terpenoids for chemotaxonomic and drug standardization purposes. *Phytochemistry* 71, 2058–2073. doi: 10.1016/j.phytochem.2010.10.001

Flores-Sanchez, I. J., and Verpoorte, R. (2008a). PKS activities and biosynthesis of cannabinoids and flavonoids in *Cannabis sativa* L. plants. *Plant Cell Physiol.* 49, 1767–1782. doi: 10.1093/pcp/pcn150

Flores-Sanchez, I. J., and Verpoorte, R. (2008b). Secondary metabolism in cannabis. *Phytochem. Rev.* 7, 615–639. doi: 10.1007/s11101-008-9094-4

Frassinetti, S., Moccia, E., Caltavuturo, L., Gabriele, M., Longo, V., Bellani, L., et al. (2018). Nutraceutical potential of hemp (*Cannabis sativa* L.) seeds and sprouts. *Food Chem.* 262, 56–66. doi: 10.1016/j.foodchem.2018.04.078

Friedman, D., and Devinsky, O. (2015). Cannabinoids in the treatment of epilepsy. *N. Engl. J. Med.* 373, 1048–1058. doi: 10.1056/NEJMra1407304

Gagne, S. J., Stout, J. M., Liu, E., Boubakir, Z., Clark, S. M., and Page, J. E. (2012). Identification of olivetolic acid cyclase from *Cannabis sativa* reveals a unique catalytic route to plant polyketides. *Proc. Natl. Acad. Sci. U.S.A.* 109, 12811–12816. doi: 10.1073/pnas.1200330109

Gallily, R., Yekhtin, Z., and Hanuš, L. O. (2015). Overcoming the bell-shaped dose-response of cannabidiol by using cannabis extract enriched in cannabidiol. *Pharmacol. Pharmacy* 6:75. doi: 10.4236/pp.2015.62010

Galvão, V. C., and Fankhauser, C. (2015). Sensing the light environment in plants: photoreceptors and early signaling steps. *Curr. Opin. Neurobiol.* 34, 46–53. doi: 10.1016/j.conb.2015.01.013

Gaoni, Y., and Mechoulam, R. (1966). Cannabichromene, a new active principle in hashish. *Chem. Commun.* 1966, 20–21. doi: 10.1039/c19660000020

Garb, S. (1981). Cannabinoids in the management of severe nausea and vomiting from cancer chemotherapy. Some additional considerations. *J. Clin. Pharmacol.* 21, 57S—59S. doi: 10.1002/j.1552-4604.1981.tb02574.x

Gertsch, J., Leonti, M., Raduner, S., Racz, I., Chen, J.-Z., Xie, X.-Q., et al. (2008). Beta-caryophyllene is a dietary cannabinoid. *Proc. Natl. Acad. Sci. U.S.A.* 105, 9099–9104. doi: 10.1073/pnas.0803601105

Ghaffari, Z., Rahimmalek, M., and Sabzalian, M. R. (2019). Variation in the primary and secondary metabolites derived from the isoprenoid pathway in the *Perovskia* species in response to different wavelengths generated by light emitting diodes (LEDs). *Indus. Crops Prod.* 140:111592. doi: 10.1016/j.indcrop.2019.111592

Giupponi, L., Leoni, V., Pavlovic, R., and Giorgi, A. (2020). Influence of altitude on phytochemical composition of hemp inflorescence: a metabolomic approach. *Molecules* 25:1381. doi: 10.3390/molecules25061381

Goldstein, B. (2016). *Cannabis in the Treatment of Pediatric Epilepsy*. Chicago, IL: O'Shaughnessy's, 7–9.

Gonçalves, J., Rosado, T., Soares, S., Simão, A. Y., Caramelo, D., Luís, Â., et al. (2019). Cannabis and its secondary metabolites: their use as therapeutic drugs, toxicological aspects, and analytical determination. *Medicines* 6:31. doi: 10.3390/medicines6010031

Grof, C. P. (2018). Cannabis, from plant to pill. *Br. J. Clin. Pharmacol.* 84, 2463–2467. doi: 10.1111/bcp.13618

Günnewich, N., Page, J. E., Köllner, T. G., Degenhardt, J., and Kutchan, T. M. (2007). Functional expression and characterization of trichome-specific (-)-limonene synthase and (+)-α-pinene synthase from *Cannabis sativa*. *Nat. Prod. Commun.* 2:1934578X0700200301. doi: 10.1177/1934578X0700200301

Gupta, S. K., Sharma, M., Deeba, F., and Pandey, V. (2017). "Plant response: UV-B avoidance mechanisms," in *UV-B Radiation: From Environmental Stressor to Regulator of Plant Growth*, eds V. P. Singh, S. M. Prasad, and P. Parihar (West Sussex: Wiley-Blackwell), 217–258. doi: 10.1002/9781119143611.ch12

Hammond, C. T., and Mahlberg, P. G. (1977). Morphogenesis of capitate glandular hairs of *Cannabis sativa* (Cannabaceae). *Am. J. Bot.* 64, 1023–1031. doi: 10.1002/j.1537-2197.1977.tb11948.x

Hawley, D. (2018). *The influence of spectral quality of light on plant secondary metabolism and photosynthetic acclimation to light quality* (Ph.D. dissertation). University of Guelph, Guelph, ON, Canada.

Hazekamp, A. (2007). *Cannabis; extracting the medicine.* Amsterdam: Print Partners Ipskamp.

Hazekamp, A., and Fischedick, J. (2012). Cannabis-from cultivar to chemovar. *Drug Test. Anal.* 4, 660–667. doi: 10.1002/dta.407

Hesami, M., Pepe, M., Alizadeh, M., Rakei, A., Baiton, A., and Jones, A. M. P. (2020). Recent advances in cannabis biotechnology. *Indus. Crops Prod.* 158:113026. doi: 10.1016/j.indcrop.2020.113026

Hilderbrand, R. (2018). Hemp and cannabidiol: what is a medicine? *Mol. Med.* 115:306.

Hong, J. C. (2016). "General aspects of plant transcription factor families," in *Plant Transcription Factors*, ed D. H. Gonzalez (Amsterdam: Elsevier), 35–56. doi: 10.1016/B978-0-12-800854-6.00003-8

Huchelmann, A., Boutry, M., and Hachez, C. (2017). Plant glandular trichomes: natural cell factories of high biotechnological interest. *Plant Physiol.* 175, 6–22. doi: 10.1104/pp.17.00727

Hudson, J. (1963). "Humulones, lupulones and other constituents of hops," in *Modern Methods of Plant Analysis/Moderne Methoden der Pflanzenanalyse*, eds K. Paech and M. V. Tracey. (Berlin; Heidelberg: Springer), 135–154. doi: 10.1007/978-3-642-94878-7_8

Hunter, W. N. (2007). The non-mevalonate pathway of isoprenoid precursor biosynthesis. *J. Biol. Chem.* 282, 21573–21577. doi: 10.1074/jbc.R700005200

Hutchison, K. E., Bidwell, L. C., Ellingson, J. M., and Bryan, A. D. (2019). Cannabis and health research: rapid progress requires innovative research designs. *Value Health* 22, 1289–1294. doi: 10.1016/j.jval.2019.05.005

Izzo, L., Castaldo, L., Narváez, A., Graziani, G., Gaspari, A., Rodríguez-Carrasco, Y., et al. (2020). Analysis of phenolic compounds in commercial *Cannabis sativa* L. inflorescences using UHPLC-Q-orbitrap HRMS. *Molecules* 25:631. doi: 10.3390/molecules25030631

Jenkins, G. I. (2017). Photomorphogenic responses to ultraviolet-B light. *Plant Cell Environ.* 40, 2544–2557. doi: 10.1111/pce.12934

Jin, D., Dai, K., Xie, Z., and Chen, J. (2020). Secondary metabolites profiled in cannabis inflorescences, leaves, stem barks, and roots for medicinal purposes. *Sci. Rep.* 10, 1–14. doi: 10.1038/s41598-020-60172-6

Jin, D., Jin, S., and Chen, J. (2019). Cannabis indoor growing conditions, management practices, and post-harvest treatment: a review. *Am. J. Plant Sci.* 10, 925–946. doi: 10.4236/ajps.2019.106067

Johnson, C. B., Kirby, J., Naxakis, G., and Pearson, S. (1999). Substantial UV-B-mediated induction of essential oils in sweet basil (*Ocimum basilicum* L.). *Phytochemistry* 51, 507–510. doi: 10.1016/S0031-9422(98)00767-5

Johnson, J. R., Burnell-Nugent, M., Lossignol, D., Ganae-Motan, E. D., Potts, R., and Fallon, M. T. (2010). Multicenter, double-blind, randomized, placebo-controlled, parallel-group study of the efficacy, safety, and tolerability of THC: CBD extract and THC extract in patients with intractable cancer-related pain. *J. Pain Sympt. Manage.* 39, 167–179. doi: 10.1016/j.jpainsymman.2009.06.008

Kessler, A., and Halitschke, R. (2007). Specificity and complexity: the impact of herbivore-induced plant responses on arthropod community structure. *Curr. Opin. Plant Biol.* 10, 409–414. doi: 10.1016/j.pbi.2007.06.001

Kessler, A., and Kalske, A. (2018). Plant secondary metabolite diversity and species interactions. *Annu. Rev. Ecol. Evol. Syst.* 49, 115–138. doi: 10.1146/annurev-ecolsys-110617-062406

Knudsen, J. T., Eriksson, R., Gershenzon, J., and Ståhl, B. (2006). Diversity and distribution of floral scent. *Bot. Rev.* 72, 1–120. doi: 10.1663/0006-8101(2006)72(1:DADOFS)2.0.CO;2

Krishnamurti, C., and Rao, S. C. (2016). The isolation of morphine by Serturner. *Indian J. Anaesth.* 60:861. doi: 10.4103/0019-5049.193696

Kulkarni, R., Pandit, S., Chidley, H., Nagel, R., Schmidt, A., Gershenzon, J., et al. (2013). Characterization of three novel isoprenyl diphosphate synthases from the terpenoid rich mango fruit. *Plant Physiol. Biochem.* 71, 121–131. doi: 10.1016/j.plaphy.2013.07.006

Kushima, H., Shoyama, Y., and Nishioka, I. (1980). Cannabis. Xii. Variations of cannabinoid contents in several strains of *Cannabis sativa* L. with leaf-age, season and sex. *Chem. Pharmaceut. Bull.* 28, 594–598. doi: 10.1248/cpb.28.594

Labandeira, C. (2005). Invasion of the continents: cyanobacterial crusts to tree-inhabiting arthropods. *Trends Ecol. Evol.* 20, 253–262. doi: 10.1016/j.tree.2005.03.002

Lapinjoki, S. P., Elo, H. A., and Taipale, H. T. (1991). Development and structure of resin glands on tissues of *Betula pendula* Roth, during growth. *New Phytol.* 117, 219–223. doi: 10.1111/j.1469-8137.1991.tb04902.x

Levin, D. A. (1973). The role of trichomes in plant defense. *Q. Rev. Biol.* 48, 3–15. doi: 10.1086/407484

Lichtenthaler, H. K. (1999). The 1-deoxy-D-xylulose-5-phosphate pathway of isoprenoid biosynthesis in plants. *Annu. Rev. Plant Biol.* 50, 47–65. doi: 10.1146/annurev.arplant.50.1.47

Lipphardt, S., Brettschneider, R., Kreuzaler, F., Schell, J., and Dangl, J. L. (1988). UV-inducible transient expression in parsley protoplasts identifies regulatory *cis-elements* of a chimeric *Antirrhinum majus* chalcone synthase gene. *EMBO J.* 7, 4027–4033. doi: 10.1002/j.1460-2075.1988.tb03296.x

Livingston, S. J., Quilichini, T. D., Booth, J. K., Wong, D. C., Rensing, K. H., Laflamme-Yonkman, J., et al. (2020). Cannabis glandular trichomes alter morphology and metabolite content during flower maturation. *Plant J.* 101, 37–56. doi: 10.1111/tpj.14516

Luo, X., Reiter, M. A., D'espaux, L., Wong, J., Denby, C. M., Lechner, A., et al. (2019). Complete biosynthesis of cannabinoids and their unnatural analogues in yeast. *Nature* 567, 123–126. doi: 10.1038/s41586-019-0978-9

Lydon, J., Teramura, A. H., and Coffman, C. B. (1987). UV-B radiation effects on photosynthesis, growth and cannabinoid production of two *Cannabis sativa* chemotypes. *Photochem. Photobiol.* 46, 201–206. doi: 10.1111/j.1751-1097.1987.tb04757.x

Maffei, M., and Scannerini, S. (2000). UV-B effect on photomorphogenesis and essential oil composition in peppermint (*Mentha piperita* L.). *J. Essent. Oil Res.* 12, 523–529. doi: 10.1080/10412905.2000.9712150

Magagnini, G., Grassi, G., and Kotiranta, S. (2018). The effect of light spectrum on the morphology and cannabinoid content of *Cannabis sativa* L. *Med. Cannabis Cannabinoids* 1, 19–27. doi: 10.1159/000489030

Mao, J., Price, D., Lu, J., Keniston, L., and Mayer, D. (2000). Two distinctive antinociceptive systems in rats with pathological pain. *Neurosci. Lett.* 280, 13–16. doi: 10.1016/S0304-3940(99)00998-2

Marks, M. D., Tian, L., Wenger, J. P., Omburo, S. N., Soto-Fuentes, W., He, J., et al. (2009). Identification of candidate genes affecting Δ^9-tetrahydrocannabinol biosynthesis in *Cannabis sativa*. *J. Exp. Bot.* 60, 3715–3726. doi: 10.1093/jxb/erp210

Mcgarvey, D. J., and Croteau, R. (1995). Terpenoid metabolism. *Plant Cell* 7:1015. doi: 10.2307/3870054

Mcpartland, J. M. (1997). Cannabis as repellent and pesticide. *J. Int. Hemp Assoc.* 4, 89–94.

Mechoulam, R., and Gaoni, Y. (1965). Hashish—IV: The isolation and structure of cannabinolic, cannabidiolic, and cannabigerolic acids. *Tetrahedron* 21, 1223–1229. doi: 10.1016/0040-4020(65)80064-3

Mirecki, R. M., and Teramura, A. H. (1984). Effects of ultraviolet-B irradiance on soybean: V. The dependence of plant sensitivity on the photosynthetic photon flux density during and after leaf expansion. *Plant Physiol.* 74, 475–480. doi: 10.1104/pp.74.3.475

Moccia, S., Russo, M., Spagnuolo, C., Tedesco, I., Picariello, G., Siano, F., et al. (2019). Activation of cytostatic autophagy by polar extract of hempseed oil (*Cannabis sativa* L.) in a colorectal adenocarcinoma cell line. *Nutr. Metab. Cardiovasc. Dis.* 29:871. doi: 10.1016/j.numecd.2019.05.003

Mudge, E. M., Brown, P. N., and Murch, S. J. (2019). The terroir of Cannabis: terpene metabolomics as a tool to understand *Cannabis sativa* selections. *Planta Medica* 85, 781–796. doi: 10.1055/a-0915-2550

Namdar, D., Charuvi, D., Ajjampura, V., Mazuz, M., Ion, A., Kamara, I., et al. (2019). LED lighting affects the composition and biological activity of *Cannabis sativa* secondary metabolites. *Indus. Crops Prod.* 132, 177–185. doi: 10.1016/j.indcrop.2019.02.016

Nazari, M., and Zarinkamar, F. (2020). Ultraviolet-B induced changes in *Mentha aquatica* (a medicinal plant) at early and late vegetative growth stages: investigations at molecular and genetic levels. *Indus. Crops Prod.* 154:112618. doi: 10.1016/j.indcrop.2020.112618

Nützmann, H. W., Huang, A., and Osbourn, A. (2016). Plant metabolic clusters–from genetics to genomics. *New Phytol.* 211, 771–789. doi: 10.1111/nph.13981

Okada, T., Mochamad Afendi, F., Altaf-Ul-Amin, M., Takahashi, H., Nakamura, K., and Kanaya, S. (2010). Metabolomics of medicinal plants: the importance of multivariate analysis of analytical chemistry data. *Curr. Comput. Aided Drug Design* 6, 179–196. doi: 10.2174/157340910791760055

Pate, D. W. (1994). Chemical ecology of Cannabis. *J. Int. Hemp Assoc.* 2, 32–37.

Pavlovic, R., Panseri, S., Giupponi, L., Leoni, V., Citti, C., Cattaneo, C., et al. (2019). Phytochemical and ecological analysis of two varieties of hemp (*Cannabis sativa L.*) grown in a mountain environment of Italian Alps. *Front. Plant Sci.* 10:1265. doi: 10.3389/fpls.2019.01265

Pellati, F., Brighenti, V., Sperlea, J., Marchetti, L., Bertelli, D., and Benvenuti, S. (2018). New methods for the comprehensive analysis of bioactive compounds in *Cannabis sativa* L. (hemp). *Molecules* 23:2639. doi: 10.3390/molecules23102639

Pillemer, E. A., and Tingey, W. M. (1976). Hooked trichomes: a physical plant barrier to a major agricultural pest. *Science* 193, 482–484. doi: 10.1126/science.193.4252.482

Piluzza, G., Delogu, G., Cabras, A., Marceddu, S., and Bullitta, S. (2013). Differentiation between fiber and drug types of hemp (*Cannabis sativa* L.) from a collection of wild and domesticated accessions. *Genet. Resour. Crop Evol.* 60, 2331–2342. doi: 10.1007/s10722-013-0001-5

Pollastro, F., Minassi, A., and Fresu, L. G. (2018). Cannabis phenolics and their bioactivities. *Curr. Med. Chem.* 25, 1160–1185. doi: 10.2174/0929867324666170810164636

Radwan, M. M., Elsohly, M. A., Slade, D., Ahmed, S. A., Wilson, L., El-Alfy, A. T., et al. (2008). Non-cannabinoid constituents from a high potency *Cannabis sativa* variety. *Phytochemistry* 69, 2627–2633. doi: 10.1016/j.phytochem.2008.07.010

Raman, V., Lata, H., Chandra, S., Khan, I. A., and Elsohly, M. A. (2017). "Morpho-anatomy of marijuana (*Cannabis sativa* L.)," in *Cannabis sativa L.-Botany and Biotechnology,* eds S. Chandra, H. Lata, and M.A. Elsohly (Cham: Springer), 123–136. doi: 10.1007/978-3-319-54564-6_5

Rea, K. A., Casaretto, J. A., Al-Abdul-Wahid, M. S., Sukumaran, A., Geddes-Mcalister, J., Rothstein, S. J., et al. (2019). Biosynthesis of cannflavins A and B from *Cannabis sativa* L. *Phytochemistry* 164, 162–171. doi: 10.1016/j.phytochem.2019.05.009

Rozema, J., Björn, L. O., Bornman, J., Gaberščik, A., Häder, D.-P., Trošt, T., et al. (2002). The role of UV-B radiation in aquatic and terrestrial ecosystems—an experimental and functional analysis of the evolution of UV-absorbing compounds. *J. Photochem. Photobiol. B Biol.* 66, 2–12. doi: 10.1016/S1011-1344(01)00269-X

Russo, E. B. (2019). The case for the entourage effect and conventional breeding of clinical cannabis: no "strain," no gain. *Front. Plant Sci.* 9:1969. doi: 10.3389/fpls.2018.01969

Ruzicka, L. (1953). The isoprene rule and the biogenesis of terpenic compounds. *Experientia* 9, 357–367. doi: 10.1007/BF02167631

Sager, J., Smith, W., Edwards, J., and Cyr, K. (1988). Photosynthetic efficiency and phytochrome photoequilibria determination using spectral data. *Trans. ASAE* 31, 1882–1889. doi: 10.13031/2013.30952

Seca, A. M., and Pinto, D. C. (2019). Biological potential and medical use of secondary metabolites. *Medicines* 6:66. doi: 10.3390/medicines6020066

Shoyama, Y., Oku, R., Yamauchi, T., and Nishioka, I. (1972). Cannabis. VI. Cannabicyclolic acid. *Chem. Pharmaceut. Bull.* 20, 1927–1930. doi: 10.1248/cpb.20.1927

Siano, F., Moccia, S., Picariello, G., Russo, G. L., Sorrentino, G., Di Stasio, M., et al. (2019). Comparative study of chemical, biochemical characteristic and ATR-FTIR analysis of seeds, oil and flour of the edible fedora cultivar hemp (*Cannabis sativa* L.). *Molecules* 24:83. doi: 10.3390/molecules24010083

Sirikantaramas, S., Morimoto, S., Shoyama, Y., Ishikawa, Y., Wada, Y., Shoyama, Y., et al. (2004). The gene controlling marijuana psychoactivity molecular cloning and heterologous expression of Δ^1-tetrahydrocannabinolic acid synthase from *Cannabis sativa* L. *J. Biol. Chem.* 279, 39767–39774. doi: 10.1074/jbc.M403693200

Sirikantaramas, S., and Taura, F. (2017). "Cannabinoids: biosynthesis and biotechnological applications," in *Cannabis sativa L.-Botany and Biotechnology,* eds S. Chandra, H. Lata, and M. A. Elsohly (Cham: Springer), 183–206. doi: 10.1007/978-3-319-54564-6_8

Small, E., and Naraine, S. G. (2016). Size matters: evolution of large drug-secreting resin glands in elite pharmaceutical strains of *Cannabis sativa* (marijuana). *Genet. Resour. Crop Evol.* 63, 349–359. doi: 10.1007/s10722-015-0254-2

Solymosi, K., and Köfalvi, A. (2017). Cannabis: a treasure trove or pandora's box? *Mini Rev. Med. Chem.* 17, 1223–1291. doi: 10.2174/1389557516666161004162133

Stojanoski, N. (1999). Development of health culture in Veles and its region from the past to the end of the 20th century. *Veles Soc. Sci.* 13, 13–34.

Taghinasab, M., and Jabaji, S. (2020). Cannabis microbiome and the role of endophytes in modulating the production of secondary metabolites: an overview. *Microorganisms* 8:355. doi: 10.3390/microorganisms8030355

Taura, F., Sirikantaramas, S., Shoyama, Y., Yoshikai, K., Shoyama, Y., and Morimoto, S. (2007). Cannabidiolic-acid synthase, the chemotype-determining enzyme in the fiber-type *Cannabis sativa*. *FEBS Lett.* 581, 2929–2934. doi: 10.1016/j.febslet.2007.05.043

Teramura, A. H. (1983). Effects of ultraviolet-B radiation on the growth and yield of crop plants. *Physiol. Plant.* 58, 415–427. doi: 10.1111/j.1399-3054.1983.tb04203.x

Theis, N., and Lerdau, M. (2003). The evolution of function in plant secondary metabolites. *Int. J. Plant Sci.* 164, S93–S102. doi: 10.1086/374190

Thirumurugan, D., Cholarajan, A., Raja, S. S., and Vijayakumar, R. (2018). "An introductory chapter: secondary metabolites," in *Secondary Metabolites - Sources and Applications,* ed R. Vijayakumar (London: IntechOpen), 3–21. doi: 10.5772/intechopen.79766

Tissier, A. (2012). Glandular trichomes: what comes after expressed sequence tags? *Plant J.* 70, 51–68. doi: 10.1111/j.1365-313X.2012.04913.x

Tomko, A. M., Whynot, E. G., Ellis, L. D., and Dupré, D. J. (2020). Anti-cancer potential of cannabinoids, terpenes, and flavonoids present in cannabis. *Cancers* 12:1985. doi: 10.3390/cancers12071985

Tossi, V. E., Regalado, J. J., Iannicelli, J., Laino, L. E., Burrieza, H. P., Escandón, A. S., et al. (2019). Beyond Arabidopsis: differential UV-B response mediated by UVR8 in diverse species. *Front. Plant Sci.* 10:780. doi: 10.3389/fpls.2019.00780

Turner, C. E., Elsohly, M. A., and Boeren, E. G. (1980). Constituents of *Cannabis sativa* L. XVII. A review of the natural constituents. *J. Nat. Prod.* 43, 169–234. doi: 10.1021/np50008a001

Urban, L., Charles, F., De Miranda, M. R. A., and Aarrouf, J. (2016). Understanding the physiological effects of UV-C light and exploiting its agronomic potential before and after harvest. *Plant Physiol. Biochem.* 105, 1–11. doi: 10.1016/j.plaphy.2016.04.004

Van Klingeren, B., and Ten Ham, M. (1976). Antibacterial activity of Δ^9-tetrahydrocannabinol and cannabidiol. *Antonie van Leeuwenhoek* 42, 9–12. doi: 10.1007/BF00399444

Vanhove, W., Van Damme, P., and Meert, N. (2011). Factors determining yield and quality of illicit indoor cannabis (*Cannabis* spp.) production. *Forensic Sci. Int.* 212, 158–163. doi: 10.1016/j.forsciint.2011.06.006

Veress, T., Szanto, J., and Leisztner, L. (1990). Determination of cannabinoid acids by high-performance liquid chromatography of their neutral derivatives formed by thermal decarboxylation: I. Study of the decarboxylation process in open reactors. *J. Chromatogr. A* 520, 339–347. doi: 10.1016/0021-9673(90)85118-F

Warner, R., Wu, B.-S., Macpherson, S., and Lefsrud, M. (2021). A review of strawberry photobiology and fruit flavonoids in controlled environments. *Front. Plant Sci.* 12:611893. doi: 10.3389/fpls.2021.611893

Wei, X., Zhao, X., Long, S., Xiao, Q., Guo, Y., Qiu, C., et al. (2021). Wavelengths of LED light affect the growth and cannabidiol content in *Cannabis sativa* L. *Indus.l Crops Prod.* 165:113433. doi: 10.1016/j.indcrop.2021.113433

Werker, E. (2000). Trichome diversity and development. *Adv. Bot. Res.* 31, 1–35. doi: 10.1016/S0065-2296(00)31005-9

Westmoreland, F. M., Kusuma, P., and Bugbee, B. (2021). Cannabis lighting: decreasing blue photon fraction increases yield but efficacy is more important for cost effective production of cannabinoids. *PLoS ONE* 16:e0248988. doi: 10.1371/journal.pone.0248988

White, A., Munson, J., Munson, A., and Carchman, R. (1976). Effects of Δ9-tetrahydrocannabinol in Lewis lung adenocarcinoma cells in tissue culture. *J. Natl. Cancer Inst.* 56, 655–658. doi: 10.1093/jnci/56.3.655

Zhou, F., and Pichersky, E. (2020). More is better: the diversity of terpene metabolism in plants. *Curr. Opin. Plant Biol.* 55, 1–10. doi: 10.1016/j.pbi.2020.01.005

Conflict of Interest: The authors declare that this study received funding from EXKA Inc. The funder was not involved in the study design, collection, analysis, interpretation of data, the writing of this article or the decision to submit for publication.

Copyright © 2021 Desaulniers Brousseau, Wu, MacPherson, Morello and Lefsrud. This is an open-access article distributed under the terms of the Creative Commons Attribution License (CC BY). The use, distribution or reproduction in other forums is permitted, provided the original author(s) and the copyright owner(s) are credited and that the original publication in this journal is cited, in accordance with accepted academic practice. No use, distribution or reproduction is permitted which does not comply with these terms.

frontiers in Plant Science

ORIGINAL RESEARCH
published: 07 July 2021
doi: 10.3389/fpls.2021.627311

Morphology, Photosynthetic Traits, and Nutritional Quality of Lettuce Plants as Affected by Green Light Substituting Proportion of Blue and Red Light

Lie Li[1,2], *Yu-xin Tong*[1,2]*, *Jun-ling Lu*[1,2], *Yang-mei Li*[1,2], *Xin Liu*[1,2] and *Rui-feng Cheng*[1,2]

[1] Institute of Environment and Sustainable Development in Agriculture, Chinese Academy of Agricultural Sciences, Beijing, China, [2] Key Laboratory of Energy Conservation and Waste Management of Agricultural Structures, Ministry of Agriculture, Beijing, China

OPEN ACCESS

Edited by:
Marie-Theres Hauser, University of Natural Resources and Life Sciences Vienna, Austria

Reviewed by:
Thomas D. Sharkey, Michigan State University, United States
Myung-Min Oh, Chungbuk National University, South Korea

***Correspondence:**
Yu-xin Tong
tongyuxin@caas.cn

Specialty section:
This article was submitted to Plant Metabolism and Chemodiversity, a section of the journal Frontiers in Plant Science

Received: *11 November 2020*
Accepted: *07 June 2021*
Published: *07 July 2021*

Citation:
Li L, Tong Y-x, Lu J-l, Li Y-m, Liu X and Cheng R-f (2021) Morphology, Photosynthetic Traits, and Nutritional Quality of Lettuce Plants as Affected by Green Light Substituting Proportion of Blue and Red Light. Front. Plant Sci. 12:627311. doi: 10.3389/fpls.2021.627311

Green light, as part of the photosynthetically active radiation, has been proven to have high photosynthetic efficiency once absorbed by plant leaves and can regulate plant physiological activities. However, few studies have investigated the appropriate and efficient way of using the green light for plant production. Thus, the objective of this study was to investigate a moderate amount of green light, partially replacing red and blue light, for plant growth and development. In this experiment, four treatments were set up by adjusting the relative amount of green light as 0 (RB), 30 (G30), 60 (G60), and 90 (G90) μmol m^{-2} s^{-1}, respectively, with a total photosynthetic photon flux density of 200 μmol m^{-2} s^{-1} and a fixed red-to-blue ratio of 4:1. Lettuce (*Lactuca sativa* cv. 'Tiberius') plant growth and morphology, stomatal characteristics, light absorptance and transmittance, photosynthetic characteristics, and nutritional quality were investigated. The results showed that: (1) shoot dry weight increased by 16.3 and 24.5% and leaf area increased by 11.9 and 16.2% under G30 and G60, respectively, compared with those under RB. Plant stem length increased linearly with increasing green-to-blue light ratio; (2) light transmittance of lettuce leaf under treatments employing green light was higher than that under RB, especially in the green region; (3) stomatal density increased, whereas stomatal aperture area decreased with the increase in the relative amount of green light; and (4) carbohydrate accumulation increased under G60 and G90. Soluble sugar contents under G60 and G90 increased by 39.4 and 19.4%, respectively. Nitrate contents under G30, G60, and G90 decreased by 26.2, 40.3, and 43.4%, respectively. The above results indicated that 15–30% green light replacing red and blue light effectively increased the yield and nutritional quality of lettuce plants.

Keywords: lettuce (*Lactuca sativa* cv. 'Tiberius'), green light, shade avoidance syndrome, light transmittance, stomata characteristics, plant photosynthesis, plant morphology

INTRODUCTION

Plants perceive not only light intensity and photoperiod but also light quality, including monochromatic and polychromatic light, as ambient growth environment signals that induce a large number of physiological responses (Kami et al., 2010). Different light qualities have distinctly different biological effects on plants (Li et al., 2020). There is a misconception that green light is less useful for plant photosynthesis, probably because the light absorption of photosynthetic pigments is relatively low within the green region compared with that within the red and blue regions, especially in the plant canopy (McCree, 1972; Smith et al., 2017). This is also the reason that red and blue light, rather than other lights, are widely used in recently developed plant factories with artificial lighting for plant production (Wang et al., 2016). Moreover, the photoreceptors of red and far-red, blue, and UV-B have been identified as phytochromes, cryptochromes and phototropins, and UV Resistance Locus 8 (Bantis et al., 2018), respectively, but no specific green light photoreceptor was detected in previous studies. Even so, the vital role of green light affecting plant physiological activities was gradually proved in previous studies (Johkan et al., 2012; Wang and Folta, 2013; Materová et al., 2017).

A recently published review suggested that green light distributed energy among plant leaves and canopies (Smith et al., 2017) because green light was capable of reaching deeper and drives CO_2 fixation under plant canopy, whereas most of the red and blue light is generally absorbed by the upper part of plant leaves (Sun et al., 1998; Schenkels et al., 2020). In addition, a green light could easily induce a shade avoidance syndrome in plants because, in natural conditions, green light transmitted through the plant canopy, causing a sharp decline in blue-to-green (B/G) ratio from the top to the bottom layers of plants (Zadoks et al., 1974). Similar to the shading response caused by far-red light, plant stem elongation and leaf area expansion also occurred under green light (Sellaro et al., 2010; Zhang et al., 2011). Besides, green light shifted cryptochromes from semi-reduced active state caused by blue light to the fully reduced and inactive state. Thus, green light could inactivate blue-mediated responses (Bouly et al., 2007; Liu et al., 2010; Sellaro et al., 2010).

Recent studies suggested that green light should not be ignored in plant growth and development. Kaiser et al. (2019) reported that, by replacing red and blue with green light, the fresh and dry weights of tomato increased linearly with an increase in the percentage of green light. Schenkels et al. (2020) have shown that additional green light significantly increased the total fresh and dry weights of plant seedlings, whereas when replacing red and blue with green light, no significant increase was found in dry weight. The above inconsistent results were mainly caused by the different proportions of green light in the light source. According to McCree (1972), once absorbed by plant leaves, green light showed a higher relative quantum efficiency than blue light. Moreover, the shade avoidance syndrome induced by green light was capable of increasing the stem length and leaf area of plants (Johkan et al., 2012). These changes in plant morphology effectively enhance the photons captured by plant leaves, improving the photosynthetic efficiency (Park and Runkle, 2017). Thus, investigating a moderate proportion of green light can optimize the photosynthesis of plant leaves to maximize the yield in plant production.

Therefore, this study aimed to investigate the optimal proportion of green light for lettuce growth and development by adjusting the relative amount of green light. Combined red and blue light were used as the fundamental light. Lettuce (*Lactuca sativa* cv. 'Tiberius') was used in this experiment because it is one of the most popular horticulture vegetables produced in plant factories with artificial lighting. Lettuce morphology, biomass, stomatal characteristics, light absorptance and transmittance, photosynthetic traits, and nutritional quality were evaluated.

MATERIALS AND METHODS

Plant Material and Growth Condition

Lettuce (*Lactuca sativa* cv. 'Tiberius') seeds were sown in sponge blocks filled in plastic trays. Seedlings were developed under fluorescent lamps (TL-D56W, Osram, Munich, Germany) with a light intensity of 150 μmol m^{-2} s^{-1} and a photoperiod of 16 h day^{-1}. Upon emerging three true leaves (15 days after sowing), seedlings were transplanted in a plant factory with artificial lighting (PFAL), in which the day/night temperature was 24/20°C, relative humidity was 60–70%, and the concentration of CO_2 (supplied by a CO_2 gas cylinder) was 1,000 μmol mol^{-1}. Plants were cultivated in a customized circulation system of nutrient solution with a planting density of 32 plants m^{-2}. The light-emitting diode (LED) panels (Datang New Energy Technology Co., Ltd., Shenzhen, China) were equipped on cultivation shelves. The distance between the LED panels and the culture bed was 0.3 m. An opaque white plastic reflective film was placed around the LED panels to ensure uniform radiation on the surface of the culture beds and to prevent light pollution from the adjacent treatments. Modified Yamasaki nutrient solution (EC = 1.2 dS m^{-1}, pH = 5.8) was applied for the plant growth. The circulation system was automatically operated for 1 h day^{-1}.

Experimental Setup

The photosynthetic photon flux density (PPFD) and red (600–690 nm, peak at 660 nm) to blue (410–490 nm, peak at 450 nm) (R/B) ratio of all treatments were maintained at 200 μmol m^{-2} s^{-1} and 4:1, respectively. The relative amount of green light (490–590 nm, peak at 525 nm) of each treatment was adjusted to 0 (RB), 30 (G30), 60 (G60), and 90 (G90) μmol m^{-2} s^{-1} (**Table 1**). The light spectrum of each treatment was presented in **Figure 1**. Plants were harvested on day 20 after transplanting. This experiment was repeated three times.

Determinations of Plant Growth and Morphology

For the growth and morphology analysis, destructive measurements were taken on five plants of each treatment on day 20 after transplanting. Lettuce samples were separated into shoot and root using sharp scalpels and forceps. The stem length was the average value of stem lengths in fully expanded leaves of each plant. The leaf area was measured by an area

meter (LI-3100C, LI-COR Biosciences, Lincoln, NE, USA). The fresh and dry weights of shoot and roots were measured by an electronic balance (Si-234; Denver Instrument, Bohemia, NY, USA). Whole-plant net assimilation was calculated by dividing shoot dry weight by total leaf area for each plant.

Measurements of Light Absorptance and Light Transmittance of Leaves

Light reflectance (Rf) and light transmittance (Tr) were measured on the fully expanded second leaves with a spectroradiometer (Ocean Optics USB2000+, Dunedin, FL, USA) in combination with two integrating spheres (FOIS-1, ISP-REF, Ocean Optics Inc., Dunedin, FL, USA). Light absorptance (Ab) was calculated as: Ab = 1 – (Rf + Tr). The diagram of the measuring apparatus is showed in **Supplementary Figure 1**.

Observation of Stomata

Leaf samples were collected from the fully expanded second young leaves of five plants in the same region of each treatment. Leaf stomatal characteristics were measured using the method of Wang et al. (2016). The stomata of plants are regarded as rhombus. Stomatal aperture area was calculated by long axis length of aperture (Al) and short axis length of aperture (As). Stomatal aperture area = Al × As/2.

TABLE 1 | Different light intensity (μmol m^{-2} s^{-1}) of red, blue, and green light of four treatments.

Treatments	Red	Blue	Green	PPFD[a]	YPFD[b]
RB	160	40	0	200	178.8
G30	136	34	30	200	173.9
G60	112	28	60	200	168.9
G90	88	22	90	200	164.0

[a] *PPFD, Photosynthetic photon flux density, μmol m^{-2} s^{-1}.*
[b] *YPFD, Yield photon flux density, which is the product of spectral photon distribution and relative quantum efficiency according to Sager et al. (1988) and McCree (1972).*

Determinations of Photosynthetic Pigments and Photosynthetic Characteristics

From the top to the bottom, the leaves of 2, 4, 6, 8, 10, 12, 14, 16, 18, and 20 from four plants in each treatment were collected at the same point with 1 cm^2 by using a punch. Subsequently, 96% ethanol was used as a solvent for these samples to measure chlorophyll a (Chl a), chlorophyll b (Chl b), and carotenoid content. The absorbance was measured at 665, 649, and 470 nm by using a spectrophotometer (UV-1800, Shimadzu Corp., Kyoto, Japan). Concentrations of chlorophyll and carotenoid were determined using the equations reported by Lichtenthaler and Wellburn (1983). All of the data measured were used for the normal distribution analysis shown in **Figure 7**.

Net photosynthetic rate (P_n), gas exchange (g_s), and intercellular CO_2 concentration (Ci) of lettuce fully expanded second leaves were measured using a portable photosynthetic instrument (LI-6400XT, LI-COR Biosciences, Lincoln, NE, USA) with a transparent leaf chamber (6400-08, LI-COR Biosciences, Lincoln, NE, USA) under the actual light condition of plant growth. The environmental conditions of the leaf chamber were maintained at 24°C, 1,000 μmol m^{-2} s^{-1} CO_2 level, and 60–70% relative humidity (Li et al., 2020). The order of measurements was arranged randomly for each repetition, and each treatment was repeated three times. P_n and g_s of lettuce leaves measured in LED leaf chamber were represented by P_{n-T} and g_{s-T}, respectively.

P_n and g_s to light intensity response curves were taken on the fully expanded second leaves by using the same portable photosynthetic instrument (LI-6400XT, LI-COR Biosciences, Lincoln, NE, USA) with a red–blue LED leaf chamber (6400-02B, LI-COR Biosciences, Lincoln, NE, USA) installed. The leaf chamber temperature, the concentration of CO_2, relative humidity, airflow rate, and leaf-to-air vapor pressure difference

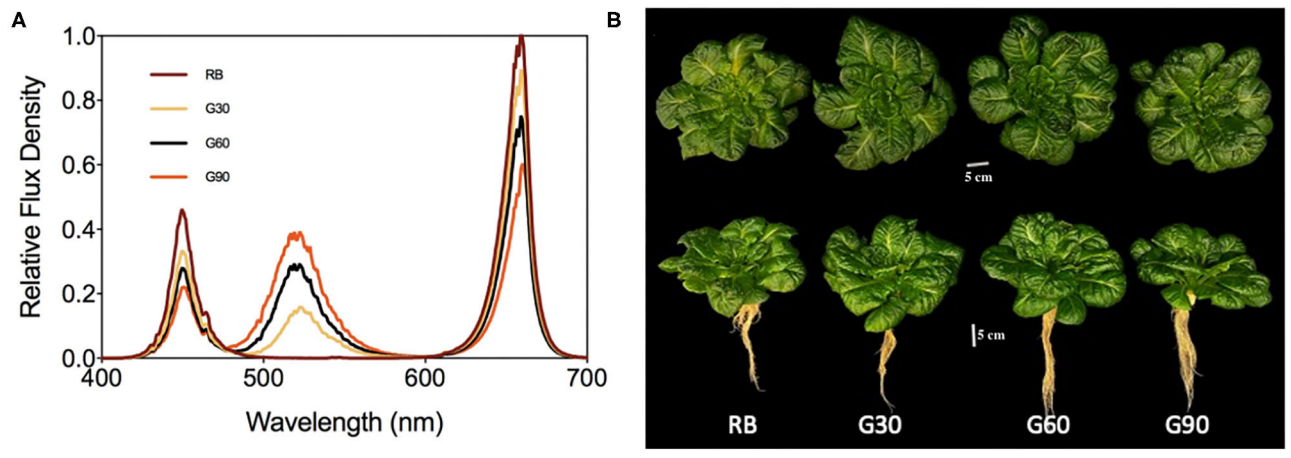

FIGURE 1 | The spectral distribution of different treatments **(A)** and photograph of lettuce grown under treatments **(B)**.

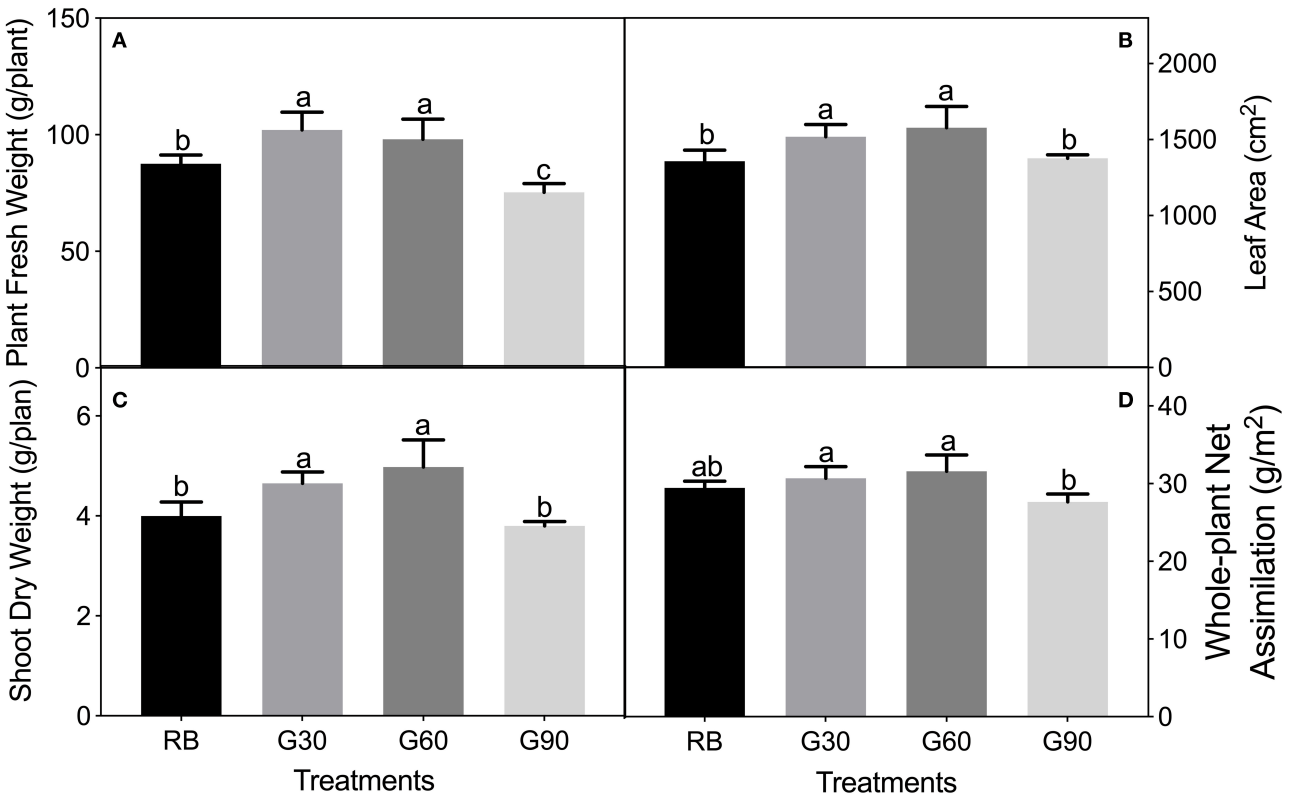

FIGURE 2 | Plant fresh weight **(A)**, leaf area **(B)**, shoot dry weight **(C)**, and whole-plant net assimilation **(D)** of lettuce plants as affected by the different proportions of green light. Different letters in each column indicate significant differences at $p < 0.05$, according to the least significant difference (LSD) test.

($VPD_{leaf-air}$) in the leaf chamber were 24°C, 1,000 μmol mol^{-1}, 60–70%, 500 μmol s^{-1}, and 1.0 ± 0.1 kPa, respectively. P_n and g_s under different light intensities were measured subsequently. The starting light intensity was 200 μmol m^{-2} s^{-1}, followed by 100, 0, 200, 400, 600, 800, 1,000, and 1,200 μmol m^{-2} s^{-1}. Light intensity decreasing from the actual growth level to dark and then gradually increasing to high light intensities was needed when measuring light intensity-photosynthesis response curves of plant leaves (Wang et al., 2016). The light source was red and blue light with an R/B ratio of 4:1. P_n and g_s were recorded when P_n reached a steady state at each light intensity. Measurement order was arranged randomly for every repetition, and each treatment was repeated three times. P_n and g_s of lettuce leaves measured in LED leaf chamber were represented by P_{n-L} and g_{s-L}, respectively.

Determinations of Sucrose, Starch, and Nutritional Quality

Lettuce leaves were collected in sample bottles, quick-frozen by using liquid nitrogen, and stored in an ultralow temperature freezer before the end of the dark period. Five plants of each treatment were taken at the end of the light period on day 20 after transplanting. The samples were used to measure sucrose, starch, and nutritional quality contents, including soluble sugar, nitrate, and crude fiber. Sucrose content was determined using the method described by Fils-Lycaon et al. (2011) and measured at 480 nm. Starch content was measured and calculated according to Clegg (1956). Soluble sugar content was determined using the method described by Fairbairn (1953). Nitrate content was determined by the method described by Cataldo et al. (1975). The ELISA performed by using the double-antibody one-step sandwich method was used to determine the crude fiber content of lettuce leaves. The absorbance was measured at 450 nm wavelength with a spectrophotometer (Shimadzu UV-1800, Shimadzu Corp., Kyoto, Japan).

Statistical Analysis

This experiment was designed as a single factor experiment. A one-way ANOVA was performed for each treatment. When the ANOVA result was significant, Duncan's multiple range test at $p < 0.05$ was used for mean separation. The linear relationships between plant stem length and G/B ratio were determined by GraphPad Prism 8 (GraphPad Software Inc., San Diego, CA, USA), using simple linear regression. The fitting light intensity response curves of P_n and g_s with non-linear regression were performed by the GraphPad Prism 8 (GraphPad Software Inc., San Diego, CA, USA), using [Agonist] vs. response–variable slope (four parameters) equation. The

data of chlorophyll concentration in different layers of lettuce plants were performed by a box-plot and drawn with the Origin 2020 software (OriginLab Inc., Northampton, MA, USA). The desperation of data is proportional to the height of the box. The lines and dots in the box represent the median and the average values, respectively. The highest and the lowest point of the vertical line represent the maximum and minimum values. All statistical analyses were performed by the IBM SPSS Statistics 26 program (SPSS Inc., Chicago, IL, USA). This experiment was repeated three times.

RESULTS

Growth and Morphology

As shown in **Figure 2**, plant fresh weight, leaf area, and shoot dry weight were 12–25% greater under G30 and G60 than those under RB or G90. The increased leaf area accounted for most of the increased plant mass so that the trend of whole-plant net assimilation was nearly constant with the leaf area among four treatments. The stem length of lettuce increased linearly with increasing G/B ratio (**Figure 3**).

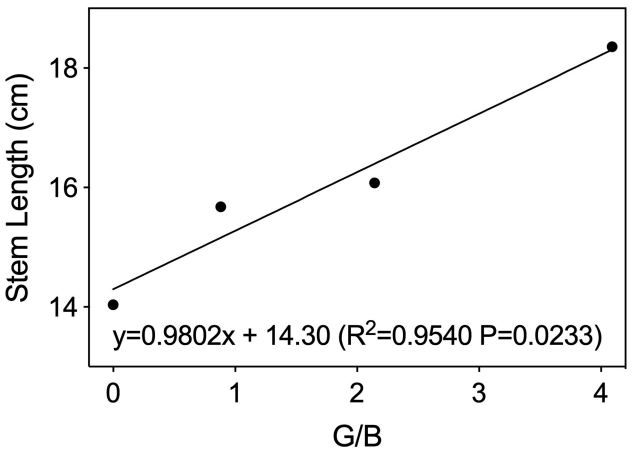

FIGURE 3 | Stem length of lettuce leaves as affected by green-to-blue (G/B) ratio. Associated correlation of coefficients (R^2) and regression equations presented here indicate significant differences at $p < 0.05$.

Light Absorptance and Light Transmittance of Lettuce Leaves

As shown in **Figure 4**, the lowest light absorptance and highest light transmittance of lettuce leaves were observed in the green range within the visible spectrum of 400–700 nm. Meanwhile, the light transmittance was higher under treatments employing green light than that under RB, whereas the light absorptance was, on the contrary, especially within the green region. The minimal absorptance and maximal transmittance found at the same wavelength point (555 nm) were 80% under G30 and 8% under G60, respectively.

Stomatal Characteristics

As shown in **Table 2**, the stomatal development was significantly affected by the relative amount of green light. Stomatal density increased by 47, 38, and 71% under G30, G60, and G90, respectively, compared with that under RB, whereas epidermal cell density only increased under G90. With the increase in green proportion from 15 to 45%, the long axis length and short axis length of aperture decreased by 7–25% and 14–51%, respectively. The reduction of long and short axis length of aperture caused a linear decrease in aperture area from 45.1 to 16.5 μm^2 with an increase in the relative amount of green light (**Figure 5**).

Leaf Photosynthetic Pigments

The concentrations of total chlorophyll and carotenoids, and Chl a/Chl b in different leaf layers of lettuce were different. As shown in **Figure 6**, these three pigment parameters increased dramatically from the 2nd to the 4th leaf. Meanwhile, the total chlorophyll and carotenoids under G60 and G90 reached their peak at the 4th leaf, whereas they decreased dramatically at the 6th leaf. Then, the curves of the three pigment parameters were relatively flat under G30, G60, and G90 from the 6th to the 14th leaf, and gradually dropped from the 14th to the 20th leaf. A significantly decrease under RB was observed on the three pigment parameters from the 12th to the 20th leaf and finally reached the lowest level among all treatments.

As shown in **Figure 7**, the data of the three pigment parameters of lettuce leaves in different layers under G60 are the most compact in all treatments, whether from the difference between the maximum and minimum values or the height of the box. Employing green light, the difference between maximum and minimum values was decreased significantly, though the highest values of the three pigment parameters were observed under RB. These results suggested that green light reduced the gap of the concentrations of pigments between upper and lower leaves of plants, especially when green light accounts for 30% (G60) in the light source.

Leaf Photosynthetic Traits

P_{n-T} under G30 decreased by 6% compared with that under RB, whereas no significant difference in P_{n-T} was found among RB, G60, and G90. g_{s-T} and Ci under treatments employing green light decreased significantly compared with those under RB (**Figure 8**).

As shown in **Figure 9**, P_{n-L} and g_{s-L} increased with the increasing light intensity. Among treatments employing green light, g_{s-L} increased with an increase in the relative amount of green light. Under G30, g_{s-L} was lower than that under RB, especially when light intensity was lower than 1,000 $\mu mol\ m^{-2}\ s^{-1}$, whereas g_{s-L} under G60 and G90 was higher than that under RB. There was no obvious difference in P_{n-L} among all treatments under the same light intensity (**Figure 9**).

Sucrose, Starch, and Nutritional Quality

As shown in **Table 3**, an increase in the carbohydrate accumulation of lettuce leaves was found under treatments

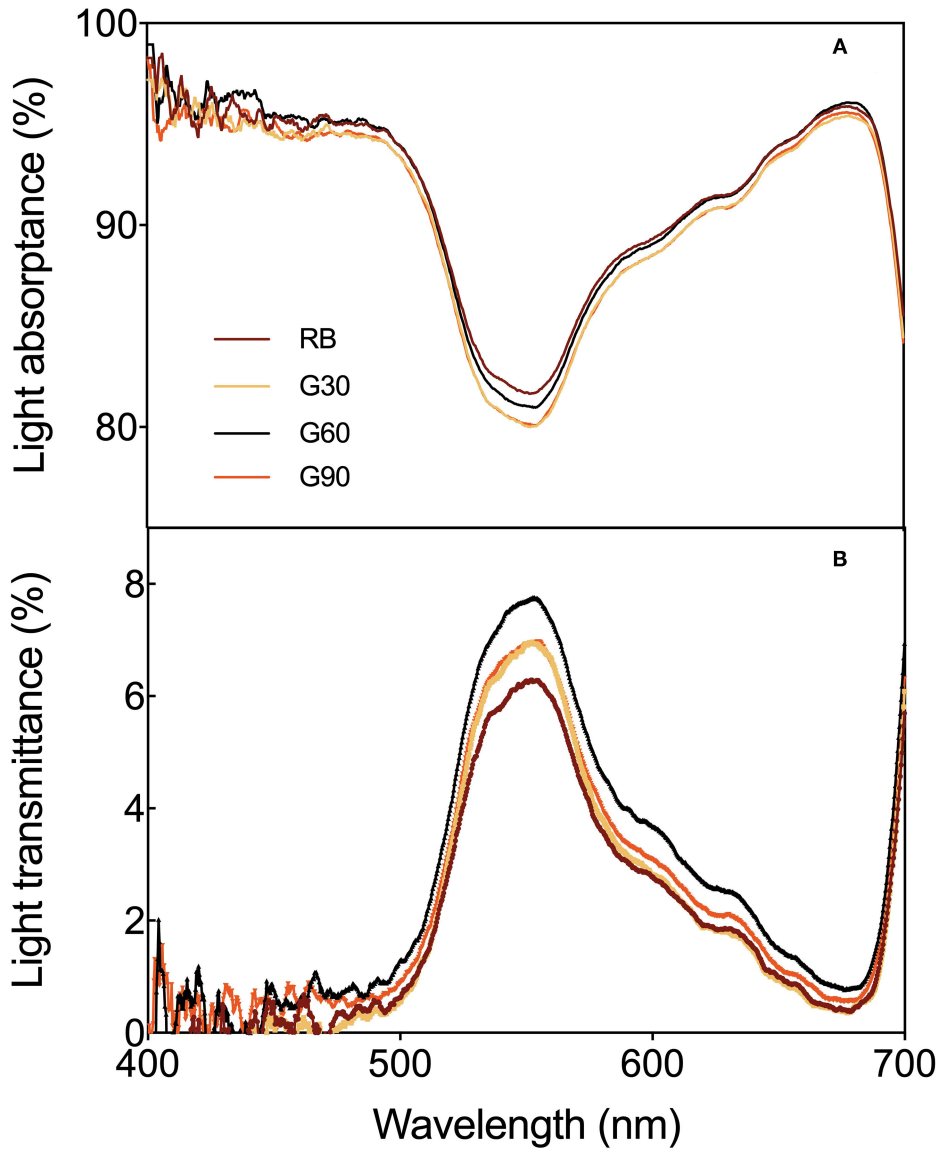

FIGURE 4 | Light absorptance **(A)** and light transmittance **(B)** as affected by the different proportions of green light.

TABLE 2 | Effects of green light on stomatal characteristics of lettuce.

	RB	G30	G60	G90
Stomatal density (N mm^{-2})	117.2 ± 26.2^{c}	172.5 ± 25.0^{b}	161.7 ± 29.4^{b}	200.0 ± 21.9^{a}
Epidermal cell density (N mm^{-2})	717.2 ± 158.0^{b}	662.5 ± 75.9^{b}	700.8 ± 99.6^{b}	1007.0 ± 89.1^{a}
Long axis length of aperture (μm)	16.2 ± 2.1^{a}	15.0 ± 2.0^{b}	14.3 ± 2.1^{b}	12.2 ± 2.6^{c}
Short axis length of aperture (μm)	5.6 ± 1.2^{a}	4.8 ± 1.3^{b}	3.8 ± 1.2^{c}	2.7 ± 1.7^{d}
Aperture area (μm^{2})	45.1 ± 1.3^{a}	35.9 ± 1.4^{b}	26.9 ± 1.3^{c}	16.5 ± 2.0^{d}

The data are means ± SDs (n = 5). Different lowercase letters in the same line show significant difference at $p < 0.05$, according to the least significant difference (LSD) test.

employing green light compared with that under RB. Sucrose and starch contents increased by 60 and 37% under G60 and by 35 and 40% under G90, respectively, compared with those under RB. In terms of nutritional quality, soluble sugar contents under G60 and G90 increased by 39 and 19%, respectively, compared with that under RB.

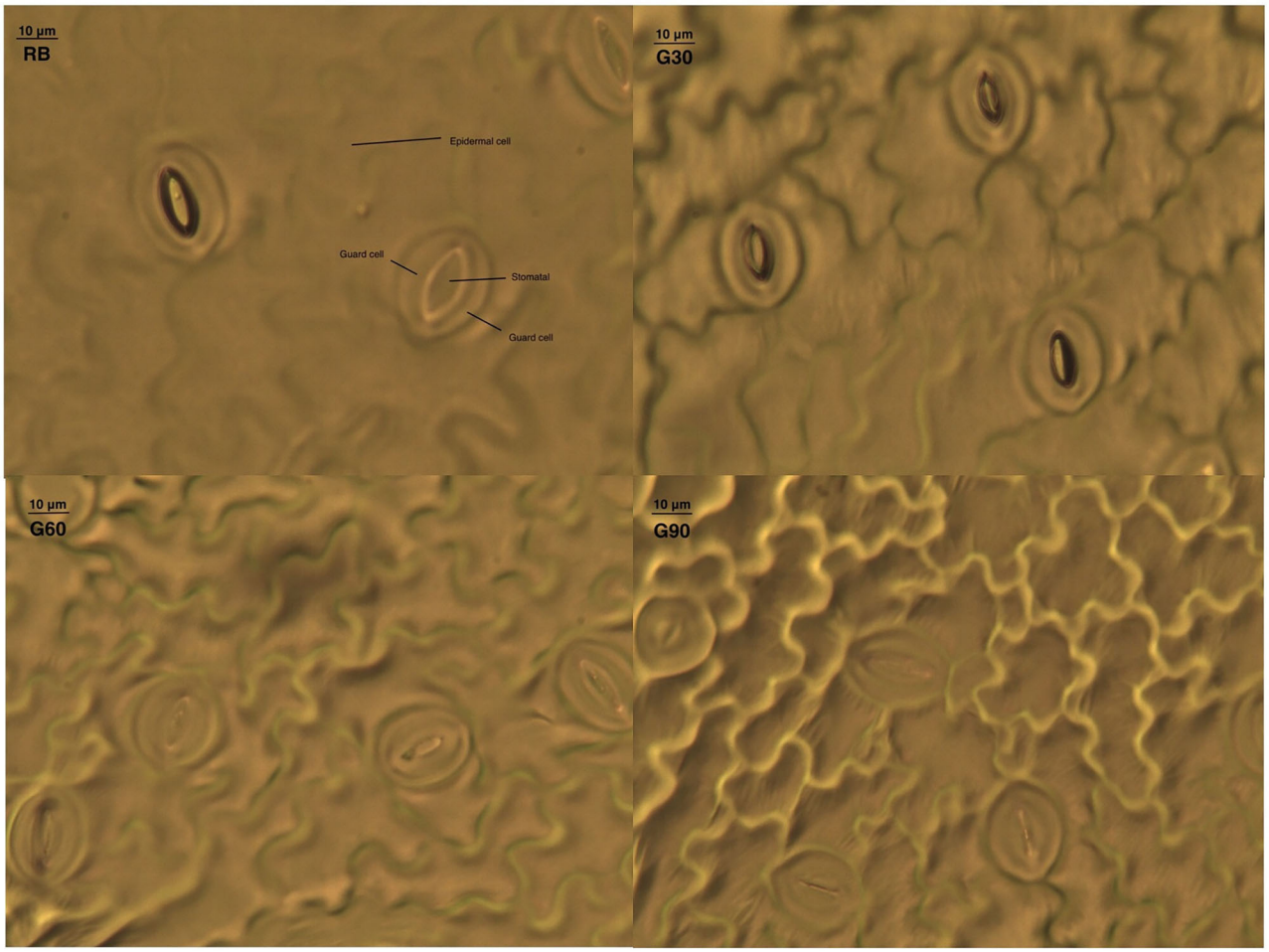

FIGURE 5 | Photos of stomatal characteristics under the different proportions of green light.

Nitrate contents of lettuce leaves significantly decreased under treatments employing green light. Nitrate contents under G30, G60, and G90 decreased by 26, 40, and 43%, respectively, compared with that under RB. No significant differences in crude fiber contents were found among all treatments.

DISCUSSION

Morphology of Lettuce Plants as Affected by Employing Green Light

Light quality, as energy and signal sources, significantly affects plant photomorphogenesis (Bantis et al., 2018). Similar to red/far-red (R/FR) ratio, the G/B ratio also could act as a shade signal within a plant canopy and could provide information about the degree of shading, triggering physiological and morphological changes of plants to best intercept available energy (Sellaro et al., 2010; Smith et al., 2017). In this experiment, lettuce stem length increased with increasing G/B ratio. This result was consistent with the finding that the hypocotyl length of Arabidopsis seedlings increased linearly with increasing G/B ratios within the range of 0.5–1.0 while cultivated in a natural environment (Sellaro et al., 2010). The above phenomenon can be explained by the shade avoidance syndrome induced by the green light. As shown in **Figure 4**, the light transmittance in the green region was higher than that in the blue region so that an increase in G/B ratio was induced under the lettuce canopy, providing a shade signal for plants. The shade signal can be detected by relevant non-photosynthetic photoreceptors, and it can then induce the shade avoidance syndrome, such as stem elongation and leaf expansion, to intercept more available light energy (Wang and Folta, 2013). Kang et al. (2016) also found that green light increased the leaf length in lettuce plants. Moreover, leaf expansion was also found under G30 and G60 in this study. This was consistent with the finding that lettuce leaf area increased dramatically when green light replaced red and blue light (Kim et al., 2004). This kind of morphological changes caused by a high G/B ratio may be attributed to cryptochromes or an unknown role of

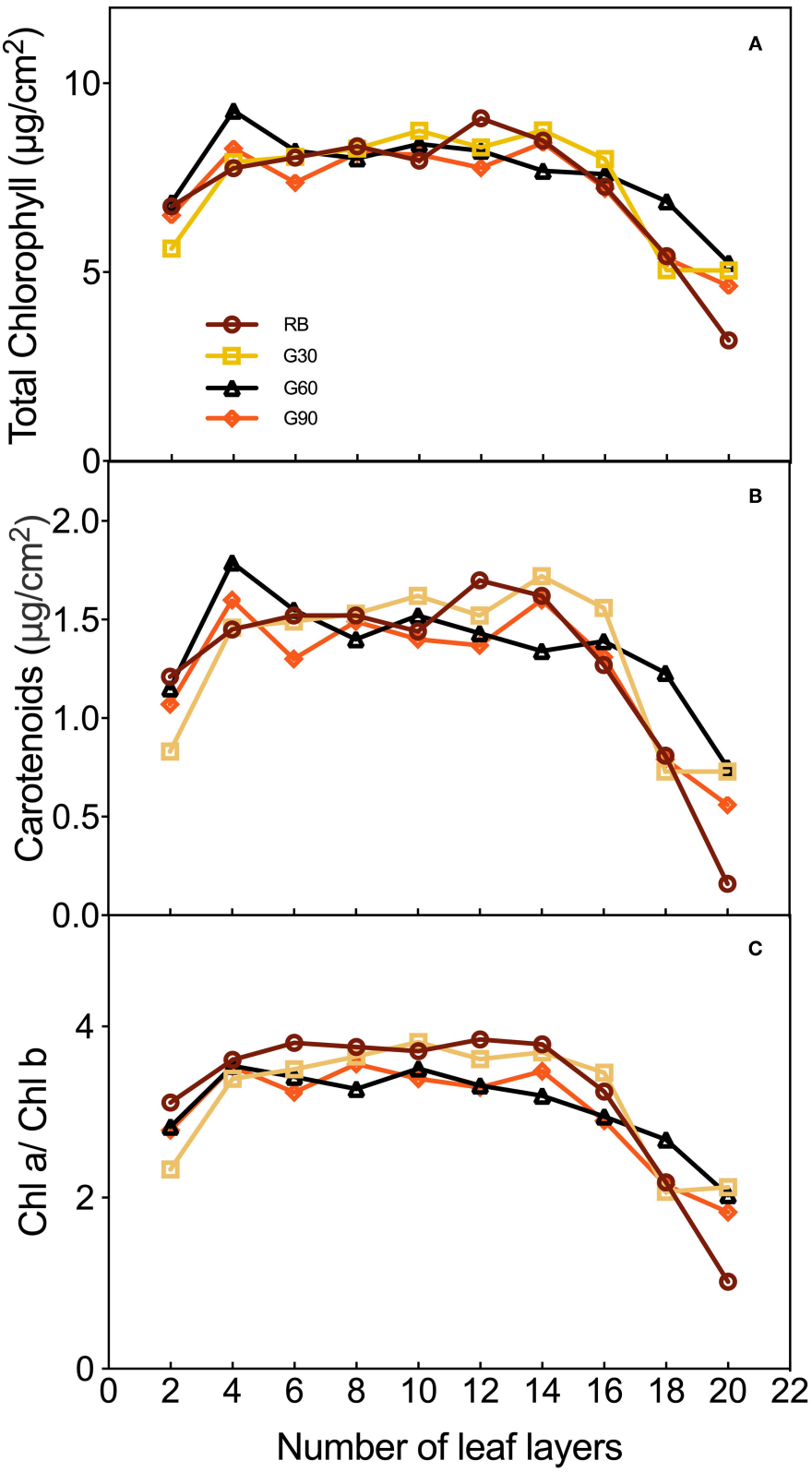

FIGURE 6 | The concentrations of total chlorophyll **(A)**, carotenoids **(B)**, and of leaves and Chl a/Chl b **(C)** of different layers of lettuce plants as affected by the different proportions of green light.

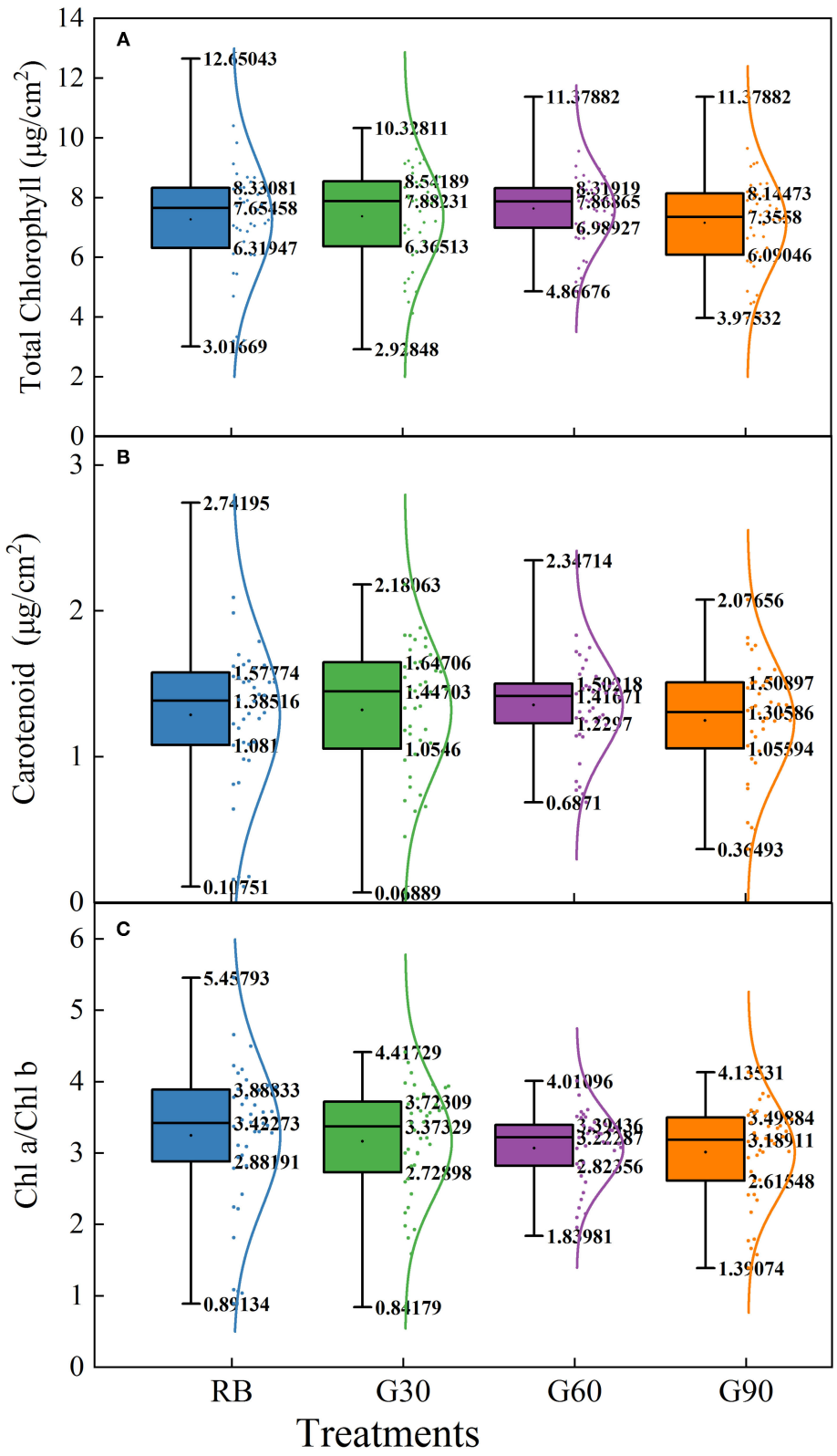

FIGURE 7 | Box-plot and normal distribution of concentrations of total chlorophyll **(A)**, carotenoid **(B)**, and Chl a/Chl b **(C)** of different layers of lettuce under different proportions of green light.

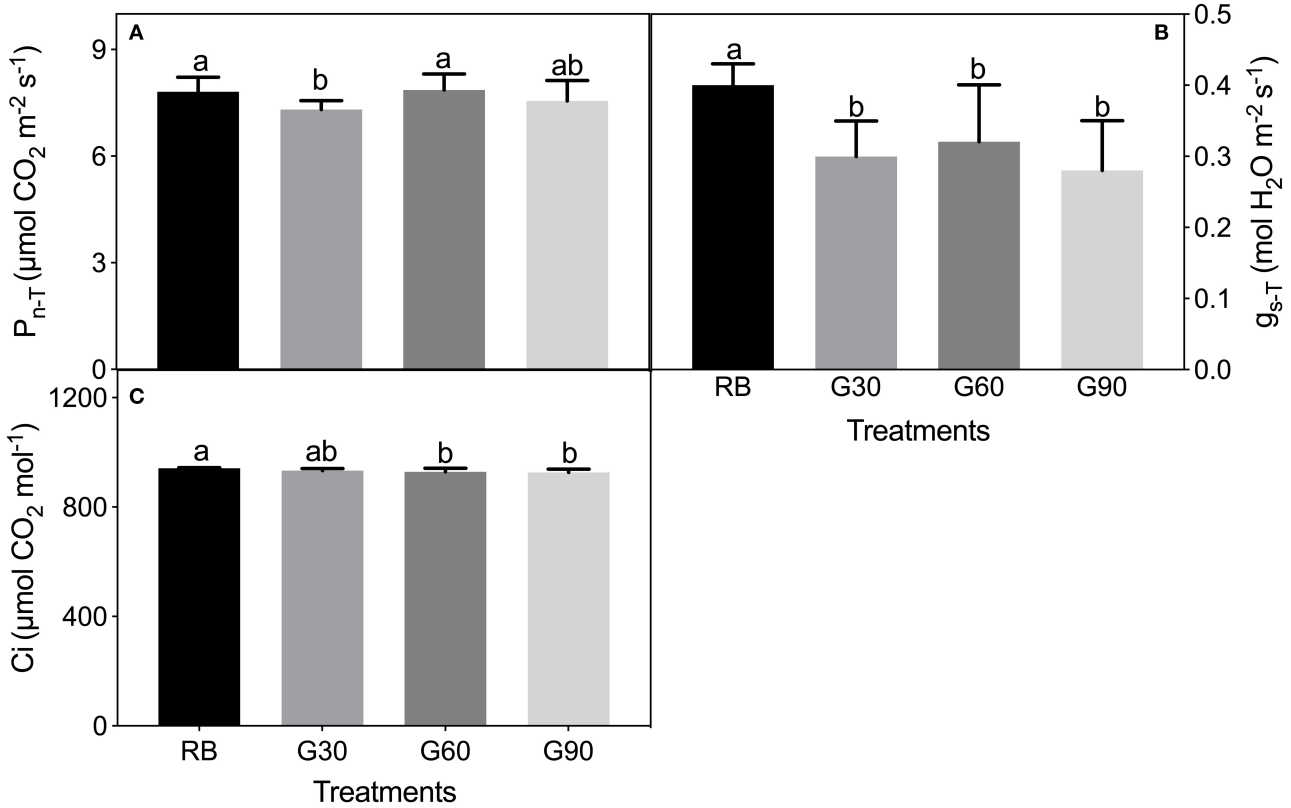

FIGURE 8 | P_{n-T} **(A)**, g_{s-T} **(B)**, and Ci **(C)** under the actual light condition of lettuce leaves as affected by different proportions of green light. Different letters in each column indicate significant differences at $p < 0.05$, according to the least significant difference (LSD) test.

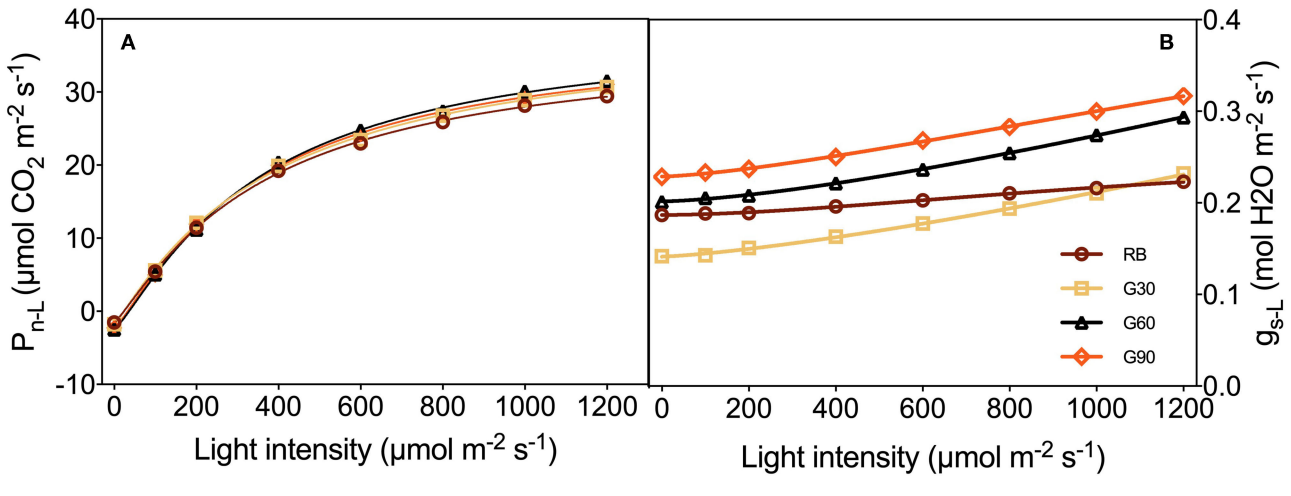

FIGURE 9 | P_{n-L} **(A)** and g_{s-L} **(B)** to light intensity response curves as affected by the different proportions of green light.

phytochromes, or perhaps a novel light photoreceptor (Sellaro et al., 2010; Zhang et al., 2011). However, the leaf area under G90 showed no significant difference with RB. This may be caused by the low yield photon flux density (YPFD) in G90 (Johkan et al., 2012).

Gas Exchange of Lettuce Leaves as Affected by Employing Green Light

Stomatal conductance was mainly affected by stomatal density and the degree of stomatal opening (Fanourakis et al., 2015). Previous studies have shown that stomatal density in newly developed leaves of C3 plants is independent of their adjacent irradiance (Lake et al., 2001; Miyazawa et al., 2006). On the contrary, exposure of mature leaves to low light conditions triggered long-distance signaling that controls the stomatal development and caused a reduction in stomatal density in young leaves (Ehonen et al., 2020). This phenomenon is called systemic signaling (Lake et al., 2001). In this experiment, stomatal density increased with an increase in the relative amount of green light. This should be attributed to green light showing a higher light transmittance to plant canopy in comparison with red and blue light. Meanwhile, the local light intensity in mature leaves of relative lower layers increased with the increasing relative amount of green light. The above result was consistent with the finding that stomatal density increased significantly when blue LEDs were replaced with green LEDs in green leaf lettuce (Son and Oh, 2015).

Green light can reverse the stomatal openings stimulated by blue light (Frechilla et al., 2000), because the fully oxidized state of the flavin chromophore of cryptochrome in darkness is shifted to a semi-reduced form by blue light, and this semi-reduced form is converted to a reduced form particularly by absorbing green light (Liu et al., 2010). This was the reason why stomatal aperture decreased linearly with increasing G/B ratio in this study. This was also the main reason that caused lower g_{s-T} under treatments employing green light than that under RB. However, the stomatal opening could be restored if the green light was followed or replaced by a second blue light in a response analogous to the R/FR reversibility of phytochrome responses (Frechilla et al., 2000; Taiz and Zeiger, 2015). In this research, the stomatal density of lettuce leaves caused by systemic signaling could not change immediately with the change of light quality; thus, under the same red and blue light condition, g_{s-L} increased with an increase in the relative amount of green light. The above phenomenon gave an efficient way to regulate stomatal behaviors. In future experiments, green light can be considered to increase the stomatal density at the early growth stage of plant leaves, whereas blue light can be considered to increase the stomatal opening at the yield-forming stage of plants so that, especially in plant factories, plant yield can be increased efficiently. Previous studies also demonstrated that stomatal response to the light environment could provide potential targets for increasing photosynthesis, water use efficiency, and overall plant yield (Matthews et al., 2020).

Green Light Affected Pigmentation, Light Energy Distribution, and Photosynthetic Characteristics in Lettuce

Most of the previous studies mainly focused on the pigment contents of individual leaves rather than the whole plant. In this study, pigment concentrations of the lettuce leaves in different layers were measured to investigate the effect of green light on pigment concentrations of leaves within the canopy. The light absorptance of red and blue light was higher, but the light transmittance was lower in the upper leaves of lettuce. Thus, the relatively scattered pigment concentrations and Chl a/Chl b were found under RB. Compact distribution of pigment concentrations and Chl a/Chl b under G60 was mainly caused by the maximal light transmittance found under G60, which helped the pigmentation of lower layer leaves of lettuce plants in this study. This was beneficial for whole-plant photosynthesis. In comparison with G60, the lower pigment level of bottom leaves under G30 may be due to the relative lower green light intensity, limiting the irradiance to transmitting through the canopy, whereas under G90, they may be related to a stronger shade condition caused by a higher G/B ratio (Smith and Whitelam, 1997). These results suggested that a moderate amount of green light can promote the pigmentation of underlying leaves in the lower layer canopy.

Green light was capable of contributing light energy to photosynthesis both at the leaf level and the canopy level of plants (Smith et al., 2017). Up to 80% of green light was detected to pass through chloroplast, when 15–25% of green light was considered to transmit through the canopy of plants, efficiently promoting green light absorbed by chloroplasts either in the deeper mesophyll of a single leaf or lower leaves within the canopy, especially in plants with a folded structure, such as lettuce (Terashima et al., 2009). Relative lower light absorptance and higher light transmittance in the green region were also found in this experiment, in comparison with red and blue light. Moreover, higher light transmittance was observed in lettuce leaves under treatments employing green light compared with that under RB, especially in green regions. This result suggested that green light promoted more light energy to transmit through leaves. However, no significant increase in the light transmittance was found by using green light in *Ocimum basilicum* L. (Schenkels et al., 2020). This inconsistent phenomenon may be because the green light accounted for only 12% of the light source in this previous study.

Green light can be transmitted into deeper mesophyll of leaves and promote photosynthesis. In addition, once absorbed by chloroplasts, green light could drive photosynthesis with the close quantum efficiency of red and blue light (McCree, 1972; Smith et al., 2017). Thus, though the YPFD, which has been used to quantify the net radiation driving photosynthesis, of G60 and G90 was lower than that of RB, no significant differences of P_{n-T} among RB, G60, and G90 were found in this research. However, P_{n-T} under G30 was found to be lower than that under RB. This may be because the YPFD of G30 was lower than that of RB, and the relatively lower amount of

TABLE 3 | The accumulation of carbohydrate and nutritional quality as affected by different relative amount of green light.

	RB	G30	G60	G90
Sucrose (mg g^{-1})	4.3 ± 1.1^{b}	5.4 ± 1.5^{ab}	6.9 ± 1.7^{a}	5.8 ± 1.7^{ab}
Starch (mg g^{-1})	1.8 ± 0.2^{b}	2.0 ± 0.5^{b}	2.8 ± 0.7^{a}	2.9 ± 0.7^{a}
Soluble sugar (mg g^{-1})	16.1 ± 1.8^{b}	15.4 ± 1.7^{b}	22.5 ± 1.7^{a}	19.24 ± 6.6^{ab}
Nitrate (mg g^{-1})	1.8 ± 0.3^{a}	1.4 ± 0.2^{b}	1.2 ± 0.3^{c}	1.2 ± 0.4^{c}
Crude fiber (mg g^{-1})	8.9 ± 2.9^{a}	10.3 ± 2.3^{a}	9.9 ± 3.4^{a}	9.9 ± 2.5^{a}

The data are means ± SDs (n = 5). Different lowercase letters in the same line show significant difference at $p < 0.05$, according to the least significant difference (LSD) test.

green light was not enough to promote photosynthesis in the deep layer of leaves. The relatively lower light absorption found under G30 was also the cause of the lowest P_{n-T} found under G30 in this study. When transferred to a similar red–blue light source, lettuce leaves of four treatments showed no differences on P_{n-L}, though g_{s-L} differed. This was mainly because g_s was no longer the limiting factor for plant photosynthesis under high CO_2 levels.

Moderate Amount of Green Light Increased the Biomass in Lettuce

Plant dry mass accumulation was mainly determined by the photosynthetic efficiency of plant leaves and total leaf area of plants. The photosynthetic efficiency was primarily affected by the net photosynthetic rate of leaves. However, the net photosynthetic rate (P_n) under the growth environment did not support the growth results in this study. This phenomenon was also found in previous studies (Kim et al., 2004; Son and Oh, 2015). The possible explanation for this result was that the P_n measured on a single leaf cannot represent the P_n of the whole plant (Yorio et al., 2001; Li et al., 2020). Thus, whole-plant net assimilation was introduced in this study because whole-plant net assimilation has been used to evaluate the photosynthesis of the whole plant (Park and Runkle, 2018). In this study, the whole-plant net assimilation under G30 and G60 showed a nearly similar trend to the dry mass. This result may indicate that G30 and G60 had the ability to improve the whole-plant photosynthesis of lettuce plants. Moreover, the total leaf area of plants affects the light energy received by the plants, because the incident radiation interception increases with increasing the total leaf area (Bugbee, 2016; Snowden et al., 2016). The promotive effects of G30 (15% green light) and G60 (30% green light) on dry matter accumulated by lettuce leaves could be mainly attributed to the increase in leaf area caused by the shade avoidance syndrome, as described in this study. Kim et al. (2004) also found that fresh and dry weights of the lettuce shoot increased significantly when 24% of red and blue light was replaced with green light.

Moderate Amount of Green Light Increased the Concentration of Carbohydrate and Nutritional Quality in Lettuce

Carbohydrate is the final product of CO_2 absorption in the progress of plant photosynthesis (Taiz and Zeiger, 2015). In this experiment, the concentration of carbohydrates under the treatments employing green light was at a higher level than that of P_{n-T} in the difference of statistical analysis. This result implicated replacing red and blue light with 15–45% of green light since the ability of plants to accumulate carbohydrates was stronger under green light than under red and blue light.

In general, higher soluble sugar concentration results in a desirable taste of the plant (Lin et al., 2013). In this study, a relatively higher soluble sugar concentration was found under G60. Chen et al. (2016) also found that supplementing green light to white LEDs increased the soluble sugar content and decreased the nitrate content in green oak leaf lettuce. However, vegetables with high nitrate concentrations are harmful to human health. Especially in China, the allowable highest nitrate concentration of leaf vegetables is 3.0 mg g^{-1}. In this study, the nitrate concentration of lettuce leaves could be significantly decreased by employing green light. Li et al. (2020) also found that partially replacing red and blue light with green light decreased the nitrate content in lettuce leaves. Bian et al. (2018) agreed with the above result that green light could decrease the nitrate contents in lettuce leaves by regulating the expression of some specific genes (e.g., *NR* and *NiR*). Crude fiber, as an important component of a plant cell wall, provided the crisp taste of and nutrients in lettuce for human beings (Taiz and Zeiger, 2015). However, no significant influence of green light on lettuce crude fiber was found in this study. Results presented in this study suggested that a moderate amount of green light could enhance the nutritional quality of lettuce plants.

CONCLUSION

The optimal proportion of green light, partially replacing red and blue light, for promoting plant growth and development was investigated in this study. Our results showed that plant growth and morphology, light absorptance and transmittance, pigment concentration, stomatal characteristics, photosynthetic characteristics, carbohydrates, and nutritional quality were affected by different proportions of green light. The best green proportion was 30% in G60 in this study because G60 not only increased the leaf expansion and lettuce yield but also improved the accumulation of carbohydrate and nutritional quality. In addition, 15% green light in G30 and 45% green light in G90 also showed some advantages in lettuce growth. G30 increased the leaf expansion and yield and decreased the nitrate content of lettuce plants. G90 increased the accumulation of carbohydrates and decreased the nitrate content in lettuce plants, but no significant influence of G90 on lettuce yield was observed. Thus, from the perspective of economic benefits, the proportion of green light substituting red and blue light should be controlled between 15 and 30% in the production of lettuce, according to

this experiment. The more accurate proportion still needs to be explored deeply in future studies.

DATA AVAILABILITY STATEMENT

The original contributions presented in the study are included in the article/**Supplementary Material**, further inquiries can be directed to the corresponding author/s.

AUTHOR CONTRIBUTIONS

LL carried out the measurements, data analysis, and drafted the manuscript. J-lL, Y-mL, and XL participated in part of measurements. Y-xT and R-fC made substantial guide about the experiment design and manuscript revision. All authors contributed to the article and approved the submitted version.

FUNDING

This work was financially supported by the National Key Research and Development Program, Ministry of Science and Technology of China (No. 2020YFE0203600) and the Science and Technology Partnership Program, Ministry of Science and Technology of China (No. KY201702008).

SUPPLEMENTARY MATERIAL

The Supplementary Material for this article can be found online at: https://www.frontiersin.org/articles/10.3389/fpls.2021.627311/full#supplementary-material

Supplementary Figure 1 | The diagram of the measuring apparatus.

REFERENCES

Bantis, F., Smirnakou, S., Ouzounis, T., Koukounaras, A., and Ntagkas, N., Radaglou, K. (2018). Current status and recent achievements in the field of horticulture with the use of light-emitting diodes (LEDs). *Sci. Hortic.* 235, 437–451. doi: 10.1016/j.scienta.2018.02.058

Bian, Z., Cheng, R., Wang, Y., Yang, Q., and Lu, C. (2018). Effects of green light on nitrate reduction and edible quality of hydroponically grown lettuce (*Lactuca sativa* L.) under short-term continuous light from red and blue light-emitting diodes. *Environ. Expt. Bot.* 153, 63–71. doi: 10.1016/j.envexpbot.2018.05.010

Bouly, J. P., Schleicher, E., Dionisio-Sese, M., Vandenbussche, F., Straeten, D. V. D., Bakrim, N., et al. (2007). Cryptochrome blue light photoreceptors are activated through interconversion of flavin redox states. *J. Biol. Chem.* 282, 9383–9391. doi: 10.1074/jbc.M609842200

Bugbee, B. (2016). Toward an optimal spectral quality for plant growth and development: the importance of radiation capture. *Acta Hortic.* 1134, 1–12. doi: 10.17660/ActaHortic.2016.1134.1

Cataldo, D. A., Maroon, M., Schrader, L. E., and Youngs, V. L. (1975). Rapid colorimetric determination of nitrate in plant tissue by nitration of salicylic acid 1. *Commun. Soil Sci Plant Anal.* 6, 71–80. doi: 10.1080/00103627509366547

Chen, X., Xue, X., Guo, W., Wang, L., and Qiao, X. (2016). Growth and nutritional properties of lettuce affected by mixed irradiation of white and supplemental light provided by light-emitting diode. *Sci. Hort.* 200, 111–118. doi: 10.1016/j.scienta.2016.01.007

Clegg, K. M. (1956). The application of the anthrone reagent to the estimation of starch in cereals. *J. Sci. Food Agric.* 7, 40–44. doi: 10.1002/jsfa.2740070108

Ehonen, S., Hölttä, T., and Kangasjärvi, J. (2020). Systemic signaling in the regulation of stomatal conductance. *Plant Physiol.* 182, 1829–1832. doi: 10.1104/pp.19.01543

Fairbairn, N. J. (1953). A modified anthrone reagent. *Chem. Ind.* 4:86.

Fanourakis, D., Giday, H., Milla, R., Pieruschka, R., Kjaer, K. H., Vasilevski, A., et al. (2015). Pore size regulates operating stomatal conductance, while stomatal densities drive the partitioning of conductance between leaf sides. *Ann. Bot.* 115, 555–565. doi: 10.1093/aob/mcu247

Fils-Lycaon, B., Julianus, P., Chillet, M., Galas, C., Hubert, O., Rinaldo, D., et al. (2011). Acid invertase as a serious candidate to control the balance source versus (glucose+fructose) of banana fruit during ripening. *Sci. Hortic.* 129, 197–206. doi: 10.1016/j.scienta.2011.03.029

Frechilla, S., Talbott, L. D., Bogomolni, R. A., and Zeiger, E. (2000). Reversal of blue light-stimulated stomatal opening by green light. *Plant Cell Physiol.* 41, 171–176. doi: 10.1093/pcp/41.2.171

Johkan, M., Shoji, K., Goto, F., Hahida, S., and Yoshihara, T. (2012). Effect of green light wavelength and intensity on photomorphogenesis and photosynthesis in *Lactuca sativa*. *Environ. Exp. Bot.* 75, 128–133. doi: 10.1016/j.envexpbot.2011.08.010

Kaiser, E., Weerherm, K., Schipper, R., and Dieleman, J. A. (2019). Partial replacement of red and blue by green light increases biomass and yield in tomato. *Sci. Hortic.* 249, 271–279. doi: 10.1016/j.scienta.2019.02.005

Kami, C., Lorrain, S., Hornitschek, P., and Fankhauser, C. (2010). Light-regulated plant growth and development. *Curr. Top. Dev. Biol.* 91, 29–66. doi: 10.1016/S0070-2153(10)91002-8

Kang, W. H., Park, J. S., Park, K. S., and Son, J. E. (2016). Leaf photosynthetic rate, growth, and morphology of lettuce under different fractions of red, blue, and green light from light-emitting diodes (LEDs). *Hortic. Environ. Biotechnol.* 57, 573–579. doi: 10.1007/s13580-016-0093-x

Kim, H. H., Goins, G. D., Wheeler, R. M., and Sager, J. C. (2004). Green-light supplementation for enhanced lettuce growth under red- and blue-light-emitting diodes. *Hort. Sci.* 39, 1617–1622. doi: 10.21273/HORTSCI.39.7.1617

Lake, J. A., Quick, W. P., Beerling, D. J., and Woodward, F. I. (2001). Plant development: Signals from mature to new leaves. *Nature* 411:154. doi: 10.1038/35075660

Li, L., Tong, Y., Lu, J., Li, Y., and Yang, Q. (2020). Lettuce growth, nutritional quality, and energy use efficiency as affected by red-blue light combined with different monochromatic wavelengths. *Hort. Sci.* 55, 613–620. doi: 10.21273/HORTSCI14671-19

Lichtenthaler, H. K., and Wellburn, A. R. (1983). Determination of total carotenoids and chlorophylls a and b of leaf extracts in different solvents. *Biochem. Soc. Trans.* 603, 591–592. doi: 10.1042/bst0110591

Lin, K., Huang, M., Huang, W., Hsu, M., Yang, Z., and Yang, C. (2013). The effects of red, blue, and white light-emitting diodes on the growth, development, and edible quality of hydroponically grown lettuce (*Lactuca sativa*, *L. var. capitata). Sci. Hortic.* 150, 86–91. doi: 10.1016/j.scienta.2012.10.002

Liu, B., Liu, H., Zhong, D., and Lin, C. (2010). Searching for a photocycle of the cryptochrome photoreceptors. *Curr. Opin. Plant Biol.* 13, 578–586. doi: 10.1016/j.pbi.2010.09.005

Materová, Z., Sobotka, R., Zdvihalová, B., Oravec, M., Nezval, J., Karlicky, V., et al. (2017). Monochromatic green light induces an aberrant accumulation of geranylgeranyled chlorophylls in plants. *Plant Physiol. Biochem.* 116, 48–56. doi: 10.1016/j.plaphy.2017.05.002

Matthews, J. S. A., Vialet-Chabrand, S., and Lawson, T. (2020). Role of blue and red light in stomatal dynamic behavior. *J. Exp. Bot.* 71, 2253–2269. doi: 10.1093/jxb/erz563

McCree, K. J. (1972). The action spectrum, absorptance and quantum yield of photosynthesis in crop plants. *J. Agric. Meteorol.* 9, 191–216. doi: 10.1016/0002-1571(71)90022-7

Miyazawa, S., Livingston, N. J., and Turpin, D. H. (2006). Stomatal development in new leaves is related to the stomatal conductance of mature leaves in poplar (*Populus trichocarpa*×*P. deltoides). J. Exp. Bot.* 57, 373–380. doi: 10.1093/jxb/eri278

Park, Y., and Runkle, E. S. (2017). Far-red radiation promotes growth of seedlings by increasing leaf expansion and whole-plant net assimilation. *Environ. Exp. Bot.* 136, 41–49. doi: 10.1016/j.envexpbot.2016.12.013

Park, Y., and Runkle, E. S. (2018). Far-red radiation and photosynthetic photon flux density independently regulate seedling growth but interactively regulate flowering. *Environ. Exp. Bot.* 155, 206–216. doi: 10.1016/j.envexpbot.2018.06.033

Sager, J. C., Smith, W. O., Edwards, J. L., and Cyr, K. L. (1988). Photosynthetic efficiency and phytochrome photoequilibria determination using spectral data. *T ASABE.* 31, 1882–1889. doi: 10.13031/2013.30952

Schenkels, L., Saeys, W., Lauwers, A., and Proft, M. P. D. (2020). Green light induces shade avoidance to alter plant morphology and increases biomass production in *Ocimum basilicum*, *L. Sci. Hortic.* 261:109002. doi: 10.1016/j.scienta.2019.109002

Sellaro, R., Creyp, M., Trupkin, S. A., Karayekov, E., Buchovsky, A. S., Rossi, C., et al. (2010). Cryptochrome as a sensor of the blue/green ratio of natural radiation in arabidopsis[1[C][W][OA]]. *Plant Physiol.* 154, 401–409. doi: 10.1104/pp.110.160820

Smith, H., and Whitelam, G. C. (1997). The shade avoidance syndrome: multiple responses mediated by multiple phytochromes. *Plant Cell Environ.* 20, 840–844. doi: 10.1046/j.1365-3040.1997.d01-104.x

Smith, H. L., McAusland, L., and Murchie, E. H. (2017). Don't ignore the green light: Exploring diverse roles in plant processes. *J. Exp. Bot.* 68, 2099–2110. doi: 10.1093/jxb/erx098

Snowden, M. C., Cope, K. R., and Bugbee, B. (2016). Sensitivity of seven diverse species to blue and green light: interactions with photon flux. *PLoS ONE* 11:e0163121. doi: 10.1371/journal.pone.0163121

Son, K., and Oh, M. M. (2015). Growth, photosynthetic and antioxidant parameters of two lettuce cultivars as affected by red, green, and blue light-emitting diodes. *Hortic. Environ. Biotechnol.* 56, 639–653. doi: 10.1007/s13580-015-1064-3

Sun, J., Nishio, J. N., and Vogelmann, T. C. (1998). Green light drives CO_2 fixation deep within leaves. *Plant Cell Physiol.* 39, 1020–1026. doi: 10.1093/oxfordjournals.pcp.a029298

Taiz, L., and Zeiger, E. (2015). *Plant Physiology*, *5th Edn*. Sunderland, MA: Sinauer Assoc Inc.

Terashima, I., Fujita, T., Inoue, T., Chow, W. S., and Oguchi, R. (2009). Green light drives leaf photosynthesis more efficiently than red light in strong white light: revisiting the enigmatic question of why leaves are green. *Plant Cell Physiol.* 50, 684–697. doi: 10.1093/pcp/pcp034

Wang, J., Lu, W., Tong, Y., and Yang, Q. (2016). Leaf morphology, photosynthetic performance, chlorophyll fluorescence, stomatal development of lettuce (*Lactuca sativa* L.) exposed to different ratios of red light to blue light. *Front. Plant Sci.* 7:250. doi: 10.3389/fpls.2016.00250

Wang, Y., and Folta, K. M. (2013). Contributions of green light to plant growth and development. *Am. J. Bot.* 100, 70–78. doi: 10.3732/ajb.1200354

Yorio, N. C., Goin, G. D., Kagie, H. R., Wheeler, R. M., and Sager, J. C. (2001). Improving spinach, radish, and lettuce growth under red light-emitting diodes (LEDs) with blue light supplementation. *Hort. Sci.* 36, 380–383. doi: 10.21273/HORTSCI.36.2.380

Zadoks, J. C., Chang, T. T., and Konzak, C. F. (1974). A decimal code for the growth stages of cereals. *Weed Res.* 14, 415–421. doi: 10.1111/j.1365-3180.1974.tb01084.x

Zhang, T., Maruhnich, S. A., and Folta, K. M. (2011). Green light induces shade avoidance synmptoms[1[C][W][OA]]. *Plant Physiol.* 157, 1528–1536. doi: 10.1104/pp.111.180661

Conflict of Interest: The authors declare that the research was conducted in the absence of any commercial or financial relationships that could be construed as a potential conflict of interest.

Copyright © 2021 Li, Tong, Lu, Li, Liu and Cheng. This is an open-access article distributed under the terms of the Creative Commons Attribution License (CC BY). The use, distribution or reproduction in other forums is permitted, provided the original author(s) and the copyright owner(s) are credited and that the original publication in this journal is cited, in accordance with accepted academic practice. No use, distribution or reproduction is permitted which does not comply with these terms.

Advantages of publishing in Frontiers

OPEN ACCESS
Articles are free to read for greatest visibility and readership

FAST PUBLICATION
Around 90 days from submission to decision

HIGH QUALITY PEER-REVIEW
Rigorous, collaborative, and constructive peer-review

TRANSPARENT PEER-REVIEW
Editors and reviewers acknowledged by name on published articles

Frontiers
Avenue du Tribunal-Fédéral 34
1005 Lausanne | Switzerland

Visit us: www.frontiersin.org
Contact us: frontiersin.org/about/contact

REPRODUCIBILITY OF RESEARCH
Support open data and methods to enhance research reproducibility

DIGITAL PUBLISHING
Articles designed for optimal readership across devices

FOLLOW US
@frontiersin

IMPACT METRICS
Advanced article metrics track visibility across digital media

EXTENSIVE PROMOTION
Marketing and promotion of impactful research

LOOP RESEARCH NETWORK
Our network increases your article's readership